AD-A191 295 PROCEEDINGS OF THE TRI-SERVICE CONFERENCE ON CORROSION (1987) HELD AT THE..(U) AIR FORCE WRIGHT AERONAUTICAL LABS WRIGHT-PATTERSON AFB OH.. F H MEYER MAY 87 1/6

UNCLASSIFIED AFWAL-TR-87-4139-VOL-1 F/G 11/6.1 NL

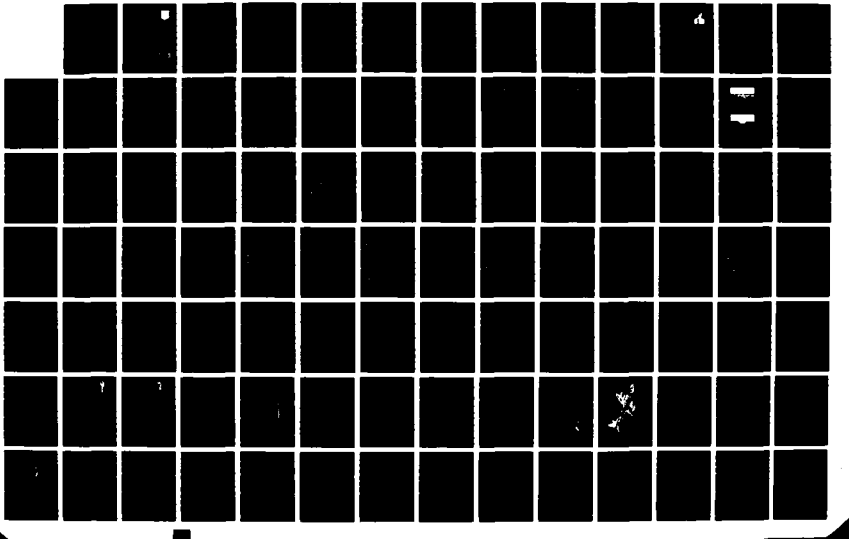

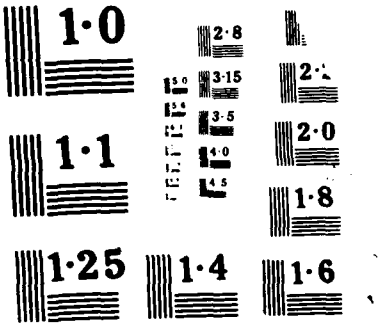
1·0
1·1
1·25
2·8
3·15
3·5
4·0
2·0
1·8
1·4
1·6

(2)

AFWAL-TR-87-4139
VOLUME I

AD-A191 295

PROCEEDINGS OF THE 1987 TRI-SERVICE CONFERENCE ON CORROSION

Fred H. Meyer Jr., Editor
Air Force Wright Aeronautical Laboratories
Materials Laboratory

MAY 1987

U.S. Air Force Academy, Colorado

Approved for public release; distribution unlimited.

MATERIALS LABORATORY
AIR FORCE WRIGHT AERONAUTICAL LABORATORIES
AIR FORCE SYSTEMS COMMAND
WRIGHT-PATTERSON AFB, OHIO 45433-6533

NOTICE

When Government drawings, specifications, or other data are used for any purpose other than in connection with a definitely related Government procurement operation, the United States Government thereby incurs no responsibility nor any obligation whatsoever; and the fact that the government may have formulated, furnished, or in any way supplied the said drawings, specifications, or other data, is not to be regarded by implication or otherwise as in any manner licensing the holder or any other person or corporation, or conveying any rights or permission to manufacture use, or sell any patented invention that may in any way be related thereto.

This report has been reviewed by the Office of Public Affairs (ASD/PA) and is releasable to the National Technical Information Service (NTIS). At NTIS, it will be available to the general public, including foreign nations.

This technical report has been reviewed and is approved for publication.

Fred H. Meyer

FRED H. MEYER
Corrosion Control/Non-Destructive
Evaluation Group
Systems Support Division

Thomas D. Cooper by RW

THOMAS D. COOPER, Chief
Materials Integrity Branch
Systems Support Division
Materials Laboratory

FOR THE COMMANDER

Warren P Johnson by RK

WARREN P. JOHNSON, Chief
Systems Support Division
Materials Laboratory

If your address has changed, if you wish to be removed from our mailing list, or if the addressee is no longer employed by your organization, please notify AFWAL/MLSA, W-PAFB, OH 45433 to help us maintain a current mailing list .

Copies of this report should not be returned unless return is required by security considerations, contractual obligations, or notice on a specific document.

CONFERENCE COMMITTEE

Chairman
Fred H. Meyer, Jr.
Air Force Wright Aeronautical Laboratories

Vice Chairman
Richard Kinzie
Warner Robins Air Logistics Center

Technical Program
Vinod Agarwala
Naval Air Development Center

Denise Aylor/Terry Morton
Naval Ship Research and Development Center

Richard Kinzie
Warner Robins Air Logistics Center

Milton Levy
Army Materials Technology Laboratory

Fred H. Meyer, Jr.
Air Force Wright Aeronautical Laboratories

Robert Reeber
Army Research Office

John Sedriks
Office of Naval Research

Unclassified
SECURITY CLASSIFICATION OF THIS PAGE

AD-A191 295

REPORT DOCUMENTATION PAGE

Form Approved
OMB No. 0704-0188

1a. REPORT SECURITY CLASSIFICATION Unclassified	1b. RESTRICTIVE MARKINGS
2a. SECURITY CLASSIFICATION AUTHORITY	3. DISTRIBUTION/AVAILABILITY OF REPORT Approved for public release; distribution is unlimited.
2b. DECLASSIFICATION/DOWNGRADING SCHEDULE	
4. PERFORMING ORGANIZATION REPORT NUMBER(S)	5. MONITORING ORGANIZATION REPORT NUMBER(S) AFWAL-TR-87-4139, Volume I
6a. NAME OF PERFORMING ORGANIZATION Materials Integrity Branch Systems Support Division 6b. OFFICE SYMBOL (If applicable) AFWAL/MLSA	7a. NAME OF MONITORING ORGANIZATION
6c. ADDRESS (City, State, and ZIP Code) AFWAL/MLSA Wright-Patterson AFB OH 45433-6533	7b. ADDRESS (City, State, and ZIP Code)
8a. NAME OF FUNDING/SPONSORING ORGANIZATION Materials Laboratory 8b. OFFICE SYMBOL (If applicable) AFWAL/MLSA	9. PROCUREMENT INSTRUMENT IDENTIFICATION NUMBER
8c. ADDRESS (City, State, and ZIP Code) AFWAL/MLSA WPAFB OH 45433-6533	10. SOURCE OF FUNDING NUMBERS PROGRAM ELEMENT NO / PROJECT NO / TASK NO / WORK UNIT ACCESSION NO.

11. TITLE (Include Security Classification)
Proceedings of the 1987 Tri-Service Conference on Corrosion

12. PERSONAL AUTHOR(S)
Fred H. Meyer, Jr. (Editor)

13a. TYPE OF REPORT	13b. TIME COVERED	14. DATE OF REPORT (Year, Month, Day)	15. PAGE COUNT
Final	FROM 1/86 TO 5/87	May 1987	546

16. SUPPLEMENTARY NOTATION

17. COSATI CODES			18. SUBJECT TERMS (Continue on reverse if necessary and identify by block number)
FIELD	GROUP	SUB-GROUP	

19. ABSTRACT (Continue on reverse if necessary and identify by block number)
This report is a compilation of the papers presented at the 1987 Tri-Service Conference on Corrosion held at the Air Force Academy, Colorado on 5-7 May 1987.

20. DISTRIBUTION/AVAILABILITY OF ABSTRACT ☒ UNCLASSIFIED/UNLIMITED ☐ SAME AS RPT ☐ DTIC USERS	21. ABSTRACT SECURITY CLASSIFICATION Unclassified
22a. NAME OF RESPONSIBLE INDIVIDUAL Fred H. Meyer	22b. TELEPHONE (Include Area Code) (513) 255-5117 22c. OFFICE SYMBOL AFWAL/MLSA

DD Form 1473, JUN 86 Previous editions are obsolete. SECURITY CLASSIFICATION OF THIS PAGE
Unclassified

FOREWORD

This report was compiled by the Materials Integrity Branch, Systems Support Division, Materials Laboratory, Air Force Wright Aeronautical Laboratories, Wright-Patterson AFB, Ohio. It was initiated under Task 24180704 "Corrosion Control & Failure Analysis" with Fred H. Meyer, Jr. as the Project Engineer. The 1987 Tri-Service Conference on Corrosion is a follow-up of eight prior conferences held in 1967, 1969, 1972, 1974, 1976, 1978, 1980 and 1983.

This Report (Vol I, Vol II) includes all available papers from the 1987 Tri-Service Conference on Corrosion.

This technical report was submitted by the editor.

Proceedings of Prior Conferences are available in:

1. AFML-TR-67-329 (1967) (AD 826-198)

2. MCIC 73-19 (1972) (AD 771345)

3. AFML-TR-75-42 Vol I, Vol II (1974) (ADA 021053, ADA 029934)

4. MCIC-77-33 (1976) (ADO 49769)

5. MCIC-79-40 (1978) (AD A- 73054)

6. AFWAL-TR-81-4019 Vol I, Vol 2 (1980) (ADA 106803)
(ADA 115785)

7. 1963 Tri-Service Corrosion Conference Proceeding Naval Ship R&D Center Annapolis, MD 20084.

The purpose of the 1987 Conference was to continue interservice Coordination in the areas of corrosion research and corrosion prevention and control. Specifically, the objectives were to make Department of Defense personnel, contractors and interest individuals aware of the important Corrosion problems in Military equipment, to present the status of significant corrosion research projects currently pursued by the military services and to provide a general forum for exchange of corrosion prevention and control information.

TABLE OF CONTENTS

VOLUME I

TABLE OF CONTENTS

VOLUME I

CONTINUED

1987 TRI-SERVICE CORROSION CONFERENCE
OPENING REMARKS
by
FRED H. MEYER JR., GENERAL CHAIRMAN

Welcome to the Ninth Biannual Tri-Service Corrosion Conference. This Conference was established in 1967. Sponsorship alternates among the Air Force, Navy and Army.

This year's Conference is sponsored by the Materials Integrity Branch, Systems Support Division of the Air Force Wright Aeronautical Laboratories, Materials Laboratory, Wright-Patterson Air Force Base, Ohio.

Corrosion of equipment continues to be a major problem for the Armed Forces, so the purpose of this Conference is to present current research and development relating to current problems in corrosion control and prevention of deterioration of military and aerospace systems due to corrosion.

Each Service has large numbers of aging weapon systems which require strong corrosion control efforts for their survival. Increasingly, more complex new weapon systems being developed by the Services also require very strong corrosion prevention design surveillance.

A free exchange of the best methods currently available for combating the serious corrosion problem will lead to the incorporation of better materials and methods in the acquisition of new systems. Discussions by leading experts in the field and the airing of current problems will not only provide valuable guidances to the Air Force, Navy, and Army programs , but will assist in stimulating high level technical people from key industrial and academic organizations to assist in solving critical DOD corrosion problems.

The earlier Tri-Service Corrosion conferences concluded that greater implementation of existing technology is especially needed within the Services. There has been considerable difficulty in the past in implementing transitioning in the state-of-the-arts in solving design and field problems.

This has been one of the major goals of the Tri-Service Corrosion Conferences in the past and will continue to be a primary goal. This Conference is dedicated to the rapid efficient transfer in advanced state-of-the-art technology in corrosion science and engineering into the direct use in the production of more effective systems for national defense.

We hope by the sponsorship of this conference to make a significant contribution to keeping our defense systems more reliable, more durable and economical by providing an open forum for the discussion of corrosion problems which at the present time plague all of the services.

The papers will be presented in concurrent sessions after lunch today, and for the balance of the Conference. They will be in this hall and the other designated hall. Please feel free to move from session to session if papers of significant interest to you are presented at different sessions.

I would like to recognize at this time the members of the Executive Planning Committee without whose considerable personal efforts this Conference would have not been possible. Also, I would like to recognize at this time members of the National Association of Corrosion Engineers Technical Committee T9 Corrosion of Aerospace Equipment. This Committee and its Subcommittees are meeting here in conjunction with the 1987 Tri-Service Corrosion Conference.

This Conference has been recognized by the DOD Joint Logistics Commanders as the prime forum for interchange of corrosion information between each of the Services and their contractors.

Our next speaker is Colonel John P. May, Acting Dean of Faculty of the Air Force Academy.

BIOGRAPHY

NAME: Fred H. Meyer, Jr.

PRESENT AFFILIATION:
AFWAL/MLSA, Wright Patterson AFB, Ohio

TITLE:
Materials Engineer (General)

FIELD OF INTEREST/RESPONSIBILITIES
Materials utilization, materials deterioration prevention and material processing in existing and new weapons systems.

PREVIOUS AFFILIATIONS/TITLES
Bendix Aerospace Systems Div - Sr Materials Engineer
U. S. Steel Applied Research Lab - Research Engineer
Honeywell, Inc - Sr Materials Engineer
Mosler Safe Co - Chief Metallurgist - Chem Eng
Aeronca Mfg Corp - Sr Materials Eng
National Lead Co of Ohio - Head, Corrosion Section
General Electric Co - Metals Chemist

ACADEMIC BACKGROUND:
BS, Chemistry - Univ of Cincinnati, 1949
Graduate level courses at: Mass Inst - Corrosion 1954
Ohio State Univ - Non-destructive Testing, 1959, Mechanistics Aspects of Stress Corrosion, 1967
Industrial Coll of Armed Forces - Economics of National Security 1961

SOCIETY ACTIVITIES/OFFICE:
National Association of Corrosion Eng (Past National Chairman)
HNO_3 - HF Committees (1958), T9B, T9D 1977 - 1981
ASM, SAMPE, SNT, accredited NACE Corrosion Specialist #1215
Presently: Member of ASTM G-1
Member of interagency chemical rocket propulsion group fuels and compatibility committee

PUBLICATIONS/PATENTS:
"Corrosion Problems Associated with Uranium Refining"
Corrosion, 15, No. 4, 168 (1959)
36 reports dealing with corrosion problems in uranium refining (published by AEC)
1967, 1974, Tri-Service Corrosion Conference Proceedings
Corrosion Performance of New Aircraft Fastener Coatings on Operational Aircraft Paper No 115, Corrosion/73
Recent Air Force Electronics Systems Corrosion Problems Corrosion/74

KEYNOTE ADDRESS

Maj. Gen. Richard F. Gillis
USAF/AFALC Commander

(Not Available At Time Of Printing)

GENERAL SESSION
OVERVIEWS

OVERVIEW OF ARMY CORROSION PREVENTION AND CONTROL PROGRAM

BRIEFER: MILT LEVY

U.S. Army Materials Technology Laboratory, LABCOM
SLCMT-MCM-SB

US ARMY
LABORATORY COMMAND
MATERIALS TECHNOLOGY
LABORATORY

ELEMENTS

- RDT&E PROGRAMS
- CENTER OF EXCELLENCE ACTIVITIES
- TRI-SERVICE AERONAUTICAL COOPERATIVE EFFORTS

US ARMY
LABORATORY COMMAND
MATERIALS TECHNOLOGY
LABORATORY

TECHNOLOGY BASE PROGRAM ACHIEVEMENTS
1987 - 1991
U.S. ARMY MATERIALS TECHNOLOGY LABORATORY

- DEVELOPMENT OF SCC RESISTANT COBALT-FREE MARAGING STEEL
- DEVELOPMENT OF AIRCRAFT QUALITY CORROSION RESISTANT STAINLESS STEEL TRANSMISSION HOUSING
- ASSESSMENT OF PROTECTIVE SCHEMES FOR Mg ALLOYS
- DEVELOPMENT OF ADVANCED LIGHTWEIGHT SCC RESISTANT Al-Li ALLOYS

US ARMY
LABORATORY COMMAND
MATERIALS TECHNOLOGY
LABORATORY

USE OF MAGNESIUM ALLOYS IN ARMY AIRCRAFT

VIETNAM ERA

216 lbs in AH-1G
280 lbs in UH-1H
1304 lbs in CH-47C

PROBLEM ⟶ **CORROSION**

RECENT CH-47D MODIFICATION
MAGNESIUM REPLACED WITH ALUMINUM
- Floor panels
- Floor beams
- Ramp hinge fittings
- Flight control bell cranks

CONCOMITANT WEIGHT PENALTY

GOAL ⟶ ARMY WANTS TO USE MAGNESIUM TO LIGHTEN THE FORCE BUT **CORROSION** REMAINS A **PROBLEM**

NEED ⟶ MORE CORROSION RESISTANT MAGNESIUM ALLOYS. IMPROVED PROTECTIVE COATING SYSTEMS

PROTECTIVE SCHEMES FOR MAGNESIUM ALLOY ZE41A-T5

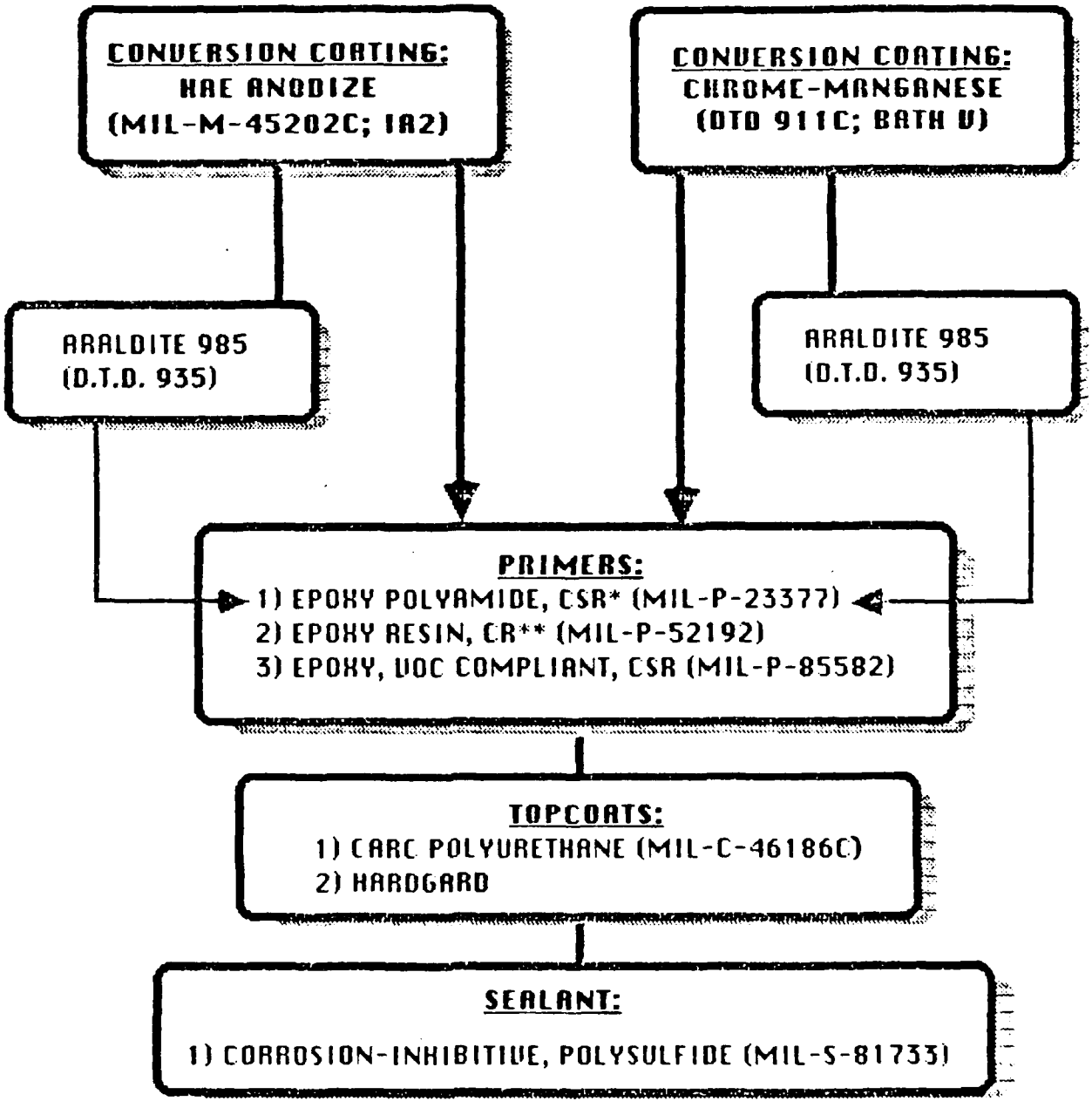

* CHEMICAL AND SOLVENT RESISTANT
** CHEMICAL RESISTANT

TECHNOLOGY BASE PROGRAM ACHIEVEMENTS

- EFFECT OF CREVICES ON STRENGTH OF HIGH STRENGTH STEELS DURING HE
- MITIGATION OF HE OF HIGH STRENGTH STEELS BY ION IMPLANTATION OF N AND B
- DEVELOPMENT OF DESIGN CRITERIA TO AVOID HE AND SCC OF HIGH STRENGTH ALLOYS
- DEVELOPMENT OF MODEL FOR GRAIN BOUNDARY SOLUTE-HYDROGEN INTERACTION IN INTERGRANULAR HE

US ARMY
LABORATORY COMMAND
MATERIALS TECHNOLOGY
LABORATORY

TECHNOLOGY BASE PROGRAM ACHIEVEMENTS

- ION IMPLANTED SURFACE TO MITIGATE CORROSION OF PENETRATOR MATERIALS
- DEVELOPMENT OF CORROSION INHIBITORS TO PREVENT PITTING OF CONTAINERS FOR BINARY WEAPONS
- NDT EDDY CURRENT TECHNIQUE FOR DETECTION OF PITTING IN CHEMICAL MUNITIONS
- DEVELOPMENT OF HIGH TEMPERATURE OXIDATION RESISTANT COATING FOR ADVANCED SINGLE CRYSTAL GAS TURBINE ALLOYS
- DEVELOPMENT OF SAND EROSION/CORROSION RESISTANT COATING FOR GAS TURBINE COMPRESSOR COMPONENTS
- AUTOMATION OF CORROSION TESTING OF METALS/COATINGS USING ROBOTICS

US ARMY
LABORATORY COMMAND
MATERIALS TECHNOLOGY
LABORATORY

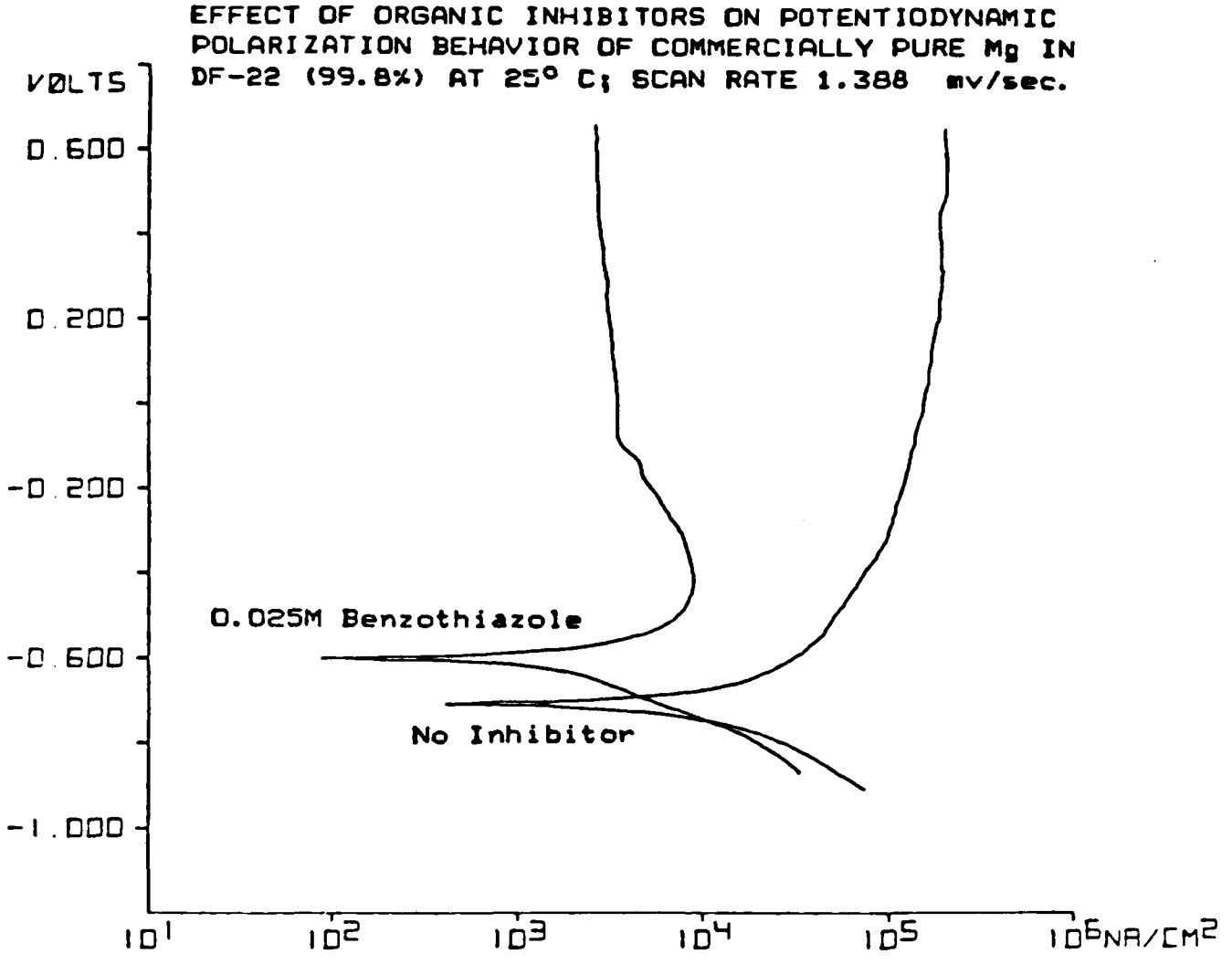
EFFECT OF ORGANIC INHIBITORS ON POTENTIODYNAMIC POLARIZATION BEHAVIOR OF COMMERCIALLY PURE Mg IN DF-22 (99.8%) AT 25° C; SCAN RATE 1.388 mv/sec.
VOLTS
0.600
0.200
-0.200
-0.600
-1.000
0.025M Benzothiazole
No Inhibitor
10¹
10²
10³
10⁴
10⁵
10⁶NA/CM²

REDUCTION OF PITTING OF COMMERCIALLY PURE Mg EXPOSED TO DF-22 VAPOR FOR 15 DAYS BY ADDITION OF 0.025M BENZOTHIAZOLE

Magnification: 40X

COMMERCIALLY PURE Mg
Mg IN DF-22 VAPOR

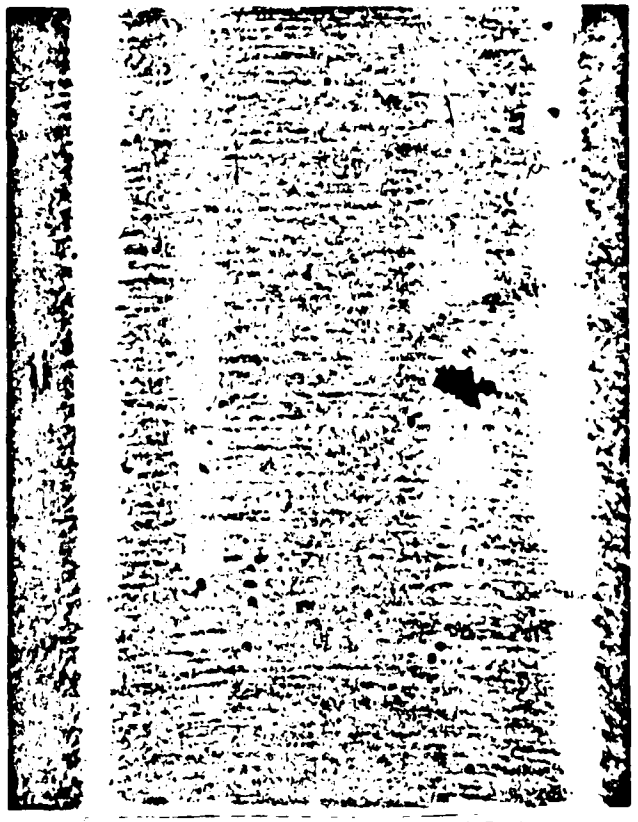

Magnification: 40X

COMMERCIALLY PURE Mg IN DF-22
VAPOR WITH 0.025M BENZOTHIAZOLE

ELIMINATION OF PITTING OF 304 STAINLESS STEEL EXPOSED TO DF-22 VAPOR FOR 30 DAYS BY ADDITION OF 0.025M BENZOTHIAZOLE

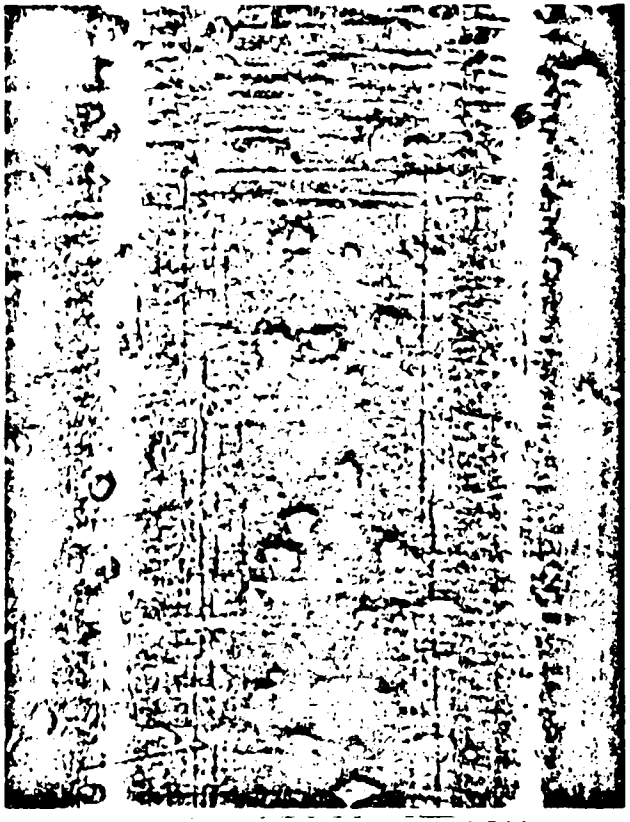

Magnification: 40X

304 STAINLESS STEEL
IN DF-22 VAPOR

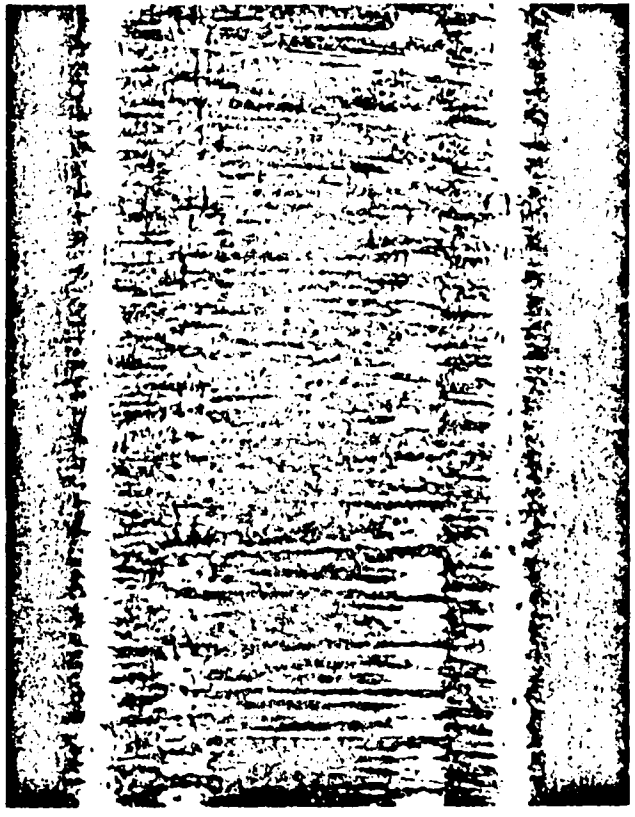

Magnification: 40X

304 STAINLESS STEEL IN DF-22
VAPOR WITH 0.025M BENZOTHIAZOLE

EFFECTS OF DECONTAMINATING SOLUTIONS ON CORROSION OF METALS

- ALUMINUM IS VERY VULNERABLE TO DECONTAMINATION SOLUTIONS (BOTH DS2 AND STB)
- MAGNESIUM IS VULNERABLE TO STB
- CARBON STEEL IS VULNERABLE TO STB
- A METAL MATRIX COMPOSITE MAY SHOW HIGHER CORROSION RATES THAN DOES ITS BASE ALLOY
- MTL DATA SUPPORTS DATA FOUND IN LITERATURE

NOTE: METALS ARE MORE SUSCEPTIBLE TO STB THAN TO DS2
POLYMERS ARE MORE SUSCEPTIBLE TO DS2 THAN TO STB

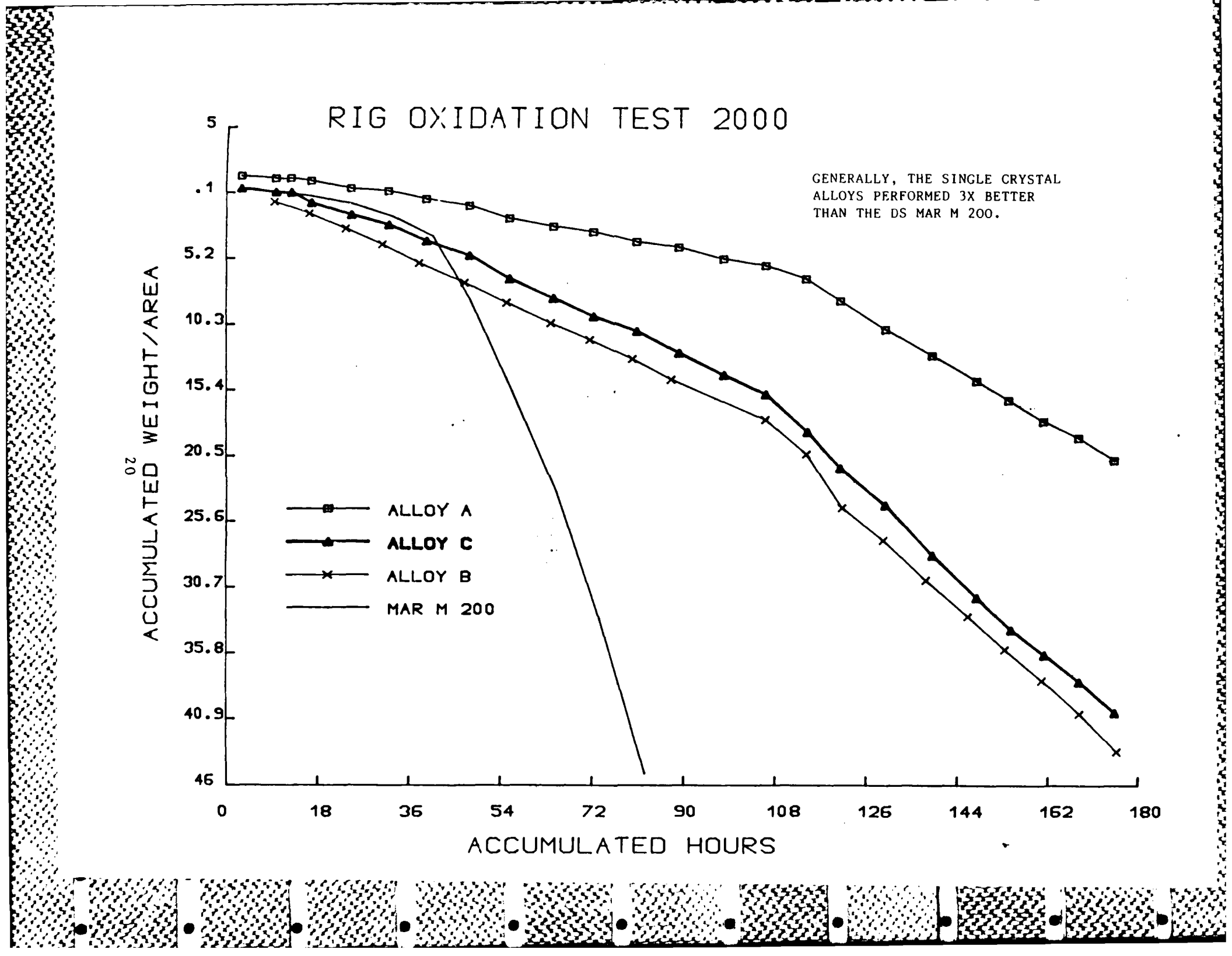
RIG OXIDATION TEST 2000
GENERALLY, THE SINGLE CRYSTAL ALLOYS PERFORMED 3X BETTER THAN THE DS MAR M 200.
ACCUMULATED WEIGHT/AREA
5
.1
5.2
10.3
15.4
20.5
25.6
30.7
35.8
40.9
46
ALLOY A
ALLOY C
ALLOY B
MAR M 200
0
18
36
54
72
90
108
126
144
162
180
ACCUMULATED HOURS

HIGH TEMPERATURE OXIDATION OF ADVANCED GAS TURBINE ALLOYS

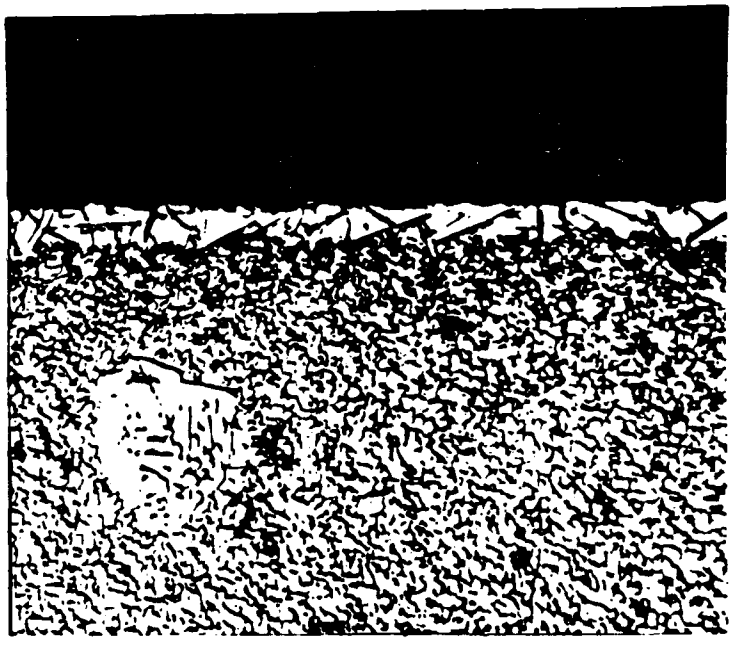

1000X

PHOTOGRAPH OF THE PLATE PHASE IN PWA 1480 AFTER 24 HOURS OF OXIDATION AT 1650 F - THE PLATE PHASE CONSISTS MAINLY OF Ni, Ta, AND W, WITH SOME Cr & Co

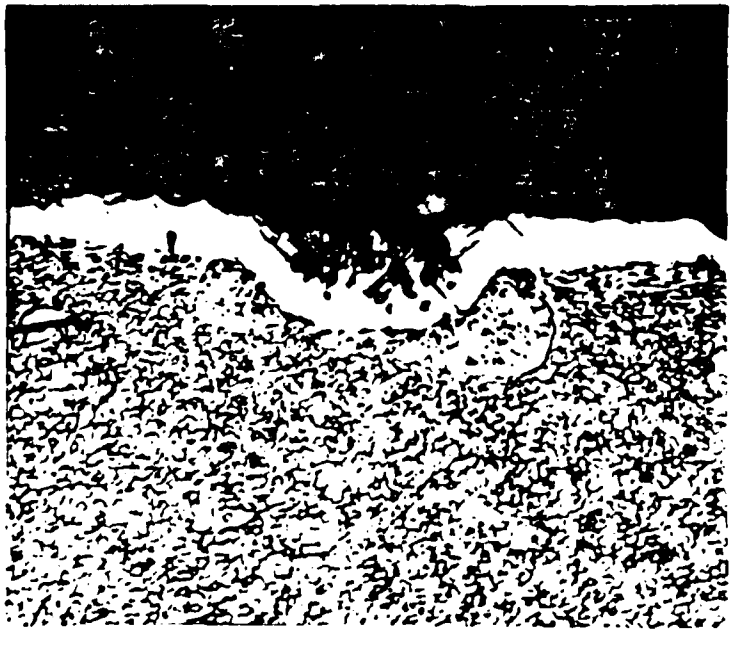

1250X

PHOTOGRAPH SHOWING PREFERENTIAL OXIDATION OF THE PLATE PHASE IN PWA 1480 AFTER 20 HOURS AT 1650 F

TECHNOLOGY BASE PROGRAM ACHIEVEMENTS

- ACCELERATED LIFE PREDICTION OF GLASS, KEVLAR, AND GRAPHITE FIBER COMPOSITES
- DEVELOPMENT OF ENVIRONMENTAL RESISTANT COATING FOR COMPOSITES
  - ACRYLIC URETHANE
  - OXOZILODINE URETHANE
- ASSESSMENT OF REPLACEMENT OF NOMEX HONEYCOMB WITH ROHACELL STRUCTURAL FOAM
  - LOWER FABRICATION COST
- EFFECTS OF PROCESSING VARIABLES ON ENVIRONMENTAL PROPERTIES OF GLASS AND KEVLAR COMPOSITES
  - FILAMENT WINDING VERSUS BRAIDING
- DURABILITY OF ADHESIVE BONDS OF CERAMICS, COMPOSITES, THERMOPLASTICS, AND ELASTOMERS TO METALS

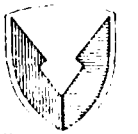

US ARMY
LABORATORY COMMAND
MATERIALS TECHNOLOGY
LABORATORY

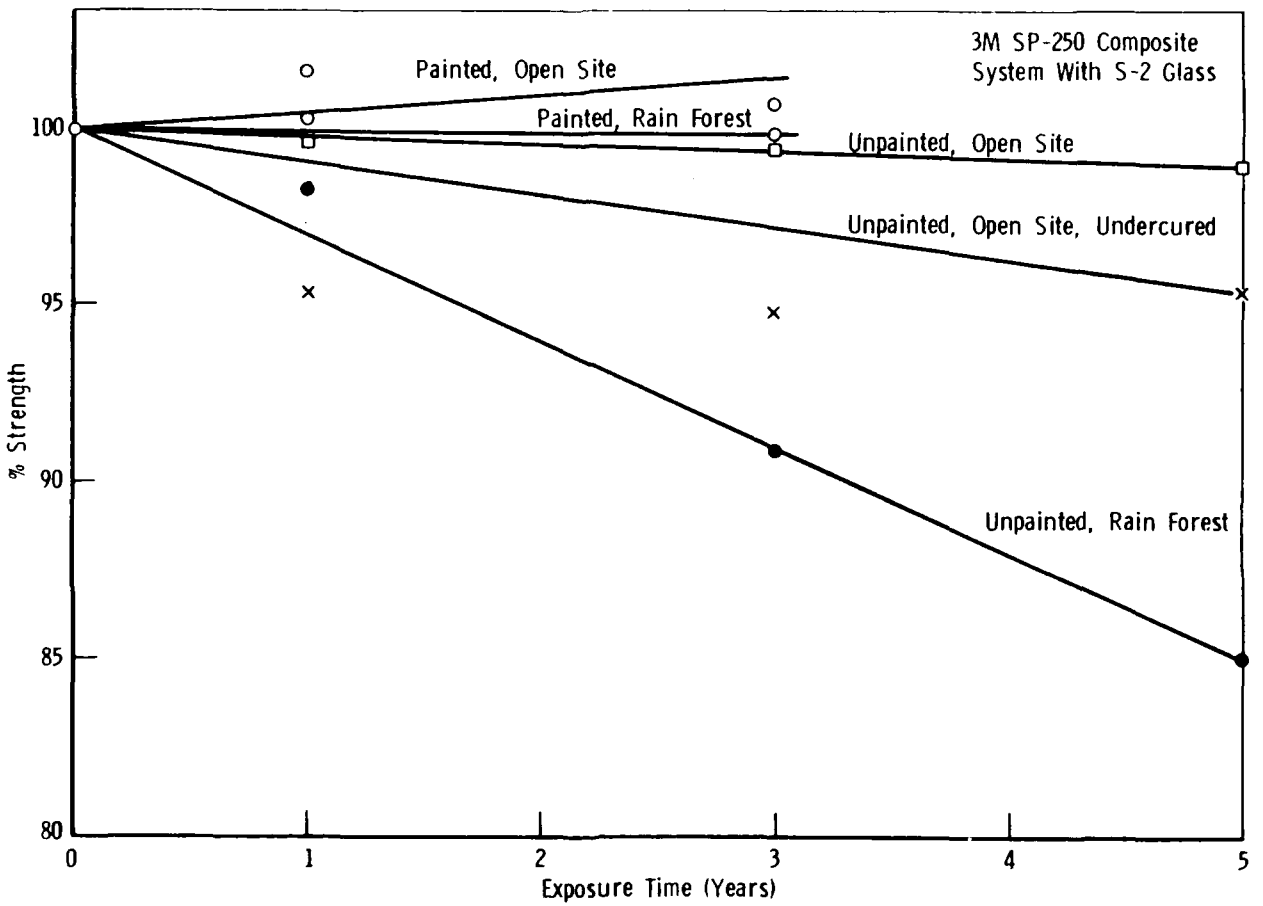

CHANGE IN TENSILE STRENGTH WITH EXPOSURE TIME

US ARMY
LABORATORY COMMAND
MATERIALS TECHNOLOGY
LABORATORY

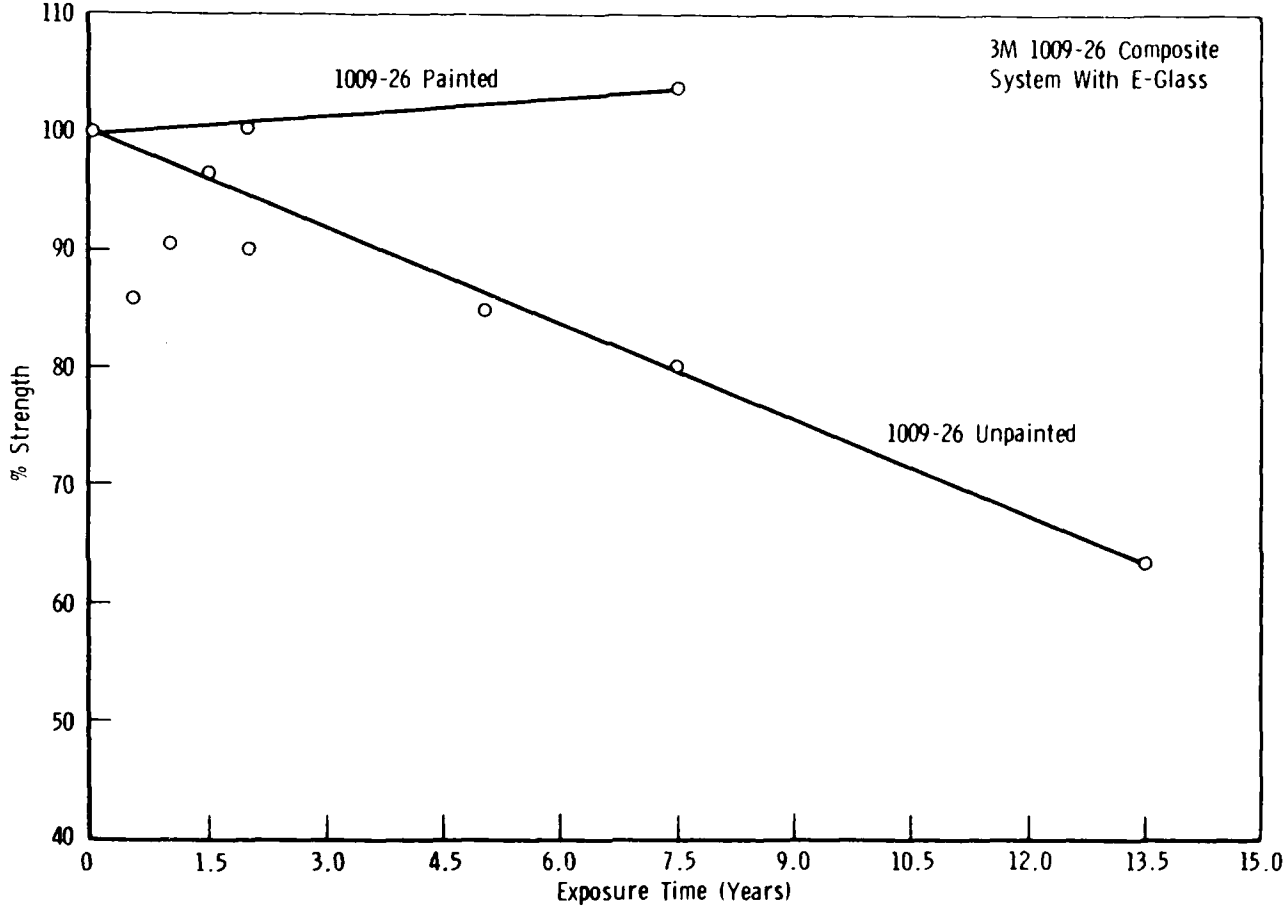

CHANGE IN SHORT BEAM SHEAR STRENGTH WITH EXPOSURE TIME

US ARMY
LABORATORY COMMAND
MATERIALS TECHNOLOGY
LABORATORY

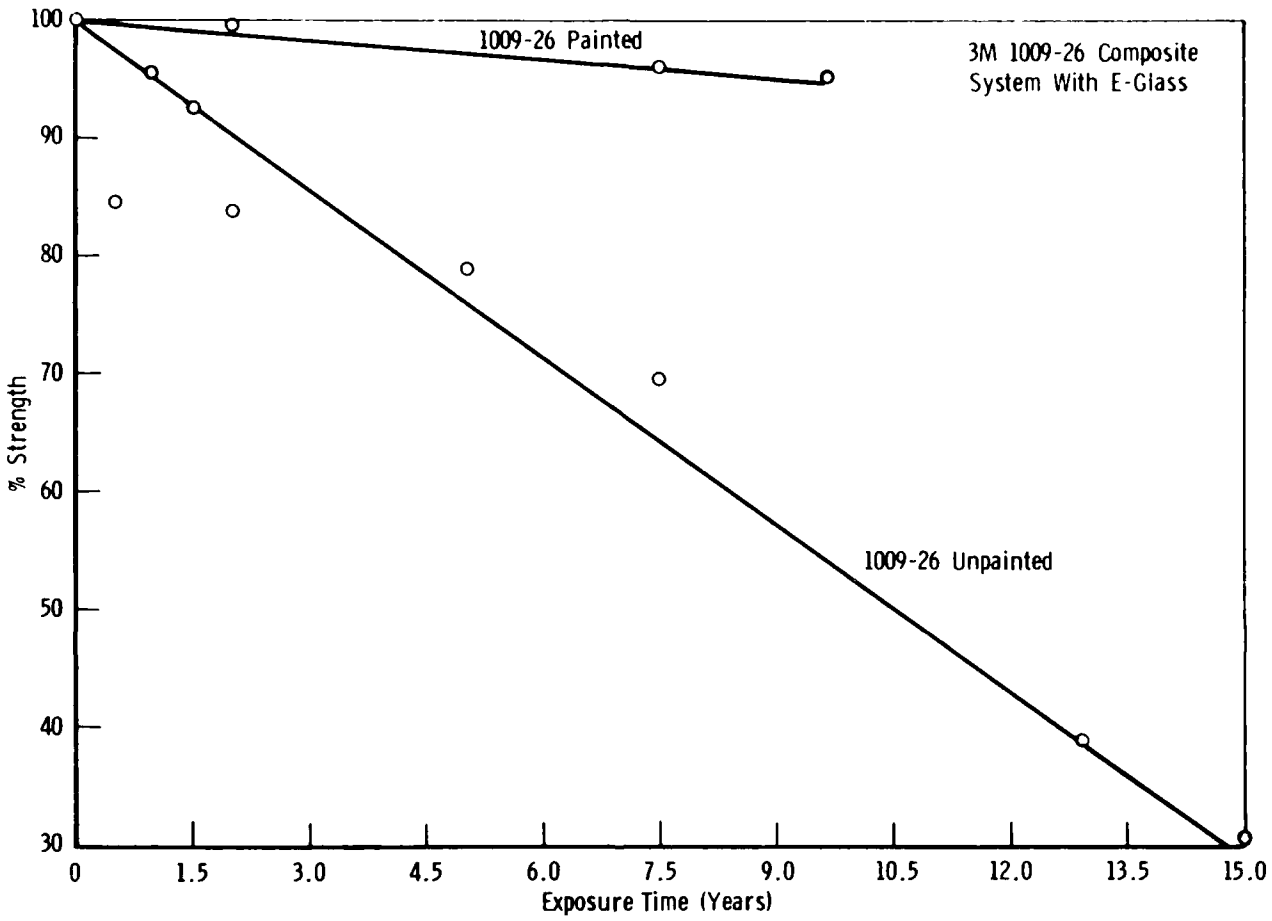

CHANGE IN FLEXURAL STRENGTH WITH EXPOSURE TIME

US ARMY
LABORATORY COMMAND
MATERIALS TECHNOLOGY
LABORATORY

TECHNOLOGY BASE PROGRAM ACHIEVEMENTS

- PLASMA TREATED KEVLAR FIBERS IMPROVES INTERFACIAL PROPERTIES
- IMPROVED EPOXY FIELD REPAIR KIT FOR BATTLE DAMAGE OF COMPOSITES
- ASSESSMENT OF NDT TECHNIQUES FOR MONITORING MOISTURE IN COMPOSITES
  - PORTABLE NEUTRON RADIOGRAPHY
  - PORTABLE NUCLEAR MAGNETIC RESONANCE
  - FIBER OPTICS EMBEDDED SENSORS
- NDT PORTABLE INFRARED PROBE FOR ASSESSING RATE OF DETERIORATION OF COMPOSITES, ORGANIC COATINGS IN THE FIELD

US ARMY
LABORATORY COMMAND
MATERIALS TECHNOLOGY
LABORATORY

BELVOIR RDE CENTER

- DEVELOPMENT AND UPGRADE NEW ADDITIVE STABILIZER INGREDIENTS FOR DIESEL FUEL APPLICATIONS
- DEVELOP MULTIPURPOSE GREASE WITH SALTWATER CORROSION RESISTANCE
- DEVELOP OPERATIONAL PRESERVATIVE ENGINE OILS AND PROCEDURES FOR IMPROVING STORAGE OF EQUIPMENT
- COMPLETE SPECIFICATION REQUIREMENTS FOR COMPATIBILITY OF WHEEL BEARING SEALS WITH NEW MILITARY GREASES
- COMPLETE DEVELOPMENT AND SPECIFICATION FOR VOC COMPLIANT ENAMELS AND PRIMERS
- COMPLETE EVALUATION OF POWDER AND RADIATION CURE COATINGS

US ARMY
LABORATORY COMMAND
MATERIALS TECHNOLOGY
LABORATORY

ARMAMENTS RDE CENTER

- CORROSION OF ARMAMENT MATERIALS
- COMPATIBILITY/DURABILITY OF EXPLOSIVES/ PROPELLANTS WITH COMPOSITE MATERIALS
- AMMUNITION DETERIORATION DUE TO ENERGETIC MATERIALS AND POLYMERS
- REPLACEMENT MATERIAL FOR NYLON 66 IN MUNITIONS

US ARMY
LABORATORY COMMAND
MATERIALS TECHNOLOGY
LABORATORY

TANK AUTOMOTIVE COMMAND

- STATIC FIELD TESTS OF NEW COATINGS TECHNOLOGY USING M151-A2 JEEP BODIES AS TEST BEDS
- DYNAMIC FIELD TESTS OF NEW COATING TECHNOLOGY
- DEVELOPMENT OF COMPUTERIZED DATABASE MANAGEMENT SYSTEMS TO TRACK CORROSION OF THE VEHICLE FLEET
- ACCELERATED CORROSION TESTING OF HIGH MOBILITY MULTIPURPOSE WHEELED VEHICLE HMMWV

TOTAL AMC CPC FUNDS $7M

US ARMY
LABORATORY COMMAND
MATERIALS TECHNOLOGY
LABORATORY

DEGRADATION, REACTIVITY AND PROTECTION

ARO

PROGRAM OBJECTIVES

- To Discover:
  The Atomic/Molecular/Macroscopic Processes Governing Deterioration Of Materials

- To Provide:
  1. New Materials/Coatings That Circumvent Such Processes
  2. Pretreatments/Materials to Improve Adhesion/Bonding

DEGRADATION, REACTIVITY AND PROTECTION

MAJOR ARMY SYSTEMS

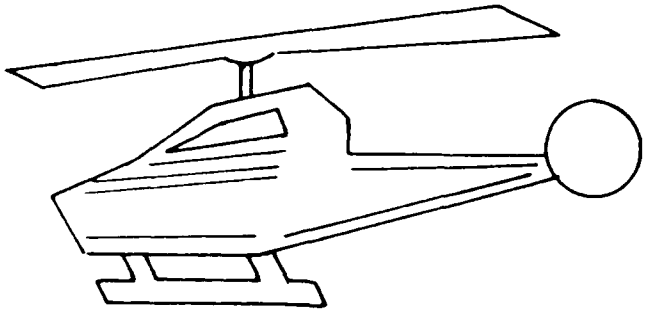

COMPOSITES → MOISTURE, ADHESION, REPAIRS

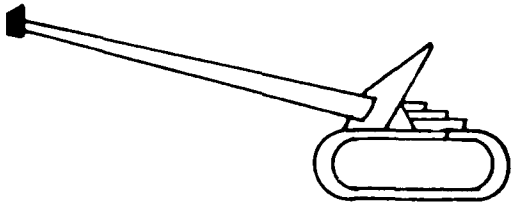

LIQUID PROPELLANTS → EROSION COATINGS

CBD → CORROSION COATINGS FABRICS/TRANSPARENT TRANSPORT DECONTAMINATION

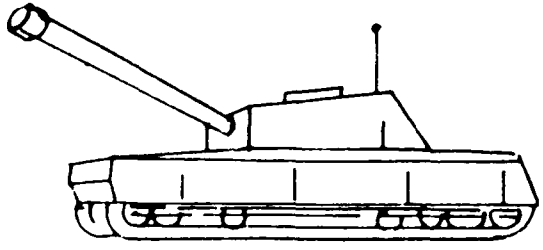

HIGH TEMPERATURE ENGINES → CERAMIC CORROSION PARTICULATE EROSION

DEGRADATION, REACTIVITY AND PROTECTION

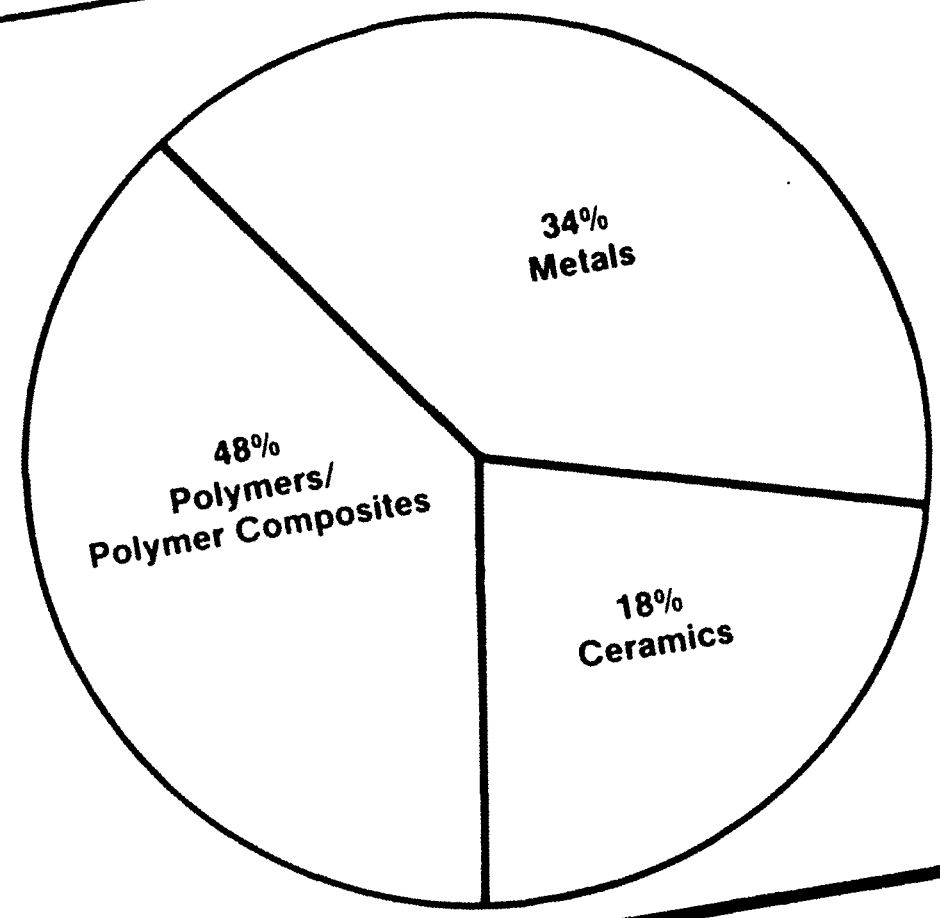

THEORY

1. Corrosion — Electron Number Diagrams
   Angus — Case Western Reserve
2. Composite Thermal Degradation
   Henderson — Univ. Rhode Island
3. Corrosion Inhibition
   White — Univ. Mo. at Columbia
4. Silica Glass/Water Interactions
   Garofalini — Rutgers Univ.
5. Simulation of Microscopic Processes at Surfaces and Grain Boundaries
   Goddard — Cal Tech
6. Magnetic Field Effects on High Heat Load Erosion Phenomena
   Gilligan — NC State
7. Irreversible Thermodynamic Approaches to Polymer Composite Reliability
   Lindenmeyer — Boeing

NOVEL COATING TECHNOLOGY

(1) Pulse Plating
(Weil — Stevens Institute)

(2) Computer Controlled CVD Ceramic Coatings
(Gallois — Stevens Institute)

(3) Metalliding
(Kendig — Rockwell Science Center)

(4) Chromium Plating From 300° C Fused Salts
(White — EIC Corp)

(5) Polyelectrolyte Zinc Phosphate Primers
(Sugama — Brookhaven)

(6) Metal/Organic Systems
(Hsu, McCarthy — Univ. Mass)

(7) Reactive Sputter Deposition
(Aita — Univ. Wisconsin/Milwaukee)

(8) Synchrotron Topography Studies of Coatings
(Bilello — Suny Stony Brook)

NOVEL CHARACTERIZATION OF SURFACES/INTERFACES

1. Photoelastic Modulated Laser Enhanced IR Spectroscopy
   (White — Univ. Mo.)
2. Photoacoustic F.T. IR Spectroscopy
   (Koenig — Case Western Reserve)
3. Photoelastic Modulated Polarization Reflectance IR Spectroscopy
   (Hsu — Univ. Mass.)
4. Pendant Drop Technique for Measuring Polymer Interfacial and Surface Tension
   (Koberstein — Princeton)
5. Synchrotron X-ray Topography
   (Bilello — Suny Stony Brook)

Applications: Adhesive Bonding, Corrosion Inhibitors, Insitu Defect Characterization

LIGHTENING THE FORCE

DEGRADATION

ELECTROCHEMICAL BEHAVIOR OF
EPOXY/GRAPHITE COMPOSITES

C. E. STONER, U. OF VIRGINIA

- FAILURE MODES IN COMPOSITES PRODUCE CHARACTERISTIC ELECTROCHEMICAL SIGNALS
- TECHNIQUE HAS POTENTIAL FOR DEVELOPING SCREENING TEST FOR RANKING ENVIRONMENTAL STABILITIES OF COMPOSITES

LIGHTENING THE FORCE

DEGRADATION

THERMAL BEHAVIOR OF POLYMER COMPOSITES EXPOSED TO HIGH TEMPERATURES

J. B. HENDERSON, U. OF RHODE ISLAND

- CHANGES IN PROPERTIES OF POLYMER COMPOSITES UNDER EXTREME TEMPERATURES EXAMINED AND MODELED
- APPLICATION IN PREDICTION OF LIFETIMES OF SINGLE USE POLYMER COMPOSITE ROCKET SYSTEMS
- HEAT/EROSION RESISTANT MATERIALS (GLASS-FIBER PHENOLIC RESINS) WIDELY USED IN MILITARY APPLICATIONS

LIGHTENING THE FORCE

DEGRADATION

CHEMICAL TREATMENT OF EPOXY RESINS
TO REDUCE MOISTURE SENSITIVITY AND
IMPROVE MECHANICAL PROPERTIES

R. D. GILBERT, NORTH CAROLINA STATE UNIVERSITY

- FIBER/MATRIX DEBONDING IS MAJOR DEGRADATION PROCESS OF POLYMER COMPOSITES

- EPOXY CHEMICAL TREATMENTS WHICH BLOCK WATER TRANSPORT ARE UNDER INVESTIGATION

TECHNOLOGY TRANSFER

1. Pulse Plating of Laminate Metals
   Stevens Institute to BWL
   Technical Report ARCCB-TR-85002
2. Electrochemistry of Epoxy/Graphite Composites
   Univ. Va./MTL
3. Characterization of Polymeric Surfaces and Interfaces
   Princeton/ATT-Bell Labs
4. Reactive Sputter Deposition Characterization
   Univ. Wisconsin — Milwaukee/
   McDonnell Douglas Astronautics

CENTER OF EXCELLENCE FOR CORROSION PREVENTION AND CONTROL AT THE U.S. ARMY MATERIALS TECHNOLOGY LABORATORY WATERTOWN, MASSACHUSETTS

US ARMY
LABORATORY COMMAND
MATERIALS TECHNOLOGY
LABORATORY

MTL-OP-1
1 May 1986

Supersedes XMR Form 160-1, 23 March 1973, which is obsolete.

WHY HAS CPC BECOME SO IMPORTANT TO THE ARMY?

- WE REQUIRE EQUIPMENT TO WORK IN MORE DIVERSE ENVIRONMENTS (WE LEARNED MANY LESSONS IN VIET NAM)
- MATERIEL IS BECOMING VERY EXPENSIVE TO REPLACE
- PRESIDENT REAGAN AND GENERAL THOMPSON PLACE A HIGH VALUE ON COMBAT READINESS

US ARMY
LABORATORY COMMAND
MATERIALS TECHNOLOGY
LABORATORY

MTL OP-1
1 May 1986

Supersedes XMR Form 160-1, 23 March 1973, which is obsolete.

WHAT IS WRONG WITH OUR EQUIPMENT THAT ALLOWS IT TO CORRODE?

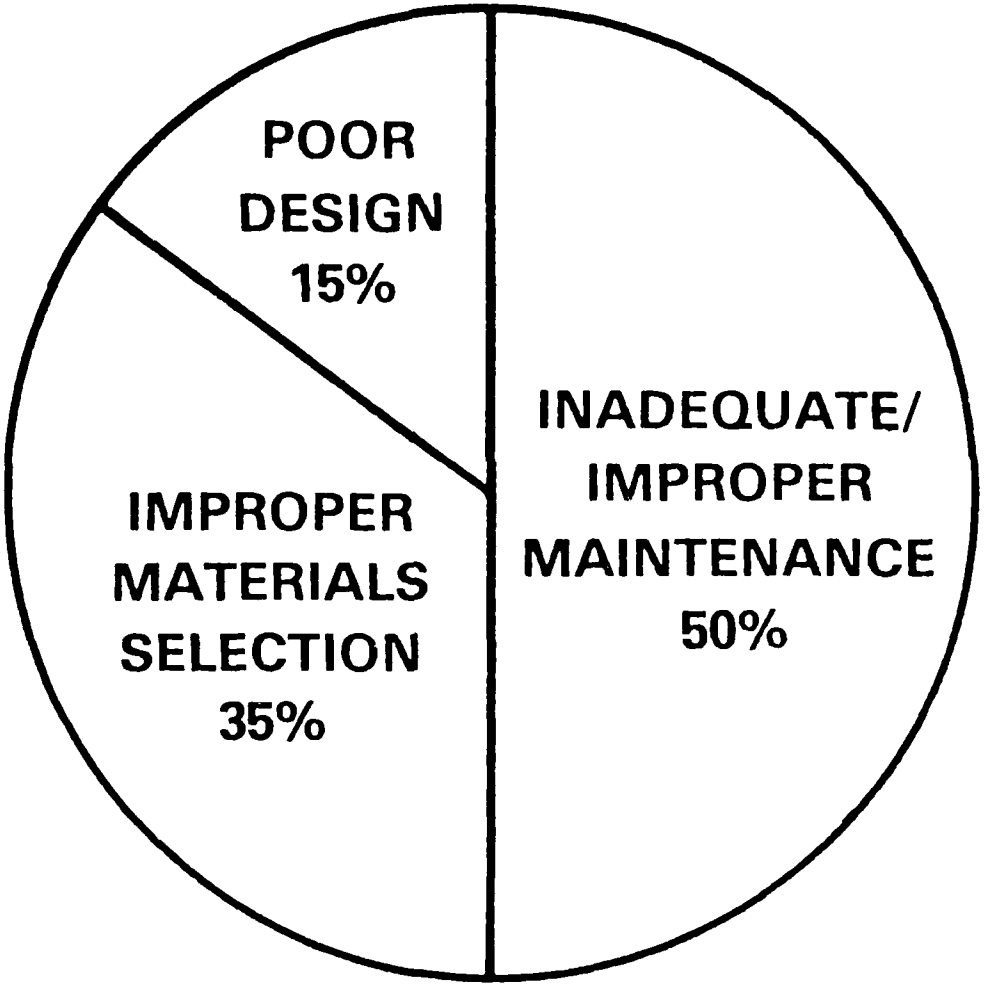

US ARMY
LABORATORY COMMAND
MATERIALS TECHNOLOGY
LABORATORY

MTL OP 1
1 May 1986

Supersedes XMR Form 160-1, 23 March 1973, which is obsolete.

CPC PROGRAMS HAVE BEEN ESTABLISHED IN 5 AREAS:

DESIGN

MANAGEMENT

MAINTENANCE

TRAINING

INDUSTRY AWARENESS

OUR AUTHORITY COMES FROM GENERAL THOMPSON's COMMANDER's GUIDANCE STATEMENT #94

US ARMY
LABORATORY COMMAND
MATERIALS TECHNOLOGY
LABORATORY

MTL OP 1
1 May 1985

Supersedes XMR Form 160-1, 23 March 1973, which is obsolete

DESIGN

- GOAL: TO ENSURE THE INCLUSION OF STATE-OF-THE-ART CPC INTO THE INITIAL DESIGN OF EQUIPMENT AND INTO CONTRACTS

- HOW: THROUGH CORROSION PREVENTION ADVISORY BOARDS THAT HAVE SIGN-OFF AUTHORITY ON DESIGN AND DESIGN MODIFICATIONS

- WHEN: IMMEDIATELY FOR NEW SYSTEMS, FIELDED SYSTEMS WILL HAVE CPAB's ESTABLISHED AS RESOURCES PERMIT

US ARMY
LABORATORY COMMAND
MATERIALS TECHNOLOGY
LABORATORY

MTL OP 1
1 May 1986

Supersedes XMR Form 160-1, 23 March 1973, which is obsolete

MANAGEMENT

- GOAL: INCORPORATE CPC INTO THE DAY-TO-DAY OPERATION OF MSC's AND PM SHOPS. TRACK CORROSION AND CORROSION COSTS THROUGH THE EQUIPMENT LIFE CYCLE.

- COST OF CORROSION STUDY - NOW UNDERWAY AT MTL

- DEPOT CORROSION SURVEYS - THE ARMY SURVEY TEAM WILL HELP IDENTIFY CORROSION PROBLEM AREAS AND OFFER SOLUTIONS WHERE POSSIBLE. THIS IS A MECHANISM FOR EDUCATING LABORATORY AND MANAGEMENT PERSONNEL ABOUT WHAT THE FIELD CONCERNS ARE.

US ARMY
LABORATORY COMMAND
MATERIALS TECHNOLOGY
LABORATORY

MTL OP 1
1 May 1986

Supersedes XMR Form 160-1, 23 March 1973, which is obsolete.

MAINTENANCE

- GOAL: APPLY CPC TECHNIQUES AND PROCEDURES TO MAINTAIN EQUIPMENT DURING AND PAST ITS DESIGN LIFE

- HOW: (1) MODIFY PRIORITIES SO THAT THE MAINTENANCE OFFICER AND COMPANY COMMANDER, ETC., CAN ALLOW TIME FOR CPC WITHOUT PENALTY

  (2) MODIFY THE TECHNICAL MANUALS TO INCORPORATE THE BEST CPC PROCEDURES

US ARMY
LABORATORY COMMAND
MATERIALS TECHNOLOGY
LABORATORY

MTL OP 1
1 May 1986

Supersedes XMR Form 160-1, 23 March 1973, which is obsolete.

TRAINING

(1) TECHNICAL CORROSION TRAINING (THIS COURSE)

(2) CORROSION CONTROL IN LIFE-CYCLE MANAGEMENT. THIS TOPIC IS BEING INCORPORATED INTO ARMY LOGISTICS MANAGEMENT COLLEGE COURSES AND DEFENSE MANAGEMENT SYSTEMS COLLEGE COURSES.

US ARMY
LABORATORY COMMAND
MATERIALS TECHNOLOGY
LABORATORY

MTL OP 1
1 May 1986

Supersedes XMR Form 160-1, 23 March 1973, which is obsolete.

INDUSTRY AWARENESS

GOAL: TO INCREASE OUR KNOWLEDGE OF CPC IN INDUSTRY AND TO BRING THIS INTO THE ARMY

- THIS WILL AUGMENT THE RESEARCH NOW UNDERWAY AT MTL. IT WILL KEEP THE DEFENSE CONTRACTORS AWARE OF THE ARMY's DESIRE TO KEEP CORROSION COSTS DOWN.

US ARMY
LABORATORY COMMAND
MATERIALS TECHNOLOGY
LABORATORY

MTL OP 1
1 May 1986

Supersedes XMR Form 160-1, 23 March 1973, which is obsolete.

TRI-SERVICE CORROSION CONTROL COOPERATIVE PROGRAMS

BRIEFING FOR

JOINT AERONAUTICAL COMMANDERS GROUP

BRIEFER: MILT LEVY
MTL, LABCOM
SLCMT-MCM-SB

US ARMY
LABORATORY COMMAND
MATERIALS TECHNOLOGY
LABORATORY

OBJECTIVE

TO PRESENT TRI-SERVICE COOPERATIVE EFFORTS IN CORROSION PREVENTION AND CONTROL

ELEMENTS

- EXCHANGE OF TECHNOLOGY
- CORROSION INFORMATION ANALYSIS CENTER
- LESSONS LEARNED
- TRI-SERVICE MANUALS
- TRAINING
- ISSUE
- TRI-SERVICE COMMITTEES
- RECOMMENDATION

EXCHANGE OF TECHNOLOGY (Cont'd)

- ANNUAL TECHNOLOGY PROGRAM REVIEW
- CONTRACTOR IRAD REVIEWS
- MATERIALS ADVISORY BOARDS
- ROUND ROBIN TESTING
- CPABs
  - H60
  - V22
- CH47 STRUCTURES CORROSION

US ARMY LABORATORY COMMAND MATERIALS TECHNOLOGY LABORATORY

EXCHANGE OF TECHNOLOGY

- CONFERENCES
  - BIENNIAL TRI-SERVICE ON CPC
  - ADPA, NEW INITIATIVES IN CPC
  - ARMY SAGAMORE MATERIALS RESEARCH ON CPC
  - ANNUAL TRI-SERVICE COATING REMOVAL
  - ANNUAL NACE CONFERENCE - T9 COMMITTEES ON MILITARY APPLICATIONS
  - DIRECT CONTACT BETWEEN PRINCIPAL INVESTIGATORS

- CH47 STRUCTURES CORROSION
  - CURRENT MOD IN ACCORD WITH NAVY PRACTICE
  - BASIC PROBLEM LIMITED PREVENTIVE MAINTENANCE
  - MORE FREQUENT INSPECTION/NONDEFERRED MAINTENANCE DIRECTED
  - TRAINING BY NAVY AT BARBERS POINT
  - WESTCOM DEVELOPED CPC PROGRAM

US ARMY
LABORATORY COMMAND
MATERIALS TECHNOLOGY
LABORATORY

CORROSION INFORMATION ANALYSIS CENTER

- OBJECTIVE
  - ESTABLISH DATA BASE
- FIRST YEAR ADD-ON BATTELLE MCIC
  - $100 K EACH SERVICE
  - 750 DOCUMENTS
  - 600 FAILURE ANALYSES
  - TWO SOARS
- SECOND YEAR
  - NEW START
  - $300 K DLA
  - $300 K SERVICES
  - FUNDING PROBLEM
  - REDUCE TOTAL FUNDS TO $300 K
  - SECOND YEAR ADD-ON TO BATTELLE

US ARMY
LABORATORY COMMAND
MATERIALS TECHNOLOGY
LABORATORY

LESSONS LEARNED

- OBJECTIVE
  - IMPROVE DESIGN
  - IDENTIFY, ADDRESS PROBLEMS
- EACH SERVICE HAS DATA BASE
  - MOA BETWEEN SERVICES FOR DATA EXCHANGE
- DISSEMINATION
  - AF QUARTERLY CORROSION SUMMARY, BULLETIN 6-12 MONTHS
  - ARMY QUARTERLY CORROSION DIGEST
  - NAVY DEVELOP CORROSION NEWSLETTER
  - CONFERENCES

US ARMY LABORATORY COMMAND
MATERIALS TECHNOLOGY LABORATORY

TRI-SERVICE AVIONICS CORROSION MANUAL

- USA/USAF ADOPTED USN MANUAL AS IS: 84
- REQUIRES UPDATE
  - SUPPORT NEW WEAPONS SYSTEMS
  - INCORPORATE STATE-OF-THE-ART TECHNOLOGY
  - INCREASE COMPATIBILITY WITH SERVICE REQUIREMENTS
- FUNDING REQUIREMENTS (K)

USN	USAF	USA
40	40	40

- UPDATE EFFORT START: THIRD QTR FY87

US ARMY
LABORATORY COMMAND
MATERIALS TECHNOLOGY
LABORATORY

PROPOSED TRI-SERVICE WEAPON SYSTEMS CORROSION MANUAL

- NAVAIR 01-1A-509, AIRCRAFT WEAPON SYSTEMS CLEANING AND CORROSION CONTROL MANUAL
  - MODIFIED TO SUPPORT TRI-SERVICE USE
  - FINAL DRAFT ADOPTED BY ALL SERVICES
  - MINOR REVISIONS COMPLETED BY 30 MAR 87
  - AVAILABLE FOR PRINTING:
    FOURTH QTR FY87

BENEFITS

- STANDARDIZATION
  - MATERIALS
  - PROCESSES
  - TRAINING
- REDUCE REDUNDANT CORROSION MANUALS
  - FROM 7 TO 2
  - COST AVOIDANCE

TRAINING

- MAINTENANCE
  - TRI-SERVICE CORROSION MANUALS
    - STANDARDIZES PROCESSES AND PROCEDURES
    - ALLOWS CROSS TRAINING
  - AF 6 WEEKS (MOS)
  - NAVY 4 ONE-WEEK COURSES AIRFRAME, AVIONICS, PAINT, AND FINAL FINISH
  - NAESU MOBILE 3-5 DAYS
  - MTL CORROSION SCHOOL - 5 DAY INTRODUCTORY, DEVELOP DESIGN, MAINTENANCE
  - AVIATION LOG CENTER MAINTENANCE TEST PILOT COURSE

TRAINING (Cont'd)

- MANAGEMENT
  - ALMC, ALL MAM COURSES
  - AFIT, DPML
  - DSMC, EFFORTS UNDERWAY TO INTRODUCE IN PM COURSE

ISSUE

- EPA/OSHA VOC RESTRICTIONS
  - TRI-SERVICE TASK GROUP ESTABLISHED NSN CLASS 8010 (ORGANIC COATINGS)
  - RECOMMENDED APPORTIONMENT $10 M TO MEET REQUIREMENTS 4 YEARS
  - CURRENT FUNDING 10 TO 11 YEARS
  - REPORT TO UNDER SECRETARY OF DEFENSE
  - AD HOC COMMITTEE ESTABLISHED UNDER JLC (NAVY LEAD)

ISSUE (Cont'd)

- OTHER EPA/OSHA RESTRICTIONS IMPACTS MAINTENANCE AND PRODUCTION
  - FEDERAL/STATE
  - CLEANING COMPOUNDS
  - SOLVENTS
  - PLATING SOLUTIONS
  - CHEMICAL PAINT REMOVAL
- NOTICES OF VIOLATIONS AT DEPOT/FIELD INCREASES
- LETTER FROM JACG(WB) REQUESTS EXPANSION OF SCOPE OF AD HOC COMMITTEE

US ARMY
LABORATORY COMMAND
MATERIALS TECHNOLOGY
LABORATORY

TRI-SERVICE COMMITTEES

- CORROSION CONFERENCE PLANNING (TECHNOLOGY)
- AIRCRAFT CPC REVIEW (MANUALS, et al.)
- OSHA-EPA AD HOC
- ORGANIZE PUBLICATIONS COMMITTEE
    - MTL AUTHORITY UNDER DoD STANDARDIZATION PROGRAM
- EVALUATION ALUMINIDE ELECTROPHORETIC PROCESS TURBINE BLADES/VANES

US ARMY
LABORATORY COMMAND
MATERIALS TECHNOLOGY
LABORATORY

RECOMMENDATION

- ESTABLISH FORMAL TRI-SERVICE CPC RELATIONSHIP
- MOA, AVSCOM (MTL), NAVAIRSYSCOM (NADC), AFLC (AFML)
- SIGNED BY PRINCIPALS
- REPORT ANNUALLY TO JACG(WB)

US ARMY
LABORATORY COMMAND
MATERIALS TECHNOLOGY
LABORATORY

BIOGRAPHY

NAME: Milton Levy

PRESENT AFFILIATION: Army Materials Technology Laboratory

TITLE: Chief, Corrosion Science Branch

FIELD OF INTEREST/RESPONSIBILITIES

Manager of technology base RDTE Program responsive to Army needs for new and improved technologies and applications in corrosion and surface science

PREVIOUS AFFILIATIONS/TITLES

Ballistic Research Laboratory, APG, MD
Coating and Chemical Laboratory, APG, MD
Research Chemist

ACADEMIC BACKGROUND

BS, MS - Boston University

SOCIETY ACTIVITIES/OFFICES/AWARDS:

American Chemical Society, The Electrochemical Society. Organized and chaired numerous conferences and sessions including Tri-Service Corrosion, NACE, Electrochemical Society, ASM-AIME, American Defense Preparedness Association. Recipient of: Army R&D Achievement Award; Army Materials Technology Laboratory Director's Awards in Science and Engineering, Army Materiel Command Special Features Award, The Federal Executive Board of Boston Award for Exceptional Achievement, The Army Materiel Command Commander's Award and Medal for Distinguished Civilian Service.

PUBLICATIONS/PAPERS:

Published more than 30 papers in Journals such as Corrosion, Corrosion Science, Journal of the Electrochemical Society, Metallurgical Transactions, ASTM, Journal of the Less-Common Metals, American Ceramic Society. Areas covered include: aqueous corrosion stress corrosion, corrosion fatigue, high temperature oxidation, and protective coatings.

BIOGRAPHY

NAME: Richard Brown

PRESENT AFFILIATION: Army Materials Technology Laboratory

TITLE: Metallurgist

FIELD OF INTEREST/RESPONSIBILITIES

Hydrogen Embrittlement, Solid Particle Erosion, Corrosion of Al alloys

~~PRESENT~~ AFFILIATIONS/TITLES

Currently Associate Professor in the Department of Chemical Engineering University of Rhode IslAND, Kingston, RI 02891

ACADEMIC BACKGROUND

PhD from Cambridge University
BSc from Nottingham University

SOCIETY ACTIVITIES/OFFICES/AWARDS:

Member NACE

PUBLICATIONS/PAPERS:

Several on Solid Particle Erosion and Fatigue Behavior of Titanium Alloys

NAVY CORROSION OVERVIEW

89

MATERIALS TECHNOLOGY

OFFICE OF NAVAL TECHNOLOGY
James J. Kelly, Manager
OCNR 225

NAVY'S CORROSIVE ENVIRONMENT

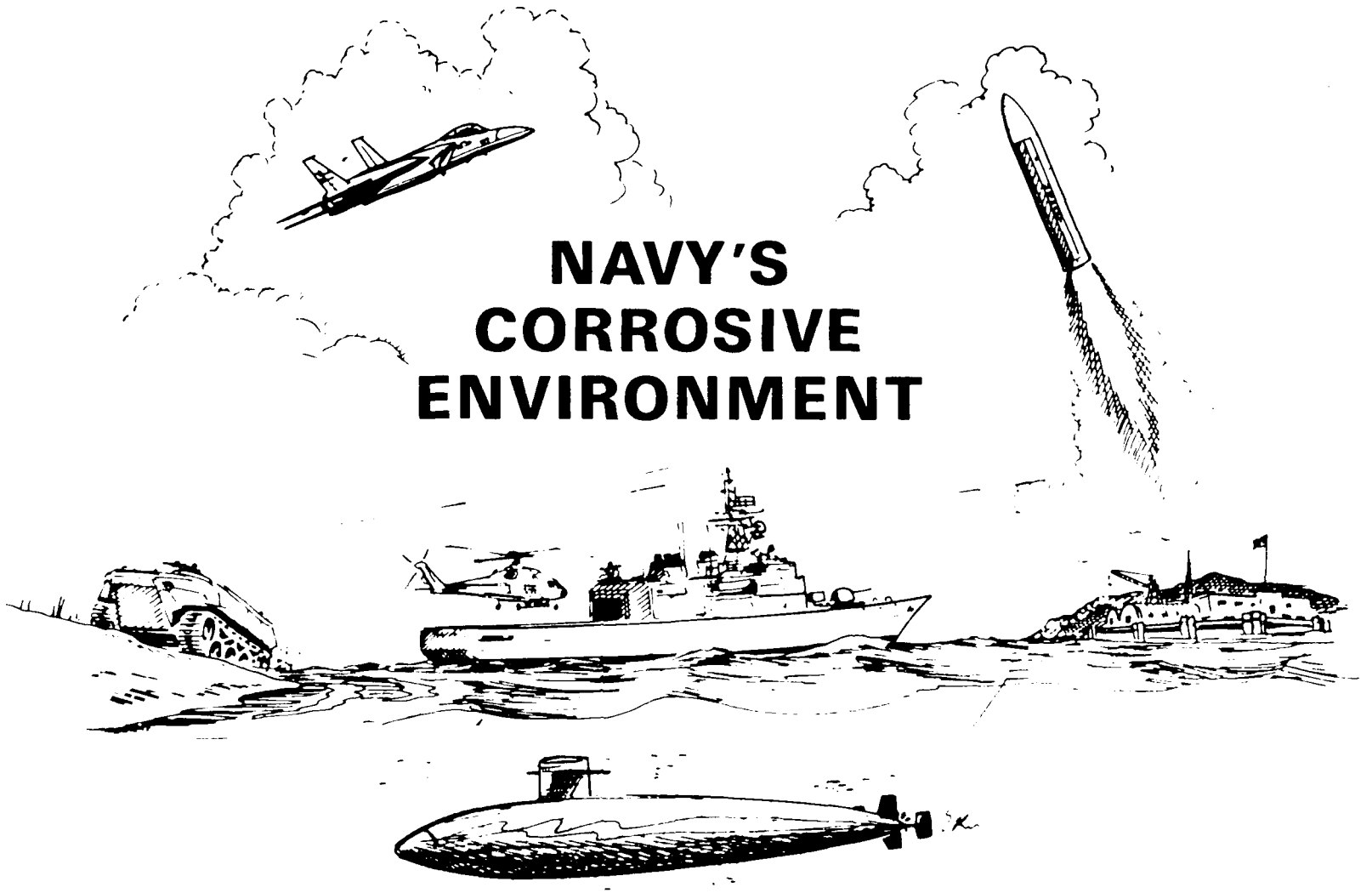

COMPLEX ENVIRONMENT

NAVAL AIR ENVIRONMENT

Characterized By:

- Operational Aircraft in Severe Conditions (Up to 0.080 Inches with Thin Cross Sections)
- Limited Maintenance Capability and Space During Deployment
- Inability To Depend on Contractor Support During Deployment
- Inability To Wash Aircraft as Frequently as Advised To Minimize Corrosion
- Continuous Readiness of Limited Aircraft Prevents Detailed Corrosion Control
- High Strength Materials Susceptible to Embrittlement Cracking (Required for Severe Launch/Recovery Demands on Carrier)
- Acidified Salt Fog Environment Due to High Sulfur Content of Stack Gases

NAVAL SHIP/SUBMARINE/SHORE FACILITY ENVIRONMENT

<u>Characterized By</u>:

- Both New and Old Ships/Submarines/Shore Facilities and Technologies
- Chlorides in the Atmoshpere/High Humidities/Salt Water
- Continuous Exposure
- Long Service Life Requirements
- Constant Changeover of Personnel
- Limited Maintenance Personnel

MAJOR PARTICIPANTS

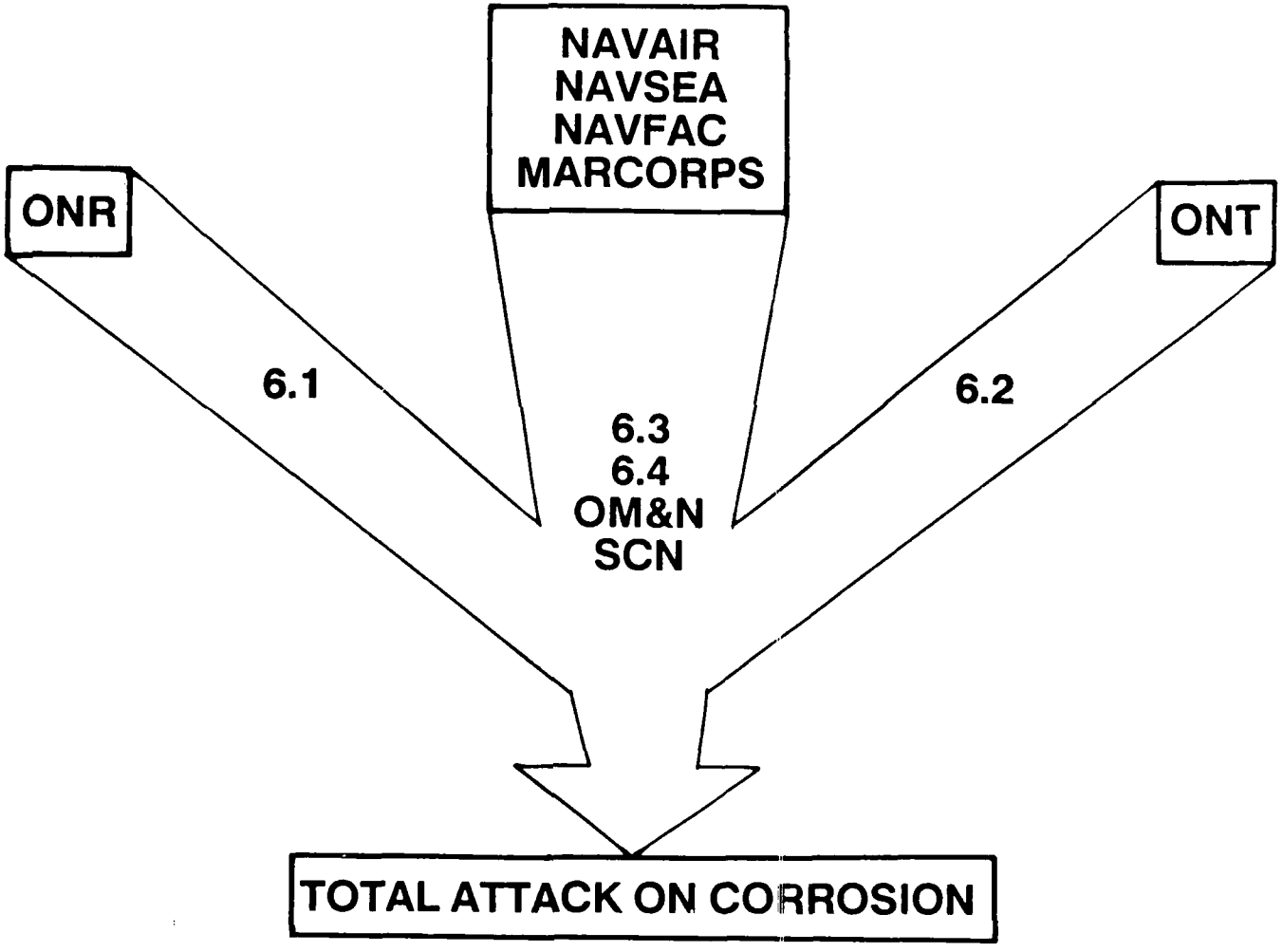

REQUIREMENTS FOR CORROSION CONTROL

- Recognition of Tough Environment Characteristics
- Amenable to Both "High Volume" Production and "One Time" Application
- Sometimes:
  - World-Wide Utilization by Non-Specialized Personnel
  - Specialized Application During Initial Manufacture
- Stringent Pollution and Safety Measures

F/A-18 AIRCRAFT CORROSION

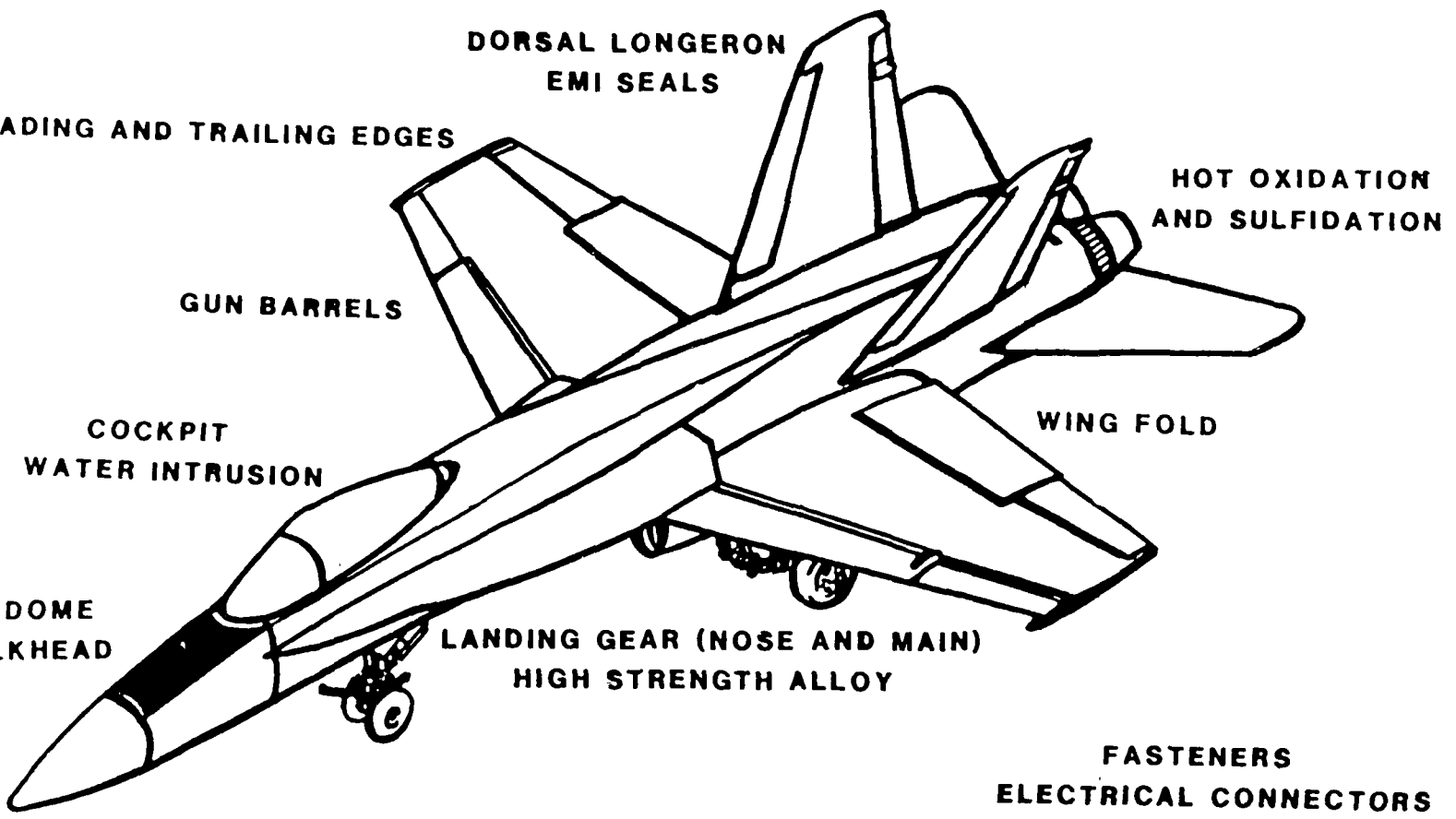

CORROSION PRONE AREAS

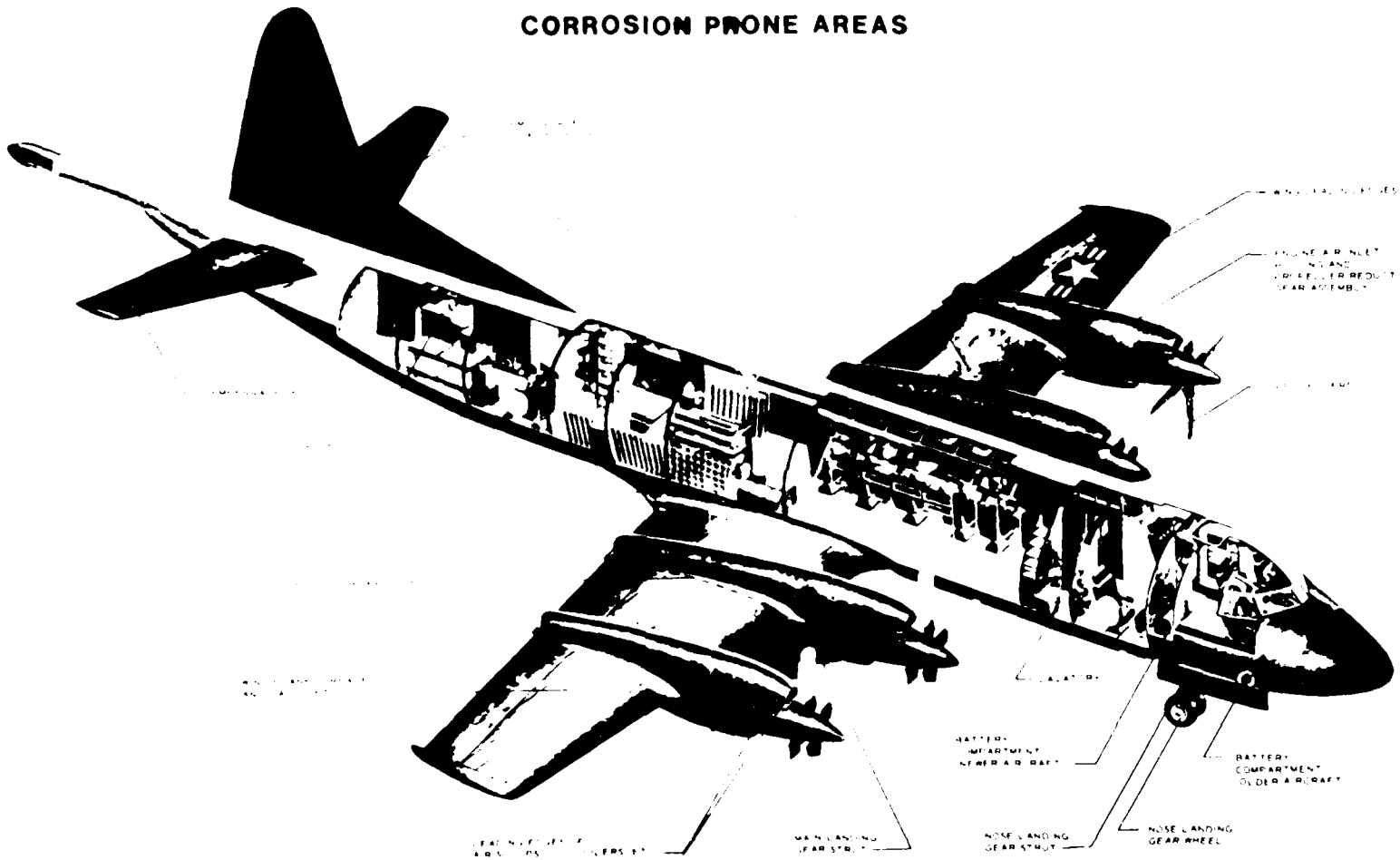

SURFACE SHIP CORROSION

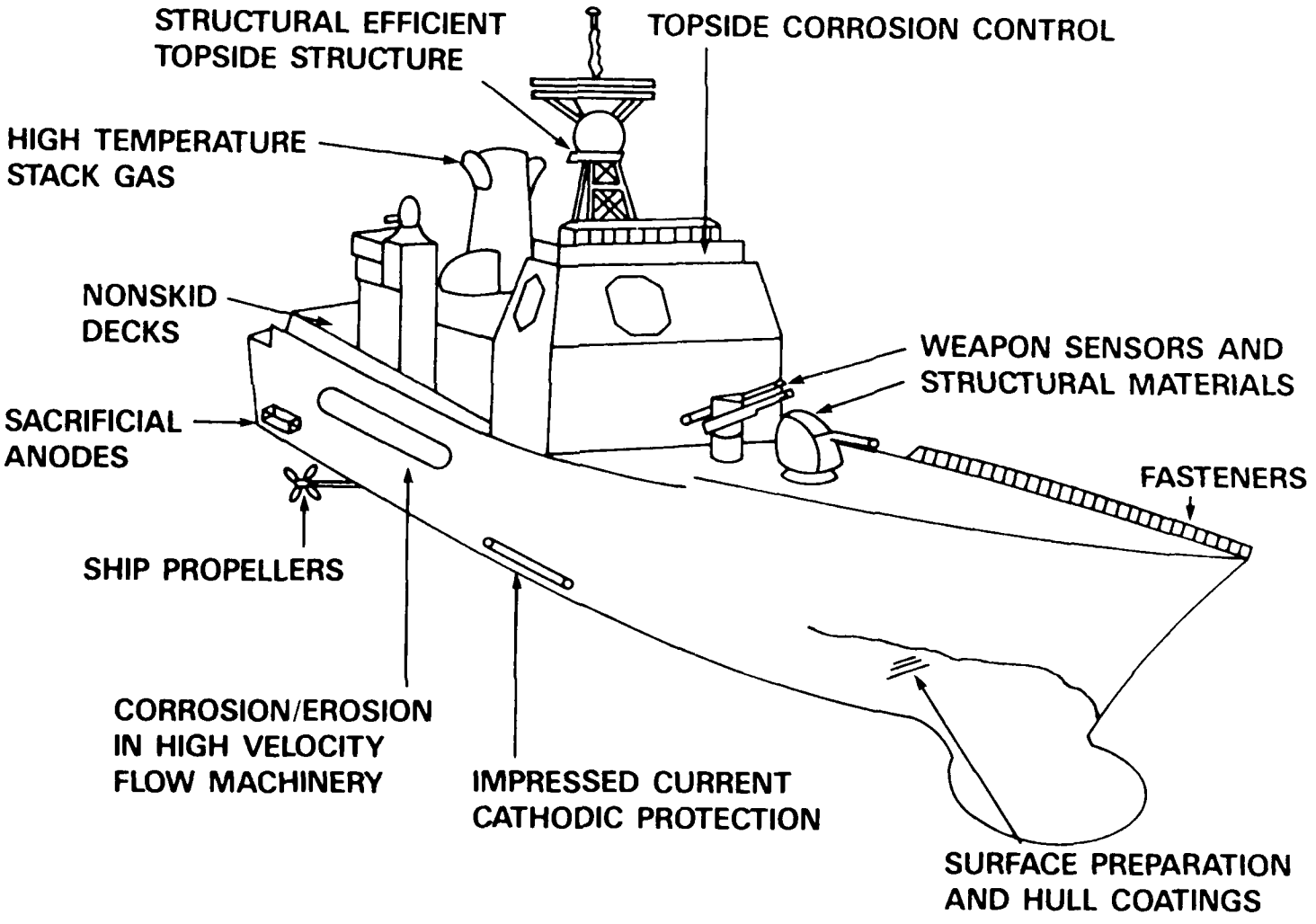

SUBMARINE CORROSION

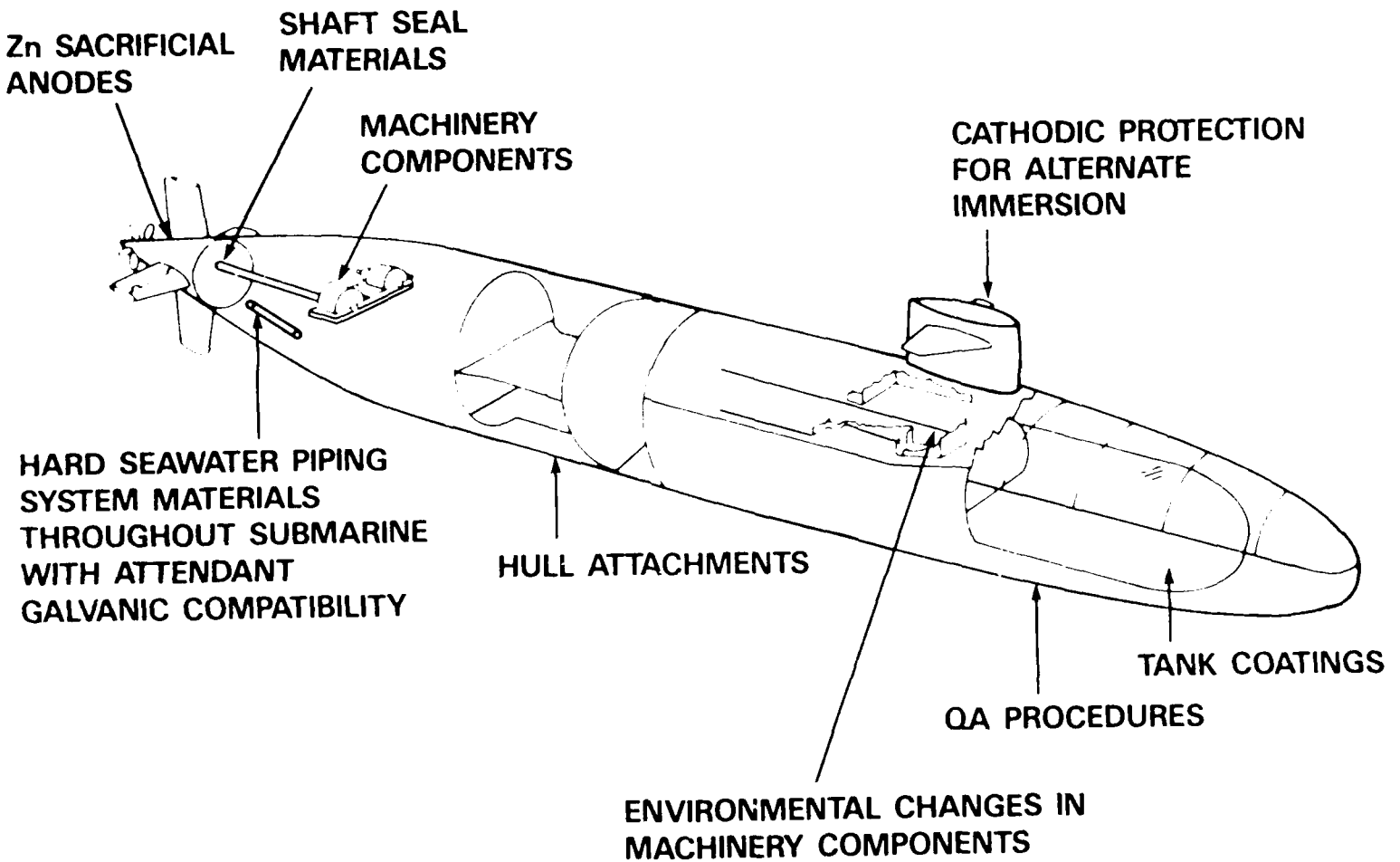

MARINE CORPS
VEHICLE CORROSION

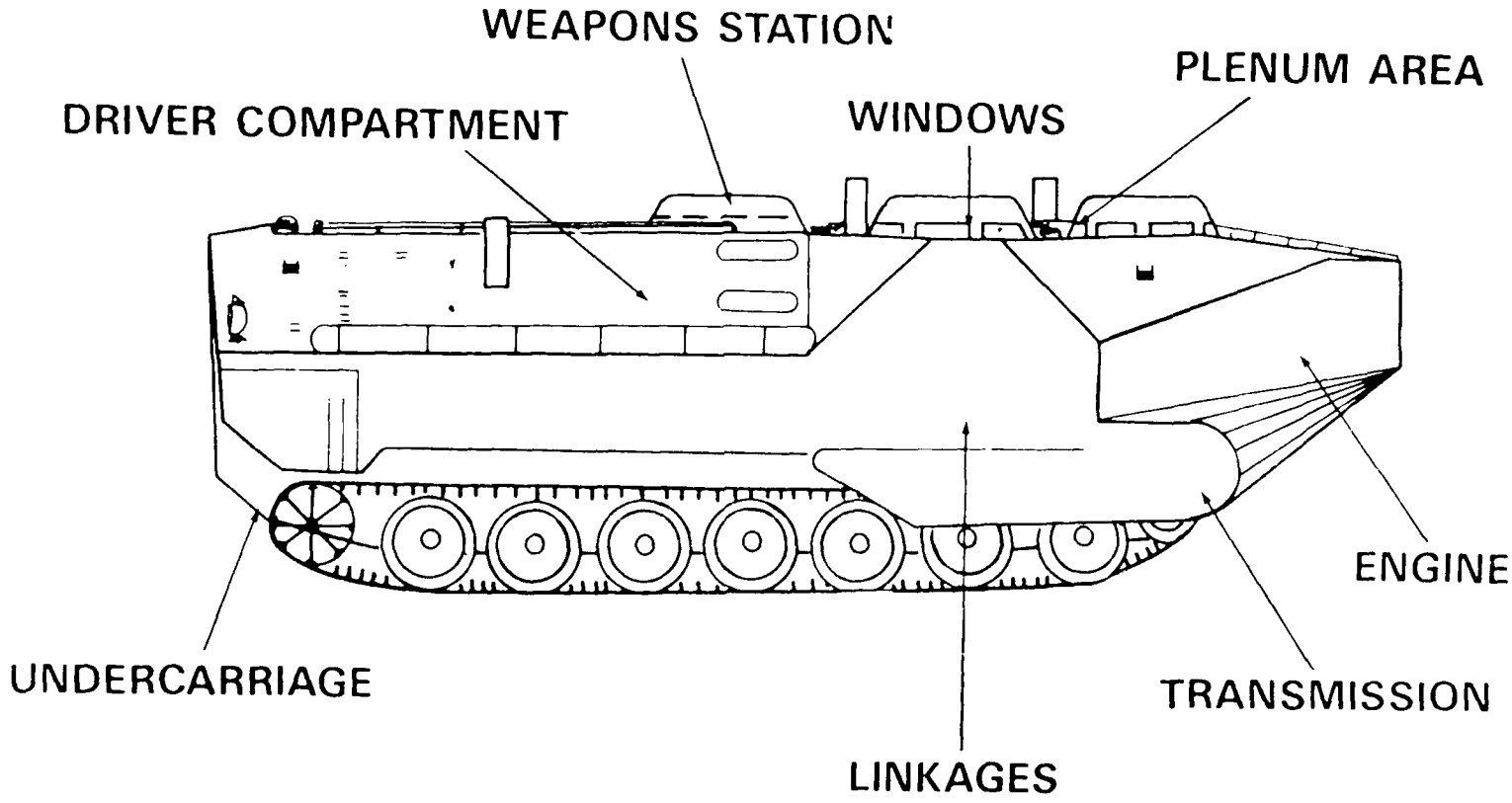

SHORE FACILITY CORROSION

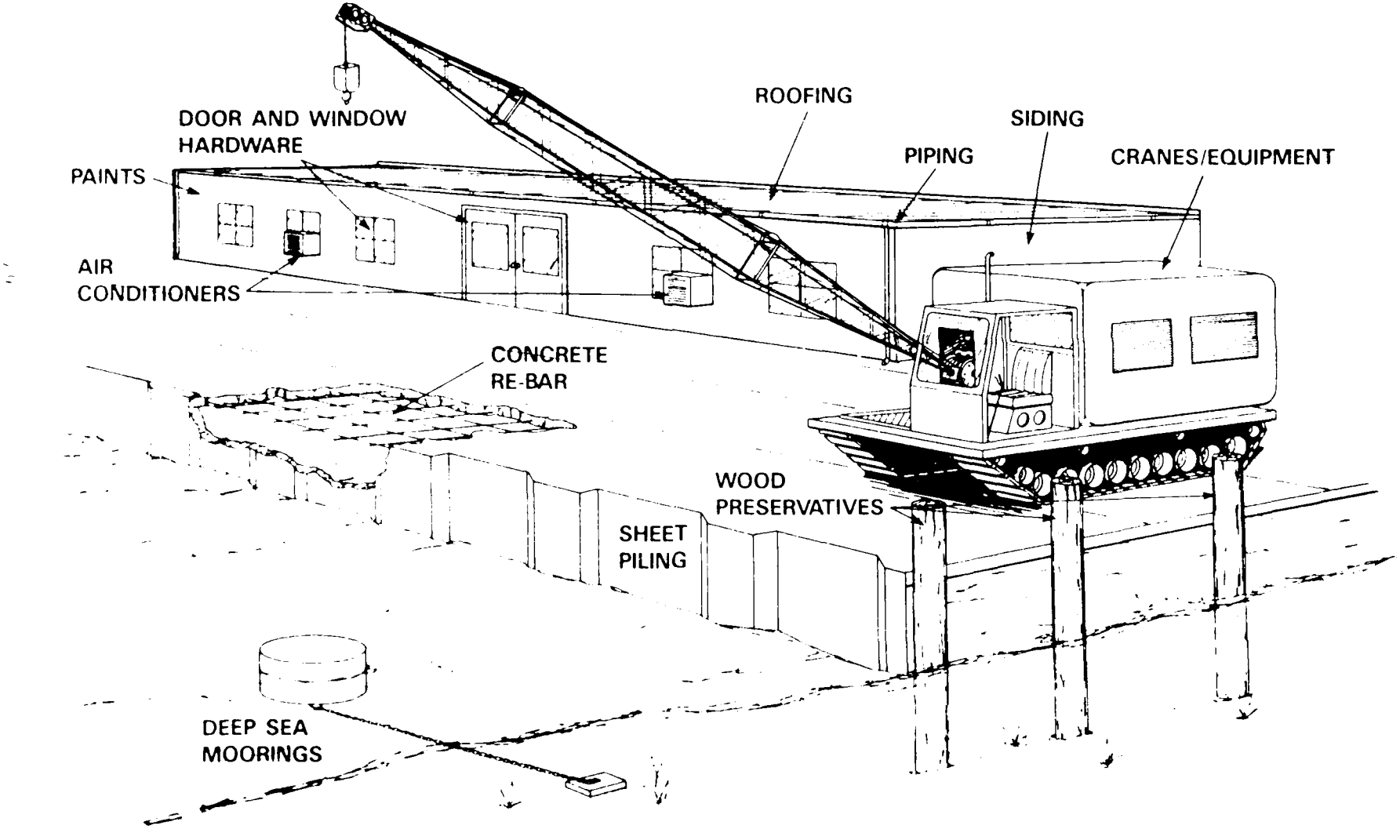

NAVY ORGANIZATIONS INVOLVED WITH CORROSION CONTROL

- CONNAVAIRLANT, COMNAVSURFLANT, COMNAVSUBLANT
- COMNAVAIRPAC, COMNAVSURFPAC, COMNAVSUBPAC
- David Taylor Naval Ship R&D Center
- NARFs, SIMAs
- NAVAIR, NAVFAC, NAVSEA
- Naval Air Development Center
- Naval Civil Engineering Laboratory
- Naval Research Laboratory
- Office of Naval Research
- Office of Naval Technology
- Shipyards
- Shore Facilities

NAVY APPROACH

- Balanced and Leveraged RDT&E Effort
- Emphasis on Mechanism and Understanding
- Emphasis on "Technologies New to the Navy"
- Minimize Corrosion Problems During Design Process
- Strong Contact/Communication Between Navy Labs, the Fleet, NARFs, SIMAs, Shipyards, and Contractors To Insure Rapid Improvement Implementation
- Insure Strong Fleet Support for Corrosion Control Efforts through Proper Education

CORROSION RESEARCH AND DEVELOPMENT

- **PASSIVITY**
  Fundamental Theory To Predict (1) Occurence of Passivity in Active/Passive Metals and (2) Effect of Alloying Elements on Passivity and Its Breakdown
- **ENVIRONMENTAL CRACKING RESISTANCE**
  Understand Processes by Which Hydrogen Induces Cracking; Develop Capability To Predict and Prevent (or Minimize) Such Cracking, Leading to Development of Resistant High Strength Steels
- **PAINTS, ADHESIVES, SEALANTS**
  Understand Loss of Adhesion Between Organic Coatings and Metal Substrate, Leading to Predictive Behavior; New Concepts for Formulating Adherent Coatings
- **HIGH TEMPERATURE COATINGS**
  Provide Science Base for New Coatings for Gas Turbine Components, Resistant to Hot Corrosion, Vanadate Attack, Oxidation, Thermal Fatigue, and Interdiffusion
- **COMPOSITES**
  Provide Knowledge Base on Composite Behavior in Environments; Repair Procedures/Technology for Composite Structure

CORROSION CONTROL

Consider Early in Design
- Design Detail
- Material Selection
- Additional Protection

CURRENT ACTIVITES:

Paints	• Standardization of Specification and Procedures • Utilization of VOC Compliant Paints • Examination of Alternatives to Grit Blasting • Development of Touch-Up Paints and Procedures • Investigation of Surface Tolerant Coatings • Inhibitors for Paints, Sealants, and Adhesives
Cathodic Protection	• Evaluation of Aluminum Anodes • Localization of Impressed Current Cathodic Protection
Non-Metallics	• Increased Utilization of Non-Metallics (Organic/Ceramic) • Increased Use of Coated Fasteners • Increased Use of Metal Spray Coatings
Metals	• Stress Corrosion Resistant Aluminum Alloys • Single Crystal Propulsion Alloys

CORROSION EDUCATION/TRAINING

PREMISE: People Want To Do a Good Job
Companies Want To Produce Quality Products

BOTH NEED THE TOOLS TO DO IT --
CORROSION COMMIUNITIES' JOB TO PROVIDE THEM

MATERIALS AVAILABLE:

- Ship, Aircraft, and Facilities Specific Manuals Issued
- Technical Data Sheets Available
- Short Courses: NACE, Naval P.G. School, NCEL
- MIL STD Documents
- NACE Publications and Magazines
- Textbooks

NAVAL AIR
CORROSION CONTROL DOCUMENTS

• SD-24	General Specification for Design and Construction of Aircraft Weapon Systems
• MIL-F-7179	Finishes, Coatings, and Sealants for the Protection of Aerospace Weapons Systems
• MIL-S-5002	Surface Treatments and Inorganic Coatings for Metal Surfaces of Weapons Systems
• NAVMAT P 4855-2	Design Guidelines for Prevention and Control of Avionic Corrosion
• NAVAIR 01-1A-509	Aircraft Weapons Systems Cleaning and Corrosion Control
• NAVAIR 16-1-540	Avionic Cleaning and Corrosion Prevention/Control

NAVAL SEA
CORROSION CONTROL DOCUMENTS

• GEN SPECS	General Specification for Design and Construction of Ships and Submarines
• MIL-HDBK-729	Corrosion and Corrosion Prevention: Metals
• MIL-STD-889B	Dissimilar Metals
• MIL-STD-1687A	Thermal Spray Processes for Naval Ship Machinery Application
• DOD-STD-2138A	Metal Sprayed Coatings for Corrosion Protestion Aboard Naval Surface Ships
• NAVSEA-S-9086-VD-STM-000	Naval Ships' Technical Manual
• NAVSEA Manuals	Corrosion Control Manuals - Specific for Ship Class (i.e., NAVSEA S9360-AB-MAN-010, Corrosion Control Manual for DD 963)

NAVAL FACILITIES
CORROSION CONTROL DOCUMENTS

- NAVFAC-MO-306 Corrosion Prevention and Control
- NAVFAC-MO-307 Cathodic Protection Systems Maintenance
- NAVFAC-MO-110 Paint and Protective Coatings
- NAVFAC-DM-11.1 Tropical Engineering
- NAVFAC-DM-25 Waterfront Operational Facilities
- NAVFAC-DM-26.5 Fleet Moorings
- NAVFAC-DM-4.10 Cathodic Protection Systems Design

CORROSION TECHNOLOGY OPPORTUNITIES

PRACTICAL DEVELOPMENT FOR:

- Alloy Surface Modification for Corrosion Control
- Design Guidance for Crevice Corrosion Control
- Miniaturization of Impressed Current Cathodic Protection
- Sacrificial Anodes ($\sim$ 200 mv) More Electropositive Than Zinc
- Nondestructive QA Techniques for Organic and Metal Spray Coatings
- Improved Coatings Performance (e.g., Underwater Hull Primers, Touch-Up Paints for Tank/Bilge Application, Aircraft Structures, Avionics Systems, and Facilities)

TECHNOLOGY TRANSITION

- Primer/Topcoat Single Coat Paint System for Aircraft
- Plastic Media Blasting for Stripping Coatings for Aircraft
- Water Displacing Paint
- Rapid Cure, High Temperature Longer Life Sealants for Aircraft
- Corrosion Monitors On-Board Aircraft Carriers
- Long Term Seawater Polarization Characteristics for Naval Alloys' Use in Seawater
- Corrosion Control Coatings for Metal Matrix Composites
- Upgraded Cathodic Protection Design Guidance for Surface Ships
- Thermal Spray Aluminum for Topside Corrosion Control of Surface Ships
- Intermediate Temperature Ceramic and Bond Coat Compositions for Surface Ship Gas Turbines
- Electrochemical Impedance Spectroscopy (EIS) Techniques and Data Analysis Procedures for Navy Underwater Primers
- Corrosion Control for Magnetic Silencing Facilities
- Inspection Methodology for Cathodic Protection of Fuel Storage Tanks

WHAT CAN WE DO?

INTER-SERVICE:

- Pool Information on Service Failures
- Improve Report Distribution
- Be Available for Consultation

INDUSTRY:

- Hardware Manufacturers
  - Raise Corrosion Consciousness Within Your Company
  - Recognize That Degradation Will Occur, and Where and How Fast on Your Products
  - Ask for Help and Advice
- Materials and Service Industries
  - Don't Oversell -- Universal Curves Are Rare
  - Blend into the Procurement System

SUMMARY

- Corrosion Conscious Design
- Detailed Specification Development
- Needs Driven Technology R&D
- Rapid Transition
- Strong Fleet Support

Overview of the Air Force Corrosion Program

The Air Force/AFLC Corrosion Program Office was established in October 1979 and is located at Robins AFB GA. This office has 12 Materials Engineers and two Sr. Enlisted Corrosion Specialists.

AFR 400-44 entitled Air Corrosion Program provides the authority for this program. This regulation covers corrosion prevention as a primary design criteria. It covers maintenance activities, command-wide corrosion programs and procurement requirements. The AFLC/AFSC supplement to this regulation further details the responsible for each organization within these commands.

The organizational network is one of the major keys to a workable corrosion program. Corrosion Managers are designated for all operating commands and ALCs, with responsibility for the programs in their respective areas. Corrosion monitors and points of contact are designated for all AF organizations with any corrosion involvement.

Corrosion Prevention Advisory Boards (CPABs) are essential to the Air Corrosion Program. These boards, established for all weapon systems and major subsystems, review all aspects of corrosion for that system and make recommendations to the program managers. These responsibilities cover design reviews, materials and processes, corrosion technical data, maintenance practices, etc.

Operating command corrosion prevention and control surveys are also a key element of the Air Program. Each command is surveyed every four years. These surveys cover all aspects of the corrosion program including training, facilities, command regulations, supply system, as well as the actual equipment itself.

The AF Corrosion Program Manager also has many other responsibilities which are essential for an effective program. These include the quarterly Corrosion Summary with nearly 2,000 copies which are circulated throughout DOD. A worldwide Corrosion Program Managers meeting is held annually to bring together those responsible for the various aspects of corrosion prevention and control. Assignment and monitoring of action items from the managers meeting and Command Surveys assures continuing effort within responsible organizations. Daily contacts with those responsible for policy, administration, research and development, etc., are keys to the program.

AD-A191 295 PROCEEDINGS OF THE TRI-SERVICE CONFERENCE ON CORROSION (1987) HELD AT THE..(U) AIR FORCE WRIGHT AERONAUTICAL LABS WRIGHT-PATTERSON AFB OH.. F H MEYER MAY 87 2/6

UNCLASSIFIED AFWAL-TR-87-4139-VOL-1 F/G 11/6.1 NL

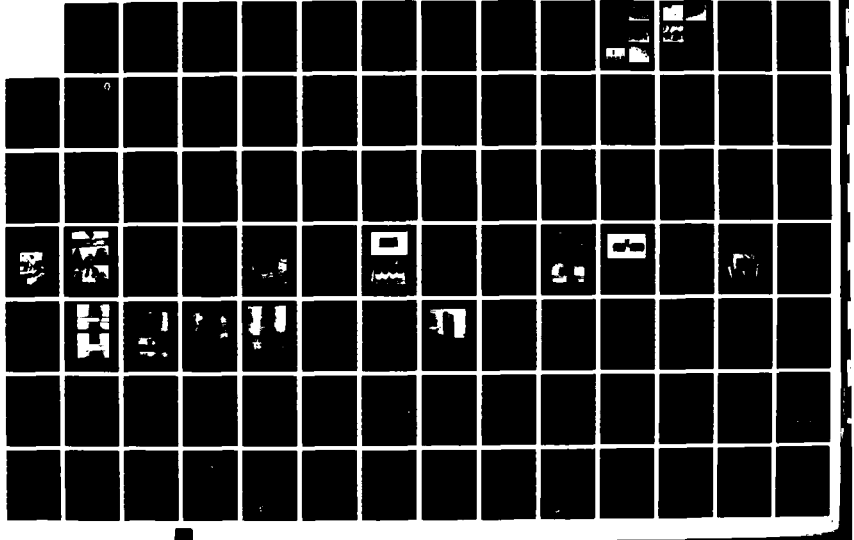

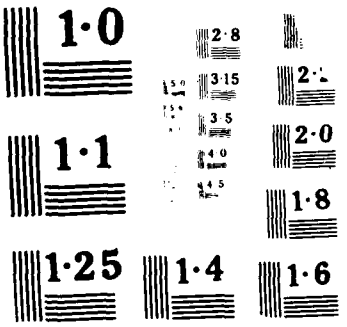
1·0
1·1
1·25
1·4
1·6
1·8
2·0
2·8
3·15
3·5
4·0
4·5

EFFECTIVE COATING SCHEMES FOR THE PROTECTION OF ALUMINUM ALLOYS IN MARINE ENVIRONMENTS

R. M. KAIN

LAQUE CENTER FOR CORROSION TECHNOLOGY, INC.

(NOT AVAILABLE AT TIME OF PRINTING)

BIOGRAPHY

NAME: Robert M. Kain

PRESENT AFFILIATION: LaQue Center for Corrosion Technology Inc.

TITLE: Corrosion Scientist

FIELD OF INTEREST/RESPONSIBILITIES: Marine Corrosion - Research, Testing, Failure Analysis

PREVIOUS AFFILIATIONS/TITLES: 38 years experience at LaQue Center and previous INCO Corrosion Section

ACADEMIC BACKGROUND: Associate of Applied Science

SOCIETY ACTIVITIES/OFFICES/AWARDS: Active in NACE, ASTM also, member of Steel Structures Painting Council and Technical Association for the Pulp & Paper Industry.

PUBLICATIONS/PAPERS: Published/Presented over 20 Technical papers Materials Performance, Corrosion, ASTM STP's, Journal of Materials for Energy Systems, Major area of interest: Corrosion of Stainless Steels and related alloys, other topics including Al Protection and MMC Corrosion and Anodic Protection.

SESSION A
MARINE CORROSION - SHIPS

Chairman
Terry Morton
Naval Ship Research
and Development Center

REFORMULATION OF MIL-SPEC

MIL P-24441 FOR SHIP PROTECTIVE COATING

S. D. RODGERS

NAVAL SEA SYSTEMS COMMAND

(NOT AVAILABLE AT TIME OF PRINTING)

BIOGRAPHY

NAME: Stephen B. Rodgers

PRESENT AFFILIATION: Naval Sea Systems Command/US Navy

TITLE: Head, Corrosion Control Branch (SEA 05M1)

FIELD OF INTEREST/RESPONSIBILITIES: All Ship Related Preservation, Corrosion Control, Cathodic Protection, Decking Materials, Biofo????? Control and Related Materials Technologies and Processes.

PREVIOUS AFFILIATIONS/TITLES: (1) David Taylor Naval Ship R&D Center, Annapolis, MD, (?) Paint Laboratory, Mare????? Shipyard, Valle??, CA

ACADEMIC BACKGROUND: B.A. in Chemistry

SOCIETY ACTIVITIES/OFFICES/AWARDS: Member National Association of Corrosion Engineers, American Chemical Society, Washington Paint Technical Group

PUBLICATIONS/PAPERS: Numerous

Additional: P.E. (Corrosion) State of California
P.E. (Nuclear Safety Related Coatings), Florida

AN EVALUATION OF MICROBIOLOGICALLY INDUCED CORROSION IN COPPER-NICKEL PIPES

Brenda Little[1], Patricia Wagner[1], and [illegible][2]

[1]Naval Ocean Research
and Development Activity
NSTL, MS 39529-5004

[2]Chemistry Laboratory
Ingalls Shipbuilding
Pascagoula, MS

ABSTRACT

Microbiologically induced corrosion in 90/10 Cu-Ni pipes was evaluated using estuarine water from the Gulf of Mexico at the mouth of the Pascagoula River maintained at a flow rate of 3 ft/sec over an 8-month period. The impact of surface preparation, batch $FeSO_4$ (50 ppb Fe^{2+} for 48 hours) pretreatment and intermittent treatment was evaluated. Surface deposits were characterized by scanning electron microscopy and energy-dispersive x-ray fluorescence spectrometry. Water analyses included pH, dissolved oxygen, dissolved sulfide and sulfate, total organic carbon, total suspended solids and dissolved heavy metal analyses, as well as quantification of bacteriological components.

Batch $FeSO_4$ treatment did not result in a persistent increase in surface-bound iron or decreased localized corrosion. Surface pitting appeared to be associated with accumulations of chlorine, sulfur, and microbiological colonization.

1. INTRODUCTION

Copper alloys have a long history of successful application in seawater piping systems due to their corrosion resistance, antifouling properties, and mechanical properties. The corrosion resistance of copper in seawater is attributable to the formation of a protective film that is predominantly cuprous oxide, irrespective of alloy composition [1]. Often, basic chloride atacamite ($Cu_2(OH)_3Cl$) or malachite ($CuCO \cdot Cu(OH_2)$), a carbonate salt, forms a bulky, green, nonprotective film that overlies the Cu_2O layer [2].

Copper alloys are susceptible to some types of corrosion and premature corrosion failures have been reported [3,4]. Failure of copper-nickel pipes in polluted estuarine water can be associated with waterborne sulfides that stimulate pitting and stress corrosion cracking [5]. 90/10 copper nickel was shown to suffer accelerated corrosion attack in seawater containing 0.01 ppm sulfide after a 1-day exposure [6]. There can also be changes in the galvanic relationships between normally compatible piping and fitting alloys in sulfide containing seawater [7]. Copper alloys are vulnerable to erosion corrosion caused by the removal or breakdown of the protective film by mechanical forces such as local turbulence and impingement [8]. Copper alloys are also susceptible to microbiologically induced corrosion (MIC). Pope [9] proposed the following mechanisms for microbial attack: production of corrosive substances, e.g., CO_2,H_2S, NH_3, organic or inorganic acids; production of metabolites that act as depolarizers; and anaerobically produced mercaptans and disulfides through the microbial transformation of sulfur compounds.

As the Cu_2O corrosion film forms in seawater, copper ions and electrons must pass through the film to support anodic and cathodic half-reactions. It has been shown experimentally that alloying additions of nickel and iron into the highly defective p-type Cu_2O corrosion product film as dopants alters the structure [1] and results in a corrosion film that possesses low electronic and ionic conductivity [10]. Such a film has been shown to be resistant to waterborne sulfides and

impingement attack [8]. CDA 706, an alloy containing 88.5% copper, 10% nickel, and 1.5% iron, has been shown to be the most corrosion-resistant copper-based alloy [11]. Both alloyed and precipitated iron are effective methods for introducing iron into the Cu_2O [9]. Ferrous ions may be added to seawater in a variety of ways, including periodic batch additions of ferrous sulfate crystals, continuous injection of ferrous sulfate solutions, or the use of naturally occurring iron corrosion products [12-19]. In the presence of naturally occurring anodes and cathodes, Fe^{+2} ions form lepidocrocite γ-FeOOH, a colloidal hydrous oxide capable of interacting with cations at pH values 6-8. It has been shown that the positively charged colloid can migrate and adhere to a negatively charged cathode. It subsequently spreads over the entire surface to form a nonconducting film that impedes electron transfer between the copper and dissolved electron acceptors. Since the corrosion of the copper-nickel alloys in aerated, unpolluted seawater is cathodically controlled by oxygen reduction (oxygen is the electron acceptor), the FeOOH is a cathodic inhibitor; furthermore, Hack [20] reported that continuous $FeSO_4$ injections prevented sulfide-induced corrosion of copper-nickel alloys by stripping corrosive sulfides from solution before reaction with the pipe surface was possible. The efficacy of $FeSO_4$ treatments has never been evaluated as a means of controlling MIC.

Both $FeSO_4$-treated and untreated CDA 706 seawater piping systems on U. S. Navy ships have experienced premature corrosion failures. Most of the failures have been attributed to turbulence and impingement attack. However, some failed sections are characterized by a nonhomogeneous, nonadherent surface film with subsurface pitting. The surface films contained calcium, sulfur, chlorine, silica and iron, in addition to copper and nickel, and accumulations of microorganisms [21].

In an attempt to understand the failure mechanism in such pipe sections and the role of $FeSO_4$, a dockside experiment was undertaken at a ship construction site at Ingalls Shipbuilding Division, Litton Industries, Pascagoula, Mississippi. The flow-through water was the naturally occurring estuarine water from the mouth of the Pascagoula River in the Gulf of Mexico. Batch ferrous sulfate surface treatment of CDA 706 copper-nickel piping systems was evaluated in the presence of biofilms containing sulfate-reducing bacteria. The corrosion of $FeSO_4$-treated pipes was compared to untreated pipes that had been cleaned according to military specifications.

2. METHODS AND MATERIALS

Eight-foot sections of CDA 706 Cu-Ni pipes were pretreated and maintained as indicated in Table 1. Pipes treated with ferrous sulfate were exposed to a 50 ppb solution of Fe^{+2} for 48 hours. The solution was prepared as follows: a 20% (by weight) stock solution (pH 1.7, stabilized with sulfuric acid) of ferrous sulfate was prepared the day it was to be used and diluted to 50 ppb, pH 7.7, prior to treatment.

The cleaning of Case 4 consisted of a soak with a general purpose detergent [22] mixed with hot tap water, a flush with tap water, and air drying. The extensive cleaning in Case 5 consisted of a soak in a mixture of tri-sodium

TABLE 1. PIPE TREATMENTS AND HISTORY

Case 1: Installed without pretreatment, allowed to biofoul (2 months)(2 weeks), stagnated and then exposed to continuous flow conditions.

Case 2: Installed without pretreatment, allowed to biofoul (5 months), then treated with $FeSO_4$.

Case 3: Pretreated with $FeSO_4$.

Case 4: Pretreated with normal shipyard cleaning (soak, flush, hydro, cleaning).

Case 5: Fabricated with bends, braze joints, socket and butt welding (exaggerated cleaning).

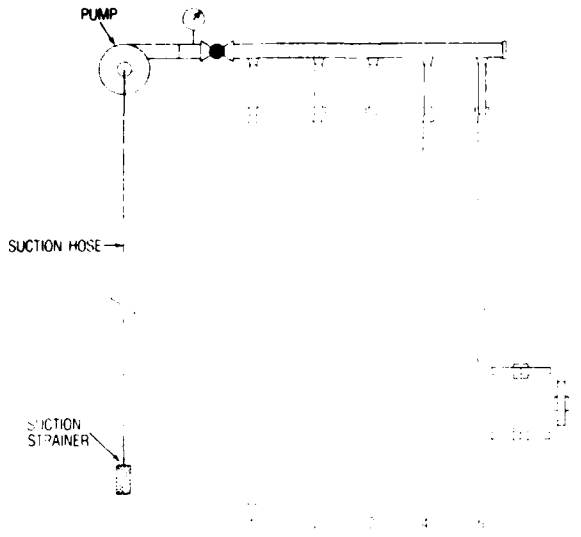

Figure 1. Flow diagram of dockside experiment.

phosphate ($Na_3PO_4 12H_2O$), [23] general purpose detergent [22] and hot tap water. This mixture was introduced into the piping system for 12 hours. The system was flushed with hot tap water. The pipe was then exposed to a mixture of citric acid [24] for a period of 6 hours, drained, flushed with tap water, and air dried.

Pipes were maintained on the Westbank Dock at Ingalls. The intake water was from a 22 ft depth and maintained at a flow rate of 3-6 ft sec^{-1}, as indicated in Figure 1. Sections from pipes 1-4 were removed biweekly, preserved in 4% buffered glutaraldehyde, and subsectioned in the laboratory. Surface chemical analyses were performed with a KEVEX-7000 energy-dispersive x-ray spectrometer (EDAX) coupled to an AMRay 1000A Scanning Electron Microscope (SEM). Subsections were sputter-coated with gold before photography with the SEM. Case 5 will be sectioned at the conclusion of the experiment.

Water samples for chemical analyses were collected at the intake depth. PH [25], chlorinity [25], dissolved oxygen [26], suspended solids [25], temperature [25], total iron [25], and total copper [25] concentrations were monitored weekly by Ingalls. Dissolved sulfides were measured biweekly using a modification of a method described by Strickland and Parsons [27]. The modification uses a 10-cm cell to increase sensitivity. The detection limit of the modified method is 6.5 ppb. Total sulfate concentration [25] was measured bimonthly. Total organic carbon [25] and ferrous iron [25] concentrations were measured intermittently. Microbiological analyses were performed periodically to determine the concentration of sulfate-reducing bacteria in the flow-through water using the American Petroleum Institute technique [28] which involves serial dilution in anaerobic bottles containing a nail as a source of iron.

3. RESULTS

Water temperature varied from 9° to 17°C over the experimental period extending from September 1986 to April 1987. The pH varied from 7.4 to 8.2. Chlorinity varied from 4.3 to 20.0 ppt Cl^-. Chlorinity can be converted to salinity using the following relationship: Salinity (ppt)=1.806 Chlorinity (ppt). Total suspended solids ranged from 10 ppm to 65 ppm during dredging operations. Dissolved oxygen varied from 5.2 ppm during September to 10.5 ppm in late December. Copper and iron concentrations in the river water fluctuated between 5 to 70 ppb and 150 to 906 ppb, respectively. Dissolved sulfides could not be detected during the experiment. The mean concentration for sulfates (SO_4^{2-}) was ≈2500 mg/l. Standard plate counts indicated bacterial populations of $1x10^4$-10^5 per cc and a sulfate-reducing bacterial population of $1x10^2$-10^3 per cc.

The EDAX spectra of the pipe surfaces were essentially identical despite the varying initial treatments. Pipe surfaces were predominantly copper, nickel, and iron. A sample spectrum is shown in Figure 2. Over the 8-month exposure period, all surfaces exposed to Pascagoula River water accumulated silica, phosphorus, sulfur, chlorine, potassium, and calcium (Fig. 3). Pipes 2 and 3 did show a temporary increase in surface Fe immediately after batch

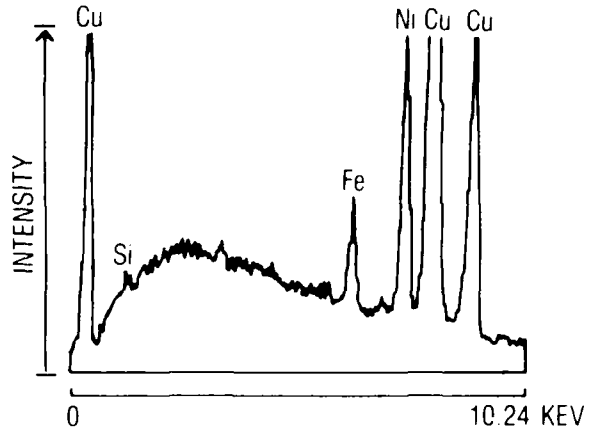

Figure 2. Representative EDAX spectrum of pipe surfaces after initial treatments.

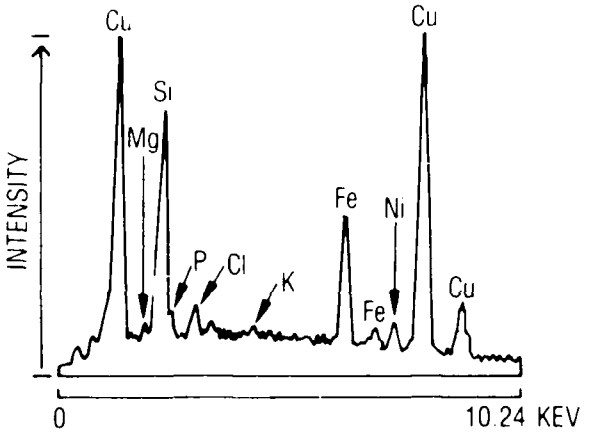

Figure 3. Representative EDAX spectrum of pipe surfaces after 6 month exposure period.

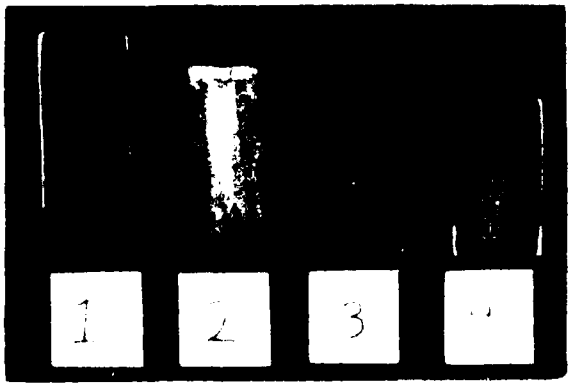

Figure 4. Pipe interiors after 6 months exposure.

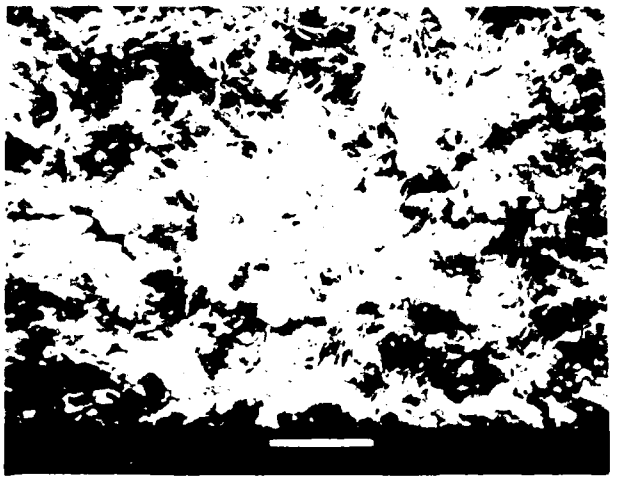

Figure 5. Biofilm on exposed surface of pipe 1.

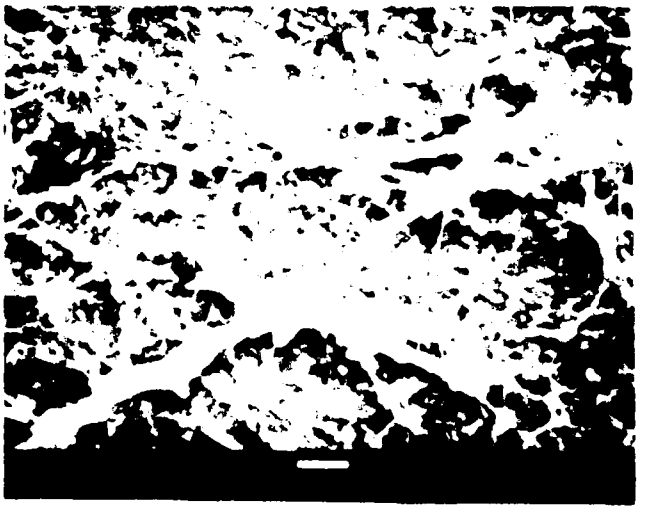

Figure 6. Biofilm on exposed surface of pipe 4.

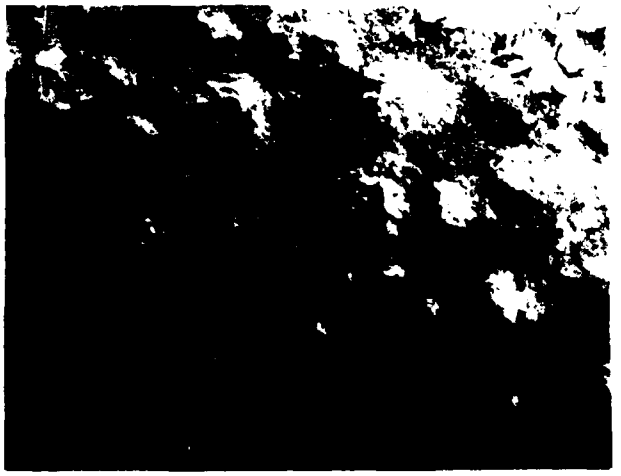

Figure 7. Blisters on pipe 2.

Figure 9. Bacterial cells observed within blister on pipe 2

Figure 10. Surface pitting beneath blisters on pipe 2

treatment. However, this increase was not evident at the next sample collection after two weeks.

The appearance of the pipe interiors was markedly different after 2 months. Despite the stagnation in pipe 1, pipes 1 and 4 had a tenacious reddish-brown film on the surface. There was no surface pitting on these two surfaces. Pipes 2 and 3 were covered with a patchy, flaky, green film characterized by blisters that have persisted over the 8-month evaluation period. Figure 4 shows the pipe interiors after 6 months of exposure. Well-defined biofilms developed on all surfaces (Figs. 5-6). Within the blisters found on pipes 2 and 3, bacterial cells were observed (Figs. 7-9). Surface pitting was found beneath the blisters (Fig. 10).

4. DISCUSSION

In the dockside experiment reported here the impact of batch $FeSO_4$ treatment in the presence of microorganisms was evaluated over an 8-month period. The straight lengths of pipe maintained at flow rates of 3-6 ft second^{-1} were designed to eliminate the possibility of impingement attack and to maximize the possibility for microbial colonization.

The mechanism of accelerated corrosion of copper-nickel alloys in sulfide-polluted seawater has been summarized by Syrett [4]. During the first few seconds of exposure to sulfide-polluted water, a thin film forms on the copper surface that is primarily cuprous oxide. Cuprous sulfide forms soon after the alloy is exposed to the polluted seawater. The chemical composition of the oxide-type film is variable, but its sulfur content never approaches that of the cuprous sulfide scale that grows on top of it. The initial anodic reaction product is Cu^+ ions that react with the dissolved sulfide and precipitate at the metal surface to produce a

porous black scale. The cathodic reaction, H^+ ion reduction, occurs at the boundary between the oxide-type and sulfide layers, and produces OH^- ions that can react with the anodically produced Cu^+ ions. However, most of the Cu^+ ions migrate through the porous Cu_2S scale, react with dissolved sulfide, and lead to a thickening of the scale. Under these conditions, corrosion is under cathodic control, limited by the transport of H^+ ions to the cathodic sites.

When sulfide-polluted, deaerated seawater is replaced by unpolluted, aerated seawater, the rate of the reaction rate increases, and the corrosion rate increases. Cu^+ ions diffusing through the porous sulfide scale combine with dissolved oxygen to produce Cu_2O, and the sulfide scale itself is slowly transformed to the oxide with the concomitant production of SO_4^{2-} ions or elemental sulfur. A reduction in the sulfur content of the oxide-type scale will also occur at a relatively low rate. The transformation of sulfide to oxide results in a change in volume that weakens the bond between the thick black scale and the oxide-type subscale and leads to spalling. Bared areas repassivate, forming cuprous oxide.

Waterborne sulfides could not be measured in the Pascagoula River water during the course of this experiment. Sulfide-induced corrosion in piping systems is often discounted because waterborne sulfides are below detection limits. However, obligate anaerobic sulfate-reducing bacteria can exist in oxygenated waters, colonize a surface in anaerobic niches, and produce sulfides. Large concentrations of sulfates and sulfate-reducing bacteria were demonstrated in the Pascagoula River water. Furthermore, sulfur and chlorine accumulated on all pipe surfaces. The concentration of Cl^- on pipes 2 and 3 was enhanced relative to pipes 1 and 4. The formation of flaky, nonadherent films only on pipes 2 and 3 and the presence of bacteria with blisters on those surfaces cannot be explained by the authors at this time.

Localized pitting of copper alloys under microbiological colonies or tubercles has been cited [29,30]. Others [31] have reported the corrosion of copper in the presence of sulfate-reducing bacteria. Sulfate-reducing bacteria have been shown to be responsible for the corrosion of copper alloys in underground pipe installations through the production of H_2S, which forms a sulfide film on the surface of the metal. Such a film is protective as long as it is continuous. Breaks in the film, however, expose areas where pitting can occur. Breaks in the wet surface films on pipes 2 and 3 were evident after 2 months exposure. Surface pitting was observed under blisters on these surfaces.

Total iron concentration in the flow-through water varied from 150 to 900 ppb. Of this amount, 65 ppb was shown to be Fe^{2+}. In the organic-rich water, a majority of the total iron concentration would be expected to be colloidal γ-FeOOH [32]. Since "oxidants are consumed in order of decreasing energy production per mole of organic carbon oxidized (O_2 > manganese oxides > nitrates > iron oxides > sulfate)" [33] ferrous iron would be produced in the flow-through water before sulfides. The iron in the flow-through water is present in concentrations an order or magnitude greater than that introduced by batch treatment. Under such circumstances it is unlikely that waterborne sulfides could cause corrosion.

5. CONCLUSIONS

The localized corrosion observed in the pipes of the dockside experiment appears to be due to microbiologically induced corrosion. Sulfate-reducing bacteria and sulfates were demonstrated in the flowthrough water and sulfur accumulated in all surface deposits, which could result in an active/passive surface. Batch FeSO$_4$ treatments did not result in a persistent increase in surface-bound iron. The persistent concentration of iron in the surface films was the same regardless of surface treatment, indicating that the iron in the surface films comes from the alloy,

or the flowthrough water, not the $FeSO_4$ treatment. These observations apply only to batch $FeSO_4$ treatment and cannot be used to predict the efficiency of $FeSO_4$ injections or other applications of Fe^{2+} to surfaces.

6. ACKNOWLEDGMENTS

This project was funded by Naval Sea Systems Command, Washington, D.C., program element 990101, Vance Saige, program manager. NORDA contribution number 333:034:87

7. REFERENCES

(1) North, R.F. and Pryor, M. J. 1970. The influence of corrosion product structure on the corrosion rate of Cu-Ni alloys. Corrosion Science, Vol. 10, pp. 297-311.

(2) Bianchi, G. and Longhi, P. 1973. Copper in sea-water, potential-pH diagrams. Corrosion Science, Vol. 13, pp. 853-864.

(3) National Materials Advisory Board, The National Research Council, National Academy of Sciences, 1977. Accelerated corrosion of copper-nickel piping. Final Report NMAB-343.

(4) Syrett, B.C. 1980. The mechanism of accelerated corrosion of copper-nickel alloys in sulfide-polluted seawater. Presented at the National Association of Corrosion Engineers, Corrosion/80, Chicago, IL, Paper No. 33.

(5) Rowlands, I.C. 1965. Corrosion of tube and pipe alloys due to polluted seawater. J. Appl. Chem., Vol. 15, pp. 57-63.

(6) Gudas, J.P. and Hack, H.P. 1979. Sulfide induced corrosion of copper-nickel alloys. Corrosion, Vol. 35, pp. 67-73.

(7) Hack, H.P. 1980. Galvanic corrosion of piping and fitting alloys in sulfide modified seawater. J. of Testing and Evaluation, Vol. 8, No. 2, pp. 74-79.

(8) Sato, S. and Nagata, K. 1978. Factors affecting corrosion and fouling of condenser tubes of copper alloys and titanium. Light Metal Technical Reports, Vol. 19, No. 3.

(9) Pope, D.H., Duquette, D.J., Johannes, A.H., and Wayner, P.C. 1984. Microbiologically influenced corrosion of industrial alloys. Materials Performance, Vol. 23, No. 4, pp. 14-18.

(10) Popplewell, J.M., Hart, R.J. and Ford, J.A. 1973. The effect of iron on the corrosion characteristics of 90-10 cupro nickel in quiescent 3·4 NaCl solution. Corrosion Science, Vol. 13, pp. 295-309.

(11) Bates, J.F. and Popplewell, J.M. 1975. Corrosion of condenser tube alloys in sulfide contaminated brine. Corrosion, Vol. 31, No. 8, pp. 269-275.

(12) Hack, H.P. and Gudas, J.P. 1980. Inhibition of sulfide induced corrosion with a stimulated iron anode. Materials Performance, Vol. 19, No. 4, pp. 49-54.

(13) Pearson, C. 1972. Role of iron in the inhibition of corrosion of marine heat exchangers-a review. Br. Corros. J., Vol. 7, pp. 61-68.

(14) $FeSO_4$ treatment to prevent corrosion of condenser and heat exchanger tubes. 1970. Technical Bulletin TB/7, Yorkshire Imperial Metals Limited, Leeds, England.

(15) Bostwick, T.W. 1961. Reducing corrosion of power plant condenser tubing with ferrous sulfate. Corrosion, Vol. 17, pp. 12-19.

(16) Lockhart, A.M. 1964-1965. Reducing condenser tube corrosion at Kincardine generating station with ferrous sulfate. Instn. Mech. Engs., Vol. 179, pt. 1, No. 16, pp. 495-509.

(17) North, R.F. and Pryor, M.J. 1968. The protection of copper by ferrous sulfate additions. Corrosion Science, Vol. 8, No. 3, pp. 149-165.

(18) Isherwood, B.F. 1907. The experiments made by Mr. Uthermann to discover a process for preventing the corrosion of copper and brass by seawater under the conditions found in the surface condensers of marine steam engines. J. Am. Soc. Nav. Engrs., Vol. 19, No. 3.

(19) Morgan, J.H., 1977. Cathodic protection, iron injection and chlorination in marine heat exchangers. In: Proceedings of Third International Congress on Marine Corrosion and Fouling, National Bureau of Standards, Gaithersburg, MD.

(20) Hack, H.P. 1977. Effectiveness of ferrous sulfate as an inhibitor for sulfide-induced corrosion of copper-nickel alloys, DTNSRDC/77-0072.

(21) November 5, 1986. Examination of copper-nickel seawater piping removed from USS Vincennes (CG-49) during post-shakedown availability (PSA). NAVSSES Memorandum.

(22) Military specification detergents, general purpose (liquid, nonionic)-MIL-D-16791F, 27 February 1985. Department of Defense Index of Specifications and Standards (D.DISS).

(23) Federal specification, sodium phosphate, tribasic, anhydrous; dodecahydrate: and monohydrate; technical, O-S-642F, 17 February 1984, Department of Defense Index of Specifications and Standards (D.DISS).

(24) Military specification, citric acid, technical, MIL-C-11029C, 20 July 1983, Department of Defense Index of Specifications and Standards (D.DISS).

(25) Annual Book of ASTM Standards (Part 31), American Society for Testing and Materials, 1978. Philadelphia, PA.

(26) Standard Methods for the Examination of Water and Waste Water, 14th Ed., 1976. American Public Health Association, Washington, D.C., p. 450.

(27) Strickland, J.D.H. and Parsons, T.R. 1968. A Practical Handbook of Seawater Analysis, Fisheries Research Board of Canada, p. 41.

(28) American Petroleum Institute Recommended Procedure 38: Section II, Paragraph 28, and Section A-11, 1983, Dallas, TX.

(29) Bengough, G.D. and May, R. 1924. Seventh report to the Corrosion Research Committee of the Institute of Metals. Inst. Metals, Vol. 32, pp. 81-256.

(30) Rogers, J. 1948. The promotion and acceleration of metallic corrosion by microorganisms. Inst. of Metals, Vol. 75, p. 19.

(31) Deshmukh, M.B., Srivastava, R.B. and Karande, A.A. 1985. Microbiological corrosion of mild steel and copper in polluted seawater. In: Proceedings of International Conference on Marine Biodeterioration, Goa, India, pp. 209-214.

(32) Strumm, W. and Morgan, J.J. 1970. Aquatic Chemistry, Wiley-Interscience, New York, p. 542.

(33) Froelich, P.N., Klinkhammer, G.P., Bender, M.L., Luedtke, N.A., Heath, G.R., Cullen, D., Dauphin, P., Hammond, D., Hartman, B. and Maynard, V. 1979. Early oxidation of organic matter in pelagic sediments of the eastern equatorial Atlantic: suboxic diagenesis. Geochimica et Cosmo Chemica, Vol. 43, pp. 1075-1090.

BIOGRAPHY

NAME: Brenda J. Little

PRESENT AFFILIATION: Naval Ocean Research and Development Activity
Code 333

TITLE: Branch Head, Biological and Chemical Oceanography Branch

FIELD OF INTEREST/RESPONSIBILITIES: Biodeterioration of metals in marine environments.

PREVIOUS AFFILIATIONS/TITLES:

Microbiologist, National Park Service
Biochemist, General Electric Company

ACADEMIC BACKGROUND:

B.S. (Biology/Chemistry), Baylor University, Waco, Texas
Ph.D. (Chemistry), Tulane University, New Orleans, Louisiana

SOCIETY ACTIVITIES/OFFICES/AWARDS:

American Chemical Society, National Association of Corrosion Engineers, The Adhesion Society, International Humic Substances Society, Sigma Xi.

PUBLICATIONS/PAPERS: (see attached)

Publications:

Little, B. - 2nd author (with) S. M. Gerchakov and P. Wagner, (in press). Probing Microbiologically Induced Corrosion. Journal of Corrosion.

Little, B., J. S. Maki, R. Mitchell and M. Walch, (in press). Factors Influencing the Adhesion of Microorganisms to Surfaces. Journal of Adhesion.

Little, B. J. and J. R. DePalma, (in press). Marine Biofouling. In: Materials for Marine Systems. D. F. Hasson and C. R. Crowe (ed.), Academic Press.

Little, B. J. - 2nd author (with) D. Wiesenburg, (in press). Chemical Oceanography. In: Handbook of Ocean Engineering. A. Berman (ed.), Academic Press.

Little, B., P. Wagner and S. M. Gerchakov, 1986. A Quantitative Investigation of Mechanisms for Microbial Corrosion. In: Proceedings of the Internation Conference on Biologically Induced Corrosion. Washington, D.C., June 1985, pp. 209-214.

Little, B. J. and P. A. Wagner, 1986. An Analytical Evaluation of Microbiologically Induced Corrosion. The NORDA Review, March 31, 1976 - March 31, 1986, Naval Ocean Research and Development Activity, NSTL, Mississippi, 39529-5004, pp. 133-136.

Little, B. J. and P. A. Wagner, 1986. An Electrochemical Assessment of Corrosion Induced by Iron Oxidizing Bacteria. In: Corrosion '86, Paper 122, Houston, TX.

Little, B. J. - 2nd author (with) P. A. Wagner, 1986. Applications of a Technique for the Investigation of Microbially-Induced Corrosion. In: Corrosion '86, Paper 121, Houston, TX.

Little, B., P. Wagner, S. M. Gerchakov, M. Walch and R. Mitchell, 1986. The Involvement of a Thermophilic Bacterium in Corrosion Processes. Journal of Corrosion. 42(9): 533-536.

Gerchakov, S. M., B. J. Little and P. Wagner, 1985. The role of microorganisms in electron transport during corrosion. Proceedings of Argentine/USA Workshop on Biodeterioration, La Plata, Argentina, Aquatic Quimica, S.A., Sao Paulo, Brazil, p. 65.

Little, B., 1985. Factors Influencing the Adsorption of Dissolved Organic Materials from Natural Waters. Journal of Colloid and Interface Science, 180(2): 331-340.

Little, B. - 2nd author (with) P. Wagner and S. M. Gerchakov, 1985. The Role of Microorganisms in Electron Transport. In: Proceedings of the Argentina/USA Workshop on Biodeterioration. LaPlata, Argentina, Aquatec Quimica, S.A., Sao Paulo, Brazil, pp. 65-72.

Little, B., 1985. Fouling and Corrosion. Naval Research Reviews, Office of Naval Research, Vol. XXXVII: 43.

Little, B. - 5th author (with) C. B. Panchal, J. Larsen Basse, L. R. Berger, J. A. Berger, H. C. Stevens, J. B. Darby, L. E. Genens and D. L. Hillies, 1985. OTEC Biofouling Control and Corrosion - Protection Study at Seacoast Test Facility : 1981-1983. Argonne National Laboratory, Argonne, Illinois. ANL/OTEC-TM-5.

Little, B. and J. Jacobuš, 1985. A comparison of two techniques for the isolation of adsorbed organic material from seawater. Organic Geochemistry, 8: 27-33.

Little, B. and A. Zsolnay, 1985. Chemical Fingerprinting of adsorbed organic materials on metal surfaces. Journal of Colloid and Interface Science, 104: 79-86.

Little, B. - 2nd author (with) C. B. Panchal and J. Larsen-Basse, 1984. Biofouling control for marine heat exchangers using intermittent chlorination. Proceedings of the 22nd National Heat Transfer Conference. Fouling in Heat Exchange Equipment. ASME Publication HTD/Vol. 35, pp. 97-103.

Little, B., M. Walch, P. Wagner, S. M. Gerchakov and R. Mitchell, 1984. The impact of extreme obligate thermophilic bacteria on corrosion processes. Proceedings of the 6th International Congress on Marine Corrosion and Fouling, pp. 511-520.

Little, B., 1984. Succession in microfouling. Marine Biodeterioration: An Interdisciplinary Study (Edited by Costlow, J. D. and Tipper, R. C.). U. S. Naval Inst. Press, Bethesda, MD, pp. 63-67.

Little, B. J., 1983. A Chemical Characterization of Adsorbed Dissolved Organic Material from an Estuarine Source. Ph.D. Dissertation, Tulane University, New Orleans, LA.

Zsolnay, A. and B. Little, 1983. Characterization of fouling films by pyrolysis and chemical ionization mass spectrometry. J. of Anal. Pyrol., 4:335-341.

Little, B., J. Morse, G. Loeb and F. Spiehler, 1981. Gulf of Mexico Study of Biofouling on OTEC heat exchanger candidate alloys. Materials Performance 8:16-21.

Little, B. 1980. Gulf of Mexico Ocean Thermal Energy Conversion (OTEC) Biofouling and Corrosion Experiment, Elsevier North Holland, Inc. (Stevens, Vander Voort, and McCall, eds.) Microstructural Sciences, Vol. 8 pp 191-215.

Berger, R. and B. Little, 1980. A Comparison of two Ocean Thermal Energy Conversion (OTEC) biofouling and corrosion experiments. 5th International Congress on Marine Corrosion and Fouling. Barcelona, Spain.

Little, B. J. and D. K. Young, 1979. Ocean Dumping Dredged Material at the Jacksonville Harbor Disposal Site: An Environmental Trend Assessment, February 1977 to April 1978. NORDA Technical Note 42, 60 pp.

Little, B. J. and D. M. Lavoie, 1979. Gulf of Mexico Ocean Thermal Energy Conversion (OTEC) Biofouling Experiment. Proceedings of Condenser Biofouling Control Symposium by Electric Power Research Institute, Inc. p. 121. Atlanta, GA.

Little, B. and R. L. Zalkan, 1978. Experiment Technical Support, (Section 3) Ocean Thermal Energy Conversion - A Study of the Feasibility and Cost Effectiveness of Deploying an Ocean Thermal Energy Conversion Experiment to an Equatorial North Pacific Site, U. S. Department of Energy.

Little, B. and R. L. Zalkan, 1978. Experimental Technical Support, (Section 3) OTEC-4 - A Study of the Feasibility and Cost Effectiveness of Deploying an Ocean Thermal Energy Conversion Experiment to an Equatorial South Atlantic Site, NOAA Data Buoy Office.

NCEL
Technical Note

N-1764
April 1987
By James F. Jenkins
Sponsored By Naval Facilities
Engineering Command

Validation of Nitronic 33 in Reinforced and Prestressed Concrete

ABSTRACT Nitronic 33 stainless steel (Trademark of Armco Steel Corporation) has a unique combination of high strength and nonmagnetic properties which make it an excellent candidate for use as prestressing strand for concrete waterfront structures where the magnetic properties of the carbon steel commonly used for prestressing strand are not acceptable. Before Nitronic 33 stainless steel prestressed concrete waterfront structures were constructed, it was necessary to establish the corrosion performance of the Nitronic 33 stainless steel in marine concrete. A test plan was developed where a series of tests which compared the performance of carbon steel to the Nitronic 33 stainless steel were to be performed. The time to initiation of attack was established as the critical parameter for the evaluation of the test results. In each test, corrosion of the carbon steel initiated prior to the initiation of the corrosion of the Nitronic 33 stainless steel. In addition, previously emplaced full scale pier pilings with both carbon steel and Nitronic 33 stainless steel prestressing were inspected. The corrosion activity of the Nitronic 33 stainless steel prestressed piling was less than that of the companion carbon steel prestressed pilings.

METRIC CONVERSION FACTORS

Approximate Conversions to Metric Measures

Symbol	When You Know	Multiply by	To Find	Symbol
		LENGTH		
in	inches	*2.5	centimeters	cm
ft	feet	30	centimeters	cm
yd	yards	0.9	meters	m
mi	miles	1.6	kilometers	km
		AREA		
in^2	square inches	6.5	square centimeters	cm^2
ft^2	square feet	0.09	square meters	m^2
yd^2	square yards	0.8	square meters	m^2
mi^2	square miles	2.6	square kilometers	km^2
	acres	0.4	hectares	ha
		MASS (weight)		
oz	ounces	28	grams	g
lb	pounds	0.45	kilograms	kg
	short tons (2,000 lb)	0.9	tonnes	t
		VOLUME		
tsp	teaspoons	5	milliliters	ml
Tbsp	tablespoons	15	milliliters	ml
fl oz	fluid ounces	30	milliliters	ml
c	cups	0.24	liters	l
pt	pints	0.47	liters	l
qt	quarts	0.95	liters	l
gal	gallons	3.8	liters	l
ft^3	cubic feet	0.03	cubic meters	m^3
yd^3	cubic yards	0.76	cubic meters	m^3
		TEMPERATURE (exact)		
°F	Fahrenheit temperature	5/9 (after subtracting 32)	Celsius temperature	°C

*1 in = 2.54 (exactly). For other exact conversions and more detailed tables, see NBS Misc. Publ. 286, Units of Weights and Measures. Price $2.25. SD Catalog No. C13.10:286

Approximate Conversions from Metric Measures

Symbol	When You Know	Multiply by	To Find	Symbol
		LENGTH		
mm	millimeters	0.04	inches	in
cm	centimeters	0.4	inches	in
m	meters	3.3	feet	ft
m	meters	1.1	yards	yd
km	kilometers	0.6	miles	mi
		AREA		
cm^2	square centimeters	0.16	square inches	in^2
m^2	square meters	1.2	square yards	yd^2
km^2	square kilometers	0.4	square miles	mi^2
ha	hectares (10,000 m^2)	2.5	acres	
		MASS (weight)		
g	grams	0.035	ounces	oz
kg	kilograms	2.2	pounds	lb
t	tonnes (1,000 kg)	1.1	short tons	
		VOLUME		
ml	milliliters	0.03	fluid ounces	fl oz
l	liters	2.1	pints	pt
l	liters	1.06	quarts	qt
l	liters	0.26	gallons	gal
m^3	cubic meters	35	cubic feet	ft^3
m^3	cubic meters	1.3	cubic yards	yd^3
		TEMPERATURE (exact)		
°C	Celsius temperature	9/5 (then add 32)	Fahrenheit temperature	°F

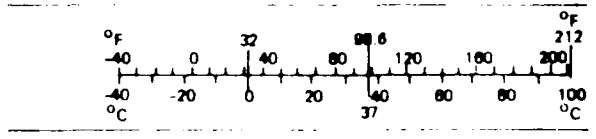

Unclassified

REPORT DOCUMENTATION PAGE

TN-1764 DN487311

VALIDATION OF NITRONIC 33 IN REINFORCED AND PRESTRESSED CONCRETE

Final; Jun 1985 - Jul 1986

James E. Jenkins

NAVAL CIVIL ENGINEERING LABORATORY
Port Hueneme, California 93043-5003

63275N;
Y1316-01-006-431

Naval Facilities Engineering Command
Alexandria, Virginia 22332

April 1987

62

Unclassified

Approved for public release; distribution unlimited

Corrosion; prestressed concrete; stainless steel

Nitronic 33 stainless steel (Trademark of Armco Steel Corporation) has a unique combination of high strength and nonmagnetic properties which make it an excellent candidate for use as prestressing strand for concrete waterfront structures where the magnetic properties of the carbon steel commonly used for prestressing strand are not acceptable. Before Nitronic 33 stainless steel prestressed concrete waterfront structures were constructed, it was necessary to establish the corrosion performance of the Nitronic 33 stainless steel in marine

DD Form 1473 continued

Unclassified

Unclassified

SECURITY CLASSIFICATION OF THIS PAGE (When Data Entered)

20. Continued

concrete. A test plan was developed where a series of tests which compared the performance of carbon steel to the Nitronic 33 stainless steel were to be performed. The time to initiation of attack was established as the critical parameter for the evaluation of the test results. In each test, corrosion of the carbon steel initiated prior to the initiation of the corrosion of the Nitronic 33 stainless steel. In addition, previously emplaced full-scale pier pilings with both carbon steel and Nitronic 33 stainless steel prestressing were inspected. The corrosion activity of the Nitronic 33 stainless steel prestressed piling was less than that of the companion carbon steel prestressed pilings.

It was concluded that prestressed concrete waterfront structures using Nitronic 33 as prestressing strand should perform at least as well as similar structures using carbon steel prestressing. Recommendations for additional work to evaluate possible differences in inspection, maintenance, and repair techniques required for Nitronic 33 stainless steel prestressed concrete waterfront structures are presented.

Library Card

Naval Civil Engineering Laboratory
VALIDATION OF NITRONIC 33 IN REINFORCED AND PRESTRESSED CONCRETE (Final), by James F. Jenkins
TN-1764 62 pp illus April 1987 Unclassified

1. Corrosion 2. Prestressed concrete I. YF316.01.006.431

Nitronic 33 stainless steel (Trademark of Armco Steel Corporation) has a unique combination of high strength and nonmagnetic properties which make it an excellent candidate for use as prestressing strand for concrete waterfront structures where the magnetic properties of the carbon steel commonly used for prestressing strand are not acceptable. Before Nitronic 33 stainless steel prestressed concrete waterfront structures were constructed, it was necessary to establish the corrosion performance of the Nitronic 33 stainless steel in marine concrete. A test plan was developed where a series of tests which compared the performance of carbon steel to the Nitronic 33 stainless steel were to be performed. The time to initiation of attack was established as the critical parameter for the evaluation of the test results. In each test, corrosion of the carbon steel initiated prior to the initiation of the corrosion of the Nitronic 33 stainless steel. In addition, previously emplaced full-scale pier pilings with both carbon steel and Nitronic 33 stainless steel prestressing were inspected. The corrosion activity of the Nitronic 33 stainless steel prestressed piling was less than that of the companion carbon steel prestressed pilings. It was concluded that prestressed concrete waterfront structures using Nitronic 33 as prestressing strand should perform at least as well as similar structures using carbon steel prestressing.

Unclassified

SECURITY CLASSIFICATION OF THIS PAGE (When Data Entered)

CONTENTS

INTRODUCTION

The purpose of this validation was to qualify Nitronic 33 stainless steel for use as prestressing strand and reinforcement in concrete construction where the magnetic properties of carbon steel are not acceptable.

This validation was directed solely to the determination of the corrosion behavior of Nitronic 33 stainless steel in concrete under conditions that are likely to be present in a pier fabricated from prestressed and reinforced concrete. Previous evaluations by others have determined that the mechanical properties, magnetic properties, fabricability, bonding strength, and other characteristics of Nitronic 33 stainless steel were suitable for construction of the type required.

While actual long term in situ testing of any material for a new application is highly desirable, this test program was based upon tests which could be completed in a relatively short period since it was necessary to determinine if Nitronic 33 prestressed and reinforced concrete could be used in the construction of urgently required facilities. The tests were developed to determine the relative susceptability of carbon steel and Nitronic 33 stainless steel to loss of passivity under various conditions which are likely to occur in an actual marine structure, and to separately assess the amounts and types of attack which are likely to occur on both carbon steel and Nitronic 33 stainless steel when, or if, active corrosion has been initiated. As both carbon steel and Nitronic 33 stainless steel were expected to behave as passive materials in concrete, the side-by-side comparison of the two was considered to be valid. By separating the determination of the initiation and propagation behavior, and by comparing the behavior of carbon steel and Nitronic 33 stainless steel in each test, an assessment of the relative corrosion performance of carbon steel and Nitronic 33 stainless steel could be made within a relatively short period. By including evaluation of previously cast sections of actual prestressed pilings (one with carbon steel prestressing and reinforcement and one with Nitronic 33 stainless teel prestressing and Nitronic 32 stainless steel reinforcement), and by the inspection of in-place pilings of each type, the test data was further validated.

If corrosion were to initiate on the Nitronic 33 stainless steel in concrete, the type, distribution, and extent of attack on the Nitronic 33 could be different from that which occurs on carbon steel in concrete. Therefore, an assessment of the effect of possible corrosion of Nitronic 33 on structural integrity of prestressed concrete pilings and slabs was made. Also, the effect of magnetic fields of the magnitude and orientation which are likely to be encountered in the vicinity of the proposed structure was assessed in order to determine the possible effects of these fields on corrosion of the reinforcement.

The direct comparison of the behavior of carbon steel and Nitronic 33 stainless steel in this validation can be used to compare the impact of corrosion of carbon steel and of Nitronic 33 stainless steel in a marine

prestressed concrete structure. It has been well established that concrete structures, prestressed and reinforced using carbon steel, can be successfully used in marine environments. This direct comparison of corrosion behavior can be used to assess whether a structure fabricated using Nitronic 33 prestressing and reinforcing can be successfully used in similar environments.

Follow-on efforts to extend the duration of the corrosion tests performed to date and to establish criteria for construction, inspection, maintenance, and repair of structures fabricated using Nitronic 33 stainless steel are also identified and described.

DEVELOPMENT AND APPROVAL OF TEST PLAN AND PRESENTATION OF INTERIM RESULTS

Development of the test plan for this validation was initiated on 14 June 1985. A preliminary test plan was reviewed by the Naval Facilities Engineering Command (NAVFAC) Code 03, 04, 05, and 07 representatives during meetings at NAVFAC on 20 June 1985. A revised test plan was reviewed by NAVFAC Code 04 representatives during a meeting at the Naval Civil Engineering Laboratory (NCEL) on 26 June 1985. The test plan was forwarded to NAVFAC by NCEL ltr Ser L52/968 of 3 July 1985 for approval. NAVFAC ltr 3902 Ser 032F/3906 of 20 August 1985 gave final approval of the test plan and directed NCEL to proceed with the validation. On 17 September 1985 a briefing on preliminary results of the validation was presented to NAVFAC. The results of the tests to that date were encouraging and it was determined that the tests should proceed as planned. A briefing was presented at NAVFAC on 17 December 1985 to present final test results and to serve as a basis for the decision to proceed with construction.

PREPARATION OF TEST SPECIMENS

All test specimens were cast from the same batch of concrete to reduce the effects of variation of concrete on the corrosion behavior of the embedded metal specimens. The mix design for the concrete was developed by Mr. Doug Burke of NCEL with consultation from Mr. Bob LaFraugh of ABAM Consulting Engineers, Tacoma, WA. The mix design was developed to represent high quality concrete of the type to be specified for construction of the deperming facilities in San Diego and Kings Bay. The mix design was as follows:

Cement - Type II	8.4 bags/yd
Water (W/C ratio = 0.40)	37.9 gal/yd
Sand (San Gabriel)	1113.0 lb/yd
Coarse aggregate (San Gabriel) 3/8 in maximum	1526.4 lb/yd

Admixture (Sika Mix 126)	200.5 fl oz/yd

Slump before admixture = 4 in
Slump after admixture = 0 in

The Nitronic 33 material was furnished by ARMCO Steel Corporation. All specimens were cut from the same coil of material. The wire diameter was 0.1875 inch. The chemical composition of the material, as determined by ARMCO, was as follows:

Composition of Nitronic 33 Test Wire

Element	%
Chromium	17.69
Manganese	12.23
Nickel	3.48
Silicon	.50
Nitrogen	.30
Molybdenum	.10
Carbon	.039
Phosphorous	.028
Sulphur	.002

The mechanical properties of the Nitronic 33 stainless steel wire, as determined by ARMCO, were as follows:

Ultimate tensile strength	136,000 psi
Yield strength	116,000 psi
Elongation	33.3%
Reduction of area	70.3%
Hardness	26 R_c

The stainless steel test material met the composition and strength requirements of ASTM Specification A580, Grade XM-29. This specification can be used for procurement of wire for prestressing strand with the additional requirement that the carbon content of the wire should be below .048% to insure adequate weldability.

The carbon steel wire specimens were center wires from prestressing strand meeting ASTM Specification A416. This is the standard specification for prestressing strand.

Both the stainless steel and carbon steel wire specimens were cut to a length of 22 inches and straightened as necessary. The specimens were degreased using mineral spirits to remove the bulk of the drawing compound on the wire and rinsed with acetone to remove any remaining surface contamination. Pairs of strands of the same materials were joined into dual strand specimens using an epoxy potting compound to be cast into 4- by 4- by 24-inch concrete prisms as shown in Figure 1.

Wires for other size test specimens were cut to the appropriate length, degreased in mineral spirits, and then in acetone. All of the molds for the test specimens were prepared in advance of casting. The dual strand specimens were placed in gang molds for the 4- by 4- by 24-inch prisms as shown in Figure 2.

After casting, all of the specimens were placed in a steam cabinet and steam cured for 16 hours. The 4- by 8-inch test cylinders cast and cured along with the test prisms were used to determine the strength of the concrete after steam curing and after 27 additional days of curing in 72-degree fog. The strength of the test cylinders was as follows:

Strength of 4- by 8-Inch Test Cylinders

16-hour steam cure	5914 psi
24-hour steam cure + 27-day fog cure	9380 psi

The 4- by 4- by 24-inch test prisms, which were to be cracked, were prepared by sawing a 1/2-inch-deep, 3/16-inch-wide "crack starter" notch in the upper "free" face of the specimen and then loading the specimen at three points as shown in Figure 3.

Eight test specimens were cut by sawing from two sections of piling furnished by ABAM Consulting Engineers, Seattle, WA. These sections were fabricated by Concrete Technology Inc., Tacoma, WA, and were used to compare the stress relaxation characteristics of the Nitronic 33 stainless steel prestressing strand with those of carbon steel. The sections are octagonal and are nominally 16 inches wide and 10 feet long. The section prestressed using Nitronic 33 stainless steel has 12 prestressing strands where the section prestressed using carbon steel has 11 prestressing strands. The section prestressed with Nitronic 33 has Nitronic 32 stainless steel spiral reinforcement. Each of the specimens cut from the Nitronic 33 prestressed section has two strands. Two of the specimens cut from the carbon steel prestressed section have one strand each and the other two specimens have two strands each. This variation in number of strands in the specimens was necessary due to the different spacing and the different number of wires in the piling sections. The test specimens and remaining sections are shown in Figure 4.

PERFORMANCE OF TESTS AND TEST RESULTS

Test Series No. 1 - Electrochemical Behavior in Mortar Extracts

Purpose of Test. To determine the chemical conditions, representative of those in marine concrete structures, which result in passivity of both carbon steel and Nitronic 33 stainless steel and to evaluate the relative stability of the passive films where they are present.

Test Specimens.

- Carbon Steel
- Carbon Steel w/crevice
- Nitronic 33
- Nitronic 33 w/crevice

Test Setup. Potentiostatic polarization per ASTM G61.

Test Measurements.

- Breakdown potential
- Repassivation potential

Test Condition Matrix.

Chloride (ppm)	pH (by dilution) 12.1	11.6	11.2	10.0
0				
40				
400				
4000				

Chloride was from seawater. Duplicate runs were made on each test specimen type for each condition.

Total Specimens.

Carbon steel	32
Carbon steel w/crevice	32
Nitronic 33	32
Nitronic 33 w/crevice	32
Total	128

Test Results. The electrochemical tests showed that the tolerance of Nitronic 33 stainless steel to both an increase in chloride ion and a decrease of pH was substantially greater than the tolerance of carbon steel. The electrochemical behavior for the specimens with crevices and those without crevices was essentially identical for both the carbon steel and Nitronic 33 stainless steel. Typical passive behavior for both the carbon steel and Nitronic 33 stainless steel as exhibited at pH 12.2 and 0 chloride are shown in Figures 5 and 6.

As the pH was lowered and/or the level of chloride increased, a point was reached where the passivity of each alloy was reduced. In the case of the carbon steel, the alloy exhibited essentially nonpassive behavior. As shown in Figures 7 and 8, the passivity of the carbon steel was reduced considerably at pH 11.6 and 200 ppm chloride and nonpassive behavior was exhibited at pH 10.0 and 200 ppm chloride. As shown in Figure 9, the level of passivity of Nitronic 33 stainless steel retained at a pH of 10.0 and 6000 ppm chloride was substantial.

Tables 1 and 2 summarize the results of the electrochemical tests. Fully passive behavior is indicated in the tables by a P. Marginal passivity is indicated by a M where passivity breaks down near the highest potential used in the tests. Lower levels of passivity are indicated by rupture potentials at increasingly negative potentials. Nonpassive behavior is indicated by a N.

Table 1. Electrochemical Behavior of Carbon Steel

Chloride (ppm)	Potential (MV) at pH (by Dilution) of--			
	12.1	11.6	11.2	10.0
0	P	P	P	P
20	P	M	+100	0
200	P	+100	-100	-200
2000	0	-100	-400	N
6000	-200	N	N	N

Table 2. Electrochemical Behavior of Nitronic 33 Stainless Steel

Chloride (ppm)	Potential (MV) at pH (by Dilution) of--			
	12.1	11.6	11.2	10.0
0	P	P	P	P
20	P	P	P	P
200	P	P	P	P
2000	P	P	P	P
6000	P	P	P	+200

Test Series No. 2 - Ion Tolerance Tests

Purpose of Test. To determine the relative tolerance of carbon steel and Nitronic 33 embedded in concrete to increased ionic content resulting from forced migration of seawater through the concrete.

Test Specimens.

- Carbon steel
- Nitronic 33

Test Setup. The apparatus used to determine the resistance of specimens embedded in concrete to accelerated ion migration is shown in Figure 10.

The voltage impressed across the test cell to drive the ions by electrophoresis was adjusted to give a voltage gradient of 1 V/in across the test specimen. Each test specimen contained one probe of Nitronic 33 stainless steel and one probe of carbon steel in order to eliminate any effects of concrete variability.

Test Measurements. Relative time (ion increase is proportional to time when applied voltage is present) for depassivation of the embedded probes.

Test Conditions.

1. Time to depassivation with diffusion potential on.

2. Run stainless steel specimen for time needed to depassivate carbon steel, then hold in seawater without diffusion voltage for 30 days to determine if delayed depassivation occurs. Duplicate runs were made for each test condition and material.

Total Specimens.

	Probes	Blocks
Carbon steel	4	2
Nitronic 33 w/crevice	8	4
Total	12	6

Test Results. The tolerance of Nitronic 33 stainless steel to ion migration was substantially greater than that of carbon steel. Figure 11 shows a typical potential versus time curve for an ion migration test run. After approximately 200 hours with voltage applied across the cell the carbon steel became active as indicated by an decrease in potential. The Nitronic 33 stainless steel remained passive for 1000 hours.

After 1600 hours of testing with the potential applied, the tests were terminated and the probes were removed from the concrete blocks by crushing the blocks. The Nitronic 33 specimens showed no evidence of attack. As shown in Figure 12, the carbon steel showed considerable attack and the Nitronic 33 stainless steel showed no attack.

Test Series No. 3 - Propagation Rates

Purpose of Test. To determine the relative rates of propagation of corrosion of carbon steel and Nitronic 33 embedded in concrete under conditions which will cause corrosion to initiate.

Test Specimens.

- Carbon steel
- Nitronic 33

Test Setup. The test setup for the determination of corrosion propagation rates is shown in Figure 13. The concrete cylinders were cut with a 1/16-inch-wide saw to a depth which exposed one of the two test probes.

Test Measurements. Corrosion current versus time measured with a zero resistance ammeter. Corrosion potential versus time.

Test Conditions. Seawater immersion. Duplicate specimens for each material.

Total Specimens.

	Probes	Blocks
Carbon Steel	4	2
Nitronic 33	4	2
Total	8	4

Test Results. The corrosion current for the carbon steel increased rapidly at the start of the test but fell to approximately 40 microamps after 50 hours. The Nitronic 33 stainless steel remained fully passive after 1000 hours with no measureable current flow. Figures 14 and 15 show the potential and current versus time for the carbon steel and Nitronic 33 stainless steel specimens.

The test probes were removed from the test blocks after 1600 hours of test exposure. The Nitronic 33 stainless steel test probes were not attacked. The carbon steel test probes showed considerable surface attack. Figure 16 shows the condition of the carbon steel and Nitronic 33 stainless steel probes after 1600 hours of exposure in the propagation rate tests.

Test Series No. 4 - Depassivation at Closed Cracks

Purpose of Test. To determine the relative susceptibility of carbon steel and Nitronic 33 embedded in concrete to depassivation in the presence of a crack in the concrete which has opened and reclosed.

Test Specimens.

- Carbon steel w/crevice
- Nitronic 33 w/crevice

Test Setup. The test setup for evaluation of depassivation at closed cracks is shown in Figure 17.

Test Measurements. Corrosion potential versus time.

Test Conditions. Seawater exposure. Duplicate specimens for each material.

Total Specimens.

	Probes	Blocks
Carbon steel w/crevice	4	2
Nitronic 33 w/crevice	4	2
Total	8	4

Test Results. Neither the carbon steel nor the Nitronic 33 stainless steel depassivated at closed cracks during the duration of this test. The corrosion potential versus time for the carbon steel is shown in Figure 18 and the corrosion potential for the Nitronic 33 stainless steel versus time is shown in Figure 19.

The test bars in these specimens were removed from the test blocks after 1200 hours of exposure in the depassivation at closed crack tests. Neither the carbon steel nor the Nitronic 33 stainless steel specimens showed any attack.

Test Series No. 5 - Ion Diffusion Tolerance at Closed Cracks

Purpose of Test. To determine the relative tolerance of carbon steel and Nitronic 33 embedded in concrete to increased ionic content resulting from forced diffusion of seawater into the concrete in the presence of a closed crack.

Test Specimens.

- Carbon steel w/crevice
- Nitronic 33 w/crevice

Test Setup. The test setup for the determination of ion diffusion tolerance at closed cracks was similar to the test setup for the determination of depassivation at closed cracks except that the inner bars were used as a counter electrode to produce a potential gradient within the specimen.

Test Measurements. Corrosion potential versus time.

Test Conditions. Seawater immersion.

1. Time to depassivation with diffusion potential on.

2. Run stainless steel specimen for time needed to depassivate carbon steel, then hold in seawater without diffusion voltage for 30 days to determine if delayed depassivation occurs. Duplicate runs were made on each material.

Total Specimens.

	Probes	Blocks
Carbon steel w/crevice	4	2
Nitronic 33 w/crevice	4	2
Total	8	4

Test Results. The carbon steel specimens depassivated after an average of 32 hours of applied current. The Nitronic 33 stainless steel remained passive after 1600 hours of applied current.

The test bars in these specimens were removed from the test blocks to determine their surface condition. The Nitronic 33 stainless steel specimens showed no attack. The carbon steel test specimens showed considerable surface attack in the area of the crack.

Test Series No. 6 - Repassivation at Closed Cracks

Purpose of Test. To determine the relative ability of carbon steel and Nitronic 33 embedded in concrete to repassivate in the presence of a closed crack if corrosion initiates when the crack is open.

Test Specimens.

- Carbon steel w/crevice
- Nitronic 33 w/crevice

Test Setup. The test setup for this series is identical to that shown for depassivation at open cracks (Figure 17).

Test Measurements. Corrosion potential versus time.

Test Conditions. Open crack until corrosion initiates. Measure time to achieve repassivation. Duplicate runs were made for test condition and material.

Total Specimens.

	Probes	Blocks
Carbon steel w/crevice	4	2
Nitronic 33 w/crevice	8	4
Total	12	6

Test Results. As the Nitronic 33 stainless steel did not depassivate at open cracks over the duration of the test in Series No. 7, it was not possible to make a comparison between the carbon steel and Nitronic No. 3 stainless steel for the ability to repassivate. The carbon steel repassivated within 35 hours of closing the crack as shown in Figure 20.

Test Series No. 7 - Depassivation at Open Cracks

Purpose of Test. To determine the relative susceptibility of carbon steel and Nitronic 33 embedded in concrete to depassivation in the presence of cracks in the concrete cover of various widths.

Test Specimens.

- Carbon steel w/crevice
- Nitronic 33 w/crevice

Test Setup. The test setup for determination of depassivation at open cracks is shown in Figure 21.

Crack Widths.

- 1/64 inch
- 1/32 inch
- 1/16 inch
- 1/8 inch

Test Measurements. Corrosion potential versus time.

Test Conditions. Seawater immersion. Duplicate specimens for each material and crack width.

Total Specimens.

	Probes	Blocks
Carbon steel w/crevice	16	8
Nitronic 33 w/crevice	16	8
Total	32	16

Test Results. None of the Nitronic stainless steel specimens showed depassivation during the duration of these tests. The carbon steel bars with 1-inch cover showed depassivation upon immersion for the 1/8-inch-wide crack, 50 hours for the 1/16-inch crack, 160 hours for the 1/32-inch crack, and 180 hours for the 1/64-inch crack. The carbon steel bar with 2-1/4-inch cover show depassivation immediately upon immersion for the 1/8-inch-wide crack but continued passive behavior for the 1/16-inch and tighter cracks. Figures 22 and 23 show the potential of the inner (2-1/4-inch cover) and outer (1-inch cover) bars versus time.

The test bars in these specimens were removed from test blocks to determine their surface condition. As shown in Figure 24 and 25, the Nitronic 33 stainless steel specimens were not attacked, but the carbon steel specimens showed considerable attack.

Test Series No. 8 - Corrosion Products

Purpose of Test. To determine [illegible] products produced in the [illegible] embedded in concrete.

Test Specimens.

- Carbon steel
- Nitronic 33

Test Setup. The test setup for the determination of corrosion product volume is shown in Figure 26.

Test Measurements.

- Change in cylinder diameter
- Visual inspection of metal-concrete interface at end of test
- Weight loss of probes

Test Conditions.

- Seawater immersion
- Anodic current from propogation rate test
- Triplicate specimens for each material

Total Specimens.

Carbon steel	3
Nitronic 33	3
Total	6

Test Results. As corrosion of the Nitronic 33 stainless steel did not initiate in the propagation rate tests it was not possible to perform the tests for the Nitronic 33 stainless steel in this series as appropriate corrosion currents could not be established.

There were no instances in the tests performed for this validation that resulted in the generation of sufficient volumes of corrosion products to establish any conclusions regarding the effects of corrosion product volume on corrosion.

Test Series No. 9 - Evaluation of Prestressed Pile Specimens

Purpose of Test. To determine the susceptibility of Nitronic 33 and carbon steel strand embedded in concrete to depassivation using specimens cut from a prestressed test piling section with cracks in the concrete cover. Original plans to test the specimens from the piling without cracks were not performed as the resistance to corrosion initiation of both the carbon steel and Nitronic 33 stainless steel in specimens without cracks was likely to be longer than the time available for these tests. Original plans to test each strand in the sections cut from the pilings were changed since it was determined that the strands were electrically connected through the spiral wrap. It was also determined after the original plans for this test that the spiral reinforcements in the Nitronic 33 stainless steel prestressed piling were Nitronic 32 stainless steel.

Test Specimens. Cut from test piling prestressed with Nitronic 33 strand and carbon steel strand.

Test Setup. The test setup for the determination of the susceptibility of carbon steel and Nitronic 33 stainless steel strand in specimens cut from test pilings is shown in Figure 27. The faces and ends of the test sections were sealed with paraffin prior to filling the reservoir with seawater.

Test Measurements. Corrosion potential versus time.

Test Conditions.

- Seawater immersion
- Crack widths - 1/8 and 1/16 inch

Total Specimens.

	Strands	Blocks
Carbon steel	2	2
Nitronic 33	2	2
Total	4	4

Test Results. The corrosion potentials versus time for the carbon steel and Nitronic 33 stainless steel piling sections showed erratic behavior. This was attributed to the more complex geometry of the specimens, the presence of the spiral reinforcement which was exposed (but coated with paraffin), and the variation of cover over the strands. The potentials indicated that there may be limited corrosion activity in both the carbon steel and Nitronic 33 stainless steel prestressed specimens.

Upon completion of the potential measurements, the strand and spiral reinforcement was removed from the test specimens. As shown in Figure 28, the carbon steel strand and spiral showed considerable surface attack in the vicinity of the cracks.

The Nitronic 32 stainless steel spiral reinforcement in the piling specimens showed several areas of incipient attack. The strand in the specimens was not attacked. The condition of the strand and spiral reinforcement is shown in Figure 29.

Test Series No. 10 - Evaluation of In-Place Pilings

Purpose of Test. To determine the short term (17-month) performance of prestressed pilings fabricated using both carbon steel and Nitronic 33 stainless steel exposed in a marine structure.

Test Specimens. Pilings in the SEA-LAND pier - Port of Tacoma.

Test Setup. The test pilings were evaluated using a developmental diver-held, surface-supported probe which measured the flow of current into or from the surface of the test pilings. The technique is described in NCEL TM 52-85-01.

Test Measurements. Corrosion currents resulting from corrosion cells on the prestressing strand or spiral reinforcement. Visual observations of surface defects on pilings.

Test Conditions. Seawater immersion of driven piling in an in-service structure.

Test Results. No significant corrosion activity was detected in either the Nitronic 33 stainless steel or the carbon steel prestressed pilings. The readings obtained on both types of pilings were statistically identical. Small locations on the Nitronic 33 stainless steel prestressed piling where limited corrosion activity was located were correlated with carbon steel "pre-ties" used in the manufacture of the test piling.

Due to instrument limitations, the readings taken during the first inspection of the test pilings on 12 September and 13 September 1985 showed no corrosion activity on either piling. The performance of the probe was substantially improved by modifying the electronics in the topside instrumentation package and the test probe. A second inspection of the pilings on 31 October 1985 and 1 November 1985 resulted in the generation of reliable and meaningful test results. The corrosion activity in the test pilings was extremely small. The maximum readings obtained were less than one-tenth of the readings typically obtained on laboratory specimens where corrosion activity was known to be occuring. Figures 30 and 31 show that the readings obtained for both the carbon steel and stainless steel were similar in the frequency of readings versus their polarity and intensity. As shown in Figure 32, which is a current profile map of the Nitronic 33 prestressed piling, there were several small sites on one surface of the piling where the majority of the corrosion activity on the pile was concentrated. The level of current was small, however the readings were reproducible and were interpreted as locations of corrosion activity. No surface indication of activity was noted by the divers at these sites or at any other location on the test pilings.

Subsequent detailed examinations of the piling sections obtained by NCEL for sectioning revealed that there were carbon steel tie wires used at some locations for securing the spiral wrap to the prestressing strand in the Nitronic 33 piling. Figure 33 shows a magnet adhering to such a tie wire. The tie wire was found on the same face of the test section where the corrosion activity was located by the test probe. The majority of the tie wires in this specimen were, however, nonmagnetic austenitic stainless steel.

Discussions with Mr. Philip Brakeland of ABAM Consulting Engineers regarding the manufacture of the test piling sections revealed that the carbon steel tie wire located in the test piling section and the corrosion activity located by the test probe were at locations where the spiral wrap was "pre-tied" to the strands. These "pre-ties" are spaced at approximately 4-foot intervals and are located along the face of the piling identified as "A" in Figure 2. This is identical to the spacing and location of the corrosion activity on the test piling. While the use of carbon steel tie wire was neither intended nor confirmed by ABAM, their use

was considered possible, particularly as their presence was confirmed in Figure 33 which shows a small bar magnet being suspended from the tie wire.

The presence of the limited number of small carbon steel ties in the exposed pilings is not considered to be significant from the standpoint of the lifetime of the pilings, however, the use of such tie wires should be avoided in future construction so that inspection using current probes can be more readily interpreted. In fact, confirmation of the ability of the test probe to detect such small sites of limited activity was considered to be a positive aspect of the presence of the carbon steel ties in the Nitronic 33 test pilings.

IMPACT OF CORROSION ON STRUCTURAL INTEGRITY

Purpose of Effort

The purpose of this effort is to assess the impact of the type and extent of corrosion which is likely to occur on Nitronic 33 stainless steel in concrete on the structural integrity of prestressed and reinforced concrete structures. As the distribution, type, and extent of corrosion of Nitronic 33 is likely to be substantially different from that of the carbon steel commonly used, the structural impact of the corrosion which is likely to occur on the Nitronic 33 may also be substantially different.

Results of Assessment

The results of this assessment are included in this report as Appendix A. This assessment was performed by Dr. George Warren of NCEL. The assessment showed that the structural impact of distributed localized attack of the type anticipated for the Nitronic 33 prestressed piling, should it occur, would be less serious than the more general attack which would be likely to occur on carbon steel prestressed structures of similar design.

ASSESSMENT OF INDUCED ELECTRICAL CURRENTS

Purpose of Effort

The purpose of this effort is to determine the magnitude and likely paths of electrical currents which may be induced in prestressed concrete structures by pulsating magnetic fields. It is possible that electrical currents which are induced can flow from the reinforcement into an electrolyte and induce corrosion.

Results of Assessment

This assessment was performed by Mr. Jim Brooks of NCEL. The results of this assessment are given in Appendix B. The assessment showed that the worst case currents are less than 1 ampere. This level

is substantially below that required to cause significant corrosion activity, and can be reduced substantially by increasing the resistance of the current path by not allowing the prestressing strand to protrude from the bottom of the pilings. As this will be required to prevent direct contact between the strands and seawater or bottom sediments, the currents in an actual structure will be insignificant from the standpoint of corrosion.

REVIEW OF TEST RESULTS

This review of test results is based upon the electrochemical tests and the actual condition of the test bars removed from the test specimens except for the evaluation of the in-place pilings.

Test Series	Results
#1	Nitronic 33 more resistant to lower pH and increased chloride.
#2	Nitronic 33 more resistant to ion migration.
#3	Carbon steel became active; Nitronic 33 remained passive.
#4	Neither alloy became active.
#5	Nitronic 33 more resistant.
#6	Carbon steel repassivated; Nitronic 33 did not depassivate.
#7	Carbon steel depassivated; Nitronic 33 did not depassivate.
#8	Carbon steel depassivated; Nitronic 33 did not depassivate. Corrosion product volume insufficient to cause measurable changes.
#9	Carbon steel corroded; Nitronic 33 did not corrode. Nitronic 32 showed incipient corrosion.
#10	No significant difference between pilings. Carbon steel in Nitronic 33 piling had become active, otherwise, no significant activity in either piling.

Test Series	Results
Structural Integrity	The type of attack expected on the Nitronic 33, should it occur, would have less impact than that of the typical corrosion of carbon steel.
Induced Currents	The effect of induced electrical currents will be insignificant and may be easily reduced further.

CONCLUSIONS

Based upon the results of all of the tests performed in this validation, it is concluded that the resistance of Nitronic 33 stainless steel to corrosion in environments representative of those found in a prestressed or reinforced structure is superior to the corrosion resistance of carbon steel.

The type of local attack which may occur if corrosion of the Nitronic 33 stainless steel is initiated will have less effect than the distributed corrosion which occurs on carbon steel prestressing.

Electrical currents induced by the operational magnetic fields associated with degaussing facilities will not result in accelerarted attack of the Nitronic 33 stainless steel.

NEED FOR ADDITIONAL EFFORTS

Construction Criteria

As the properties and performance of Nitronic 33 stainless steel have been found to be substantially different from the commonly used carbon steel, it is necessary to develop different criteria for the construction and construction inspection of structures using Nitronic 33 stainless steel. This has already been accomplished for the design of Nitronic 33 prestressed and reinforced structures where such differences in strength, elasticity, stress relaxation, bond strength, and weldability were assessed and changes to the design and fabrication of the structural elements were modified as necessary. This must also be done for the differences in corrosion behavior. The most critical factors related to corrosion performance are likely to be the tolerable limits for cracking in the cover over prestressing strand and reinforcing bars, and the method for repairing such cracks and encapsulating the exposed ends of the prestressing strands.

Maintenance, Repair Methods, and Criteria

As for construction criteria, it will be necessary to develop different methods and criteria for the in-service inspection of structures using Nitronic 33. The most critical factors related to corrosion performance are likely to be the detection of corrosion activity and the location of the position of the prestressing strands. The test probe

used experimentally in the validation should be developed into a field unit which can be used for the inspection of Nitronic 33 prestressed structures and for carbon steel prestressed and reinforced structures as well.

As for construction criteria, it will be necessary to develop different methods and criteria for the in-service maintenance and repair of structures using Nitronic 33. The most critical factors related to corrosion performance are likely to be the methods for repair of in-service cracking in the cover over prestressing strand and reinforcing bars, and the the methods for spalled elements.

Continuation of Test Exposures

Long term exposure is the most reliable method of determining actual performance of any material. The tests performed in this validation were designed to determine the relative performance of Nitronic 33 stainless steel and carbon steel under artificially produced conditions and in small samples. While the results of such tests can be used to compare performance, they should not be used to predict the lifetime of the materials tested when they are in use in full-scale structures.

Selected test exposures of Nitronic 33 should be continued to both support the recommended methods and criteria efforts and to serve as a basis for the prediction of the long term performance of Nitronic 33 stainless steel in full-scale structures.

RECOMMENDATIONS

1. The design and construction of the deperming facilities should proceed.

2. The design drawings should be carefully reviewed to insure that adequate cover is provided over all of the Nitronic 33 stainless steel.

3. Construction and construction inspection criteria should be developed for the facilities constructed using Nitronic 33 stainless steel.

4. In-service inspection methods and criteria should be developed for facilities constructed using Nitronic 33 stainless steel.

5. Maintenance and repair methods and criteria should be developed for facilities constructed using Nitronic 33 stainless steel.

6. Selected test exposures of Nitronic 33 should be continued to support the recommended methods and criteria efforts and to obtain long term performance data on Nitronic 33 stainless steel.

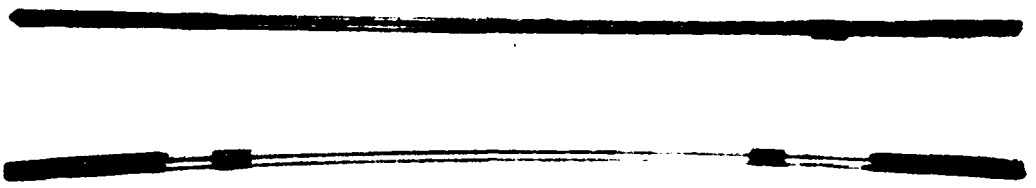

Figure 1. Dual strand prestressing wire specimens.

Figure 2. Gang molds for 4- by 4- by 16-inch prisms.

Figure 3. Cracking of 4- by 4- by 24-inch prisms.

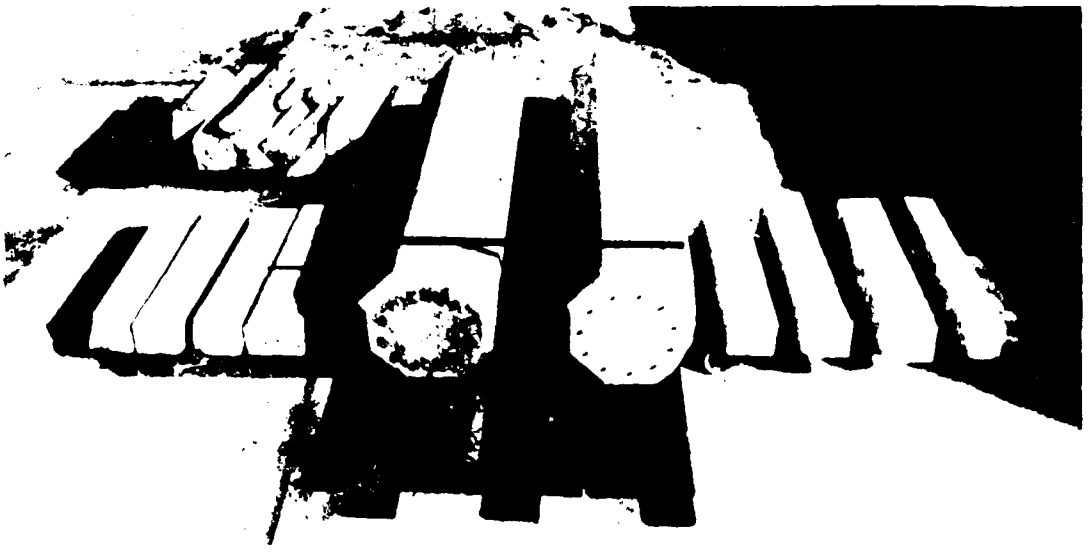

Figure 4. Test sections and specimens after sawing.

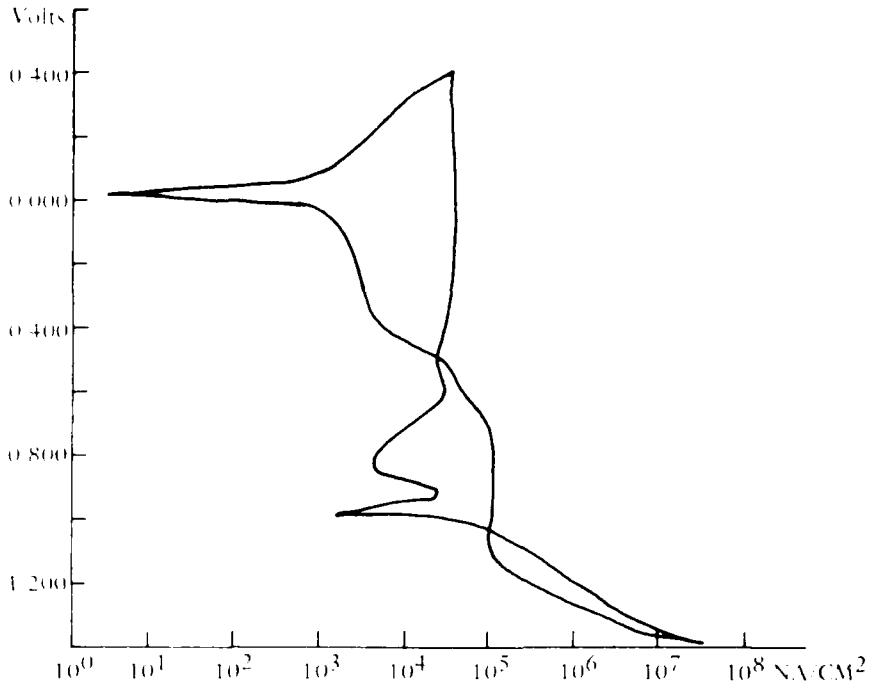

Figure 5. Polarization behavior of Nitronic 33 stainless steel - pH = 12.1, Cl^- = 0.

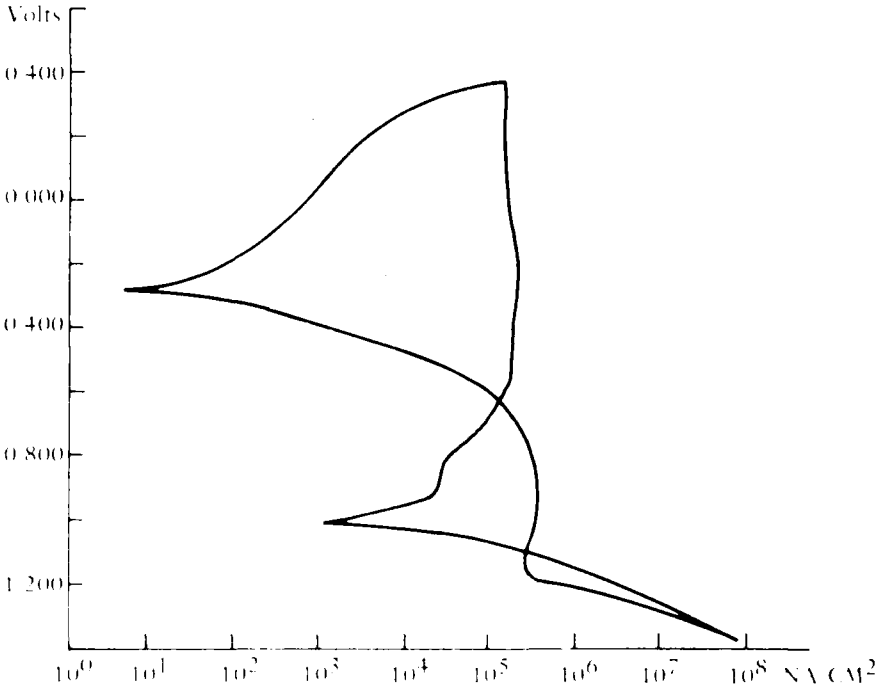

Figure 6. Polarization behavior of carbon steel - pH = 12.1, Cl^- = 0.

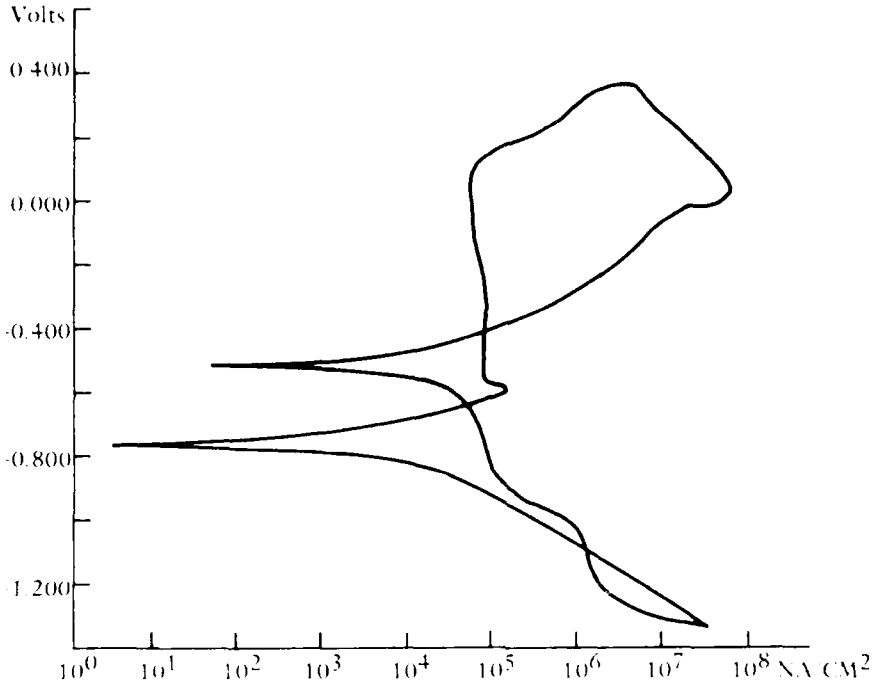

Figure 7. Carbon steel - pH = 11.6, Cl^- = 200 ppm.

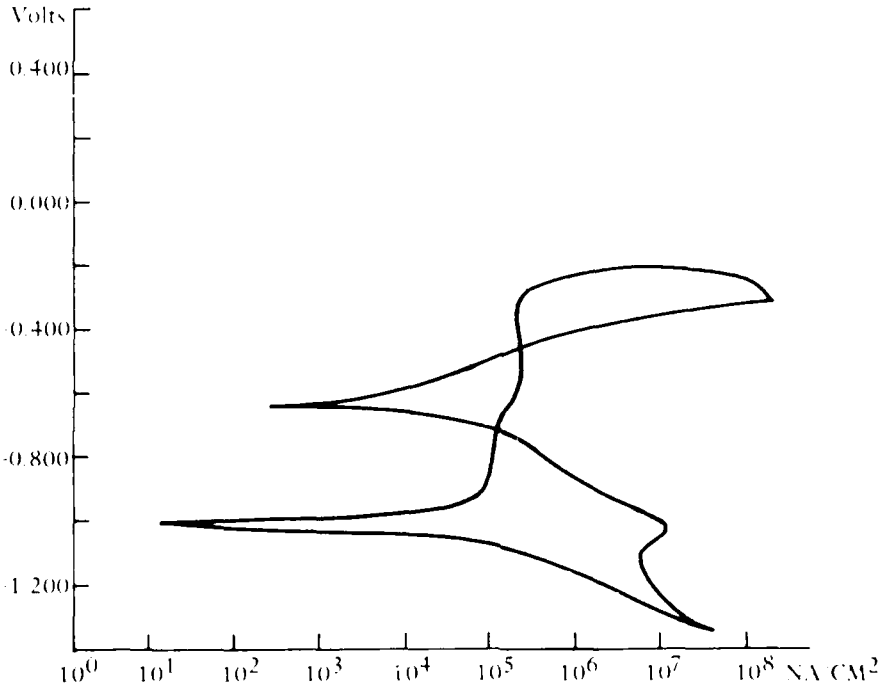

Figure 8. Carbon steel - pH = 10.0, Cl^- = 200 ppm.

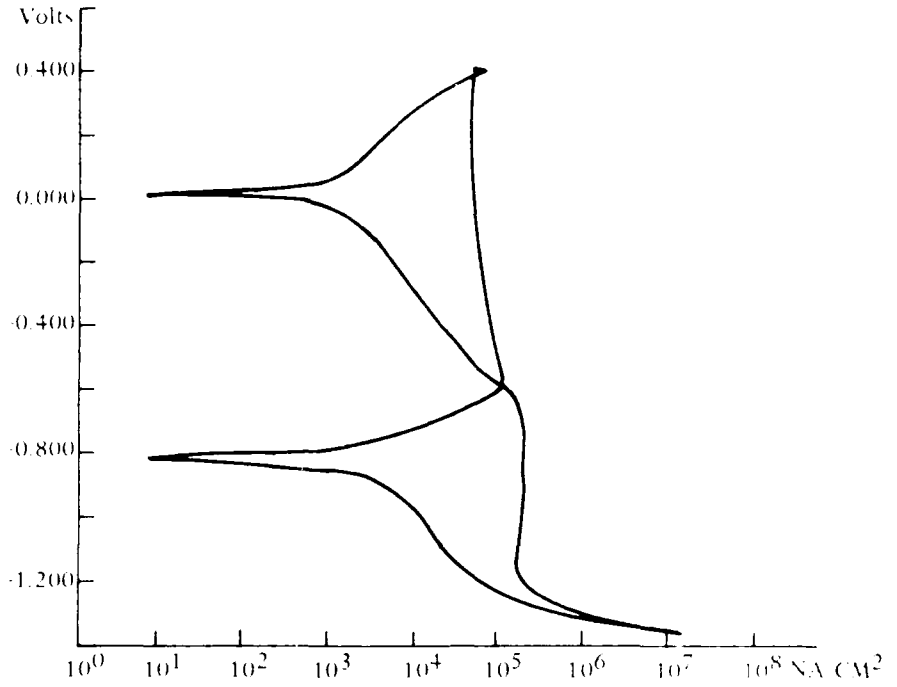

Figure 9. Nitronic 33 stainless steel - pH = 10.0, Cl^- = 6,000 ppm.

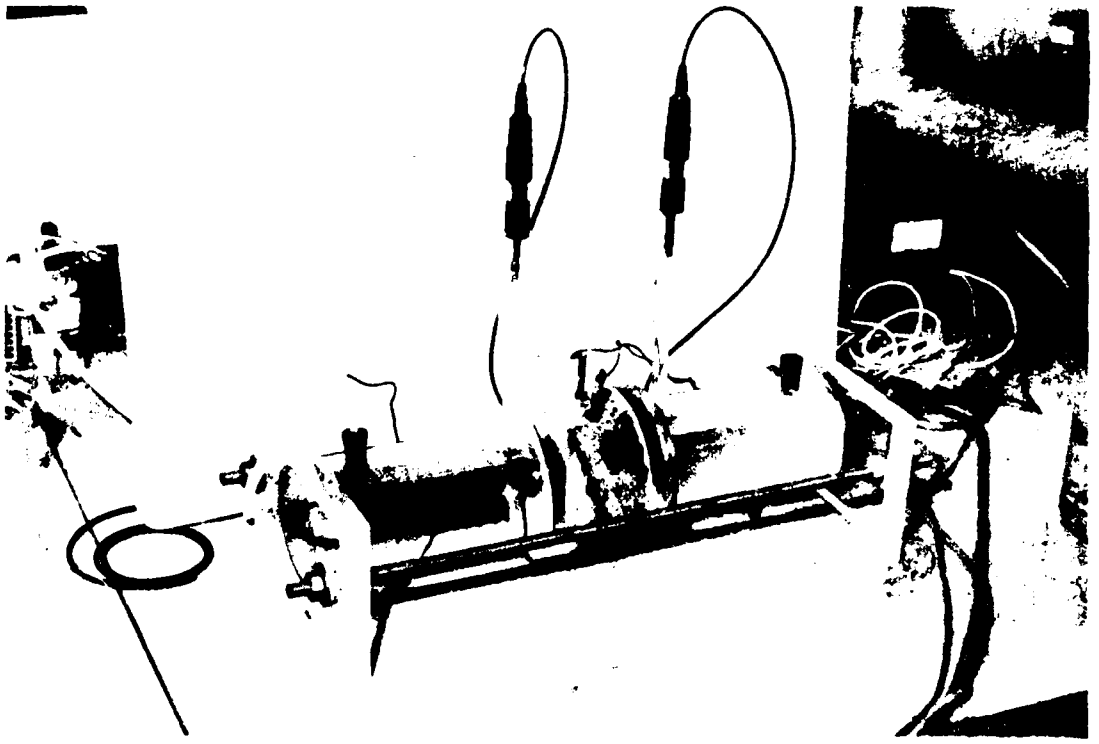

Figure 10. Apparatus for determining resistance to ion migration.

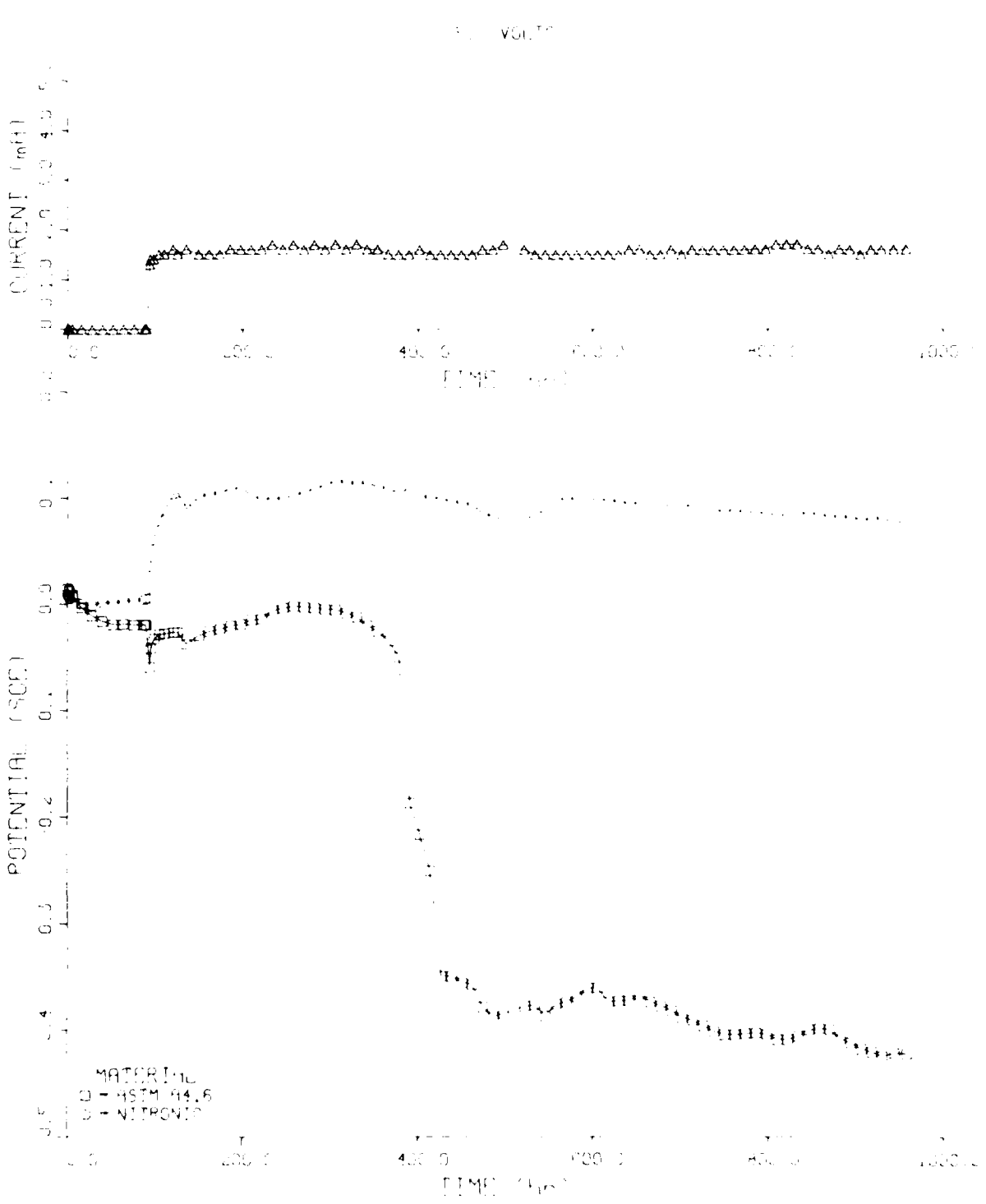

Figure 11. Tolerance of Nitronic 33 stainless steel and carbon steel to ion migration.

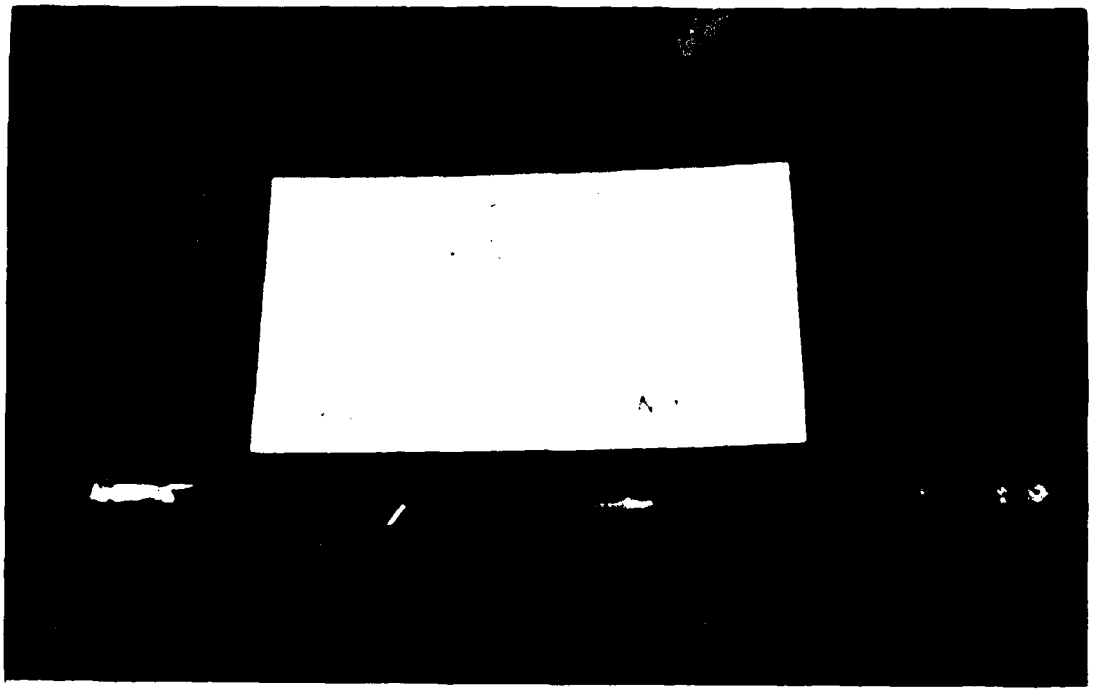

Figure 13. Setup for preparation of the test

Figure 14. Corrosion current and potential versus time for carbon steel.

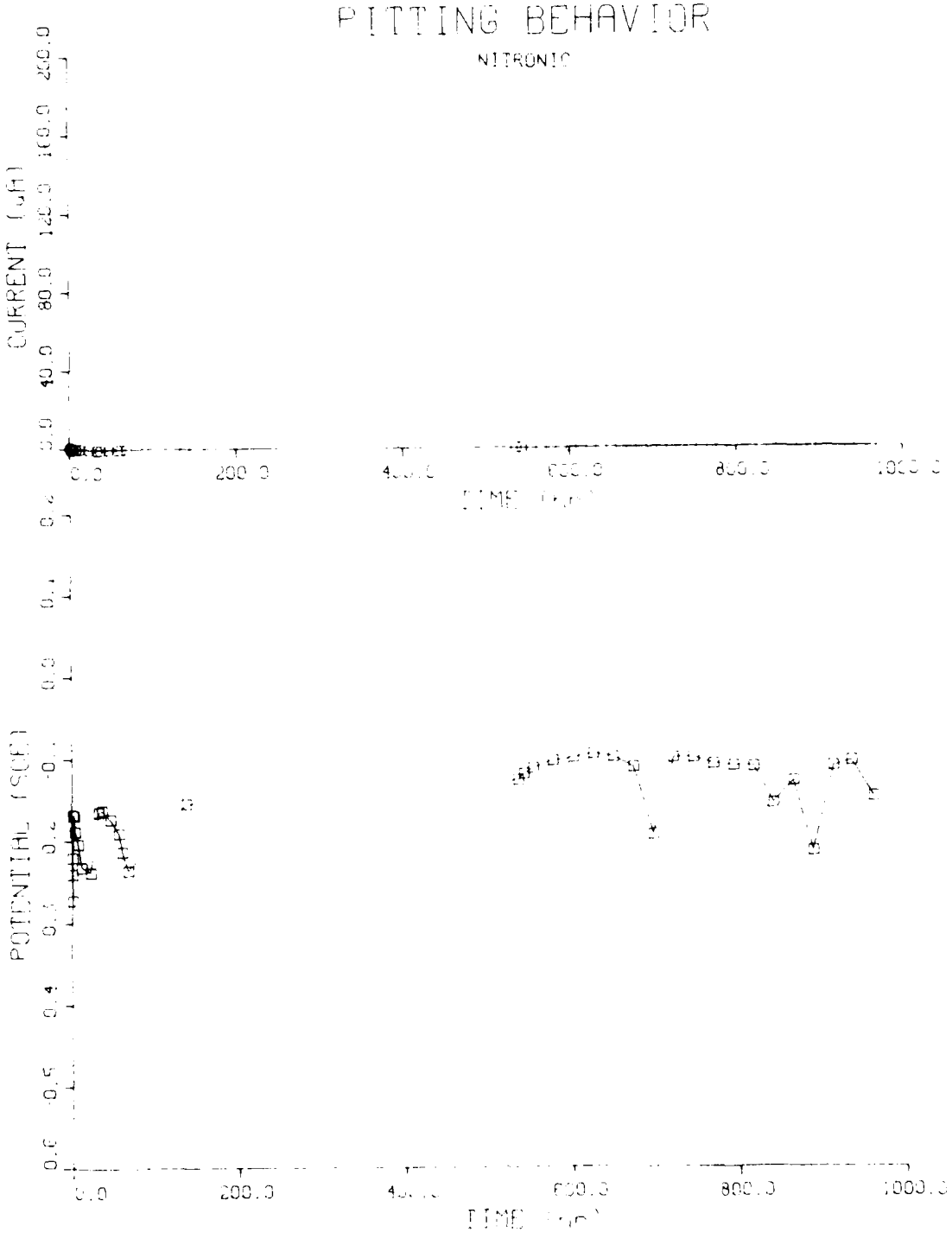

Figure 15. Corrosion current and potential versus time for Nitronic 33 stainless steel.

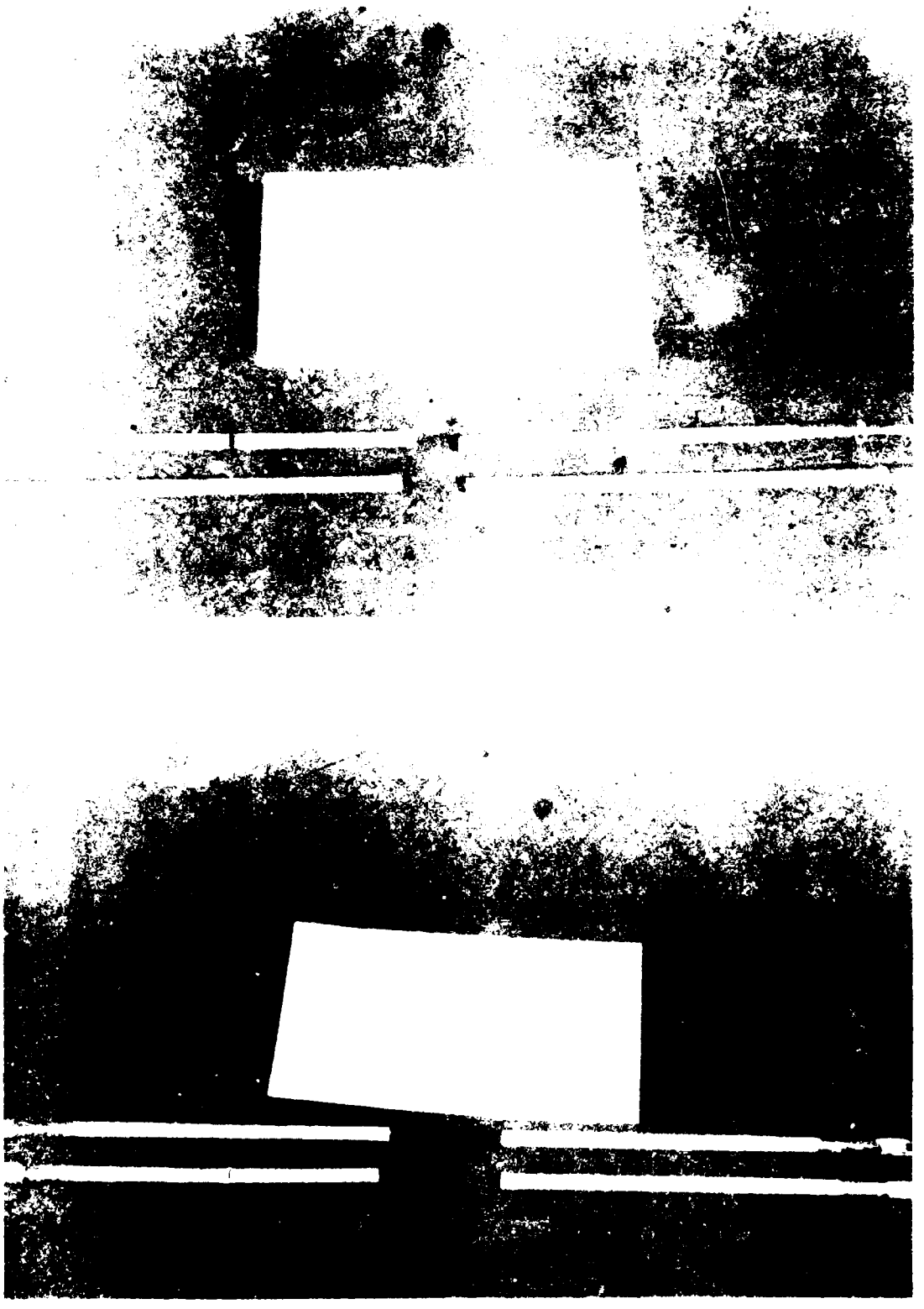

[illegible] condition of carbon steel and Nitronic 33 stainless steel test probes after 1600 hours of exposure in propagation rate tests.

Figure 17. Test setup for depassivation at closed cracks.

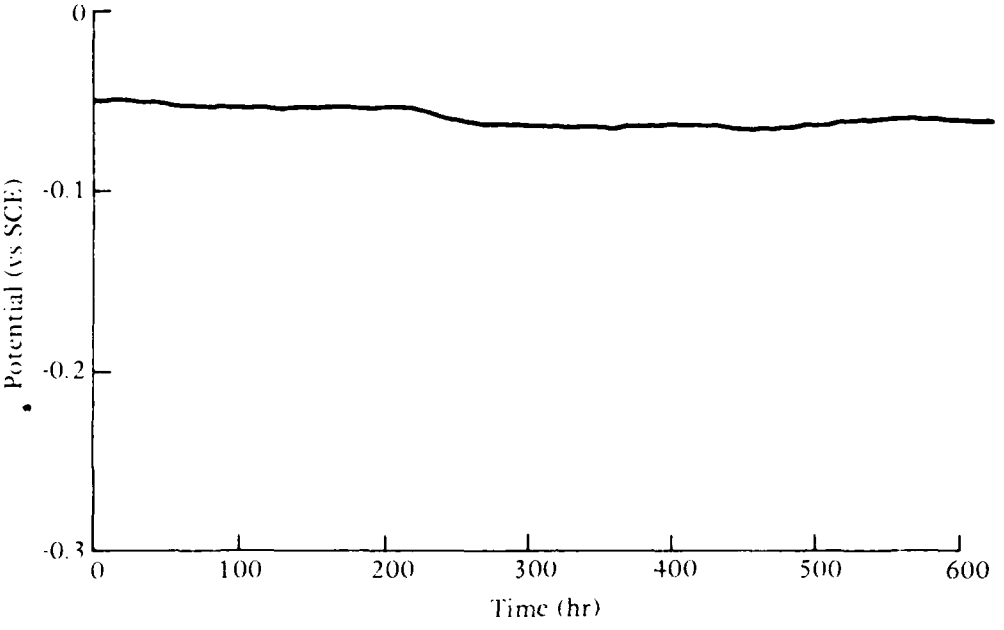

Figure 18. Corrosion potential versus time for carbon steel at a closed crack.

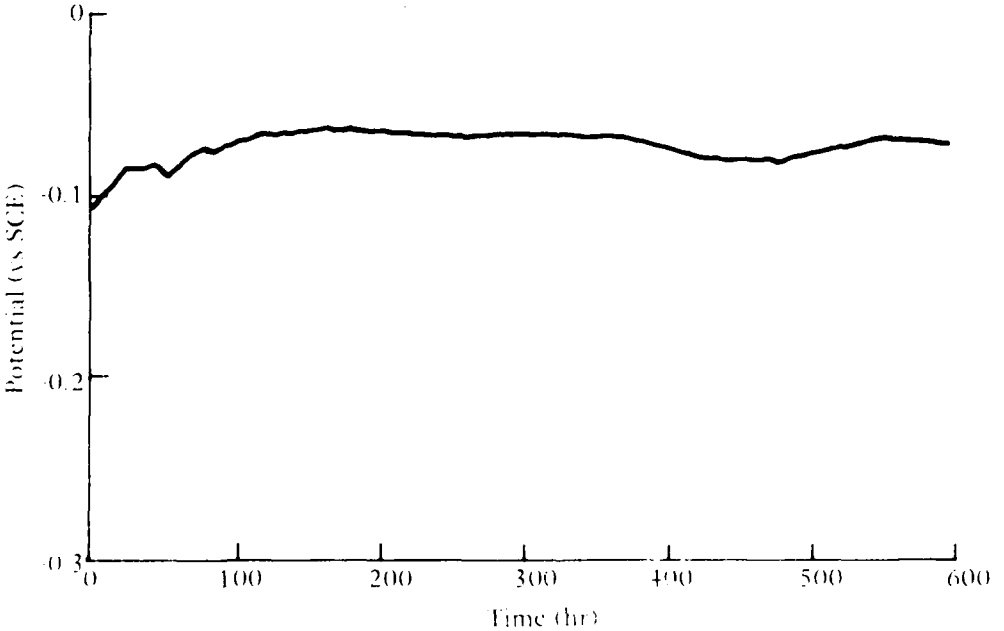

Figure 19. Corrosion potential versus time for Nitron 33 stainless steel at a closed crack.

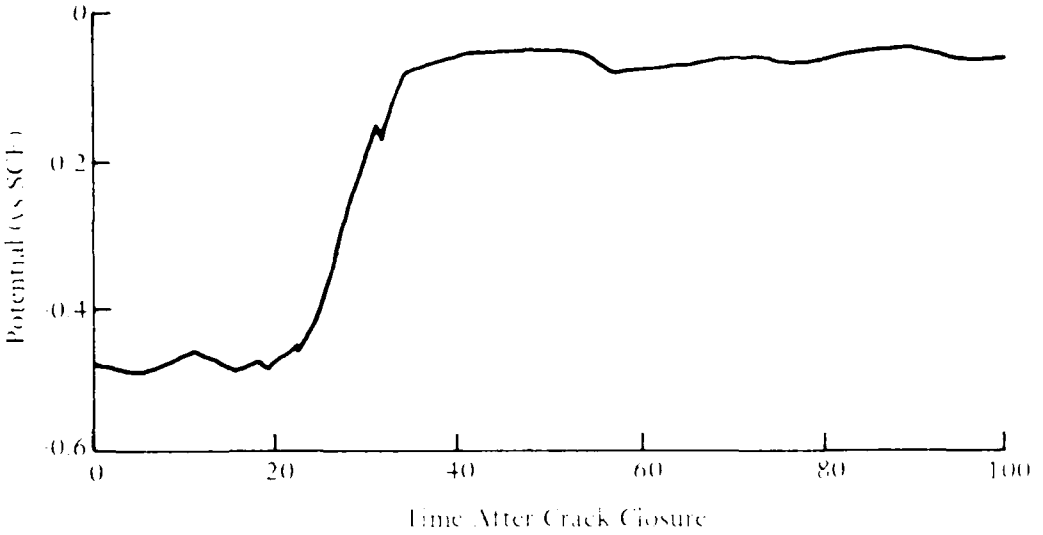

Figure 20. Repassivation of carbon steel after initiation of corrosion

Figure 21. Setup for determination of depassivation at open cracks.

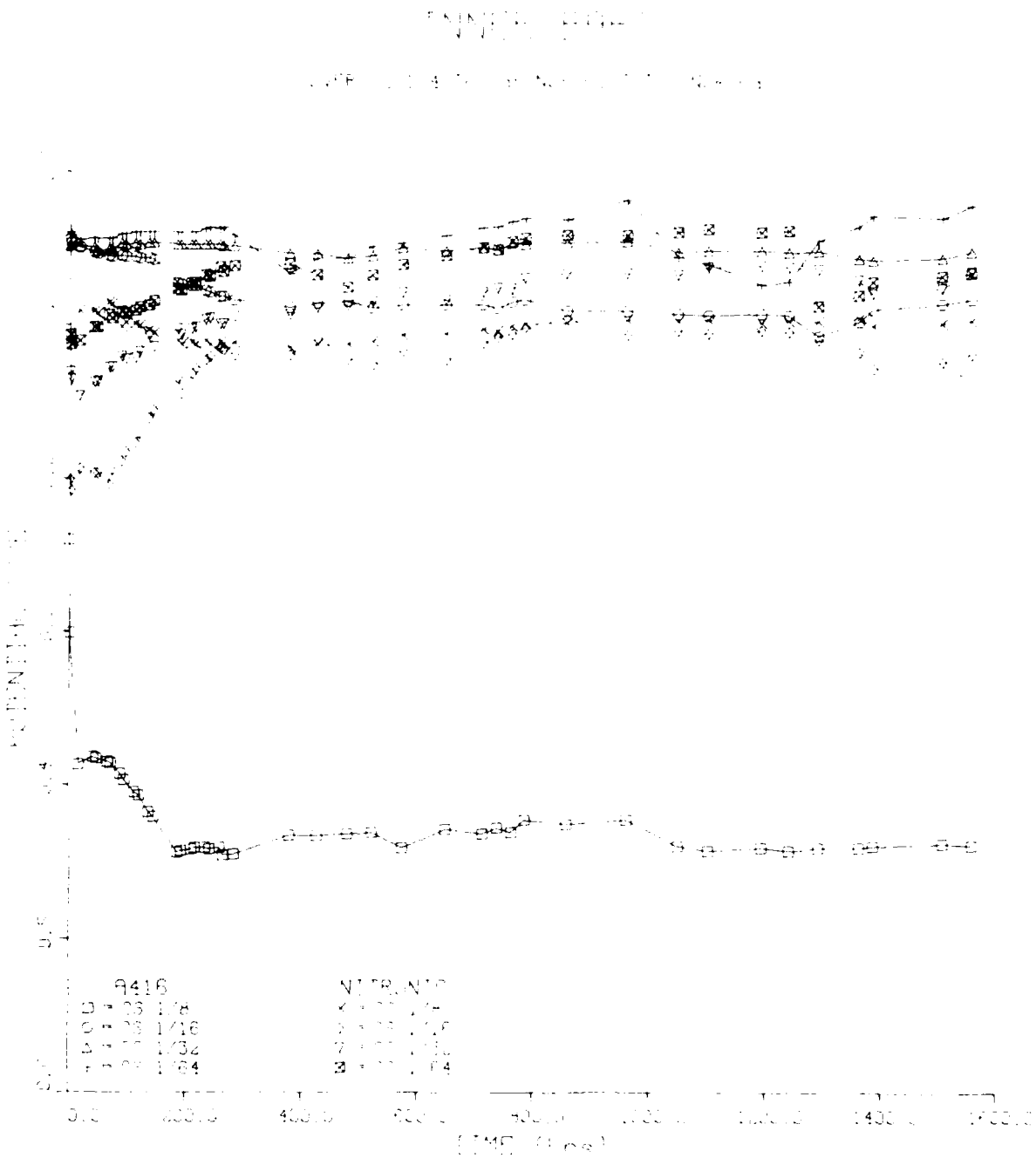

Figure 22. Potential versus time for inner bars at cracks.

Cover 1 in. at Notch, 1-3/4 in. Nominal

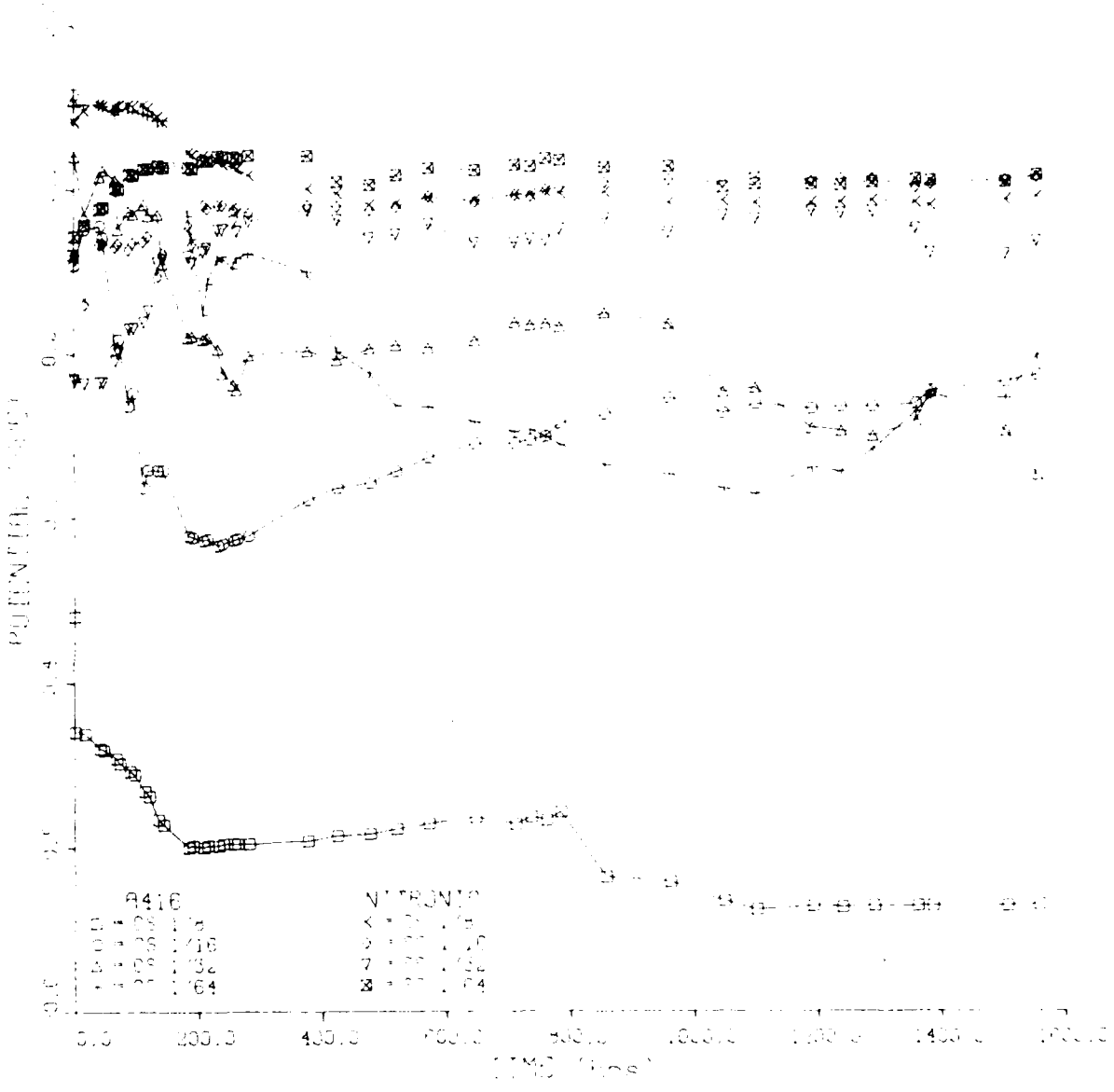

Figure 23. Potential versus time for outer bars at cracks.

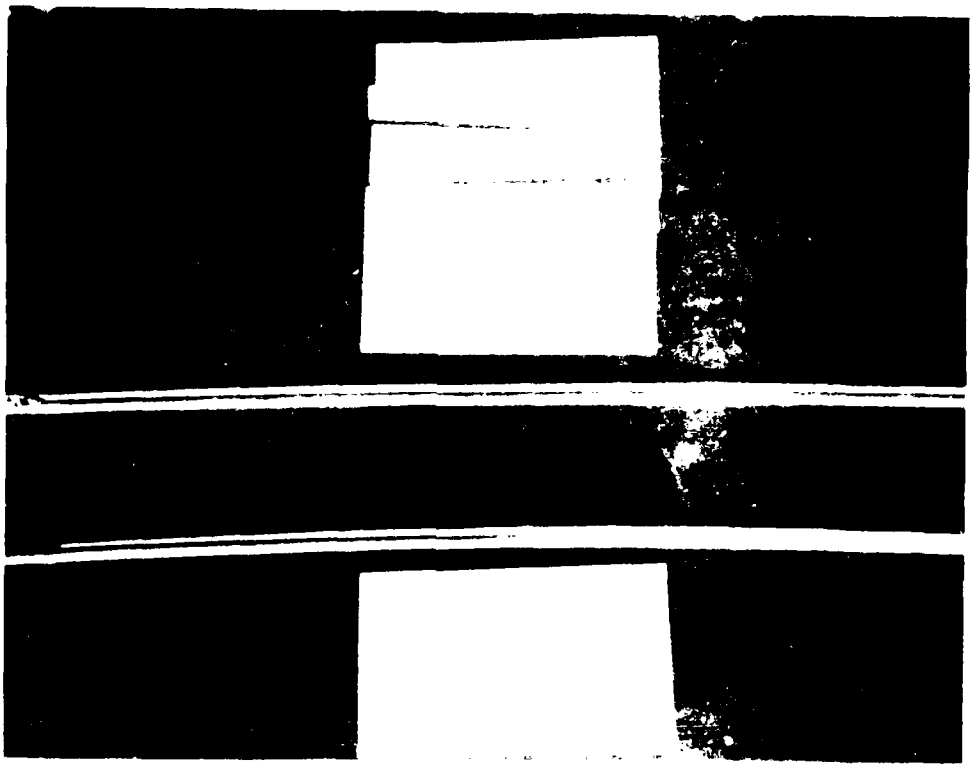

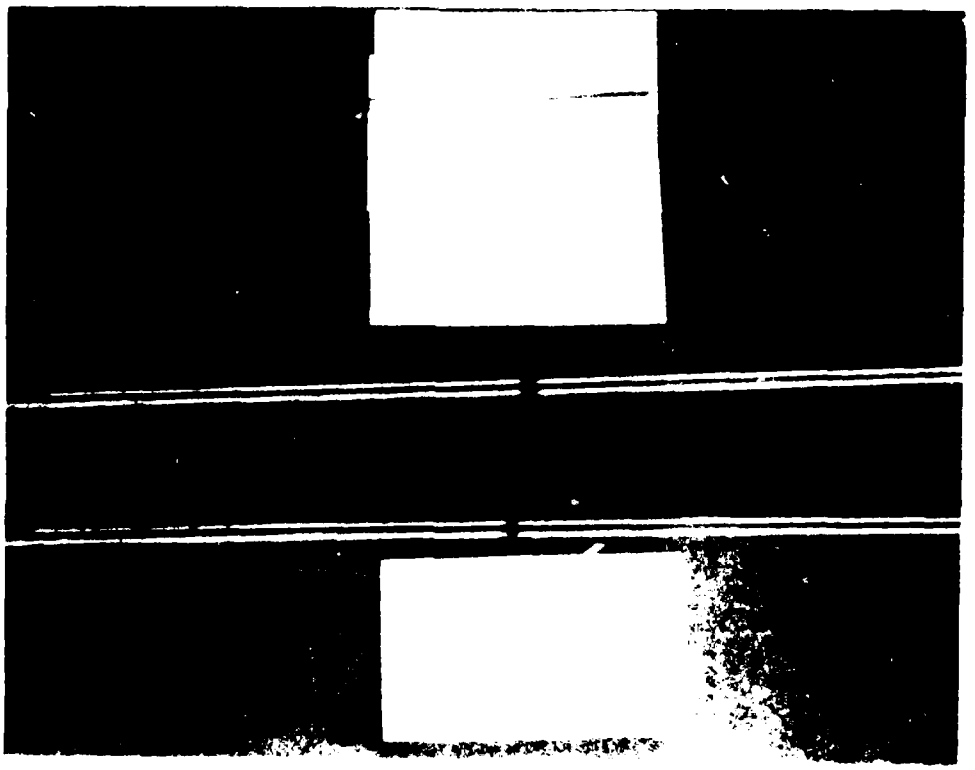

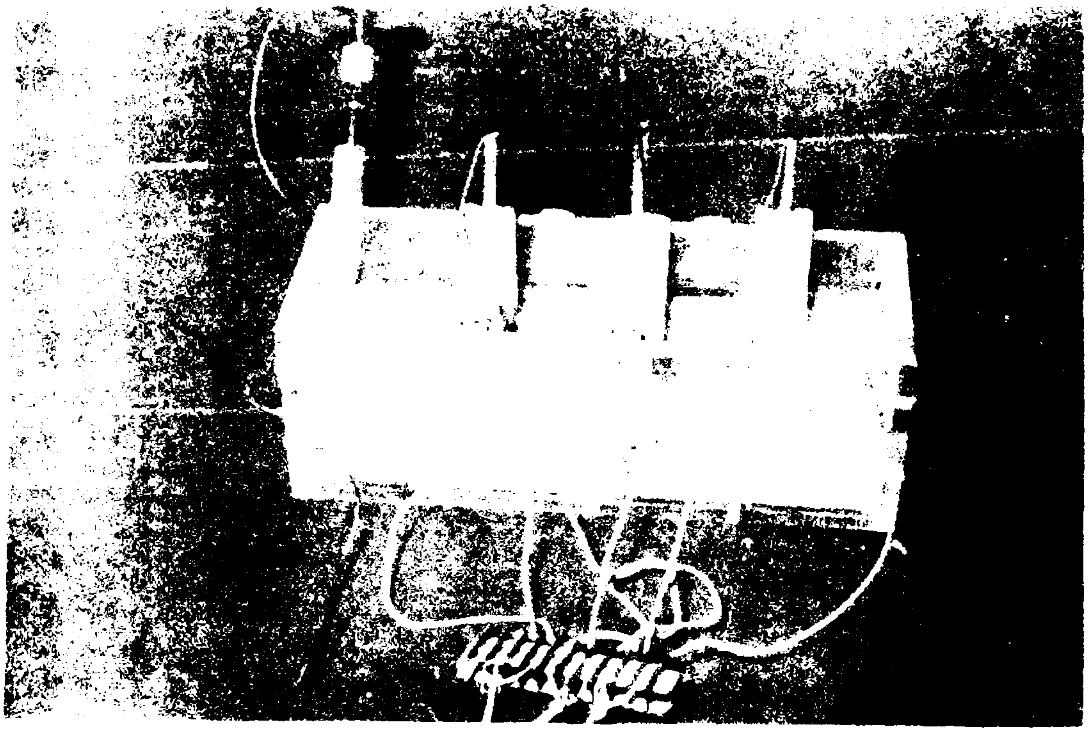

[illegible] the determination of relative corrosion product [illegible] volumes.

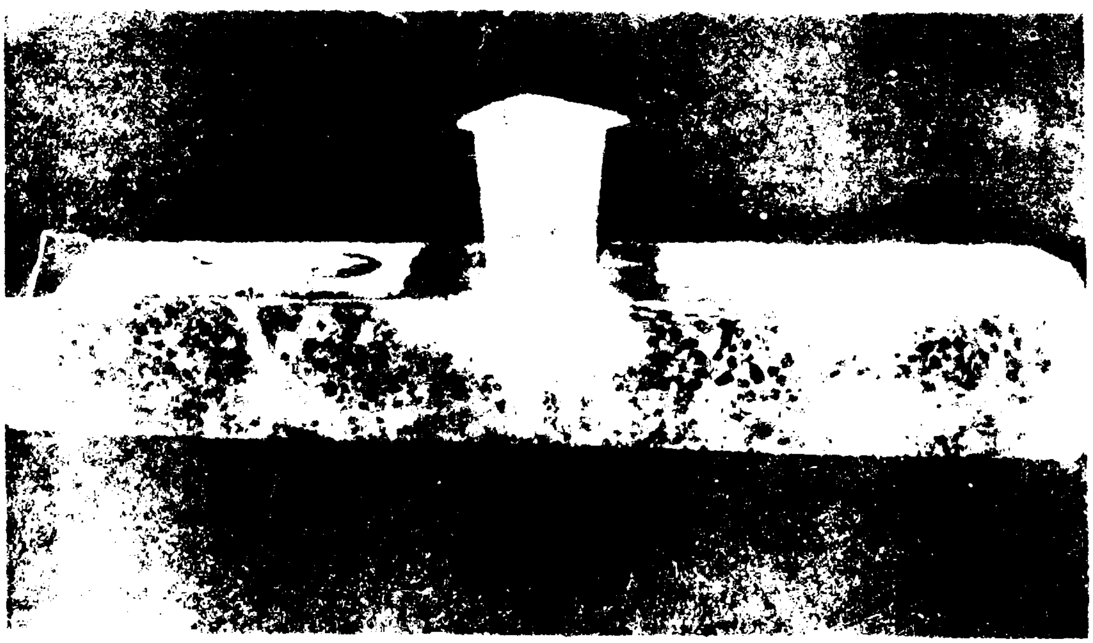

[illegible] determination [illegible] of carbon [illegible] specimens [illegible]

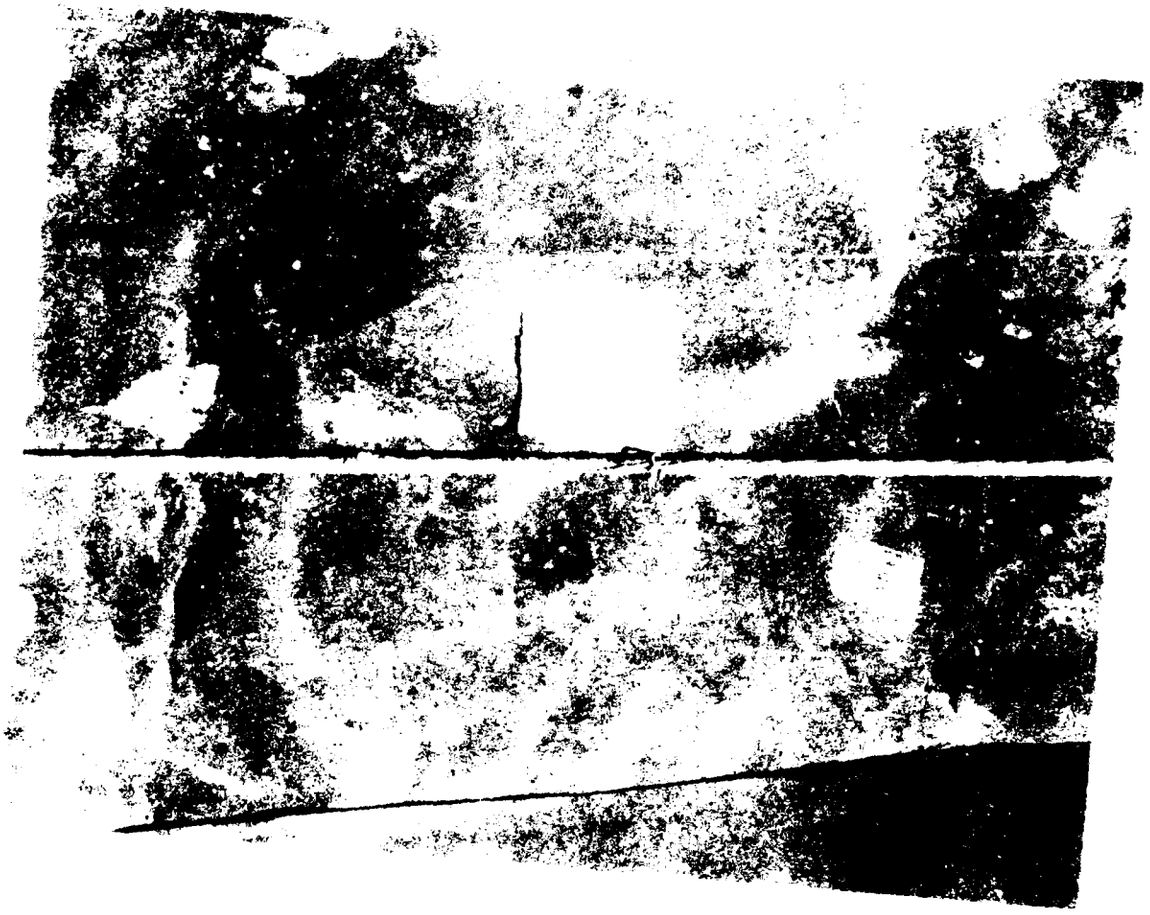

Figure 28. Carbon steel strand from piling specimen.

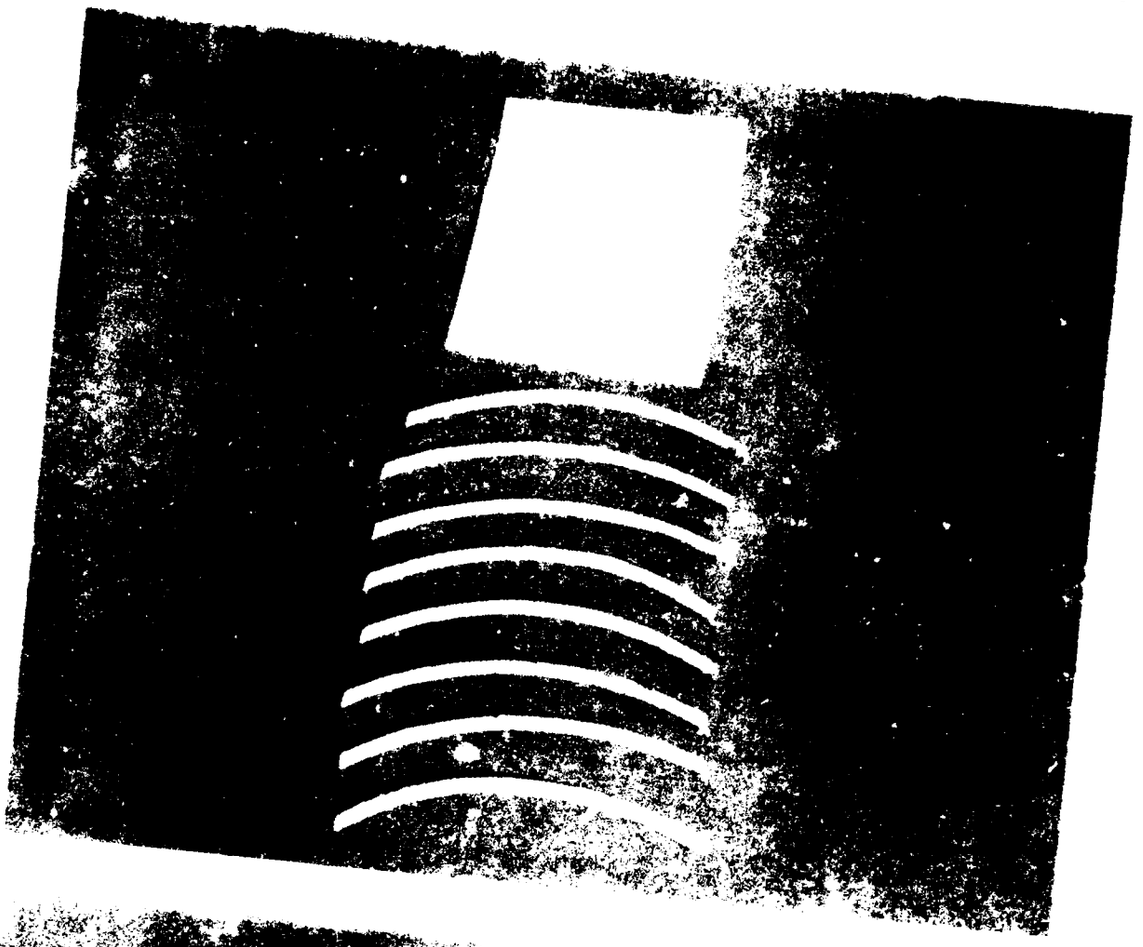

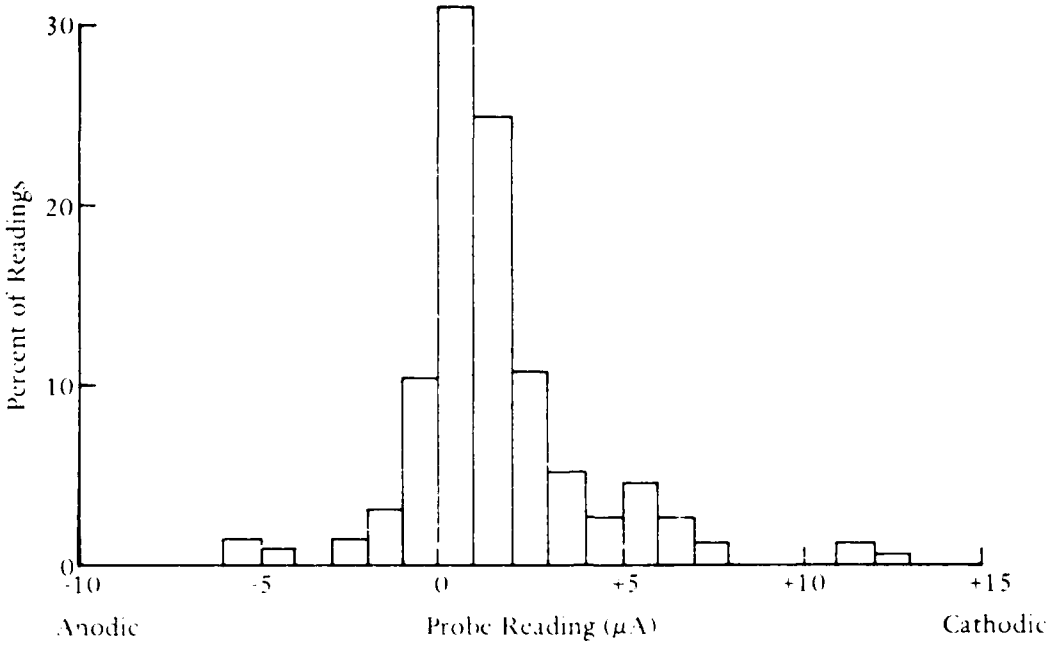

Figure 30. Frequency of readings versus values - carbon steel.

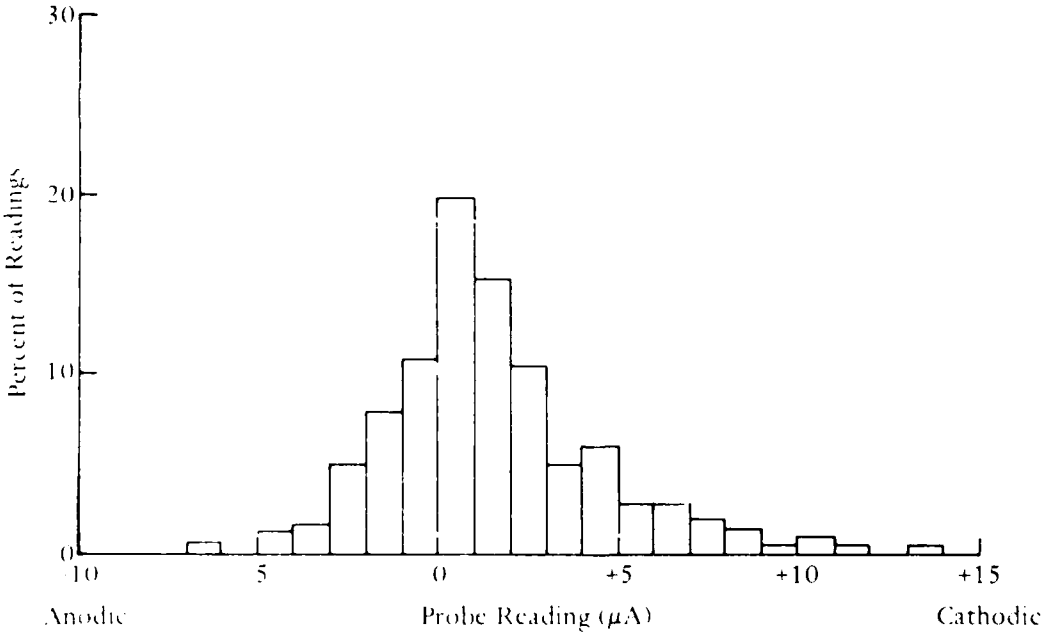

Figure 31. Frequency of readings versus values - Nitronic 33.

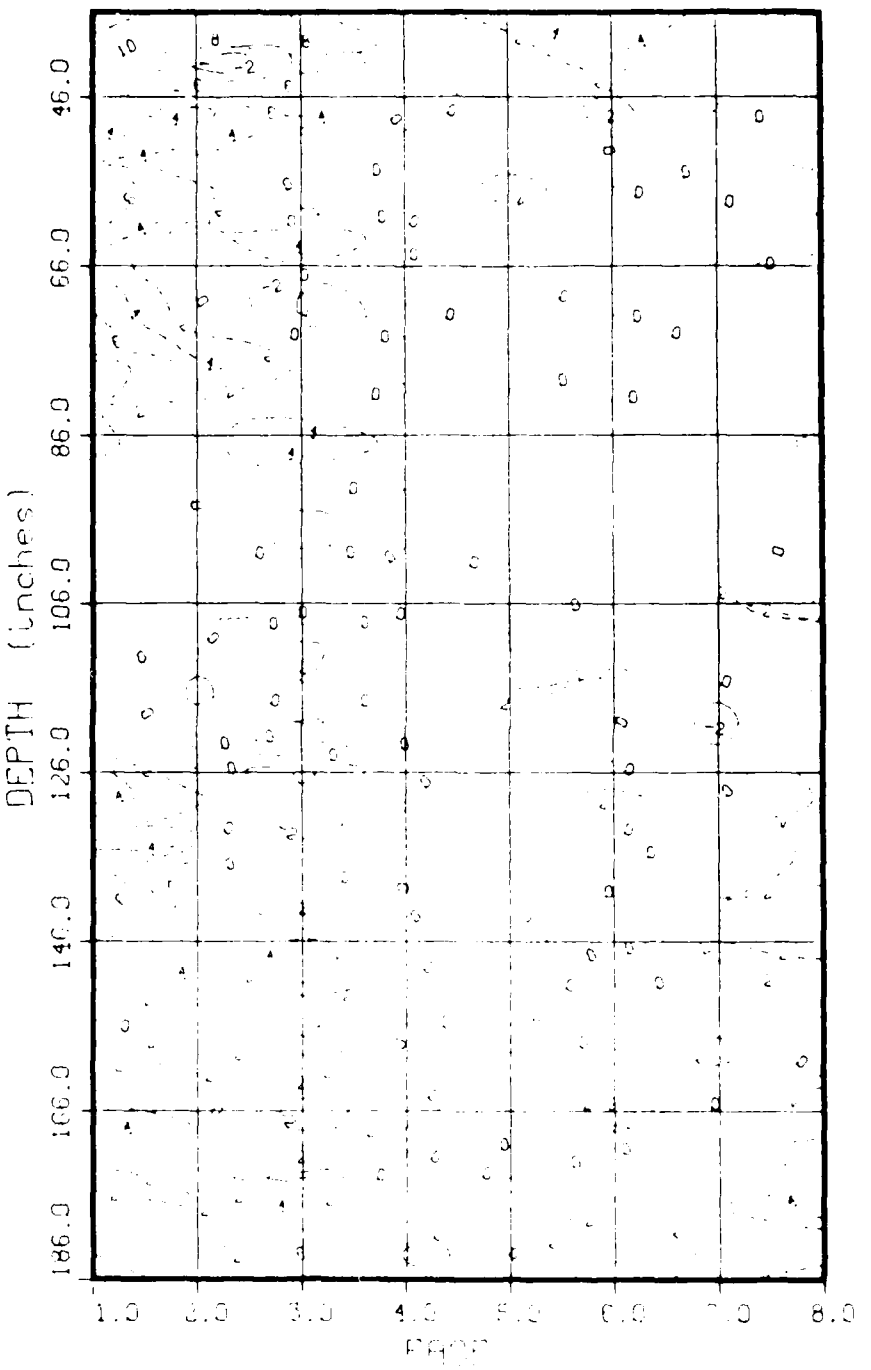

Figure 32. Current profile map - Nitronic 33 piling.

Figure 43. Carbon steel tie wire in Nitronic 33 stainless steel prestressed piling section.

Appendix A

ASSESSMENT OF IMPACT OF CORROSION ON STRUCTURAL INTEGRITY

26 November 1985

MEMORANDUM

FROM: L51/WARREN

TO: L52/JENKINS

VIA: L51
L52
L50

SUBJ: Structural analysis of deperming pier - NAVSTA San Diego

REF: (a) Final 35% Submittal Engineering Calculations Contract N62474-84-C-4194 by ABAM Consulting Engineers

(b) Final 35% Submittal Engineering Drawings Contract N62474-84-C-4194 by ABAM Consulting Engineers

1. This memorandum is to formalize our conversations of 11 and 26 November on the subject requested analysis.

2. The structural analysis was conducted on the deck panels subjected to critical crane loading. The objective was to determine the structural response to the loss of individual prestressing strands and reinforcing bars by corrosion. Critical loading occurs as the 20 kip wheel loads of the 30 ton portable crane are positioned near midspan of the deck (between pile bents). A review of Reference (a) showed that the pier deck was the weakest link in the structure which included the curb beam, pile caps and the piles.

3. The most sensitive mechanism in the deck panels was flexure. Critical loading will cause the prestress strands to fail at panel midspan prior to reinforcement yielding at the supports (pile caps) or before any distress occurs due to shear or reactions. Critical crane loading will produce a panel maximum midspan moment of 140 ft-kips in addition to the dead load (weight of the structure) moment of 115 ft-kips. Using load factors of 1.4 for dead load and 1.7 for live load, then the maximum design ultimate moment at panel midspan is 400 ft-kips.

4. A graph of the midspan flexural capacity versus loss of prestress strand for each deck panel is attached. The development length of the 1/2 inch diameter strand is 20 inches, so the graph reflects the ultimate capacity of the deck panel as strands are sequentially corroded through at discrete points within 20 inches of midspan. The ultimate moment capacity is 4[illegible] ft-kips which is well above the required design strength of 400 ft-kips. Even with the loss of one strand, the capacity is still

sufficient to resist the ultimate design moment and there would be little if any noticeable deflection increase. After the loss of 6 strands (randomly placed), the panel capacity approaches the load response of 255 ft-kips (without load factors applied). Before such losses occurred there would be a noticeable increase in deflection as the 30 ton crane rolled over the deck.

5. I will retain the calculations on file if you need them for your reporting. I shall also continue to review and checking References (a) and (b), although I doubt I will find anything to revise my estimates of the structural response. If you need further assistance please contact me at ext 4765.

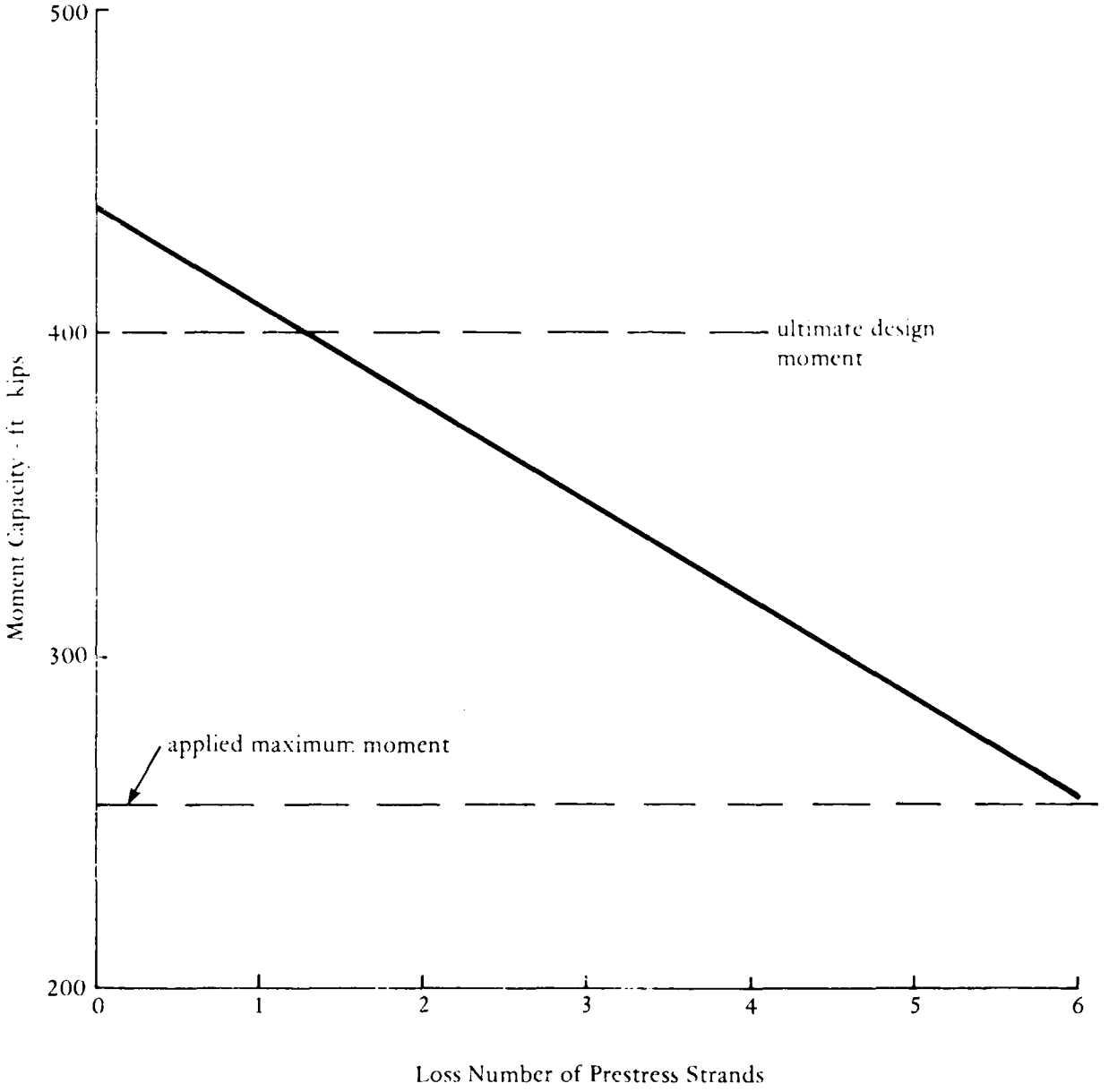

Figure A-1. Effect of prestressing strand corrosion damage on midspan flexural capacity of pier deck.

Appendix B

ASSESSMENT OF INDUCED ELECTRIC CURRENTS

L72/JLB/at
5095201
26 Nov 85

MEMORANDUM

From: L72/Brooks
To: L51/Jenkins
Via: L72
L70

Subj: CORROSION CURRENTS ASSOCIATED WITH NAVY DEPERMING PIERS

Ref: (a) L51 memo of 7 Oct 85 requesting assistance

1. As requested by reference (a), the 35% design reports of the Deperming Pier for San Diego have been reviewed. Preliminary analysis shows that the X-loops of the structure can induce currents of up to one ampere in the pier structure when the separation between loops is 10 ft. All other configurations are not expected to present a problem including the Z-loop. If currents of up to one ampere present a corrosion problem, then the following steps are recommended:

(a) Choose a configuration where the pier structure is outside the X-loops.

(b) Coat the rebar steel with a non-conducting epoxy prior to imbedding in the concrete.

(c) Do not allow the rebar steel to protrude out the bottom of the concrete piling.

(d) Do not connect the rebar steel of the piling with the rebar of the pier top structure.

JAMES L. BROOKS

Copy to:
L72/Miller

DISTRIBUTION LIST

AF 18 CESS DEEEM, Kadena, JA; 6550 ABG DER, Patrick AFB, FL; AFLC DET, Wright-Patterson AFB, OH
AFB HQ MAC DEET, Scott AFB, IL; HQ TAC DEMM (Schmidt), Langley, VA; SAMSO MNND, Norton AFB CA
AFESC DEB, Tyndall AFB, FL; HQ AFESC TST, Tyndall AFB, FL; HQ RDC, Tyndall AFB, FL; HQ TST, Tyndall AFB, FL
AF HQ ESD OCMS
NATL ACADEMY OF ENGRG Alexandria, VA
ARMY AFZF-DE-EPS, Ft Hood, TX; AMCSM-WS, Alexandria, VA
ARMY-ARADCOM STINFO Div, Dover, NJ
ARMY BMDSC-RL (H McClellan), Huntsville, AL; Ch of Engrs, DAEN-CWE-M, Washington, DC; Ch of Engrs, DAEN-MPU, Washington, DC; Comm Cmd, Tech Ref Div, Huachuca, AZ; ERADCOM Tech Supp Dir, (DELSD-L), Ft Monmouth, NJ; FESA-E (J Havell), Ft Belvoir, VA; FESA-EM (Krajewski), Ft Belvoir, VA; Facs Engr Dir, Contr Br, Ft Ord, CA; HQDA (DAEN-ZCM); POJED-O, Okinawa, Japan
ARMY CERL, CERL ZN, Champaign, IL; Library, Champaign IL
ARMY CORPS OF ENGINEERS HNDED-CS, Huntsville, AL; HNDED-SY, Huntsville, AL; Library, Seattle, WA
ARMY CRREL, CRREL-EG (Rsch Ctr), Hanover, NH
ARMY DEPOT Letterkenny, Fac Engr (SDSLE-SF), Chambersburg, PA
ARMY EWES Library, Vicksburg MS; WESCV-Z (Whalin), Vicksburg, MS; WESGP-E (Green), Vicksburg, MS; WESGP-EM (CJ Smith), Vicksburg, MS
ARMY ENGR DIST Library, Portland OR; Phila, Lib, Philadelphia PA
ARMY MAT & MECH RSCH CEN DRXMR-SM (Lenoe), Watertown, MA
ARMY MTMC MTT-CE, Newport News, VA
ARMY TRANSPORTATION SCHOOL, ASTP-CDM, Fort Eustis, VA; ATSP-CDM (Civilla), Fort Eustis, VA
ARMY-BELVOIR R&D CTR STRBE-AALO, Ft Belvoir, VA; STRBE-BLORE, Ft Belvoir, VA; STRBE-CFLO, Ft Belvoir, VA; STRBE-WC, Ft Belvoir, VA
ADMINSUPU PWO, Bahrain
BUREAU OF RECLAMATION D-1512 (GW DePuy), Denver, CO
CBC Code 10, Davisville, RI; Code 155, Port Hueneme, CA; Code 430, Gulfport, MS; Dir, CESO, Port Hueneme, CA; Library, Davisville, RI; PWO (Code 80), Port Hueneme, CA; PWO, Davisville, RI; PWO, Gulfport, MS; Tech Library, Gulfport, MS
CBU 401, OIC, Great Lakes, IL; 405, OIC, San Diego, CA; 411, OIC, Norfolk, VA; 417, OIC, Oak Harbor, WA
CINCUSNAVEUR London, England
CNO Code NOP-964, Washington, DC; Code OP-987J, Washington, DC; OP-098, Washington, DC
COMCBLANT Code S3L, Norfolk, VA
COMCBPAC Diego Garcia Proj Offr, Pearl Harbor, HI
COMDT COGARD Library, Washington, DC
COMFAIRMED SCE, Naples, Italy
COMFLEACT PWO (Engr Dir), Sasebo, Japan; PWO, Sasebo, Japan; SCE, Yokosuka Japan; PWO, Kadena, Okinawa
COMNAVACT PWO, London, England
COMNAVAIRLANT Nuc Wpn Sec Offr, Norfolk, VA
COMNAVLOGPAC Code 4348, Pearl Harbor, HI
COMNAVRESFOR Code 08, New Orleans, LA
COMNAVSUPPFORANTARCTICA DET, PWO, Christchurch, NZ
COMOCEANSYSLANT Fac Mgmt Offr, PWD, Norfolk, VA
COMOCEANSYSPAC SCE, Pearl Harbor, HI
COMTRALANT SCE, Norfolk, VA
NAVOCEANCOMCEN CO, Guam, Mariana Islands; Code 141S, Guam, Mariana Islands
DIRSSP Tech Lib, Washington, DC
DOE Wind Ocean Tech Div, Tobacco, MD
DTIC Alexandria, VA
DTNSRDC Code 172, Bethesda, MD; Code 4111, Bethesda, MD; Code 42, Bethesda MD; DET, Code 284, Annapolis, MD; DET, Code 1720, Annapolis, MD
FAA Code APM-740 (Donaldt), Washington, DC
FCTC LANT, PWO, Virginia Bch, VA
FMFLANT CEC Offr, Norfolk, VA
GIDEP OIC, Corona, CA
GSA Chief Engrg Br, Code PQB, Washington, DC
INTL MARITIME, INC D Walsh, San Pedro, CA
IREHTED Input Proc Dir (R Danforth), Eagan, MN
KWAJALEIN MISRAN BMDSC-RKE-C
LIBRARY OF CONGRESS Sci & Tech Div, Washington, DC

MARCORDIST 32 Code 4 San Francisco CA
MARCORPS FIRST FSSG Engr Supp Offr Camp Pendleton CA
MARINE CORPS BASE ACOS Fac Engr Okinawa Code 4.01 Camp Pendleton CA Code 406 Camp Lejeune NC Dir Maint Control PWD Okinawa Japan M & R Division Camp Lejeune NC Maint Ofc Camp Pendleton CA PWO Camp Lejeune NC PWO Camp Pendleton CA
MARINE CORPS HQTRS Code LFF-2 Washington DC
MCAF Code C144 Quantico VA
MCAS Dir Ops Div Fac Maint Dept Cherry Point NC Dir Util Div Fac Maint Dept Cherry Point NC PWO Kaneohe Bay HI PWO Yuma AZ
MCDEC M & E Div Quantico VA PWO Quantico VA
MCRD SCE San Diego CA
NAF Dir Engrg Div PWD Atsugi Japan PWO Atsugi Japan
NAFF OIC San Diego CA
NAS Chase Fld Code 18300 Beeville TX Code 01 Alameda CA Code 163 Keflavik Iceland Code 182 Bermuda Code 18700 Brunswick ME Code 62344 C Arnold Point Mugu CA Code 70 Marietta GA Code 72E Willow Grove PA Code 83 Patuxent River MD Code 8E Patuxent River MD Code 8EN Patuxent River MD Dir Engrg Div Millington TN Dir Maint Control Div Key West FL Director Engrg Div Engrg Dir PWD Adak AK Engrg Dir PWD Corpus Christi TX Fac Plan Br Mgr (Code 183) NI San Diego CA Fleet CPO PWD Self Help Div Beeville TX Code 1821A Miramar San Diego CA PWD Maint Div New Orleans LA PWD Maintenance Control Dir Bermuda PWO Beeville TX PWO Cecil Field FL PWO Dallas TX PWO Glenview IL PWO Keflavik Iceland PWO Key West FL PWO Kingsville TX PWO Millington TN PWO Miramar San Diego CA PWO Moffett Field CA PWO New Orleans LA PWO Sigonella Sicily PWO South Weymouth MA PWO Willow Grove PA SCE Barbers Point HI SCE Cubi Point R.P. Security Offr (Code 151) Alameda CA Security Offr Kingsville TX
NAVE BUREAU OF STANDARDS B348 BR Gaithersburg MD
NAVE RESEARCH COUNCIL Naval Studies Board Washington DC
NAVAIRENGCEN Code 182 Lakehurst NJ
NAVAIREWORKFAC Code 300 Cherry Point NC Code 640 Pensacola FL Code 64136 San Diego CA Code 65000 Pensacola FL SCE Norfolk VA
NAVAIRPROPTESTCEN CO Trenton NJ
NAVAIRTESTCEN PWO Patuxent River MD
NAVAUDSVCHQ Director Falls Church VA
NAVAVIONICCEN Deputy Dir PWD (Code D70E) Indianapolis IN PW Div Indianapolis IN
NAVCAMS PWO Norfolk VA SCE (Code N-5) Naples Italy SCE (Code W-60) Wahiawa HI SCE Guam Mariana Islands
NAVCHAPGRU Code 60 Williamsburg VA
NAVCOASTSYSCEN Code 2360 Panama City FL Code 423 Panama City FL Code 630 Panama City FL Code 715 C Mittlemann Panama City FL Tech Library Panama City FL
NAVCOMMSTA Code 401 Nea Makri Greece Dir Maint Control PWD Diego Garcia Dir Maint Control PWD Thurso UK PWO Exmouth Australia
NAVCONSTRACEN Code B-2 Port Hueneme CA
NAVEDTRAPRODEVCEN Tech Dev Pensacola FL
NAVELEXCEN DEL OIC Winter Harbor ME
NAVEODTECHCEN Tech Library Indian Head MD
NAVFAC PWO Centerville Bch Ferndale CA
NAVFACENGCOM CO (Code 00) Alexandria VA Code 03 Alexandria VA Code 03T (Essoglou) Alexandria VA Code 04B3 Alexandria VA Code 04M Alexandria VA Code 04MEA Alexandria VA Code 05A Alexandria VA Code 09M123 (Lib) Alexandria VA Code 100 Alexandria VA Code 1002B Alexandria VA Code FPO-3A2 (Bloom) Alexandria VA Code FPO-3C Alexandria VA
NAVFACENGCOM CHES DIV Code 101 Washington DC Code 403 Washington DC Code 405 Washington DC Code 406 Washington DC Code 407 (Dr Schexnider) Washington DC Code FPO-1C Washington DC Code FPO-1PF Washington DC
NAVFACENGCOM LANT DIV Br Off Dir Naples Italy
NATL BUREAU OF STANDARDS Bldg Mat Div (Rossiter) Gaithersburg MD
NAVFACENGCOM LANT DIV Code 403 Norfolk VA Library Norfolk VA
NAVFACENGCOM NORTH DIV CO Philadelphia PA Code 04 Philadelphia PA Code 04AL Philadelphia PA Code 11 Philadelphia PA Code 111 Philadelphia PA Code 202.2 Philadelphia PA Code 405 AE Philadelphia PA
NAVFACENGCOM PAC DIV Code 101 (Keto) Pearl Harbor HI Code 09P Pearl Harbor HI Code 2011 Pearl Harbor HI Code 402 RDT&E Fac0 Pearl Harbor HI Library Pearl Harbor HI
NAVFACENGCOM SOUTH DIV Code 2111 Charleston SC Code 505 Charleston SC Code 806 Charleston SC Geotech Section (Code 402) Charleston SC Library Charleston SC
NAVFACENGCOM WEST DIV 09P20 San Bruno CA Code 03B San Bruno CA Code 402 San Bruno CA Dir PWD (Code 04N) San Bruno CA Library (Code 04A2) San Bruno CA RDT&E Fac0 San Bruno CA

NAVFACENGCOM CONTRACTS AROICC, Quantico, VA; Code 460, Portsmouth, VA; DOICC, Diego Garcia; DROICC, Lemoore, CA; DROICC, Santa Ana, CA; OICC, Guam; OICC, Rota Spain; OICC, Virginia Beach, VA; OICC ROICC, Norfolk, VA; ROICC (Code 495), Portsmouth, VA; ROICC, Code 61, Silverdale, WA; ROICC, Corpus Christi, TX; ROICC, Crane, IN; ROICC, Jacksonville, FL; ROICC, Keflavik, Iceland; ROICC, Key West, FL; ROICC, Point Mugu, CA; ROICC, Rota, Spain; ROICC, Twentynine Plams, CA; ROICC AROICC, Brooklyn, NY; ROICC AROICC, Colts Neck, NJ; ROICC OICC, SPA, Norfolk, VA; SW Pac, OICC, Manila, RP

NAVFLTACT DET OIC, Yokohama, Japan

NAVHOSP CL, Newport, RI; CO, Millington, TN; Dir, Engrg Div, Camp Lejeune, NC; PWO, Guam, Mariana Islands; PWO, Okinawa, Japan; SCE (Knapowski), Great Lakes, IL; SCE, Camp Pendleton CA; SCE, Pensacola FL; SCE, Yokosuka, Japan

NAVMAG Engr Dir, PWD, Guam, Mariana Islands; SCE, Guam, Mariana Islands; SCE, Subic Bay, RP

NAVMEDCOM MIDLANT REG, PWO, Norfolk, VA; NWREG, Head, Fac Mgmt Dept, Oakland, CA; SE REG, Hd, Fac Mgmt Dept, Jacksonville, FL; SWREG, Head, Fac Mgmt Dept, San Diego, CA; SWREG, OICC, San Diego, CA

NAVMEDRSCHINSTITUTE, Code 47, Bethesda, MD

NATL BUREAU OF STANDARDS Bldg Mat Div (Mathey), Gaithersburg, MD

NAVOCEANO Code 6200 (M Paige), Bay St Louis, MS; Library, Bay St Louis, MS

NAVOCEANSYSCEN Code 94 (Talkington), San Diego, CA; Code 964 (Tech Library), San Diego, CA; Code 9642B (Bayside Library), San Diego, CA

NAVORDMISTESTSTA Dir, Engrg, PWD, White Sands, NM

NAVORDSTA PWO, Louisville, KY

NAVPETOFF Code 30, Alexandria, VA

NAVPGSCOL Code 68 (C S Wu), Monterey, CA

NAVPHIBASE Harbor Clearance Unit Two, Norfolk, VA; PWO, Norfolk, VA; SCE, San Diego, CA

NAVRADREDFAC Kamiseya, Japan

NAVRESREDCOM Commander (Code 072), San Francisco, CA

NAVSCOLCECOFF Code C44A, Port Hueneme, CA

1 PWO, Athens, GA

NAVSEACENPAC Code 32, Sec Mgr, San Diego, CA

NAVSEASYSCOM Code 05M, Washington, DC; Code 06H4, Washington, DC; Code CEL-TD23, Washington, DC; Code SEA 05M, Washington, DC

NAVSECGRUACT CO, Galeta Island, Panama Canal; PWO (Code 40), Edzell, Scotland; PWO, Adak, AK; PWO, Sabana Seca, PR

NAVSECGRUCOM Code G43, Washington, DC

NAVSECSTA Dir, Engrg, PWD, Washington, DC

NAVSHIPREPFAC Library, Guam; SCE, Subic Bay, RP; SCE, Yokosuka Japan

NAVSHIPYD CO, Philadelphia, PA; Carr Inlet Acoustic Range, Bremerton, WA; Code 134, Pearl Harbor, HI; Code 202.4, Long Beach, CA; Code 202.5 (Library), Bremerton, WA; Norfolk, Code 380, Portsmouth, VA; Code 382.3, Pearl Harbor, HI; Mare Island, Code 410, Vallejo, CA; Code 440, Bremerton, WA; Code 440, Portsmouth, NH; Norfolk, Code 440, Portsmouth, VA; Code 440.4, Bremerton, WA; Mare Island, Code 457, Vallejo, CA; Code 903, Long Beach, CA; Code 420, Long Beach, CA; Norfolk, Code 420, Portsmouth, VA; Library, Portsmouth, NH; Norfolk, Code 450.D, Portsmouth, VA; Norfolk, Code 457L, Portsmouth, VA; PWO, Bremerton, WA; Mare Island, PWO, Vallejo, CA; SCE, Pearl Harbor, HI

NAVSTA A Sugihara, Pearl Harbor, HI; CO, Brooklyn, NY; CO, Long Beach, CA; CO, Roosevelt Roads, PR

NAF AROIC, Midway Island

NAVSTA Dir, Engr Div, PWD (Code 18200), Mayport, FL; Dir, Engr Div, PWD, Guantanamo Bay, Cuba; Engrg Dir, Rota, Spain; WC 93, Guantanamo Bay, Cuba; PWO, Guantanamo Bay, Cuba; PWO, Mayport, FL; SCE, Guam, Marianas Islands; SCE, San Diego CA; SCE, Subic Bay, RP; Util Engrg Offr, Rota, Spain

NAVSUPPACT PWO, Holy Loch, UK; PWO, Naples, Italy

NAVSUPPFAC Dir, Maint Control Div, PWD, Thurmont, MD

NAVSUPPO Security Offr, La Maddalena, Italy

NAVSWC Code E211 (C Rousey), Dahlgren, VA; DET, PWO, White Oak, Silver Spring, MD; PWO, Dahlgren, VA

NAVTECHTRACEN SCE, Pensacola FL

NAVTRASTA SCE, San Diego, CA

NAVWARCOL Fac Coord (Code 24), Newport, RI

NAVWPNCEN Code 2630B, China Lake, CA; Code 2636, China Lake, CA; DROICC (Code 702), China Lake, CA; PWO (Code 266), China Lake, CA

NAVWPNSFAC Wpns Offr, St Mawgan, England

NAVWPNSTA Code 092, Colts Neck, NJ; Code 092, Concord CA; Dir, Maint Control, PWD, Concord, CA; Dir, Maint Control, Yorktown, VA; Engrg Div, PWD, Yorktown, VA; K T Clebak, Colts Neck, NJ; PWO, Charleston, SC; PWO, Code 09B, Colts Neck, NJ; PWO, Seal Beach, CA

NAVWPNSTA PWO, Yorktown, VA

NAVWPNSTA Supt Gen Engr, PWD, Seal Beach, CA

NAVWPNSUPPCEN Code 09, Crane, IN

NETC Code 42, Newport, RI; PWO, Newport, RI

NCR 20: CO, Gulfport, MS; 20, Code R70, Gulfport, MS
NMCB 3: Operations Offr, 40, CO, 5, Operations Dept; 74, CO
NOAA Library, Rockville, MD
NORDA Code 352, Bay St Louis, MS; Ocean Rsch Off (Code 440), Bay St Louis, MS
NRL Code 2511 (Civil Engrg), Washington, DC; Code 5800, Washington, DC; Code 6123 (Dr Brady), Washington, DC
NSC Cheatham Annex, PWO, Williamsburg, VA; Code 54.1, Norfolk, VA; Code 700, Norfolk, VA; Fac & Equip Div (Code 43) Oakland, CA; SCE, Charleston, SC; SCE, Norfolk, VA
NSD SCE, Subic Bay, RP
NUSC DET Code 3322 (Brown), New London, CT; Code 3232 (Varley) New London, CT; Code 44 (RS Mann), New London, CT, Code TA131 (G. De la Cruz), New London, CT
OCNR Code 1234, Arlington, VA
OFFICE SECRETARY OF DEFENSE OASD, Energy Dir, Washington, DC
ONR DET, Dir, Boston, MA
PACMISRANFAC PWO, Kauai, HI
PHIBCB 1, CO, San Diego, CA; 1, P&E, San Diego, CA; 2, Co, Norfolk, VA
PMTC Code 5054, Point Mugu, CA
PWC ACE Office, Norfolk, VA; Code 10, Great Lakes, IL; Code 10, Oakland, CA; Code 100, Guam, Mariana Islands; Code 101 (Library), Oakland, CA; Code 110, Oakland, CA; Code 123-C, San Diego, CA; Code 30, Norfolk, VA; Code 400, Oakland, CA; Code 400, Pearl Harbor, HI; Code 400, San Diego, CA; Code 420, Great Lakes, IL; Code 420, Oakland, CA; Code 422, San Diego, CA; Code 423, San Diego, CA; Code 424, Norfolk, VA; Code 425 (L.N. Kaya, P.E.), Pearl Harbor, HI; Code 438 (Aresto), San Diego, CA; Code 500, Norfolk, VA; Code 500, Oakland, CA; Code 505A, Oakland, CA; Code 590, San Diego, CA; Code 610, San Diego Ca; Code 500, Great Lakes, IL; Code 400, Great Lakes, IL; Code 700, Great Lakes, IL; Code 600, Great Lakes, IL; Fac Plan Dept (Code 1011), Pearl Harbor, HI; Library (Code 134), Pearl Harbor, HI; Library, Guam, Mariana Islands; Library, Norfolk, VA; Library, Pensacola, FL; Library, Yokosuka JA; Tech Library, Subic Bay, RP; Util Offr, Guam, Mariana Island
SPCC PWO (Code 08X), Mechanicsburg, PA
SUBASE Bangor, PWO (Code 8323), Bremerton, WA; SCE, Pearl Harbor, HI
SUPSHIP Tech Library, Newport News, VA
HAYNES & ASSOC H. Haynes, P.E., Oakland, CA
UCI ONE CO, Norfolk, VA
UCI TWO CO, Port Hueneme, CA
U.S. MERCHANT MARINE ACADEMY Reprint Custodian, Kings Point, NY
US DEPT OF INTERIOR Nat'l Park Svc, RMR/PC, Denver, CO
US GEOLOGICAL SURVEY Marine Geology Offc (Piteleki), Reston, VA
USAF SCHOOL OF AEROSPACE MEDICINE Hyperbaric Med Div, Brooks AFB, TX
USCINC PAC, Code J44, Camp HM Smith, HI
USDA Forest Serv, Reg 8, Atlanta, GA
USNA Mech Engrg Dept (Hasson), Annapolis, MD; Mgr, Engrg, Civil Specs Br, Annapolis, MD; PWO, Annapolis, MD
USS USS FULTON, Code W-3, New York, NY
WATER & POWER RESOURCES SERVICE Smoak, Denver, CO
ADVANCED TECHNOLOGY Ops Cen Mgr (Moss), Camarillo, CA
CALIF DEPT OF NAVIGATION & OCEAN DEV G Armstrong, Sacramento, CA
CALIF MARITIME ACADEMY Library, Vallejo, CA
CITY OF BERKELEY PW, Engr Div (Harrison), Berkeley, CA
CITY OF LIVERMORE Dawkins, PE, Livermore, CA
CLARKSON COLL OF TECH CE Dept (Batson), Potsdam, NY
COLORADO SCHOOL OF MINES Dept of Engrg (Chung), Golden, CO
CORNELL UNIVERSITY Library, Ithaca, NY
DAMES & MOORE LIBRARY Los Angeles, CA
DUKE UNIV MEDICAL CENTER CE Dept (Muga), Durham, NC
FLORIDA ATLANTIC UNIVERSITY Ocean Engrg Dept (Hartt), Boca Raton, FL; Ocean Engrg Dept (McAllister), Boca Raton, FL
FLORIDA INSTITUTE OF TECHNOLOGY CE Dept (Kalajian), Melbourne, FL
INSTITUTE OF MARINE SCIENCES Dir, Morehead City, NC; Library, Port Aransas, TX
WOODS HOLE OCEANOGRAPHIC INST Proj Engr, Woods Hole, MA
LEHIGH UNIVERSITY CE Dept, Hydraulics Lab, Bethlehem, PA; Linderman Libr, Ser Cataloguer, Bethlehem, PA; Marine Geotech Lab (A. Richards), Bethlehem, PA
LOS ANGELES COUNTY Rd Dept (J Vicelja), Los Angeles, CA
MAINE MARITIME ACADEMY Lib, Castine, ME
MICHIGAN TECHNOLOGICAL UNIVERSITY CE Dept (Haas), Houghton, MI
MIT Engrg Lib, Cambridge, MA; Lib, Tech Reports, Cambridge, MA
NATURAL ENERGY LAB Library, Honolulu, HI
NEW MEXICO SOLAR ENERGY INST, Dr. Zwibel, Las Cruces, NM
NEW YORK NEW JERSEY PORT AUTH R&D Engr (Yontar), Jersey City, NJ

NY CITY COMMUNITY COLLEGE Library, Brooklyn, NY
OREGON STATE UNIVERSITY CE Dept (Grace), Corvallis, OR; CE Dept (Hicks), Corvallis, OR; Oceanography Scol, Corvallis, OR
PENNSYLVANIA STATE UNIVERSITY Rsch Lab (Snyder), State College, PA
PORT SAN DIEGO Proj Engr, Port Fac, San Diego, CA
PURDUE UNIVERSITY CE Scol (Altschaeffl), Lafayette, IN; CE Scol (Leonards), Lafayette, IN; Engrg Lib, Lafayette, IN
SAN DIEGO STATE UNIV, CE Dept (Noorany), San Diego, CA
SEATTLE UNIVERSITY CE Dept (Schwaegler), Seattle, WA
SOUTHWEST RSCH INST J Hokanson, San Antonio, TX; R DeHart, San Antonio TX
STATE UNIV OF NEW YORK CE Dept (Reinhorn), Buffalo, NY; CE Dept, Buffalo, NY
TEXAS A&M UNIVERSITY CE Dept (Ledbetter), College Station, TX; CE Dept (Niedzwecki), College Station, TX; Ocean Engr Proj, College Station, TX
UNIVERSITY OF ALASKA Marine Sci Inst, Lib, Fairbanks, AK
UNIVERSITY OF CALIFORNIA CE Dept (Gerwick), Berkeley, CA; CE Dept (Taylor), Davis, CA; Marine Rsrs Inst (Spiess), La Jolla, CA
UNIVERSITY OF DELAWARE Engrg Col (Dexter), Lewes, DE
UNIVERSITY OF HAWAII Library (Sci & Tech Div), Honolulu, HI
UNIVERSITY OF ILLINOIS Arch Scol (Kim), Champaign, IL; CE Dept (Hall), Urbana, IL; CE Dept (W. Gamble), Urbana, IL; Library, Urbana, IL; M.T. Davisson, Urbana, IL; Metz Ref Rm, Urbana, IL
UNIVERSITY OF MASSACHUSETTS ME Dept (Heroneumus), Amherst, MA
UNIVERSITY OF MICHIGAN CE Dept (Richart), Ann Arbor, MI
UNIVERSITY OF NEBRASKA-LINCOLN Polar Ice Coring Office, Lincoln, NE
UNIVERSITY OF NEW MEXICO NMERI (Falk), Albuquerque, NM; NMERI (Leigh), Albuquerque, NM
UNIVERSITY OF PENNSYLVANIA Schl of Engrg & Applied Sci (Roll), Philadelphia, PA
UNIVERSITY OF TEXAS AT AUSTIN Breen, Austin, TX; CE Dept (Thompson), Austin, TX
UNIVERSITY OF WASHINGTON CE Dept (Mattock), Seattle, WA
UNIVERSITY OF WISCONSIN Great Lakes Studies, Ctr, Milwaukee, WI
VENTURA COUNTY Deputy PW Dir, Ventura, CA; PWA (Brownie), Ventura, CA
ALFRED A YEE DIV L.A. Daly, Honolulu, HI
AMERICAN CONCRETE INSTITUTE Library, Detroit, MI
AMETEK OFFSHORE RSCH Santa Barbara, CA
APPLIED SYSTEMS R. Smith, Agana, Guam
ARVID GRANT & ASSOC Olympia, WA
ATLANTIC RICHFIELD CO RE Smith, Dallas, TX
BATTELLE D Frink, Columbus, OH
BECHTEL NATL, INC Woolston, San Francisco CA
BETHLEHEM STEEL CO Engrg Dept (Dismuke), Bethlehem, PA
BROWN & ROOT Ward, Houston, TX
CANADA Viateur De Champlain, D S A , Matane, Canada
CHEMED CORP Dearborn Chem Div Lib, Lake Zurich IL
COASTAL SCI & ENGRG C Jones, Columbia, SC
COLUMBIA GULF TRANSMISSION CO, Engrg Lib, Houston, TX
CONSTRUCTION TECH LABS, INC AE Fiorato, Skokie, IL
CONTINENTAL OIL CO O Maxsen, Ponca City, OK
DILLINGHAM PRECAST (HD&C), F McHale, Honolulu, HI
DRAVO CORP Wright, Pittsburg, PA
EASTPORT INTL, INC Mgr (JH Osborn), Ventura, CA
ENERCOMP H Amstadt, Brunswick, ME
EVALUATION ASSOC, INC MA Fedele, King of Prussia, PA
GENERAL DYNAMICS Dept 443 (DeLeone), Groton, CT
GEOTECHNICAL ENGINEERS INC (R E Murdock) Principal, Winchester, MA
GOULD INC Ches Instru Div, Tech Lib, Gen Burme, MD
HALEY & ALDRICH, INC HP Aldrich, Jr, Cambridge, MA
NUSC DET Library (Code 4533) Newport, RI
KATSURA CONSULTING ENGRS Y Katsura, PE, Ventura, CA
LIN OFFSHORE ENGRG P Chow, San Francisco CA
LINDA HALL LIBRARY Doc Dept, Kansas City, MO
M C D E Marek, Orangevale, CA
MARATHON OIL CO Houston TX
MARINE CONCRETE STRUCTURES INC W A Ingraham, Metairie, LA
MOBIL R & D CORP Offshore Eng Library, Dallas, TX
MOFFATT & NICHOL ENGRS R Palmer, Long Beach, CA
MUESER RUTHLEDGE CONSULTING ENGRS Richards, New York, NY
NEW ZEALAND NZ Concrete Rsch Assoc, Library, Porirua
PROF SVCS INDUSTRIES, INC Dir, Roots (Evons), Houston TX
PACIFIC MARINE TECHNOLOGY (M Wagner) Duvall WA

PITTSBURG TESTING LAB M. Kocak, Pittsburg, PA
RAYMOND INTL, INC Soil Tech Dept (F. Colle), Pennsauken, NJ
SAUDI ARABIA King Saud Univ, Rsch Cen, Riyadh
SEATECH CORP Peroni, Miami, FL
SHELL OIL CO E&P Civil Engrg, Houston, TX
SIMPSON, GUMPERTZ & HEGER, INC F. Hill, CE, Arlington, MA
TEXTRON, INC Rsch Cen Lib, Buffalo, NY
TIDEWATER CONSTR CO J Fowler, Virginia Beach, VA
TILGHMAN STREET GAS PLANT (Sreas), Chester, PA
TREMCO, INC M Raymond, Cleveland, OH
WESTINGHOUSE ELECTRIC CORP Library, Pittsburg, PA
WISS, JANNEY, ELSTNER, & ASSOC DW Pfeifer, Northbrook, IL
WOODWARD-CLYDE CONSULTANTS R Cross, Walnut Creek, CA; R Dominguez, Houston, TX; W Reg. Lib, Walnut Creek, CA
YOUTSEY, DJ Architect, Kansas City, KS
BULLOCK, TE La Canada, CA
CHAO, JC Houston, TX
DOBROWOLSKI, JA Altadena, CA
HAYNES, B Austin, TX
LAYTON, JA Redmond, WA
PAULI, DC Silver Spring, MD
PETERSEN, CAPT N.W. Pleasanton, CA
PRESNELL ASSOC, INC DG Presnell, Jr. Louisville, KY
SETHNESS, D Austin, TX
SPIELVOGEL, L Wyncote, PA
STEVENS, TW Long Beach, MS

INSTRUCTIONS

The Naval Civil Engineering Laboratory has revised its primary distribution lists. The bottom of the label on the reverse side has several numbers listed. These numbers correspond to numbers assigned to the list of Subject Categories. Numbers on the label corresponding to those on the list indicate the subject category and type of documents you are presently receiving. If you are satisfied, throw this card away (or file it for later reference).

If you want to change what you are presently receiving

- Delete — mark off number on bottom of label
- Add — circle number on list
- Remove my name from all your lists — check box on list
- Change my address — line out incorrect line and write in correction (PLEASE ATTACH LABEL).
- Number of copies should be entered after the title of the subject categories you select

Fold on line below and drop in the mail

Note: Numbers on label but not listed on questionnaire are for NCEL use only, please ignore them.

DEPARTMENT OF THE NAVY

NAVAL CIVIL ENGINEERING LABORATORY
PORT HUENEME, CALIFORNIA 93043-5003

OFFICIAL BUSINESS
PENALTY FOR PRIVATE USE, $300
NAVFAC-NCEL-2700/4 (REV. 12-73)
0930-LL-L70-0044

POSTAGE AND FEES PAID
DEPARTMENT OF THE NAVY
DOD-316

U.S. MAIL

Commanding Officer
Code L08B
Naval Civil Engineering Laboratory
Port Hueneme, California 93043-5003

DISTRIBUTION QUESTIONNAIRE

The Naval Civil Engineering Laboratory is revising its primary distribution lists.

SUBJECT CATEGORIES

1 **SHORE FACILITIES**
2 Construction methods and materials (including corrosion control, coatings)
3 Waterfront structures (maintenance/deterioration control)
4 Utilities (including power conditioning)
5 Explosives safety
6 Aviation Engineering Test Facilities
7 Fire prevention and control
8 Antenna technology
9 Structural analysis and design (including numerical and computer techniques)
10 Protective construction (including hardened shelters, shock and vibration studies)
11 Soil/rock mechanics
13 BEQ
14 Airfields and pavements
15 ADVANCED BASE AND AMPHIBIOUS FACILITIES
16 Base facilities (including shelters, power generation, water supplies)
17 Expedient roads/airfields/bridges
18 Amphibious operations (including breakwaters, wave forces)
19 Over-the-Beach operations (including containerization, materiel transfer, lighterage and cranes)
20 POL storage, transfer and distribution
28 ENERGY/POWER GENERATION
29 Thermal conservation (thermal engineering of buildings, HVAC systems, energy loss measurement, power generation)
30 Controls and electrical conservation (electrical systems, energy monitoring and control systems)
31 Fuel flexibility (liquid fuels, coal utilization, energy from solid waste)
32 Alternate energy sources (geothermal power, photovoltaic power systems, solar systems, wind systems, energy storage systems)
33 Site data and systems integration (energy resource data, energy consumption data, integrating energy systems)
34 ENVIRONMENTAL PROTECTION
35 Solid waste management
36 Hazardous waste materials management
37 Wastewater management and sanitary engineering
38 Oil pollution removal and recovery
39 Air pollution
44 OCEAN ENGINEERING
45 Seafloor soils and foundations
46 Swimming construction systems and operations (including divers and manipulator tools)
47 Undersea structures and materials
48 Anchors and moorings
49 Undersea power systems, electromechanical cables, and connectors
50 Pressure vessel facilities
51 Physical environment (including site surveying)
52 Ocean based concrete structures
53 Hyperbaric chambers
54 Undersea cable dynamics

TYPES OF DOCUMENTS

85 Techdata Sheets
86 Technical Reports and Technical Notes
82 NCEL Guide & Updates
None remove my name
83 Table of Contents & Index to TDS
91 Physical Security

COMNAVSURFPAC

SHORE INTERMEDIATE MAINTENANCE ACTIVITY (SIMA)

CORROSION CONTROL (CC) SHOPS

by

ROBERT A. SULIT AND A. MARIE ROBINSON

INTEGRATED SYSTEMS ANALYSTS, INC.
740 BAY BOULEVARD
CHULA VISTA, CA 92010
(619) 422-7100

1987 TRI-SERVICE CONFERENCE ON CORROSION
USAF ACADEMY, COLORADO SPRINGS, CO
5 - 7 MAY 1987

Abstract: The Commander Naval Surface Force, U.S. Pacific Fleet (COMNAVSURFPAC) Shore Intermediate Maintenance Activities (SIMA) are now being outfitted to provide corrosion-control (CC) services to tended ships. Services include wire-sprayed-aluminum (WSA) and electrostatic-sprayed-powder (ESP) coating and installation kits (i.e., 316-SS and ceramic-coated fasteners, gaskets/insulators, anti-seize and sealing compounds) for all ship-to-shop and shipboard preserved components/areas. This paper discusses the need, planning/screening policy, CC-Shop capabilities and capacity (equipment and layout, process instructions, quality control, standard production times for 120 shipboard items, crew training/certification), modus operandi for planning, screening and production management, records and follow-up customer-ship inspections for CC program effectiveness feedback.

References:

1. Sulit, Robert A. and Owen G. O'Brien, ASW and Support-Ship Corrosion-Control (CC) Program: Pilot SIMA CC Shop, ISA(WC)-101, 14 September 1984, Contract N66001-84-D-0032, Delivery Order 0003.

2. Adkins, W. et al., Corrosion-Control (CC) Program, SIMA Pilot CC-Shop Service Test and Technical Support (Final Report), ISA(WC)-107, 30 November 1985, Final Report, ISA(WC)-107, 3 Volumes, Contract N66001-85-C-0350.

3. Schlunt, P., Corrosion-Control (CC) Program: Pilot Powder Coating Service Test, ISA(WC)-ITR-108, 31 December 1985, Contract N66001-85-D-0015, Delivery Order 0012.

4. Sulit, R.A., Corrosion-Control (CC) Shop Technician Training Curriculum in the Shop-Qualification-Improvement-Program (SQIP) Format, August 1986 Revision, ISA(WC)-110, 15 August 1986, Contract N66001-86-D-0086, Delivery Order 0002.

5. Robinson, M. et al., SIMA(SD) Production CC Shop and Ship Work Package Guide, Interim Technical Report, ISA(WC)-Interim-112, 31 December 1986, Contract N66001-86-D-0086, Delivery Order 0001.

6. Kullerd, S. et.al., Corrosion-Control (CC) Program: SIMA, Pearl Harbor, Production CC Shop, ISA(WC)-ITR-113, 31 December 1986, Contract N66001-86-D-0086, Delivery Order 0002.

7. Kullerd, S., P. Schlunt and M. Robinson, Corrosion-Control Program: COMNAVSURFPAC SIMA CC Support, ISA(WC)-Interim-114, 31 March 1987, Contract N66001-86-D-0086, Delivery Order 0004.

OVERVIEW

- PROBLEM
- BACKGROUND AND REQUIREMENT
- MISSION/FUNCTIONS OF CC - SHOP
- CC - SHOP SERVICES

  ❶ TECH ASSIST ❷ - WSA CTG ❸ - PC ❹ - INSTALLATION KITS
- STANDARD TIMES FOR WSA
- SHIP - SIMA - TYCOM PLANNING
- SHIP'S CC WORK PACKAGE GUIDE
- SUMMARY

BACKGROUND AND REQUIREMENT

Refs. 1,2,7

BACKGROUND & REQUIREMENT

1977 • COMNAVSURFPAC INITIATES SERVICE TEST OF WSA

1979 • NAVSEA AUTHORIZES USE OF WSA

• CNO DIRECTS ACCELERATED IMPLEMENTATION OF WSA IN FLEET

1980 • NAVSEA INITIATES USE OF IMPROVED CC SYSTEMS IN NEW SHIP CONSTRUCTION
-- SPECS FOR BUILDING: SECTIONS 078 AND 630
-- NAVSEA DWG NO. 631-5751754 (FOR CG-47 CL)

1981 • NAVSEA ISSUES SHIP CLASS CC MANUALS

• NAVSEA ISSUES DoD-STD-2138(SH), METAL-SPRAYED COATING SYSTEMS FOR CORROSION PROTECTION ABOARD NAVAL SHIPS

BACKGROUND & REQUIREMENT (CONT'D)

1983 • NMAB COMMITTEE ON THERMAL-SPRAY COATINGS FOR *CORROSION CONTROL,REPORT (NMAB-409, FEB 83)*: WSA CTGS CAN PROVIDE UP TO 10-20 YEARS SERVICE LIFE AND ON A LIFE-CYCLE BASIS ARE MORE ECONOMICAL THAN PAINT

1984 • COMNAVSURFPAC INITIATES PILOT SIMA CC SHOP FOR NAVY

1985 • PILOT CC SHOP 1-YEAR SERVICE TEST COMPLETE AND RECS ADOPTED AS MODEL FOR SIMA UPGRADE PROGRAM

1986 • CC SHOP DESIGNED INSTALLED SIMA (PH): IOC - JUL 87

• CC SHOP MILCON UPGRADE: SIMA (LB): IOC - FY88
SIMA (SD): IOC - FY88
SIMA (SF): IOC - FY89

PROBLEM

6

PROBLEM

- EXCESSIVE S/F LABOR SPENT ON RECURRING CORROSION PREVENTION AND CONTROL REDUCING READINESS TRAINING AND MAINTENANCE ACTION

- SHORTENED COMPONENT/STRUCTURE SERVICE LIFE AND ATTENDANT MATERIAL, LABOR AND SCHEDULE COST TO REPAIR/REPLACE

Refs. 1,2,7

7

MISSION/FUNCTION

OF

SIMA CC - SHOP

MISSION OF
SIMA CORROSION CONTROL SHOP

SIMA PLANNING and PRODUCTION CAPABILITY → DELIVER and SUPPORT → NAVSEA CC SYSTEMS
- Ships-in- Service
- New Construction

SIMA CC - SHOP FUNCTIONS

CORROSION CONTROL (CC) SERVICES

(1) TECH ADVICE ON THE CAUSES AND PREVENTION OF TOPSIDE CORROSION PROBLEMS AND THE APPLICATION OF THE 15 NAVSEA SYSTEMS

(2) PRODUCTION FOR:

- WIRE-SPRAYED ALUMINUM
- POWDER COATING
- INSTALLATION KITS FOR PRODUCTS PRESERVED WITH SYS 1, 2, & 4

	NAVSEA CC SYSTEMS
1	WSA - HIGH TEMPERATURE
2	WSA - LOW TEMPERATURE
3	EXTERIOR TOPSIDE PAINT COATINGS
4	POWDER COATINGS
5	NON-SKID DECK COATINGS
6	CERAMIC COATING
7	WATER DISPLACING COMPOUNDS
8	ANTI-SEIZE COMPOUNDS
9	IMPROVED FASTENERS
10	SEAL AND COATING COMPOUNDS
11	POLYSULFIDE SEALANTS
12	MULTI-PIN CONN. PROT.
13	PLASTIC DIELECTRIC BARRIER
14	VAPOR PHASE INHIBITOR
15	STRIPPABLE COATING

Refs. 1,2

SIMA CC - SHOP FUNCTIONAL WORK FLOW

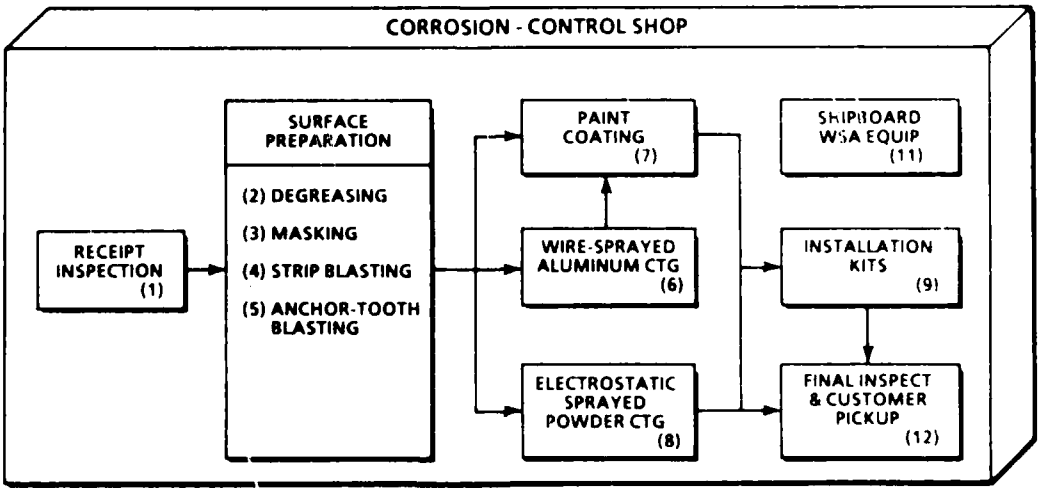

NOTIONAL CC - SHOP MANNING

FUNCTION	RATING/RATE	NUMBERS
SHOP MASTER	BMC or HTC	1
ASSISTANT SHOP MASTER	HT-1 or BM-1	1
QUALITY CONTROL	BM-2 or HT-2	2
SUPPLY	SK-1 2	1
WSA PRODUCTION	BM-1 2 3	2
	HT-1 2 3	2
	BM SN 3	2
	HT FN 3	2
ESP PRODUCTION	BM-1	1
	BM-2 3	2
	BM SN 3	1
INSTALLATION KIT MAKEUP	SK-2 3	1
	TOTAL	20

Refs: 1,2

SIMA SAN DIEGO
CC SHOP

SIMA San Diego
Naval Station
San Diego, CA

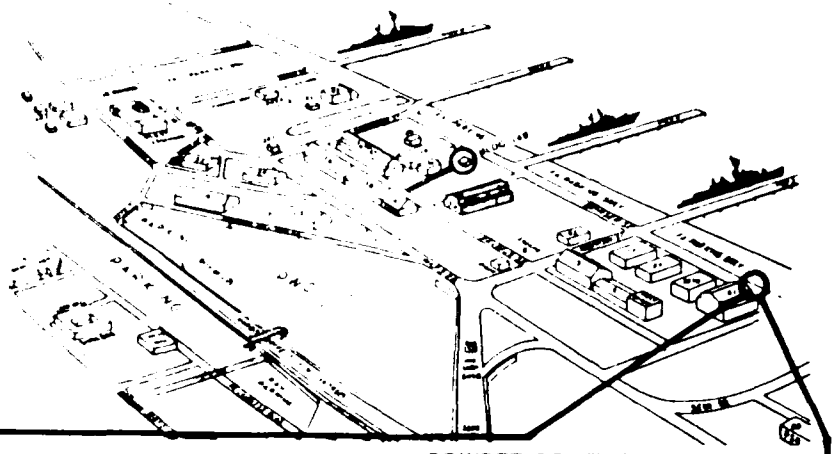

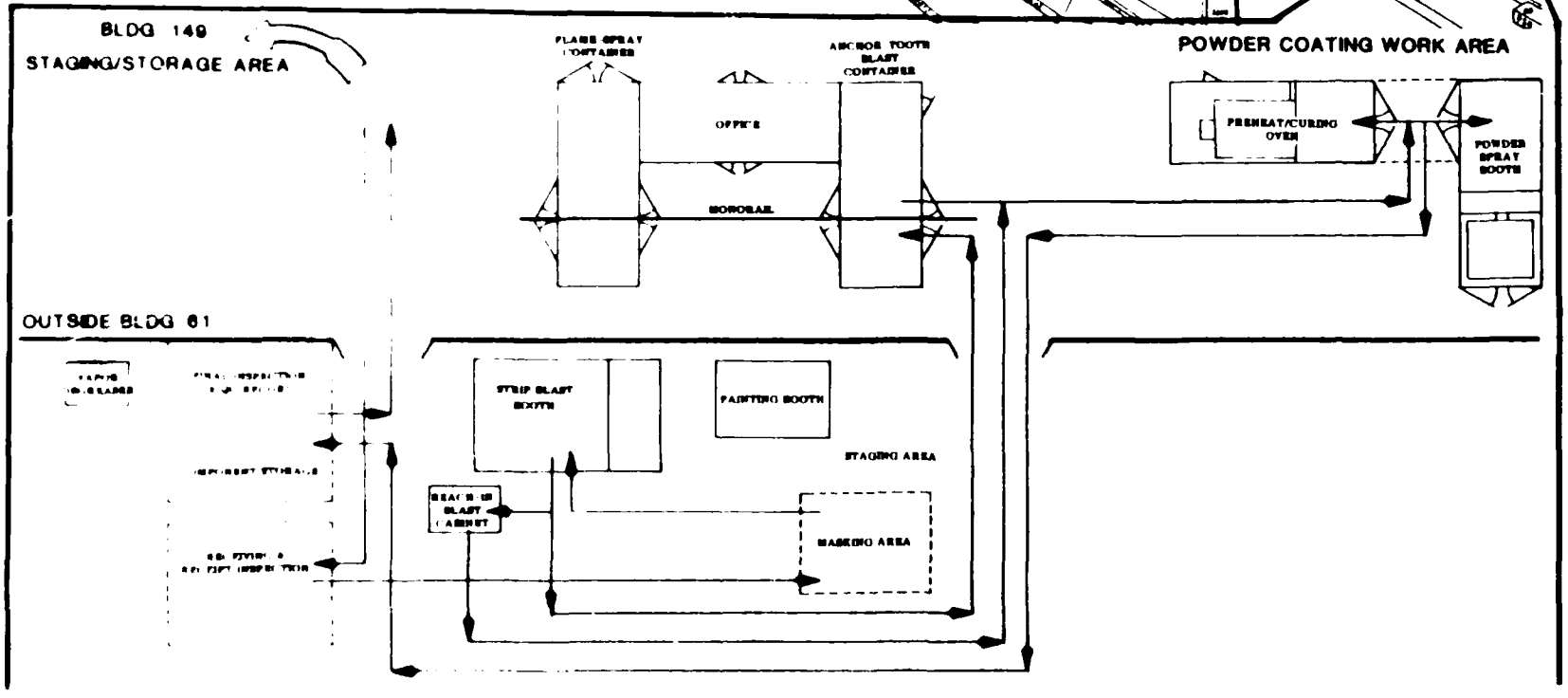

SIMA (PEARL HARBOR)
CC - SHOP PLOT PLAN

SIMA CC-Shop
PEARL HARBOR, HAWAII

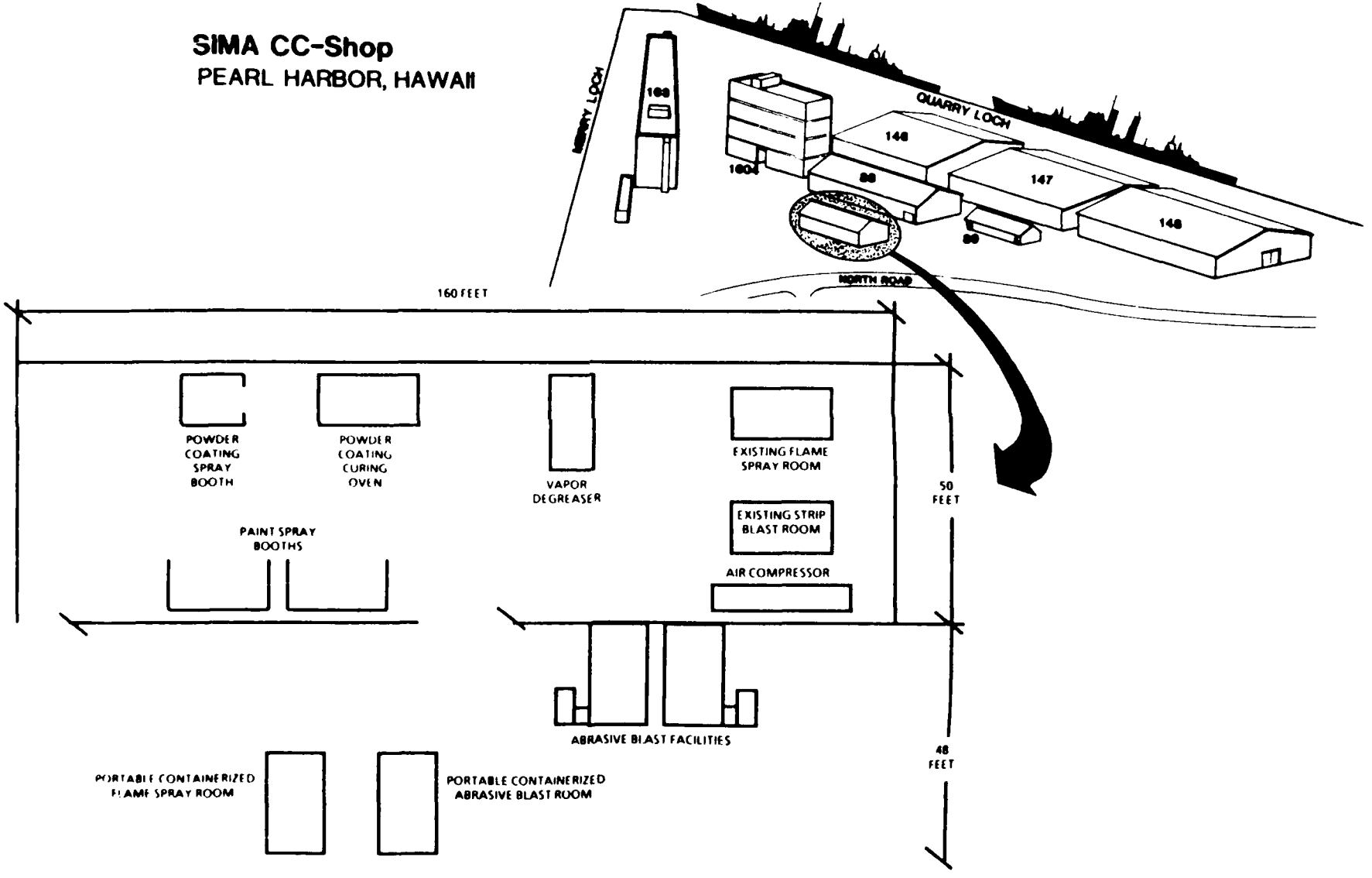

Ref. 6

PROCESS INSTRUCTION
WIRE - SPRAYED ALUMINUM

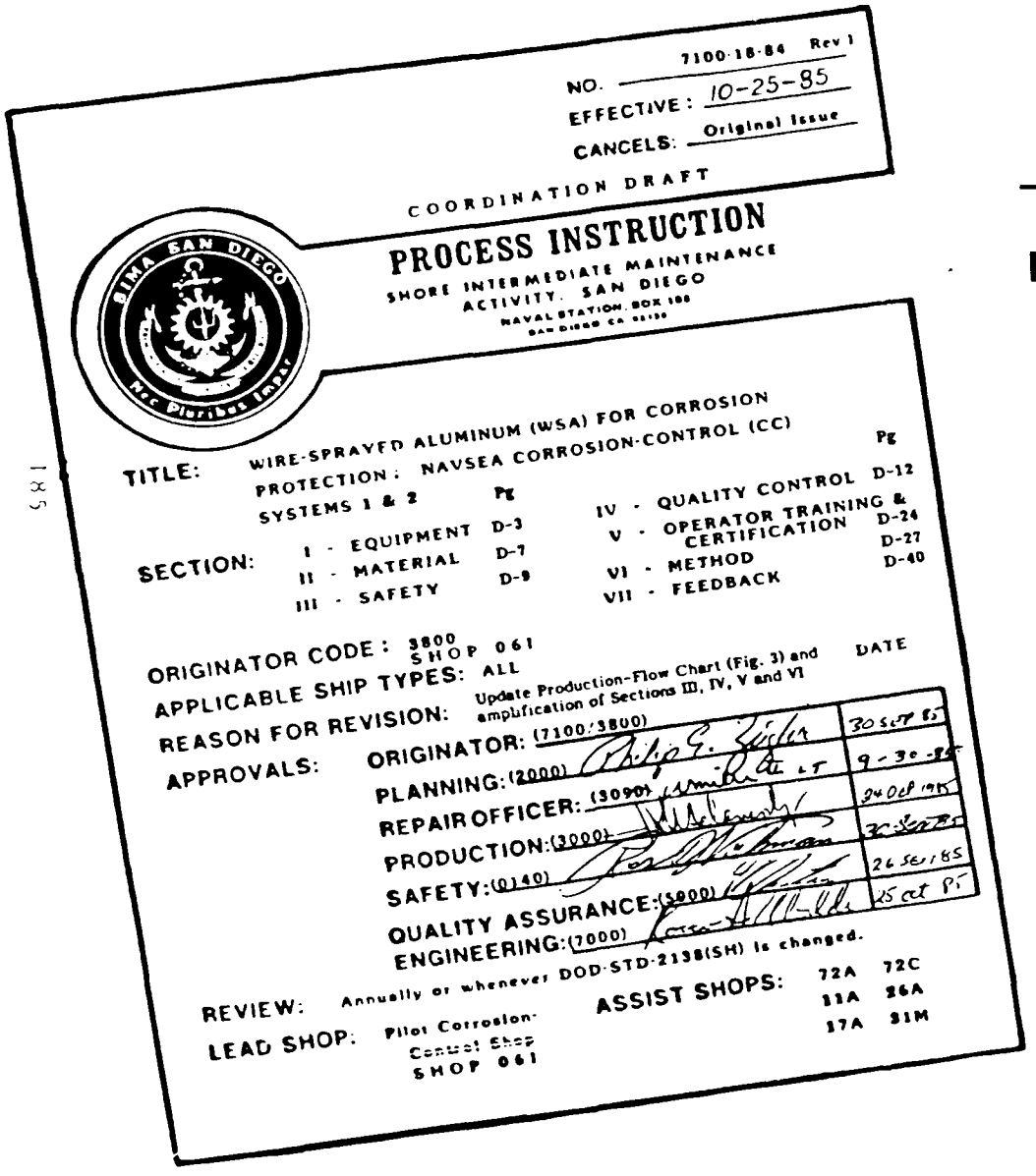

NO. 7100-18-84 Rev 1
EFFECTIVE: 10-25-85
CANCELS: Original Issue

COORDINATION DRAFT

PROCESS INSTRUCTION
SHORE INTERMEDIATE MAINTENANCE ACTIVITY: SAN DIEGO
NAVAL STATION, BOX 160
SAN DIEGO CA 92136

TITLE: WIRE-SPRAYED ALUMINUM (WSA) FOR CORROSION PROTECTION: NAVSEA CORROSION-CONTROL (CC) SYSTEMS 1 & 2

SECTION:	Pg		Pg
I - EQUIPMENT	D-3	IV - QUALITY CONTROL	D-12
II - MATERIAL	D-7	V - OPERATOR TRAINING & CERTIFICATION	D-24
III - SAFETY	D-9	VI - METHOD	D-27
		VII - FEEDBACK	D-40

ORIGINATOR CODE: 3800 SHOP 061
APPLICABLE SHIP TYPES: ALL
REASON FOR REVISION: Update Production-Flow Chart (Fig. 3) and amplification of Sections III, IV, V and VI

APPROVALS:	DATE
ORIGINATOR: (7100/3800)	30 SEPT 85
PLANNING: (2000)	9-30-85
REPAIR OFFICER: (3090)	24 Oct 1985
PRODUCTION: (3000)	30 SEP 85
SAFETY: (0140)	26 SEP 85
QUALITY ASSURANCE: (3000)	25 oct 85
ENGINEERING: (7000)	

REVIEW: Annually or whenever DOD-STD-2138(SH) is changed.
LEAD SHOP: Pilot Corrosion Control Shop SHOP 061
ASSIST SHOPS: 72A 72C 11A 26A 37A 31M

Ref. 7

SECTION

I EQUIPMENT

II MATERIALS

III SAFETY

IV QUALITY CONTROL

V OPERATOR TRAINING & CERTIFICATION

VI METHOD

VII FEEDBACK

SECTION VI - METHOD

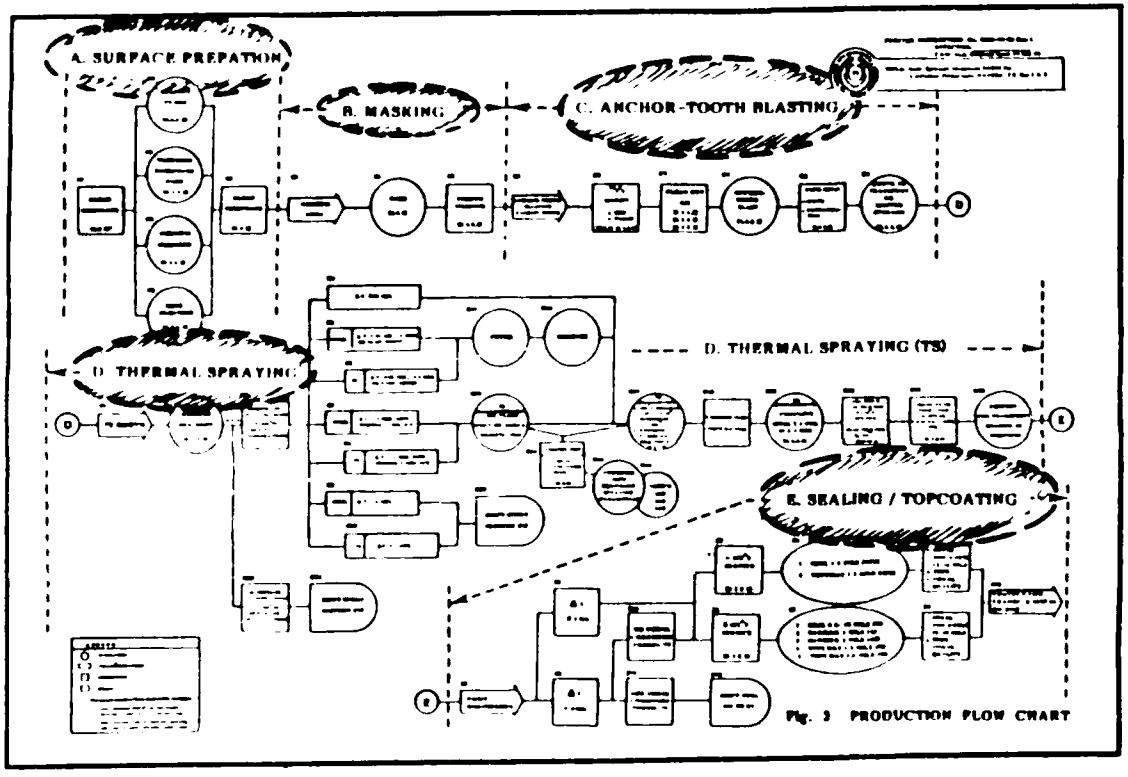

Fig. 3 PRODUCTION FLOW CHART

MAJOR FUNCTIONS & WORK STATIONS

A - SURFACE PREPARATION

B - MASKING

C - ANCHOR-TOOTH BLASTING

D - THERMAL SPRAYING

E - SEALING/TOPCOATING

Ref. 2

WSA - LOW TEMP. (< 175° F)

7 -10 MILS WSA + 5-COMPONENT PAINT SCHEDULE PER DoD-STD-2138 (SH)

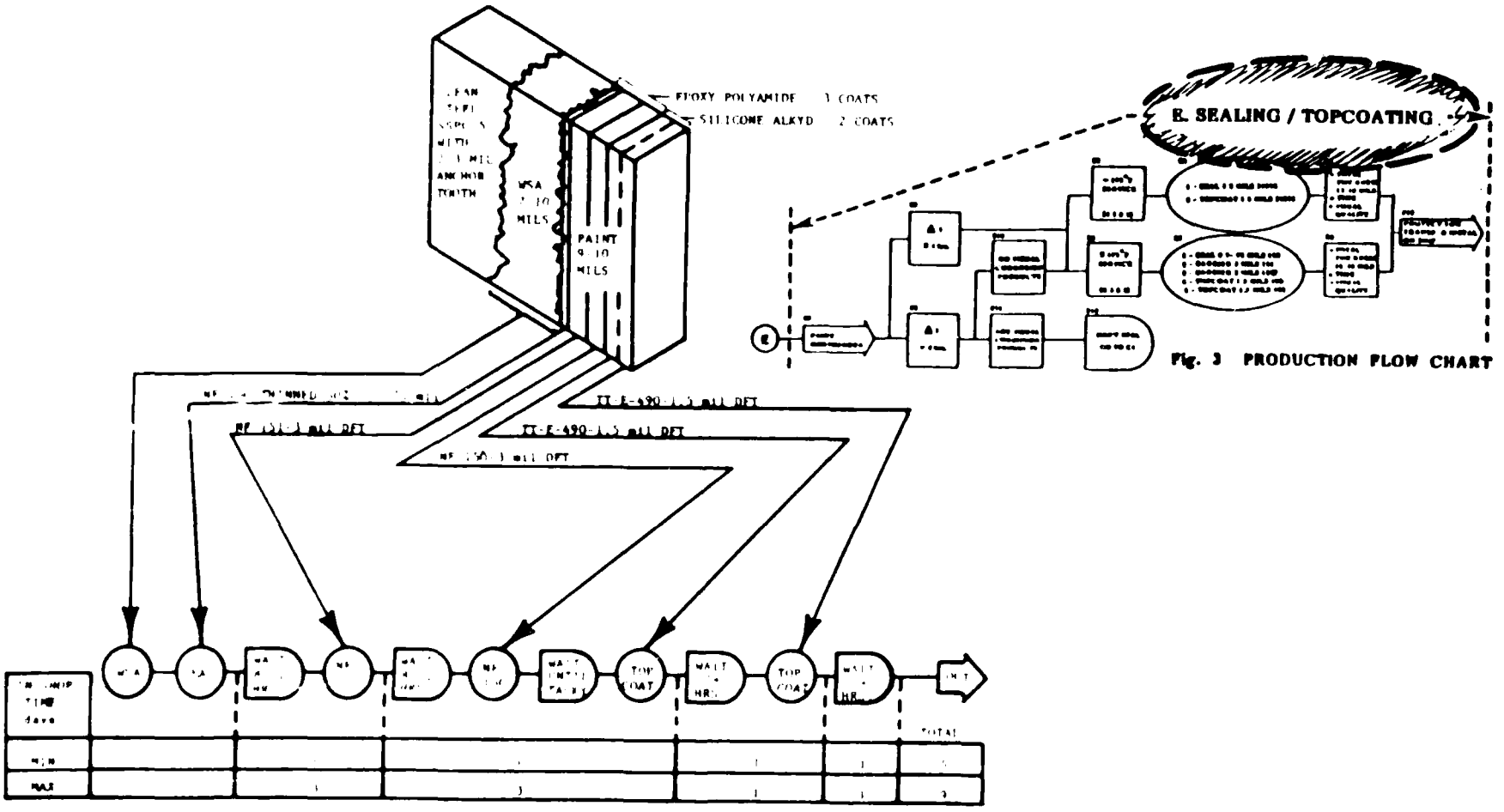

Fig. 3 PRODUCTION FLOW CHART

CC SHOP CONSUMABLES OF REPRESENTATIVE ITEMS

STATION	STATION	STATION
DEGREASING	TRICHLORETHANE	75 GAL
MASKING	DUCT TAPE 2-INCH ALUMINUM TAPE 1-INCH	15 ROLLS 9 ROLLS
STRIP BLASTING	GARNET SAND #36	5000 LBS
ANCHOR-TOOTH BLASTING	ALUMINUM OXIDE #16 (for WSA) ALUMINUM OXIDE #36 (for PC) PRESS-O-FILM TAPE (X-coarse)	4000 LBS 1000 LBS 10 ROLLS
FLAME SPRAYING	ALUMINUM WIRE, 1 8-IN OXYGEN ACETYLENE	4 ROLLS 16 BTLS 8 BTLS

Refs. 2,5,6,7

CC SHOP CONSUMABLES OF REPRESENTATIVE ITEMS

CONT'D

STATION	ITEM		MONTHLY USE
POWDER COATING	POWDER	HAZE GREY	175 LBS
		RED	50 LBS
		YELLOW	25 LBS
		BLACK	50 LBS
		WHITE	70 LBS
PAINTING	TT E 781 EGM THINNER		20 GAL
	NF 150 GREEN PRIMER		60 GAL
	NF 151 HAZE GREY		50 GAL
	NF 20 EXTERION DK GREY		10 GAL
	TT E 490 HAZE GREY		20 GAL
	DoD P 2455 (SH) HEAT RESISTANT ALUM PAINT		20 GAL

Refs. 2,5,6,7

INSTALLATION KIT
TECHNICAL DATA SHEET

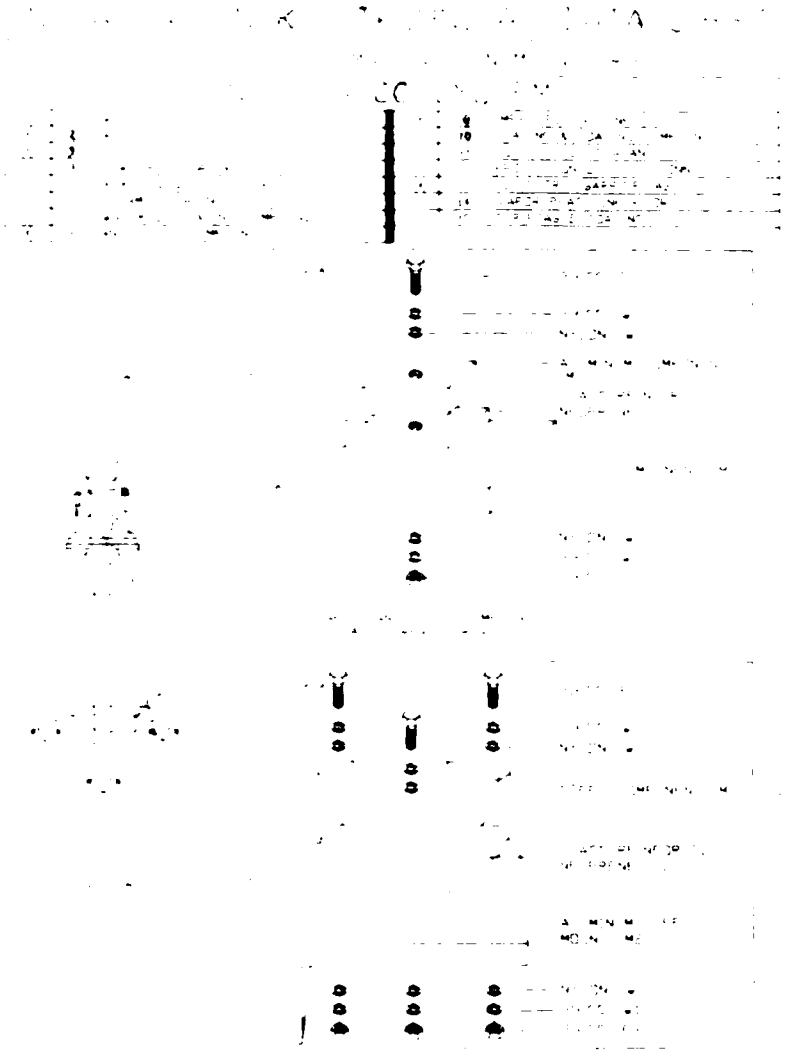

Ref. [illegible]

INSTALLATION KIT TECHNICAL DATA SHEET

[illegible] CALIBER MACHINE GUN MOUNT TRIPOD

[illegible] SCREWS				WASHERS				GASKETS	
	DIM	QTY	MATERIAL		DIM	QTY	MATERIAL		MATERIAL
	3/8	2	[illegible]	W1	[illegible]	[illegible]	[illegible]	G1	[illegible] REINFORCED NEOPRENE
	3/8	[illegible]	[illegible]	W2	[illegible]	36	NYLON	G2	
	5/8	[illegible]	[illegible]	W3		18	[illegible]		
				W4					COMPONENT
				W5					MATERIAL
								M1	STEEL
								M2	ALUMINUM/STEEL
								M3	

INSTALLATION INSTRUCTIONS

PREPARE ALUMINUM MOUNTING AS FOLLOWS

- REMOVE ANY OIL OR GREASE USING APPROPRIATE SOLVENTS
- PREPARE MOUNTING SURFACE BY REMOVING ALL CORROSION PRODUCTS USING AN [illegible] ABRASIVE DISC
- APPLY A PRIMER COAT OF FORMULA 150 IMMEDIATELY TO A DRY FILM THICKNESS OF [illegible] MILS
- APPLY A BARRIER COAT OF FORMULA 151 TO A DFT OF 15 MILS AFTER A MINIMUM OF [illegible] BUT NOT MORE THAN 72 HOURS HAS ELAPSED SINCE THE APPLICATION OF THE PRIMER
- APPLY A TOP COAT OF TT-E-490 TO A DFT OF 15 MILS WHILE THE BARRIER COAT IS [illegible] APPROXIMATELY 2-4 HOURS
- APPLY A TOP COAT OF TT-E-490 WITHIN 24 HOURS TO A DFT OF 15 MILS
- ALLOW PAINT SYSTEM TO DRY THOROUGHLY BEFORE REINSTALLATION OF THE COMPONENT

PREPARE STEEL MOUNTING AS FOLLOWS

- REMOVE ANY OIL OR GREASE USING APPROPRIATE SOLVENTS
- PREPARE MOUNTING SURFACE BY REMOVING ALL CORROSION PRODUCTS USING A [illegible] POWER WIRE BRUSH
- APPLY A MINIMUM COAT OF INORGANIC ZINC PRIMER IMMEDIATELY TO A DRY FILM [illegible] OF 3 MILS
- APPLY A BARRIER COAT OF FORMULA 150 TO A DFT OF [illegible] MILS AFTER A MINIMUM OF [illegible] BUT NOT MORE THAN 72 HOURS HAS ELAPSED SINCE THE [illegible] OF PRIMER COAT
- APPLY A BARRIER COAT OF FORMULA 151 TO A DFT OF 3 MILS AFTER A MINIMUM OF 6 HOURS
- APPLY A TOP COAT OF TT-E-490 TO A DFT OF 15 MILS WHILE THE SECOND BARRIER [illegible] APPROXIMATELY 2-4 HOURS
- APPLY A TOP COAT OF TT-E-490 TO A DFT OF 15 MILS WITHIN 24 HOURS
- ALLOW PAINT SYSTEM TO DRY THOROUGHLY BEFORE REINSTALLATION OF THE COMPONENT

MOUNTING COMPONENT AS FOLLOWS

- APPLY ANTI-SEIZE COMPOUND TO ALL FASTENER THREADS
- APPLY [illegible] SEALANT TO ALL MATING SURFACES AS SHOWN IN THE ILLUSTRATION
- IN ALL THE FASTENER ASSEMBLIES PROVIDED AS SHOWN IN THE ILLUSTRATION ENSURE [illegible] NYLON WASHERS ARE INSTALLED NEXT TO THE MOUNTING SURFACE AND OF THE COMPONENT TO FORM A PROTECTIVE BARRIER FOR THE COATINGS
- REPAIR ANY CHIPS OR SCRATCHES IMMEDIATELY BY FEATHERING THE EDGES AND APPLYING AN APPROPRIATE PAINT SYSTEM IN ACCORDANCE WITH NSTM [illegible]

FASTENER RQMTS FOR VARIOUS SHIP CLASSES (17 Ship Classes Surveyed)

AO-177	AR-5	ATS-1	CG-16	CGN-38
DD-963	DDG-2	FF-1040	FF-1052	FFG-1
FFG-7	LHA-1	LKA-113	LPD-1	LPH-2
LSD-36	LST-1179			

DD963 SHIP CLASS

316 – SS FASTENERS

DIAMETER	LENGTH (IN)											HEX NUTS	LOCK NUTS	FLAT WSHRS	NYLON WSHRS	PYRO CLIP	
	1/2	3/4	1	1 1/4	1 1/2	1 3/4	2	2 1/2	3	3 1/2	4						
.413	112	0	1444	0	0	0	0	0	0	0	0	1084	0	2288	2388	0	
.3[illegible]	0	198	3[illegible]	0	0	0	0	0	0	0	0	3[illegible]8	24	7844	8656	234	10,000
.4[illegible]6	0	[illegible]6	1[illegible]2	0	0	0	0	16	0	0	0	1474	0	1784	1832	1474	
.[illegible]8	0	856	1[illegible]4	28	648	144	764	132	0	0	0	3852	364	8784	9618	352	
1.0	0	48	96	0	600	0	1[illegible]	32	0	0	0	484	368	1784	1928	0	
1.[illegible]8	0	0	0	0	0	0	0	16	0	0	24	16	24	98	248	0	
1.5	0	0	48	0	0	0	0	0	2	2	0	44	0	88	588	0	

CERAMIC COATED FASTENERS

DIAMETER (IN)	LENGTH (IN)								HEX NUTS	FLAT WSHRS	
	1 1/4	1 1/2	1 3/4	2	2 1/2	3	3 1/2	4			
.2[illegible]8	16	0	0	0	0	0	0	0	16	32	500
1.[illegible]	0	16	12	36	24	0	0	0	32	168	
.[illegible]6	0	0	0	0	76	96	0	0	172	344	
1.0	0	16	0	0	0	64	64	64	208	416	

316 – SS FORGED PINS

DIAMETER (IN)	LENGTH (IN)	
	2 1/2	6
1.[illegible]	[illegible]	0
5.0	0	216

WATERTIGHT CLOSURE PARTS

DESCRIPTION	QUANTITY
HINGE PIN (RAISED HATCH)	28
WASHER (RAISED HATCH)	28
COTTER PIN	232
HINGE PIN (SCUTTLE)	8
COLLAR (SCUTTLE)	8
UPPER LINK PIN (SCUTTLE)	4
LOWER LINK PIN (SCUTTLE)	4
COLLAR (LINK PIN)	4
HINGE PIN (DOOR)	284
COLLAR (DOOR)	284

Ref.

STANDARD (SHOULD COST)

TIMES FOR

WSA CTGS

STANDARD TIMES (Should Cost) FOR WSA PRESERVATION

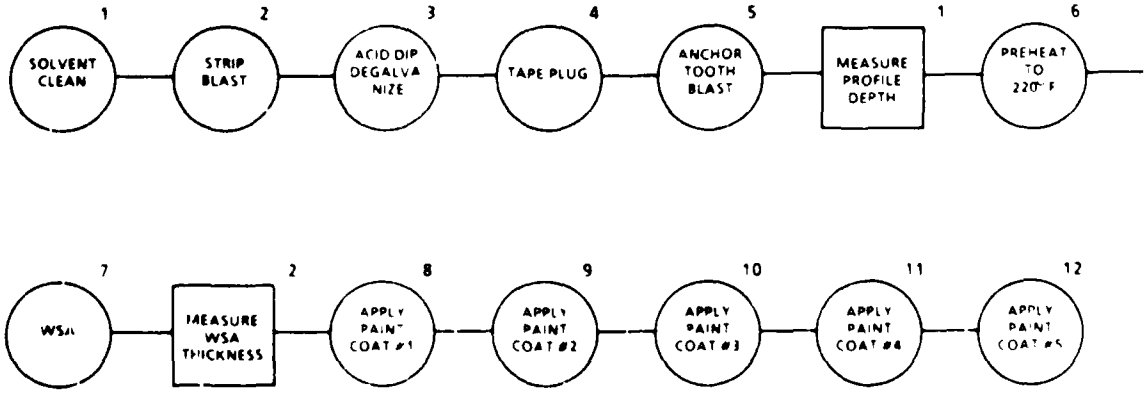

Ref. 2

PROCESS ELEMENT TIME SUMMARY

STANDARD TIMES

COMPONENT	SOLVENT CLEAN	STRIP BLAST	ACID/ BASE DIP	TAPE/ PLUG	ANCHOR TOOTH	QA	PREHEAT	THERMAL SPRAY	QA	PAINT #1	PAINT #2	PAINT #3	PAINT #4	PAINT #5	TOTAL M-MIN	TOTAL M-HR
Chain Bar		25.0			32.5	1.0	6.5	12.5	1.0	1.5	1.5	1.5	1.5	1.5	86.0	1.43
Baxter bolt		5.0		5.0	5.0	1.0	4.0	4.0	1.0	1.0	1.0	1.0	1.0	1.0	30.0	0.50
J-Bolt	2.0	10.0		10.0	5.0	1.0	2.0	4.0	1.0	1.0	1.0	1.0	1.0	1.0	40.0	0.67
Accom Ladder Brace		21.7		1.4	13.1	2.0	3.9	13.6	1.0	3.8	3.7	3.6	3.6	3.6	74.9	1.25
Big Eyes Bracket		7.0			6.0	2.0	4.0	14.0	2.0	3.0	4.0	4.0	4.0	4.0	54.0	0.90
Bottle Rack Bracket	1.6	10.4			6.0	1.0	2.5	3.8	1.0	1.8	1.8	1.8	1.8	1.8	35.3	0.59
CO2 Bottle Bracket		18.0		2.0	18.0	2.0	2.0	13.0	2.0	2.5	2.5	2.5	2.0	2.0	68.5	1.14
Light Bracket/Plate	2.0	13.7			7.4	1.0	3.4	4.8	1.0	1.4	1.4	1.4	1.4	1.4	40.2	0.67
Light Bracket/Pipe	1.9	14.7			9.4	1.0	5.0	6.3	1.3	1.6	1.6	1.6	1.6	1.6	47.7	0.79
Halo Net Securing Bracket		3.0			2.5	1.0	0.5	2.0	1.0	1.5	1.0	1.0	1.0	1.0	15.5	0.26
Scupper Bracket	0.2	14.1			6.8	1.9	3.6	6.4	1.0	1.6	1.6	1.6	1.6	1.6	42.0	0.70
Sliding Padeye Bracket	3.7	5.3			7.7	1.0	1.0	9.7	1.0	3.0	2.5	2.5	2.5	2.5	42.3	0.71
Capstan Controller	4.0	28.0			15.0	2.0	3.5	10.0	1.0	3.0	2.5	3.0	3.0	3.0	78.0	1.30
Portable Cleat	5.0	4.3		2.0	16.6	0.9	3.8	7.3	1.0	3.8	3.9	3.8	3.8	3.8	60.0	1.00
Director Counterweight		6.2			5.0	1.0	4.0	5.8	1.0	1.6	1.6	2.3	2.4	2.2	33.1	0.55
Dir. Cntrst. (Cylindrical)		29.5			26.0	2.0	16.0	46.0	1.0	7.5	7.0	8.0	8.0	8.0	159.0	2.65
Pipe Coupling	5.0	10.0		8.0	6.0	1.0	3.0	5.0	1.0	2.0	2.0	2.0	2.0	2.0	49.0	0.82
IMI Speaker Cover		20.0		5.0	12.0	1.0	2.0	20.0	1.0	8.0	4.0	4.0	4.0	5.0	86.0	1.43
BPDMS Cable Cover	3.2	8.4			10.8	2.4	2.2	17.6	1.6	5.4	6.5	6.6	5.9	6.3	77.0	1.28
Chain Locker Cover	5.9	27.8			20.0	1.5	3.8	26.1	1.2	5.3	5.4	5.5	5.3	5.6	113.3	1.89
Chock Cover	0.8	17.7		7.7	10.8	1.3	3.4	7.5	1.0	3.8	3.3	3.3	3.3	3.3	67.0	1.12
Fuel Oil Vent Cover		3.0		1.0	2.0	1.0	0.5	1.0	1.0	1.0	1.0	1.0	1.0	1.0	14.5	0.24
Edge Light Cover	2.0	10.0			10.0	1.0	2.0	6.0	1.0	1.0	1.0	1.0	1.0	1.0	37.0	0.62
Hawse Pipe Cover	5.0	26.7			40.7	1.1	6.5	20.1	1.1	6.4	6.7	6.1	6.0	6.0	132.3	2.21
Junction Box Cover	2.0	14.0			7.0	1.0	3.0	5.0	1.0	1.0	1.0	1.0	1.0	1.0	38.0	0.63
Handwheel Cover		6.0			12.0	1.0	1.0	6.0	1.0	1.0	1.0	1.0	1.0	1.0	32.0	0.53
VDS 3 Dog Cover		4.0		2.0	2.5	1.0	1.0	5.0	1.0	1.5	1.5	1.5	1.5	1.5	24.0	0.40
Life Raft Cradle		15.0			14.0	2.0	2.0	15.0	2.0	5.0	5.0	4.5	4.5	5.0	75.0	1.25
Portable Davit	2.0	41.8		4.2	32.2	1.6	14.4	28.5	1.4	6.0	5.6	6.2	6.0	5.6	153.5	2.59
Port. Davit Socket	4.1	15.1		3.8	11.8	2.5	3.0	15.0	1.0	4.8	4.1	3.8	4.0	5.3	95.3	1.59

PROCESS ELEMENT TIMES FOR WATERTIGHT DOOR

STANDARD TIMES

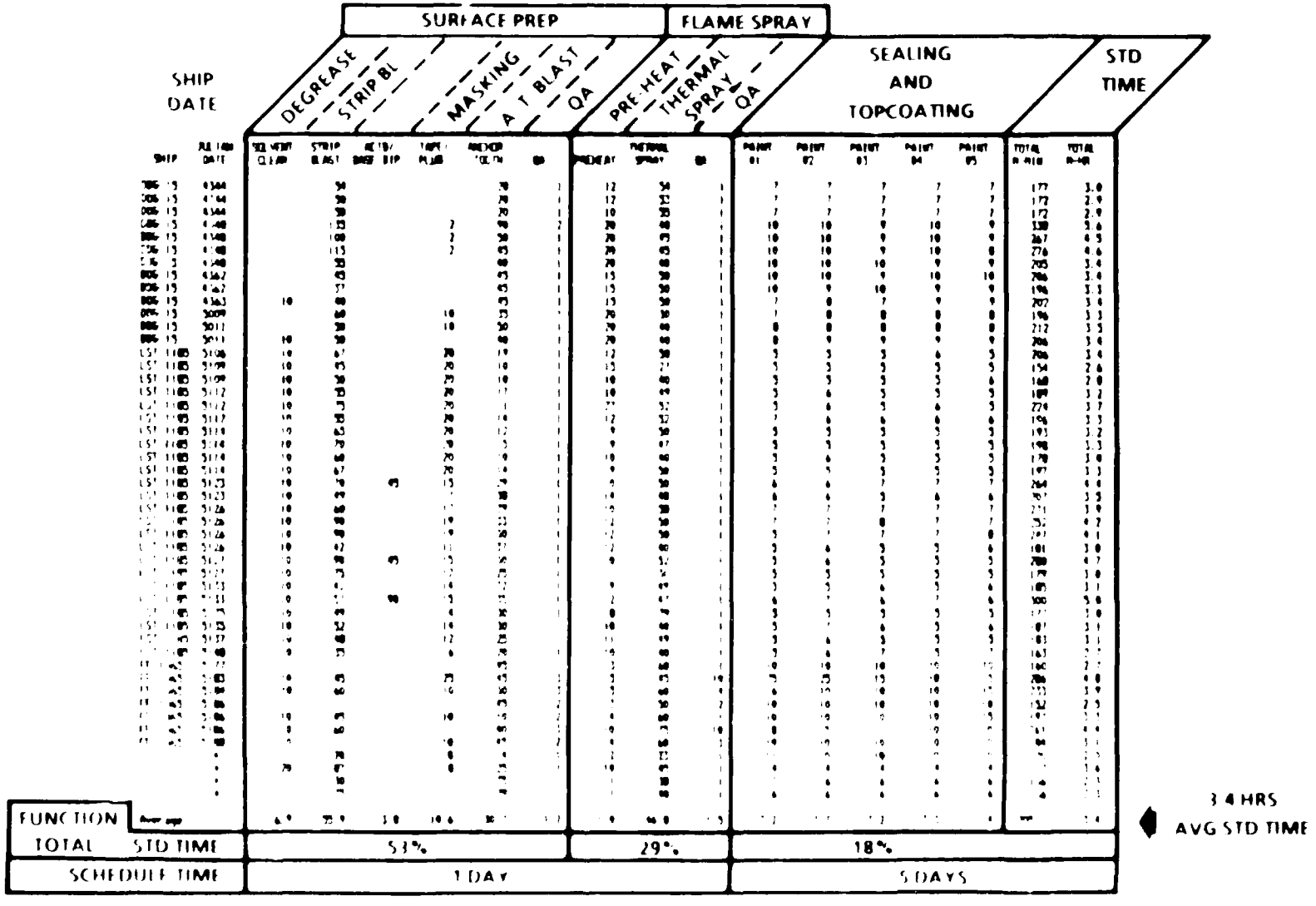

CC SHOP STANDARD TIMES
(121 Components Measured)

COMPONENT	STANDARD TIME (MAN HRS)	
	IDEAL*	NOTIONAL CC SHOP**
[illegible]	[illegible]	4.1
[illegible]	[illegible]	7.2
[illegible]	[illegible].6	8.4
[illegible]	[illegible].8	5.6
[illegible]	[illegible].6	2.5
[illegible]	[illegible].1	5.2
[illegible]	[illegible].2	3.7
[illegible]	[illegible].5	2.1
[illegible]	[illegible]	1.6
[illegible]	[illegible].4	8
[illegible]	[illegible].4.4	16.4
[illegible]	[illegible].1	4.8

[illegible]

[illegible]

SHIP - SIMA - TYCOM

PLANNING

AD-A191 295 PROCEEDINGS OF THE TRI-SERVICE CONFERENCE ON CORROSION (1987) HELD AT THE.. (U) AIR FORCE WRIGHT AERONAUTICAL LABS WRIGHT-PATTERSON AFB OH.. F H MEYER MAY 87 1/6

UNCLASSIFIED AFWAL-TR-87-4139-VOL-1 F/G 11/6.1 NL

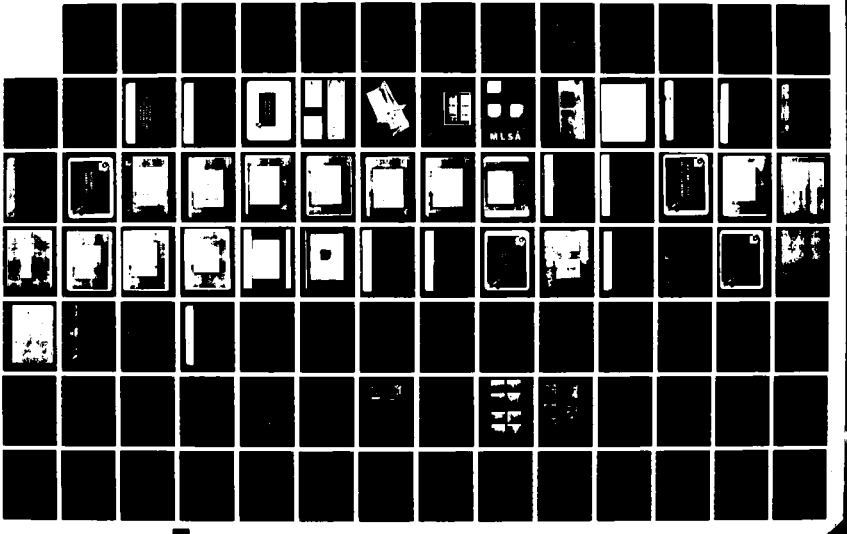

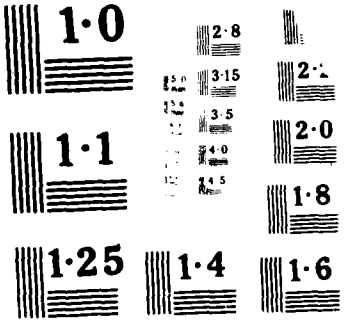
1·0
1·1
1·25
1·4
1·6
1·8
2·0
2·8
3·15
3·5
4·0

CC PLANNING & WORK ACCOMPLISHMENT

PRE-AVAILABILITY ACTIVITIES

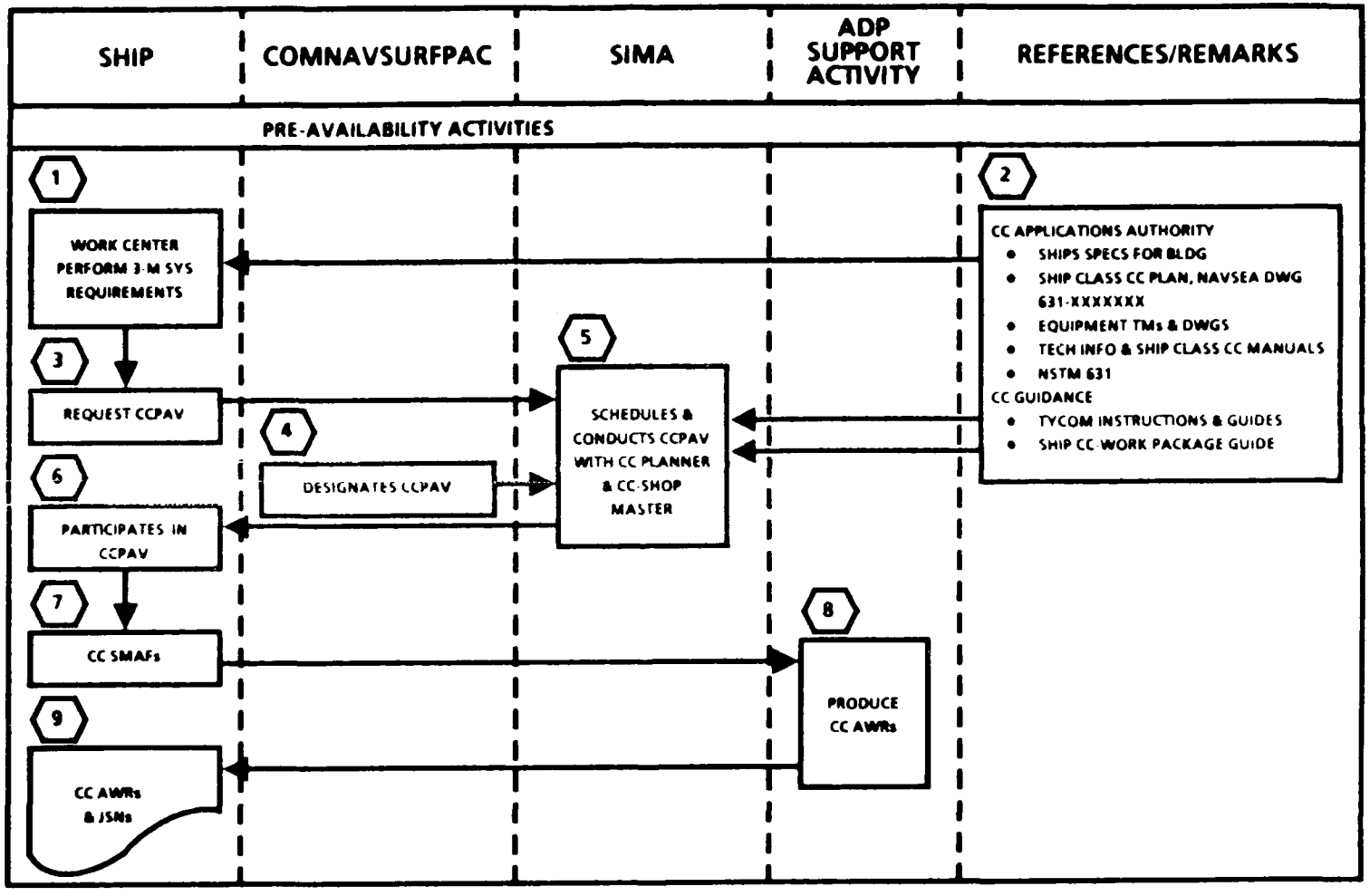

Refs. 2,5

CC PLANNING & WORK ACCOMPLISHMENT

AVAIL. PLANNING, SCREENING & WORK ACCOMPLISHMENT

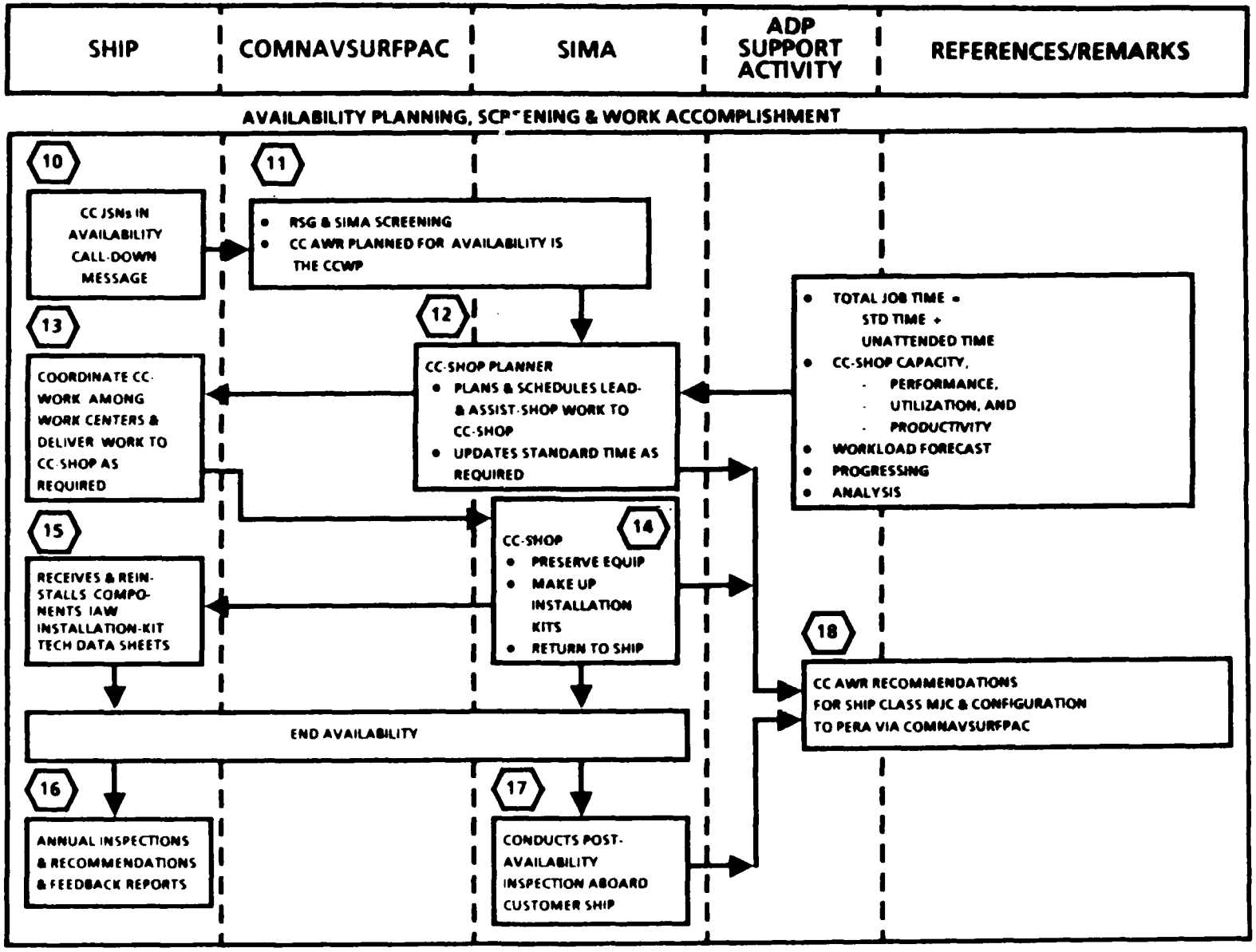

SHIP'S
CC WORK PACKAGE
GUIDE

30

SHIP'S CC WORK PACKAGE GUIDE
OBJECTIVE/SCOPE

- PROCEDURES FOR IDENTIFICATION AND SCREEENING ITEMS FOR CC AVAILABILITIES
- MAINTENANCE AND REPAIR OF THE 15 NAVSEA CC COATING SYSTEMS
  - --- THREE MAINTENANCE REQUIREMENT CARDS
  - --- INSTALLATION KIT TECH DATA SHEETS
  - --- CORROSION DISCUSSION
  - --- THE 15 NAVSEA CODIFIED CC SYSTEMS
- CONFIGURATION CONTROL AND CORPORATE HISTORY

Ref. 5

31

SHIP'S CC WORK PACKAGE GUIDE

AVAILABILITY PLANNING AND ACCOMPLISHMENT

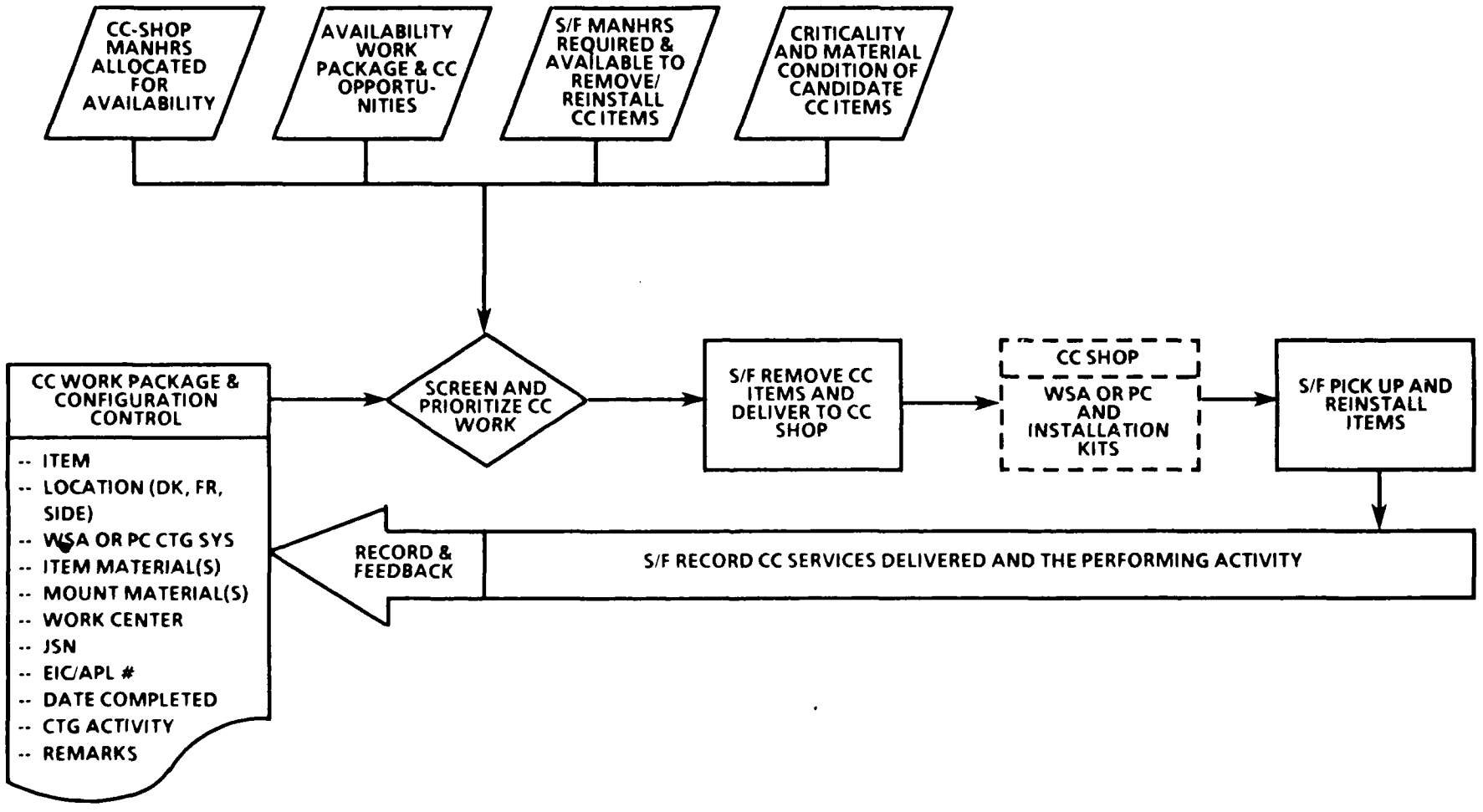

Ref. 5

SHIP'S WORK PACKAGE GUIDE
CANDIDATE ITEMS

ITEM | LOCATION | CTG SYS | COMP. MAT. | MT. MAT. | NOTES | SHIP'S DRI | DATE COMP. | CTG ACTIVITY | REMARKS

FOR NOTES 1-4 & a-d, SEE PAGES B1-2

CORROSION-CONTROL WORK PACKAGE LIST
FOR THE
USS WHIPPLE (FF-1062)

LEGEND: WSA = WIRE-SPRAYED ALUMINUM; PC = POWDER COATING; ST = STEEL; GRP = FIBERGLASS; AL = ALUMINUM; BR = BRASS/BRONZE; SS = STAINLESS STEEL; PVC = PLASTIC PIPE

ITEM	LOCATION	COATING SYSTEM	COMPONENT MATERIAL	MOUNT MATERIAL	NC	JSN	SHOP MHRS	BLOCK 35	SHIP'S PRIORITY	DATE COMPL	COATING ACTIVITY	REMARKS
Jack Staff	Bow	PC	AL	ST			6.0	Note 4				
Electrical Outlet Box	Bow	PC	BR	ST			1.8	Note 4				
Jack Staff Braces (2 ea)	Bow	PC	AL	ST			8.0	Note 4				
Portable Stanchions (9 ea)	Port Fc'sle	WSA	ST	ST			22.5	Note 2				
Portable Stanchion Braces (3 ea)	Port Fc'sle	WSA	ST	ST			3.0	Note 2				
Stanchion Braces (2 ea)	Stbd Fc'sle	WSA	ST	ST			6.0	Note 2				
Removable Stanchions (9 ea)	Stbd Fc'sle	WSA	ST	ST			22.5	Note 2				(b)
Hawse Pipe Cover	1-000-0	PC	ST	ST			5.6	Note 4				
Jack Staff Deck Bracket	1-000-1	PC	ST	ST			3.0	Note 4				
S/P Telephone & Jack Box (Double)	1-002-1	PC	BR	ST			1.8	Note 4				
S/P Telephone & Jack Box (Fairway)	1-002-1	PC	BR	ST			1.8	Note 4				
1-MC Speaker	1-002-1	PC	AL	ST			2.5	Note 4				
Lane Roller	1-004-1	WSA	ST	ST			7.9	Note 2				
Chain Locker Cover	1-005-0	WSA	ST	ST			4.8	Note 2				
Raised Deck Hatch	1-005-2	WSA	ST	ST			8.6	Note 2				(a)
Capstan Control Pedestal	1-008-2	WSA	ST	ST			3.0	Note 2				
Capstan Control Box & Lever	1-008-2	WSA	ST	ST			2.5	Note 2				
Windlass Brake Pedestal	1-009-2	WSA	ST	ST			3.0	Note 2				
Windlass Brake Handwheel	1-009-2	PC	BR	ST			1.5	Note 4				
Chain Locker Cover	1-012-0	WSA	ST	ST			4.8	Note 2				
Hawse Pipe Cover	1-013-0	WSA	ST	ST			5.6	Note 2				
Port Bbr Vlve, Piping, Elbows & Hndwhls (2 ea)	1-014-1	PC	BR	AL			5.5	Note 4				
2-1/2" Firemain Valve	1-016-1	PC	BR	ST			5.5	Note 4				
2-1/2" Firemain Handwheel	1-016-1	PC	BR	BR			1.0	Note 4				
2-1/2" Firemain Strainer	1-016-1	PC	BR	BR			2.5	Note 4				
2-1/2" Firemain Strainer Handle	1-016-1	WSA	ST	BR			1.4	Note 2				
Raised Deck Hatch	1-016-2	WSA	ST	ST			8.6	Note 2				(a)
Hand-Hold Bars (10 ea)	1-021-0	WSA	ST	BR/			15	Note 2				
Defroster Pipes	1-021-0	PC	AL	GRP			3.0	Note 4				
Door Hinges (4 ea)	1-021-0	WSA	ST	GRP			4.0	Note 2				
Ladders (2 Steel, 1 ea)	1-021-0	WSA	ST	ST			4.1	Note 2				
Telescope Cover	1-021-0	PC	AL	AL			6.0	Note 4				
Electrical Outlet Box								Note 4				

Ref: a

199

MAINTENANCE REQUIREMENT CARDS (MRC)

NAVY JOB PERFORMANCE AID FOR SHIP'S FORCE

- WHAT
- WHEN
- HOW
- WHO

THREE DRAFT CC MRC DEVELOPED

1 - CC INSPECTION FOR AN AVAILABILITY

2 - CC INSPECTION MAINTENANCE AND REPAIR

3 - FASTENERS CC INSPECTION, MAINTENANCE AND REPLACEMENT

Ref. 5

MAINTENANCE REQUIREMENT CARD (MRC)
FOR
CC-INSPECTION FOR AN AVAILABILITY

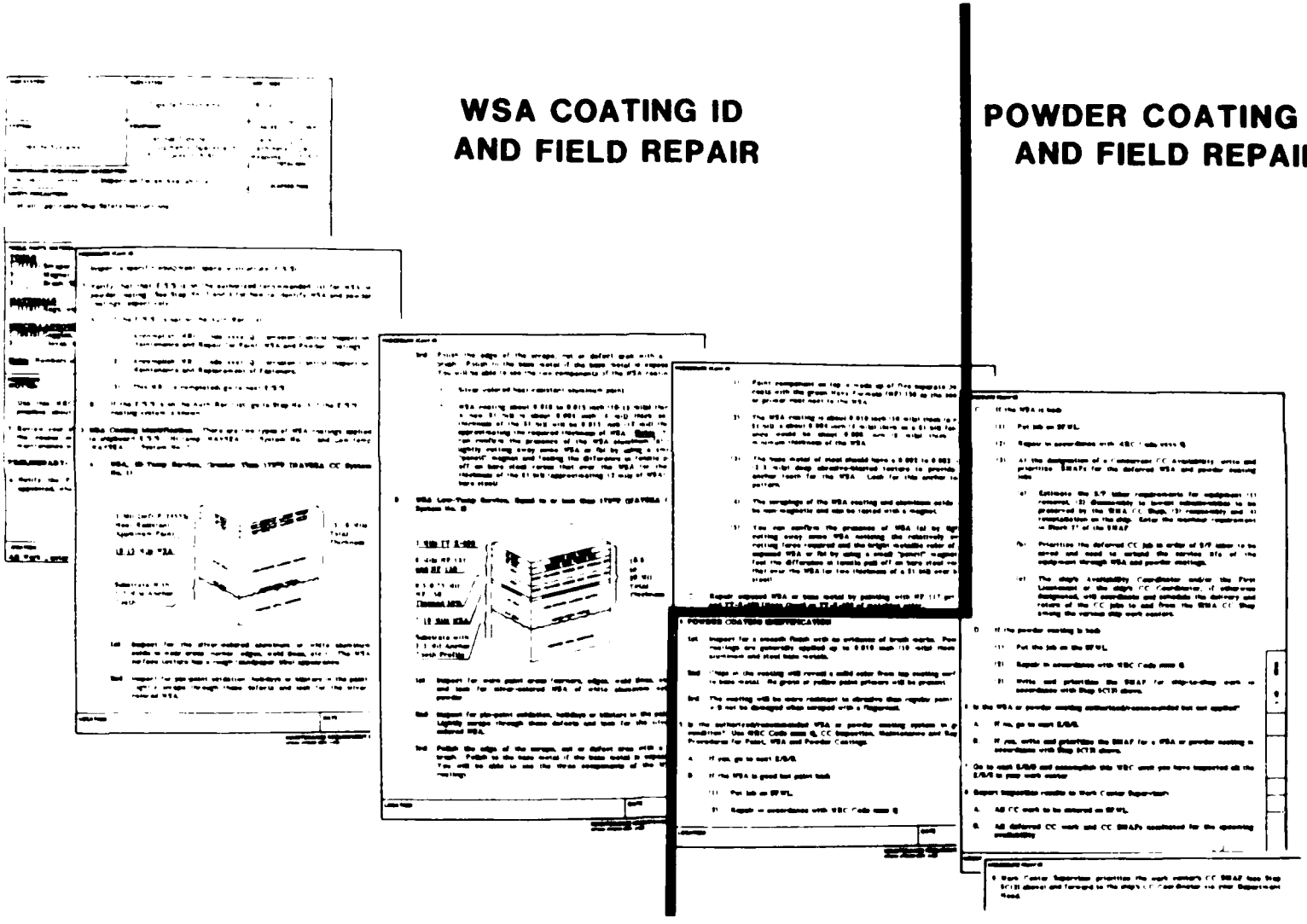

Ref. 5

MAINTENANCE REQUIREMENT CARD (MRC) FOR CC-INSPECTION MAINTENANCE AND REPAIR

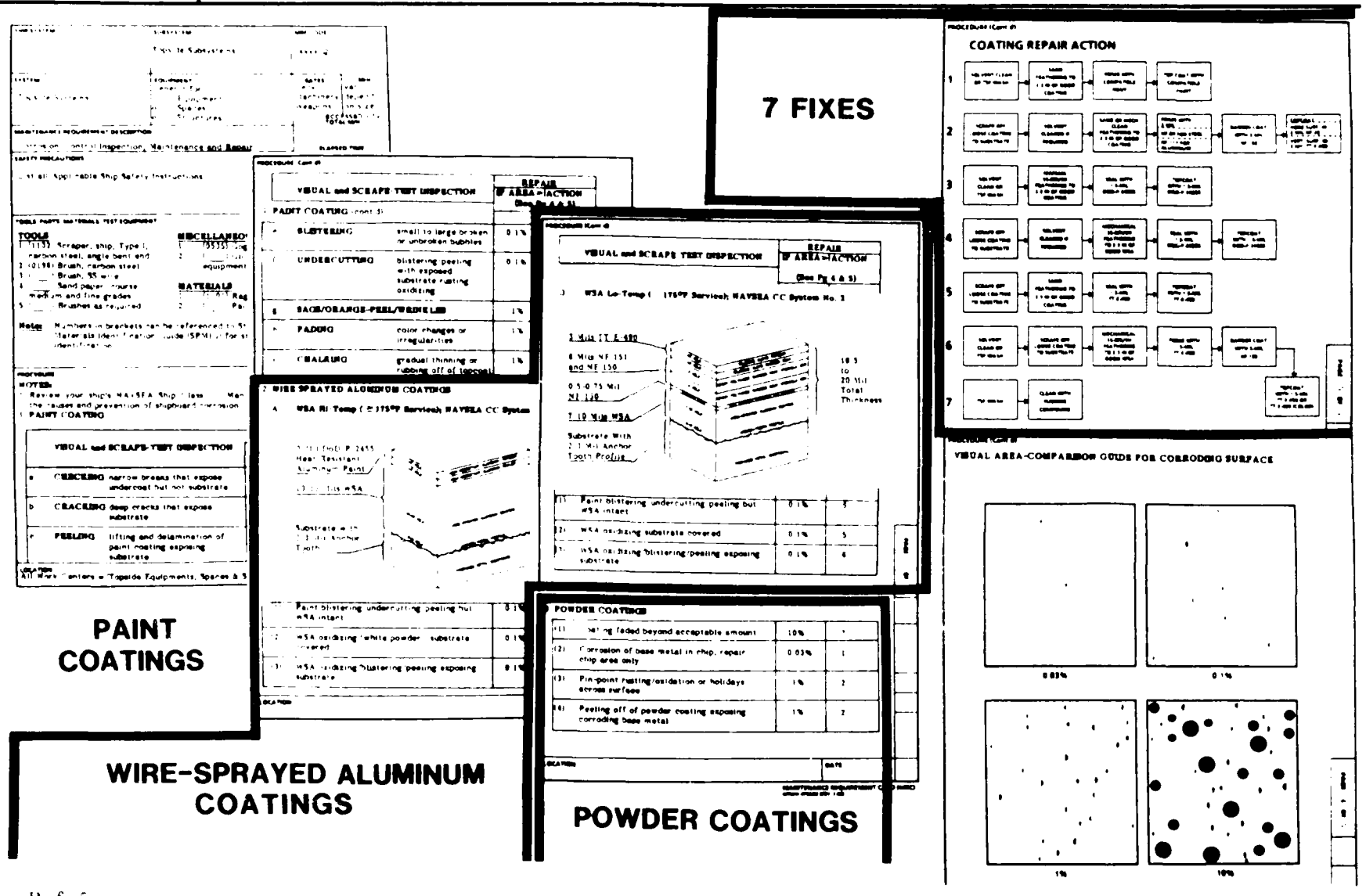

Ref. 5

MAINTENANCE REQUIREMENT CARD (MRC) FOR FASTENERS, CC-INSPECTION AND REPLACEMENT

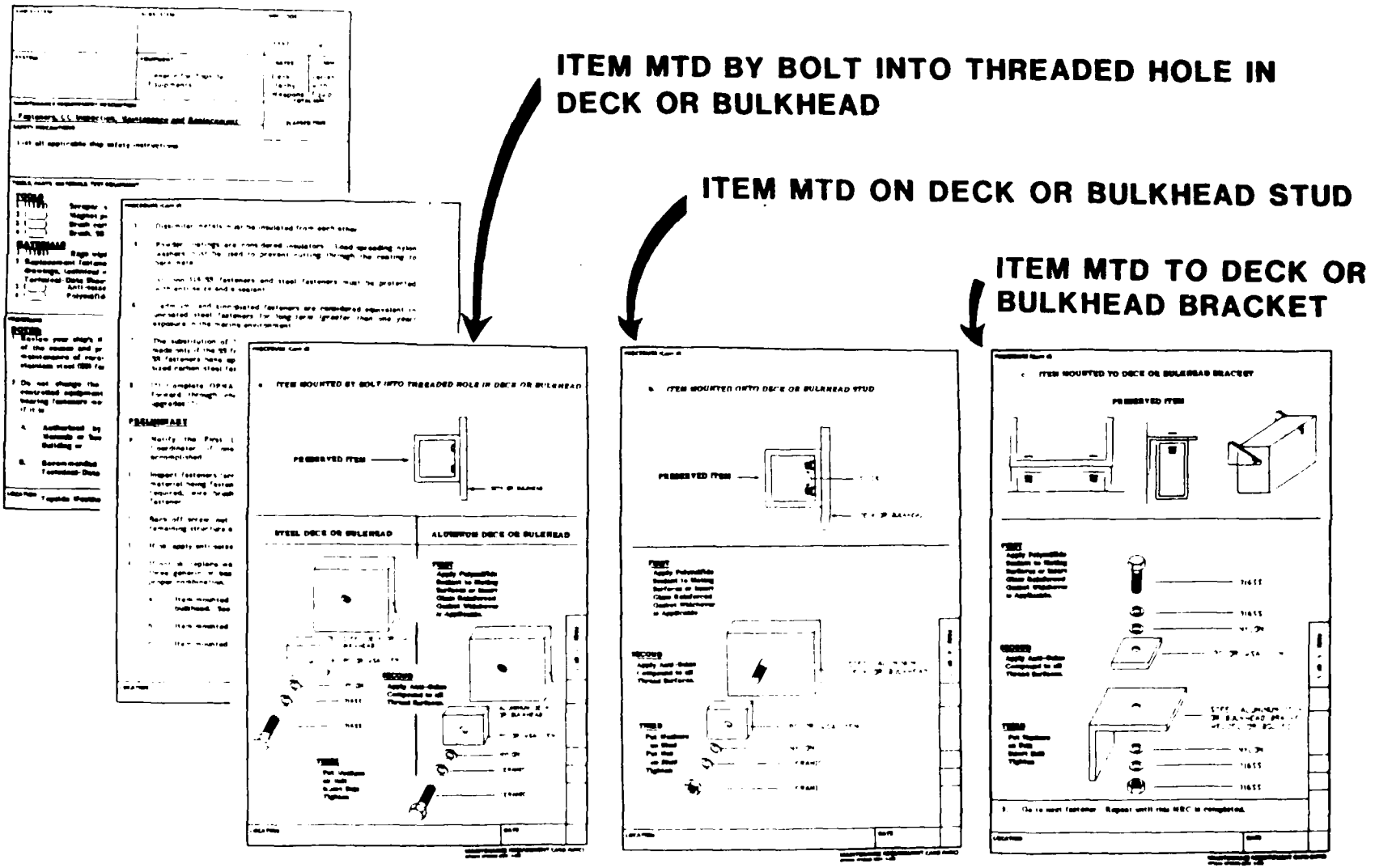

Ref. 5

- 27 COMPLETED — AUG 86 TO MAY 87
- 6 IN PROGRESS

SHIP	# CANDIDATE ITEMS		
	WSA CTG	PDR CTG	TOTAL
USS BREWTON (FF 1086) (KNOX CL)	277	659	936
USS GRIDLEY (CG 21) (LEAHY CL)	198	434	632
USS JOSEPH STRAUSS (DDG 16) (ADAMS CL)	185	480	665
USS ALAMO (LSD 33) (THOMASTON CL)	409	524	933
USS CHANDLER (DDG 996) (KIDD CL)	232	870	1102
USS LONG BEACH (CGN 9) (LONG BEACH CL)	675	1118	1793

Refs. 5,7

SHIP'S CC WORK PACKAGE GUIDE

SUMMARY

SUMMARY

- DEMONSTRATED FEASIBILITY OF SIMA CC SHOP
- $1.5 M/YR FOR CC SHOPS IN SIMA UPGRADE PROGRAM FY-86 THROUGH FY-91
- IPE, INDUSTRIAL PROCESSES AND QC ESTABLISHED

  BUT

  REFINEMENT REQUIRED FOR WSA TOP COATING AND POWDER COATING MATERIAL SPECIFICATION
- FLEET-WIDE, POLICY PROCEDURES AND TRAINING REQUIRED

40

CC SERVICES DELIVERY

SUMMARY

- PLANNING AND CONFIGURATION CONTROL
- PRODUCTION
- QUALITY CONTROL
- RECORDS, AUDIT AND FEEDBACK

41

PRODUCTION

SUMMARY

PERSONNEL

FACILITY

IPE

PROCESS INSTRUCTIONS

CONSUMABLES

QUALITY CONTROL

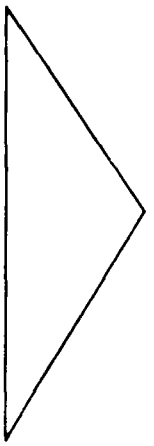

PRODUCTION

SERVICES

42

POLICY, PROCEDURES & TRAINING (REFINEMENTS & IMPROVEMENTS)

SUMMARY

CC SERVICES	PERSONNEL
• CONFIGURATION CONTROL	• CAREER PATH FOR BOATSWAIN MATE (BM) & HULL TECH (HT)
• PLANNING & SCHEDULING SMAF→CSMP→WORK ORDER	• RATE TRAINING MANUAL
• PRODUCTION	• ON-BOARD TRAINING
• QC & FEEDBACK	• SHOP QUALIFICATION IMPROVEMENT PROGRAM (SQIP) TRAINING

43

SESSION B
SPECIAL TOPICS-I

Chairman
Richard Carlston
TRW

Corrosion Prevention and Control Surveys

AFR 400-44 requires a Corrosion Prevention and Control Survey of each operating command every four years. This results in two to three surveys being conducted each year. This comprehensive survey covers all aspects of the command program including the command corrosion regulation, local Maintenance Operating Instructions, corrosion facilities, training, manpower and quality control as well as the condition of the equipment itself.

The survey team is made up of a cross section of personnel with expertise over a broad range of the corrosion discipline. An Air Corrosion Program representative leads the team which includes a Sr. NCO with specific corrosion shop experience, the command corrosion manager, ALC corrosion program managers, an AF Materials Lab representative, as well as members from AFALC and SA-ALC (with responsibility for corrosion control chemicals). Often representation from System Program Managers will also enhance the team capability. The benefits from such surveys are numerous. In addition to the obvious benefits there are intangible benefits in the solving of local problems at the local level and firsthand AFLC/AFSC knowledge of field problems. The cross feed of information between team members also serves as a valuable avenue of technology transfer.

Many times previously identified problems of significance are discovered. Action items are assigned to address all problems other than those which are unique to a particular base. The action is then reported quarterly until the item is closed. These items are included in a final survey report which is circulated throughout the Air Force.

AIR FORCE FAILURE ANALYSIS — CORROSION OF STRUCTURAL MATERIALS

RON WILLIAMS

FY	STRUCTURAL	ELECTRONIC	CORROSION	NDI	TOTAL
1983	39	16	16	---	71
1984	53	21	5	---	79
1985	65	29	4	1	99
1986	51	26	6	7	90
1987	13	10	3	5	31

SAUDIA ARABIA
SAND PROBLEM

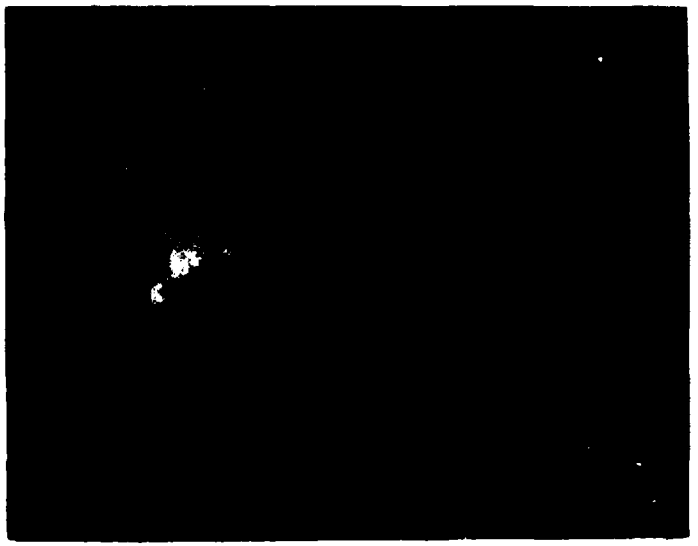

F-16 AIRCRAFT

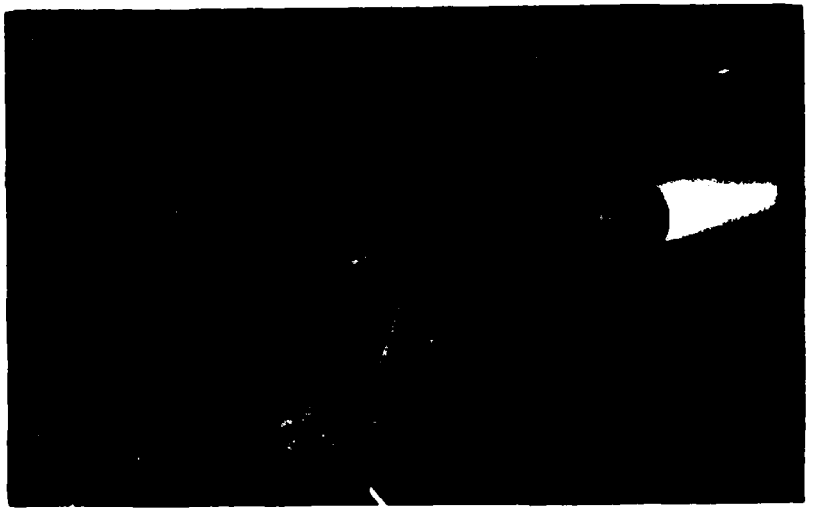

F-100 ENGINE

1st STAGE TURBINE
BLADE DISTRESS

AIRFOIL CLOSE-UP SAND WING
ATTACHED SAND RESIDUE

SAND POWDER PARTICLES
BELOW BLADE PLATFORM

ANALYSES PERFORMED

A. CHEMISTRY OF SUBMITTED SAND AND ROCK SAMPLES TAKEN AT SEVERAL IN COUNTRY AIR BASES

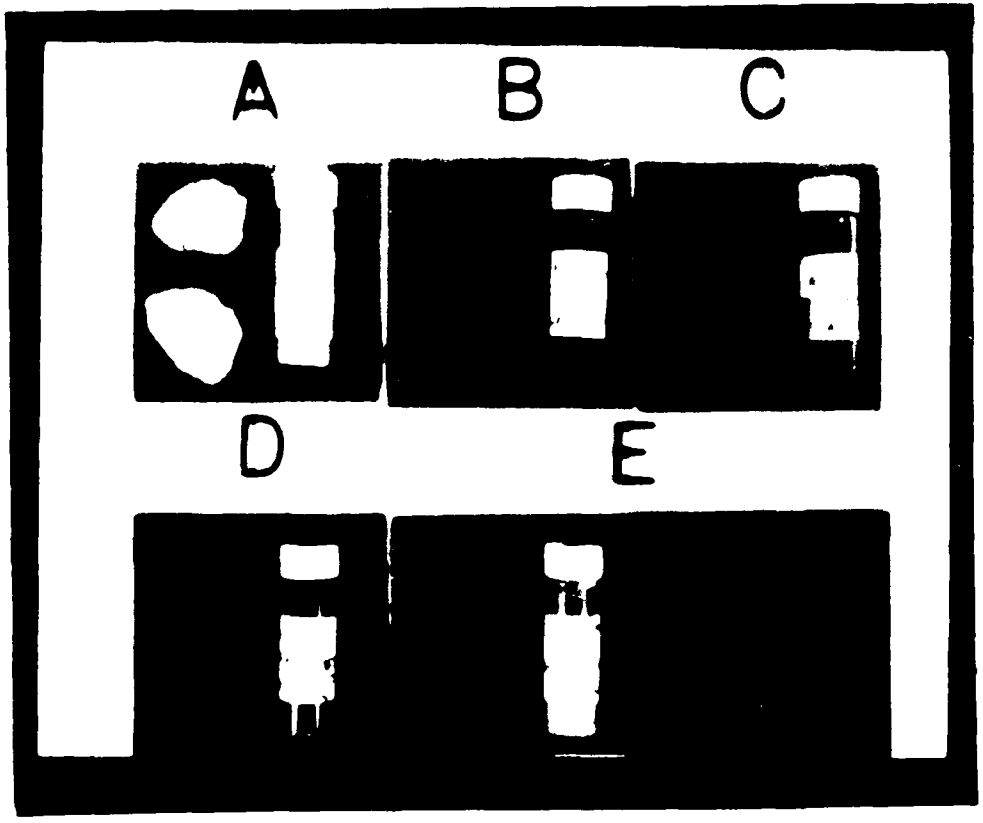

ELMENDORF AFB

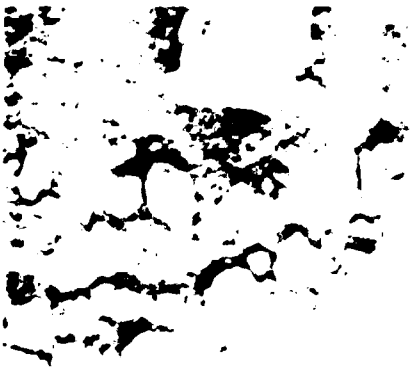

NELLIS AFB

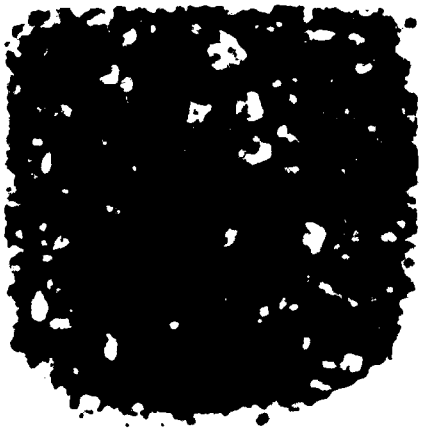

McENTIRE AFB

SHAW AFB

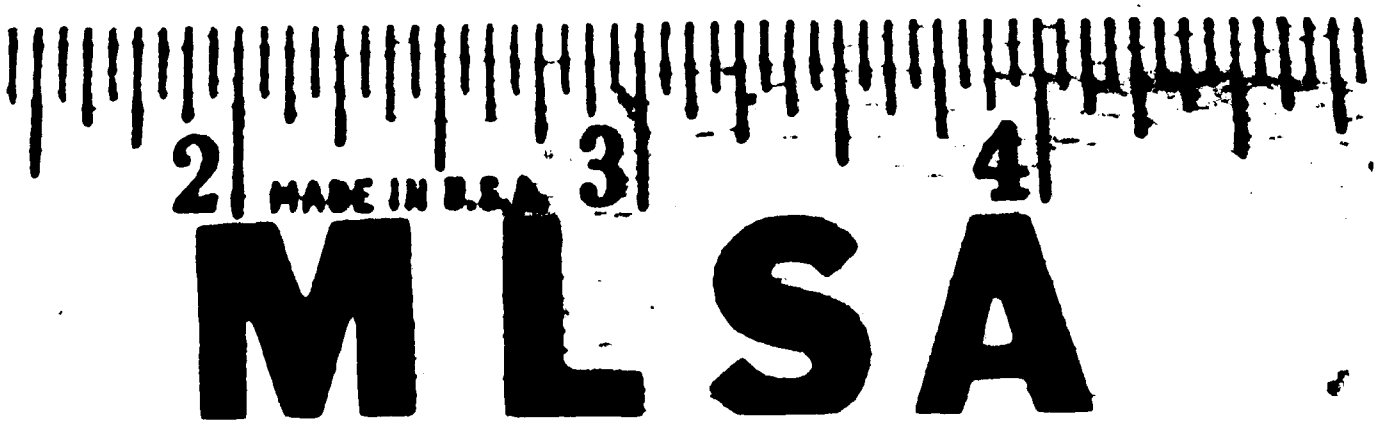

B. MATERIAL IDENTIFICATION ON AIR FOIL SURFACES USING SCANNING ELECTON MICROSCOPY

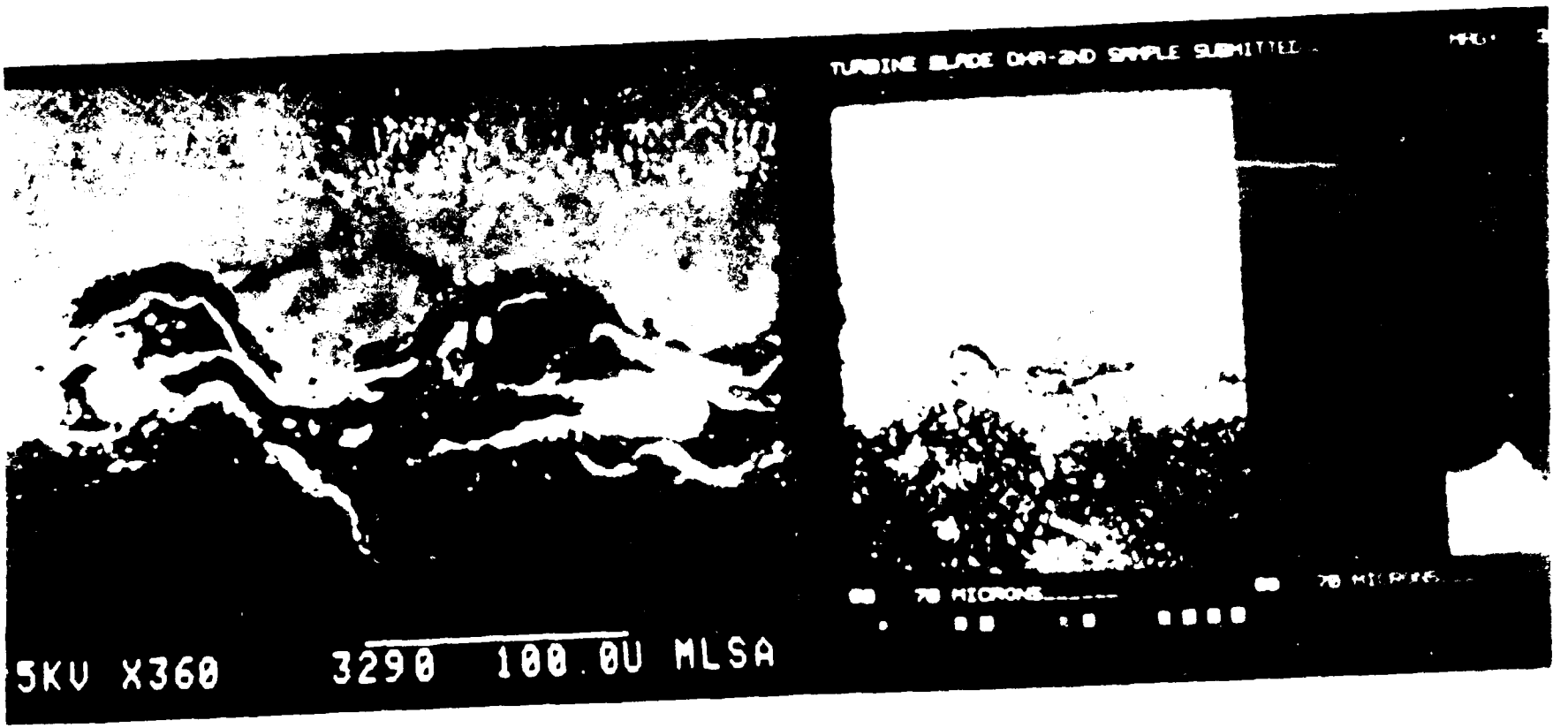

BLADE CROSS SECTION
SHOWING FLUXING OF COATING

ENERGY DISPERSING ANALYSIS
SHOWING CALCIUM CONTAMINATION

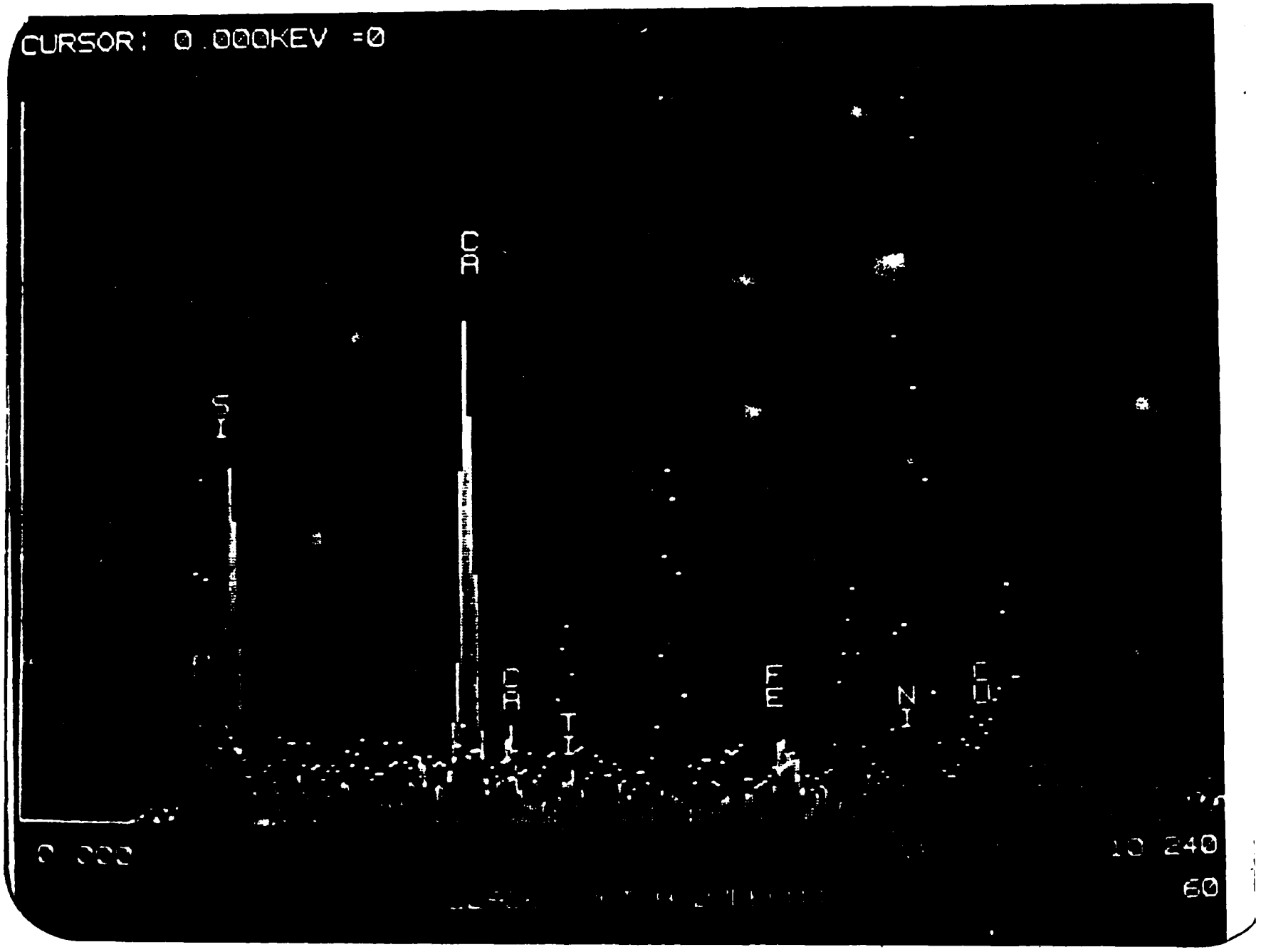
CURSOR: 0.000KEV =0
CA
SI
CA
TI
FE
NI
CO
0.000
10.240
60

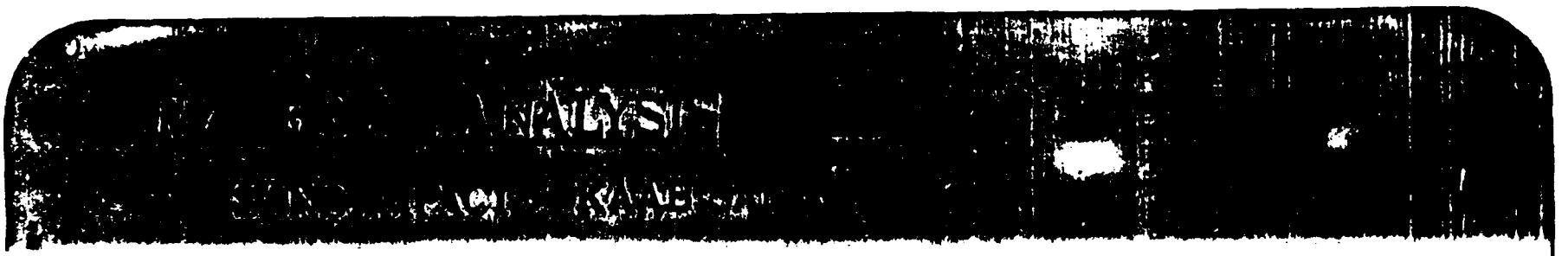

KAAB SAND

- OXIDES AND CARBONATES OF CALCIUM AND MAGNESIUM 70% BY WEIGHT
- SILICON DIOXIDE 25% BY WEIGHT

CHARACTERISTICS

- MORE CHEMICALLY REACTIVE THAN SAE J726B
- MOLTEN AT ABOUT 2100°F (1148°C)
- ≈ 1000°F (538°C) LOWER THAN SAE J726B SAND

F100 VS. OTHER ENGINES AT KAAB

- HIGHER TURBINE INLET TEMP ALLOWS SAND TO ADHERE TO AIRFOILS
- COOLED AIRFOILS ARE IMPACTED BY INCREASED HEAT FLUX FROM ROUGH (GLAZED) AIRFOILS

CONCLUSIONS

- THE PRESENCE OF LOW MELTING ELEMENTS IN THE SAND DEPOSITS AND SUBSEQUENT RESIDUE BUILD-UP CAUSED MELTING OF AIRFOIL COATING AND SUBSTRATE MATERIAL

- SAND PARTICLE BLOCKAGE OF AIRFOIL COOLING HOLE PASSAGES CONTRIBUTED TO INTERRUPTED AIR FLOW AND SUBSEQUENT DISTRESS TO AIRFOILS

PROPOSED CLEANING SOLUTION

SOLUTION A

- HYDROXYLAMINE SULFATE & WATER
- PH 3-4

SOLUTION B

- AMMONIUM HYDROXIDE & ETHYLENE DIAMINE & WATER

&

HYDROXYETHYLETHYLENE DIAMINETRIACETIC ACID (HEDTA)

&

AMMONIUM SULFAMATE

- PH 9-10

PROPOSED CLEANING SOLUTION (CONT'D)

- INGESTED FORWARD OF 1ST STAGE TURBINE VANES
- DOSAGE - 8 TO 10 GALLONS / WASHING
- 8-10 GALLONS OF WATER FOR RINSE
- RECENTLY ADOPTED IN SAUDI ARABIA ON TRIAL BASIS

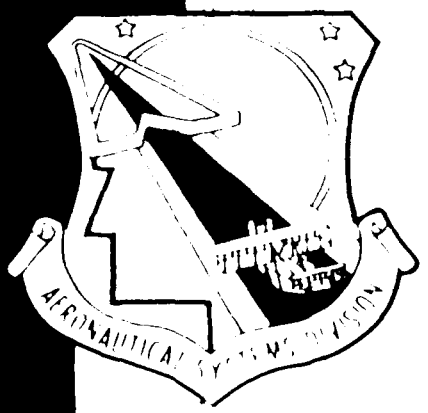

SEAT ARMREST CORROSION

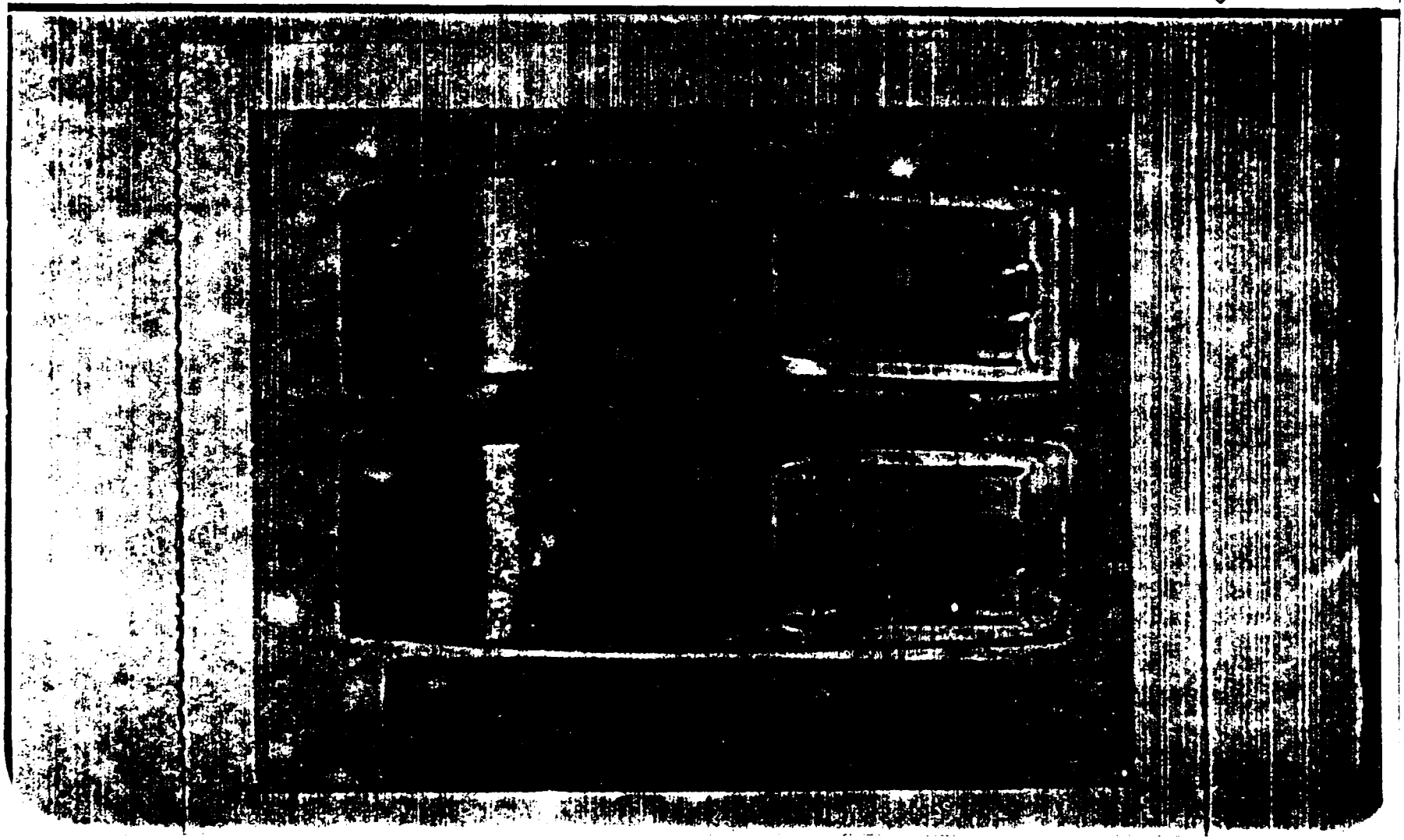

Structural and Electronic Failure Analysis
Materials Integrity Branch
Systems Support Division

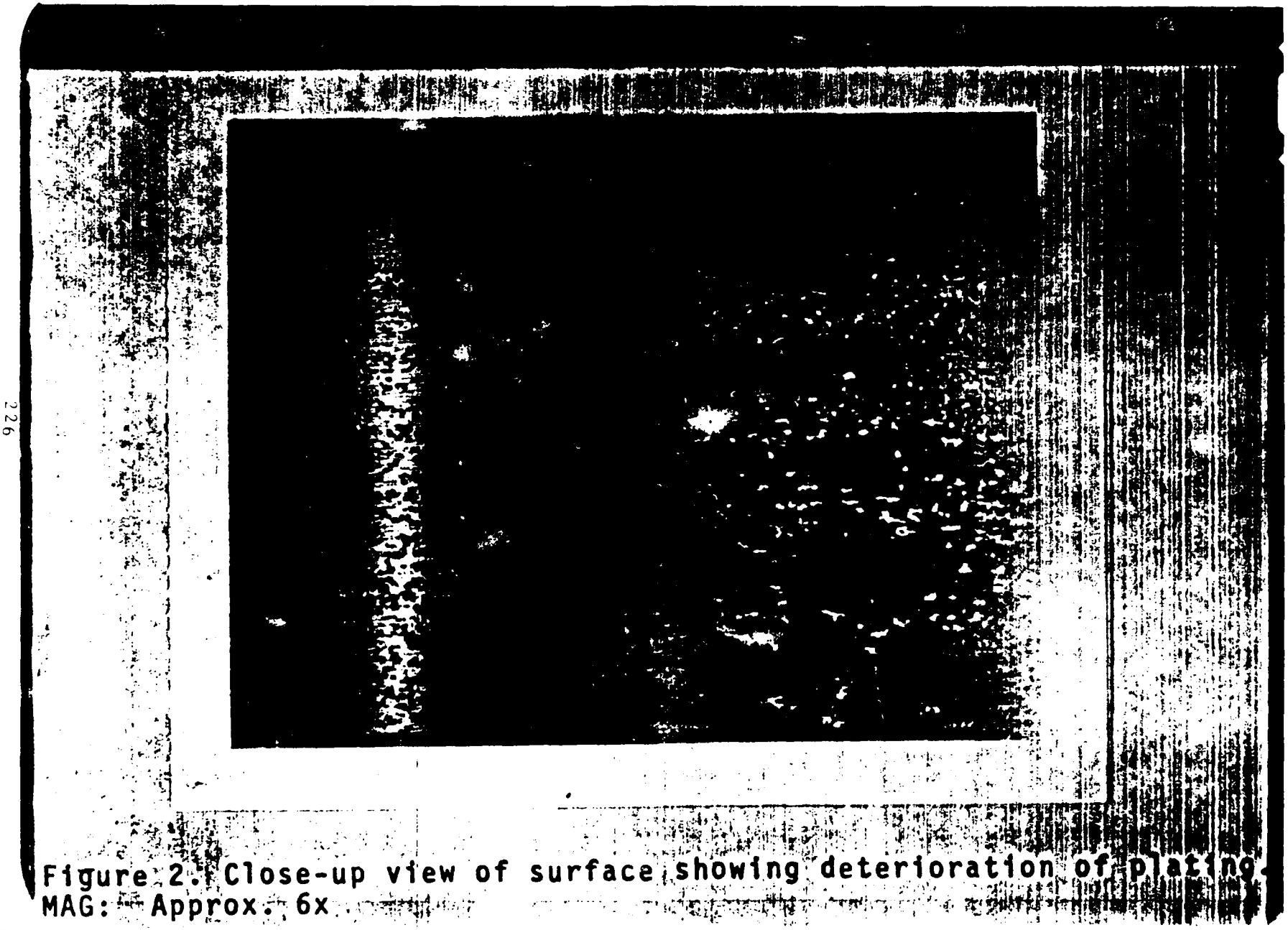

Figure 2. Close-up view of surface showing deterioration of plating.
MAG: Approx. 6x

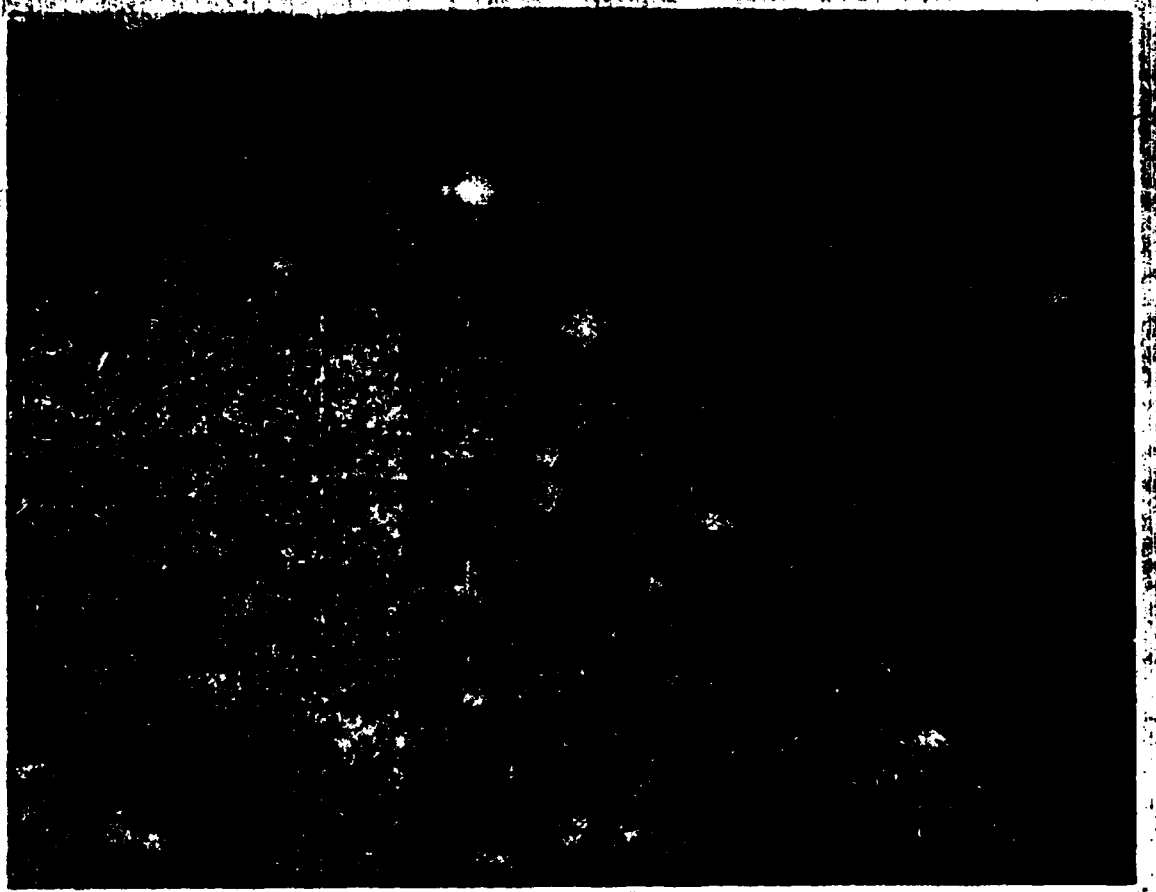

Figure 3. Cracks and separation of plating from aluminum base material. MAG: 325x

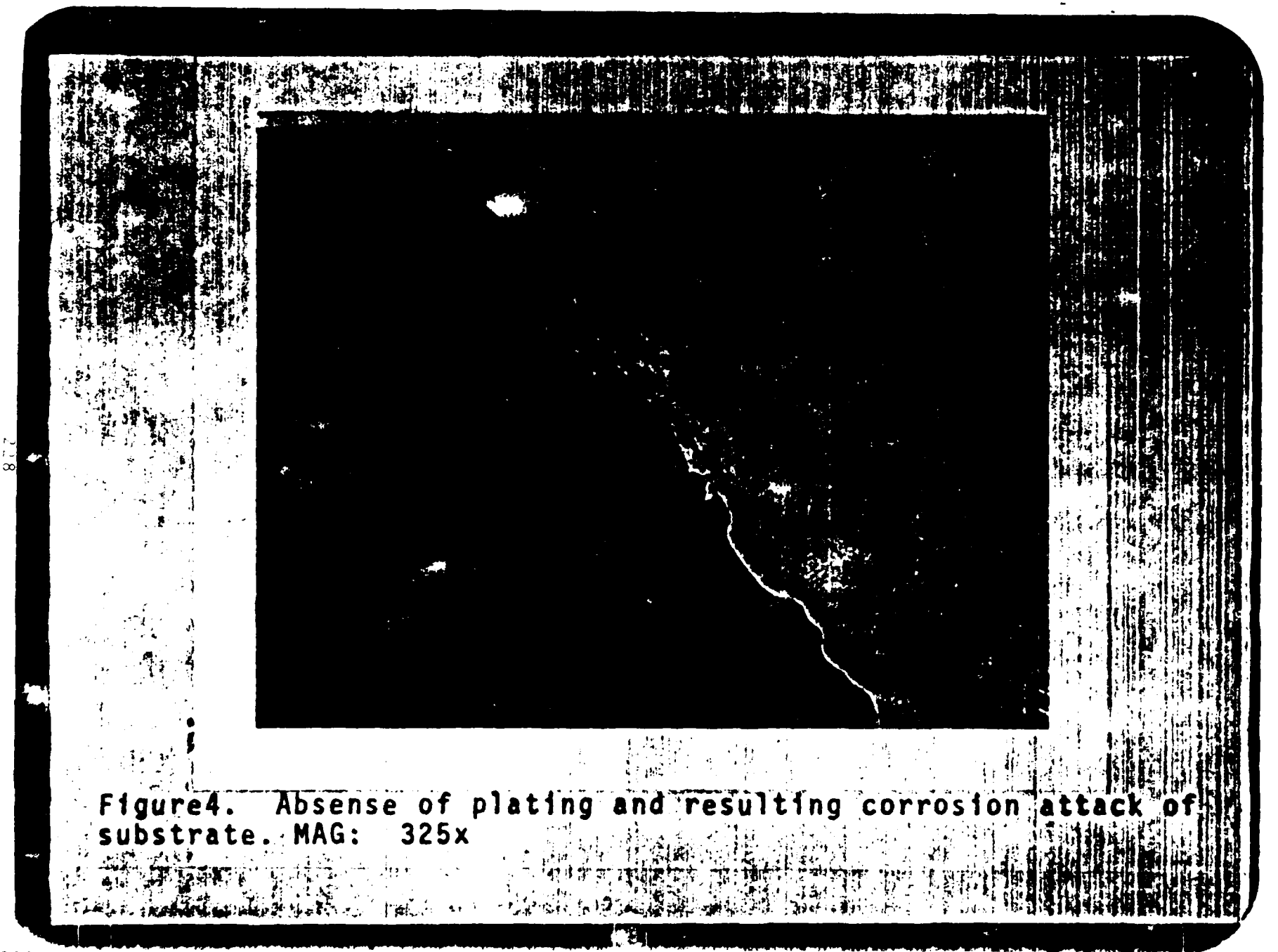

Figure4. Absense of plating and resulting corrosion attack of substrate. MAG: 325x

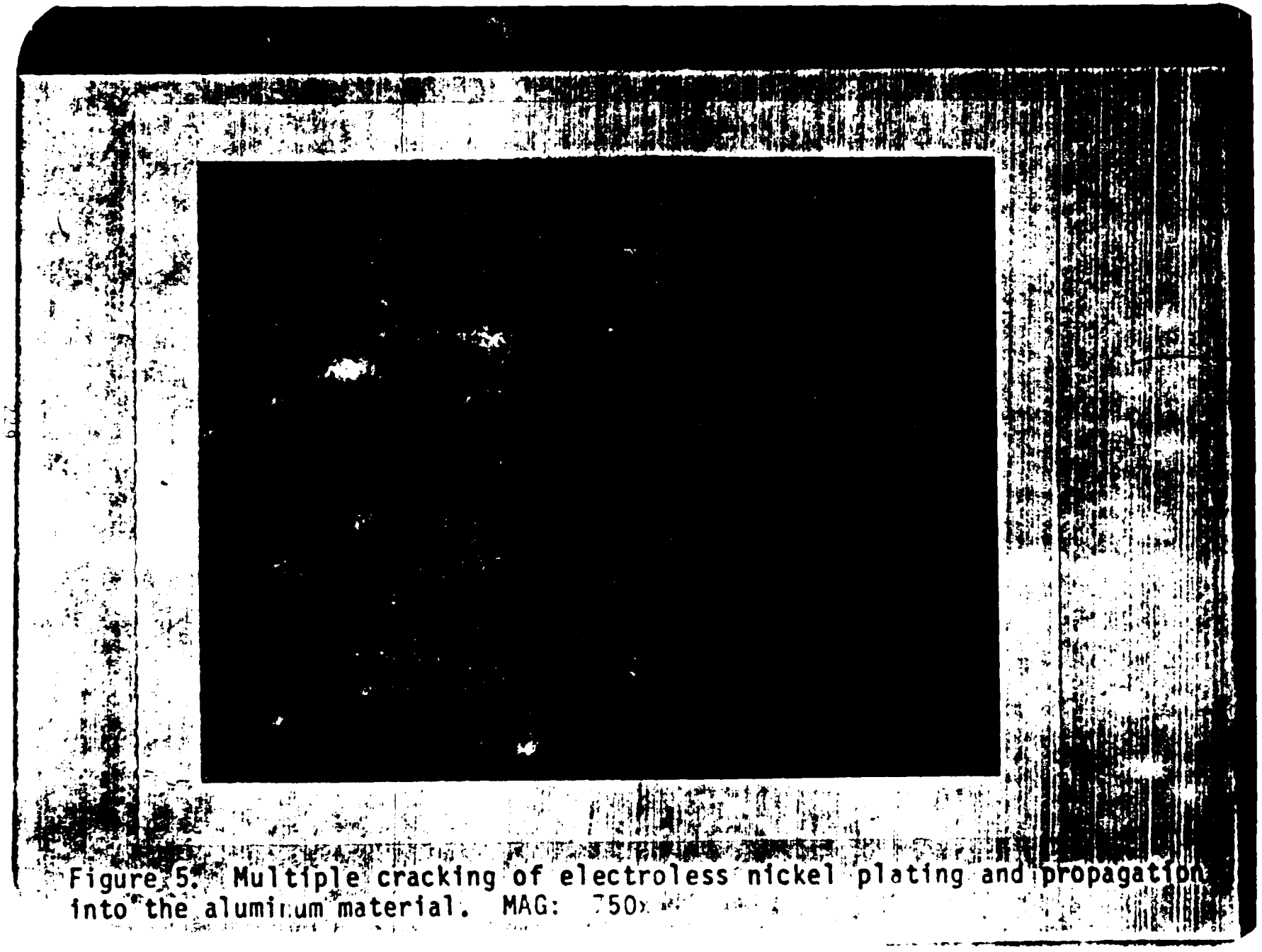

Figure 5. Multiple cracking of electroless nickel plating and propagation into the aluminum material. MAG: 750x

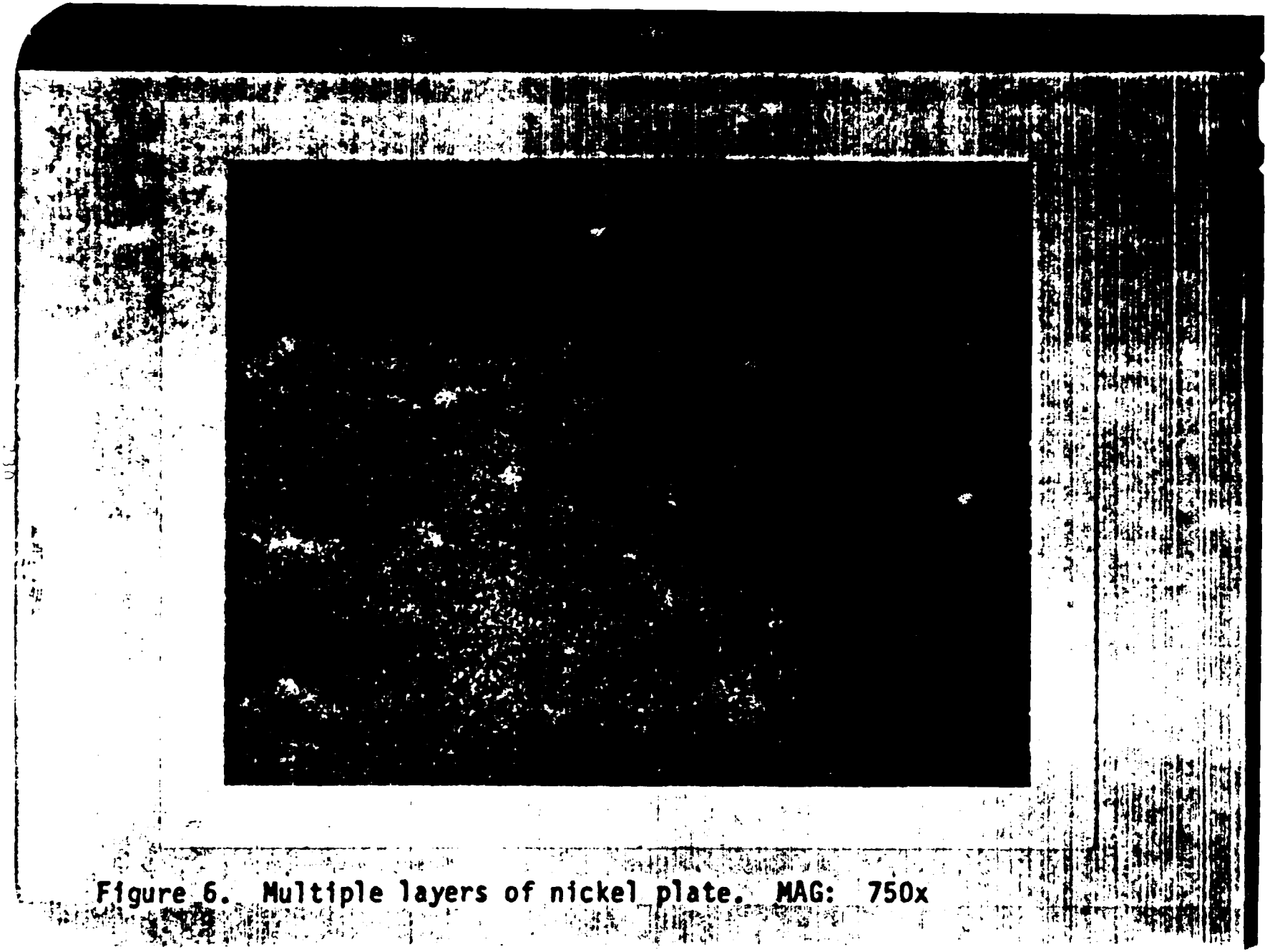

Figure 6. Multiple layers of nickel plate. MAG: 750x

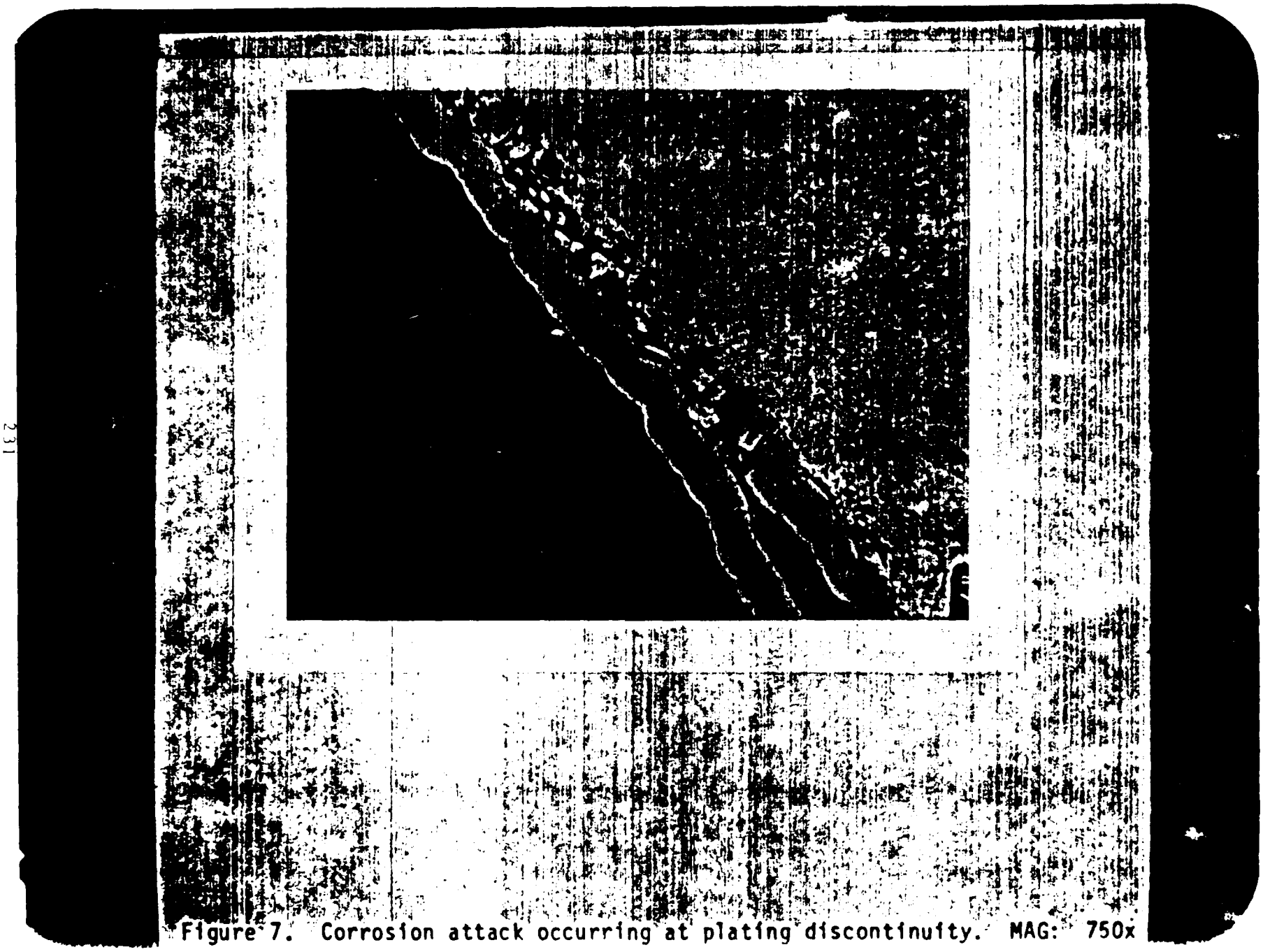

Figure 7. Corrosion attack occurring at plating discontinuity. MAG: 750x

RECOMMENDATIONS

- THE USE OF ELECTROLESS NICKEL PLATING SHOULD BE DISCONTINUED DUE TO ITS SUSCEPTIBILITY TO GALVANIC CORROSION WITH ALUMINUM.

- CANDIDATE ALTERNATIVES WOULD BE EITHER BARE ALUMINUM OR 300 SERIES STAINLESS STEEL. ANOTHER CHOICE WOULD BE WATER-SEALED SULFURIC ACID ANODIZED ALUMINUM.

CONCLUSION

- VOIDING OF THE ELECTROLESS NICKEL PLATING CAUSED A GALVANIC CELL BETWEEN THE PLATING AND SUBSTRATE AND ULTIMATE CORROSION OF THE ALUMINUM MATERIAL.

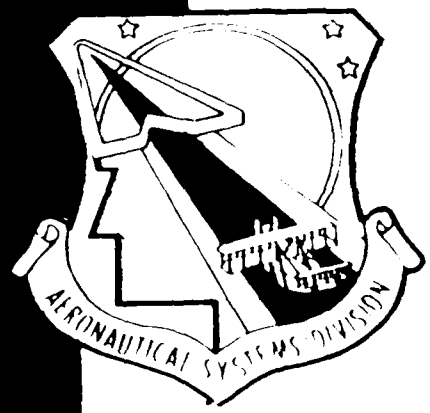

ARMAMENT EJECTOR RACK CORROSION

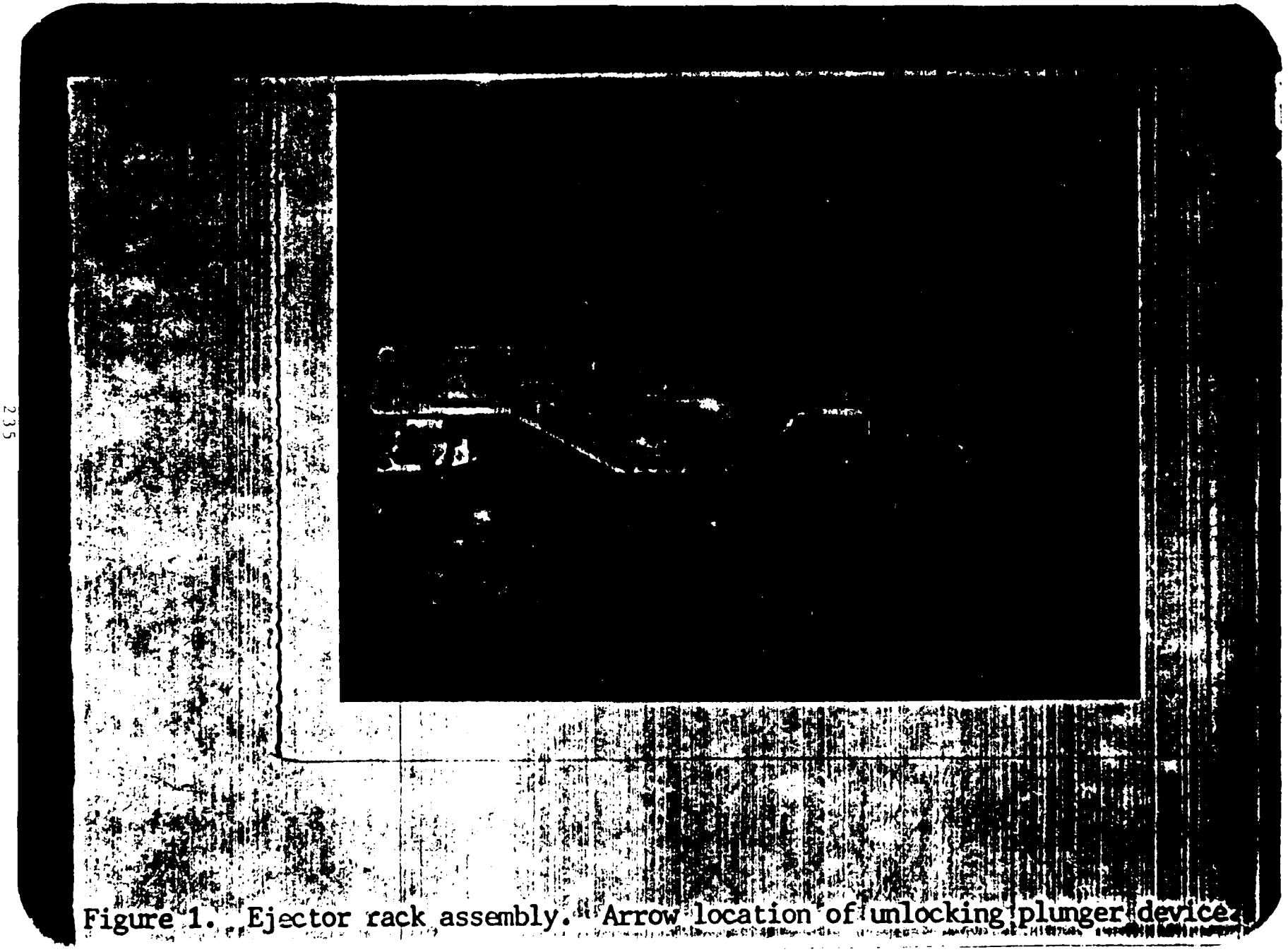

Figure 1. Ejector rack assembly. Arrow location of unlocking plunger device.

Figure 2. Unlocking plunger assemblies each fractured at [illegible] threads and cylinder wall surfaces.

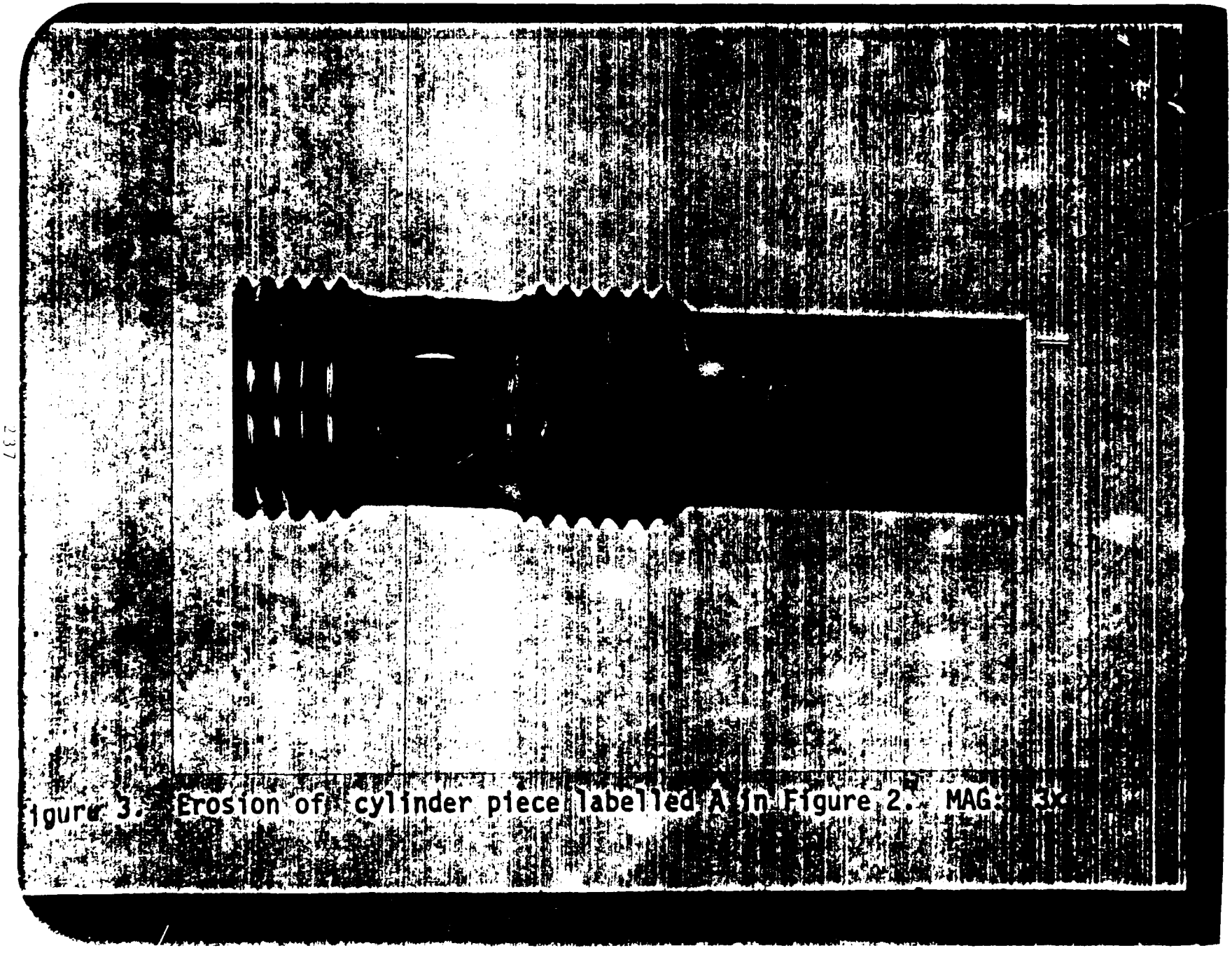

Figure 3. Erosion of cylinder piece labelled A in Figure 2. MAG: 3X

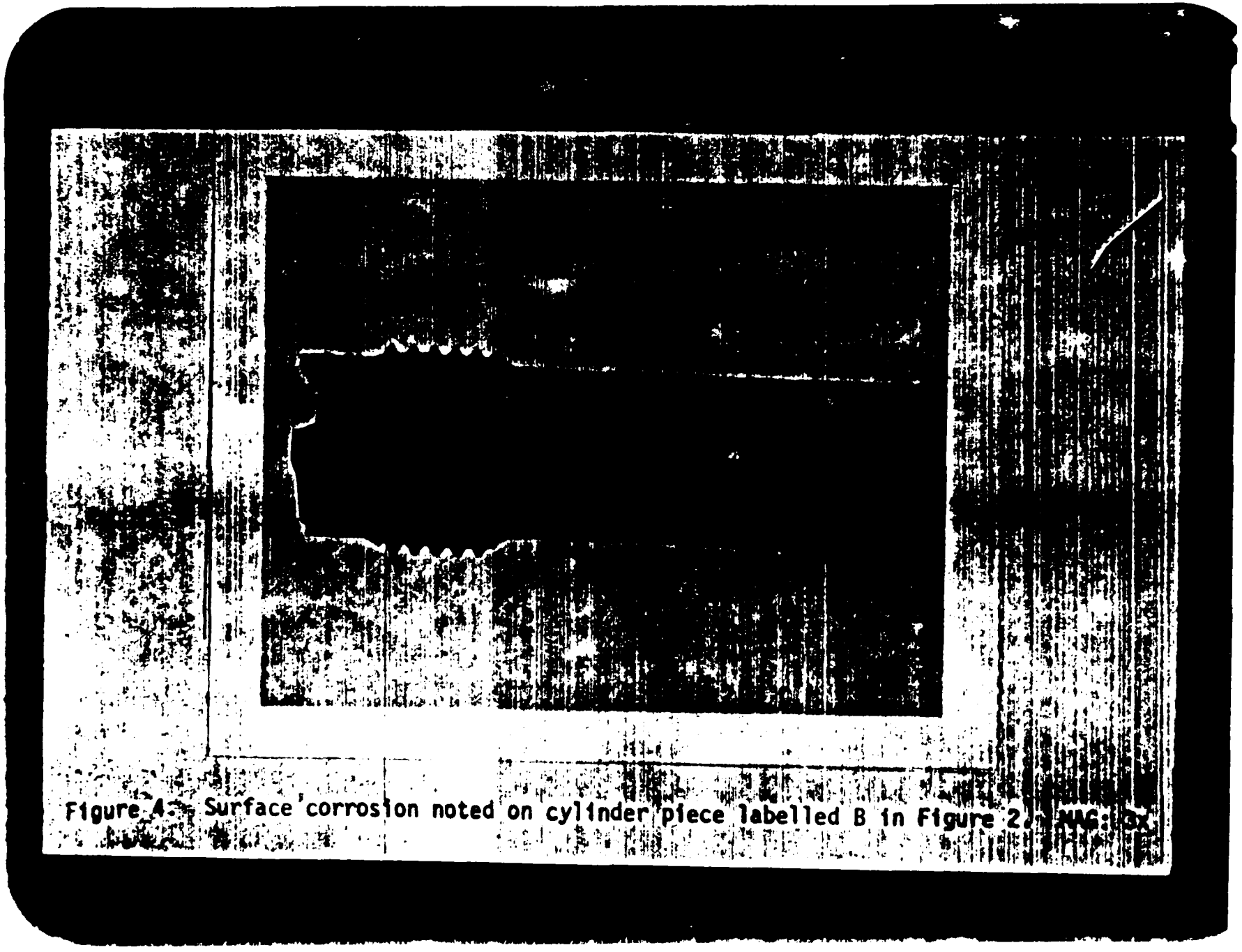

Figure 4: Surface corrosion noted on cylinder piece labelled B in Figure 2. MAG: 8X

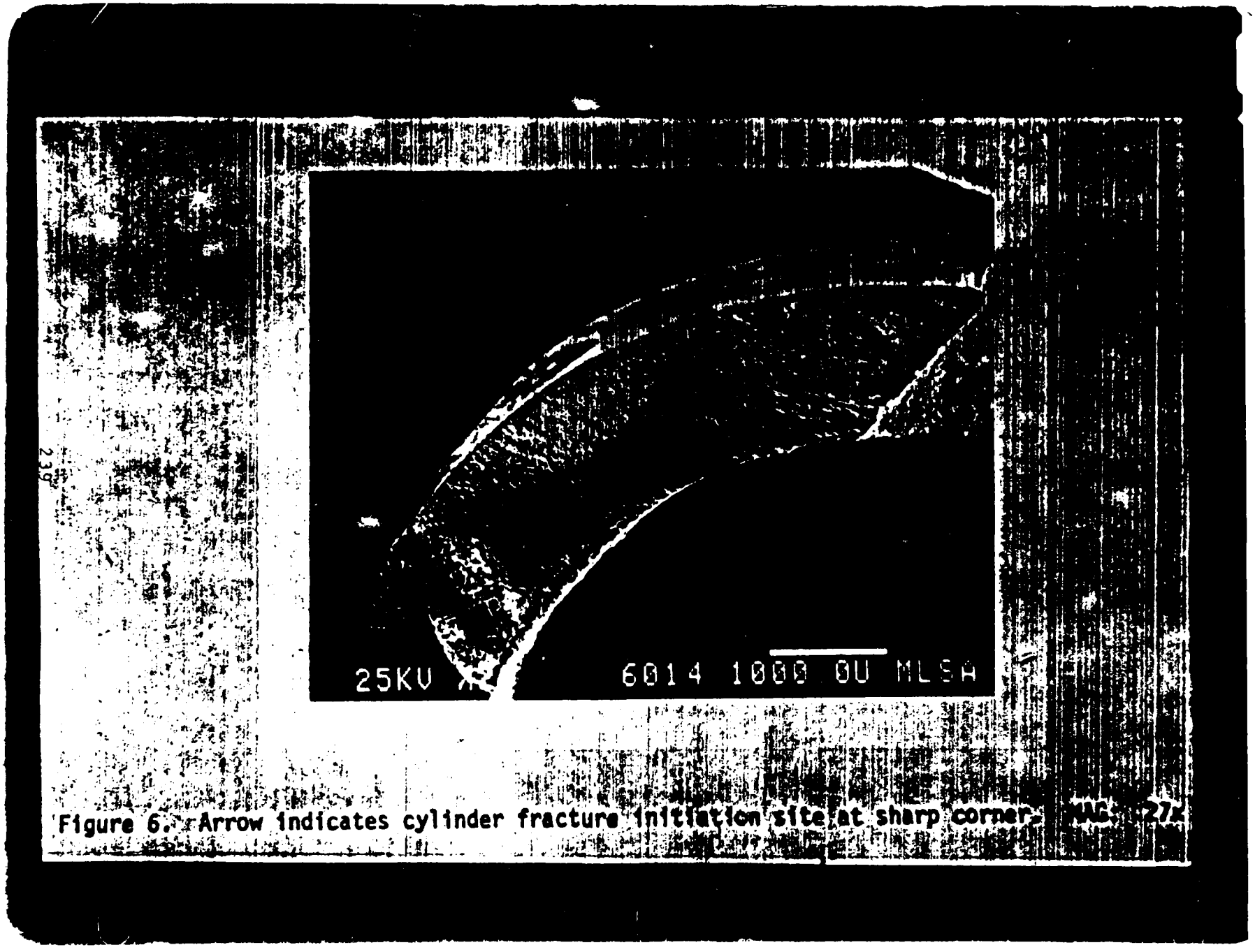

Figure 6. Arrow indicates cylinder fracture initiation site at sharp corner. MAG. 27X

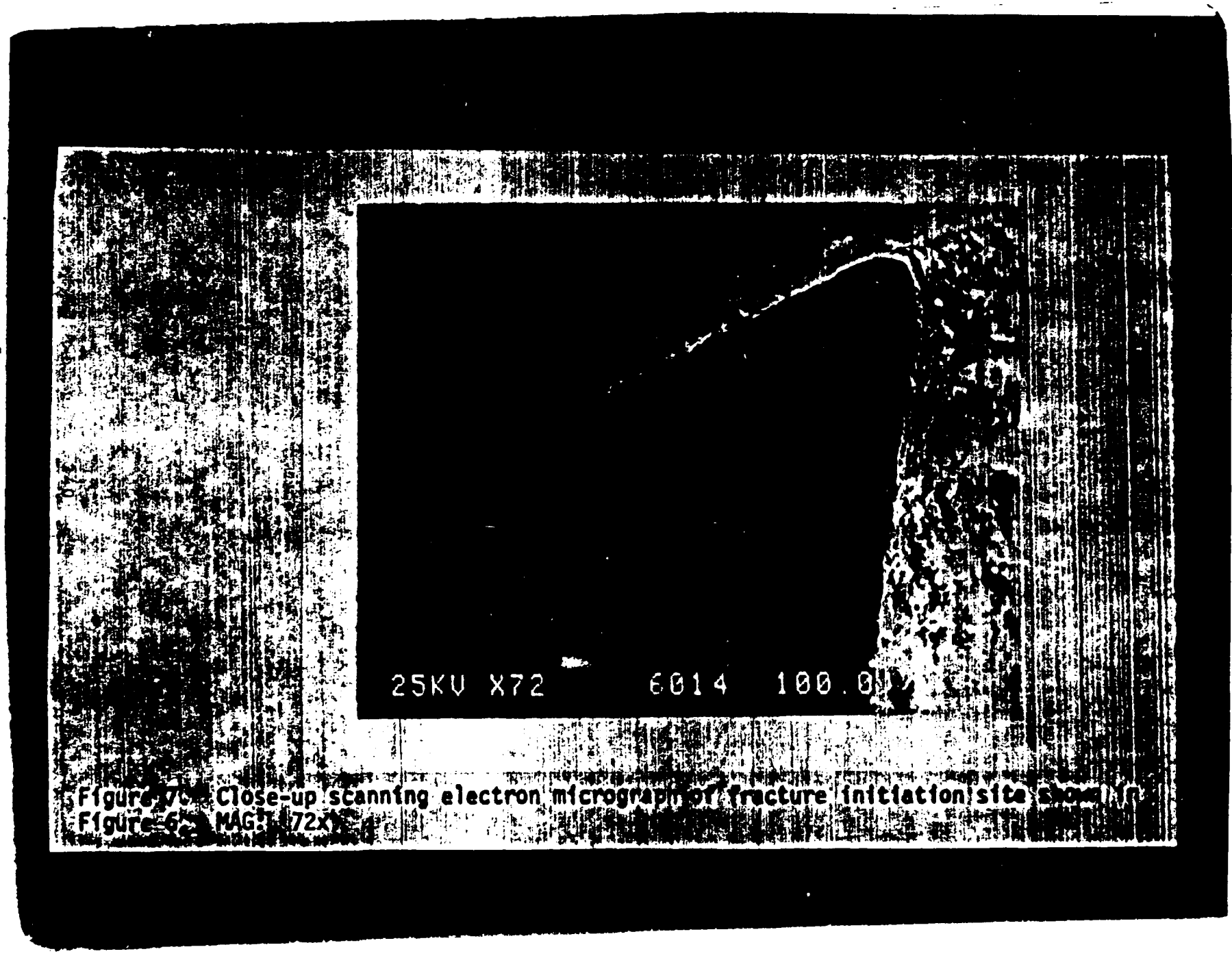

Figure 6. Close-up scanning electron micrograph of fracture initiation site shown in Figure 6. MAG: (72X)

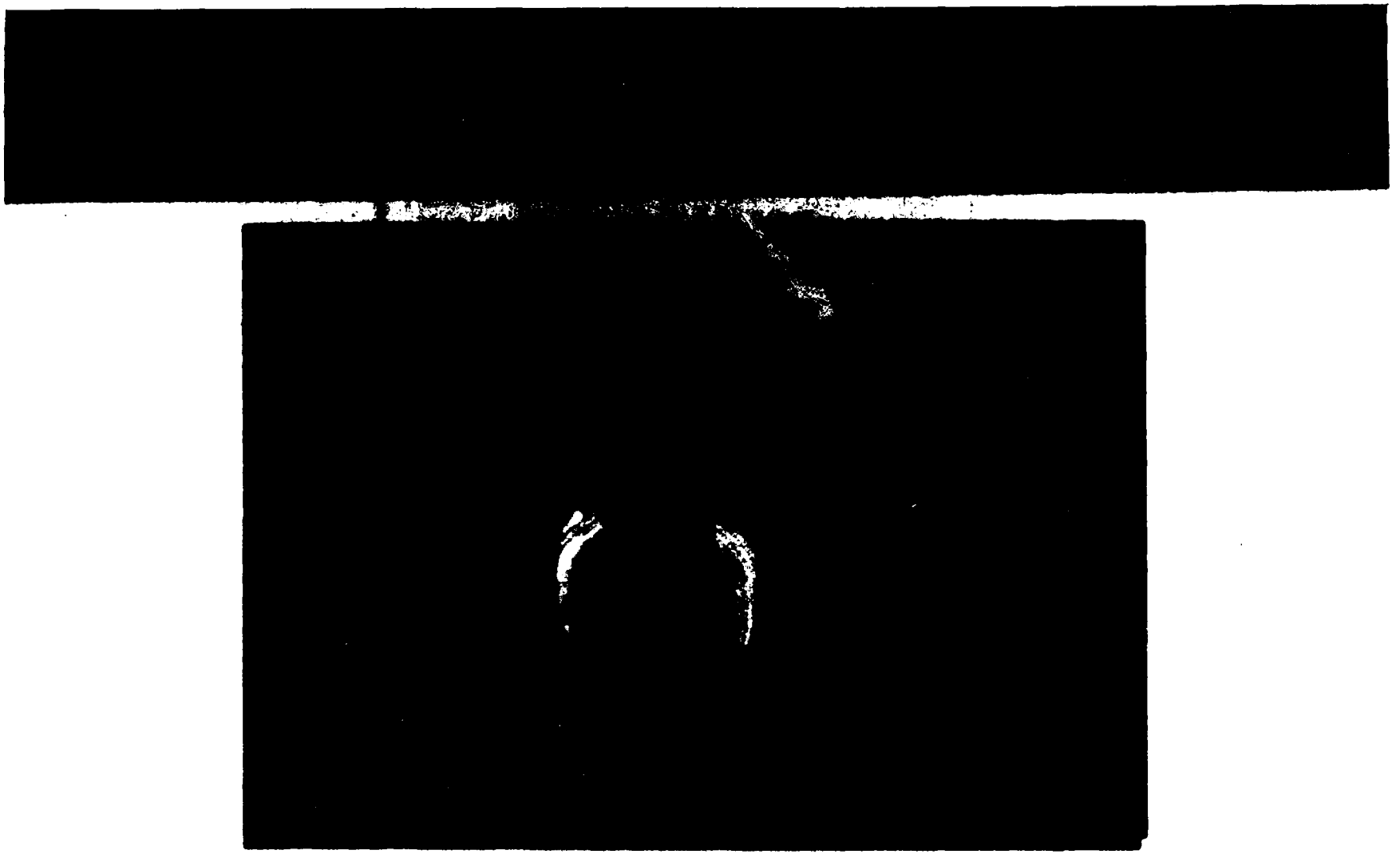

Figure 8. Erosion and corrosion of the ejector rack cylinder assembly housing at threaded area.

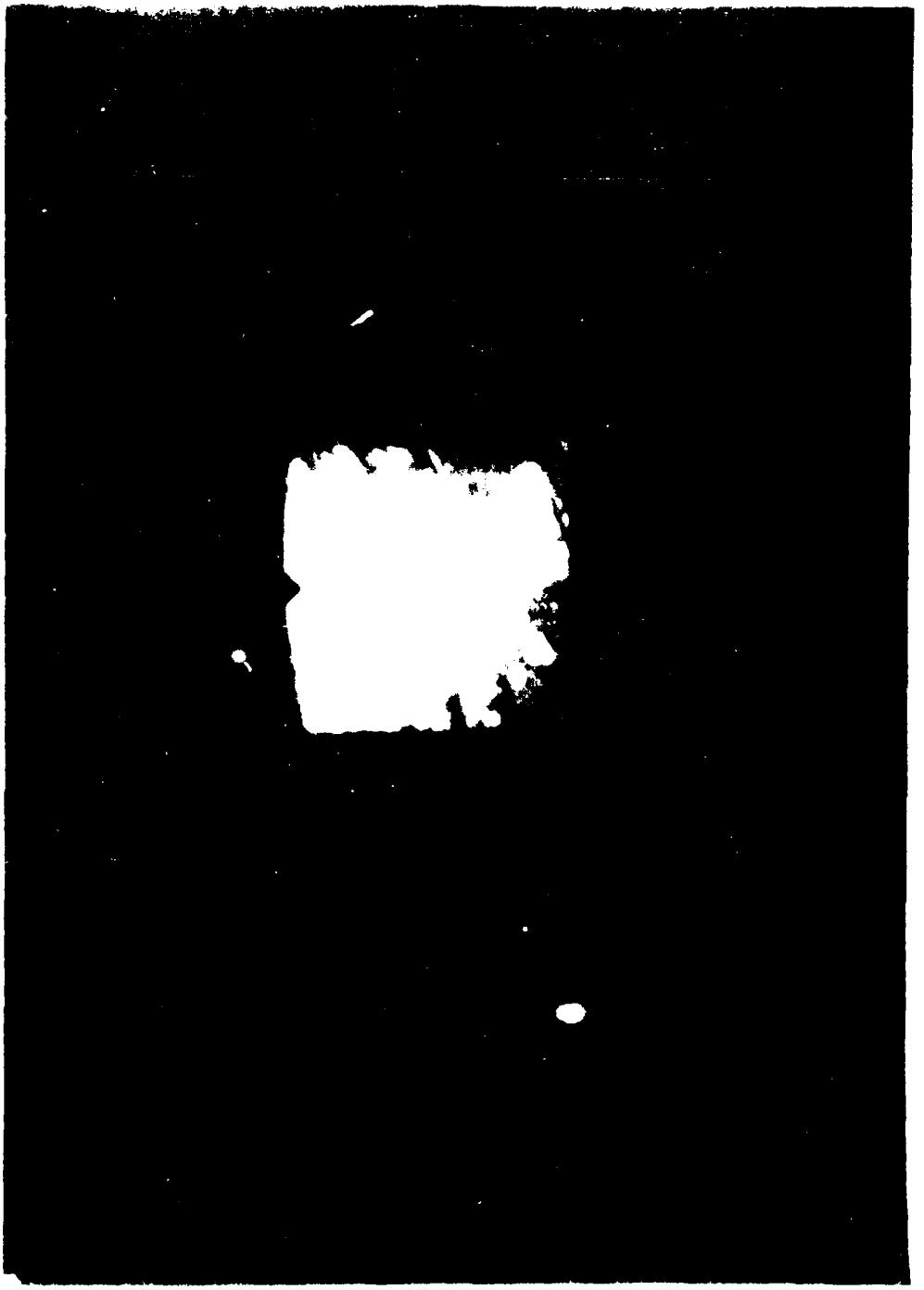

[redacted]

CONCLUSIONS

- FRACTURE OF THE UNLOCKING PLUNGERS INITIATED AT SHARP CORNER STRESS RAISERS.

- HOT GAS IMPINGEMENT AND SUBSEQUENT EROSION/CORROSION OF THE GLAND AND CYLINDER ASSEMBLY HOUSING SURFACES CONTRIBUTED TO REDUCTION IN INTEGRITY OF THE EJECTOR RACK.

RECOMMENDATIONS

- BLENDING OF PLUNGER SHARP CORNERS

- CONSIDER MATERIAL SUBSTITUTE FOR 440C STAINLESS STEEL GLAND. CANDIDATE CHOICES WOULD BE MP35N OR INCO 718 ALLOYED TO RESIST HIGH TEMPERATURE EROSION/CORROSION.

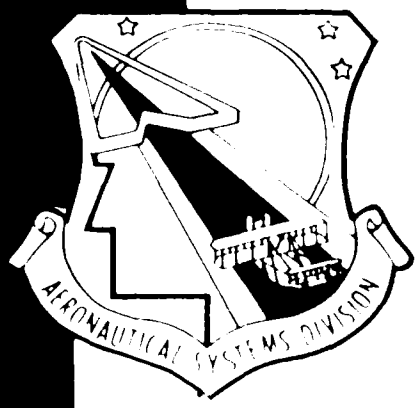

FUEL LINE CORROSION

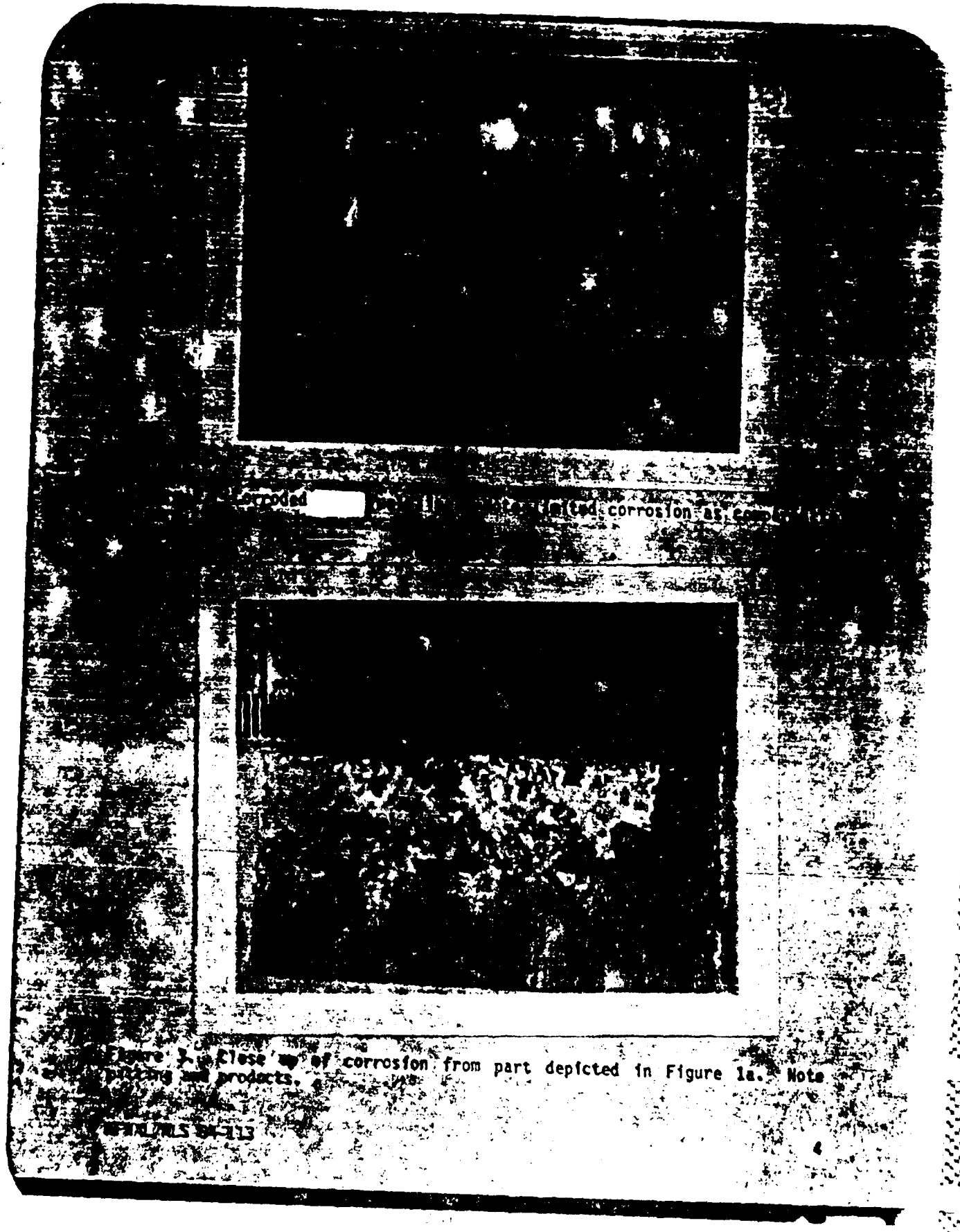

Figure 1b. Close up of corrosion from part depicted in Figure 1a. Note pitting and products.

- CONCLUSIONS -

- THE MARKING ELECTROLYTE USED FOR LABELING FUEL LINES WAS TRAPPED BETWEEN THE 6061-T6 TUBING AND THE FERRULE. THIS FOSTERED INTERGRANULAR CORROSION.

- RECOMMENDATIONS -

0 USE OF ANOTHER MARKING PROCESS WHICH DOES NOT INVOLVE CORROSIVE MATERIALS.

0 PREVENT THE TRAPPING OF IMPACTING ELECTROLYTE BETWEEN THE GG41-16 TUBING AND FERRULES. MIL-S-8802 SEALANTS WERE RECOMMENDED AS CANDIDATES.

AIRCRAFT ATTACHMENT BOLT FAILURE

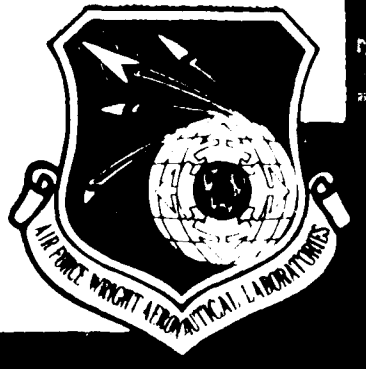

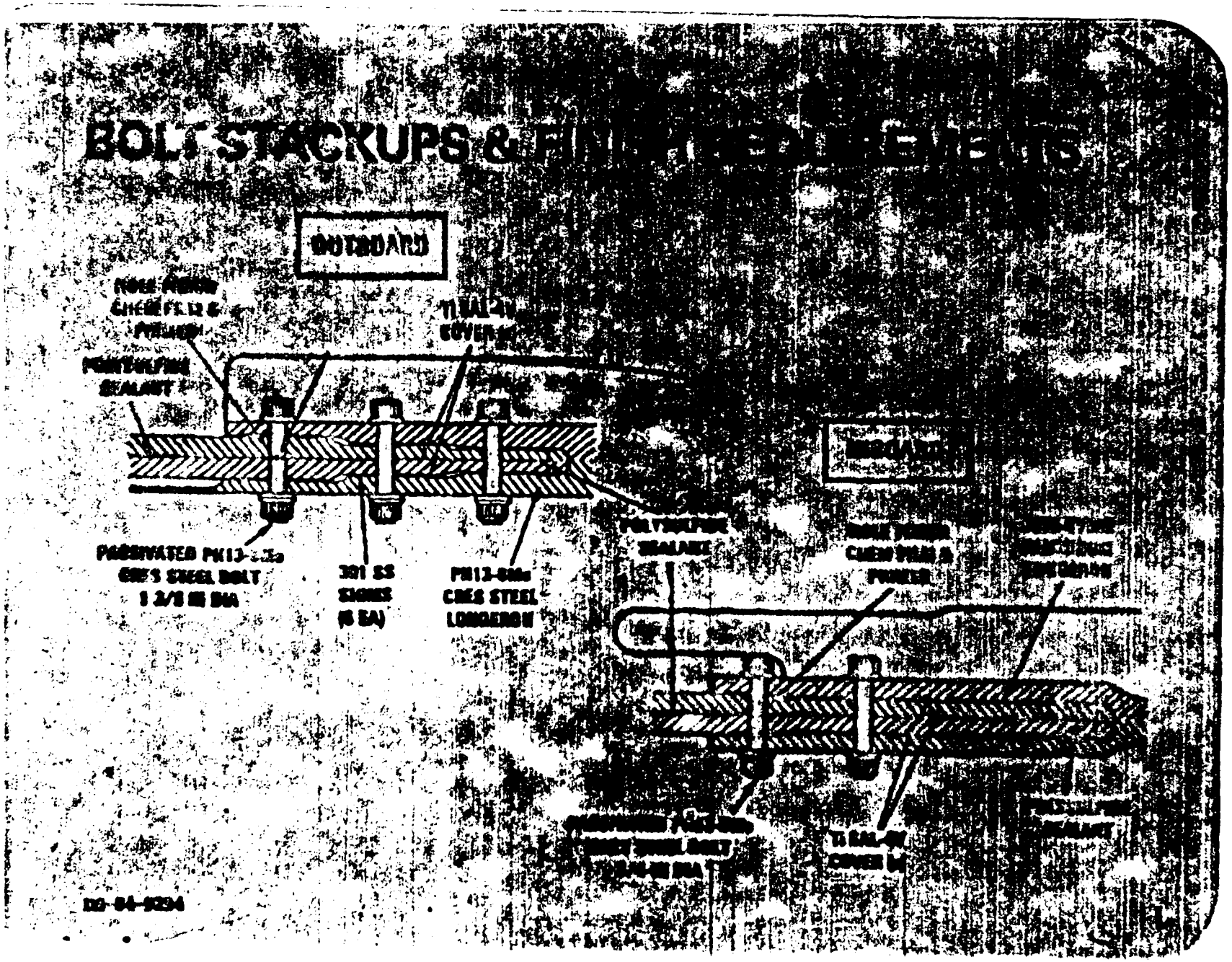
BOLT STACKUPS & FI
OUTBOARD
POLYSULFIDE
SEALANT
PASSIVATED PH13-
CRES STEEL BOLT
301 SS
SLEEVE
PH13-8Mo
CRES STEEL
LONGERON
POLYSULFIDE
SEALANT
FILLER
DG-84-9294

SYSTEM SUPPORT FAILURE ANALYSIS

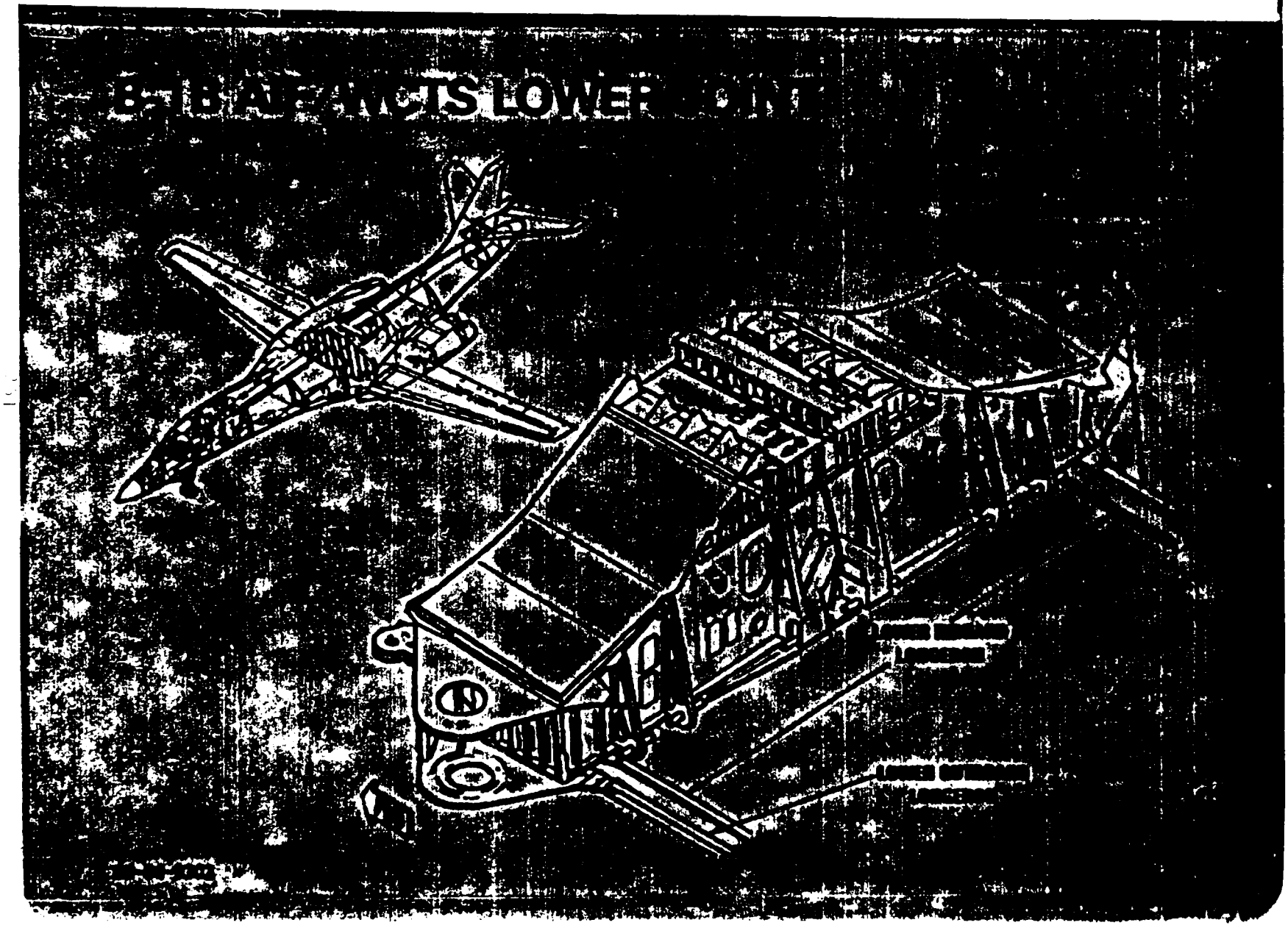

1. PITTING CORROSION WAS FOUND ON THE SIDE OF THE BOLT.

2. STRESS CORROSION PROGRESSED FROM THE SURFACE PITS.

3. ULTIMATE FAILURE OCCURRED BY OVERLOAD.

RECOMMENDATIONS

1. REMOVE ALL ATTACHMENT BOLTS WHICH WERE INSTALLED USING THE WATER SOLUBLE COOLANT.

2. RINSE ALL MACHINED FASTENER HOLES WITH A NON-CORROSIVE AGENT.

3. INSTALL NEW 13-8PH STAINLESS STEEL BOLTS USING A POLYSULFIDE SEALANT.

- CORROSION RELATED FAILURES OF STRUCTURAL MATERIALS CONTINUE TO SHOW THEIR PRESENCE AT AFWAL / MLSA

- THE VAST MAJORITY OF THESE INCIDENCES, HOWEVER, ARE EITHER MANUFACTURING / QUALITY CONTROL RELATED OR MATERIALS AND / OR HEAT TREATMENTS USED ON OLDER SYSTEMS

- THE INTRODUCTION OF IMPROVED CORROSION RESISTANT MATERIALS INTO NEWER AEROSPACE SYSTEMS WILL CERTAINTLY EXTEND PART LIVES AND REDUCE THE NUMBER OF CORROSION FAILURES

- THE PERFORMANCE OF THESE MATERIALS, HOWEVER, WILL BE AS GOOD AS THE UP FRONT PROCESSES EMPLOYED AT THE MANUFACTURER COUPLED WITH THE FOLLOW ON MAINTENANCE ACTIVITIES IN THE FIELD

SESSION A
CORROSION ASSISTED FAILURES

Chairman
Bennie Cohen
Air Force Wright
Aeronautical Laboratories

STRESS CORROSION EVALUATION OF POWDER METALLURGY ALUMINUM ALLOY 7091 WITH THE BREAKING LOAD TEST METHOD

Marcia S. Domack

ABSTRACT

The stress corrosion behavior of powder metallurgy (PM) aluminum alloy 7091 has been evaluated using a new technique called the breaking load test method, which was developed by Alcoa Laboratories under NASA contract NAS1-16424. Direct tension specimens machined from extruded material in the T7E69 and T7E70 conditions were tested in both the longitudinal and transverse orientations. Specimens were exposed to a 3.5 percent NaCl solution in alternate immersion for up to 9 days at stress levels as high as 90 percent of the material yield strength. Optical and scanning electron microscopy were used to evaluate specimen fracture surfaces to determine the extent of stress corrosion and to identify attack by other mechanisms. Breaking stress data were analyzed with extreme value statistics to determine threshold stress levels for stress corrosion cracking, probability of survival at specific stress levels, and 99 percent survival stresses. The results of this study are in agreement with data reported in the literature, and indicate that PM 7091 aluminum is highly resistant to stress corrosion cracking for the orientations tested. Preliminary data analysis indicates that the effects of test variables such as heat treatment, specimen orientation, and exposure conditions can be better discriminated by the breaking load test method than by conventional pass-fail data analysis.

INTRODUCTION

The use of powder metallurgy (PM) processing technology for the production of advanced aluminum alloys has resulted in materials which have combinations of properties which are superior to those of similar materials produced by ingot metallurgy (IM) techniques. The improved properties can be attributed to microstructural refinements achieved through rapid solidification during powder production and also to the development of alloy chemistries which cannot be attained through conventional IM processing. One of the goals of aluminum PM technology has been the development of alloys having improved combinations of strength and stress corrosion cracking (SCC) resistance.

A powder metallurgy alloy developed by Alcoa which shows promise in meeting this goal is 7091. This material is one of the first powder metallurgy alloys to become commercially available, and is characterized by a combination of high strength and toughness as well as good corrosion resistance. The 7091 powder is produced by air atomization of the melt, and is subsequently consolidated and then wrought by extrusion or forging.

7091 is a 7XXX-type chemistry, with Zn the major alloying element, but is more heavily alloyed than conventional ingot metallurgy 7XXX-type chemistries, and also contains cobalt for grain refinement. Cobalt is generally associated with slightly higher strength and better SCC resistance, but cannot be added by conventional processing due to its low solubility in solid aluminum at ambient temperatures. Rapid solidification technology has enabled incorporation of up to 1.6 wt percent concentrations of Co without the formation of coarse segregates.

Cobalt provides strengthening and enhanced resistance to SCC by the formation of Co_2Al_9 dispersoids. Several explanations for the enhanced stress corrosion resistance associated with Co additions have been proposed (ref. 1) and include: grain boundary pinning by the Co_2Al_9 particles, which makes the grain boundaries less favorable for SCC; blunting of stress corrosion cracks by Co_2Al_9 particles; and enhanced desorption of atomic hydrogen from the crack surfaces, which reduces the amount of damaging hydrogen entering the material. Christodoulou, et. al., (ref. 2), have observed matrix dissolution around Co_2Al_9 particles, indicating the particles are cathodic with respect to the matrix, and suggesting they serve as sites for hydrogen recombination.

The present study evaluates the SCC resistance of 7091 in two overaged heat treatments and compares the results with conventional ingot metallurgy alloy 7075 at comparable strength levels. Stress corrosion testing is conducted according to the breaking load test method (ref. 3), an improved, accelerated technique for assessing the stress corrosion cracking behavior of aluminum alloys which was developed by Alcoa Laboratories under NASA Langley Research Center contract NAS1-16424. When compared with other currently used test methods, the breaking load method is capable of providing more information with fewer specimens and shorter exposure times, and is a better discriminator of SCC performance among relatively resistant materials. The breaking load method also provides a quantitative estimate of SCC resistance, rather than general material rankings, which is amenable to statistical analysis and fracture mechanics evaluations.

The breaking load method involves determination of breaking strengths of replicate groups of smooth tensile specimens after exposure to static stresses and corrosive environment for various lengths of time. The degree of degradation due to SCC is determined by comparison of the various breaking strengths with the material ultimate tensile strength. In general, the larger the strength decrease, the greater the degree of SCC attack. Comparing the breaking strength of specimens exposed with and without stress provides a means of separating SCC response from that due to general corrosion.

The breaking stress values determined from the breaking load technique are analyzed with extreme value statistics principles to determine several quantitative parameters including threshold stress levels for stress corrosion cracking, probability of survival at specific stress levels, and 99 percent survival stresses.

Extreme value statistics principles have been used in previous work (refs. 4-8) to evaluate fracture data, and the analysis methods are well developed. The rationale for application of extreme value statistics to the analysis of fracture data is that materials contain flaws which have a wide range of sizes, but fracture will occur at the largest of these flaws (the weakest link). For statistical purposes, the distribution of all flaw sizes in a group of specimens is not as important as the distribution of largest flaw sizes (the extreme value). The fracture stress of a specimen is inversely related to the size of the largest flaw; therefore, the breaking strengths of replicate specimens would be expected to follow an extreme value distribution of the smallest values. Prior analysis of corrosion pitting data (refs. 9-11) indicated that pit depth followed an exponential distribution, but that maximum pit depth followed the related extreme value distribution. Pit depth and occurrence are related to microstructural features, as is stress corrosion cracking. The assumption is made that flaw sizes in SCC specimens

would also follow the exponential distribution, with the maximum flaw sizes (or the related minimum breaking strengths) then following the related extreme value distribution (ref. 3).

A conventional pass-fail test is conducted with similar specimens and test parameters as the breaking load method to define a threshold stress. Specimen exposure continues until failure, however, which can be defined as either complete specimen fracture or the first appearance of corrosion cracking, and resulting exposure times can be as long as 30 days. The breaking load test method can be considered an accelerated test technique for two reasons. As in the conventional technique the stress corrosion damage is accelerated through the application of alternate immersion exposure. However, more significantly, the exposure times required to define a threshold stress are reduced by about a factor of three from that associated with pass-fail testing.

This report contains data collected with the breaking load test method for PM 7091 in both T7E69 and T7E70 conditions in both the longitudinal and transverse orientations. The results are compared with data for ingot metallurgy 7075 and are discussed in terms of test variables and microstructural features.

MATERIAL AND PROCEDURES

Material and Mechanical Properties

The PM alloy 7091 evaluated in this study was supplied as extrusions with cross section 4.5 by 1.5 inches. Nominal composition for 7091 is given in table I and compared with that of ingot metallurgy alloy 7075. Alloy 7091 contains more Zn than 7075, and contains Co as a grain refiner and strengthening addition rather than Cr. The 7091 extrusions were supplied in both the T7E69 and T7E70 conditions. Both heat treatments consist of solution treatment followed by stress relief by stretching and then artificial aging. Material in the T7E69 condition has been overaged for 4 hours, and the T7E70 condition has been overaged for 14 hours (ref. 12). Polished metallographic sections, shown in figure 1, indicate elongated grain structures with grain size varying from 2 by 2 by 2 microns up to 2 by 2 by 15 microns with an average value of about 2 by 2 by 6 microns. Tensile mechanical properties were determined using a closed loop electrohydraulic mechanical test machine, according to ASTM Standard E8 (ref. 13). Tensile specimens were 0.25-inch diameter by 2.0-inch long, and were machined in both the longitudinal (L) and long transverse (T) orientations. Properties measured included 0.2 percent offset yield strength, ultimate strength, Young's modulus, and percent elongation. Results were found to agree with manufacturer's data and are presented in table II. The yield and ultimate strengths for 7091 are presented in figure 2 with data for IM 7075 in both the peak aged (T651) and overaged (T73) conditions (ref. 14). The longitudinal yield strength of 7091-T7E69 is about 10 percent greater than that for T7E70 and about 6 percent greater than the peak aged 7075. The longitudinal yield strength of 7091-T7E70 is about 10 percent greater than the overaged 7075-T73.

Stress Corrosion Testing

Stress corrosion specimens were tested in groups of five replicates according to the test matrix shown in table III. Groups of five replicates were

selected for statistical considerations. The exposure stress levels correspond to 0, 50, and 90 percent of the material yield strength measured for each heat treatment and orientation. Test specimens were 0.125 inch diameter by 2.0-inch long direct tension specimens, which are described in ASTM standard G49 (ref. 15), and shown in figure 3. Test specimens were machined in both the longitudinal and transverse orientations, but due to size constraints of the supplied extrusions, it was not possible to evaluate the short transverse orientation. The specimens were loaded in tension by means of constant deflection stressing frames made of 6061 aluminum. Specimens are assembled in the frames as shown in figure 3 and the end bolts are hand tightened. The loading device shown in figure 4 is then used to push the sides of the frame inward along the tapered end members, extending the specimen in tension. Both the specimen frame and a similar loading device are described in reference 15. Specimen extension was monitored with an extensometer during the loading process, and the output used to calculate the exposure stress. Specimens were exposed to a 3.5 percent NaCl solution under alternate immersion test conditions according to ASTM standard G44 (ref. 16). The 1-hour cycle consists of ten minutes immersion followed by a 50 minute drying period. Specimens were observed daily for stress corrosion cracks or other indications of corrosive attack. Specimen frames were coated with paraffin after specimen loading to prevent degradation of the frames during environmental exposure, as well as any galvanic interaction between the frame and the specimen.

According to the breaking load test method, specimens are removed from solution after the discrete exposure time intervals and failed in tension to determine the breaking strength. The test method requires that the specimens be failed in tension on the same day as their removal from solution. The breaking load tests were conducted with a screw-driven mechanical test machine, at a load rate of 0.02 inch/minute and the failure load was recorded.

Data Analysis

The measured specimen failure loads were converted to breaking stress values by division by the original specimen cross sectional area. The sample mean ($\bar{x}$) and standard deviation ($\bar{\delta}$) were determined for each group of five replicates.

The probability of survival (Ps) is calculated based on the mean and standard deviation of breaking stress values for a group of replicate specimens, and reflects the probability of specimens surviving for a given environmental exposure period at a specific stress level. The probability of survival is calculated with the Gompertz survival equation (ref. 8), given as follows:

$$Ps = \exp\left[-\exp\left(\frac{S - \hat{\mu}}{\hat{\sigma}}\right)\right]$$

where s is the exposure stress, and $\hat{\sigma}$ and $\hat{\mu}$ are the extreme value distribution scale and location parameters, respectively, calculated as follows:

$$\hat{\sigma} = \frac{\bar{\delta}}{S_N} \qquad \hat{\mu} = \bar{X} + Y_N \hat{\sigma}$$

The values Y_N and σ_N are the calculated estimates of the mean and standard deviation, respectively, of the reduced extremes as functions of sample size, N. For a sample size of five, Y_N=0.4565 and σ_N=0.7932. Values for other sample sizes can be found in reference 8.

The 99 percent survival stress, S_{99}, is the tensile stress 99 percent of a group of replicates would be expected to survive after environmental exposure for a specified time and stress level combination. Calculation of the 99 percent survival stress is achieved by rearranging the Gompertz survival equation and setting the probability of survival at 99 percent.

$$S = \hat{\mu} + \hat{\sigma} \ln [-\ln Ps]$$

$$S_{99} = \hat{\mu} - 4.6\ \hat{\sigma} \qquad (Ps = 0.99)$$

The 99 percent survival stress is a parameter which provides for a direct comparison of stressed and unstressed specimens exposed to identical conditions, as well as comparison of material performance for identical test conditions.

The 99 percent survival stress is unique for a given material exposed under specific test conditions but does not reflect a threshold below which no SCC occurs. A series of 99 percent survival stresses, however, can be used to determine a satistically defined threshold stress, σ_{Th}, which is the exposure stress for which there is a 95 percent confidence that the probability of specimen failure under specified test conditions is less than one percent.

The threshold stress is determined by applying a confidence interval to the mean of point estimates of the threshold determined from the 99 percent survival stress data. The point estimates can be obtained from the 99 percent survival stress data as a function of the exposure stress by determining, either graphically or by linear regression, the point at which these stresses are equal. Figure 5 illustrates the estimation procedure for 0.125 inch-diameter specimens of ingot metallurgy alloy 7075-T651 (ref. 3). The estimates of the threshold stress correspond to the point where the data trend intersects the dotted 1:1 line indicating equal exposure stresses and survival stresses. By using various combinations of the data, several estimates can be made for each exposure time. The threshold stress can then be calculated from this series of point estimates.

The threshold stress is given by the lower limit of the 90 percent confidence band for the point estimates, and can be calculated from the student's t distribution by the equation:

$$\sigma_{Th} = X + Z\ \delta$$

where X and δ are the mean and standard deviation, respectively, of the point estimates and z is the variate for the appropriate degrees of freedom.

RESULTS AND DISCUSSION

Breaking stress data for both the T7E69 and T7E70 conditions in both longitudinal and transverse orientations are summarized in table IV as mean and standard deviations for each set of replicate specimens. As a percentage of the mean, the standard deviations of each test set are typical of corrosion test data. The Alcoa developmental study (ref. 3) revealed that greater standard deviations were associated with greater SCC susceptibility. This is in contrast to trends observed in data collected by conventional pass-fail testing, and occurs because the data in the breaking load test is dependent on a reduction in load carrying ability of each specimen and not upon specimen failure during exposure. The mean breaking stresses are also presented graphically in figures 6 and 7 for the T7E69 and T7E70 conditions, respectively. The data for each test case displays trends typical of materials which are very resistant to stress corrosion cracking; i.e., increasing exposure time or exposure stress level has only a small effect on breaking stress. The reduction in breaking stress with time observed for specimens exposed at zero stress level for both material conditions can be attributed to the effects of pitting or general corrosion. The data for the T7E69 longitudinal orientation specimens displays no significant reduction in mean breaking stress with increased exposure stress and time. All of these data curves display a similar reduction in mean breaking stress as is observed for the zero exposure stress specimens. For the T7E69 transverse orientation specimens, however, there is a greater reduction in mean breaking stress for specimens exposed at a stress of 90 percent of the material yield strength than for the specimens exposed at lower stresses. Results for the T7E70 specimens display little effect of increased exposure stress on the mean breaking stress for either longitudinal or transverse orientation. Rather, for each orientation, the data curves exhibit similar reductions in mean breaking stress with time regardless of exposure stress. The data indicate that transverse orientation specimens exhibit a somewhat greater reduction in mean breaking strength than longitudinal specimens. Under the most severe exposure conditions used, 9 days at 90 percent of the yield strength, reductions on the order of 6 percent were observed in the longitudinal orientation and 9 percent in the transverse orientation.

Breaking stress data were collected for 7091-T7E69 in the short transverse orientation by researchers at Alcoa (ref. 3) for stress levels as high as 75 percent of the short transverse yield strength. They reported mean breaking stress values for short transverse orientation direct tension specimens exposed to alternate immersion in 3.5 percent NaCl solution at 30 ksi exposure stress (approximately 45 percent of the short transverse material yield strength). The reduction in mean breaking stress after nine days exposure was about nine percent, which is very similar to that determined in the current study for the transverse orientation, T7E69 specimens.

Metallographic sections were prepared from selected specimens in order to evaluate the type of corrosive attack occurring in each test case. Sections of both longitudinal and transverse specimens exposed for 9 days at the 0 and 90 percent yield strength exposure stress levels are shown in figures 8 and 9 for both the T7E69 and T7E70 specimens, respectively. The micrographs support

the trends observed in the breaking stress data. The depth of penetration of corrosive attack is greatest in the transverse orientation T7E69 specimens exposed at 90 percent of the material yield strength and correlates with the greater reduction in mean breaking stress observed for these specimens. The corrosive attack in this case is in the form of intergranular cracks propagating perpendicular to the applied stress, as would be expected in stress corrosion cracking. In the longitudinal orientation T7E69 specimens the crack path tends to curve around to follow grain boundaries along the specimen length, creating a corrosion morphology which resembles the onset of exfoliation rather than stress corrosion.

The morphology of the corrosive attack observed in the zero exposure stress level specimens for both orientations is similar to that observed in the higher stress level specimens. The short intergranular cracks seen in the transverse orientation T7E69 specimens exposed at zero stress level are probably due to residual machining stresses in the specimens. The depth of corrosive attack is greater in the transverse orientation T7E69 specimens exposed at high stress levels than in the lower and zero stress level specimens, again correlating with the observed variation in mean breaking stress observed for these conditions. The depth of attack in the longitudinal orientation specimens appears similar for both zero and high exposure stress, which correlates with the absence of any exposure stress level effect on mean breaking stress.

There is a significant difference in the morphology of the corrosion damage observed in the T7E70 specimens (fig. 9) than was observed in the T7E69 specimens (fig. 8). In the T7E70 specimens the damage appears to be severe surface pitting attack with a slight directionality due to grain orientation. The depth of attack is similar when comparing specimens exposed at zero and high exposure stress levels, for each orientation. This correlates with the absence of any exposure stress level effect observed for the T7E70 specimens. The depth of attack is greater in the transverse specimens than in the longitudinal specimens at equal exposure stress level, which explains the greater reduction in mean breaking stress observed for the transverse orientation.

Scanning electron microscopy was used to further characterize the regions of corrosive attack. On the higher stress level T7E69 specimens, regions of transgranular cracking were observed occasionally about the circumference of the fracture surface, as shown in figure 10a. These regions always occurred at the intersection of stress corrosion cracking and overload fracture. Similar regions of transgranular cracking have been observed in bolt-loaded precracked stress corrosion specimens of 7XXX aluminum alloys in T7 conditions exposed to marine atmospheric conditions (ref. 17). The transgranular cracks were observed to propagate along uncracked ligaments between stress corrosion cracks, thereby joining these regions, with only slight penetration into uncracked material. At the magnification shown in fig. 10a there is little difference in appearance between the regions of stress corrosion cracking and overload fracture, but differences become apparent at higher magnification. The intersection of the stress corrosion and overload regions (fig. 10b) and of the transgranular and overload regions (fig. 10c) illustrate the expected ductile dimple morphology associated with the tensile overload fracture. These features are absent from the regions of stress corrosion and transgranular cracking. At very high magnification (fig. 11) the presence of microdimpling is evident in the overload fracture region, but is still absent in both the stress corrosion and transgranular regions. Similar analysis of the T7E70

specimen fracture surfaces revealed a mix of microdimpling and smooth grain boundary surfaces in the regions of corrosive attack, suggesting this attack is other than stress corrosion cracking. Similar fractographic features have been observed in stress corrosion cracking studies of 7091 with precracked specimens (refs. 2, 18).

The calculated probability of survival and 99 percent survival stress for each exposure condition are presented in table V for each combination of heat treatment and orientation. The 99 percent survival stress data is also presented graphically in figure 12 as a function of exposure stress for each exposure time. The probability of survival is very high in all cases, reflecting the excellent stress corrosion resistance of the material. The data presented in figure 12 indicate that for the time intervals tested the condition of equal exposure and survival stress was reached with the T7E69 specimens but not with the T7E70 specimens.

Point estimates of the threshold stress, determined by the linear regression method, are presented in table VI for each test case. The calculated values of threshold stress, σ_{Th}, for each heat treatment-orientation combination are presented at the bottom of table VI. The threshold stress levels vary as might be expected for the material condition-specimen orientations evaluated, but the differences for each of the four test conditions are relatively small. This data illustrates one of the strengths of the breaking load test method, the ability to discriminate differences in stress corrosion performance of relatively resistant materials. While both heat treatment conditions evaluated are overaged, T7E70 has been aged for a longer time and would be expected to be more resistant to stress corrosion. This greater resistance is indicated as a higher threshold than is seen for T7E69. The least resistant of the test conditions evaluated, i.e., that exhibiting the lowest threshold value, was the transverse orientation of the less overaged T7E69, as might be expected.

The developmental study conducted by Alcoa (ref. 3) indicated that threshold values determined with the breaking load method for materials with high stress corrosion resistance reflected differences in material performance where the same materials were rated equally with pass-fail test data. It is nearly certain that pass-fail testing would have equally rated the T7E69 and T7E70 conditions of PM 7091. The study also indicated that threshold values determined with the breaking load test method for well characterized materials agreed extremely well with threshold values determined by pass-fail testing.

A useful comparison of threshold values can be made by considering the thresholds as a percentage of the material yield strength. Figure 13 presents threshold values and yield strengths for PM 7091 in the T7E69 and T7E70 conditions in longitudinal and transverse orientations. Data for IM 7075 in both the peak aged T6bl and overaged T73 conditions in longitudinal, transverse, and short transverse orientations are also presented (ref. 14). The threshold values given for IM 7075 were determined by using the pass-fail method, and are values for rolled plate 0.25 to 4.5-inches thick. Threshold values are shown for short transverse IM 7075 for familiarity and illustrate the often documented improved stress corrosion resistance of overaged material when compared to peak aged material in this orientation. A comparison of material performance for PM 7091 and IM 7075 can be made for the longitudinal and transverse orientations. The threshold stress level for T7E69 is about 80 percent of the yield strength for both the longitudinal and transverse

orientations. These percentages are comparable to threshold percentages for 7075-T73, and are 5 and 10 percent higher than for peak aged 7075. The threshold values for 7091-T7E70 are 90 and 95 percent of the material yield strength for the transverse and longitudinal specimens, respectively. The superiority of the PM material is evident when the threshold values as a percentage of yield strength are considered in conjunction with the improved tensile properties of 7091. An interesting point to note here is that while the threshold values were determined by the breaking load test method for 7091 with testing of several hundred specimens, the data presented for 7075 required testing of thousands of specimens using the pass-fail method.

CONCLUDING REMARKS

The stress corrosion behavior of powder metallurgy alloy 7091 was evaluated in two overaged heat treatment conditions, T7E69 and T7E70. Stress corrosion testing was performed with the breaking load test method, a new accelerated technique developed by Alcoa Laboratories under NASA contract NAS1-16424. Direct tension specimens were exposed in both longitudinal and transverse orientations to 3.5 percent NaCl solution at stress levels corresponding to 9, 50 percent, and 90 percent of the material yield strength. Specimen exposure by alternate immersion was continued for as long as 9 days with residual load carrying ability of the specimens determined by tensile failure after periods of 2, 4, 6, and 9 days. Breaking stress values were evaluated with extreme value statistics principles to determine the probability of specimen survival for specific exposure conditions, 99 percent survival stresses, and threshold stresses for stress corrosion cracking. The results were compared with literature data on ingot metallurgy alloy 7075 determined by conventional pass-fail testing.

The breaking load test method was found to be sensitive to small differences in material stress corrosion performance. This allows the method to be useful for evaluating more resistant materials, including advanced aluminum alloys. The technique provides quantitative estimates of stress corrosion behavior rather than general material rankings. Test results determined can be further evaluated by statistical methods to calculate a statistically defined threshold stress level for stress corrosion cracking.

Threshold stress levels can be determined with the breaking load test method with testing of an order of magnitude fewer specimens and with exposure times reduced by about one third when compared with conventional pass-fail testing. The breaking load test method is capable of discriminating differences in stress corrosion performance between materials which would be equally rated by pass-fail test data.

The breaking load data collected in this study indicate PM 7091 is highly resistant to stress corrosion cracking in both longitudinal and transverse orientations at stress levels up to 90 percent of the material yield strength. Reduction in mean breaking stress as a result of corrosive attack was smallest for material in the more overaged T7E70 condition. In this case the corrosive damage appeared to be limited to gross surface pitting, with no evidence of stress corrosion cracking observed. The only significant reduction in mean breaking stress observed in this investigation occurred for transverse orientation specimens in the T7E69 condition exposed at the 90 percent yield strength stress level. The corrosive damage in these

specimens was intergranular stress corrosion cracks. Threshold stress levels determined from test data ranged from 80 to 95 percent of the material yield strength. In comparison, threshold stress levels are typically 80 percent of the yield strength for IM 7075 in the overaged T73 condition. Mechanical properties determined for 7091 indicated tensile yield strengths as much as 10 percent greater than IM 7075-T73. The very high stress corrosion threshold values combined with the improved tensile properties of 7091 reflect the superior property combinations possible with powder metallurgy technology.

REFERENCES

1. Lyle, J. P.; and Cebulak, W. S.: Met. Trans. A, Vol 6A, 1975, p. 685-699.

2. Christodoulou, L.; Gordon, J. R.; and Pickens, J. R.: Effect of Co Content on the Stress-Corrosion Cracking Behavior of 7091-Type Aluminum Powder Alloys. Met. Trans. A, Vol 16A, May 1985, p.945-951.

3. Sprowls, D. O.; Bucci, R. J.; Ponchel, B. M.; Brazill, R. L.; Bretz, P. E.: A Study of Environmental Characterization of Conventional and Advanced Aluminum Alloys for Selection and Design. Phase II- The Breaking Load Test Method, NASA CR 172387, August 1984.

4. Fisher, J. C.; and Hollomon, J. H.: A Statistical Theory of Fracture," Tech. Pub. No. 2218, Metals Technology, AIME, Vol. 14, 1947, p. 5.

5. Epstein, B.: Statistical Aspects of Fracture Problems. Journal of Applied Physics, Vol. 19, 1948, p. 140.

6. Epstein, B.: Application of the Theory of Extreme Values in Fracture Problems. Journal of American Statistics Association, Vol. 43, 1948, p. 403.

7. Gumbel, E. J.: Statistical Theory of Extreme Values and Some Practical Applications. U. S. Department of Commerce, Applied Mathematics Series 33, 1954.

8. Gumbel, E. J.: Statistics of Extremes. Columbia University Press, New York, 1958.

9. Mears, R. B.; and Brown, R. H.: Ind. Eng. Chem., Vol. 29, No. 10, 1937, p. 1087.

10. Aziz, P. M.: Application of the Statistical Theory of Extreme Values to the Analysis of Maximum Pit Depth Data for Aluminum. Corrosion, Vol. 12, 1956, pp. 495t-506t.

11. Persons, R.: Statistical Analysis: A Decision Making Approach. Second Edition, 1978, Harper & Row Publishers, p. 240.

12. Billman, F. R.; Petit, J. I.; Sanders, R. E., Jr.; Paris, H. G.: Microstructure and Processing Control for Aluminum P/M Wrought Products. Technical Report RSCD-CR-83001, June 1983.

13. ASTM Standard E8: Standard Methods of Tension Testing of Metallic Materials. 1985 Annual Book of ASTM Standards, Vol. 03.01.

14. Mehr, P. L., et al.,: Alcoa Alloy 7075-T73. Alcoa Green Letter, Aluminum Company of America, Aug. 1965.

15. ASTM Standard G49: Standard Practice for Preparation and Use of Direct Tension Stress Corrosion Test Specimens. 1986 Annual Book of ASTM Standards, Vol 03.02.

16. ASTM Standard G44: Standard Recommended Practice for Alternate Immersion Stress Corrosion Testing in 3.5 percent Sodium Chloride Solution. 1986 Annual Book of ASTM Standards, Vol. 03.02.

17. Hasse K. R.; and Dorward, R. C.: Flaw Growth of 7075, 7475, 7050, and 7049 Aluminum Alloy Plate in Stress Corrosion Environments: 4-Year Marine Atmosphere Exposure Results. Kaiser Aluminum CFT RR 81-15, Oct. 1981.

18. Pickens, J. R.; and Christodoulou, L.: The Stress Corrosion Cracking Behavior of High-Strength Aluminum Powder Metallurgy Alloys. Met Trans A, Vol 18A, Jan. 1987, p. 135-149.

Element	PM 7091	IM 7075
Zn	6.47	5.80
Mg	2.58	2.39
Cu	1.57	1.57
Cr	0.03	0.19
Co	0.40	0.00
Mn	0.00	0.05
Fe	0.12	0.26
Si	0.02	0.11

Table I. Nomonal compositions for powder metallurgy alloy 7091 and ingot metallurgy alloy 7075.

Material Condition	Orientation	UTS (ksi)	YS (ksi)	E (msi)	%el
T7E69	L	85.1	77.9	9.8	17.5
	T	79.9	72.1	10.0	14.9
T7E70	L	78.5	70.0	10.4	19.9
	T	75.3	66.7	9.9	19.7

Table II. Mechanical properties determined for PM 7091 extrusions in both longitudinal (L) and transverse (T) orientations.

Exposure Stress		Exposure Time (days)			
		T7E69		T7E70	
(ksi)	(% YS)	L	T	L	T
0	0	0,2,4,6,9	0,2 4 6 9	0,2,4,6,9	0,2,4,6,9
35	50		2,4,6,9	2,4,6,9	2,4,6,9
40	50	2,4,6,9			
60	90				2,4,6,9
65	90		2,4,6,9	2,4,6,9	
70	90	2,4,6,9			

Table III. Exposure stresses and times for each test condition.

Exposure Time (days)	Exposure Stress (% YS)	Breaking Stress (ksi) T7E69 L $\bar{X}$	T7E69 L $\bar{\delta}$	T7E69 T $\bar{X}$	T7E69 T $\bar{\delta}$	T7E70 L $\bar{X}$	T7E70 L $\bar{\delta}$	T7E70 T $\bar{X}$	T7E70 T $\bar{\delta}$
0	0	85.53	0.48	77.65	1.06	79.67	0.38	77.72	0.91
2	0	82.89	1.87	79.61	2.44	78.07	1.95	79.15	4.08
2	50	82.55	1.79	77.96	1.23	78.63	2.15	79.05	2.69
2	90	83.23	0.53	77.00	2.16	80.30	0.92	78.16	1.73
4	0	82.54	1.22	77.61	1.74	75.58	1.73	74.22	1.52
4	50	84.39	2.49	78.35	2.13	77.49	1.83	74.88	1.04
4	90	82.14	0.85	74.69	3.79	77.39	1.38	73.70	2.45
6	0	83.55	1.79	78.49	3.08	79.18	0.69	76.11	1.40
6	50	82.47	2.08	77.42	2.95	79.78	1.92	74.42	3.98
6	90	79.27	3.38	75.42	1.93	79.07	1.80	74.39	1.53
9	0	80.78	0.86	75.12	2.52	73.86	0.75	70.58	1.85
9	50	79.72	1.09	75.24	1.52	75.72	0.72	70.53	1.54
9	90	80.22	1.31	71.18	1.29	75.58	0.58	70.53	1.54

Table IV. Mean, $\bar{X}$, and standard deviation, $\bar{\delta}$, of breaking stress data for each set of replicate specimens of PM 7091.

Exposure Time (days)	Exposure Stress (% YS)	T7E69 L Ps	T7E69 L S_{99}	T7E69 T Ps	T7E69 T S_{99}	T7E70 L Ps	T7E70 L S_{99}	T7E70 T Ps	T7E70 T S_{99}
0	0	1	82.93	1	71.86	1	77.47	1	72.73
2	0	1	73.09	1	67.36	1	68.29	1	58.68
2	50	1	73.52	1	71.79	1	67.86	1	65.50
2	90	1	80.55	0.99	66.14	1	75.67	0.99	69.50
4	0	1	76.43	1	68.89	1	66.89	1	66.58
4	50	1	71.88	1	67.65	1	68.28	1	69.64
4	90	1	77.86	0.93	55.62	0.99	70.47	0.99	61.37
6	0	1	74.18	1	63.02	1	75.69	1	69.07
6	50	1	72.63	1	62.62	1	70.17	0.99	54.45
6	90	0.94	62.29	0.99	65.31	0.99	70.01	0.99	66.69
9	0	1	76.45	1	62.49	1	70.11	1	61.30
9	50	1	74.20	1	67.61	1	72.12	1	62.26
9	90	0.99	73.62	0.98	64.72	1	72.68	0.99	62.79

Table V. Probability of survival, P_s, and 99 percent survival stress, S_{99}, values calculated for each test condition for PM 7091.

Exposure Time (days)	Exposure Stresses (% YS)	T/E69 L	T/E69 T	T/E70 L	T/E70 T
2	0-50	73.90	77.10	67.50	72.90
2	0-90	81.80	66.10	77.00	71.60
2	50-90	83.80	66.00	79.40	71.30
2	0-50-90	80.10	67.90	75.20	71.80
4	0-50	68.60	66.50	69.70	73.00
4	0-90	78.00	57.20	70.80	61.30
4	50-90	79.80	58.30	70.90	61.00
4	0-50-90	75.90	58.90	70.60	63.50
6	0-50	70.40	62.30	65.40	48.70
6	0-90	63.40	65.30	69.60	66.40
6	50-90	64.20	65.30	70.00	73.10
6	0-50-90	64.90	64.70	68.80	61.50
9	0-50	72.40	73.20	74.40	63.60
9	0-90	73.50	64.70	73.00	62.90
9	50-90	73.60	64.70	72.80	62.90
9	0-50-90	73.20	66.20	73.20	62.90
Calculated	σ_{Th}	61.65	56.83	67.09	60.91

Table VI. Point estimates of the threshold stress for each test case and calculated threshold stresses, σ_{Th}, for each condition of PM 7091.

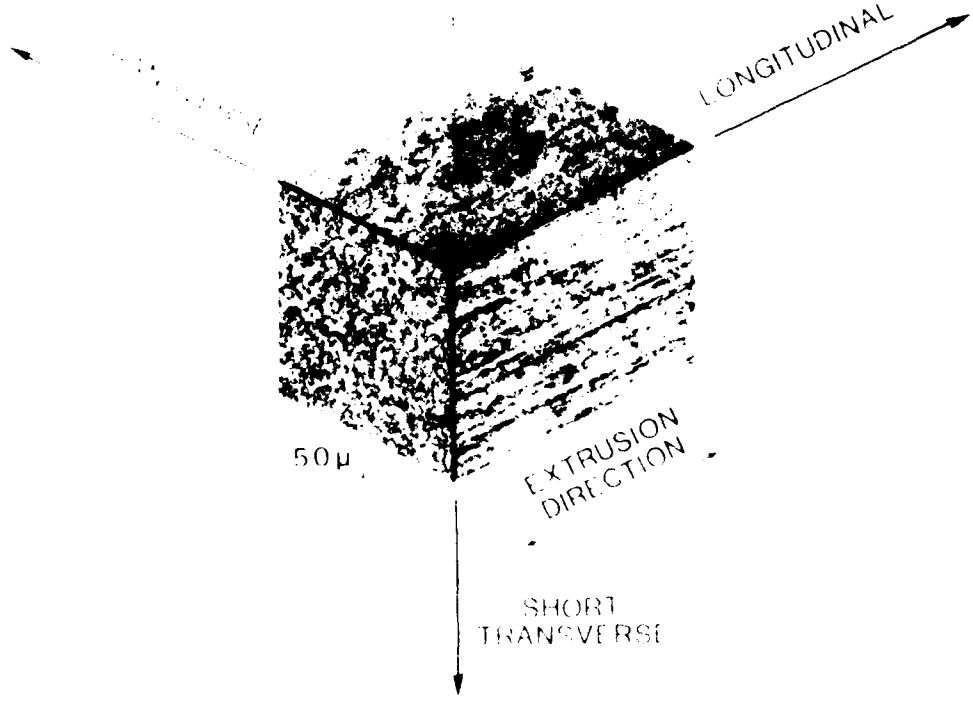

Figure 1. Grain structures at mid-plane of 1.5-inch thick PM 7091 extruded bar in both (a) T/E69 and (b) T/E70 conditions.

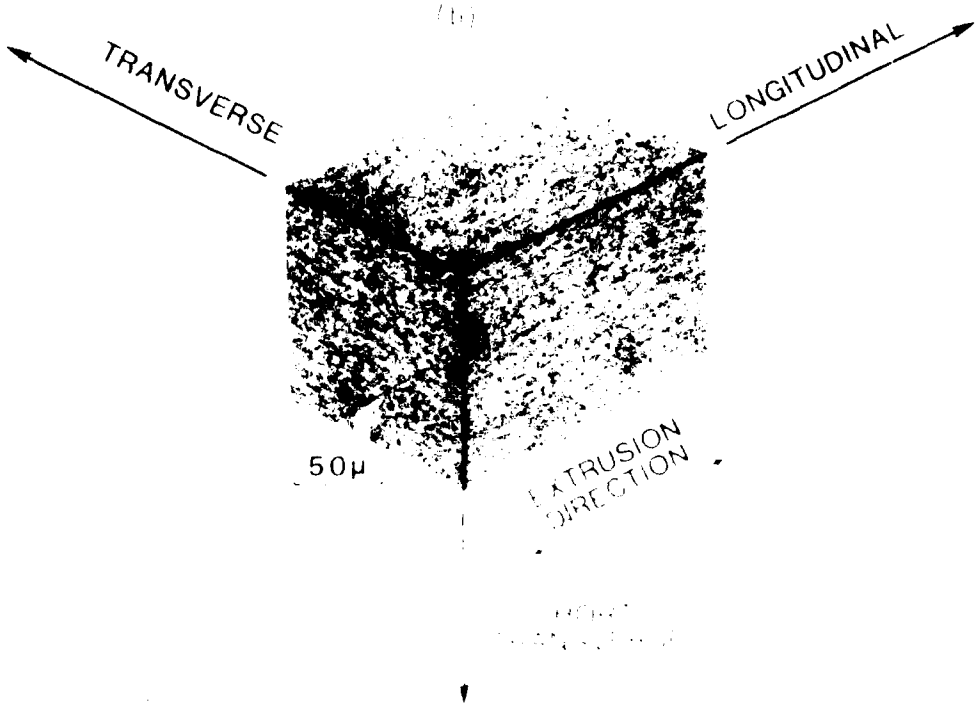

Figure 1. Continued.

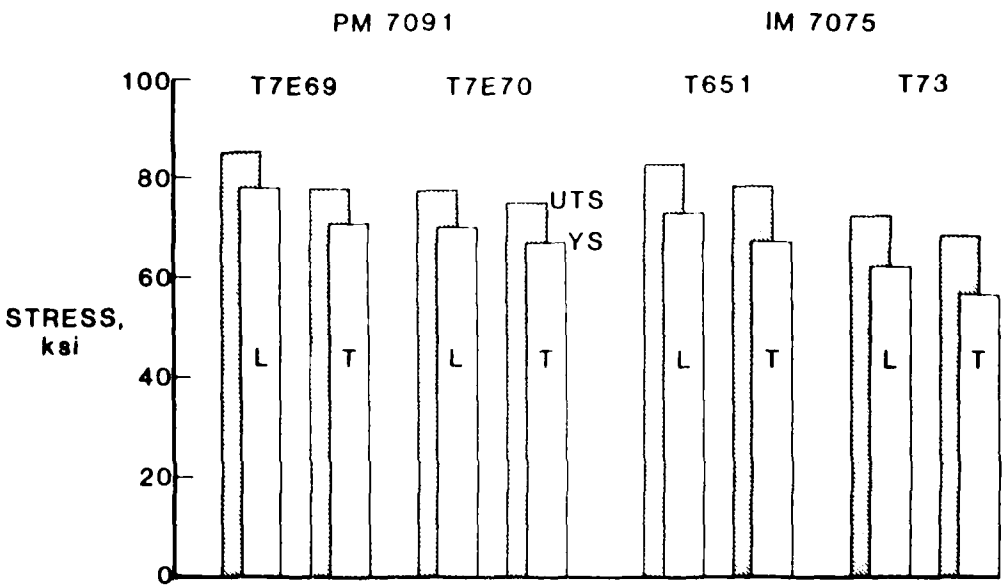

Figure 2. Tensile yield and ultimate strengths of overaged PM 7091 and peak and overaged IM 7075 in both longitudinal (L) and transverse (T) orientations.

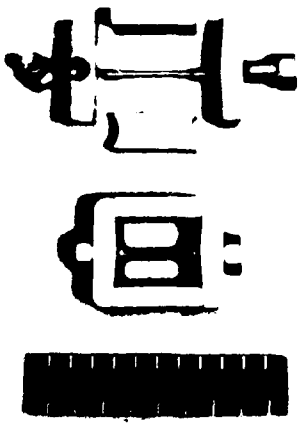

Figure 3. Constant deflection stressing frame and direct tension specimen.

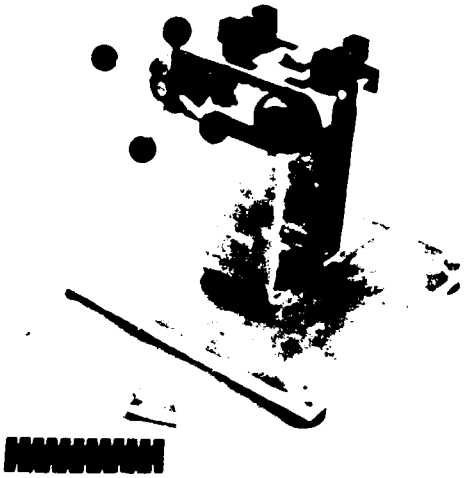

Figure 4 Device for loading specimens in tension with constant deflection stressing frames.

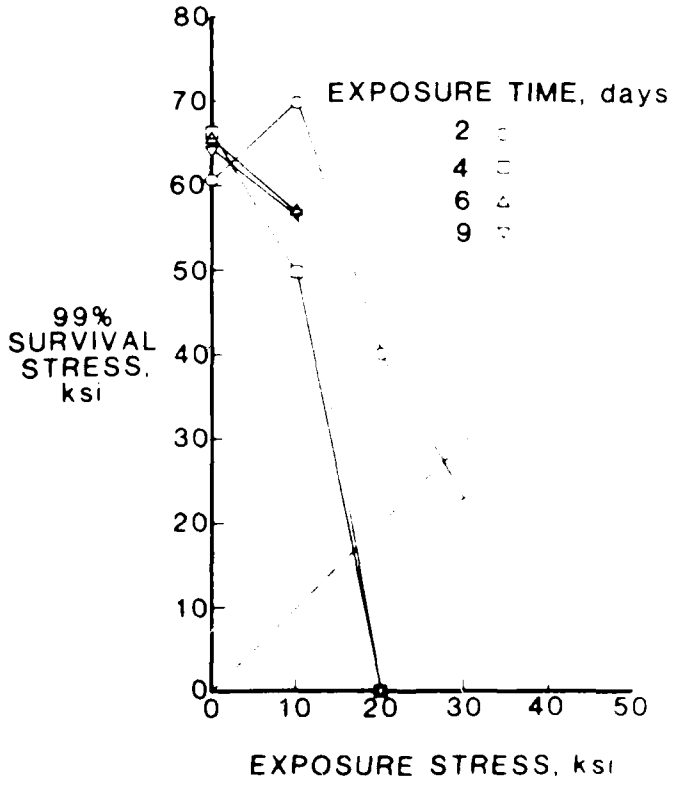

Figure 5. 99 percent survival stresses for IM 7075-T651 as a function of exposure stress and time. (Ref. 3)

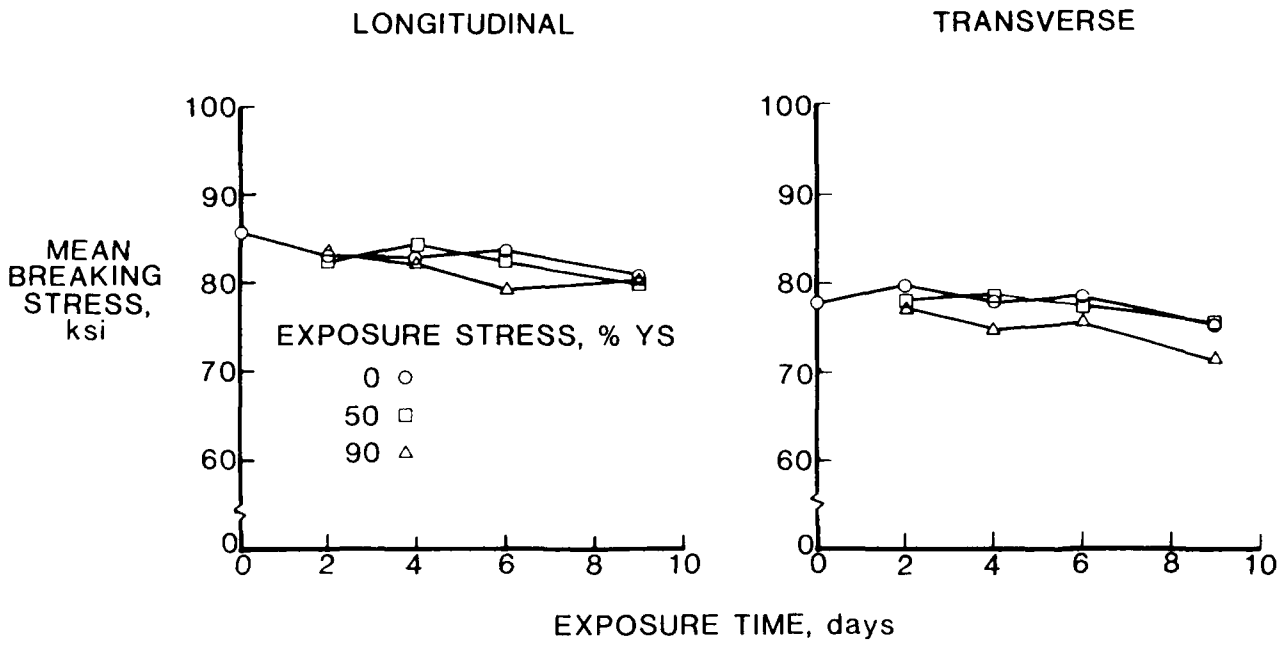

Figure 6. Mean breaking stresses for PM [illegible]-T[illegible].

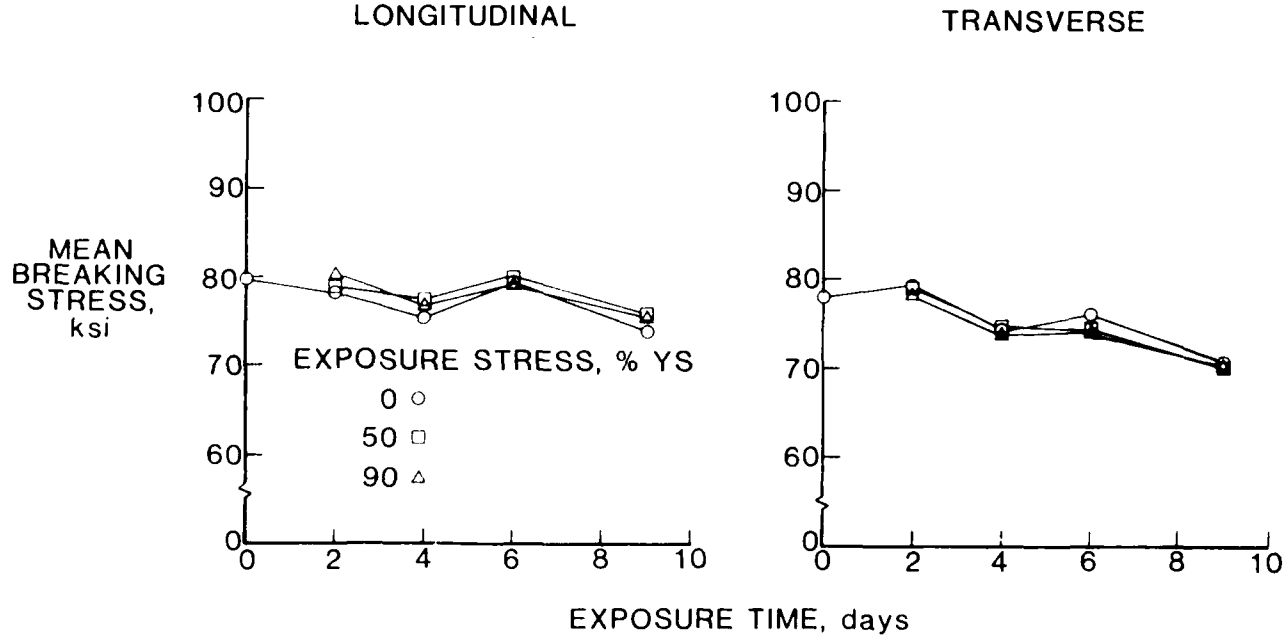

Figure 7. Mean breaking stresses for [illegible]-T[illegible].

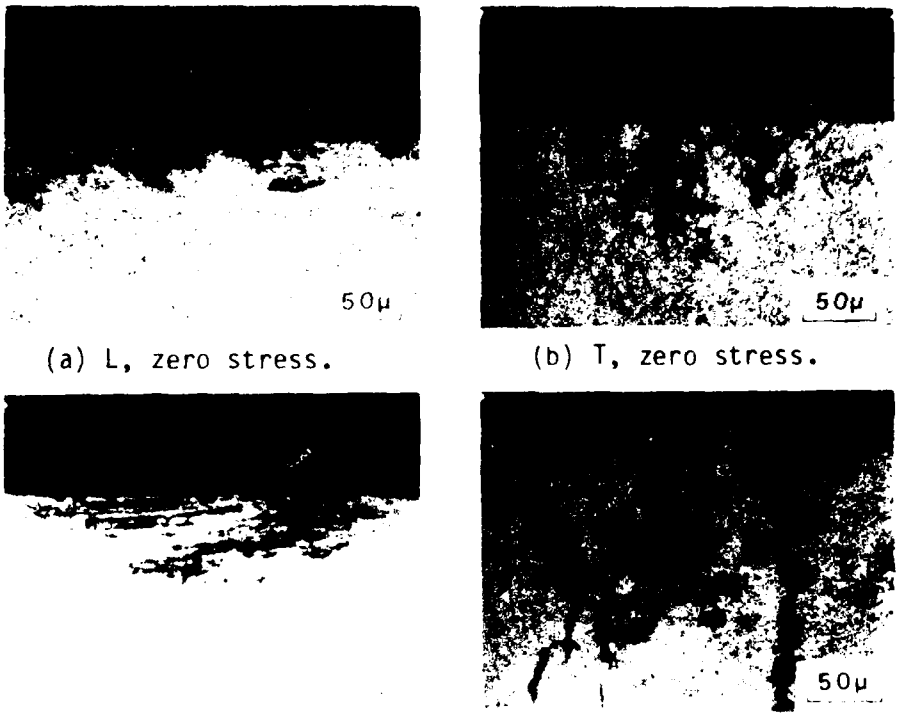

(a) L, zero stress. (b) T, zero stress.

(c) L, 90 percent YS. (d) T, 90 percent YS.

Figure 8. Longitudinal (L) and transverse (T) orientation metallographic sections of PM 7091-T7E69 specimens exposed for 9 days at zero and 90 percent yield strength.

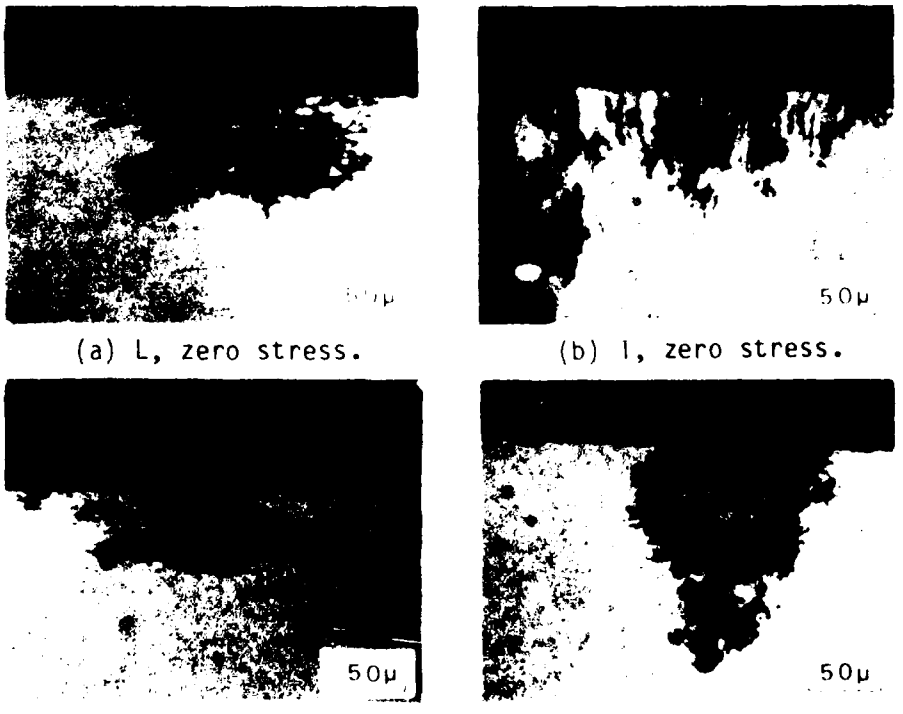

(a) L, zero stress. (b) T, zero stress.

(c) L, 90 percent YS. (d) T, 90 percent YS.

Figure 9. Longitudinal (L) and transverse (T) orientation metallographic sections of PM 7091-T7E70 specimens exposed for 9 days at zero and 90 percent yield strength.

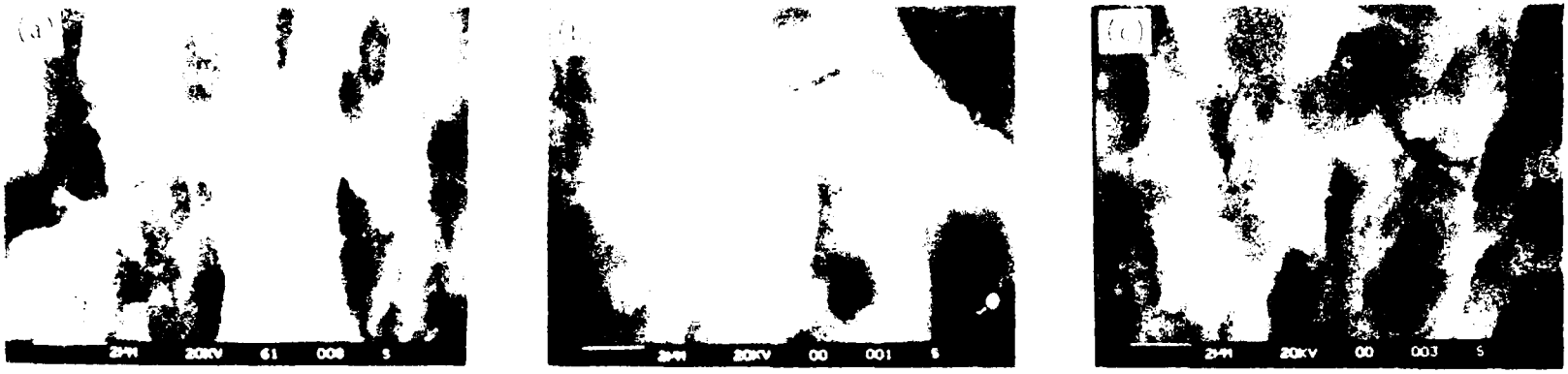

Figure 10. Fractographs of PM 7091-T7E69 transverse orientation specimen exposed for 9 days at 50 percent material yield strength. (a) Transgranular fracture regions; (b) Intersection of stress corrosion cracking (SCC) and overload (OL) fracture; (c) Intersection of transgranular (TG) and overload (OL) fracture.

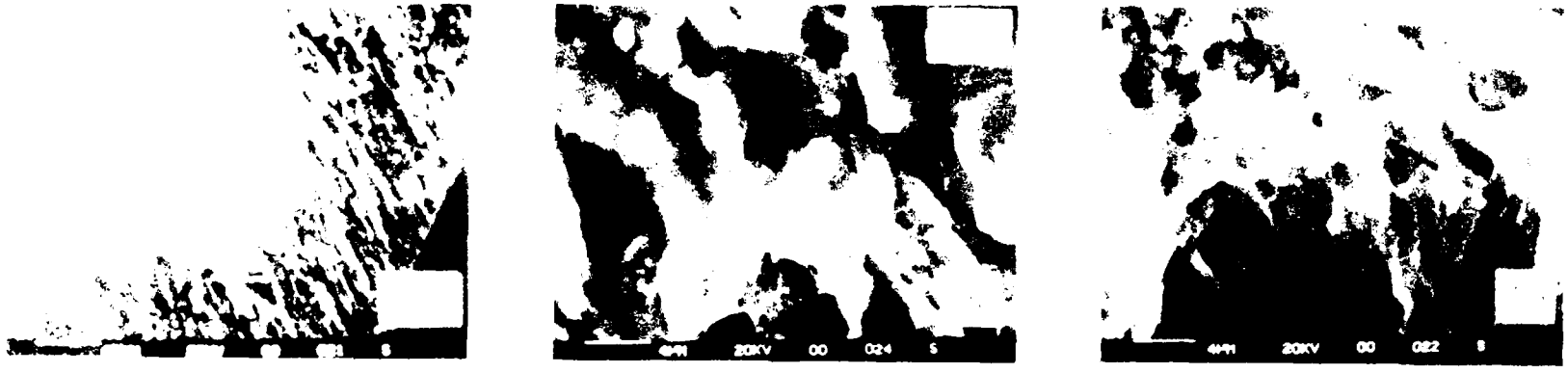

Figure 11. Fractographs of PM 7091-T7E69 transverse orientation specimen exposed for 9 days at 50 percent material yield strength. (a) Overload fracture; (b) Stress corrosion cracking; (c) Transgranular fracture.

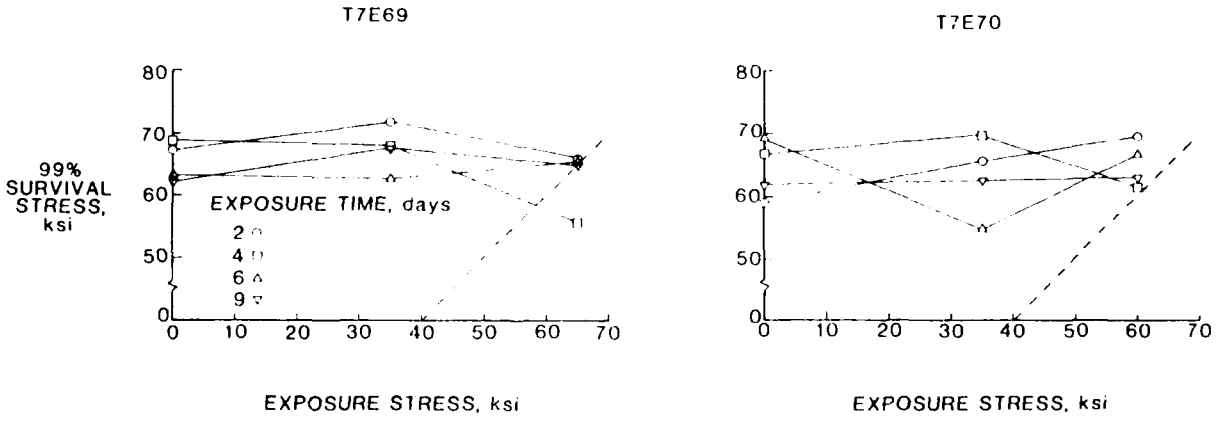

Figure 12. 99 percent survival stresses for transverse orientation of 7091 specimens.

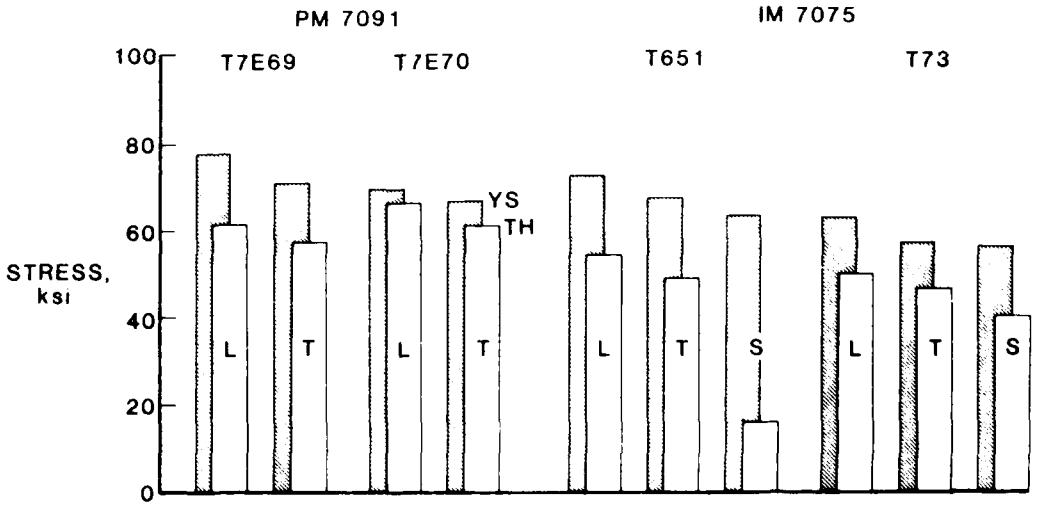

Figure 13. Threshold stresses (TH) and material yield strengths (YS) for overaged PM 7091 and peak and overaged IM 7075 (Ref. 14) in longitudinal (L), transverse (T), and short transverse (S) orientations.

ANALYSES AND CORRELATIONS OF ENVIRONMENT ASSISTED FATIGUE CRACK PROPAGATION FOR ATTACHMENT LUGS

J.T. Huang
Specialist Engineer
Lockheed-Georgia Company
Marietta, Georgia 30063-0001

Abstract

Fatigue crack growth rate data were generated for the 4340 steel (H.T. 180-200 ksi) in salt water. At lower frequencies and in the lower delta-K region, they are higher than those obtained in lab air. To properly account for environment effects, an existing crack growth prediction program was modified, and a table-lookup scheme for describing the FCGR's as functions of stress ratio, frequency, and delta-K was added. Using the new capability, crack growth life predictions were made for attachment lugs, with and without bushings, subjected to spectrum loads, in salt water and in lab air. Overall, the predictions correlate well with test results. The tests also demonstrated that, during the test periods, interference-fit bushings had a beneficial effect on corrosion-fatigue lives of attachment lugs made of 4340 steel. Future works are recommended.

Introduction and Objectives

Modern aircraft are designed to tolerate flaws and fly safely until the next scheduled inspection and repair. Crack growth predictions are intended to provide information for making such assessment; and for evaluating design and repair options, including the use of new materials.

Attachment lugs are among the most commonly used fracture critical components in aircraft structures. Due to corrosion, stress-corrosion cracking, human-induced damage, material defects, fretting, and fatigue, cracks may nucleate in attachment lugs. Such cracks significantly elevate the high stresses and strains around the hole edges which exist before crack initiation. Because of the narrow net section and high stress concentrations, it is particularly important to develop accurate analytical procedures and verify them experimentally so that damage tolerance of attachment lugs is assured.

Crack growth prediction procedures became sophisticated during the Seventies and early Eighties. At Lockheed, Hsu developed a general purpose crack growth prediction program [1] and a load-interaction model [2] to account for crack growth retardation/acceleration. In addition, with funding provided by Lockheed's IRAD projects and AFWAL Contract No. F33615-80-C-3211, Hsu, Kathiresan, and Brussat developed and test-verified analytical procedures for predicting crack growth in attachment lugs [3, 4, 5, 6].

The need to consider corrosion fatigue has long been recognized. As stipulated in the military specification "Airplane Damage Tolerance Requirements," MIL-A-83444 for metallic aircraft structures, crack growth

analyses shall account for cyclic mechanical loads and chemical environments to which components are subjected in service. In recent years, corrosion assisted fatigue has attracted even more attention. For attachment lugs, as shown in Figure 1, the two leading causes of failure in service have been found to be stress-corrosion cracking and (corrosion) fatigue crack growth. These statistics are the outcome of a Lockheed survey [5], with assistance from five Air Force Logistics Centers.

Many attachment lugs are made of high strength steels, including 4340 steels. Crooker and Lange [7] found that the fatigue crack growth rates (FCGR's) of 4340 steel in salt water subjected to cyclic loads at lower frequencies are higher than those obtained in lab air. Since some aircraft are stationed on coastal bases, it is reasonable to include salt water and salt water spray as upper bound conditions in the service environment spectra. Thus, additional database and a new capability to properly account for environmental effects become desirable.

The objectives of this work are: (1) Add capability to an existing crack prediction program for attachment lugs to account for the effect of varying frequencies of spectrum loads. (The existing program considers constant frequency for the entire loading spectrum in an analysis.) (2) Evaluate the effect of interference-fit bushing on the crack growth life of attachment lugs made of 4340 steel in 3.5% NaCl solution.

Case Studies

Figure 2 shows the configuration of a straight shank attachment lug without bushing. All lugs, with or without bushing, that were selected in this work are straight shank lugs containing a through-the-thickness crack and having a hole radius of 0.75 inch, thickness of 0.5 inch, and R_o/R_i ratio of 2.25, which is the medium of 1.5 to 3.0 for most lugs in service. They are made of 4340 steel (H.T. 180-200 ksi), having a tensile yield strength of 179.7 ksi. The bushing was made of 4130 steel (H.T. 125-145 ksi). Its wall thickness is 0.09 inch. The diametral interference is 0.008 inch. The target environment was 3.5% NaCl solution at room temperature, in which the 4340 steel is known to be corrosion-susceptible.

Figure 3 summarizes all case studies. For each case, an analytical prediction was made and correlated by test result. The lab air cases were included to gain a better perspective of the prediction/test correlations. For these cases, lab air test data were taken from Ref. 5; new predictions based on an improved method for crack growth rate description were accomplished.

To verify the prediction procedures against variable amplitude loads, three flight-by-flight cyclic load spectra, with or without an amplification factor, were used. The spectrum loads {F} are cyclic loads derived from an A-7 trainer spectrum (Ref. 5). The spectrum loads {C}, consisting of 120 flights, were derived from C-5 mission profiles (Ref. 5). The block spectrum loads {B}, shown in Figure 4, were altered from a typical flight in {C}. Those numbers in the parentheses are artificial,

with the intent to accelerate the tests. The cyclic loads in the spectrum {B} have varying amplitude, stress ratio, and frequency. The wave form is sinusoidal. All stresses in Figure 4 are far-field stresses applied to a lug.

Experimental Procedures

The target environment was 3.5% NaCl solution at room temperature. The solution was contained in a small transparent plexiglass chamber with an open top end; the specimen was totally immersed. A small pump and a flexible tube were employed to continuously circulate the salt water from the chamber bottom to the specimen region, where salt water was gently injected from a nozzle toward the crack tip. This setup created bubbles, but no slushing or massive fluid flow. The debris generated by corrosion spread out in suspension; some of which eventually settled. As the test progressed, the entire chamber of dirty fluid was occasionally replaced with fresh solution.

The specimen was precracked in lab air. A microscope, aided by local illumination and rulers attached to the specimen, was used to visually read the crack lengths on the two outer surfaces.

Cyclic mechanical loads were provided by electrohydraulic servo controlled testing systems. Each system contains the necessary elements to control the servo loop, generate and monitor the predetermined cyclic loads, as well as perform failsafe functions. The system is interfaced to a digital computer.

The plain end of a lug was clamped in a hydraulic grip. Loads were applied through a hardened steel pin in a steel fork fitting, which was slotted to render visual access to the crack path during the tests.

Spectrum loads such as those in a block shown in Figure 4 were applied sequentially according to the load numbers. After the completion of one block, the same block was repeated over and over again until the specimen failed.

FCGR DATA

For the generation of FCGR data, compact type (CT) specimens were used. The measured crack growth increments, da, and corresponding elapsed numbers of constant amplitude load cycles, dN, were fitted into a polynomial equation to obtain the da/dN vs. delta-K curve. The procedures were in accordance with the ASTM Standard E647 for constant-load-amplitude FCGR's above 10^{-8} m/cycle.

FCGR data were generated for 4340 steel (H.T. 180-200 ksi) in salt water. The wave form is sinusoidal. The stress ratios, R, of cyclic loads are 0.01, 0.2, 0.5; the frequencies, Ω, are 1, 2, and 15 Hz. They amount to 9 test conditions. Additional data were also generated at R = 0.75 and Ω = 15 Hz.

Figure 5 shows the FCGR data at R = 0.2 and Ω = 1.0 Hz, in salt water and in lab air. At lower delta-K, the FCGR's in salt water are higher than those in lab air. This indicates a significant contribution to the total

crack growth by environmental enhancement. At higher delta-K, there is a merging of the FCGR's obtained in the two environments - the crossover in Figure 5 would most likely disappear if many coupons were tested. The merging data trends indicate that at higher delta-K and for the exposure time of 1 second per cycle, cyclic mechanical effects are the predominant contributors to the total crack growth. Similar qualitative behavior has been reported by Crooker and Lange [7]. It should be noted that the lab air is also an aggressive environment. In Marietta, Georgia, the relative humidity of lab air all year round is mostly 50-60%.

Figure 6 shows the FCGR data for three different combinations of frequency and stress ratio. Given the same stress ratio, the crack growth rate is higher for lower frequency; given the same frequency, the crack growth rate is higher for higher stress ratio. Such behavior has also been reported by Miller, Hudak, and Wei [8].

Crack Growth Prediction Procedures

Prediction of crack growth from an initial length involves three steps: (1) computation of stress intensity factors (SIF's) as functions of the structure and crack geometry/length, (2) calculation of FCGR's from data table or fitted functions, and (3) accumulation of crack growths in response to the time varying cyclic loads, crack geometry/length, and crack tip plastic zone. At Lockheed, for a number of structural components or lugs containing typical cracks, these steps are automated in the computer program "CRACKGROWTH/TH79" [1] and its offspring "LUGRO" [5].

To calculate the SIF's for lugs, the program "LUGRO" takes stress distribution in an uncracked lug (obtained from finite element analysis) as input, and performs convolution integration involving Green's functions [3, 4, 5]. The Green's functions, obtained from two-dimensional finite element models with a crack tip element, are stored in data form in the program.

For predicting the damage accumulation, both "CRACKGROWTH/TH79" and "LUGRO" use a layer-by-layer integration technique to calculate the incremental crack growth per load block, da/dB, as function of crack length "a". Its inverse function dB/da is then integrated with respect to the crack length "a" to obtain the number of load blocks required to grow a crack from "a" to "a + da".

Hsu's load-interaction model [2] was applied to account for the crack growth retardation due to tensile overload. For lugs, there is no crack growth acceleration due to compressive overload to consider. This is because a lug is designed primarily to carry tensile loads; and when it is subjected to compressive loads, small tensile hoop stresses are developed at the crack site shown in Figure 2.

Both "CRACKGROWTH/TH79" and "LUGRO" consider constant frequency for the entire loading spectrum in an analysis. Since the environment enhanced crack growth rate is frequency dependent, the program "LUGRO" was modified in this work so that the effect of varying frequencies of spectrum loads can be accounted for.

A scheme for describing the FCGR's as functions of stress ratio, frequency, and delta-K was added. This was accomplished by setting up the FCGR "tables" for various material/environment/wave-form/frequency combinations. In each table, the FCGR's are stored in the form of fitted data or Forman equation constants for a number of stress ratio R's and delta-K ranges. The FCGR's at frequencies not tested are calculated from a linear combination of the FCGR's for two encompassing frequencies for which data were tested and data or equation constants were stored.

Effect of Interference-Fit Bushing

The installation of an interference-fit bushing results in substantial reduction in peak local stress concentration in a lug. Simultaneously, residual hoop stresses are introduced because the lug hole is enlarged; the latter is due to compressive stresses exerted in the radial direction onto the lug hole boundary by the bushing. In the presence of a fatigue crack and a mechanical load cycle, this means a lower stress-intensity factor range but a higher stress-intensity factor ratio. In lab air, the net effect on fatigue life is beneficial when an optimum amount of interference is used [9]. In salt water, the effect of a lower stress-intensity factor range should remain beneficial. The effects of residual stress and higher stress ratio are qualitatively negative. To determine their net combined effect is one objective of this investigation.

Figure 7 shows the fatigue lives of three lugs that were cyclic load tested in salt water. Let lives be compared on the same basis: the number of load blocks required for the crack to grow from an initial length of 0.13 inch to 0.60 inch. Here a load block is equivalent to 3642 cycles. The unbushed lug SW-1 survived about 200 load blocks; whereas the bushed lug SW-2 survived about 400 load blocks. Even the bushed lug SW-3, which was subjected to 50% higher cyclic loads, lasted longer than the unbushed lug SW-1. Clearly, the net effect of bushing on fatigue life is beneficial for the tested cases.

Comparison of Predicted and Tested Lives

Figure 8 shows the ratios of predicted to tested crack growth lives. A prediction is conservative if its life ratio is less than 1. Incidentally, because of the inherent randomness in material properties and structural details, life ratios and FCGR data normally fall in scatter bands. For the purpose of development here, the best fit or average FCGR data were used. In application, the upper bound of the "real" scatter band of FCGR data should be used when conservative predictions are desired [10].

For unbushed lugs, in lab air and salt water, the life ratios here vary from 0.90 to 1.70. For lugs, such accuracy is good in view of the high stress concentrations and the clearance that may have existed at the pin/lug interfaces.

For bushed lugs, in lab air and in salt water, the life ratios are 0.96, 0.48, 0.26, and 0.42, respectively. The trend is conservative; and it may be due to bush/lug interface modeling. As to the low ratio of 0.26 for the lug SW-2, test records show that the initial crack lengths on the two outer surfaces are highly unequal. A crack of such shape can be expected to grow slower than a through-the-thickness crack. For the other three lugs, the life ratios fall within a factor of 2.4. Although such accuracy is acceptable, improvement is desirable.

Summary

The FCGR's of the 4340 steel (H.T. 180-200 ksi) in salt water are functions of cyclic load frequency and stress ratio. They are higher than those obtained in lab air at lower frequencies and in the lower delta-K region. Since structures spend most of their crack growth lives at crack shape/length corresponding to lower delta-K's, it is important to consider the service environments and the effect of cyclic load frequencies.

An existing crack growth prediction program was modified, and a table-lookup scheme for describing the FCGR's as functions of stress ratio, frequency, and delta-K was added. Using the new capability, crack growth life predictions were made for three attachment lugs that were spectrum load tested in salt water; and for eight attachment lugs that were previously spectrum load tested in lab air. Compared with test results, predictions for unbushed lugs are satisfactory; predictions for bushed lugs need improvement. Overall, the prediction procedures have properly accounted for the salt water environment.

The tests also demonstrated that interference-fit bushings had a beneficial effect on corrosion-fatigue lives of attachment lugs made of 4340 steel during the test periods.

The following works are recommended: (1) Improve prediction procedures for analyzing a lug with an interference-fit bushing; (2) Determine the effect of pin/lug clearance on the stress intensity factor of a cracked lug; (3) Investigate the long term effect of an interference-fit bushing on the fatigue life of a 4340 steel lug in an aggressive environment; (4) Evaluate the performance of lugs made of more corrosion resistant, high strength steel alloys.

Acknowledgement

This work was performed at the Lockheed-Georgia Company under 1986-87 IRAD Project R523. The author would like to thank the Lockheed-Georgia Company for granting unlimited release, and Mr. H.S. Pearson for preparing test equipment and conducting all tests reported in this paper. He also wishes to thank Mr. M.D. Goodyear for his encouragement.

References

1. Hsu, T.M., "Computer Program for Prediction of Fatigue Crack Propagation," Lockheed-Georgia Report SMN 370, Rev. A, November 1979.

2. Hsu, T.M., "Development of Load-Interaction Model," Lockheed-Georgia Report SMN 390, February 1976.

3. Hsu, T.M., "Analysis of Cracks at Attachment Lug," Proceedings of the AIAA/ASME 21st SSDMS, May 12-14, 1980, Seattle, Washington.

4. Hsu, T.M., and K. Kathiresan, "Analysis of Cracks at an Attachment Lug Having an Interference-Fit Bushing," Fracture Mechanics, ASTM STP 791, ASTM, 1982.

5. Kathiresan, K., T.M. Hsu, and T.R. Brussat, "Advanced Life Analysis Methods," AFWAL-TR-84-3080, Vol. I-VI, AFWAL, September 1984.

6. Kathiresan, K., T.R. Brussat, and J.L. Rudd, "Crack Growth Analyses and Correlations for Attachment Lugs," Journal of Aircraft, Vol. 22, No. 9, September 1985.

7. Crooker, T.W., and E.A. Lange, "Fatigue Crack Growth in Three 180 ksi Yield Strength Steels in Air and in Salt-Water Environments," NRL Report 6761, Naval Research Laboratory, Washington, DC, September 1968.

8. Miller, G.A., S.J. Hudak, and R.P. Wei, "The Influence of Loading Variables on Environment-Enhanced Fatigue Crack Growth in High Strength Steels," Journal of Testing and Evaluation, JTEVA, Vol. 1, No. 7, November 1973.

9. Smith, C.R., "Tips on Fatigue," NAVWEPS 00-25-559, Bureau of Naval Weapons, Dept. of the Navy, 1963.

10. Gallagher, J.P., F.J. Giessler, A.P. Berens, and R.M. Engle, Jr., "USAF Damage Tolerant Design Handbook: Guidelines for the Analysis and Design of Damage Tolerant Aircraft Structures," University of Dayton Research Institute, Dayton, Ohio, March 1984.

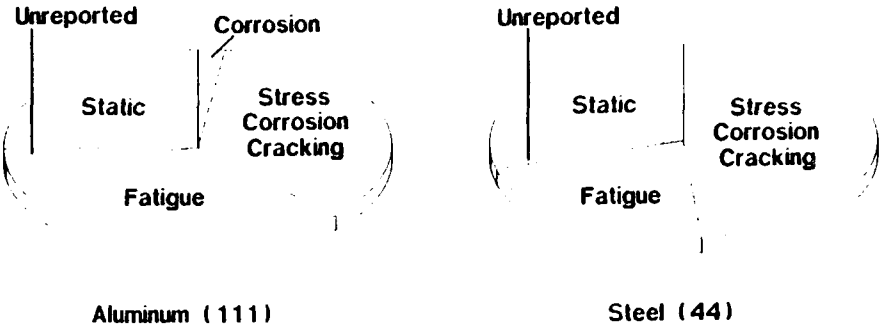

Figure 1. Causes of Failure of Lugs in Service

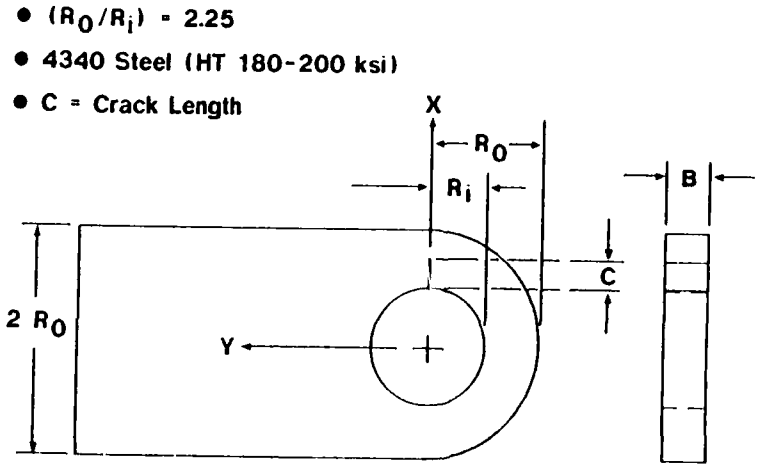

Figure 2. Straight Attachment Lug with a Through-the-Thickness Crack

- 4340 Steel (HT 180-200)
- Thru Crack

Coupon ID	Interference-Fit Bushing	Environment	Spectrum Loads
SB-75 & 77	No	Lab Air	{F}
SB-78 & 94	No		{C}
SB-76 & 46	No		{C} X 1.5
SV-43 & 45	Yes		{C} X 1.5
SW-1	No	3.5% Salt Water	{B} X 1.2
SW-2	Yes		{B} X 1.2
SW-3	Yes		{B} X 1.5

Figure 3. Case Studies for Straight Shank Lugs

Load No.	(σ_0) Max ksi	(σ_0) Min ksi	No. of Cycles	Frequency
1	18.1	-1.8	1	1
2	15.6	0.0	2	1
3	(6.4)	(0.4)	3330	30
4	13.5	(7.5)	270	15
5	15.1	9.1	32	15
6	15.9	7.9	5	15
7	16.9	5.6	2	1

Figure 4. Block Spectrum {B}

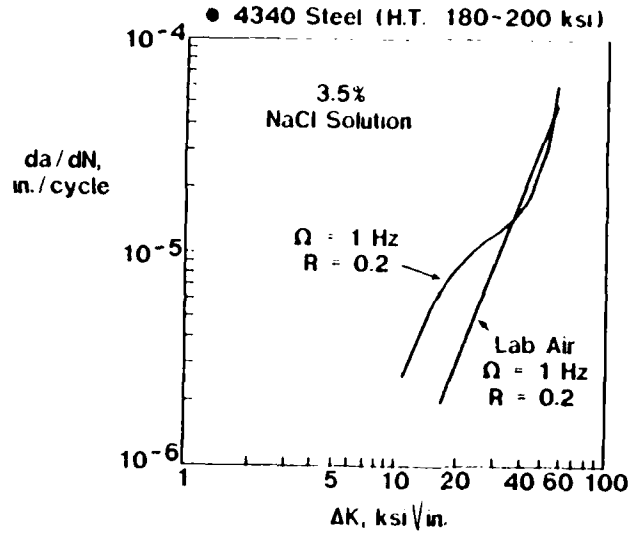

Figure 5. FCGR Data in Salt Water and Lab Air

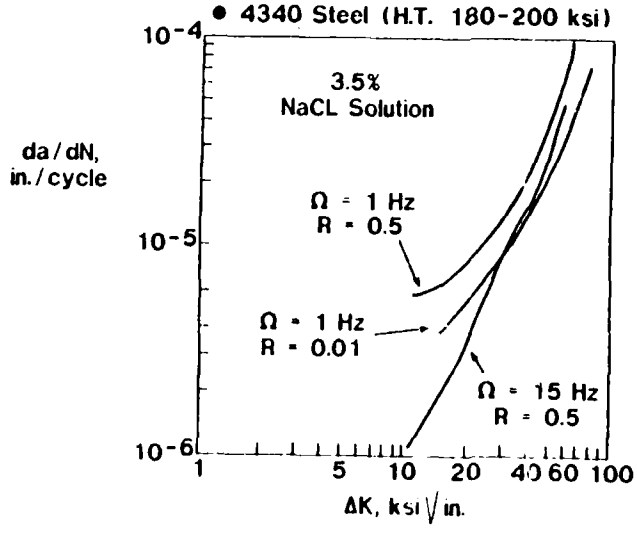

Figure 6. FCGR Data in Salt Water

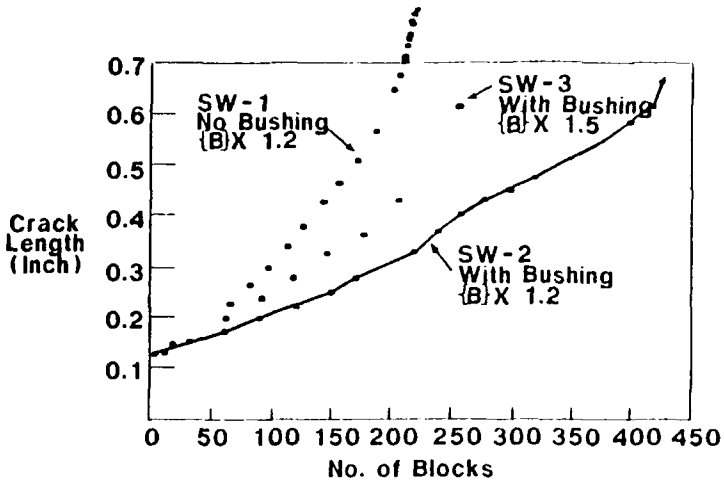

Figure 7. Tested Crack Growths in Attachment Lugs

Coupon ID	$\left(\frac{\text{Predicted Life}}{\text{Tested Life}}\right)$
SB-75 & 77	1.70 & 1.38
SB-78 & 94	1.50 & 1.32
SB-76 & 46	0.90 & 1.41
SV-43 & 45	0.96 & 0.48
SW-1	1.42
SW-2	0.26
SW-3	0.42

Figure 8. Accuracy of Crack Growth Life Predictions

BIOGRAPHY

NAME:

J.T. HUANG

PRESENT AFFILIATION:

LOCKHEED-GEORGIA COMPANY

TITLE:

SPECIALIST ENGINEER

FIELD OF INTEREST/RESPONSIBILITIES :

FRACTURE MECHANICS; COMPOSITE JOINTS

PREVIOUS AFFILIATIONS/TITLES:

ALCOA LABORATORIES, PITTSBURGH, PA; SENIOR ENGINEER

ACADEMIC BACKGROUND:

UNIVERSITY OF PITTSBURGH, STRUCTURAL MECHANICS

SOCIETY ACTIVITIES/OFFICES/AWARDS:

ASCE, ASTM

PUBLICATIONS/PAPERS:

ENVIRONMENTAL CRACKING OF A SUPERFERRITIC STAINLESS STEEL UNDER SLOW STRAIN RATE CONDITIONS

J. A. Smith
Material Science and Technology Division
Naval Research Laboratory
Washington, DC 20375-5000

Abstract

Computer aided slow strain rate testing together with electrochemical/permeation measurements were performed on a superferritic stainless steel in 0.6 N NaCl solution. Data show that in the absence of applied stress permeation current density (i_p), hydrogen diffusivity (D_H), and hydrogen concentration (C_o) all decrease with increased deformation. In the presence of applied stress, i_p and D_H values decrease but C_o values increase in going from elastic to plastic strains. The observed pseudo-invariant in the ductility vs electropotential plot for this material is ascribed to the increase in C_o values with increases in plastic strain.

ENVIRONMENTAL CRACKING OF A SUPERFERRITIC STAINLESS STEEL UNDER SLOW STRAIN RATE CONDITIONS

Introduction

Materials utilized for critical components in marine applications typically require both passivity and resistance to environmental cracking. The emergence of a new class of alloys, namely, the superferritic stainless steels have created considerable interest because of their excellent resistance to pitting and crevice corrosion in chlorinated environments (1,2). The essential features of these alloys are their low interstitial levels and their high chromium and molybdenum contents.

In many applications these new ferritic steel alloys are required to be in contact with other less corrosion-resistant alloys. To prevent galvanic corrosion such multi-metal systems are usually protected by the application of cathodic potentials (3,4). However, at modest cathodic potentials, a totally unexpected and surprising tendency toward cracking occurs in these medium strength alloys.

Generally, in most passive metal systems, the crack initiation mechanism is considered from the standpoint of surface dissolution effects related to the competition between passivation and depassivation kinetics. Since the surface dissolution process of passive metals in Cl^- solutions at open circuit potential (OCP) is dependent in part on the pH and electropotential of the system and the stress state of the material, the influence of these parameters requires critical analysis.

The purpose of the present work is to study the role of hydrogen absorption/permeation and stress state in determining the mechanism of crack initiation in Fe-29Cr-4Mo superferritic stainless steel (Allegheny Ludlum Steel Corporation Al29-4C).

Experimental Procedure

The experimental approach utilized in these tests consists of a computer-aided slow-strain-rate technique which incorporates facilities for electrochemical and hydrogen permeation monitoring. Great advantages are afforded by computer-aided systems because they bring enormous data acquisitions and manipulative capabilities, as well as, consistency, reliability, and high speed to the field of experimental corrosion testing. The slow-strain-rate (SSR) apparatus used to assess susceptibility to environmental cracking consists of a gear driven system mounted in a sturdy load frame (Figure 1). In the SSR tests, smooth tensile bars with a cross-section of approximately 6.35 mm x 0.8 mm were pulled to fracture at a strain rate of 1.45×10^{-6}/sec, while being exposed to the relevant environmental conditions either at the free corrosion potential or potentiostatically controlled at a predetermined potential. Alloy chemical compositions and as received mechanical properties are listed in Tables 1 and 2.

Slow-strain-rate/H-permeation testing was carried out with each specimen having an exposed diameter of 19 mm and a thickness of approximately 0.127 mm. All permeation specimens are given a 600-grit finish and then the exit side is immediately coated with Pd.

A schematic diagram of the permeation cell is shown in Figure 2. Briefly, the technique (5,6) requires the establishment of a diffusion gradient within a metal specimen by utilizing two electrochemical cells, one on either side of the metal specimen. On one side, the conditions within the cell are adjusted via a potentiostat so that hydrogen is charged into the specimen; on the other side of the specimen is put under anodic control so that hydrogen is continually being extracted. Analyzing the permeation current-time transients by known mathematical and graphical methods provides information concerning hydrogen absorption and movement.

Results

Table 3 gives a summary of SS tests for superferritic steel, Al29-4C, in air and 0.6N NaCl solutions. These results show a shift from ductile to brittle behavior as one progresses from anodic to cathodic potentials. This shift is attributed totally, or in part, to material embrittlement due to hydrogen absorption.

Slow-Strain-Rate Tests

A representation of the damage to Al29-4C via environmental corrosion is expressed in terms of ductility degradation versus potential in Figure 3. This graph shows a low ductility region stretching from -1400 mV to circa -600 mV. By using the pH value of the test solution, one may calculate the hydrogen equilibrium potential, $V_{H/H2}$, by the Nerst equation: $V_{H/H2} = -0.242 - 0.059$ pH (SCE). At pH = 6.3, the calcualted potential is $V_{H/H2} = -610$ mV. Since this potential is more negative than the observed open circuit potential of +17 mV, crack propagation at the open circuit potential is not expected to be controlled by hydrogen related processes. However, at controlled potentials more cathodic than -610 mV, crack propagation is expected to be influenced or controlled by hydrogen diffusion processes.

In Figure 4 at OCP, the SEM fractograph shows a predominance of microvoid coalescence while, in Figure 5 at -600 mV, alpha-cleavage is seen to predominate. At -1400 mV (Figure 6) large cathodic currents produce copious amounts of H_2 at the metal/solution interface. The adsorption of this hydrogen on the surface and subsequent adsorption into the metal result in the fractured specimen showing little reduction in area and possessing all transgranular alpha-cleavage, numerous secondary cracks, and some microvoids. The observed microvoids are consistent with the findings of other investigators (7).

Electrochemical/Permeation Tests

The superior environmental cracking behavior of super ferritic stainless steel, Al20-4C, appears to be vested in an oxide film possessing considerable Cr and some Mo enrichment, based on Auger data. As seen in

Figures 7 and 8, observed open circuit potential in aerated 0.6N NaCl solutions at pH 6.3 is approximately +17 mV and resides in a low current density passive regime. Additionally, referring back to Figure 3, one notes that no area of low ductility exists outside the potential range where the evolution of hydrogen is possible. This is consistent with a cracking mechanism attributable to hydrogen embrittlement and not to a process dependent on anodic dissolution.

Table 4 shows the behavior of pure iron, some binary iron alloys, and A129-4C in 0.6N NaCl at pH 6.3. this table illustrates that, given a certain amount of adsorbed hydrogen, as primarily determined by pH and system potential, the amount of absorbed hydrogen is greatly influenced by oxides, films, etc. at the metal/solution surface. Additionally, one notes in Figure 9 that the amount of deformation influences the amount of hydrogen in a metal. By plotting ip @ -610 mV as a function of stress, a significant decrease in ip values is noted after the yield strength (σy) is exceeded while ip values are found to be relatively uniform below σy. This reduction in ip values suggests that hydrogen is being trapped within the metal (8). Such an occurrence together with the increase in C_o values (Table 5) at stress levels greater than σy suggests that the constancy of low ductility values in the cathodic potential range (-1400 mV to circa -600 mV) results from the increased hydrogen generated in the plastic stress range and from hydrogen trapped at and below -610 mV. Together they conjointly act to embrittle the metal.

Discussion

The environmental cracking behavior of superferritic stainless steel, A129-4C, may be explained on the basis of hydrogen movement and surface film breakdown. Movement of hydrogen is usually accomplished through diffusion when an appropriate potential exists. It may be accelerated by the movement of dislocations during deformation processes or restricted by their trapping action.

In iron and ferritic steels, dislocation cores and grain boundaries are considered to contribute greatly to hydrogen trapping (9). Oriani (10) and McLellan (11) estimated trap densities caused by these lattice defects (for deformed ferritic steels) to be on the order of 10^{17} - 4 x 10^{19} cm^{-3}. For non-deformed ferritic steels the value is expected to be somewhat less (12). It is reasonable to assume that increased dislocation density effectively traps some hydrogen and reduces H-permeation (13-15). This is noted in Figure 9. A consideration of the data in Tables 4 and 5 also support this premise. For ferritic stainless steel, A129-4C, an 85 percent decrease in ip and circa 19 percent decrease in diffusivity (D_{ip}) result upon deformation via cold rolling to 85 per cent reduction in thickness.

Under conditions of plastic deformation, plastic strains can break down surface films and induce local electrochemical reactions. These reactions depending on the pH, electropotential, and chemistry of the system may either result in dissolution or hydrogen generation effects. In the aforementioned tests, one would expect an increase in the amount of hydrogen absorbed into the metal because of the film breakdown at the

higher plastic strain levels. Table 5 shows the variation of ip and D_H with increasing stress levels for Al29-4C material deformed 85 percent by cold rolling. Although slight, a definite increase in hydrogen concentration values is indicated with ascending plastic stress levels.

It has been shown that the cracking behavior of superferritic stainless steel, Al29-4C, in chloride solutions is controlled by a hydrogen related mechanism. The experimental results presented in this paper indicate that the movement/trapping of hydrogen within the metal is of great importance in interpreting cracking behavior. In the absence of applied stress ip, D_H, and C_o values decrease as the degree of deformation increases. However, in the presence of stress ip and D_H values decrease but C_o values increase as we go from elastic to plastic behavior. The appearance of a pseudo-invariant line in the cathodic region of the ductility vs electropotential plot is ascribed to this increase in metal hydrogen content with increasing plastic strain. This conclusion is in agreement with current observations of H-permeation in Al29-4C under conditions of continuous cathodic hydrogen charging.

Conclusions

1. The inherently low H-permeation value evident in superferritic stainless steel, Al29-4C, appears to result from the high Cr and Mo content of its surface film.

2. As defined by the solution pH of 0.3, hydrogen evolution is possible in this metal/solution system at V_{SCE} = -[illegible] mV.

3. The time necessary to develop hydrogen embrittlement and material ductility (measured as $\epsilon_{fa}/\epsilon_{fa}$(air)) [illegible] decreases as the potential becomes more electronegative than -[illegible] mV.

4. Fractographic analysis [illegible] microvoid coales[illegible] alpha-ferrite at -[illegible] and to alpha-ferrite at -1400 mV.

5. Room temperature [illegible] substantially decreases H-permeation [illegible] a decrease in the hydrogen concentration within the metal.

6. H-permeation is [illegible] stress-strain [illegible]

7. [illegible] the metal hydrogen concentration [illegible]

8. [illegible] beyond it is possible [illegible] potentials between [illegible]

AD-A191 295 PROCEEDINGS OF THE TRI-SERVICE CONFERENCE ON CORROSION (1987) HELD AT THE..(U) AIR FORCE WRIGHT AERONAUTICAL LABS WRIGHT-PATTERSON AFB OH.. F H MEYER MAY 87 4/6

UNCLASSIFIED AFWAL-TR-87-4139-VOL-1 F/G 11/6.1 NL

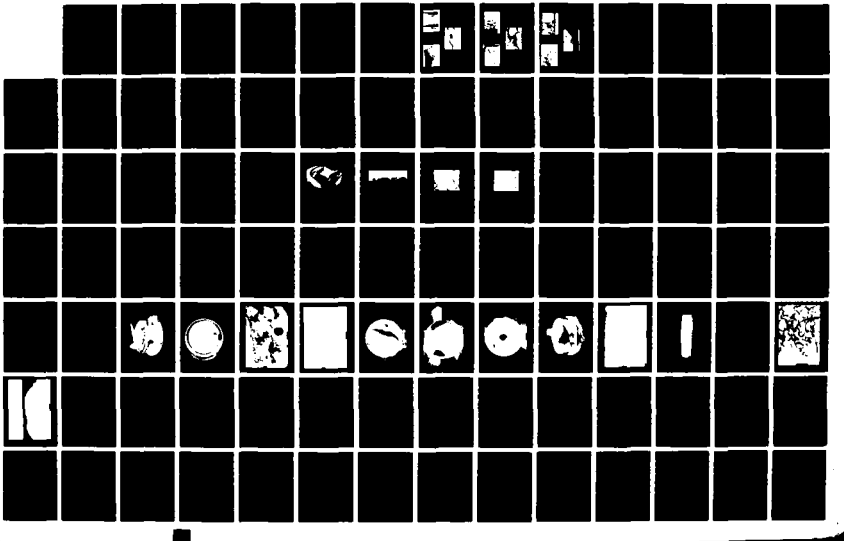

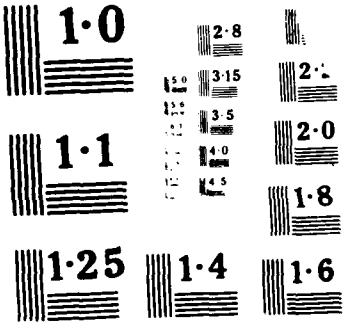
1·0
1·1
1·25
2·8
3·15
3·5
4·0
4·5
2·0
1·8
1·4
1·6

References

1. A. John Sedriks, Corrosion of Stainless Steels, New York, John Wiley and Sons, Inc., 1979, p. 30

2. M. A. Streicher, Corrosion, 30 (3), 1974, pp. 77-91.

3. R. W. Staehle, J. Hochman, R. McCright, and J. E. Slater (eds.) in Stress Corrosion Cracking and Hydrogen Embrittlement of Iron Base Alloys, NACE, Houston, TX, 1977, pp. 286, 306, and 405.

4. J. F. Grub and J. R. Maurer, Corrosion/84 Paper No. 28, New Orleans, Louisiana, 1984.

5. M. A. V. Devanathan and Z. Stachurski, Proc. R. Soc., A270, 1962, p. 90.

6. M. A. V. Devanathan and Z. Stachurski, J. Electrochem. Soc., Vol. 111, 1966, p. 619.

7. R. A. Oriani and P. H. Josephic, Scr. Metall., Vol. 13, 1979, pp. 469-471.

8. W. M. Robertson and A. W. Thompson, Metal Trans A, Vol. 11A, 1980, pp. 553-557.

9. J. P. Hirth, Metal Trans A, Vol. 11A, 1980, pp. 861-889.

10. R. A. Oriani, Fundamental Aspects of Stress Corrosion Cracking, NACE - 1, Houston, TX, 1969, pp. 32-49.

11. R. B. McLellan, Acta Meta, Vol. 27, 1979, pp. 89-100.

12. A. J. Kumnick and H. H. Johnson, Acta Meta, Vol. 28, 1980, pp. 33-40.

13. P. Bastien and P. Azou, C. R. Acad. Sci., Paris, Vol. 232, 1951, pp. 1845-1848.

14. R. Broudeur, J. P. Fidelle, and H. Auchere, Proc. Int. Congr. Hydrogen in Metals, Paris, Editions Science et Industrie, Paris, 1972, pp. 106-107.

15. M. R. Louthan, Jr.., G. R. Caskey, Jr., J. A. Donovan, and D. E. Rawl, Jr., Mater. Sci. Eng., Vol. 10, 1972, pp. 357-368.

FIGURES

TABLES

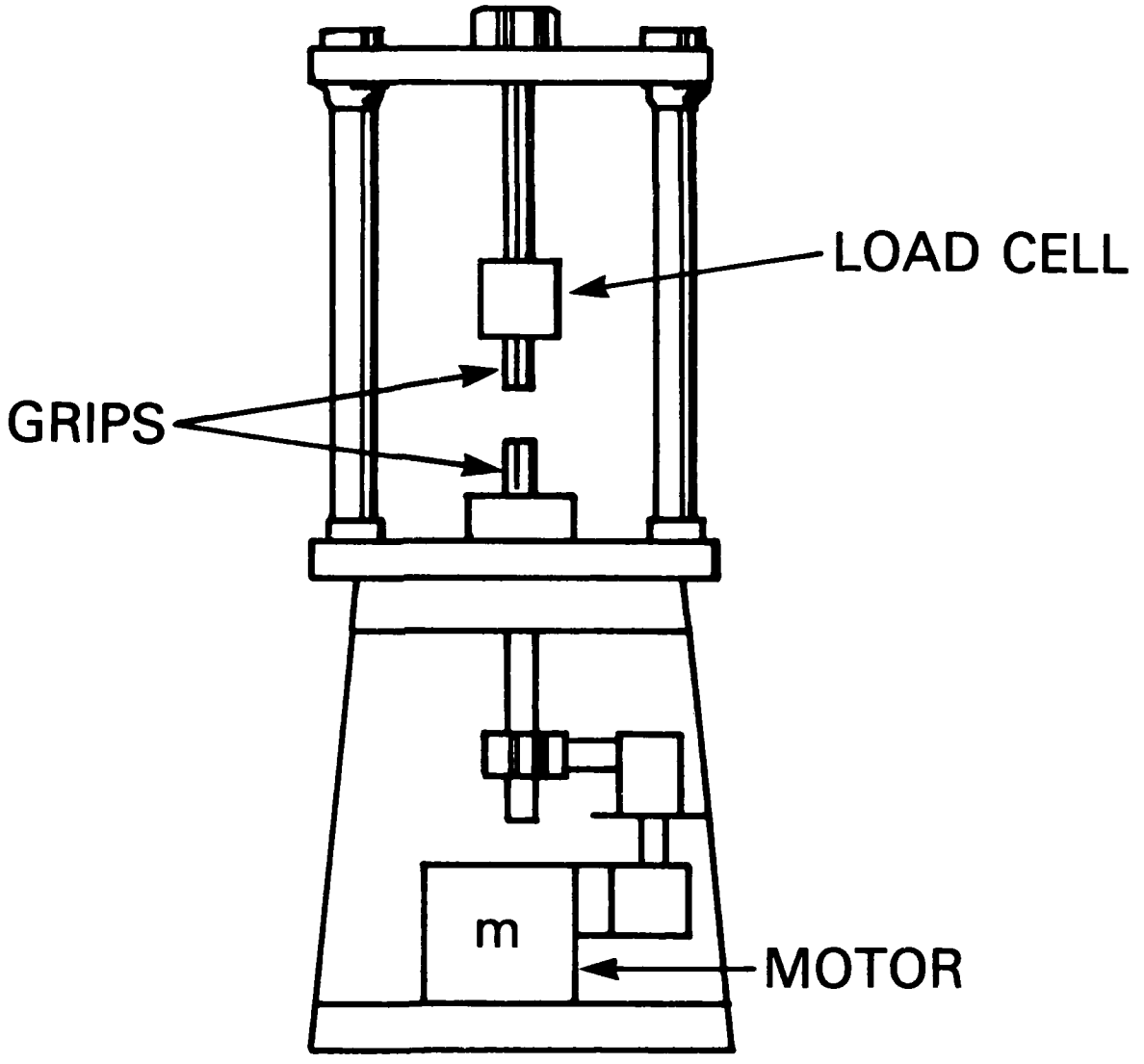

Figure 1 - Slow strain rate apparatus.

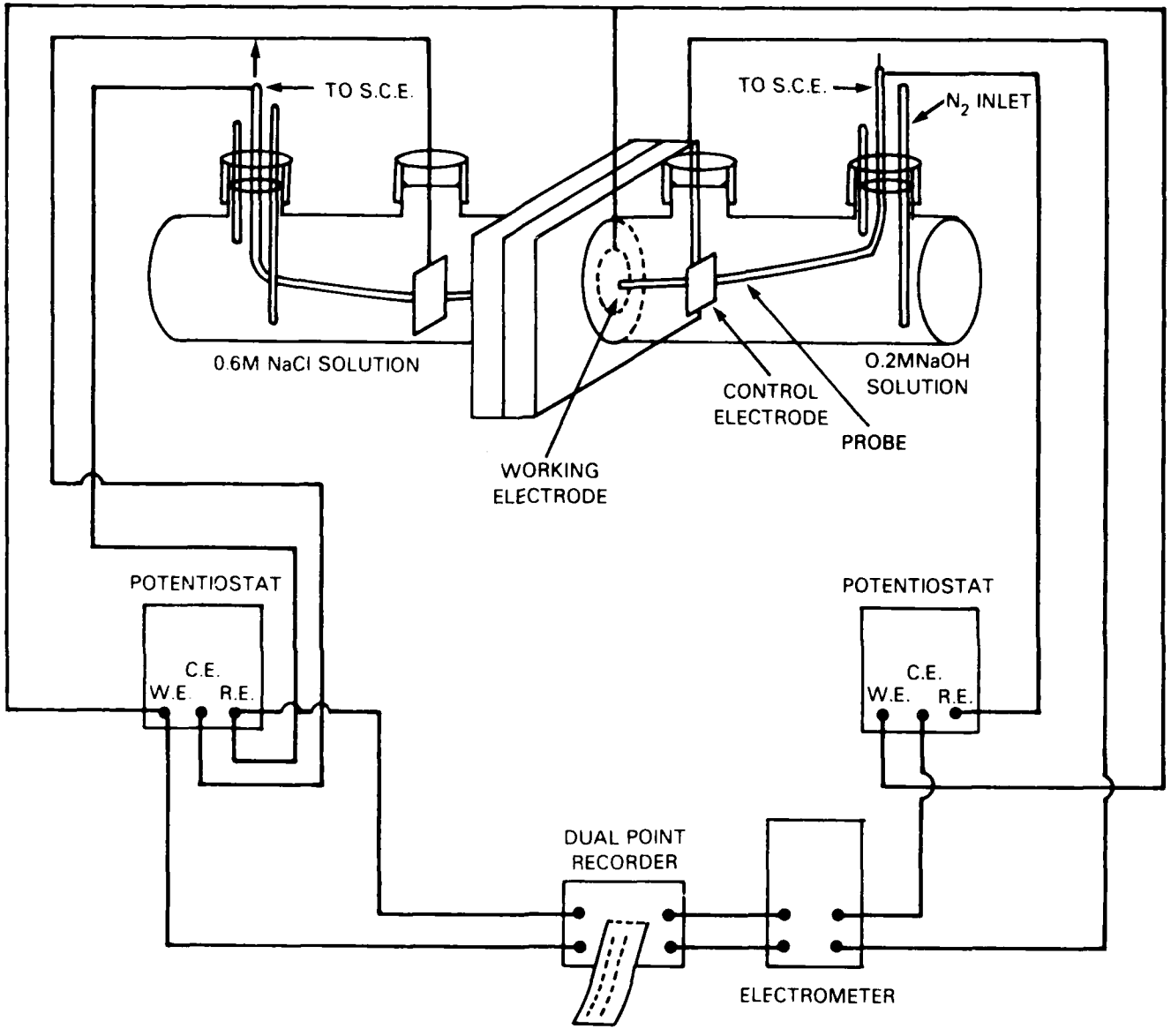

SCHEMATIC OF HYDROGEN PERMEATION APPARATUS

Figure 2 - Electrochemical/H-permeation test cell.

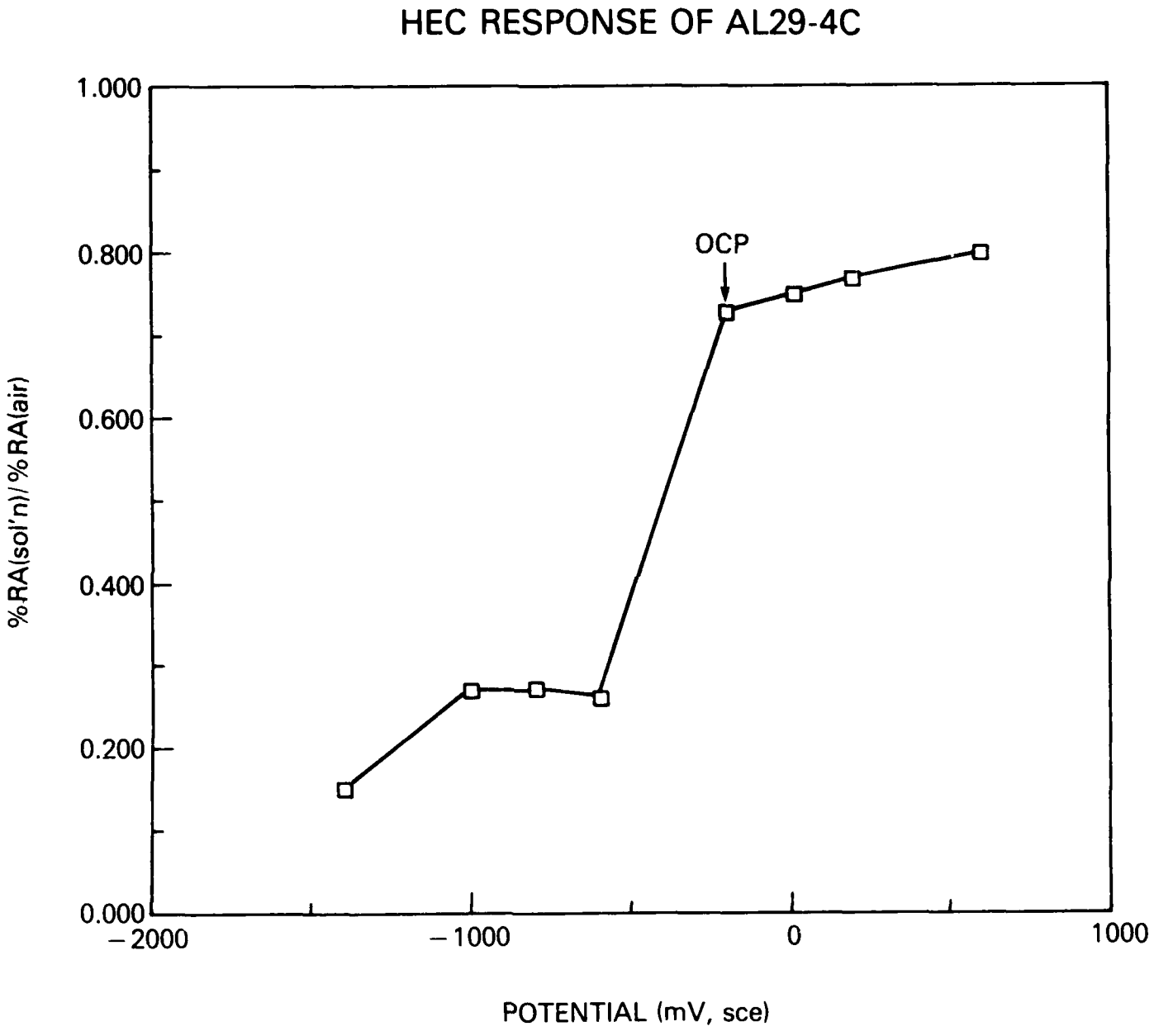

Figure 3 - The influence of polarization potential on reduction in area ratio ($\%RA_{sol'n}/\%RA_{air}$) for Al29-4C in 0.6N NaCl solutions.

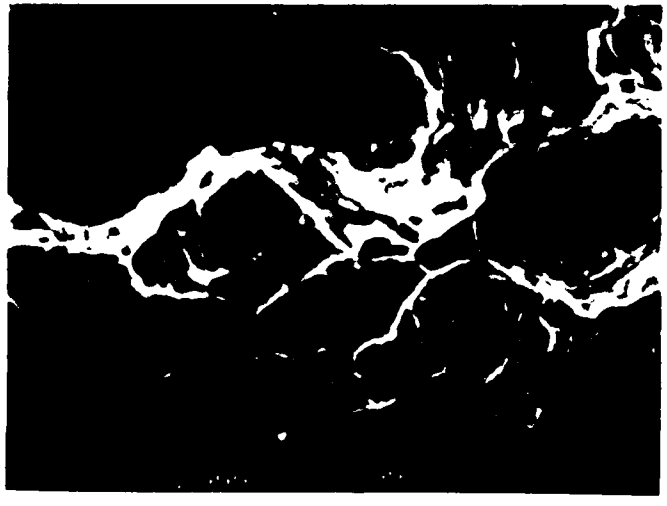

S.E.M. of fracture surfaces of a ferritic stainless steel after test in 0.6N NaCL solution. ($1.4X10^{-6}$).

OPEN CIRCUT

Figure 4 - SEM fractograph of A129-4C tested in 0.6N NaCl solution at open circuit potential.

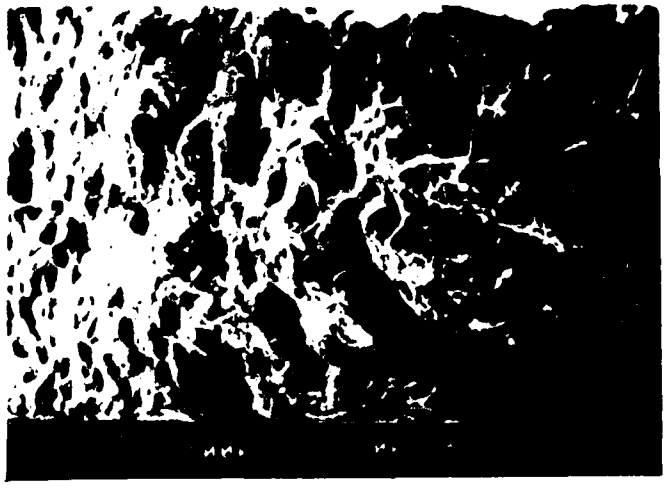

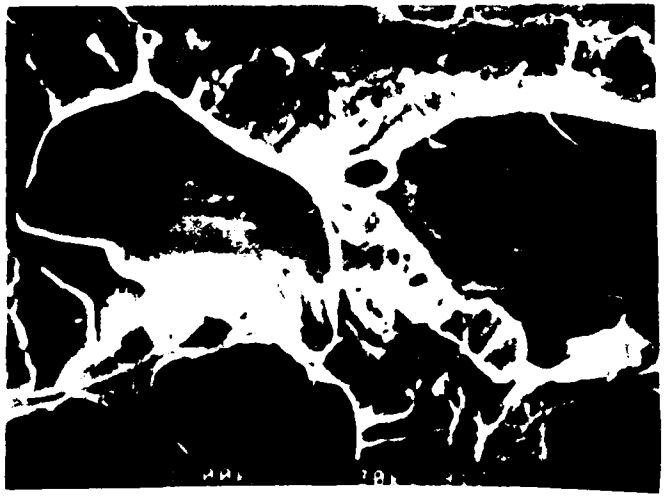

S.E.M. of fracture surfaces of a ferritic stainless steel after test in 0.6N NaCL solution. ($1.4X10^{-6}$).

-600MV

Figure 5 - SEM fractograph of A129-4C tested in 0.6N NaCl solution at -600 mV.

S.E.M. of fracture surfaces of a ferritic stainless steel after test in 0.6N NaCL solution. ($1.4X10^{-6}$).

-1400MV

Figure 6 - SEM fractograph of A129-4C tested in 0.6N NaCl solution at -1400 mV.

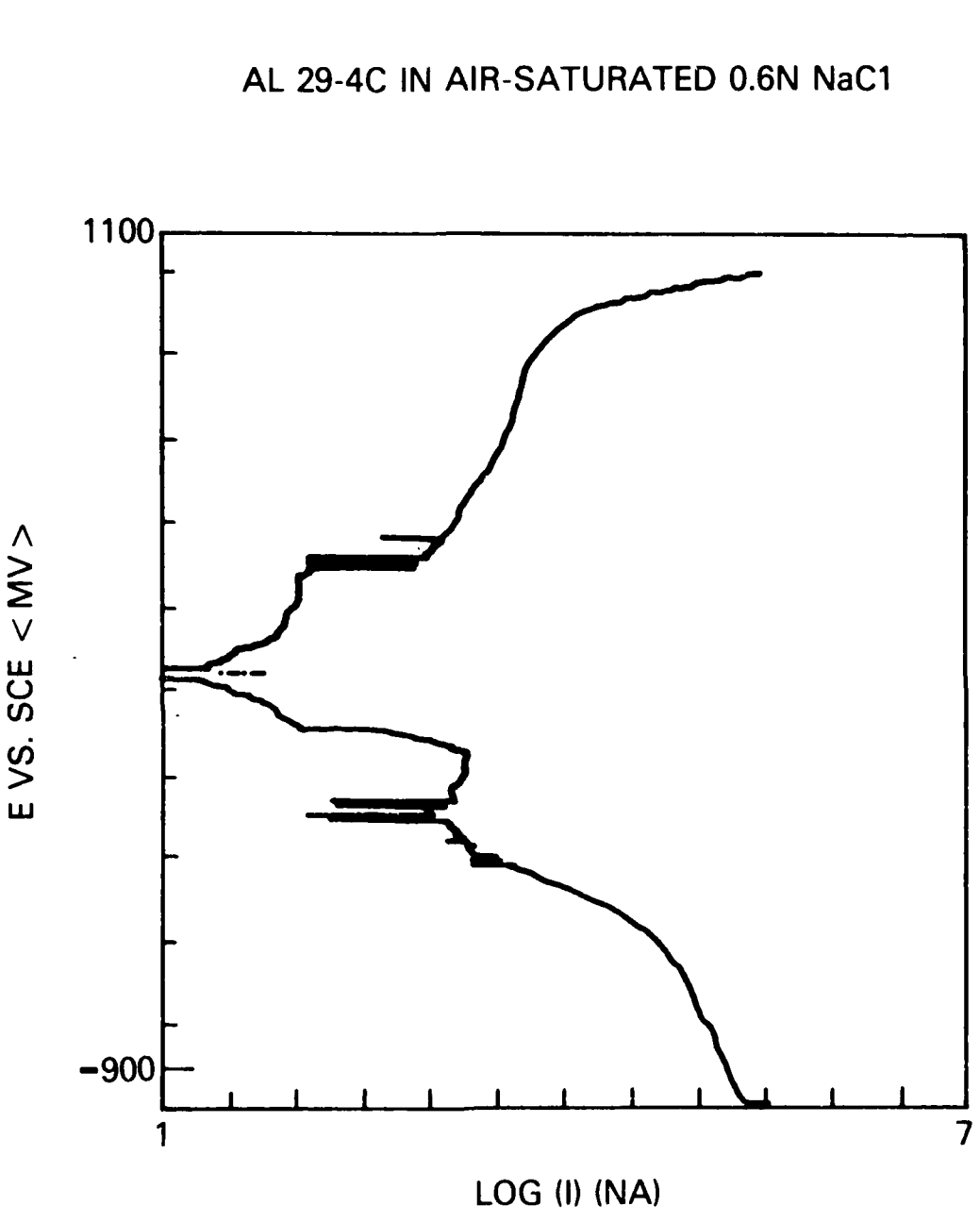

Figure 7 - The anodic polarization curve obtained for Al29-4C in 0.6N NaCl solution.

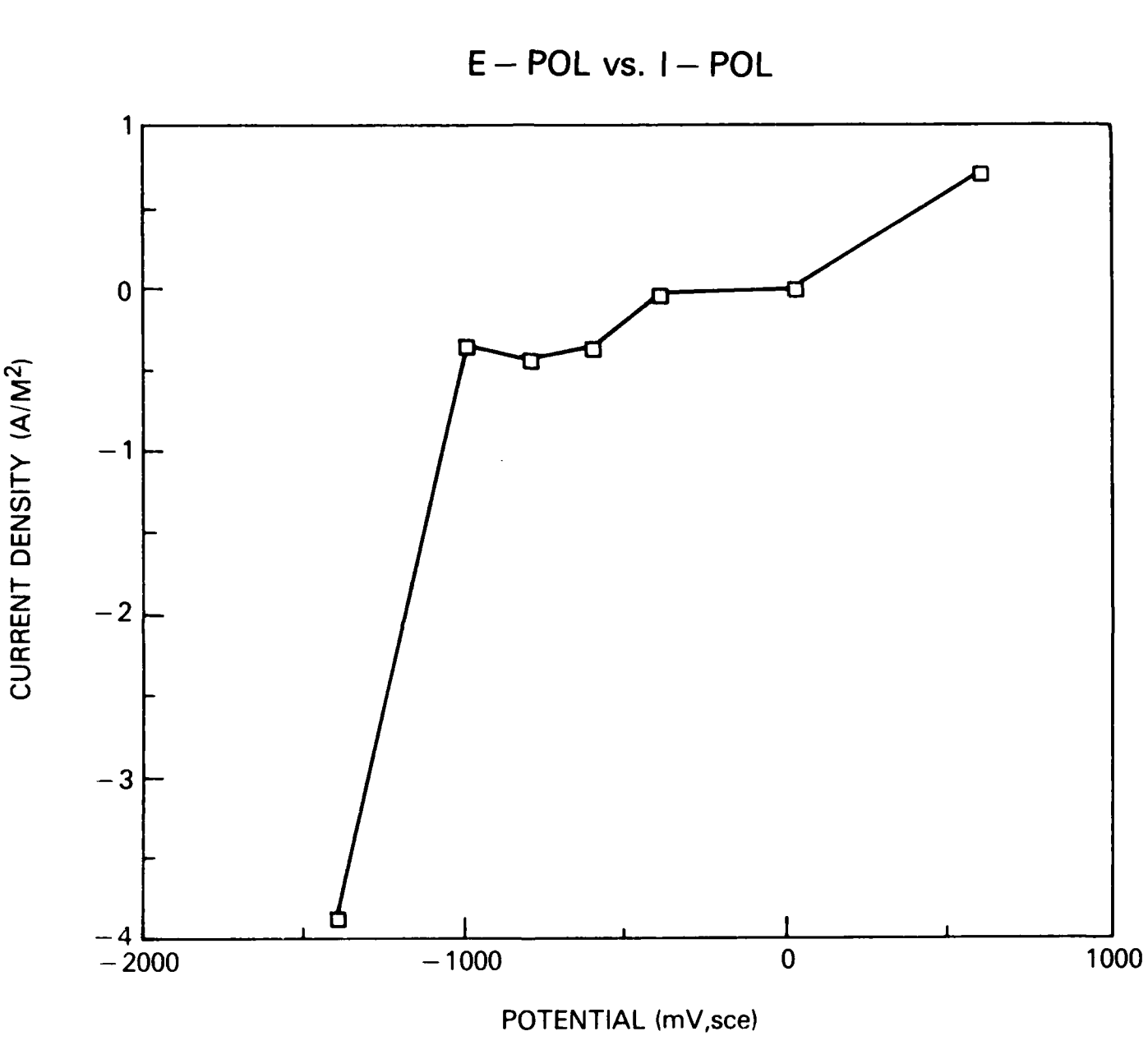

Figure 8 - The straining electrode polarization curve for A129-4C in 0.6N NaCl solution.

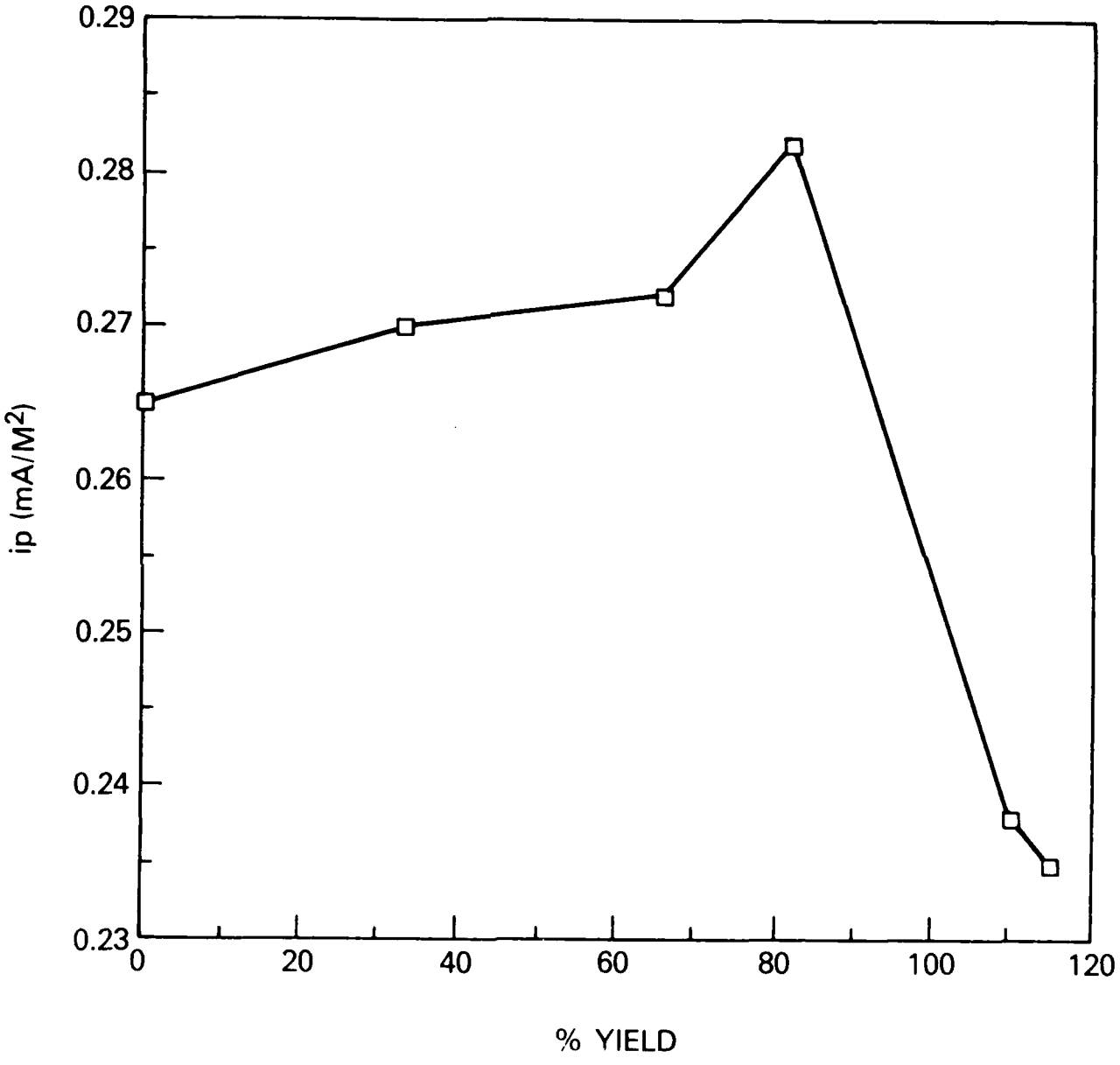

Figure 9 - The influence of stress level on H-permeation (ip) for A129-4C in 0.6N NaCl solutions.

CHEMICAL COMPOSITION (WEIGHT PERCENT) OF AL 29-4C

C	Cr	Ni	Mn	Mo	Ti	N	S	P	Si	Fe
0.018	29.5	0.42	0.29	3.80	0.76	0.25	0.002	0.028	0.26	BAL

Table 1 - Chemical composition of superferritic stainless steel A129-4C.

MECHANICAL PROPERTIES

YIELD STRENGTH MPA	ULTIMATE TENSILE STRENGTH MPA	ELONGATION %	HARDNESS RB
517	620	27	94

Table 2 - The mechanical properties of superferritic stainless steel A129-4C.

SUMMARY OF SSR TESTS AND RESULTS

APPLIED POTENTIAL (MV VS SCE)	MEDIUM	STRAIN RATE (SEC-1)	UTS MPA	%RA(sol'n) / %RA(air)	TTF HR	OBSERVATIONS
—	AIR	1.4×10^{-6}	510.1	—	104.0	DIMPLES
+600	0.6M NaCl	1.4×10^{-6}	470.9	.80	121.8	DIMPLES
+200	0.6M NaCl	1.4×10^{-6}	470	.77	108.0	DIMPLES
OC	0.6M NaCl	1.4×10^{-6}	470	.75	60.9	DIMPLES, α-CLEAVAGE
−200	0.6M NaCl	1.4×10^{-6}	439	.73	59.0	DIMPLES, α-CLEAVAGE
−600	0.6M NaCl	1.4×10^{-6}	439	.26	47.0	α-CLEAVAGE, DIMPLES
−800	0.6M NaCl	1.4×10^{-6}	425	.27	31.0	α-CLEAVAGE, DIMPLES
−1000	0.6M NaCl	1.4×10^{-6}	368	.27	10.8	α-CLEAVAGE
−1400	0.6M NaCl	1.4×10^{-6}	350	.15	4.1	α-CLEAVAGE
−800	0.6M NaCl	7.2×10^{-8}	—	—	>1000	—

Table 3 - Summary of slow strain rate tests.

PERMEATION BEHAVIOR OF F_E AND F_E ALLOYS IN 0.6N NaCl, pH 6.3

ALLOY	Ip@-610 mA (MA/M^2)	D_H (M^2/sec)
F_E	23	1.3×10^{-9}
F_E-25%C_R	0.45	1.4×10^{-12}
F_E-4.3%M_0	12	1.2×10^{-10}
F_E-24%C_R-4.5%M_0	0.55	5.0×10^{-12}
Al29-4C	0.90	7.0×10^{-12}

Table 4 - The permeation behavior of iron and some iron alloys in 0.6N NaCl solutions.

STRESS LEVEL % YIELD	$i_{p@-610\ mV}$ (mA/M^2)	D_H ($M^2/sec) \times 10^{12}$	C_o ($\times 10^3$ mole-H/M^3)
0	.265	5.74	5.59
33	.270	4.98	6.56
66	.272	4.87	6.76
82	.282	4.75	6.80
110	.238	4.13	6.83
115	.235	4.07	6.99

Table 5 - The influence of stress level on the ip, D_H, and C_o values of superferritic stainless steel A129-4C in 0.6N NaCl solutions.

CORROSION AND STRESS CORROSION

OF METALS IN DECONTAMINATION SOLUTIONS

Elizabeth Hall and Milton Levy
U.S. Army Materials Technology Laboratory
Watertown, Massachusetts 02172-1000

ABSTRACT

Highly alkaline decontamination solutions can damage Army materiel. To evaluate alloys used in its equipment, the Army is undertaking electrochemial studies in sodium carbonate, DS2 and STB. General corrosion rates are reported for full-strength and diluted solutions. Ferrous alloys, titanium, aluminum alloys, magnesium and two metal matrix composites are tested. Research in progress on susceptibility of alloys to stress corrosion cracking and CARC coating durability is discussed.

INTRODUCTION

The longevity of equipment with potential exposure to toxic chemical environments is a priority for the U.S. Army. The solutions most effective for decontamination, however, pose corrosion concerns. These solutions are highly caustic and neutralize toxic agents either by oxidation or by hydrolysis. Thus they may attack metal as well as organic coatings. This paper delineates the research in progress at the U.S. Army Materials Technology Laboratory to obviate materiel degradation during decontamination.

At present, electrochemical techniques are used to investigate the effects of three decontamination solutions: sodium carbonate, DS2 (an organic/hydroxide solution) and STB (supertropical bleach) on alloys of steel, titanium, aluminum, and magnesium as well as composites of aluminum and magnesium. Decontamination solution and alloy compositions are shown in Tables 1 and 2. General corrosion rates are quantified and localized attack is noted. Susceptibility to stress corrosion cracking (SCC) is evaluated using the method of Parkins.[1] In a later portion of the study, electrochemical impedance techniques will be used to evaluate the durability of chemical agent resistant coating (CARC) on alloys decontaminated with these three solutions.

EXPERIMENTAL METHODS

The electrochemical corrosion measuring system includes a Greene cell, a microcomputer controlled Potentiostat/Galvanostat (PAR Model 273), and a printer/plotter. Two graphite counter

electrodes are used. The reference electrode is a saturated calomel electrode (SCE) separated by a glass bridge with a Vycor tip. The working electrode disc is fastened in a polytetrafluoroethylene holder and has a surface area of 1.0 cm^2. Cell volume is 1 liter. The scan rate is .2 mV/sec.

Tests are run at room temperature. Solutions are not purged. Equilibrium time required varied between fifteen minutes and overnight depending on the solution. Line syncronization and IR compensation are used for low conductivity solutions such as distilled water and full-strength DS2. Distilled water is used for dilution to keep results as consistant as possible. Due to the irritant nature of DS2 and STB, runs are conducted in a hood with 100 fpm +/- 20 fpm face-flow. Gloves are used when working with DS2 and STB to avoid contact with skin.

For each alloy, data is gathered by three techniques: potentiodynamic scan, Tafel plot, and polarization resistance. Tafel slopes of 100 mV are assumed. Computer calculated corrosion rates are hand-checked before they are reported.

Calculation of corrosion rates for metal matrix composites assume that the silicon carbide particles and the aluminum oxide fibers do not contribute to the corrosion current. The volume percentage is used to approximate the surface area covered by the particles. Thus, the corrosion rate is calculated using the surface area of metal exposed.

Susceptibility to SCC is measured by the method of Parkins.[1] The technique involves comparing a fast potentiodynamic sweep (17 mV/sec) wherein film formation is minimized, to a slow potentiodynamic sweep (.2 mV/sec). Overlaying the two curves will indicate any ranges of potential within which there is significant current density difference and thus, SCC is likely. The following boundary conditions are used:

(a) Current densities below 1 mA/cm^2 on the fast sweep are considered negligible.

(b) At any given point, the current density difference between fast and slow sweeps, divided by the slow sweep current density, shall exceed 1000.

The software controlling the potentiostat has been modified to allow 17 mV/sec to be run.

The slow/fast scan technique will not quantify SCC incubation time or crack growth rate, but it may allow a ranking of alloy vulnerability to SCC. Because sodium carbonate is so well-known a system, it will be used as the basis of comparison for results in DS2 and STB.

Electrochemical impedance techniques on a PAR Model 5208 will be used to rate CARC coating on samples as "good", "fair", or "poor". Coated samples will be soaked in solution for 24 hours. After the open circuit potential has stabilized, Nyquist, Bode and phase plots will be generated. Using these plots to

find "equivalent circuits" the physical behavior of the coating will be characterized. These equivalent circuits will serve as the criterion for relative ranking.

TEST MATRIX

Five alloys are being investigated: Carbon Steel 1020, Carpenter 20CB3 (a Ni-Cr steel), Titanium 6Al-4V (grade 5), Aluminum alloys 5083, 6061, 7039, Magnesium ZE41A, Al 6061/25 vol% SiC, and Mg ZE41A/35 vol% FP (fine polished Al_2O_3). They are in the most commonly used heat treatments. Composition data are given in Table 2. The specimen are prepared by grinding with dry 600 grit paper and ultrasonic cleaning in acetone.

Samples are tested in 10% sodium carbonate. They are then tested in 100% DS2, and in dilutions of 50%, 30% and 20% and pure water. STB is tested as a saturated solution and as a 50% dilution with water.

Fast and slow scans are being run in 10% sodium carbonate. These data are evaluated with the Parkins criteria.

CARC samples will be tested in 10% sodium carbonate, full-strength DS2, and STB. Dilutions will be limited by the number of samples available.

RESULTS

Only a few alloys were tested in sodium carbonate. The results are found in Table 3. Sodium carbonate is agressive to aluminum, but benign to steel and titanium. This same test matrix was evaluated via the Parkins technique. Preliminary data indicate that none of these alloys has a tendency to crack. However, experiments with a system known to produce cracking also showed a low tendency to crack. Discussions with Dr. Parkins have lead the author to conclude that this method may not be a good indicator of cracking for these particular alloys. Further investigation will be needed before finalizing this conclusion.

Full-strength DS2 is benign to all alloys. When diluted, DS2 is more aggressive to all alloys. Aluminum, however, is acutely susceptible to dilutions in the range of 20 to 30% DS2. Metal matrix composites behaved similarly to the base alloy. Results are listed in Tables 4 - 7.

STB is very agressive to steel and aluminum. Diluting STB mitigates the corrosion rate for most alloys. Metal matrix composites had higher corrosion rates than did the base alloy in some cases. Results are listed in Table 8.

Preliminary stress corrosion cracking data in sodium carbonate, using the Parkins technique, have been inconclusive. Normalized differences in corrosion current density have been below 1000 in the passive region for each of the five alloys.

Normalized differences exceeded 1 mV only at very high potentials. Further refining of the technique is required, especially for reactive metals such as the titanium and aluminum.

DISCUSSION

This corrosion rate data [illegible] corroborated by data in the literature. Work has been done by other researchers in long and short term immersion including cyclic testing. Short exposure studies may be correlated with a single decontamination. Longer exposures may be correlated with repeated decontaminations or situations where rinse water is not available. The effects of agents and their decomposition products will be considered to have a negligable effect on corrosion rate because of their low concentration relative to the decontaminants.

Sodium Carbonate

Sodium carbonate (Na_2CO_3) is used as a 10 wt% solution in water. It is excellent in hydrolyzing one agent but slow or ineffective on others.[3] It is non-flammable and non-toxic. It is particularly recommended for cotton or rubberized fabrics, although it is available to the user for use on metallic equipment.[3,4] It is inexpensive and may be stored as a powder.

From the literature, sodium carbonate in low concentrations is only mildly corrosive to ferritic steels and titanium, although it does attack aluminum. Sodium carbonate threatens ferritic alloys because of its tendency to promote SCC.[5] Data in Table 3 support this.

DS2

DS2 (decontaminating solution 2) is composed of 70% diethylenetriamine, 28% methyl cellosolve and 2% sodium hydroxide. It has a pH of 13.5, a specific gravity of 1.04, and a viscosity of 14.[3] It neutralizes all agents and has been used extensively.[3] It is flammable with a low flashpoint, 141°F.[3] This limits it to not suitable for use near running engines or for electrical equipment. It is not highly toxic, but will irritate the eyes and the respiratory system.[2] In sealed containers, the solution has been stored for months at ambient or elevated temperatures.[3] If exposed to air, it will absorb moisture diminishing its effective mass.

DS2 is reported [illegible] to most metals other than zinc or cadmium.[3] In [illegible], cadmium plating is reported as durable.[3] For [illegible], DS2 has not been reported to cause localized [illegible].

When DS2 is [illegible] rinsing, corrosivity may [illegible] diethylenetriamine and methyl cellosolve are [illegible]. Water increases the mobility of the [illegible] making them more aggressive.[5] The per[illegible] the important

factor. Tarantino found that pure DS2 was non-reactive with aluminum alloys but very corrosive upon dilution with water. Maximum corrosion rates occurred at 30 percent DS2. Table 9 presents some of these results.[9] A Canadian study of DS2 containers showed corrosion only on those with defects allowing DS2 to contact the atmosphere.[10]

Two studies, however, contradicted these findings. The Naval Civil Engineering Laboratory tested coupons by partial and cyclic immersion for two weeks.[8] The cyclic immersion coupons allow moisture to absorb, forming an unknown dilution. These showed slightly increased corrosion rates for most metals. Corrosion rates for aluminum however, decreased slightly. Table 10 presents some of this data. A study by Roberts in 1947 showed no detectable corrosion on aluminum or titanium in DS2/10% H_2O solution.[11]

Because of its organic constituents, DS2 attacks many non-metallics. Hughes Aircraft reported an uncross-linked urethane coating exposed to DS2 was turned to syrup within 24 hours. Even after 2 hours, the urethane was damaged.[7] Because the urethane used in CARC is cross-linked, CARC is expected to withstand DS2 after 24 hours. Roberts showed that polyurethane sheet dissolved in DS2. He tested two types of polyurethane coatings in pure DS2 and DS2/10%H_2O. In both cases significant deterioration was noted. However, in this same test, a glass fiber/epoxy resin composite showed no deterioration after 24 hours.[11] Roberts' results contrast with those reported by Hughes. That study showed some epoxy disolved from an epoxy-glass laminate exposed to DS2 for 24 hours.[7] Tests on two epoxy coatings have shown similarly mixed results. One coating peeled off in less than 10 days, while another in the same test lasted almost 45 days. On an epoxy adhesive, DS2 caused peel strength to decrease to 24 percent of the original strength after 24 hours at 23°C.[12]

STB

STB, supertropical bleach, is a mixture of calcium oxide (CaO) and calcium hypochlorite ($CaOCl_2$). It contains 10-30 percent active chlorine, compared with 3-5 percent in commercial bleach.[2,4] It has a pH of 11.8, or when diluted 11.5. STB is a strong oxidizer making it effective on most agents. It is recommended for broad usage.[3,4] Like any bleach, it is dangerous to eyes, skin , the respiratory system and clothing. As a slurry with water, STB is non-flammable, albeit less effective in decontamination.[2]

As a powder, STB will not penetrate crevices. It can ignite in contact with agent and produces an exothermic reaction with anti-freeze (ethylene glycol). In reactions with some agents it produces toxic vapors.[2-4] It may be stored as an anhydrous powder for 2 years or more. It is stable as a solution for 6 weeks at 158°F and for 10 years in hermetically sealed bottles at

ambient temperatures.[2,3]

STB is severely corrosive to most metals.[7,8,13] Hughes Aircraft reported pitting and discoloration on aluminum alloys after only 1 hour coupon immersion. Copper, brass and electroless nickel plating were also discolored. Martensitic stainless steel remained passivated for the 24 hour immersion.[7] The Naval Civil Engineering Laboratory study showed very low corrosion rates for Al 5052 and 6061, and titanium alloys; moderate rates for stainless and Inconel; high rates for Al 1100, 2024, 3003, and other metals.[8] A subset of this data is presented in Table 10. Harris reported only Stellite, Hastelloy and tungsten alloys as having "excellent" corrosion resistance. Stainless steel, high silicon iron and Inconel were rated "good".[13]

Dilution is expected to mitigate the aggressiveness of STB. Unlike DS2, STB solutions are inherently conductive. Dilution will reduce the chloride concentration.

Most nonmetallics are stable in STB. Hughes Aircraft reports that a urethane circuit-board coating was intact after 24 hours in STB; a diminished gloss was noted.[7] No physical change or strength loss was seen on an epoxy-glass laminated in STB.[7] Epoxy adhesive showed no change in appearance or physical properties in STB after 24 hours.[12]

CONCLUSIONS

Aluminum is very vulnerable to decontamination solutions.

Magnesium and carbon steel are vulnerable to STB.

Metal matrix composites may show higher corrosion rates than does its base alloy.

The Parkins method of SCC evaluation may not be useful for the Army's engineering alloys. Further investigation is required.

REFERENCES

1. R.N. Parkins, Corrosion Science, Vol. 20, No.2, p. 147 (1980)

2. "An Evaluation Study to Select a Standard Navy BWA/CWA Decontaminant", U.S. Naval Air Engineering Laboratory, NAEL-Eng-7102, April, 1964.

3. "Chemical Reference Handbook", U.S. Army Field Manual FM 3-8, January 1967.

4. "Safety Regulation for Chemical Agents GB and VX", DARCOM-R 385-102, 6 May 1982.

5. N.E. Hamner, "Corrosion Data Survey", Metals Section, edition National Association of Corrosion Engineers, p. 164.

6. R.N. Parkins, R.R. Fessler, International Journal of Materials in Engineering Applications, No. 12, p. 80 (1978).

7. "NBC Materials Handbook", Hughes Aircraft Company, Report No. ROL 6109-1, August 1982.

8. C.V. Brouilette, "Corrosion Studies on BW-CW Decontaminants" U.S. Naval Civil Engineering Laboratory, USNCEL Report R-229, 30 April 1963.

9. P.A. Tarantino, P.M. Davis, "Electrochemical Corrosion Rates of DS-2 with Some Aluminum Alloys" U.S. Army Armament Research and Development Command Technical Report, ARCSL-TR-83051, June 1983.

10. A.A. Casselman, R.A.R. Bannard, K.B. Shaw "Analysis of Decontaminating Agent CI by Gas-Solid Chromatography" (Canadian) Technical Support Document TSD 350 Ca 230/70-16 June 1970.

11. W.B. Roberts, "Development of Apparatus, Decontaminating, 2 Quart, Expendable E3 and E3R1" U.S. Army Technical Division Memo Report, TDMR 1273, 24 March 1947.

12. T.E. Lawler, "Analytical Methodology and Testing Task 1-Development and Conduct of Material/Decontaminant Test Streams", U.S. Army Chemical Research and Development Center Technical Report, CRDC-CR-84006, September 1984.

13. R.W. Harris "Decontaminating Apparatus, Power-Driven, Multi-purpose, 200 Gallon and 500 Gallon, July 1961.

Table 1. Decontamination Solution Compositions

Sodium Carbonate - 10 wt% solution in water

DS2 - 70 wt% Diethylenetriamine
28 wt% Methyl Cellosolve (Ethylene glycol monomethyl ether)
2 wt% Sodium Hydroxide

STB - Calcium Hypochlorite
Calcium Oxide - added as a stabilizer
Water - optional; used to form a slurry

Table 2. Specimen Composition Data

Alloy	Density gm/cm^3	Equivalent weight	Composition wt%
C 1020	7.86	28.98	C-.17, Mn-.42, P-.009, S-.006
20CB3	7.86	24.53	C-.019, Mn-.34, Si-.40, P-.021, S-.002, Cr-19.40, Ni-32.91, Mo-2.22, Cu-3.26, Cb+Ta-.58
Ti-6Al-4V	4.43	11.70	C-.02, N-.014, Fe-.14, Al-6.0, V-3.9, O-.132
Al 5083-H112	2.66	9.18	Si-.40, Fe-.4, Cu-.10, Mn-.40/1.0, Mg-4.0/4.9, Cr-.05/.25, Zn-.25, Ti-.15
Al 6061	2.70	9.15	Si-.60, Cu-.10, Mn-.75, Mg-.10, Cr-.20, Zn-.125
Al 7039	2.70	10.01	Cr-.16/.25, Cu-.10, Fe-.4, Mg-2.3/3.3, Mn-.10/.40, Si-.30, Ti-.10, Zn-3.5/4.5
Mg ZE41A	1.85	13.33	Zn-.04, Ce-.012, Zr-.007

Note: Metal matrix composites use same data as matrix alloy. Surface area exposed is modified.

Table 3. Alloys in Sodium Carbonate

Alloy	Corrosion Rate (mpy)
Carbon Steel	0.14
Alloy 20CB3	0.08
Titanium	0.08
Aluminum 5083	28.4
Aluminum 7039	37.4

Table 4. Ferrous and Titanium Alloys in DS2

DS2 Volume %	Carbon Steel (mpy)	Alloy 20CB3 (mpy)	Titanium (mpy)
100	0.01	0.03	0.01
50	0.03	0.04	0.04
30	0.20	0.10	0.03
20	0.34	0.25	0.18
0	1.00	0.10	0.02
USNCEL Data (100%)	0.3	-	0.0

Table 5. Aluminum Alloys in DS2

DS2 Volume %	Al 5083 (mpy)	Al 7039 (mpy)
100	0.13	0.02
50	180	400
30	490	990
20	360	980
0	0.04	0.08
USNCEL data (100%)	(Al 5052) 0.6	(Al 7178) 0.3

Table 6. Aluminum Metal Matrix Composites in DS2

DS2 Volume %	Al 6061 (mpy)	Al 6063 (mpy)	Al 6061/SiC (mpy)
100	0.23	0.12	0.22
50	445	421	69
30	>1000	766	444
20	>1000	717	888
0	0.05	7.1	0.24
USNCEL data (100%)	0.6	-	-

Table 7. Magnesium Metal Matrix Composites in DS2

DS2 Volume %	Mg ZE41A (mpy)	Mg/FP (mpy)
100	0.03	0.03
50	0.29	0.48
30	0.24	1.92
20	0.50	0.34
0	4.80	4.90
USNCEL data (100%)	(Mg-FS) 0.5	-

Table 8. Corrosion of Alloys in Super Tropical Bleach

Alloy	Full Strength (mpy)	USNCEL (mpy)	50% Dilution (mpy)
C.S. 1020	156	12.6	97
Alloy 20CB3	1.28	-	0.28
Titanium Gr. 5	0.14	0.1	0.14
Al 5083	10	1.3	23
Al 7039	50	45.5	20
Al 6061	27	1.1	10
Al 6061/SiC	24	-	64
Mg ZE41A	125	43.0	290
Mg ZE41A/FP	330	-	575

Table 9. Corrosion Rates of Aluminum 6063-T6 in DS2 Diluted with Distilled Water Using Tafel Extrapolation

DS2 (Vol %)	Corrosion Rate mpy
100	0.12
95	1.7
90	19
75	84
60	219
50	421
35	724
25	808
10	539
5	387
2	80
0	7.1

Source: Reference 9

Table 10. Corrosion Rates of Coupons in DS2 or STB for 2 Hours

Alloy	Partial Immersion 100°F mpy		Cyclic Immersion* 75°F mpy	
	DS2	STB	DS2	STB
Steel 1020	0.3	12.6	0.3	5.7
Aluminum 1100	0.8	37.4	0.4	7.8
2024	0.4	48.3	0.2	9.7
3003	0.7	32.5	0.4	6.4
5052	0.6	1.3	0.3	3.3
6061	0.6	1.1	0.3	3.8
7178	0.3	45.5	0.2	6.8
Ti-6Al-4V	0.0	0.1	0.0	0.0
Ti-4Al-3Mo-1V	0.0	0.1	0.0	0.0
Stainless 304	0.1	4.0	0.1	4.2
Stainless 15-7PH	0.0	3.6	0.0	2.4
Inconel MIL-N-6840	0.1	8.5	0.1	7.6
Magnesium-FS	0.5	43.0	1.6	4.3
Cr plate on steel	0.7	11.4	1.1	4.7
Cd plate on steel	0.0	6.5	0.0	0.9

*Immersions were 5 seconds long followed by 15 minutes of atmospheric exposure.

Source: Reference 8

HYDROGEN EMBRITTLEMENT OF STEEL

RICHARD BROWN

MATERIALS TECHNOLOGY LAB.

WATERTOWN, MA 02172.

INTRODUCTION

- MIXER SUPPORT BOLT FAILED MARCH 12, 1986.
- BOLT MATERIAL 4340 ESR STEEL Rc 55
- 286 DAYS FROM MANUFACTURE.
- FAILED IN THREADED REGION.
- BOLT TORQUED TO 250 ft.lbs IN SERVICE.
- VACUUM CADMIUM PLATING ON COMPONENT.

OBJECTIVES

- DETERMINE FAILURE MECHANISM OF BOLT.
- CONDUCT TESTS ON BOLTS REMOVED FROM SERVICE TO DETERMINE STRENGTH LEVEL OF MATERIAL.
- OBTAIN INFORMATION OF DEGRADATION MECHANISMS.

APPROACH

- FRACTOGRAPHY OF FAILED BOLT.
- METALLOGRAPHY OF FAILED BOLT.
- MECHANICAL TEST PROGRAM ON SPECIMENS FROM SERVICE BOLTS.
- RESEARCH PROGRAM TO STUDY MITIGATION OF THE PROBLEM.

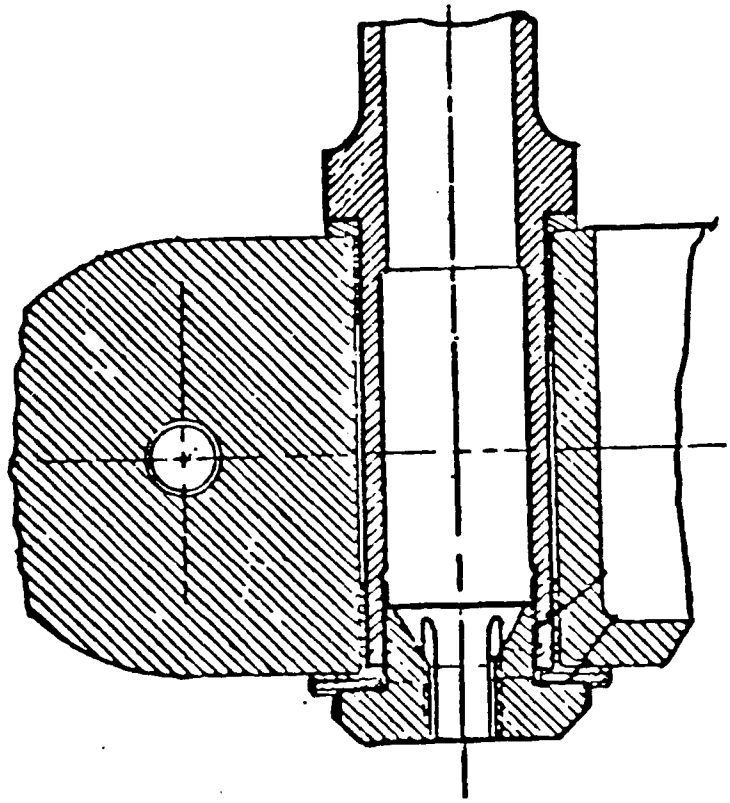

FAILURE OCCURRED IN BETWEEN ARROWS

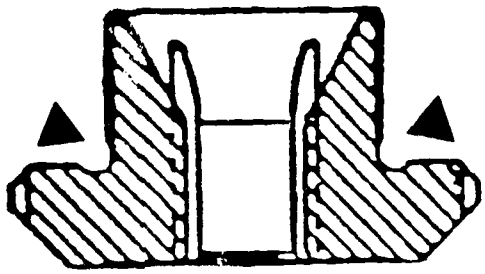

MIXER SUPPORT BOLT SCHEMATIC.

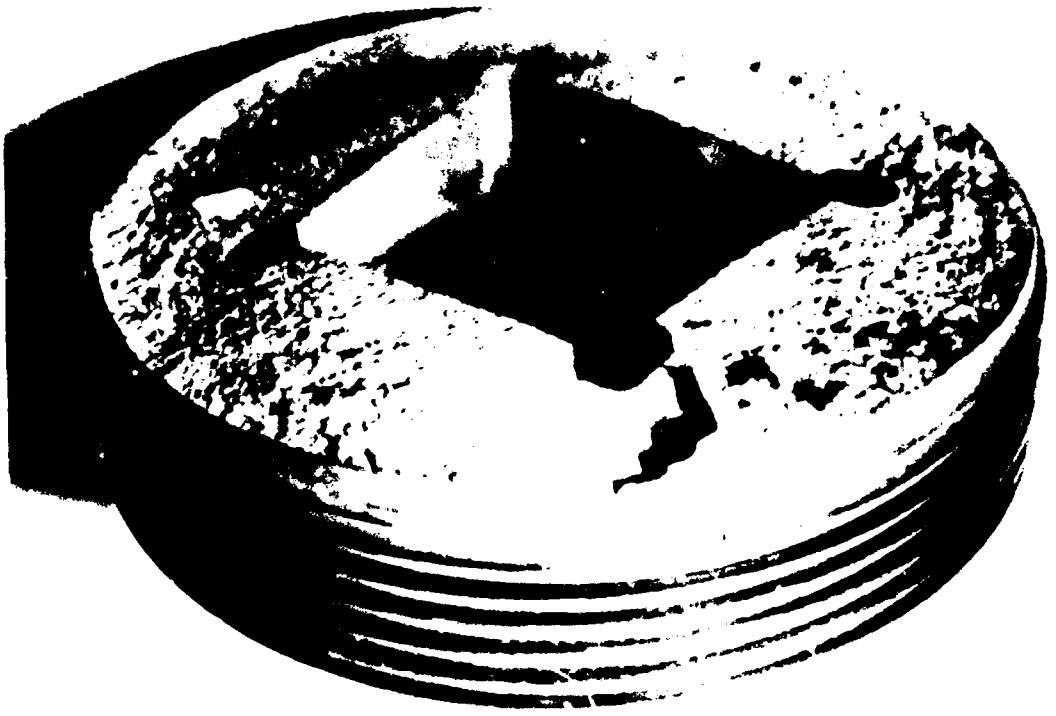

MIXER SUPPORT BOLT FAILURE.

METALLOGRAPHIC SECTION SHOWING FACETTED NATURE OF CRACK GROWTH.
SOME SECONDARY INTERGRANULAR CRACKS CAN BE SEEN.

FRACTURE SURFACE AT ORIGIN EXHIBITING INTERGRANULAR FACETS.

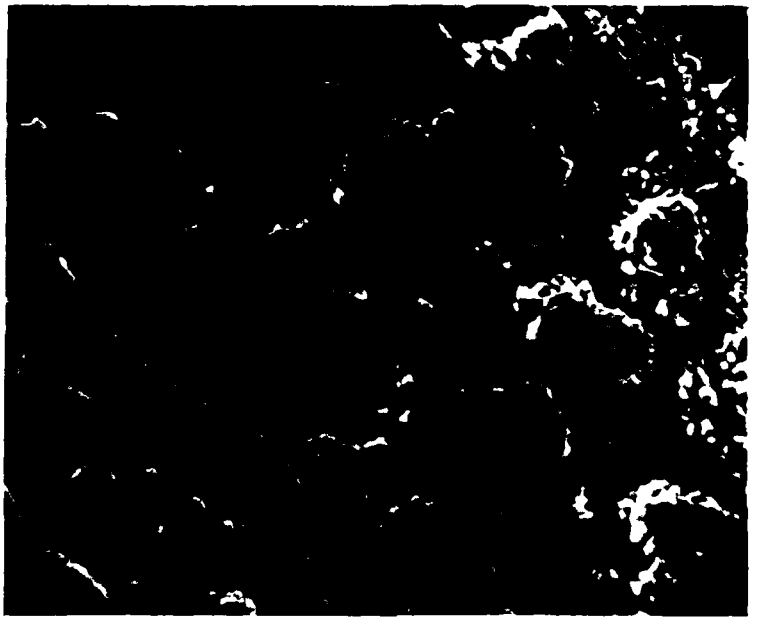

VACUUM CADMIUM PLATING MORPHOLOGY ON SURFACE.

SMOOTH TENSILE DATA

- 4340 ESR STEEL BATCH FOR MIXER SUPPORT BOLT. SMOOTH BAR 0.002"/MIN STRAIN RATE.

- LONGITUDINAL

%RH	UTS (ksi)	%RA	TR 82-1
0	296	37	47
50/55	292	39	41
75/85	291	37	43
100	292	24	12

- TRANSVERSE

0	294	38	
50/55	290	39	
75/85	295	38	
100	296	19	

MIXER BOLT MATERIAL

- NOTCHED BAR TESTS, 0.00002"/MIN SRAIN RATE.
- CREVICE FORMED BY NYLON FILAMENT IN NOTCH.

ENVIRON.	CREVICE	LOAD AT FAILURE. (lbs)
AIR	NO	6900
DIST. WATER	NO	7500
3.5% NaCl	NO	GRIPS
3.5% NaCl	YES	3250
0.2M SOD. SULF.	YES	2770
3.5% NaCl,-1.2V(SCE)	YES	1860
0.2M SOD. SULF.,-1.2V	YES	1770
3.5%NaCl, Al 6061 T6	YES	2750

MECHANISMS.

- HYDROGEN SEGREGATES TO GRAIN BOUNDARIES AND WEAKENS THEM. POSTULATED BY LATANISON THAT WEAK BONDING BETWEEN H,S,AND P RESULTS IN LOSS OF STRENGTH.

- DISLOCATION LOCKING OCCURS DUE TO INTERSTITIAL HYDROGEN. IN ITSELF IT CANNOT EXPLAIN THE DRAMATIC AND CATASTROPHIC STRENGTH DECREASES.

- IN ADDITION CREVICE CORROSION MECHANISMS OPERATE WHICH DECREASE ph IN AREA OF CREVICE. FILM REMOVAL TO EXPOSE SUBSTRATE WILL OCCUR AND HIGH HYDROGEN ION CONTENT WILL RESULT IN INCREASED HYDROGEN CONTENT IN STEEL. A FURTHER DECREASE IN STRENGTH WILL BE FOUND UNDER THESE CONDITIONS.

CONCLUSIONS.

- MIXER SUPPORT BOLT FAILED BY HYDROGEN EMBRITTLEMENT. POSSIBLY ENVIRONMENTAL EXPOSURE AND A CREVICE FORMED BY THE THREADS BOTH CONTRIBUTED TO THE EMBRITTLEMENT.

- THE 4340 ESR STEEL USED FOR MANUFACTURE WAS GOOD.

- EXPOSER TESTS INDICATE THAT A CREVICE APPEARS TO FURTHER DEGRADING THE STEEL, POSSIBLY BY CREVICE CORROSION PROVIDING EXTRA HYDROGEN IN THE HIGH STRESS AREAS AT NOTCHES.

- A RESEARCH PROGRAM IS UNDER WAY TO INVESTIGATE MITIGATION BY ION IMPLANATION TO BLOCK HYDROGEN DIFFUSION PATHS.

- COMPONENT TESTING IS BEING CONDUCTED TO AID DESIGN BY PROVIDING INPUT DATA TO STRESS ANALYSIS PACKAGES SO BETTER PREDICTION OF THE USEFUL SERVICE STRENGTH LEVELS CAN BE ACHIEVED.

BIOGRAPHY

NAME: Chester V. Zabielski

PRESENT AFFILIATION: Army Materials Technology Laboratory

TITLE: Research Metallurgist

FIELD OF INTEREST/RESPONSIBILITIES

Metal Processing, Corrosion and Protection
Principal Investigator of R&D projects involving thermomechanical processing of Depleted Uranian, Corrosion and Protection of munition metals/alloys

PREVIOUS AFFILIATIONS/TITLES

Professor of Metallurgy, University of Pittsburg
Metallurgical Engineer, Westinghouse Electric Corp.

ACADEMIC BACKGROUND

BS Columbia University
MS Rensselaer Polytechnic Institute
PhD University of Pittsburgh

SOCIETY ACTIVITIES/OFFICES/AWARDS:

NACE, Electrochemical Society, ASM-AIME, ACS

PUBLICATIONS/PAPERS:

Publications in Metallurgical Characterization of Depleted Uranium (DU) Alloys, Corrosion and Protection of DU Alloys, Electrochemical Behavior of Metals/Alloys in DU Solutions

A1-6 2

ENVIRONMENTALLY ASSISTED CRACK INITIATION IN IGNITION STARTER BREECH CHAMBERS

by

R. D. Daniels, D. M. Egle, A. S. Khan
University of Oklahoma
Norman, OK

and

A. B. Gillies
Oklahoma City Air Logistics Center
Tinker Air Force Base, OK

Abstract

Failures of steel breech chambers in cartridge-ignition aircraft jet engine starters, although rare occurrances, are a matter of serious concern. Failures have taken several forms, but usually involve fracture and unzipping of the chamber dome. The interior surface of the dome is subject to corrosion because of the accumulation of combustion products and moisture behind heat shields. The corrosion frequently involves pitting.

Twenty-five used but serviceable breech chambers were taken from service for examination and pressure testing. Corrosion products were collected and analyzed and the interior surfaces of the domes were cleaned and inspected before hydraulic pressure testing of the chambers to 5000 psi, a pressure well above the nominal operating pressure. Seventeen of the chambers ruptured. The ruptured chambers were examined to determine the origin and nature of the failures. Three of the fractures initiated at pits; one of these involved preexisting cracks emanating from pits.

The evidence gathered in this study indicates that failures encountered in the field are often a consequence of environmentally assisted crack initiation associated with the pitting corrosion. Significant wall thinning due to pitting did not correlate with failure load or origin. However, finite element analysis showed that a crack of depth 12 percent of the wall thickness could extend subcritically under service loads.

Introduction

Cartridge-pneumatic starters are mechanical systems used to accelerate jet engine turbines to speeds sufficient to start the engines [1]. The starters are used in two modes: (a) the cartridge mode, in which a rapidly burning solid propellant cartridge is ignited within a closed chamber (the breech chamber/cartridge chamber assembly) and the rapidly expanding combustion gases provide the energy to start the engine, and (b) the pneumatic mode, in which air from another engine or a ground support compressor provides the necessary energy. The benefits of the cartridge mode are that it provides a self-sufficient starting capability, not dependent on ground support, and that it provides a quick start capability in which all engines can be started simultaneously.

Failure of breech chambers during firing is a rare occurrance, about one out of 20,000 firings, but is nevertheless prevalent enough to cause serious concern. A number of steel breech chamber failures that have occurred since 1978 have been investigated at the University of Oklahoma. Reports on some of these investigations have been published [2,3]. Early-on, corrosion was identified as a significant factor in most of the failures, and stress-corrosion cracking was suggested as a possible failure mechanism [2]. A study was undertaken in 1983 to determine the operating conditions within the steel breech chambers used on B-52 aircraft [4]. The work included measurement of temperatures, pressures, and stresses that occur in a chamber during actual firings, a finite element stress analysis of the chamber based on these actual operating conditions [5], and studies of the propensity of the steel to initiate and propagate cracks under the combined influence of stress and the residues left in the chamber after firing of cartridges. Stress-corrosion cracking studies were carried out, using the slow strain rate technique, on steel samples in an environment consisting of moistened residues removed from failed breech chambers [6]. These studies demonstrated that the residues can cause stress-corrosion cracking.

Based on the knowledge gained in these earlier studies, twenty-five used but serviceable breech chambers for B-52 aircraft were removed from service for examination and pressure testing to determine the condition of the chambers and the size and shape of flaws and/or cracks that might be present in the chambers [7]. The chambers, manufactured by the Sundstrand Corporation, had been in service for undetermined lengths of time and each had undergone an undetermined number of firings. All 25 chambers were considered to be in operational condition by existing criteria.

Service failures in the steel breech chambers have been primarily of the type shown in Figure 1, wherein the chamber dome splits open during a cartridge burn. The fracture typically initiates in the knuckle region, on the side of the dome diametrically opposite the gas exhaust port. Subsequent to initiation, the fracture propagates around the circumference of the dome toward the exhaust port and the top of the dome is bent away from the chamber to form a flap. Erosion of the fracture surfaces by escaping hot gases generally makes it impossible to detect pre-existing flaws and/or cracks at the location of the fracture origin.

In the present study the 25 used breech chambers were pressurized hydraulically. The goal of the project was to determine the flaw configurations that might be present in a chamber after some period of service. It was hoped to determine flaw sizes, shapes, and locations that are responsible for the service failures in a typical chamber. The project was divided into three tasks: (a) pressure testing and nondestructive evaluation of flaws, (b) stress and fracture analysis, and (c) metallographic analysis [7]. This paper touches on all phases of the study, with emphasis on the significance of corrosion on the general degradation of the chambers and on the development of critical flaws.

Examination and Testing of the Breech Chambers

Task (c) included visual examination and photography of the chambers initially and subsequent to each procedure or test that altered the appearance or condition of the chambers.

Examination of Uncleaned Chambers

After an initial examination of a chamber as-received, the internal heat shields were removed by dry cutting. The inner surface of the chamber dome was then examined before any attempt was made to remove corrosion product and other residues from the surface (except for the loose products that were collected during removal of the heat shields).

In general, there were two distinct types of residue on the interior surface of the chamber dome. A thick, adherent scale tended to cover the surface surrounding the exhaust port. It was up to one-quarter inch thick in places. This scale on some chambers covered up to 50 percent of the interior surface area of the dome. The remaining surface was covered by a light to heavy rust colored scale. This scale, where present in quantity, was less adherent than the scale around the exhaust port. Examples of both types of scale are shown in Figures 2 and 3. Figure 2 shows the interior surface of chamber 7. The thick, adherent scale is at the bottom of the photograph around the exhaust port. The smoother looking surface above is covered with a thin layer of rust colored scale. The thick, adherent scale is gray-yellow and gray-brown in color. A portion of this scale is shown close up in Figure 3. Table 1 summarizes results of observations on the interior surfaces of the uncleaned chamber domes.

Removal and Analysis of Surface Scales

The surface scales were collected from the breech chambers for study by x-ray diffraction. The loose scale could be removed by light brushing of the surface but the adherent scale had to be picked or chipped away. An attempt was made to segregate the loose scale from the adherent scale, so that there were two distinct residue samples for each chamber. The loose scale was identified with the chamber number and the adherent scale with the additional modifier "A". In all instances the "A" scale represented the scale removed from the area around the exhaust port.

X-ray diffraction patterns were obtained for each of the residue samples. The principal compounds identified in each of the samples are listed in Table II. The compounds are listed in order of decreasing intensity of the strongest diffraction line produced by the compound. Because of the number of compounds probably present in residues, many only in trace quantities, only compounds present in substantial quantities could be identified.

The average pH of the residues was 5, with the lowest value found being 3.5. This contrasts with the results for residues from chambers failed in service that showed an average pH of 3.

Examination of Cleaned Chambers

Scale that could not be removed by mechanical means without damage to the interior surface of the dome was removed by cleaning in an ultrasonic bath with a detergent cleaner. The cleaned surface was then visually examined and photographed. Particular note was made of the location and severity of pitting of the surface. The results of these visual observations are presented in summary form in Table III. Also included in the table are notations on the presence of electroless nickel plating on the interior surface. A portion of the interior surface around the exhaust port is plated when the chamber is immersed in a bath to plate the external surfaces during manufacture. Small, shallow pits referred to in the table are less than 1 mm in diameter and 0.25 mm in depth. Larger pits are 2 to 5 mm in diameter and more than 0.5 mm in depth. Examples of deep pitting in chamber 17 are shown in Figure 4.

Ultrasonic spectroscopy was employed to obtain an approximate picture of the roughness and the thickness of pitted areas of the dome surface. The method was shown to be capable of detecting shallow isolated pits of depth less than 0.03 inch [6]. The method was also employed to map the wall thickness of the chamber domes. The nominal wall thickness of the chamber dome is 0.10 inches out to the knuckle radius where the wall begins to thicken. Because of general thinning of the wall due to corrosion, thickness values of 0.07 to 0.09 inches were common.

Proof Testing and Chamber Fractures

The cleaned chambers were proof tested to a design maximum pressure of 5000 psi in a hydraulic pressurization system. Automotive automatic transmission fluid was used as the pressure medium. During pressurization the chambers were monitored for acoustic emission.

Seventeen of the 25 chambers ruptured. The results of the proof tests and classification of the dome ruptures are presented in Table IV. Not all of the chambers that ruptured failed on the first pressure cycle. Some chambers failed only after several cycles to the proof test pressure. The majority of the fractures initiated at the weld located at the exhaust port. The fracture either initiated at the weld as in Figure 5 or went around the weld as in Figure 6. Several chambers fractured across the center of the top of the dome as in Figure 7. Only one chamber, chamber 7, fractured at a location diametrically opposite the exhaust port. In this instance a 0.75 inch long through-wall crack developed in the knuckle area, Figures 8 and 9.

Fracture Surface Examination

The crack in chamber 7 was cut out of the breech chamber and split open. As shown in Figure 10, the crack consists of three semi-elliptical pre-cracks. Discoloration of the cracks was due to corrosion, indicating that the cracks were present prior to the pressurization test. Dimensions of these cracks are illustrated in Figure 11. The fracture surfaces of the pre-cracks were examined using the scanning electron microscope. An SEM photograph of the pre-crack fracture surface, Figure 12, indicates intergranular fracture. Outside the pre-crack area the fracture surface exhibited features of ductile overload fracture.

Preexisting cracks were also found in chambers 10 and 20. In both cases the domes had completely separated from the chambers during the pressurization tests. The cracks were semi-elliptical and similar in configuration to those in chamber 7. Both fractures contained one large crack with small satellite cracks adjacent to it. In chamber 10 the largest crack penetrated through approximately 50 percent of the dome wall. In chamber 20, the largest crack penetration was 80 percent. The cracks in chamber 10 were about one-third inch in total length; the cracks in chamber 20 were about one-half inch long. SEM examination revealed the fracture modes to be ductile overload even in the pre-cracked areas. The fracture surfaces were not discolored and showed no evidence of corrosion as did those in chamber 7. The cracks originated from well defined pits on the dome inner surface.

Wall Thickness Measuements

Measurements of wall thickness were made on cross-sections taken for metallographic examination on a number of the chambers. The chambers examined included the range of failure types observed. The cross-sections were taken in areas adjacent to the fracture origins. The results are presented in Table V. Maximum, minimum, and typical observed wall thicknesses are recorded. As noted above, the nominal wall thickness of the dome is 0.10 inch. Figure 13 shows an example of extreme wall thinning in chamber 1 caused by corrosion. The wall thickness has been reduced by 90 percent.

Finite Element Fracture Analysis

The failure pressures to be expected in the breech chambers were analyzed as a function of crack geometry using a finite element elasto-plastic program. The details of the program are given elsewhere [8,9]. The analysis was carried out for a 4340 steel with a true stress-true strain curve corresponding to a 800°F temper (hardness of R_c 43) [10]. The results of the several models examined are presented in Table VI. The models include: no crack or cavity, random variations in thickness, discontinuous variation in thickness, partly spherical cavity, and semi-elliptical crack. The partly spherical cavity (PSC) would be analogous to a pit shaped as a portion of a sphere. The semi-elliptical crack (SEC) would be a sharp crack with a semi-elliptical contour. Both the PSC and the SEC can be characterized by the parameters c/t and a/t, where c is one-half the crack width (or cavity diameter), a is the crack or cavity depth, and t is the wall thickness.

The operating pressure of a breech chamber during firing is about 1200 psi [4]. Thus only the models with an SEC could produce crack extension at pressures on the order of 1200 psi. These models assume some wall thinning due to overall corrosion (t = 0.08 inch). In addition, the ratio of crack width c/t to crack depth a/t must be large as in models 15, 19, 20, and 22. The reason for this is that if c/t is small, the neutral plane does not shift too much when the crack grows in the thickness direction. Since the stresses in the cap change from tensile at the inside surface to compressive at the outside surface with a very steep gradient [5], most of the crack tip will sit in a stress field of lower magnitude than a crack with a smaller a/t ratio. With a large c/t ratio the neutral plane shifts toward the outside as the crack grows.

Discussion and Conclusions

Only one of the twenty-five breech chambers tested failed in a manner that could be predicted from our experience with service failures. This was chamber 7 where fracture initiated from preexisting cracks located diametrically opposite the exhaust port at the radius where the knuckle region begins. This is the location where the spherical dome intersects the cylindrical side wall of the chamber. The maximum tensile stresses produced in the chamber wall during the burn of a cartridge are located at this radius [4,5]. Hydraulic pressurization of chamber 7 produced only a through-wall fracture at this location, Figures 8 and 9. Pneumatic pressurization would probably have produced a failure similar to the service failure shown in Figure 1.

In the absence of preexisting cracks or other major defects in the dome wall, overload failures initiating at the weld around the exhaust port are to be expected. The weld reinforcement introduces a stiffness at this location which acts to concentrate the stress. In those instances where the chambers failed across the top of the dome, the ultrasonic thickness maps of the domes showed that the fracture paths approximately matched the boundaries where there was a distinct discontinuity in wall thickness. However, these maps did not identify the fracture origins.

The residues removed from the chambers included oxides of iron and potassium chloride. The potassium chloride will increase the corrosion rate in the presence of moisture and tend to increase the acidity in pits through the hydrolysis reaction involving the chloride ion. Observations on cleaned chambers indicated that pitting was more severe in areas which were plated with electroless nickel. Since the temperature on the inside surface of the dome reaches 500°F to 800°F during a cartridge burn [4], the electroless nickel is expected to crack due to brittleness of the coating produced by heating to these temperatures and the differential expansion with the steel. Cracks in the coating will in turn set up galvanic cells that promote pitting of the steel.

The wall thinning, mapped ultrasonically and measured in particular locations by taking cross-sections, did not correlate with failure load or origin. The finite element analysis showed that thickness variations were insufficient to cause failure at the chamber operating pressure. The analysis also showed that the presence of a pit could cause yielding at the bottom of the pit but not failure under operating conditions.

The finite element analysis showed that cracks could extend subcritically under chamber operating pressures if crack geometry is favorable. For a semi-elliptical crack the c/t ratio must be large compared to the a/t ratio. One model (model 19 in Table VI) demonstrates that a crack with a depth 12 percent of the wall thickness will extend sub-critically under loads of only one-half the chamber operating pressure.

Cracking appears to initiate at the base of pits. It is speculated that when isolated pits reach a certain size, the stresses produced by firing a cartridge cause yielding to occur at the base of a pit. Yielding induces tensile residual stresses localized at the pit. Corrosive agents in the combustion residue (combined with moisture which collects behind the heat shields between firings) and the residual tensile stresses must promote environmentally assisted cracking. This process starts a microcrack at the base of the pit. If microcracks of several adjacent pits coalesce, as in Figure 10, a crack large enough to permit subcritical crack growth under service conditions is produced. This crack grows slowly (presumably over a period involving a number of cartridge firings) until it becomes critical under the chamber operating conditions and failure occurs. The process of subcritical crack growth can be considered as a form of low cycle corrosion-fatigue.

While this mechanism is plausible, there are unanswered questions. First, it is not understood why some of the chambers had more acidic residues than others. Second, it has been observed in examination of service failures that some secondary cracks found in chambers appeared to initiate from a surface which was essentially free of pits [3]. Finally, the rate of crack growth in the low cycle fatigue region is not addressed. These observations do not invalidate the mechanism proposed, but they do indicate that the process may be more complex than outlined.

Two possible remedies for preventing failures in service emerge. First, the chamber could be redesigned so that the heat shields could be removed for regular inspection and cleaning of the inside surface of the dome. Cleaning would likely reduce the overall corrosion and visual inspection would facilitate removal of pitted chambers from service. Second, if cracks of 25 to 50 percent of the dome thickness can exist before failure, then it should be possible to develop an NDE technique to inspect the chambers.

Acknowledgement

This work was supported under U. S. Air Force Contract No. F34601-85-C-0791.

References

1. J. A. Anderson, and C. R. Galasinski, "Jet Engine Starters, Cartridge-Pneumatic", ASME Paper No. 67-GT-49, ASME Gas Turbine Conference, Houston, TX, March 5-9, 1967.

2. W. R. Coleman, R. J. Block, and R. D. Daniels, "Corrosion Problems in Aircraft Components -- Case Studies of Failures", **Proceedings, 1980 Tri-Service Conference on Corrosion**, AFWAL-TR-81-4019, Vol. II, 241-270, (1981).

3. P. C. Perkins, R. D. Daniels, and A. B. Gillies, "Failure Analyses of Steel Breech Chambers Used With Aircraft Cartridge-Ignition Starters", **Analyzing Failures: The Problems and the Solutions**, V. S. Goel, Editor, 143-150, American Society for Metals, Metals Park, (1986).

4. D. M. Egle, A. S. Khan, A. G. Striz, and R. D. Daniels, "A Comprehensive Stress and Life-Cycle Analysis of Jet Engine Starter Breech Chambers", AMNE Report 85-5, University of Oklahoma, USAF Contract F43601-83-C-3448, May 1985.

5. A. G. Striz and F. P. Brueckner, "Finite Element Analysis and Redesign of Jet Engine Starter Breech Chamber", ASME Paper No. 86-WA/DE-20, ASME Winter Meeting, Anaheim, CA, December 7-12, 1986.

6. K. J. Kennelley and R. D. Daniels, "Stress-Corrosion Cracking of 4340 Steel in Aircraft Ignition Starter Residues", **Corrosion Cracking**, V. S. Goel, Editor, 199-204, American Society for Metals, Metals Park, (1986).

7. D. M. Egle, A. S. Khan, and R. D. Daniels, "Determination of Initial Flaw Configuration and Fracture Analysis for Breech Chambers", AMNE Report 86-2, University of Oklahoma, USAF Contract F34601-85-C-0791, July 1986.

8. A. R. Kukreti, A. S. Khan, and A. Iranmanesh, "Fracture Prediction in Elastoplastic Problems Using Finite Element Method", **Proceedings of the International Conference on Application of Fracture Mechanics to Materials and Structures**, G. C. Sih, E. Sommer, and W. Dahl, Editors, 619-637, Martinns Nijhoff, (1984).

9. A. R. Kukreti, A. S. Khan, and A. Kumar, "A Three-Dimensional Finite Element Program for Crack Initiation and Propagation in Solids", **Proceedings of International Conference on Finite Elements in Computational Mechanics**, T. Kant, Editor, Pergamon Press, (1985).

10. **Structural Alloys Handbook**, Mechanical Properties Data Center, Belfour Stulen, Inc. Traverse City, MI, (1977).

List of Tables

List of Figures

Table I

Condition of Breech Chamber Dome Interior Surfaces (uncleaned)

Chamber No.	Heavy Scale			Rust		
	Color	% Coverage	Location	Light	Heavy	% Coverage
1	Grey-green	20	on plated area and also encircles chamber in knuckle region		X	80
2	Grey-green	20	on plated area	X		80
3	Green-blue	25	on plated area	X		75
4	Red-orange	3	confined to knuckle region behind exhaust port		X	97
5	Black	70	area opposite exhaust port not covered	X		30
6	Grey-yellow	50	1/2 dome opposite exhaust port not covered		X	50
7	Grey-yellow Grey-brown	50	"		X	50
8	Brown	35	area opposite exhaust port not covered	X		65
9	Grey-brown	55	"	X		45
10	Grey	40	"		X	60
11	Grey	30	on either side of exhaust port		X	70
12	Yellow-black	50	area opposite exhaust port not covered	X		50
13	---	0	---	X		100
14	Grey	30	around exhaust port	X		70
15	Grey	5	in knuckle region behind exhaust port		X	95
16	Grey-black	50	in plated area and a patch opposite exhaust port	X		50
17	Brown	15	around exhaust port	X		85
18	Grey	20	only on one side of exhaust port	X		80
19	Black	3	in knuckle region behind exhaust port	X		97
20	Black	15	only on one side of exhaust port	X		35
21	Grey-black	25	around exhaust port	X		75
22	Grey	20	only on one side of exhaust port		X	30
23	Brown	15	"	X		85
24	Black	70	middle domed portion not covered		X	30
25	Brown	10	scattered patches over entire dome	X		90

Table II

Compounds Identified in Chamber Residues

Corrosion Product No.	Compounds Present	Major Peak
4	Fe_3O_4, FeOOH	Fe_3O_4
5	Fe_2O_3, KCl, FeOOH	Fe_2O_3
6	KCl, Fe_3O_4, Fe_2O_3	KCl
7	Fe_2O_3, KCl, Fe_3O_4	Fe_2O_3
7A	KCl, Fe_2O_3, Fe_3O_4	KCl
8	KCl, Fe_3O_4, Fe_2O_3	KCl
8A	KCl, Fe_3O_4, Fe_2O_3	KCl
9	KCl, Fe_3O_4, Fe_2O_3	KCl
9A	KCl, Fe_3O_4, Fe_2O_3	KCl
10	KCl, Fe_3O_4, Fe_2O_3	KCl
10A	KCl, Fe_3O_4, Fe_2O_3	KCl
11	Fe_2O_3, Fe_3O_4	Fe_2O_3
11A	Fe_3O_4, Fe_2O_3	Fe_3O_4
12	KCl, Fe_3O_4, Fe_2O_3	KCl
12A	Fe_3O_4, Fe_2O_3, KCl	Fe_3O_4
13	Fe_3O_4, FeOOH	Fe_3O_4
14	KCl, Fe_3O_4, Fe_2O_3	KCl
14A	KCl, Fe_2O_3, Fe_3O_4	KCl
15	Fe_2O_3, Fe_3O_4, KCl	Fe_2O_3
15A	Fe_3O_4, Fe_2O_3, KCl	Fe_3O_4
16	KCl, Fe_2O_3, Fe_3O_4	KCl
16A	KCl, Fe_2O_3, Fe_3O_4	KCl
17	Fe_3O_4, Fe_2O_3, KCl	Fe_3O_4
17A	Fe_3O_4, Fe_2O_3, KCl	Fe_3O_4
18	Fe_3O_4, Fe_2O_3, KCl	Fe_3O_4
18A	Fe_3O_4, Fe_2O_3, KCl	Fe_3O_4
19	Fe_3O_4, Fe_2O_3, KCl	Fe_3O_4
19A	Fe_3O_4, Fe_2O_3, KCl	Fe_3O_4
20	KCl, Fe_3O_4, Fe_2O_3	KCl
20A	Fe_2O_3, Fe_3O_4, KCl	Fe_2O_3
21	KCl, Fe_3O_4	KCl
21A	KCl, Fe_3O_4	KCl
22	Fe_2O_3, Fe_3O_4, FeOOH	Fe_2O_3
22A	Fe_2O_3, Fe_3O_4, FeOOH	Fe_2O_3
23	Fe_3O_4, Fe_2O_3	Fe_3O_4
23A	Fe_3O_4, Fe_2O_3	Fe_3O_4
24	KCl, Fe_3O_4, Fe_2O_3	KCl
24A	Fe_2O_3, KCl, Fe_3O_4	Fe_2O_3
25	Quartz, Fe_3O_4	Quartz

Table III

Condition of Breech Chamber Dome Interior Surfaces (cleaned)

Chamber No.	Severity	Location	Electroless Nickel Plating	
			Present	Location
1	Small shallow pits	Dome center	Yes	Isolated patches between exhaust hole & knuckle region
2	Small shallow pits Large deep pits	Entire surface Near exhaust hole	No	---
3	Small shallow pits Large deep pits	Entire surface Near exhaust port	No	---
4	None		Yes	Circular patch around exhaust hole
5	Shallow pits Large deep pits	Across dome center At dome center & around exhaust hole	No	
6	Large deep pits	Around exhaust port	Yes	Small patches near exhaust hole
7	Small shallow pits Large deep pits	Dome center To left of exhaust port	No	
8	Large deep pits	Around exhaust hole	No	
9	Large deep pits	Entire surface	Yes	Large patch covers 1/3 of dome left of exnaust hole
10	Large deep pits Isolated pits	Knuckle region behind exhaust port Over entire surface	Yes	Small patches to left of exhaust hole
11	Small shallow pits Large deep pits	Covered 1/2 of dome Near exhaust hole	No	
12	Isolated shallow pits Large deep pits	Over surface Near exnaust hole	No	
13	None	---	Yes	Large patch surrounding exhaust hole
14	Shallow small pits	Entire surface	No	
15	Isolated pits	Knuckle region	Yes	Large patch at dome center
16	Large deep isolated pits	Around exhaust hole	No	
17	Large deep pits	Entire surface	No	
18	Shallow pits Isolated deep pits	Entire surface At dome center	No	
19	Isolated small pits	Over entire surface	No	
20	Isolated small pits	Over entire surface	Yes	Patch near exnaust hole
21	None		No	
22	Large deep pits Shallow pits	Across dome center Elsewnere	No	
23	Large deep pits Shallow pits	Around exnaust hole Elsewnere	No	
24	Shallow pits	Dome center	No	
25	None		No	

Table IV

Classification of Breech Chamber Dome Failures

Chamber No.	Ruptured	Across Dome Apex	Origin at or near Exhaust Port Weld	Includes Exhaust Port	Total Separation	Inital Flaw Detected	Initial Flaw Location
1	Yes	---	X	---	Yes	No	---
2	Yes	X	---	---	No	No	---
3	Yes	---	X	---	No	No	---
4	No	---	---	---	---	---	---
5	Yes	---	X	---	Yes	No	---
6	No	---	---	---	---	---	---
7	Yes	---	---	---	No	Yes	3/4" crack in knuckle opposite exhaust port
8	No	---	---	---	---	---	---
9	Yes	X	---	---	No	No	---
10	Yes	---	X	---	Yes	Yes	1/3" semi-elliptical crack adjacent to exhaust port
11	Yes	X	---	---	No	No	---
12	Yes	---	X	---	No	No	---
13	Yes		X		No	No	---
14	Yes		X		No	No	---
15	Yes		X		No	No	---
16	No						
17	Yes			X	No	No	---
18	Yes			X	No	No	---
19	Yes		X		No	No	
20	Yes	X			Yes	Yes	1/2" semi-elliptical crack opposite exhaust port
21	No						
22	No						
23	No						
24	Yes		X		No	No	---
25	No						

Table V
Wall Thickness Measurements
(Adjacent to Failure Origins)

Chamber No.	Failure History	No. of Samples	Minimum (inch)	Maximum (inch)	Typical (inch)
1	1st cycle, 4300 psi at weld	2	0.009	0.065	0.055-0.060
3	1st cycle, 4100 psi at weld	3	0.020	0.047	0.035-0.040
5	1st cycle, 4920 psi at weld	1	0.043	0.072	0.045-0.060
6	No failures, circular yield marks in knuckle	3	0.082	0.092	0.086-0.088
7	1st cycle, 3810 psi 3/4 in. through-crack	3	0.086	0.093	0.086-0.091
9	1st cycle, 4940 psi across dome apex	2	0.077	0.105	0.090-0.095
13	3rd cycle, 5140 psi at weld	3	0.083	0.095	0.087-0.092
14	1st cycle, 4900 psi at weld	3	0.082	0.095	0.089-0.093
17	1st cycle, 4580 psi includes exhaust port	3	0.051	0.091	0.075-0.085
18	1st cycle, 4480 psi includes exhaust port	3	0.047	0.079	0.060-0.075
20a	1st cycle, 5100 psi across dome apex	2	0.073	0.091	0.085-0.090
20b	1st cycle, 5100 psi across dome apex	2	0.075	0.090	0.080-0.088
24	1st cycle, 4660 psi at weld	3	0.080	0.088	0.083-0.086

Table VI

Pressures at the First Yield and First Crack Extension* with Different Sizes of Partly Spherical Cavity (PSC) or Semi-Elliptic Crack (SEC)

Model No.	Thickness (in.)	Cavity or Crack Size (c/T x a/T)	Pressures (psi)
2	0.09	No crack or cavity	2724, 6216
4	0.10	No crack or cavity	2796, 6816
6	0.09	PSC (0.25 x 0.20)	1032, 5004
7	0.077-0.0916	Random variation in thickness	1968, 5976
8	0.063-0.094	Random variation in thickness	1920, 5820
10	0.06-0.09	Discont. variation in thickness	1596, 3929
11	0.08	PSC (0.62 x 0.62)	492, 4320
12	0.08	PSC (0.78 x 0.62)	492, 4296
13	0.08	SEC (0.69 x 0.12)	420, 4104
14	0.08	SEC (0.69 x 0.12)	420, 2100
15	0.08	SEC (1.00 x 0.12)	48, 948
16	0.08	SEC (1.00 x 0.24)	276, 1224
17	0.08	SEC (1.00 x 0.36)	528, 2424
18	0.08	SEC (1.00 x 0.50)	480, 3072
19	0.08	SEC (1.50 x 0.12)	24, 624
20	0.08	SEC (1.50 x 0.24)	120, 1032
21	0.08	SEC (1.5 x 0.36)	240, 1224
22	0.08	SEC (1.5 x 0.50)	264, 1200

* When the average stress in any element reaches yield stress or ultimate stress.

Note: The first number under pressure column is for the yield, while the second number is for crack extension.

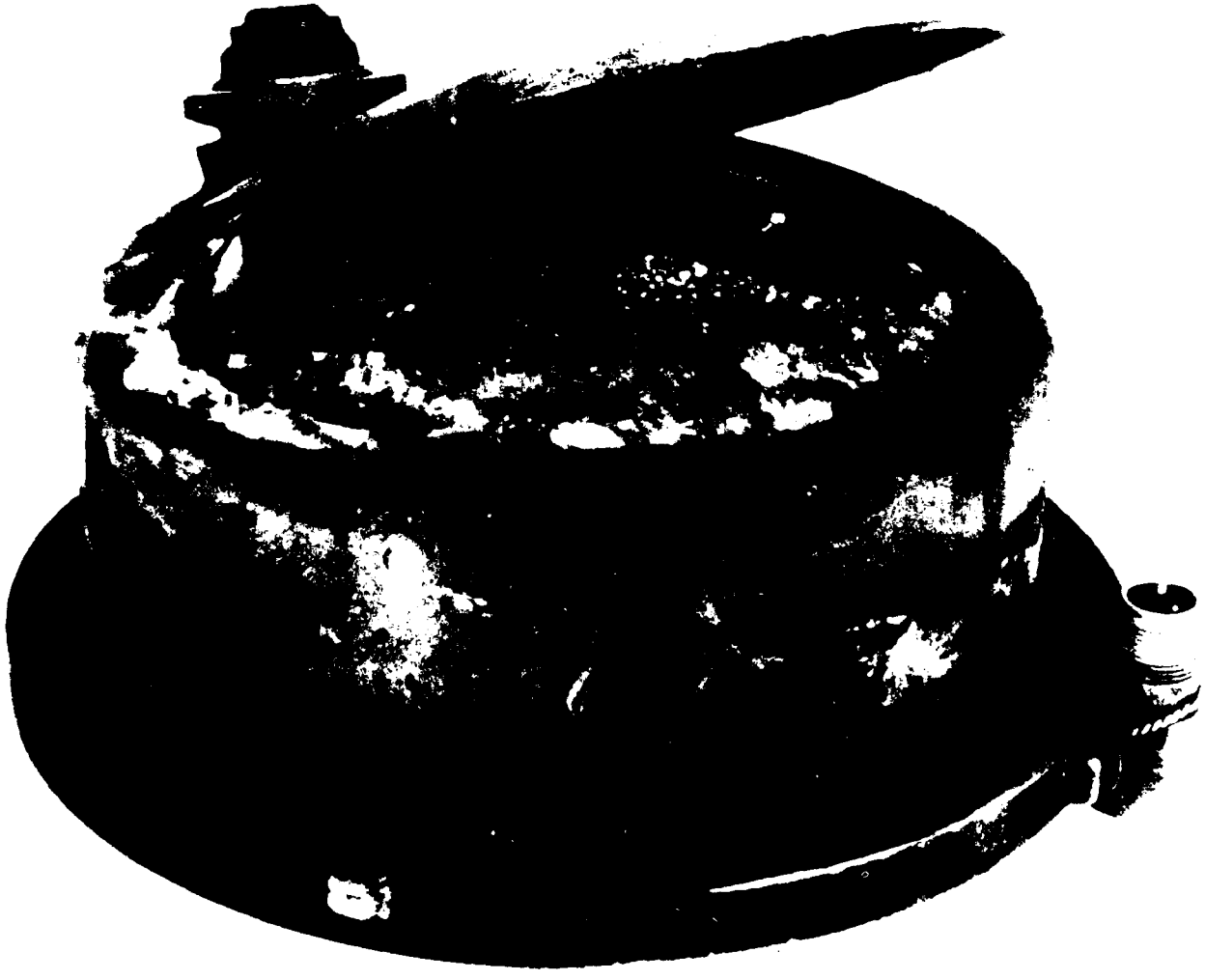

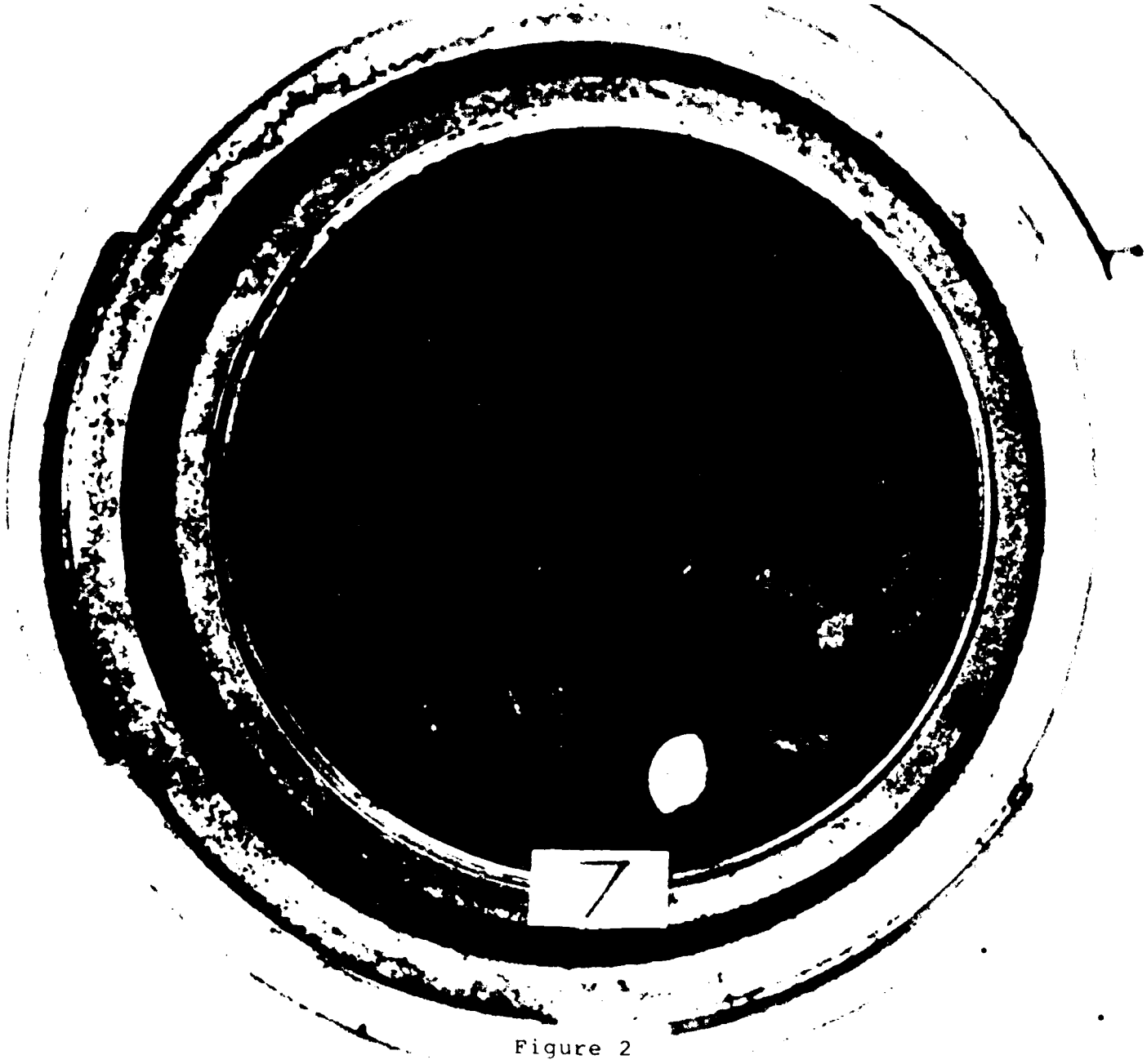

Figure 2

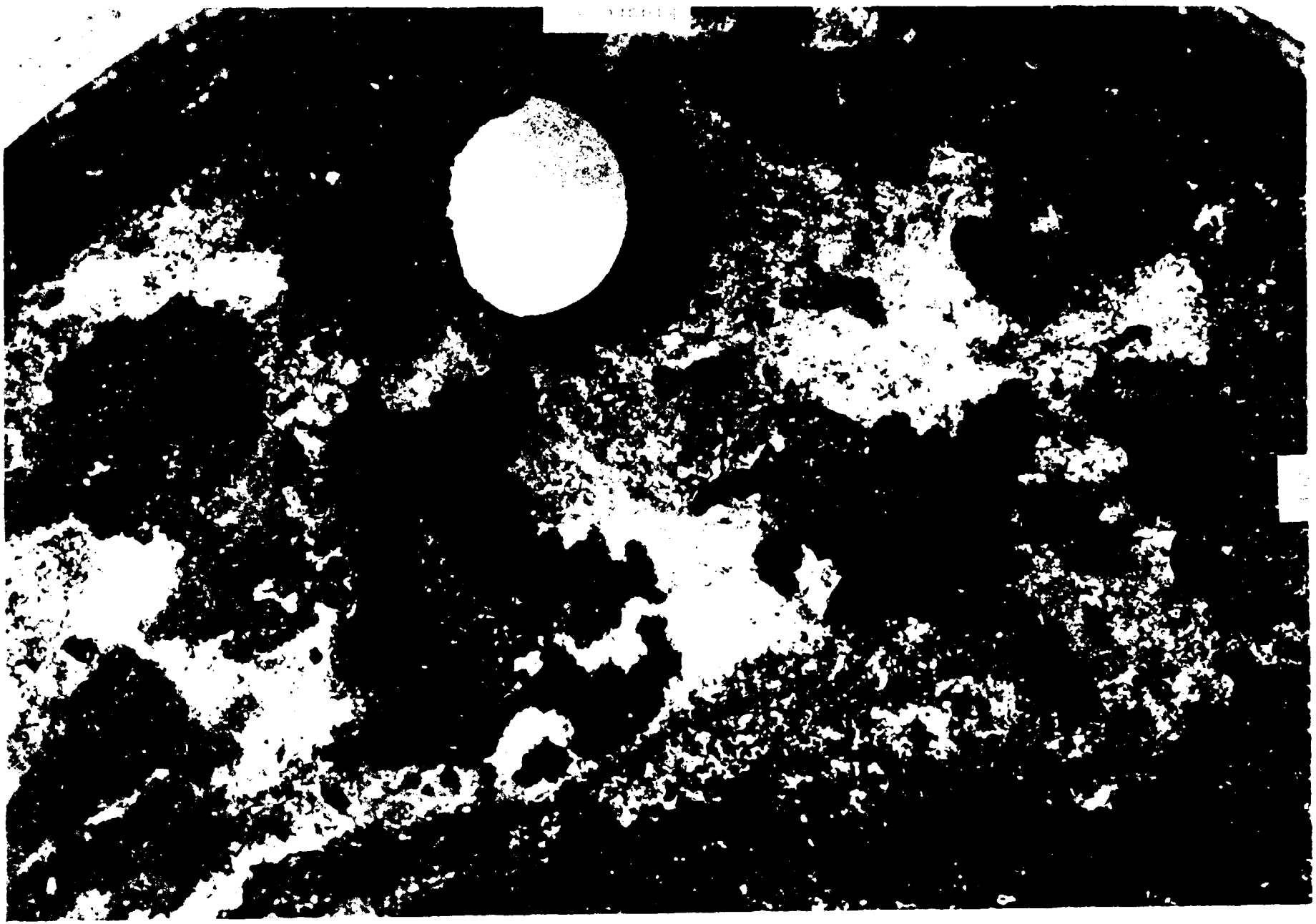

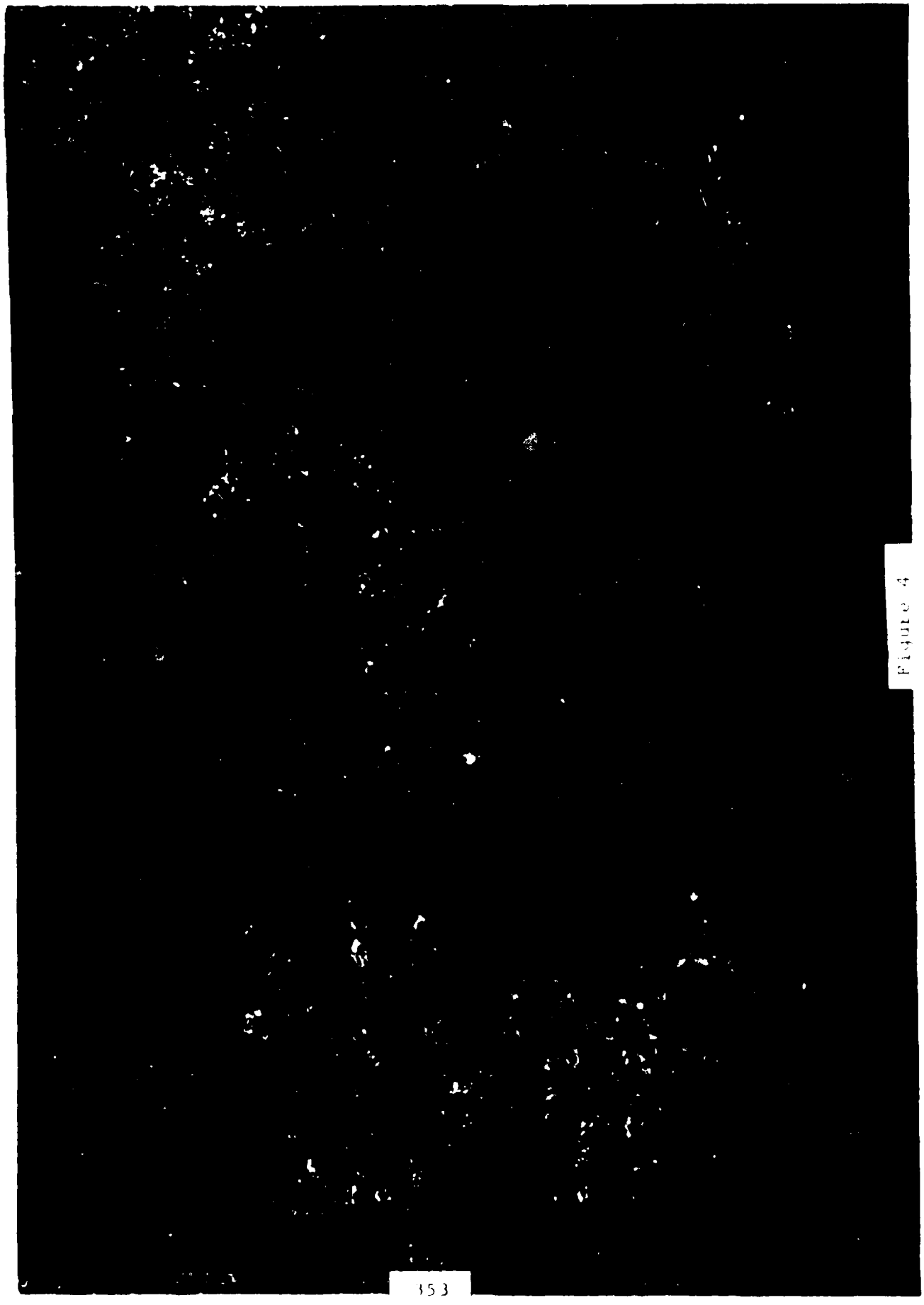

Figure 4

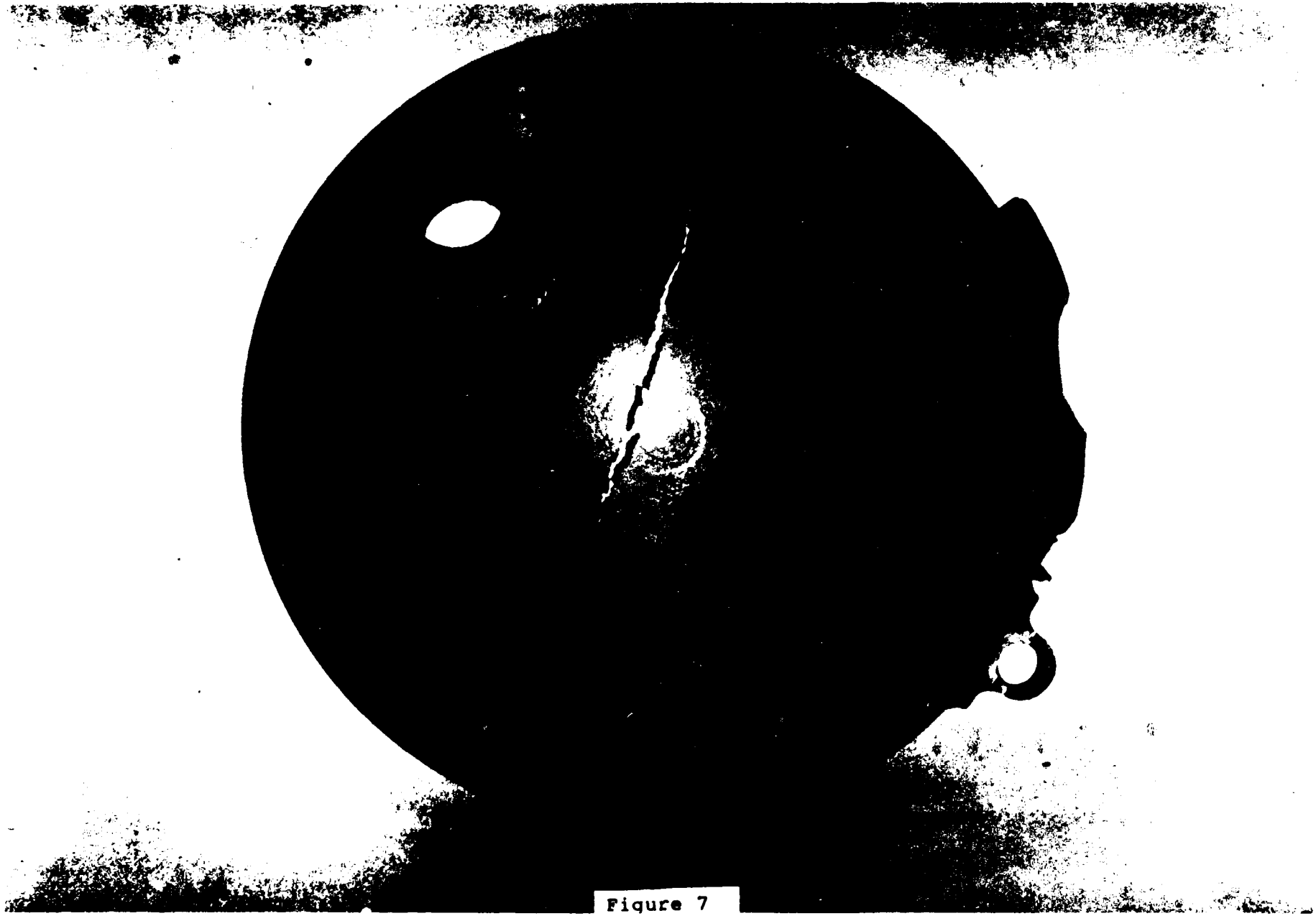

Figure 7

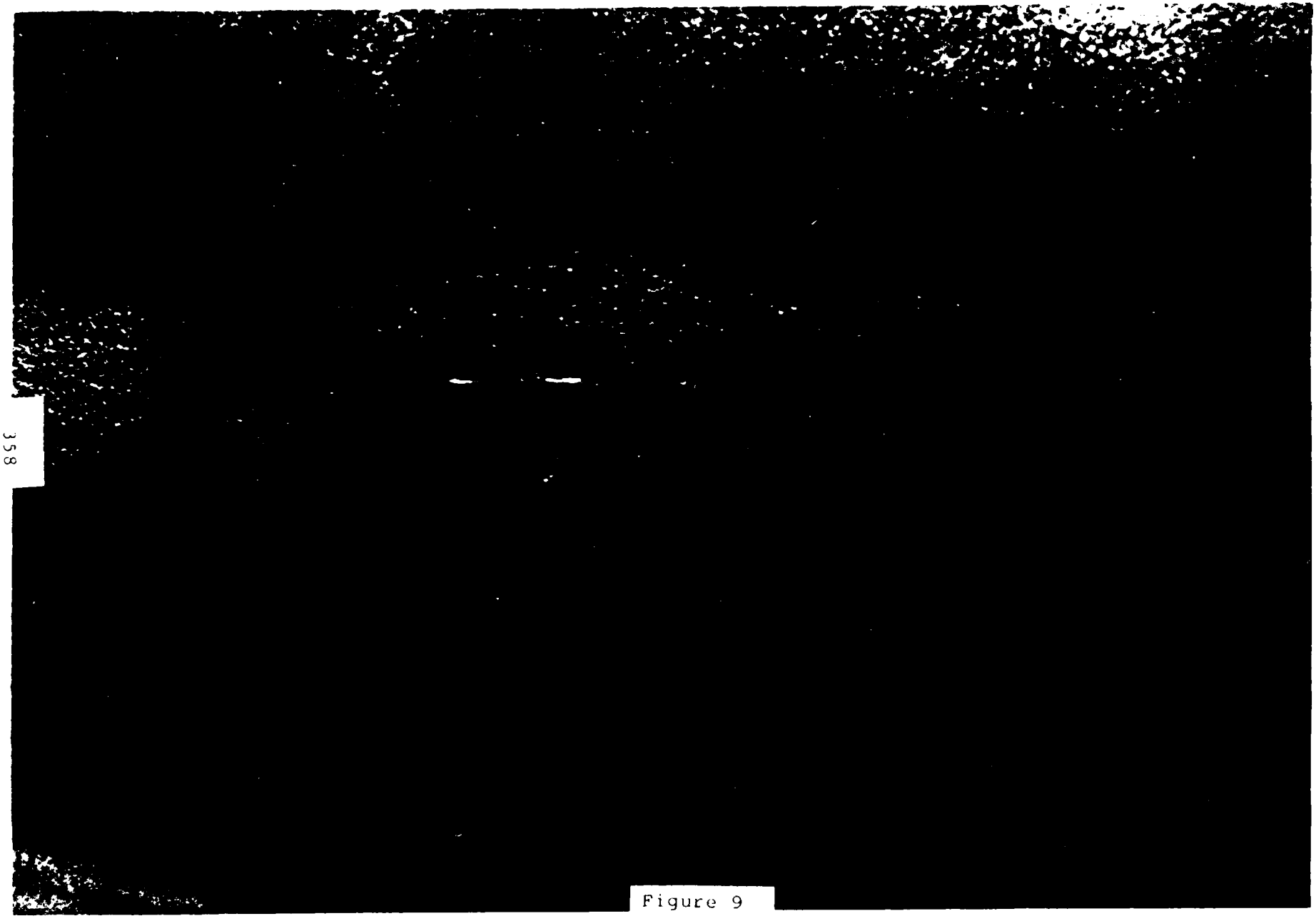

Figure 9

Figure 10

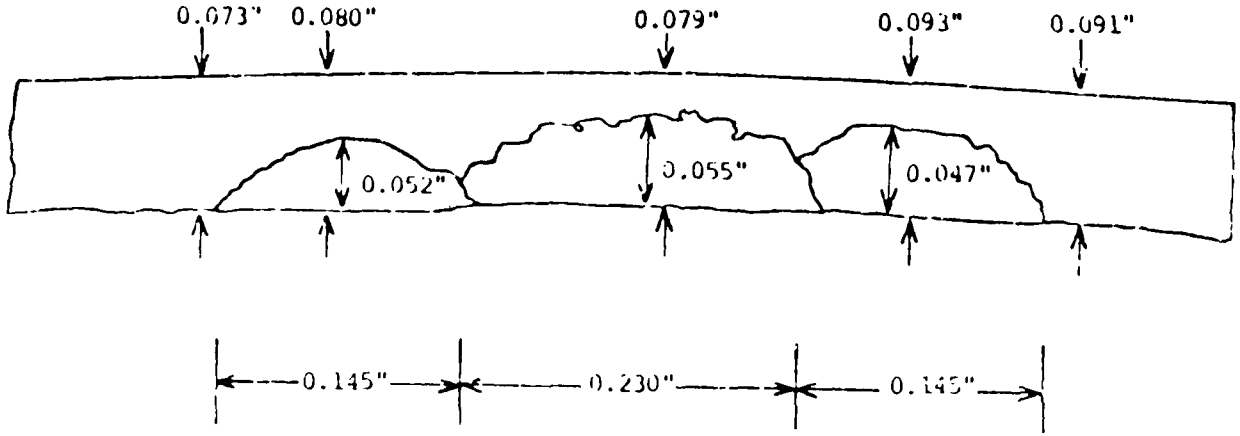

Fig. 11 Dimensions of Preexisting Cracks Seen in Figure 10

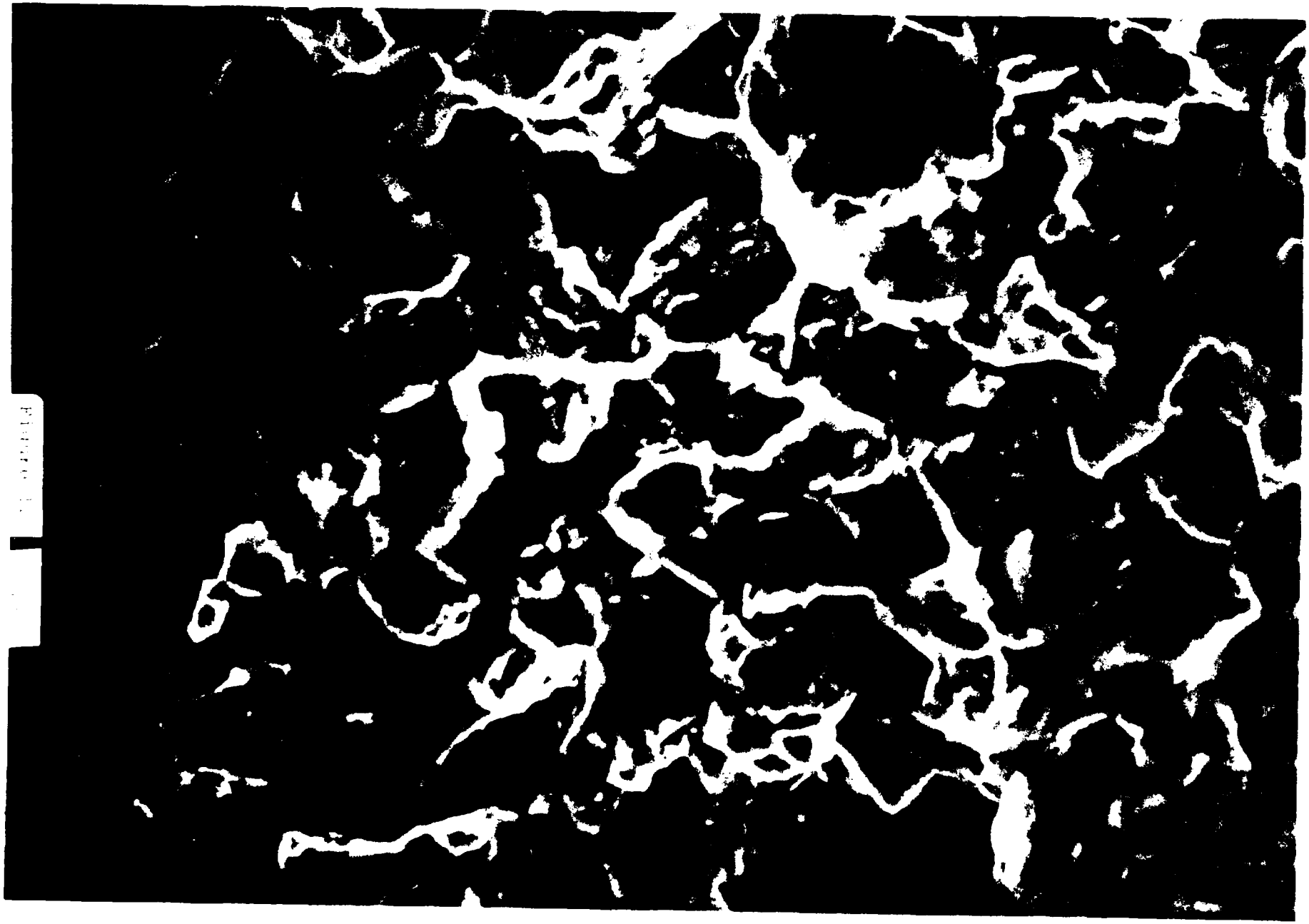

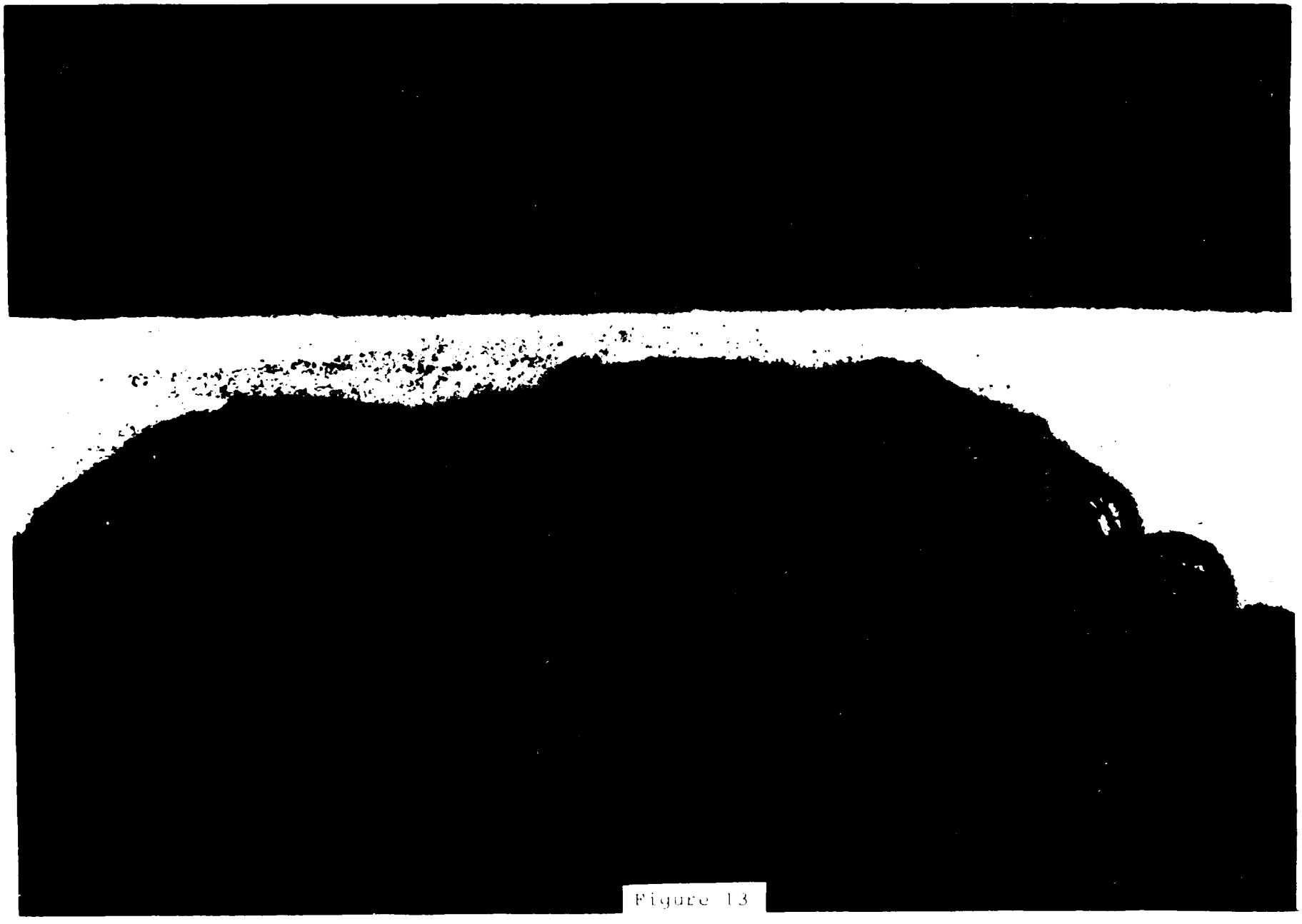

Figure 13

BIOGRAPHY

NAME:

Raymond P. [illegible]

PRESENT AFFILIATION:

School of [illegible] and Materials Science
University of [illegible]
Norman, OK [illegible]

TITLE:

Professor and [illegible]

FIELD OF INTEREST/RESPONSIBILITIES:

PREVIOUS AFFILIATIONS/TITLES:

ACADEMIC BACKGROUND:

SOCIETY ACTIVITIES/OFFICES/AWARDS:

PUBLICATIONS/PAPERS:

BIOGRAPHY

NAME:

Davis M. Egle

PRESENT AFFILIATION:

School of Aerospace, Mechancial and Nuclear Engineering
University of Oklahoma

Norman, OK 73019

TITLE:

Professor and Director

FIELD OF INTEREST/RESPONSIBILITIES :

PREVIOUS AFFILIATIONS/TITLES:

ACADEMIC BACKGROUND:

SOCIETY ACTIVITIES/OFFICES/AWARDS:

PUBLICATIONS/PAPERS:

BIOGRAPHY

NAME:

Akhtar S. Khan

PRESENT AFFILIATION:

School of Aerospace, Mechanical and Nuclear Engineering
University of Oklahoma
Norman, OK 73019

TITLE:

Professor

FIELD OF INTEREST/RESPONSIBILITIES :

PREVIOUS AFFILIATIONS/TITLES:

ACADEMIC BACKGROUND :

SOCIETY ACTIVITIES/OFFICES/AWARDS:

PUBLICATIONS/PAPERS:

BIOGRAPHY

NAME:

A. Bruce Gillies

PRESENT AFFILIATION:

Oklahoma City Air Logistics Center
Tinker Air Force Base, OK 73045

TITLE:

Senior Project Engineer

FIELD OF INTEREST/RESPONSIBILITIES:

PREVIOUS AFFILIATIONS/TITLES:

ACADEMIC BACKGROUND:

SOCIETY ACTIVITIES/OFFICES/AWARDS:

PUBLICATIONS/PAPERS:

SESSION B
ELECTRONICS CORROSION AND DATA BASES

Chairman
Jack Guttenplan
Rockwell International

AVIONICS CORROSION TRI-SERVICE 87

NAVAL AIR FORCE, U.S. ATLANTIC FLEET

AVIONIC AND ELECTRICAL SYSTEM CORROSION PREVENTION AND CONTROL MAINTENANCE

BY

C. T. BROWNE

MATERIAL ADVISOR, COMNAVAIRLANT

NORFOLK, VA 23511-5188

1. A STUDY OF PREMATURE FAILURES OF INSTALLED AVIONICS, ELECTRICAL EQUIPMENT, AND SYSTEMS EXPERIENCED IN U.S. NAVY OPERATIONAL AIRCRAFT IN THE 1960'S AND EARLY 1970'S WAS REPORTED IN REFERENCE (1). THESE FAILURES WERE CAUSED BY CORROSION, WATER INTRUSION AND OTHER CONTAMINATING AGENTS. IN ORDER TO REVERSE THIS TREND, THE COMMANDERS NAVAL AIR FORCES, U.S. ATLANTIC AND PACIFIC FLEETS (COMNAVAIRLANT) (COMNAVAIRPAC) REQUESTED THAT COMMANDER, NAVAL AIR SYSTEMS COMMAND (COMNAVAIRSYSCOM) DEVELOP A CORROSION PREVENTION AND CONTROL PROGRAM FOR AVIONICS, ELECTRICAL AND INSTALLED SYSTEMS USED IN NAVAL AIRCRAFT. COMNAVAIRSYSCOM TASKED THE NAVAL AIR DEVELOPMENT CENTER (NAVAIRDEVCEN) TO DEVELOP THE PROGRAM TOGETHER WITH A TECHNICAL MANUAL. A CONFERENCE WITH ALL INTERESTED PARTIES WAS HELD IN 1976 AND ACTION INITIATED TO DEVELOP THE PROGRAM AND TECHNICAL MANUAL FOR USE BY THE FLEET TECHNICIANS.

2. A REVIEW WAS CONDUCTED TO ASSESS THE OVERALL PROBLEM.

A. HOW TO CLEAN AVIONICS, REMOVE CORROSION, RESTORE PROTECTIVE FINISHES; WHAT CORROSION PREVENTIVES COULD BE USED ON AVIONICS WITHOUT DEGRADING PERFORMANCE OF THE EQUIPMENT; HOW TO RECLAIM EQUIPMENT THAT HAD BEEN EXPOSED TO CORROSIVE AGENTS. EACH ISSUE REQUIRED ANSWERS.

B. THE AGENTS CAUSING CORROSION WERE IDENTIFIED, I.E., SALT WATER, SEA ENVIRONMENT WITH 100% HUMIDITY, MAINTENANCE CHEMICALS, STACK GASES, HIGH TEMPERATURE, CYCLIC TEMPERATURES, MOISTURE, GALVANIC ACTION IN THE OPERATING ENVIRONMENT BETWEEN DISSIMILAR MATERIALS, MICROBIAL, INSECT, BACTERIA, FUNGI PRODUCING ENVIRONMENT, ETC.

C. METALLIC

WHAT KINDS OF CORROSION CAN WE EXPECT TO SEE? (SEE FIGURE 1-10.)

(1) UNIFORM SURFACE ATTACK

(2) GALVANIC

(3) PITTING

(4) CREVICE (CONCENTRATED CELL)

(5) INTERGRANNULAR

(6) STRESS

(7) EXFOLIATION

(8) EROSION

(9) WHAT DOES IT LOOK LIKE? (SEE ENCLOSURE (1).)

D. NON-METALLIC DETERIORATION

(1) MECHANICAL FAILURE

(2) CRACKING

(3) SWELLING

3. THE RESULTS OF CORROSION OR CONTAMINATION CAN CAUSE FAILURE OF THE EQUIPMENT OR UNDESIRABLE ALTERATION OF ITS ELECTRICAL CHARACTERISTICS. THE LIST OF ALL TYPES OF MATERIAL USED IN AVIONICS WOULD BE EXTENSIVE; MOST HAVE AN ABILITY TO FUNCTION WELL INDIVIDUALLY AND WOULD LAST THE LIFE OF THE COMPONENT. HOWEVER, THE SYNERGISTIC EFFECT WHEN DISSIMILAR MATERIALS ARE EXPOSED TO A CORROSIVE ENVIRONMENT IS OFTEN CORROSION.

A. SPECIAL CONSIDERATION. THE CONTROL OF CORROSION IN AVIONIC SYSTEMS IS NOT UNLIKE THAT IN AIRFRAMES, WITH PROCEDURES USEFUL FOR AIRFRAMES BEING APPLICABLE TO AVIONICS, WITH APPROPRIATE MODIFICATIONS. THE GENERAL DIFFERENCES IN CONSTRUCTION AND PROCEDURES BETWEEN AIRFRAME AND AVIONICS RELATIVE TO CORROSION CONTROL ARE AS FOLLOWS:

(1) LESS DURABLE PROTECTION SYSTEM.

(2) VERY SMALL AMOUNTS OF AVIONICS CORROSION CAN MAKE EQUIPMENT INOPERATIVE, AS COMPARED TO AIRFRAMES.

(3) DISSIMILAR METALS ARE OFTEN IN ELECTRICAL CONTACT.

(4) STRAY CURRENTS CAN CAUSE CORROSION.

(5) ACTIVE METALS AND DISSIMILAR METALS IN CONTACT ARE OFTEN UNPROTECTED.

(6) CLOSED BOXES CAN PRODUCE CONDENSATION DURING NORMAL TEMPERATURE CHANGES DURING FLIGHT.

(7) AVIONIC SYSTEMS HAVE MANY AREAS TO TRAP MOISTURE.

(8) HIDDEN CORROSION IS DIFFICULT TO DETECT IN MANY AVIONIC SYSTEMS.

(9) MANY MATERIALS USED IN AVIONIC SYSTEMS ARE SUBJECT TO ATTACK BY BACTERIA AND FUNGI.

(10) ORGANIC MATERIALS ARE OFTEN USED WHICH, WHEN OVERHEATED OR IMPROPERLY OR INCOMPLETELY CURED, CAN PRODUCE VAPORS WHICH ARE CORROSIVE TO ELECTRONIC COMPONENTS AND DAMAGING TO COATINGS AND INSULATORS.

B. INVESTIGATION REVEALED A SECOND SPECIAL CONSIDERATION WAS MICROBIAL, FUNGI, INSECTS AND ANIMALS CAUSING CORROSION IN AVIONICS. (SEE ENCLOSURE (2).)

(1) MICROBIAL, INSECT AND ANIMAL ATTACK

(A) GENERAL. MICROBIAL ATTACK (WHICH INCLUDES MOLD, BACTERIA AND FUNGI) CREATES BYPRODUCTS THAT WILL CAUSE CORROSION. MODERN AVIONIC EQUIPMENTS, BECAUSE OF THEIR COMPLEXITY, DENSE PACKAGING AND HIGHER SENSITIVITY, ARE MORE SUSCEPTIBLE TO DAMAGE FROM MICROBIAL ATTACK THAN EARLIER SYSTEMS. MOLDS, BACTERIA AND FUNGI ARE LIVING MEMBERS OF THE PLANT WORLD AND, IN MOST CASES, MUST HAVE WATER TO LIVE. THE ORGANISMS CAUSING THE GREATER CORROSION

PROBLEMS ARE BACTERIA AND FUNGI. IN ADDITION TO MICROBIAL ATTACK, AVIONIC EQUIPMENT IS SUSCEPTIBLE TO INSECT AND ANIMAL DAMAGE WHICH CAN RESULT IN CORROSION.

(B) BACTERIA. BACTERIA MAY BE EITHER AEROBIC OR ANAEROBIC. AEROBIC BACTERIA REQUIRE OXYGEN TO LIVE. OXYGEN CAN ACCELERATE A CORROSION ATMOSPHERE BY OXIDIZING SULFUR TO PRODUCE SULFURIC ACID OR BY OXIDIZING AMMONIA TO PRODUCE NITRIC ACID. BACTERIA LIVING ADJACENT TO METALS WILL PROMOTE CORROSION BY DEPLETING THE OXYGEN SUPPLY OR BY RELEASING METABOLIC PRODUCTS. ANAEROBIC BACTERIA, ON THE OTHER HAND, CAN SURVIVE ONLY WHEN FREE OXYGEN IS NOT PRESENT. THE METABOLISM OF THESE BACTERIA REQUIRES THEM TO OBTAIN PART OF THEIR SUSTENANCE BY OXIDIZING INORGANIC COMPOUNDS SUCH AS IRON, SULFUR, HYDROGEN AND NITROGEN. THE RESULTANT CHEMICAL REACTION CAUSES CORROSION. BECAUSE OF THE ACIDIC NATURE OF BACTERIAL MICROORGANISMS, METALS ARE SUSCEPTIBLE TO MICROBIAL ATTACK. MINOR SURFACE CONTAMINATION CAN BE ACCELERATED INTO A MAJOR CORROSION PROBLEM BY LOCAL BACTERIAL CORROSION CELLS, OR BY ADDITIONAL ACIDS LIBERATED BY THE BACTERIA.

(C) FUNGUS. FUNGUS IS A MICROORGANISM GROWTH THAT FEEDS ON ORGANIC MATERIALS AND GENERALLY TAKES THE FORM OF MOLDS, RUSTS, MILDEWS AND SMUTS. FUNGAL GROWTH REQUIRES SPECIFIC ENVIRONMENTS AND NUTRIENTS FOR SURVIVAL. FUNGI ARE COMMONLY FOUND IN THE FOLLOWING COLORS:

BLACK

YELLOW

GREEN

BLUE-GREEN

(D) FUNGI-PRODUCING ENVIRONMENTS. WHILE LOW HUMIDITY DOES NOT KILL THE FUNGI MICROBES, IT SLOWS THEIR GROWTH. IDEAL GROWTH CONDITIONS FOR MOST FUNGI MICROBES ARE TEMPERATURES BETWEEN 68°F (20°C) AND 104°F (40°C) AND A RELATIVE HUMIDITY BETWEEN 85 AND 100%. IT WAS FORMERLY THOUGHT THAT FUNGI ATTACK COULD BE PREVENTED BY APPLYING MOISTURE-PROOF COATINGS TO NUTRIENT MATERIAL OR BY DRYING THE INTERIOR OF COMPARTMENTS WITH DESSICANTS. IT WAS NOT KNOWN THAT SOME MICROORGANISMS REMAIN IN SPORE FORM FOR LONG PERIODS, EVEN UNDER EXTREMELY DRY CONDITIONS. FURTHERMORE, ELECTRICAL INSULATING VARNISHES AND SOME MOISTURE-PROOFING COATINGS ARE ATTACKED BY MOLD, BACTERIA, OR OTHER MICROBES, ESPECIALLY IF THE SURFACES ON WHICH THEY ARE USED ARE CONTAMINATED. DIRT, DUST AND OTHER AIRBORNE CONTAMINANTS ARE THE LEAST RECOGNIZED CONTRIBUTORS TO MICROBIAL ATTACK. EVEN SMALL AMOUNTS OF AIRBORNE DEBRIS CAN BE SUFFICIENT TO PROMOTE FUNGAL GROWTH.

(E) FUNGI NUTRIENTS. IT HAS LONG BEEN THOUGHT THAT MATERIALS SUCH AS WOOL, COTTON, ROPE, FEATHER AND LEATHER WERE THE ONLY MATERIALS KNOWN TO PROVIDE SUSTENANCE FOR FUNGI MICROBES. THE INCREASING COMPLEXITY OF SYNTHETIC MATERIAL MAKES IT DIFFICULT OR IMPOSSIBLE TO DETERMINE FROM THE NAME ALONE WHETHER A MATERIAL WILL SUPPORT THE GROWTH OF FUNGUS. MANY OTHERWISE RESISTANT SYNTHETICS ARE RENDERED SUSCEPTIBLE FOR FUNGI ATTACK BY THE APPLICATION

OF A PLASTICIZER OR HARDENER. THE SERVICE LIFE, SIZE, SHAPE, SURFACE SMOOTHNESS AND CLEANLINESS OF THE EQUIPMENT, ITS ENVIRONMENT AND THE TYPE OF FUNGI MICROORGANISM INVOLVED ALL DETERMINE THE DEGREE OF FUNGAL ATTACK.

(F) DAMAGE. DAMAGE RESULTING FROM MICROBIAL ATTACK CAN OCCUR WHEN ANY OF THREE BASIC MECHANISMS OR A COMBINATION OF MECHANISMS IS BROUGHT INTO PLAY: FUNGI ARE DAMP AND HAVE A TENDENCY TO HOLD MOISTURE, WHICH CONTRIBUTES TO OTHER FORMS OF CORROSION; BECAUSE FUNGI ARE LIVING ORGANISMS, THEY NEED FOOD TO SURVIVE. THE FOOD IS OBTAINED FROM THE MATERIAL ON WHICH THE FUNGI ARE GROWING; THESE MICROORGANISMS SECRETE CORROSIVE FLUIDS THAT ATTACK MANY MATERIALS, INCLUDING SOME THAT ARE NOT FUNGI NUTRIENT. OPTICAL DEVICES CAN ALSO BE DAMAGED BY MICROORGANISMS. LENS COATINGS ARE EXTREMELY SUSCEPTIBLE TO FUNGAL ATTACK WHICH WILL TAKE ANY OF THREE FORMS: A SPIDERWEB, A FLAT STARFISH SHAPE WHICH LEAVES A MILKY STAIN, OR MINUTE CIRCULAR SPOTS THAT ETCH THE GLASS. UNDER PROPER ATMOSPHERIC CONDITIONS, FUNGI CAN GROW ON ALMOST ANY SURFACE. (SEE FIGURE II-12

(G) CORROSION CAUSED BY INSECTS AND ANIMALS. DAMAGE TO AVIONICS EQUIPMENT CAN BE CAUSED BY SMALL INSECTS AND ANIMALS, ESPECIALLY IN TROPICAL ENVIRONMENTS. EQUIPMENT IN STORAGE IS SUSCEPTIBLE TO THIS TYPE OF ATTACK, SINCE INSECTS AND SMALL ANIMALS MAY ENTER THROUGH VENT HOLES OR TEARS IN PACKAGING. IN SOME CASES, INSECTS HAVE ENTERED SMALL OPENINGS, PITOT LINES AND AIR VENTS IN AIRCRAFT, CAUSING BLOCKAGE. IN THE CASE OF PACKAGED EQUIPMENT, THEY MAY BUILD NESTS WHICH TEND TO ABSORB MOISTURE. THIS MOISTURE, PLUS EXCRETIONS AND SALTS FROM THE INSECTS AND ANIMALS, CAN CAUSE CORROSION AND DETERIORATION THAT GO UNNOTICED UNTIL THE EQUIPMENT OR SYSTEM IS PUT TO USE AND FAILS. ANOTHER TYPE OF DAMAGE CAN OCCUR WHEN ELECTRICAL INSULATION, VARNISHES AND CIRCUIT BOARD COATINGS BECOME FOOD FOR INSECTS. ONCE BARE WIRES OR CIRCUIT COMPONENTS ARE EXPOSED, MORE AREAS BECOME AVAILABLE FOR CORROSION AND SHORTING TO OCCUR. (SEE ENCLOSURE (3).)

D. DESIGN, PACKAGING AND LOCATION OF AVIONICS IN AIRCRAFT. PRIME CONTRACTOR AIRCRAFT MANUFACTURERS ALLOCATE SPACE INSIDE AIRCRAFT FOR AVIONICS EQUIPMENT, AND PROCURE AVIONICS FROM SUBCONTRACTORS. THE SUBCONTRACTOR DESIGNS THE EQUIPMENT TO MEET ALLOCATED SPACE AND PERFORMANCE STANDARDS PROVIDED BY THE PRIME CONTRACTOR. THE EQUIPMENT MAY REQUIRE VENTED COOLING OR THE EQUIPMENT MAY BE PLACED IN THE AIRCRAFT IN AN AREA SUSCEPTIBLE TO WATER LEAKS THROUGH AIRFRAMES, RESULTING IN WATER INTRUSION AND EQUIPMENT FAILURE.

(1) REQUIREMENT. EACH UNIT OF AVIONICS EQUIPMENT MUST BE DESIGNED TO STAND ON ITS OWN IN THE OPERATING ENVIRONMENT AND TO BE RESISTANT TO WATER INTRUSION, MOISTURE, ELECTROMAGNETIC INTERFERENCE (EMI) AND CORROSION.

(A) LIDS SHOULD BE SHOE BOX TYPE.

(B) FASTENERS SHOULD BE LOCATED IN VERTICAL WALLS OF THE BOX VICE ON THE LID.

(C) COOLING AND VENTING SHOULD BE DESIGNED TO ENSURE THAT WATER CANNOT ENTER THROUGH COOLING OR VENTING DUCT HOLES.

(D) CABLES CONNECTING SYSTEM TO BOXES MUST HAVE DRIP LOOPS.

(E) AVIONICS MANUFACTURERS MUST GET FEEDBACK INFORMAION ON RELIABILITY OF EQUIPMENT.

(F) ELECTRICAL CONNECTORS MUST BE PROTECTED FROM THE ENVIRONMENT.

4. LESSONS OF THE FOREGOING SHORT HISTORY AND FINDINGS OF THE ASSESSMENT HAVE BEEN APPLIED AND HAVE RESULTED IN THE DEVELOPMENT OF A VERY SUCCESSFUL AVIONICS AND ELECTRICAL CORROSION PREVENTION AND CONTROL PROGRAM BEING CONDUCTED THROUGH THE U.S. NAVY.

5. WE WILL NOW GO THROUGH A STANDARD MAINTENANCE CYCLE OF A FAILED COMPONENT. A FAILED COMPONENT IS REMOVED FROM THE AIRCRAFT AND INDUCTED INTO THE SECOND LEVEL OF MAINTENANCE, THE AIRCRAFT INTERMEDIATE MAINTENANCE DEPARTMENT (AIMD), TO DETERMINE AND CORRECT THE PROBLEM IN THE FAILED EQUIPMENT. THE EQUIPMENT IS OPENED AND VISUALLY INSPECTED FOR CORROSION OR CONTAMINANTS. IF CORROSION IS DETECTED, THE EQUIPMENT IS FORWARDED TO THE CLEANING AND CORROSION WORK CENTERS OR SHOPS. THE EQUIPMENT IS DISASSEMBLED BY A TRAINED TECHNICIAN. THE CORROSION IS REMOVED BY MINIATURE GRINDING TOOLS, SIMPLE ERASER, MINIATURE GRIT BLASTER, OR HAND POLISHER. THE MILDEST METHOD IS ALWAYS USED. GENERAL CLEANING: THE COMPONENTS ARE MADE READY TO ENSURE WATER OR CLEANING AGENT DOES NOT DAMAGE INTERNAL COMPONENTS. (SEE ENCLOSURE (4).) THE COMPONENT IS THEN WATER WASHED, USING A DETERGENT/WATER MIX OF NINE PARTS WATER TO ONE PART DETERGENT. DETERGENTS USED ARE UNDER MIL-SPECIFICATION MIL-D-16791 (NONIONIC) OR MIL-C-43616 WITH A 16 TO ONE MIX, WITH A pH UNTER TEN. THE CLEAN COMPONENTS ARE THEN PLACED IN A DRYING OVEN AND DRIED AT 130°F (54°C) WHERE THE DRYING TIME IS DEPENDENT ON THE COMPLEXITY OF THE EQUIPMENT OR COMPONENT BEING DRIED--NORMALLY THREE TO FOUR HOURS ARE REQUIRED. A HOT AIR GUN MAY ALSO BE USED FOR SPOT DRYING. ENCLOSURE (5) CONTAINS BASIC AVIONICS CLEANING REQUIREMENTS, A LIST OF CLEANING CHEMICALS, RECOMMENDED CLEANING PROCESSES, AND CLEANING AND DRYING RESTRICTIONS. (SEE FIGURE 13-17.)

A. SOME COMPONENT BOXES, CHASSIS, METAL COMPONENTS MAY BE CLEANED USING THE ULTRASONIC CLEANING METHOD WITH SOLVENT, I.E., TRICHORTRIFLUORETHANE, MIL-C-81302. CARE MUST BE TAKEN NOT TO EXPOSE THE TECHNICIAN TO THIS MATERIAL, AS THE MATERIAL WILL REMOVE OILS FROM THE BODY EXPOSED TO A SOLVENT VAPOR AND DISPLACES OXYGEN. THIS MATERIAL SHOULD ALWAYS BE USED IN SMALL AMOUNTS IN A WELL VENTILATED AREA. FACE SHIELD, RUBBER GLOVES AND COVERALLS SHOULD BE USED WHEN ULTARSONIC CLEANING IS CONDUCTED. AN ADVANTAGE TO ULTRASONIC CLEANING IS DRYING TIME, WHICH IS REDUCED TO BETWEEN 15 SECONDS AND THREE MINUTES. A DISADVANTAGE TO ULTRASONIC CLEANING IS THAT SOME FREQUENCIES IN THE CLEANING UNIT CAN DAMAGE SOME CIRCUITS AND COMPONENTS. THEREFORE, COMPONENTS TO BE ULTRASONICALLY CLEANED MUST BE IDENTIFIED BY ENGINEERING AUTHORITY.

B. HAND CLEANING WITH MIL-C-81302 CAN BE ACCOMPLISHED BY USING A SOFT BRISTLE BRUSH.

C. WHEN THE EQUIPMENT HAS BEEN CLEANED AND ANY CORROSION DISCOVERED HAS BEEN REMOVED AND ARRESTED, THE EQUIPMENT IS RETURNED TO THE REPAIR AND CHECK TECHNICIAN. THE EQUIPMENT IS REPAIRED AND TESTED IF REQUIRED, AND CORROSION PREVENTION COMPOUND MIL-C-81309 TYPE 3 CLASS 2 AEROSOL IS APPLIED TO INTERNAL AREAS OF THE EQUIPMENT. (SEE ENCLOSURE (5).) THE MATERIAL IS SPREAD ON AND THE EXCESS IS WIPED OFF, LEAVING A THIN, NON-CONDUCTIVE FILM OF WATER DISPLACING CORROSION PREVENTIVE COMPOUND. IF CONTACT POINTS ARE INVOLVED, POINTS MUST BE WIPED TO ENSURE NON-CONDUCTIVE FILM IS REMOVED. THE EQUIPMENT IS THEN CLEANED AND SEALING MATERIALS ARE USED AS REQUIRED TO ENSURE WATER OR CORROSIVE FLUIDS OF ANY FORM CANNOT ENTER THE BOX. THREE BASIC SEALANTS ARE USED MEETING MIL-SPECIFICATION MIL-S-8802, MIL-S-81733, OR ROOM TEMPERATURE VULCANIZING (RTV) MIL-A-46146. NORMALLY SEALED AREAS ARE LIDS AROUND FASTENERS AND CONNECTOR PORTS. THE READY FOR ISSUE (RFI) COMPONENT IS THEN PACKAGED AND RETURNED TO THE USER OR HELD IN A STOREROOM UNTIL NEEDED. (SEE ENCLOSURE (6).)

D. THE FIRST MAINTENANCE LEVEL (SQUADRON) RECEIVES THE RFI COMPONENT AND BEGINS INSTALLING THE COMPONENT IN THE AIRCRAFT. THE TECHNICIAN OPENS THE ACCESS PANEL AND INSPECTS THE AREA IN WHICH THE COMPONENT IS TO BE INSTALLED (USUALLY IN A SHOCK MOUNTED RACK) TO ENSURE THE AREA AND SHOCK MOUNTED RACK ARE CLEAN AND FREE FROM CORROSION OR CONTAMINANTS. WHEN SATISFIED THE AREA IS CLEAN, THE COMPONENT IS INSTALLED. THE TECHNICIAN THEN INSPECTS AND HAND CLEANS THE ELECTRICAL CONNECTOR. THE FEMALE CONNECTOR IS TREATED USING MIL-C-81302 AND A SOFT BRISTLE BRUSH AFTER CLEANING. MIL-C-81309 TYPE 3 CLASS 2 AVIONICS GRADE WATER DISPLACING CORROSION PREVENTION COMPOUND IS APPLIED TO THE FEMALE CONNECTOR, THE EXCESS IS WIPED OFF AND THE CONNECTOR IS CONNECTED TO THE COMPONENT. THE COMPONENT IS THEN TESTED USING AIRCRAFT POWER TO COMPLETE THE INSTALLATION.

6. ELECTRICAL CONNECTORS. ELECTRICAL CONNECTORS HAVE HISTORICALLY BEEN PRONE TO CORROSION PROBLEMS, AS DISCUSSED IN REFERENCE (1). HOWEVER, SINCE THE AVIONICS CORROSION PREVENTION AND CONTROL PROGRAM HAS BEEN IMPLEMENTED, THE PROBLEMS ARE DISAPPEARING. PERIODIC MAINTENANCE IS CONDUCTED ON ALL AIRCRAFT CONNECTORS RANGING FROM DAILY TO 180 DAYS OR LONGER IN SOME INSTALLATIONS. MAINTENANCE OF CONNECTORS CONSISTS OF KEEPING THE CONNECTORS CLEAN AND DRY, FREE FROM CORROSION INTERNALLY AND EXTERNALLY. THIS IS ACCOMPLISHED AS FOLLOWS:

A. CONNECTORS DIRECTLY EXPOSED TO THE ENVIRONMENT. THE CONNECTOR IS OPENED AND INSPECTED; IF CORROSION IS DETECTED ON PINS OR BODY OF THE CONNECTOR, IT IS REMOVED BY THE MILDEST METHOD POSSIBLE. THE CONNECTOR IS THEN INSPECTED WITH A 10X GLASS TO ENSURE ALL CORROSION PRODUCT HAS BEEN REMOVED; THE CONNECTOR IS THEN CLEANED USING AN ACID BRUSH AND MIL-C-81302. THE FEMALE END OF THE CONNECTOR IS SPRAYED WITH MIL-C-81309 TYPE 3 CLASS 2 WATER DISPLACING CORROSION PREVENTION COMPOUND AND THE EXCESS IS WIPED OFF. IT IS RECONNECTED AND WIPED OFF WITH A CLEAN CLOTH WET WITH MIL-C-81302 TO REMOVE BODY OILS, FINGERPRINTS, ETC. THE EXTERNAL AREA OF THE CLOSED CONNECTOR IS SPREAD WITH MIL-C-85054 AMLGARD. THE AMLGARD IS ALLOWED TO DRY 30 MINUTES AND A SECOND COAT IS APPLIED. IN EXTREME CASES, THE CONNECTOR IS WRAPPED WITH ELECTRICAL INSULATING TAPE PAINTED WITH RTV 3140. (SEE FIGURE 18-20.)

B. TEST CONNECTORS TREATED IN THIS MANNER HAVE BEEN EXPOSED ON AIRCRAFT CARRIERS FOR AS LONG AS 18 MONTHS WITH NO DEGRADATION TO THE CONNECTORS. (SEE FIGURE 23.)

7. CONNECTORS INTERNAL TO THE AIRCRAFT ARE CLEANED IN THE SAME MANNER AS DESCRIBED ABOVE FOR THE EXTERNAL CONNECTOR WITH MIL-C-81309 TYPE 2 CLASS 2 APPLIED OUTSIDE THE CONNECTOR. FREQUENCY OF PREVENTIVE MAINTENANCE IS DICTATED BY THE OPERATING ENVIRONMENT.

A. ADDITIONAL CONNECTOR MAINTENANCE - SEALING. SEALING THE BACK SHELL OF MULTI-PIN ENVIRONMENTAL CONNECTORS BECOMES NECESSARY UNDER SOME CONDITIONS; I.E., WHEN SIDE LOADS ARE APPLIED TO PINS, WHEN WETTING AGENTS ARE USED IN THE CONNECTOR BACK SHELL AREA. WHEN THESE CONDITIONS EXIST, THE BACK SHELL OF THE CONNECTOR IS SEALED AS FOLLOWS: THE RETAINER RING AND BACK SHELL ARE LOOSENED AND SLID UP THE WIRE BUNDLE, EXPOSING THE RUBBER GROMMET CONTAINING WIRE RECEPTACLES.

B. THE AREA OF THE RUBBER GROMMET IS CLEANED USING AN ACID BRUSH AND MIL-C-81302, VERIFYING THAT SEALING PLUGS (DOG BONES) ARE INSTALLED IN UNUSED WIRE RECEPTACLE CAVITIES. SEALANT IS APPLIED (RTV-3140 ALCOHOL CURE) TO THE BACK SIDE OF THE RUBBER GROMMET, WORKING THE NOZZLE OF THE APPLICATOR THROUGH THE WIRE BUNDLE TO ENSURE COMPLETE COVERAGE. SEALANT THICKNESS SHOULD NOT EXCEED 1/16" (1.59 mm). ADDITIONAL SEALANT MAY BE ADDED; HOWEVER, AT NO TIME SHALL SEALANT EXCEED 1/8" (3.2 mm) THICKNESS). POSITION CONNECTOR FACE PARALLEL TO THE FLOOR/DECK FOR 30 MINUTES FOR INITIAL CURE OF SEALANT. AFTER 30 MINUTES, THE CONNECTOR MAY BE RECONNECTED; HOWEVER, THE SEALANT WILL REQUIRE 24 HOURS FOR COMPLETE CURE.

8. WHEN THIS PROCEDURE WAS DEVELOPED, RTV-118, WHICH IS AN ACETIC ACID CURE MATERIAL, WAS SELECTED BECAUSE IT IS CLEAR, ALLOWING THE ELECTRONIC TECHNICAN TO READ PIN NUMBERS ON THE SEALED BACK OF THE GROMMET. WIRES CAN BE CHANGED WITH SEALANT IN PLACE USING STANDARD TOOLS. WHEN A WIRE IS REPLACED, A DROP OF SEALANT IS PLACED IN THE AREA WHERE WORK WAS ACCOMPLISHED. RTV-118 HAS BEEN REPLACED WITH A CLEAR RTV-3140 WHICH IS A CLEAR, ALCOHOL CURE MATERIAL ELIMINATING THE CORROSIVE ACETIC ACID. RTV-118 CAN BE USED; BUT TIME FOR A FULL 24 HOUR CURE MUST BE USED, WHICH REQUIRES CONNECTOR TO REMAIN OPEN, PREVENTING CORROSION CAUSED BY GAS OFF OF THE ACETIC ACID. THE ONLY ACETIC ACID CURE MATERIAL IN USE IS RTV-730 WHICH IS A WHITE, HIGH TEMPERATURE MATERIAL WITH A WORKING TEMPERATURE OF 550°-600°F (287°-315°C). USE OF RTV-730 MUST BE AUTHORIZED BY ENGINEERING AUTHORITY.

A. FIGURE 21-24 SHOWS THE WAY NOT TO INSTALL AN AVIONICS SYSTEM.

(1) FIGURE 21 SHOWS AN ENVIRONMENTAL CONNECTOR INSTALLED VERTICALLY ON TOP OF A BOX IN A WET AREA.

NOTE: SIDE LOADS ON WIRES ENTERING GROMMET WHICH WILL ALLOW WATER TO ENTER THE CONNECTOR MAY CAUSE CORROSION/ELECTRICAL SHORTS IN MATING SURFACES.

B. FIGURE 22

NOTE: CORROSION EXISTS WHERE NICKEL PLATE HAS BEEN DAMAGED.

C. FIGURE 23/24 SHOW THE RESULTS OF USE OF A COMBINATION OF MATERIALS WHEN JOINED TOGETHER NOT COMPATIBLE TO THE NAVY OPERATING ENVIRONMENT.

ELECTROLYSIS NICKEL PLATED CONNECTOR

STAINLESS STEEL BRAID

NOMAX PROTECTIVE COVER (NOMAX IS KNOWN TO HAVE A WICKING PROBLEM WHEN EXPOSED TO WATER SUPPLYING THE ELECTROLYTE TO INITIATE CORROSION.)

9. EMI BONDING CORROSION. OVER THE PAST 20 YEARS, THE ELECTRONIC WORLD HAS MADE TREMENDOUS ADVANCES IN TECHNOLOGY. IN THE DEVELOPMENT OF LOW POWER MICROELECTRONIC SYSTEMS, THE NEW EQUIPMENT IS LIGHT IN WEIGHT, SMALL IN SIZE, IDEAL FOR USE IN AIRCRAFT WHERE WEIGHT AND SIZE ARE FACTORS. THE NEW SYSTEMS ARE GENERALLY VERY DEPENDABLE AND ARE REPLACING THE MORE CUMBERSOME MECHANICAL SYSTEMS USED IN TODAY'S AND EARLIER AIRCRAFT, I.E., FLY BY WIRE, AUTOPILOTS, WEAPONS CONTROL SYSTEMS, ETC. HOWEVER, THE NEW LOW POWER MICROELECTRONIC EQUIPMENT AND SYSTEMS ARE SUSCEPTIBLE TO ELECTROMAGNETIC INTERFERENCE (EMI) CAUSED BY HIGH POWER ELECTRONIC/ELECTRICAL SOURCES EXTERNAL TO THE AFFECTED SYSTEM OR EQUIPMENT, RESULTING IN SYSTEM/EQUIPMENT MALFUNCTION. TO PREVENT EMI PROBLEMS, THE EQUIPMENT/SYSTEMS ARE SHIELDED AND GROUNDED BY BONDING TO THE AIRCRAFT. MOST OF THE MATERIAL SELECTED FOR BONDING BY THE ELECTRONIC ENGINEERS HAVE BEEN GOOD CONDUCTORS OF ELECTRICITY BUT ARE CATHODIC TO THE ALUMINUM SUBSTRATE THEY ARE ATTACHED TO, CAUSING GALVANIC CELLS TO BE FORMED, RESULTING IN CORROSION.

FACTS:

A. CORROSION OF THE AIRFRAME IS CAUSED BY BONDING MATERIAL.

B. AIRFRAME CORROSION REQUIRES CORRECTION OR STRUCTURAL REPAIR.

C. BOND IS LOST, MAKING THE BONDED EQUIPMENT AND SYSTEM SUSCEPTIBLE TO EMI, AS BOND CANNOT BE MAINTAINED DUE TO CORROSION PRODUCT.

D. EMI PROTECTION SYSTEMS ARE REQUIRED TO ENSURE OPERATION OF MODERN MICROELECTRONIC SYSTEMS.

SOME BONDING SYSTEMS THAT HAVE BEEN USED:

A. BERRYLIUM COPPER STRIPS (SEE FIGURE 25.)

B. SILVER FILLED EPOXY BONDING MATERIAL WHICH IS HYDROSCOPIC

C. ALUMINUM TO STEEL, ETC.

D. SILVER LOADED SILICON RUBBER EMI SEALS

ACTION NEEDED:

A. DEVELOPMENT OF EMI PROTECTIVE SYSTEMS/MATERIALS THAT WILL PROVIDE REQUIRED PROTECTION THAT WILL NOT CAUSE CORROSION IN THE OPERATING ENVIRONMENT.

B. DEVELOPMENT OF ELECTRONIC SYSTEMS THAT WILL STAND ON THEIR OWN AND IN AN EMI ENVIRONMENT.

10. THE U.S. NAVY IS INVESTIGATING A AND B ABOVE TO DETERMINE THE BEST, MOST ECONOMICAL METHOD TO PROVIDE REQUIRED PROTECTION TO ELECTRONIC SYSTEMS AND STOP THE CORROSION FROM OCCURRING. AS STATED ABOVE, THIS SUCCESSFUL PROGRAM IS ESTABLISHED THROUGHOUT THE U.S. NAVAL AVIATION COMMUNITY. IT WAS ESTABLISHED IN ACCORDANCE WITH CHIEF OF NAVAL OPERATIONS (CNO) INSTRUCTION 4790.2C AND AMPLIFIED BY COMNAVAIRLANT/COMNAVAIRPAC INSTRUCTIONS. TECHNICAL INFORMATION IS PROVIDED IN THE AVIONICS CLEANING AND CORROSION PREVENTION/CONTROL MANUAL, NAVAIR 16-1-540. TRAINING IS PROVIDED TO SUPERVISORS, ELECTRONIC TECHNICIANS AND MECHANICS BY NAVAL AIR MAINTENANCE TRAINING DETACHMENTS (NAMTRADET), NAVAL AIR REWORK FACILITIES (NAVAIREWORKFAC) AND ON-SITE NAVAL AVIATION ENGINEERING SERVICE UNITS (NAESU). DETAILED REQUIREMENTS FOR AIMD AND OPERATIONAL SQUADRONS ARE CONTAINED IN COMNAVAIRLANT/COMNAVAIRPAC INSTRUCTIONS AS FOLLOWS:

A. EACH ACTIVITY SHALL ESTABLISH AN AVIONICS CLEANING AND CORROSION PREVENTION/CONTROL PROGRAM THAT WILL FUNCTION ON A DAY TO DAY BASIS.

B. AVIONICS CORROSION TEAM MEMBERS SHALL RECEIVE NAMTRADET TRAINING BEFORE THEY ARE CONSIDERED QUALIFIED.

C. AVIONICS OFFICER SHALL HAVE NAMTRADET TRAINING.

D. ESTABLISH AN AVIONICS EQUIPMENT EMERGENCY RECLAMATION TEAM IN EACH FLEET ACTIVITY. EMERGENCY RECLAMATION TEAM SHALL CONSIST OF ELECTRONIC TECHNICIANS WHO ARE TRAINED TO RECOVER AVIONICS EQUIPMENT THAT HAVE BEEN EXPOSED TO UNUSUALLY SEVERE CORROSIVE CONDITIONS, E.G., SALT WATER IMMERSION, FIRE EXTINGUISHING AGENTS, BATTERY ACID, ETC.

11. IN ORDER TO ENSURE THAT FUTURE DESIGNS FOR AVIONICS COMPONENTS ARE MORE CORROSION RESISTANT, THE CHIEF OF NAVAL MATERIAL (CHNAVMAT) HAS ISSUED GUIDELINES FOR PREVENTION AND CONTROL OF AVIONICS CORROSION (NAVMAT P4855-2 DATED JUNE 1983). THIS DOCUMENT WAS DEVELOPED AND MADE AVAILABLE TO INDUSTRY.

12. CONCLUSION

A. AVIONICS CORROSION DAMAGE CAN BE MINIMIZED ON AIRCRAFT AND OTHER MILITARY EQUIPMENT BY A DYNAMIC CORROSION PREVENTION/CONTROL PROGRAM.

B. DETAILED TRAINING OF INVOLVED PERSONNEL MUST BE PROVIDED.

C. AS NEW MATERIAL BECOMES AVAILABLE, THE OCCURRENCE OF AVIONICS CORROSION CAN BE REDUCED THROUGH DESIGNING BOXES THAT WILL NOT LEAK AND MATERIAL SELECTION, I.E., NON-CORROSIVE MATERIALS FOR CONSTRUCTION OF COMPONENT EQUIPMENT. SEE FIGURE 26

D. CLOSE COOPERATION BETWEEN ALL FACETS. I.E., THE AVIONICS/AEROSPACE COMMUNITY, IS NEEDED TO ENSURE THAT THE MOST DURABLE, RELIABLE AVIONICS/ELECTRONICS ARE PROVIDED IN THE ARMED FORCES.

ENCLOSURES

(1) CORROSION OF METALS - NATURE AND APPEARANCE OF CORROSION PRODUCTS

(2) EFFECTS OF MOISTURE AND FUNGI ON VARIOUS MATERIALS

(3) EFFECTS OF CORROSION AND AVIONIC EQUIPMENT

(4) BASIC AVIONICS CLEANING REQUIREMENTS/4.2 - 4.6 AVIONIC CLEANING MATERIALS

(5) RECOMMENDED CLEANING PROCESS VERSUS TYPE OF AVIONIC EQUIPMENT/5.2 CLEANING AND DRYING RESTRICTION

(6) AVIONIC PRESERVATION MATERIALS

REFERENCES

(1) G. T. BROWNE, COMNAVAIRLANT U.S. FLEET AIRCRAFT CORROSION AGARD CP-315 1981

(2) U.S. NAVAL AIR SYSTEMS COMMAND AVIONICS CLEANING AND CORROSION PREVENTION/ CONTROL MANUAL NA 16-1-540

(3) IRVING S. SHAFFER NAVAIRDEVCEN WARMINSTER PA CORROSION IN NAVAL AIRCRAFT ELECTRONIC SYSTEMS AGARD CR-315 1981

CORROSION OF METALS - NATURE AND APPEARANCE OF CORROSION PRODUCTS

ALLOY	TYPE OF ATTACK TO WHICH ALLOY IS SUSCEPTIBLE	APPEARANCE OF CORROSION PRODUCT
ALUMINUM ALLOY	SURFACE, PITTING AND INTERGRANNULAR.	WHITE OR GRAY POWDER.
TITANIUM ALLOY	HIGHLY CORROSION RESISTANT. EXTENDED OR REPEATED CONTACT WITH CHLORINATED SOLVENTS MAY RESULT IN EMBRITTLEMENT. CADMIUM PLATED TOOLS CAN CAUSE EMBRITTLEMENT OF TITANIUM.	NO VISIBLE CORROSION PRODUCTS.
MAGNESIUM ALLOY	HIGHLY SUSCEPTIBLE TO PITTING.	WHITE POWDER SNOWLIKE MOUNDS, AND WHITE SPOTS ON SURFACE.
CARBON AND LOW ALLOY STEEL (1000-8000 SERIES)	SURFACE OXIDATION AND PITTING, SURFACE AND INTERGRANNULAR.	REDDISH-BROWN OXIDE (RUST)
STAINLESS STEEL (300-400 SERIES)	INTERGRANNULAR CORROSION. SOME TENDENCY TO PITTING IN MARINE ENVIRONMENT (300 SERIES MORE CORROSIN RESISTANT THAN 400 SERIES).	CORROSION EVIDENCED BY ROUGH SURFACE; SOMETIMES BY RED, BROWN, OR BLACK STAIN.
NICKEL-BASE ALLOY (INCONEL)	GENERALLY HAS GOOD CORROSION-RESISTANT QUALITIES. SOMETIMES SUSCEPCTIBLE TO PITTING.	GREEN POWDERY DEPOSIT.
COPPER-BASE ALLOY (INCONEL)	SURFACE AND INTERGRANNULAR CORROSION.	BLUE OR BLUE-GREEN POWDER DEPOSIT.
CADMIUM (USED AS A PROTECTIVE PLATING FOR STEEL)	GOOD CORROSION RESISTANCE. WILL CAUSE EMBRITTLEMENT IF NOT PROPERLY APPLIED.	WHITE, POWDERY CORROSION PRODUCTS.
CHROMIUM (USE AS A WEAR-RESISTANT PLATING FOR STEEL)	SUBJECT TO PITTING IN CHLORIDE ENVIRONMENTS.	CHROMIUM, BEING CATHODIC TO STEEL, DOES NOT CORRODE ITSELF, BUT PROMOTES RUSTING OF STEEL WHERE PITS OCCUR IN THE COATING.
SILVER	WILL TARNISH IN PRESENCE OF SULFUR.	BROWN TO BLACK FILM.
GOLD	HIGHLY CORROSION RESISTANT.	DEPOSITS CAUSE DARKENING OF REFLECTIVE SURFACES.
TIN	SUBJECT TO WHISKER GROWTH.	WHISKER-LIKE DEPOSITS.

ENCLOSURE (1)

EFFECTS OF MOISTURE AND FUNGI ON VARIOUS MATERIALS

PART OR MATERIAL	EFFECTS OF MOISTURE AND FUNGI
FIBER: WASHERS, SUPPORTS, ETC.	MOISTURE CAUSES SWELLING WHICH CAUSES THE SUPPORT TO MISALIGN, RESULTING IN BINDING OF SUPPORTED PARTS. DESTROYED BY FUNGI.
FIBER: TERMINAL STRANS AND INSULATORS	ELECTRICAL LEAKAGE PATHS ARE FORMED, CAUSING FLASHOVERS AND CROSSTALK. INSULATING PROPERTIES ARE LOST. DESTROYED BY FUNGI.
LAMINATED PLASTICS: TERMINAL STRIPS AND BOARDS, SWITCHBOARD PANELS, ETC., TUBE SOCKETS AND COIL FORMS AND CONNECTORS	INSULATING PROPERTIES ARE LOST. LEAKAGE PATHS CAUSE FLASHOVERS AND CROSSTALK. DELAMINATION OCCURS AND FUNGI GROW ON SURFACE AND AROUND EDGES. EXPANSION AND CONTRACTION UNDER EXTREME TEMPERATURE CHANGES.
MOLDED PLASTICS: TERMINAL BOARDS, SWITCHBOARD PANELS, CONNECTORS, ETC., TUBE SOCKETS AND COIL FORMS	MACHINED, SAWED, OR GROUND EDGES OF SURFACES AND SUPPORTERS OF FUNGI, CAUSING SHORTS AND FLASHOVERS. FUNGI GROWTH REDUCES RESISTANCE BETWEEN PARTS MOUNTED ON PLASTIC TO SUCH AN EXTENT THAT THE PARTS ARE USELESS.
COTTON LINEN, PAPER AND CELLULOSE DERIVATIVES: INSULATION, COVERINGS, WEBBING, BELTING, LAMINATIONS, DIELECTRICS, ETC.	INSULATING AND DIELECTRIC PROPERTIES ARE LOST OR IMPAIRED, CAUSING ARCING, FLASHOVERS AND CROSSTALK. DESTROYED BY FUNGI.
WOOD: CASES, HOUSES AND HOUSINGS, PLASTIC FILLERS, MASTS, ETC.	DRY ROT, SWELLING AND DELAMINATION CAUSED BY MOISTURE AND FUNGI.
LEATHER: STRAPS, CASES, GASKETS, ETC.	MOISTURE AND FUNGI DESTROYING TANNING AND PROTECTIVE MATERIALS, CAUSING DETERIORATION.
GLASS: LENSES, WINDOWS, ETC.	FUNGI GROW ON ORGANIC DUST, INSECT TRACK, INSECT FECES, DEAD INSECTS, ETC. DEAD MITES AND FUNGI GROWTH ON GLASS OBSCURE VISIBILITY AND CORRODE NEARBY METAL PARTS.
WAX: FOR IMPREGNATION	FUNGI-INHIBITING WAXES WHICH ARE NOT CLEAN SUPPORT THE GROWTH OF FUNGI, CAUSE DESTRUCTION OF INSULATING AND PROTECTIVE QUALITIES, AND PERMIT ENTRANCE OF MOISTURE WHICH DESTROYS PARTS AND UNBALANCES ELECTRICAL CIRCUITS.
METALS:	HIGH TEMPERATURE AND MOISTURE VAPOR CAUSE RAPID CORROSION. FUNGI AND BACTERIAL GROWTH PRODUCE ACID AND OTHER PRODUCTS WHICH SPEED CORROSION, ETCHING OF SURFACES AND OXIDATION.

	THIS INTERFERES WITH THE OPERATION OF MOVING PARTS, SCREWS, ETC., AND CAUSES DUST BETWEEN TERMINALS, CAPACITORS, PLATES OR AIR CONDENSERS, ETC., WHICH IN TURN CAUSE NOISE, LOSS IN SENSITIVITY AND ARC-OVERS.
METALS, DISSIMILAR:	METALS MAY HAVE DIFFERENT POTENTIALS. WHEN MOISTURE IS PRESENT, ONE OF THE METALS (ANODE) CORRODES.
SOLDERED JOINTS:	RESIDUAL SOLDERING FLUX ON TERMINAL BOARDS HOLDS MOISTURE, WHICH SPEEDS UP CORROSION AND GROWTH OF FUNGI. SOLDERING IRON SHOULD NOT COME IN CONTACT WITH WIRE INSULATION.

EFFECTS OF CORROSION ON AVIONIC EQUIPMENT

COMPONENT	FAILURE MODE
ANTENNA SYSTEM	SHORTS OR CHANGES IN CIRCUIT CONSTANTS AND STRUCTURAL DETERIORATION.
CHASSIS, HOUSINGS, COVERS AND MOUNT FRAMES	CONTAMINATION, PITTING, LOSS OF FINISH AND STRUCTURAL DETERIORATION.
SHOCK MOUNTS AND SUPPORTS	DETERIORATION AND LOSS OF SHOCK EFFECTIVENESS.
CONTROL BOX MECHANICAL AND ELECTRICAL TUNING LINKAGE AND MOTOR CONTACTS	INTERMITTENT OPERATION AND FAULTY FREQUENCY SELECTION.
WATER TRAPS	STRUCTURAL DETERIORATION.
RELAY AND SWITCHING SYSTEMS	MECHANICAL FAILURE, SHORTS, INTERMITTENT OPERATION AND SIGNAL LOSS.
PLUGS, CONNECTORS, JACKS AND RECEPTACLES	SHORTS, INCREASED RESISTANCE, INTERMITTENT OPERATION AND REDUCED SYSTEM RELIABILITY.
MULTI-PIN CABLE CONNECTORS	SHORTS, INCREASED RESISTANCE, INTERMITTENT OPERATION AND WATER SEAL DETERIORATION.
POWER CABLES	DISINTEGRATION OF INSULATION, AND WIRE/CONNECTOR DETERIORATION.
DISPLAY LAMPS AND WING LIGHTS	INTERMITTENT OPERATION, MECHANICAL AND ELECTRICAL FAILURES.
WAVEGUIDES	LOSS OF INTEGRITY AGAINST MOISTURE, PITTING, REDUCTION OF EFFICIENCY AND STRUCTURAL DETERIORATION.
RADAR PLUMBING JOINTS	FAILURE OF GASKETS, PITTING AND POWER LOSS.
PRINTED CIRCUITS AND MICROMINIATURE CIRCUITS	SHORTS, INCREASED RESISTANCE, COMPONENT AND SYSTEM FAILURES.
BATTERIES	HIGH RESISTANCE AT TERMINALS, FAILURE OF ELECTRICAL CONTACT POINTS AND STRUCTURAL DETERIORATION OF MOUNTING.
BUS BARS	STRUCTURAL AND ELECTRICAL FAILURES.
COAXIAL LINES	IMPEDANCE FLUCTUATIONS, LOSS OF SIGNALS AND STRUCTURAL DETERIORATION OF CONNECTORS.

ENCLOSURE (3)

BASIC AVIONICS CLEANING REQUIREMENTS

ALWAYS USE THE MILDEST CLEANING METHOD

1. PRE-CLEANING:

A. DISCONNECT POWER SUPPLY.

B. ENSURE ALL DRAIN HOLES ARE OPEN.

C. REMOVE COVERS, ETC.

D. DISASSEMBLE WHERE PRACTICAL.

E. USE ONLY AUTHORIZED MATERIALS.

F. ASSURE COMPATIBILITY OF MATERIAL BEFORE USE.

G. MASK, PROTECT ACCESSORIES, COMPONENTS TO PREVENT ENTRANCE OF WATER, SOLVENT/ CLEANING COMPOUND.

2. CLEANING EQUIPMENT HAND CLEANING TOOLS FOR HAND CLEANING:

A. COTTON LINT-FREE CLOTH

B. CHEESECLOTH

C. COTTON TIP APPLICATORS (Q TIPS)

D. ACID BRUSH

E. TOOTHBRUSH

3. CLEANING EQUIPMENT INSTALLED/MATERIALS:

A. SPRAY CLEANING BOOTH

(1) WATER

(2) WATER DETERGENT

(3) SOLVENT

B. ULTRASONIC

(1) AQUEOUS

(2) CHEMICAL

ENCLOSURE (4)

AVIONIC CLEANING MATERIALS

WARNING

SOLVENTS ARE FLAMMABLE AND SOLVENT VAPORS ARE TOXIC. KEEP SOLVENTS AWAY FROM OPEN FLAMES AND USE ONLY IN A WELL VENTILATED AREA. AVOID SOLVENT CONTACT WITH SKIN.

DESCRIPTION	CHARACTERISTICS	APPLICATION	RESTRICTIONS
CLEANING COMPOUND, AIRCRAFT SURFACE, MIL-C-43616, CLASS 1, OR CLASS 1A * OR EQUIVALENT	GENERAL CLEANING AGENT FOR LIGHT SOIL AND DIRT IN EQUIPMENT BAYS, ON EXTERNAL CASES AND COVERS, AND ANTENNA ASSEMBLIES.	MIX ONE PART CLEANER IN 16 PARTS WATER AND APPLY WITH CLEANING CLOTH. RINSE WITH FRESH WATER AND WIPE DRY.	DO NOT USE AROUND OXYGEN, OXYGEN FITTINGS, OR OXYGEN REGULATORS, SINCE FIRE OR EXPLOSION MAY RESULT.
* AEROSOL CAN TO BE USED AS PACKAGED WITHOUT ADDITIONAL DILUTION.	HEAVY CONCENTRATION OF SURFACE GRIME, OIL, EXHAUST SMUDGE AND FIRE EXTINGUISHING CHEMICALS IN EQUIPMENT BAYS AND ON EXTERNAL CASES AND COVERS.	MIX ONE PART CLEANER IN NINE PARTS WATER AND APPLY WITH CLEANING CLOTH. RINSE WITH FRESH WATER AND WIPE DRY WITH COTTON CLOTH.	NEVER USE FULL STRENGTH NOR EVER ALLOW TO DRY ON SURFACE. REFER TO SECTION IX FOR EMERGENCY CLEANING PROCEDURES AFTER IMMERSION OR EXPOSURE TO GROSS AMOUNTS OF SALT WATER, FIRE EXTINGUISHING CHEMICALS, SMOKE, OR VAPOROUS GASES.
DETERGENT, LIQUID, NONIONIC MIL-D-16791, TYPE I	CLEANING OF TRANSPARENT AND ACRYLIC PLASTICS AND COCKPIT INDICATOR GLASS COVERS. ALSO USED IN THE WATER BASED SOLVENT SPRAY CLEANING BOOTH AND THE AQUEOUS ULTRASONIC CLEANER FOR REMOVING CONTAMINANTS.	FOR HAND CLEANING, APPLY WITH FLANNEL. LET DRY, THEN REMOVE WITH DRY FLANNEL CLOTH.	MIX ONE FLUID OUNCE PER GALLON WATER.
CLEANING AND LUBRICATING COMPOUND, ELECTRICAL CONTACT, MIL-C-83360, TYPE I	A CLEANER-LUBRICANT COMPATIBLE WITH POTTING COMPOUNDS, RUBBERS AND INSULATIONS. CONTAINS THREE TO FIVE PERCENT SILICONE. MAY BE USED FOR CLEANING AND LUBRICATING ELECTRICAL CONTACTS.	APPLY BY SPRAYING AN EVEN FILM TO THE SURFACE. WIPE CLEAN WITH DISPOSABLE APPLICATOR, OR PIPE CLEANER.	DO NOT USE AS A SUBSTITUTE FOR MIL-C-81302 TYPE I OR TYPE II. AVOID APPLICATION TO AREAS REQUIRING SOLDERING OR COATING.

CLEANING COMPOUND, SOLVENT TRICHLOROTRI-FLUOROETHANE, MIL-C-81302, TYPE I (ULTAR-CLEAN)	GENERAL CLEANER FOR LIGHT TO MEDIUM SURFACE DUST, DIRT AND CONTAMINANTS ON PRECISION EQUIPMENT, INSTRUMENTS, ETC., WHERE ULTRA-CLEAN SOLVENT IS REQUIRED. USE IN CLEAN ROOM APPLICATIONS. MAY BE USED TO CLEAN DIRT AND DUST FROM AREAS WHERE CRITICAL SOLDERING IS REQUIRED.	APPLY BY WIPING OR SCRUBBING ON AFFECTED AREA WITH ACID BRUSH OR TOOTHBRUSH. AIR DRY OR OVEN DRY, AS APPLICABLE.	DO NOT USE ON ACRYLIC PLASTICS AND ACRYLIC CONFORMAL COATINGS. DO NOT USE ON UNSEALED ALUMINUM ELECTROLYTIC CAPACITORS. DAMAGE MAY RESULT TO END CAPS AND CAUSE LEAKAGE.
CLEANING COMPOUND, SOLVENT TRICHLOROTRI-FLUOROETHANE, MIL-C-81302, TYPE II	GENERAL CLEANER FOR LIGHT TO MEDIUM SURFACE DUST, DIRT AND CONTAMINANTS ON ALL INTERNAL AREAS OF AVIONIC EQUIPMENT. MAY BE USED TO CLEAN DIRT AND DUST FROM AREAS WHERE SOLDERING IS REQUIRED.	SAME AS ABOVE.	SAME AS ABOVE.
DRY CLEANING SOLVENT, P-D-680, TYPE II (HIGH FLASH POINT)	GENERAL PURPOSE CLEANER FOR MEDIUM TO HEAVY DIRT, DUST, CONTAMINANTS AND FIRE EXTINGUISHING CHEMICALS IN EQUIPMENT BAYS AND ON EXTERNAL CASES, COVERS, STRUCTURAL HARDWARE, MOUNTS, RACKS, ETC.	APPLY BY WIPING OR SCRUBBING AFFECTED AREA WITH CLEANING CLOTH, CHEESECLOTH OR BRUSH, TYPEWRITER, AS APPROPRIATE. WIPE CLEAN WITH CLEANING CLOTH.	DO NOT USE AROUND OXYGEN OR OXYGEN FITTINGS OR OXYGEN REGULATOR SINCE FIRE OR EXPLOSION MAY RESULT.
	CLEANER FOR SMOKE DAMAGE REMOVAL ON INTERNAL CHASSIS COMPONENTS.	APPLY BY SCRUBBING AFFECTED AREA WITH CLEANING CLOTH, COTTON, TOOTHBRUSH, OR BRUSH, TYPEWRITER, AS APPROPRIATE. WIPE CLEAN WITH CLEANING CLOTH.	WHEN USED FOR SMOKE DAMAGE REMOVAL, ALWAYS FOLLOW UP WITH SOLUTION OF ONE PART DEIONIZED WATER AND ONE PART ISOPROPYL ALCOHOL, TT-I-735.

	CLEANER FOR SMOKE DAMAGE REMOVAL ON CIRCUIT COMPONENTS AND LAMINATED CIRCUIT BOARDS.	APPLY BY WIPING OR SCRUBBING AFFECTED AREA WITH CLEANING CLOTH, COTTON, OR TOOTHBRUSH. WIPE CLEAN WITH CLEANING CLOTH.	MAY CAUSE SWELLING OF SILICONE RUBBER SEALS IN EQUIPMENT EXPOSED TO IMMERSION FOR LONG PERIODS.
	CLEANER FOR REMOVAL OF WATER-DISPLACING CORROSION PREVENTIVE COMPOUNDS, MIL-C-81309, TYPE III; MIL-C-81309, TYPE II; MIL-C-85054; AND CORROSION PREVENTIVE COMPOUND, MIL-C-16173, GRADE 4.	APPLY WITH BRUSH, OR TOOTHBRUSH, AS APPROPRIATE. WIPE CLEAN WITH CLEANING CLOTH, COTTON.	MAY SOFTEN SOME PLASTICS, WIRE HARNESS TUBING, OR PLASTIC COATING ON WIRING. TEST AFFECTED AREA FOR ADVERSE REACTIONS PRIOR TO GENERAL APPLICATION.
ISOPROPYL ALCOHOL, TT-I-735	GENERAL PURPOSE CLEANER AND SOLVENT FOR REMOVAL OF SALT RESIDUE AND CONTAMINANTS COMMON TO INTERNAL AVIONIC EQUIPMENT. GENERAL CLEANER FOR INTERNAL CHASSIS COMPONENTS.	APPLY A SOLUTION OF ONE PART DEIONIZED OR DISTILLED WATER AND ONE PART ISOPROPLY ALCOHOL, TT-I-735, TO THE AFFECTED AREA WITH CLEANING CLOTH OR TOOTHBRUSH.	ISOPROPYL ALCOHOL, TT-I-735, IS HIGHLY FLAMMABLE. ALL APPLICATIONS OF ISOPROPYL ALCOHOL, TT-I-735, AND WATER MAY BE AIR DRIED OR DRIED BY PORTABLE AIR BLOWER OR OVENS.
	SOLVENT CLEANER FOR SOLDER FLUX RESIDUE IN ALL APPLICATIONS OF ELECTRONICS, ELECTRICAL EQUIPMENT AND MICROMINIATURE CIRCUITS.	APPLY A SOLUTION OF ONE PART DEIONIZED OR DISTILLED WATER TO THREE PARTS ISOPROPYL ALCOHOL, TT-I-735, AND SCRUB THE SOLDER JOINT AND ADJACENT AREA WITH ACID BRUSH OR TOOTHBRUSH. WIPE CLEAN WITH CLEANING CLOTH, COTTON.	
	CLEANER FOR FINGERPRINT REMOVAL ON METALS AND NONMETALLICS.	APPLY A SOLUTION OF ONE PART DEIONIZED OR DISTILLED WATER AND ONE PART ISOPROPYL ALCOHOL, TT-I-735, TO AFFECTED AREA WITH CLEANING CLOTH, COTTON. WIPE CLEAN.	

	CLEANER FOR BACTERIA AND FUNGI ATTACK ON ALL METALS AND NON-METALLICS.	APPLY A SOLUTION OF ONE PART SOLVENT TRICHLOROTRIFLUOR-ETHANE, MIL-C-81302, TYPE 1I AND ONE PART ISOPROPYL ALCOHOL, TT-1-735, TO AFFECTED AREA WITH CLEANING CLOTH, COTTON. WIPE CLEAN. AIR DRY.	
	CLEANER FOR SALT WATER IMMERSION AND FIRE EXTINGUISHING CHEMI-CALS ON ALL INTERNAL CIRCUIT BOARDS.	APPLY A SOLUTION OF ONE PART ISOPROPYL ALCOHOL, TT-I-735, AND NINE PARTS SOLVENT TRICHLOROTRIFLUOR-ETHANE, MIL-C-81302, TYPE II TO AFFECTED AREA WITH CLEANING COTTON CLOTH, ACID BRUSH, OR TOOTHBRUSH, AS APPROPTIATE.	
	CLEANER FOR ELECTRI-CAL CONTACT SURFACES.	APPLY A SOLUTION OF ONE PART DEIONIZED OR DISTILLED WATER AND ONE PART ISOPROPYL ALCOHOL, TT-I-735, TO AFFECTED AREA WITH ACID BRUSH OR PIPE CLEANER. WIPE CLEAN AND AIR DRY.	
WATER, DISTILLED	CLEANER FOR SOLDER FLUX RESIDUE IN ALL APPLICATIONS OF ELECTRONICS, ELEC-TRICAL EQUIPMENT AND MICROMINIATURE CIRCUITS.	APPLY A SOLUTION OF ONE PART DEIONIZED OR DISTILLED WATER TO THREE PARTS ISOPROPYL ALCOHOL, TT-I-735, AND SCRUB JOINT AND ADJACENT AREA WITH ACID BRUSH OR TOOTH-BRUSH. WIPE CLEAN WITH CLEANING COTTON CLOTH.	DEIONIZED WATER, OBTAINABLE FROM COMMERCIALLY AVAIL-ABLE PROCESSING UNITS THAT ARE PLUMBED INTO SOME SHORE ACTIVITY SHOPS, IS AN AUTHO-RIZED SUBSTITUTE.

AD-A191 295 PROCEEDINGS OF THE TRI-SERVICE CONFERENCE ON CORROSION (1987) HELD AT THE..(U) AIR FORCE WRIGHT AERONAUTICAL LABS WRIGHT-PATTERSON AFB OH.. F H MEYER MAY 87 5/6

UNCLASSIFIED AFWAL-TR-87-4139-VOL-1 F/G 11/6.1 NL

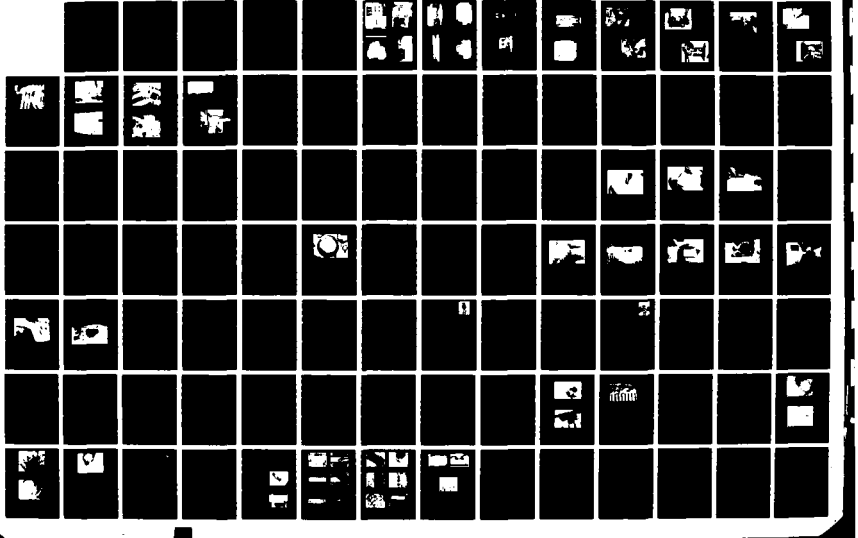

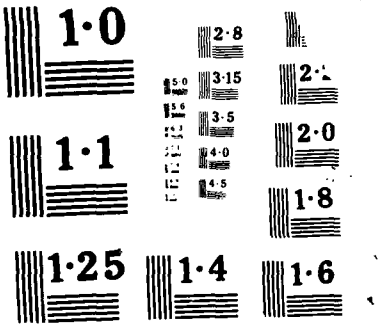
1·0
1·1
1·25
1·4
1·6
1·8
2·0
2·8
3·15
3·5
4·0
4·5

RECOMMENDED

CLEANING PROCESS VERSUS TYPE OF AVIONIC EQUIPMENT

TYPE EQUIPMENT	AQUEOUS ULTRA-SONICS	SOLVENT ULTRA-SONICS	WATER BASE SPRAY BOOTH	ABRA-SIVE TOOL	MINI-ABRA-SIVE	HAND CLEAN
HOUSINGS/COVERS	X	X	X	X	X	X
CHASSIS	X	X	X	X	X	X
RACKS/MOUNTS	X	X	X	X	X	X
CONTROL BOXES	X	X(1)	X		X	X
INSTRUMENTS					X(1)	X
LIGHT ASSEMBLIES	X	X	X	X(1)	X	X
WAVEGUIDES	X	X	X	X(1)	X	X
WIRE HARNESSES			X		X	X
SERVOS/SYNCHROS					X(1)	X
ANTENNAS, BLADE	X	X	X		X	X
ANTENNAS, DOME	X(1)	X(1)	X	X(1)	X	X
ANTENNAS, RADAR			X	X(1)	X	X
ANTENNAS, ECM					X	X
MOTORS	X	X(1)	X	X(1)	X	X
GENERATORS	X	X(1)	X	X(1)	X	X
BATTERIES						X
CIRCUIT BREAKER PANELS	X	X	X		X	X
GYROSCOPES			X(1)		X(1)	X
PLUGS AND CONNECTORS			X		X	X
HIGH DENSITY CONNECTORS					X	X
EDGE CONNECTORS			X		X	X
COAXIAL CONNECTORS					X	X
PRINTED CIRCUIT BOARDS			X			X

ENCLOSURE (5)

CLEANING AND DRYING RESTRICTIONS

COMPONENT	PROBLEM	SOLUTION
TRANSFORMERS	TRAP SOLUTION IN HOUSING	SEAL
SYNCHROS AND SERVOS	REMOVES LUBRICANT FROM BEARING	SEAL OR REMOVE
METERS AND INSTRUMENT GAUGES	TRAP SOLUTION THROUGH OPEN BACK	SEAL
SLIDING ATTENUATORS (RF)	TRAP SOLUTION IN SLIDE HOUSING	SEAL OR REMOVE
TUNABLE CAVITIES	TRAP SOLUTION IN CAVITY AREA	SEAL OR REMOVE
VARIABLE ATTENUATORS (MICRO-WAVE)	TRAP SOLUTION IN HOUSING	SEAL OR REMOVE
WAVEGUIDE (MICROWAVE)	TRAP SOLUTION IN GUIDE HOUSING (WHEN INSTALLED)	SEAL OR REMOVE
ROTARY SWITCHES	TRAP SOLUTION THROUGH OPEN HOUSING	SEAL
POTENTIOMETERS	TRAP SOLUTION THROUGH OPEN HOUSING	SEAL
DELAY LINES (PHYSICAL)	TRAP SOLUTION IN HOUSING	SEAL
KLYSTRON CAVITY	TRAP SOLUTION IN SOCKETS	REMOVE TUBE AND SEAL SOCKET
FAN MOTORS	TRAP SOLUTION IN HOUSING	SEAL OR REMOVE
PAPER CAPACITORS	DISINTEGRATE	SEAL
PRINTED CIRCUIT BOARD	TRAP SOLUTION (WHEN INSTALLED)	REMOVE (CLEAN SEPARATELY)
VACUUM TUBES	SHOCK DAMAGE	REMOVE
SLIDING CAM SWITCHES	SHOCK DAMAGE TO CAM	REMOVE OR HAND CLEAN ONLY
CRYSTAL DETECTORS	HEAT DAMAGE FROM OVEN	DRY AT 130°F (54°C) MAXIMUM
APC CONNECTORS (MICROWAVE)	SHOCK DAMAGE TO CENTER CONDUCTOR	SEAL AND HAND CLEAN ONLY
WIRE WRAP CONNECTORS	SHOCK DAMAGE	HAND CLEAN ONLY
GYROSCOPES	TRAP SOLUTION IN HOUSING	SEAL

ENCLOSURE (5).2

AVIONIC PRESERVATION MATERIALS

DESCRIPTION	CHARACTERISTICS	APPLICATION	RESTRICTIONS
CORROSION PREVENTIVE COMPOUND, WATER-DISPLACING, ULTRA-THIN FILM, AVIONICS GRADE, MIL-C-81309, TYPE III	GENERAL PRESERVATIVE FOR INTERNAL AREAS OF AVIONIC EQUIPMENT; INTERNAL AREAS OF ELECTRICAL CONNECTORS, PLUGS, RECEPTACLES; AND SOLDER JOINTS. CONTAINS WATER-DISPLACING PROPERTIES.	APPLY BY SPRAYING AN EVEN, THIN FILM TO THE SURFACE.	NOT INTENDED FOR USE ON EXTERIOR SURFACES OF AVIONIC EQUIPMENT. DEPOSITS A THIN, NON-CONDUCTIVE FILM WHICH MUST BE REMOVED FOR PROPER FUNCTION OF CONTACT POINTS AND OTHER ELECTROMECHANICAL DEVICES WHERE NO SLIPPING OR WIPING ACTION IS INVOLVED. DO NOT USE AROUND OXYGEN, OXYGEN FITTINGS, OR OXYGEN REGULATORS, SINCE FIRE OR EXPLOSION MAY RESULT. CAN BE REMOVED WITH DRY CLEANING SOLVENT, P-D-680, TYPE II.
CORROSION PREVENTIVE COMPOUND, WATER-DISPLACING, ULTRA-THIN FILM, AVIONICS GRADE, MIL-C-81309, TYPE II	GENERAL PRESERVATIVE FOR INTERNAL AREAS OF CHASSIS, EQUIPMENT COVERS, HARDWARE, MOUNTING BRACKETS, LATCHES, HINGES, TERMINAL BOARDS, BUS BARS, GROUND STRAPS AND INTERNAL/EXTERNAL AREAS OF JUNCTION BOXES.	APPLY BY SPRAYING AN EVEN, THIN FILM TO THE SURFACE.	NOT INTENDED FOR USE ON EXTERIOR SURFACES OF AVIONIC EQUIPMENT. DO NOT USE IN INTERIOR SURFACES OF COAXIAL CONNECTORS. DEPOSITS A THIN, NON-CONDUCTIVE FILM WHICH MUST BE REMOVED FOR PROPER FUNCTION OF CONTACT POINTS AND OTHER ELECTROMECHANICAL DEVICES WHERE NO SLIPPING OR WIPING ACTION IS INVOLVED. DO NOT USE AROUND OXYGEN, OXYGEN FITTINGS, OR OXYGEN REGULATORS, SINCE FIRE OR EXPLOSION MAY RESULT. CAN BE REMOVED WITH DRY CLEANING SOLVENT, P-D-680, TYPE II.

CORROSION PREVENTIVE COMPOUND, WATER-DISPLACING, CLEAR, MIL-C-85054	GENERAL PRESERVATIVE FOR EXTERNAL SURFACES EXPOSED TO ELEMENTS AND MOISTURE, INCLUDING: CHASSIS, EQUIPMENT COVERS, HARDWARE, MOUNTING RACKS, EQUIPMENT RACKS, SHELVING, BRACKETS, RADAR PLUMBING, ANTENNA HARDWARE, LATCHES, TERMINAL BOARDS, BUS BARS, GROUND STRAPS, JUNCTION BOXES, FASTENERS AND EXTERIOR SURFACES OF ELECTRICAL CONNECTORS, COAXIAL CONNECTORS, PLUGS AND RECEPTACLES.	APPLY BY SPRAYING AN EVEN, THIN FILM OR BRUSHING ONTO THE SURFACE.	NOT INTENDED FOR USE ON INTERIOR SURFACES OF AVIONIC EQUIPMENT. DO NOT USE ON INTERIOR SURFACES OF ELECTRICAL CONNECTORS, COAXIAL CONNECTORS, PLUGS, OR RECEPTACLES. DO NOT USE AROUND OXYGEN, OXYGEN FITTINGS, OR OXYGEN REGULATORS, SINCE FIRE OR EXPLOSION MAY RESULT. CAN BE REMOVED WITH DRY CLEANING SOLVENT, P-D-680, TYPE II OR ISOPROPYL ALCOHOL, TT-I-735.
CORROSION PREVENTION COMPOUND, SOLVENT CUTBACK, COLD APPLICATION, MIL-C-16173 GRADE 4	GENERAL PRESERVATIVE FOR EXTERNAL SURFACES EXPOSED TO ELEMENTS AND MOISTURE, INCLUDING: MOUNTING RACKS, SHELVING, BRACKETS, RADAR PLUMBING, SHOCK MOUNTS, RIGID MOUNTS, ANTENNA HARDWARE, GENERAL HARDWARE, HINGES, FASTENERS, GROUND STRAPS; AND EXTERIOR SURFACES OF ELECTRICAL CONNECTORS, COAXIAL CONNECTORS, PLUGS AND RECEPTACLES.	APPLY BY BRUSH OR SPRAYING AN EVEN, THIN FILM TO THE SURFACE. MATERIAL PRESENTS A SEMITRANSPARENT FILM.	NOT INTENDED FOR USE ON INTERIOR SURFACES OF AVIONIC EQUIPMENT. DO NOT USE ON INTERIOR SURFACES OF ELECTRICAL CONNECTORS, COAXIAL CONNECTORS, PLUGS, OR RECEPTACLES. DO NOT USE AROUND OXYGEN, OXYGEN FITTINGS, OR OXYGEN REGULATORS, SINCE FIRE OR OR EXPLOSION MAY RESULT. CAN BE REMOVED WITH DRY CLEANING SOLVENT, P-D-680, TYPE II. MUST BE APPLIED OVER WATER-DISPLACING CORROSION PREVENTIVE COMPOUND, MIL-C-81309, TYPE II, TO ACCOMPLISH A COMPLETE "WATER-DISPLACING AND PRESERVATIVE SYSTEM" ON ALL AREAS EXPOSED TO ELEMENTS AND MOISTURE.

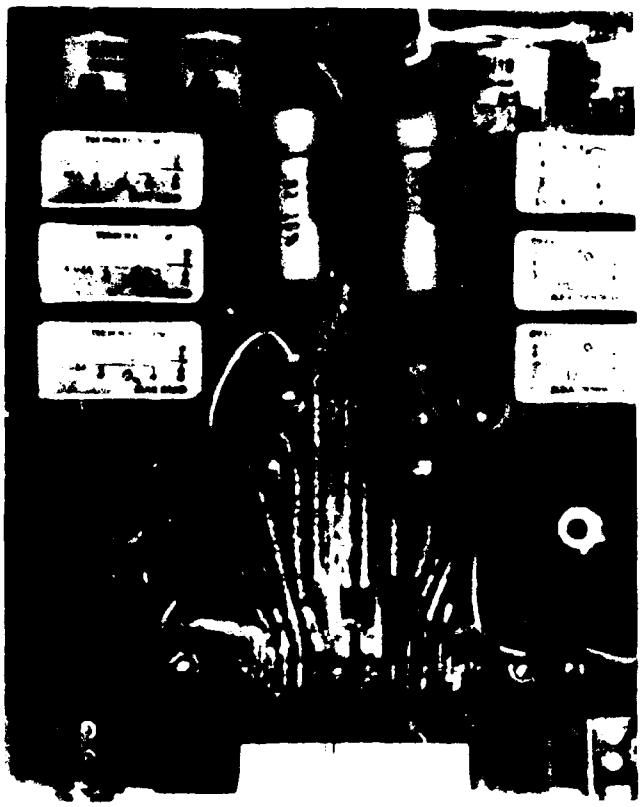

1. EXPOSURE TO SALT WATER

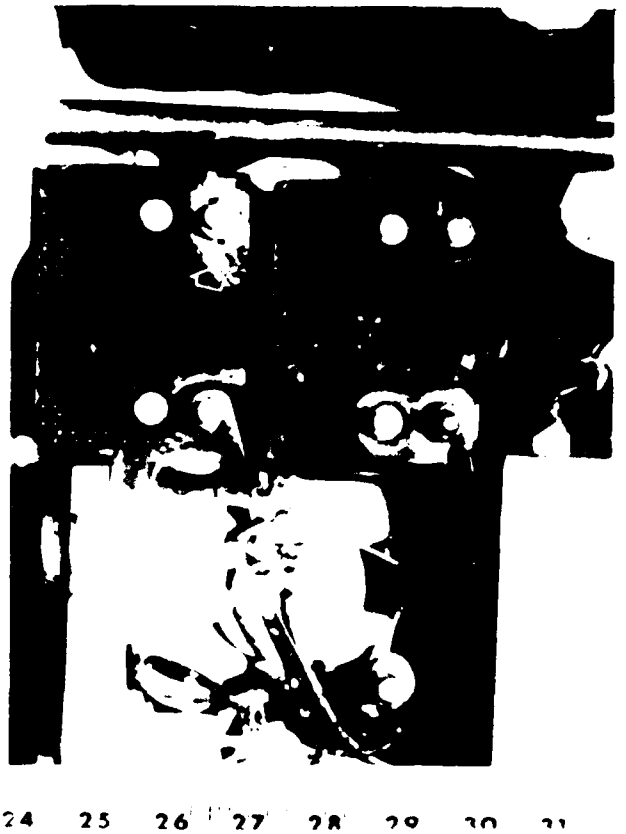

2. RUST ON STEEL COMPONENTS

3. WATER INTRUSION

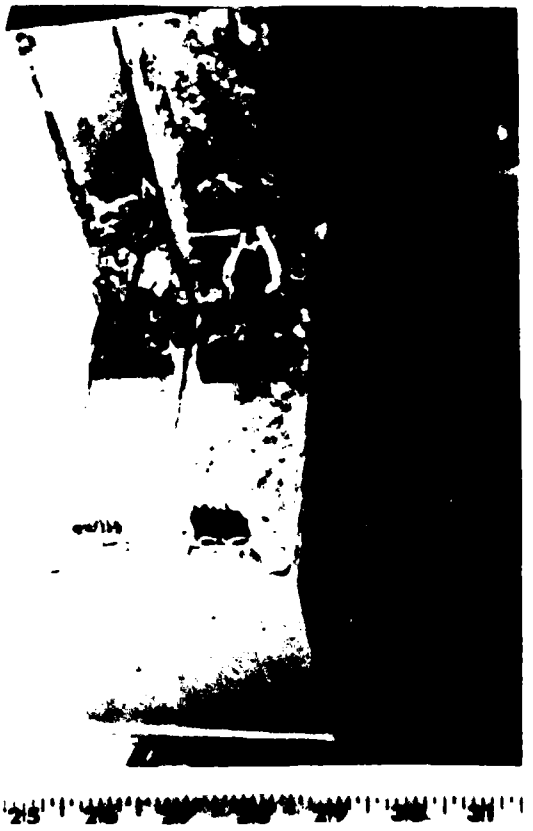

4. WATER INTRUSION

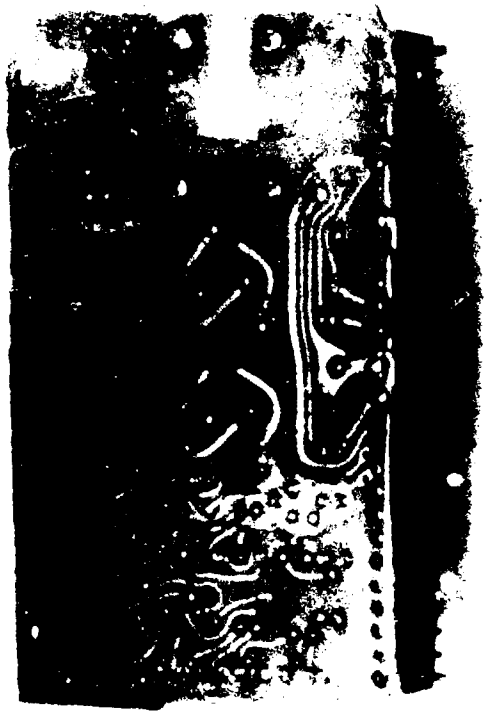

5. PIN CORROSION WATER INDUCED

6. SOLDER FLUX CORROSION

7. END VIEW SOLDE FLUX CORROSION

8. WATER INTRUSION ON PRINTED CIRCUIT

9. LONG TIME ENVIRONMENTAL CORROSION

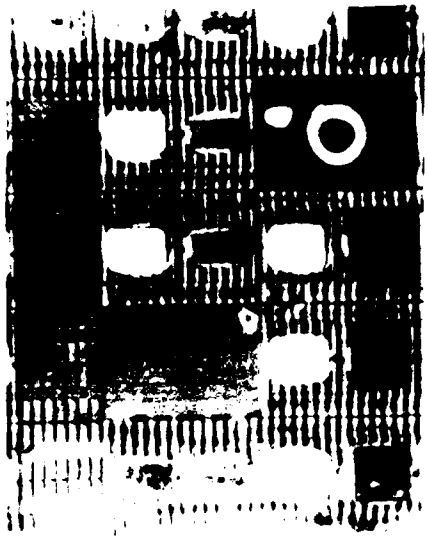

10. SOLDER FLUX CORROSION

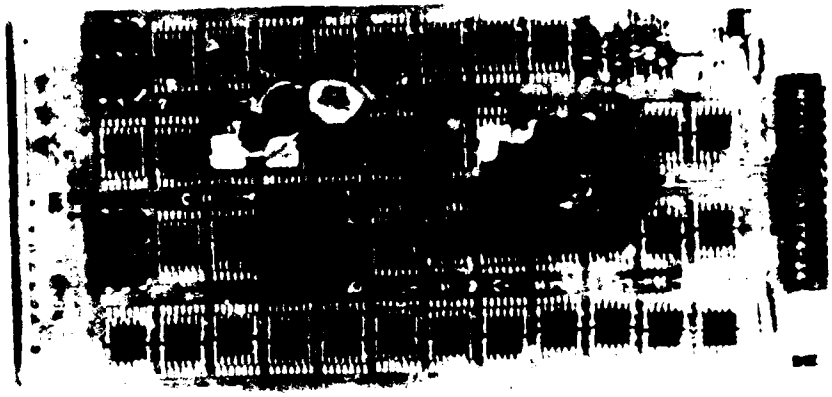

11. FUNGI GROWTH

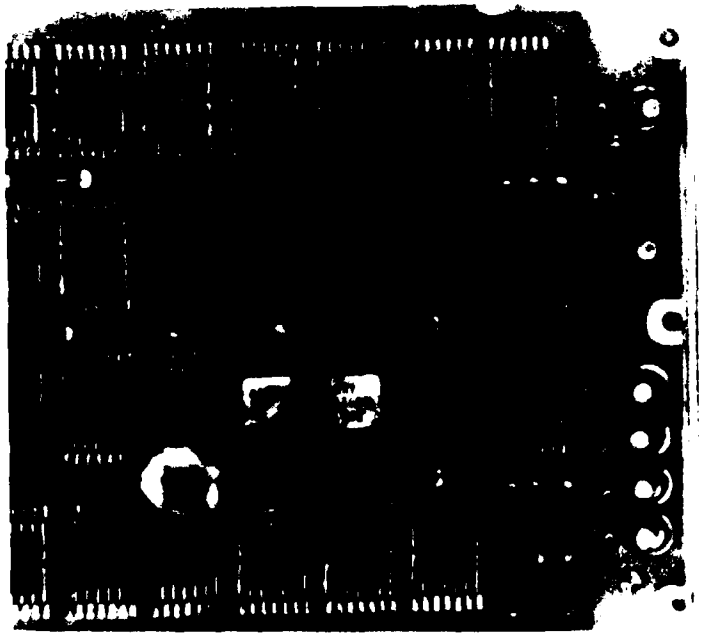

12.

13. CORROSION NOTED DURING INSPECTION

14. CORROSION BEING REMOVED WITH MINI GRINDER

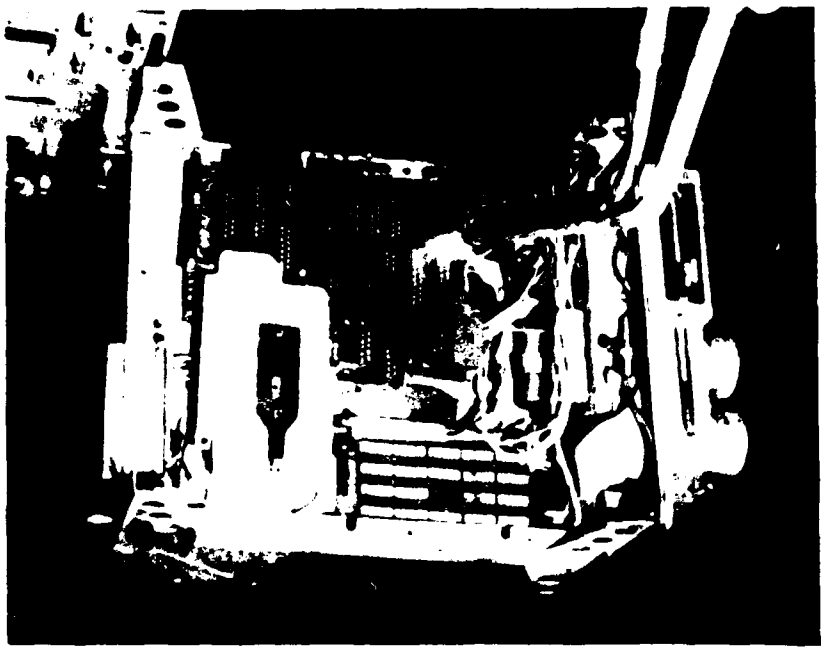

15. WATER DETERGENT CLEANING

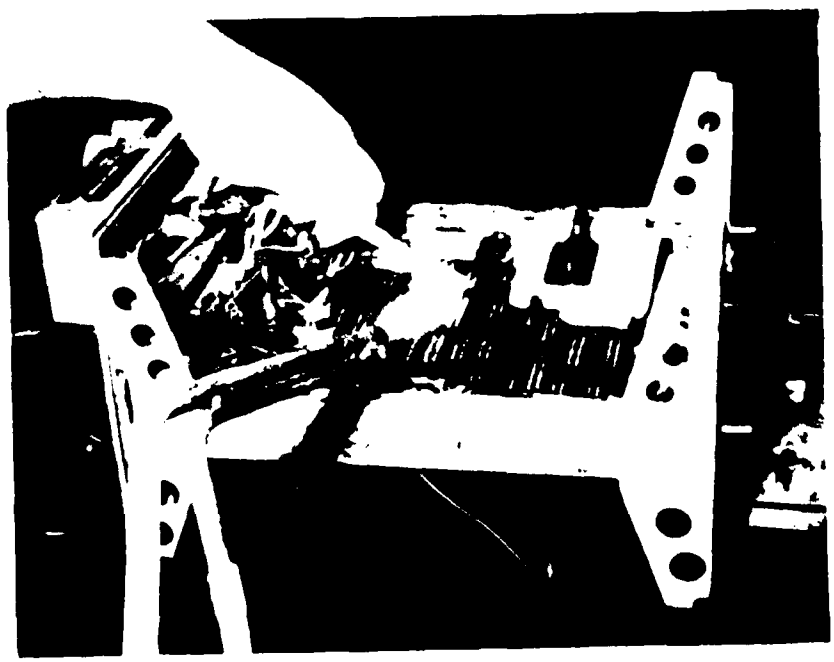

16. WATER DETERGENT CLEANING BRISTLE BRUSH

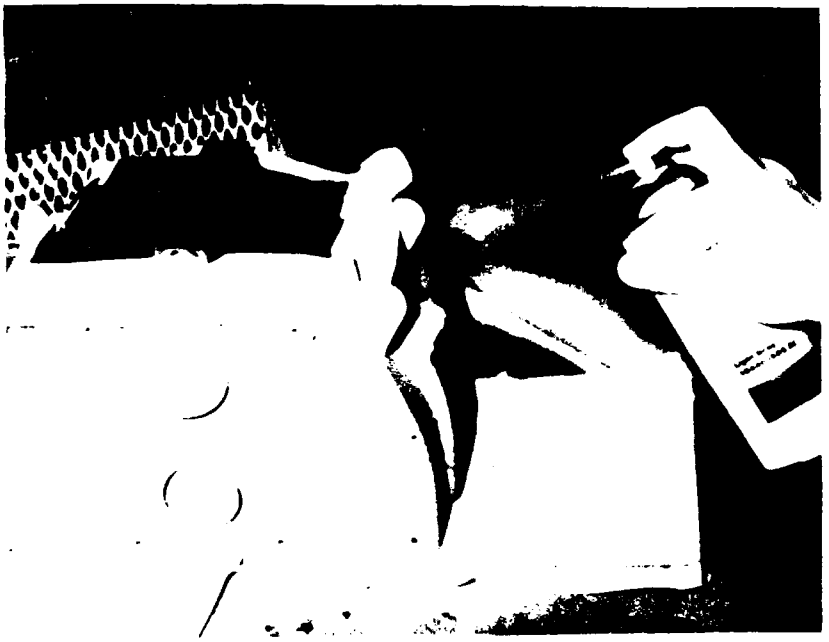

17. AVIONICS BOX REFINISHED AT
IMA CORROSION WORK CENTER

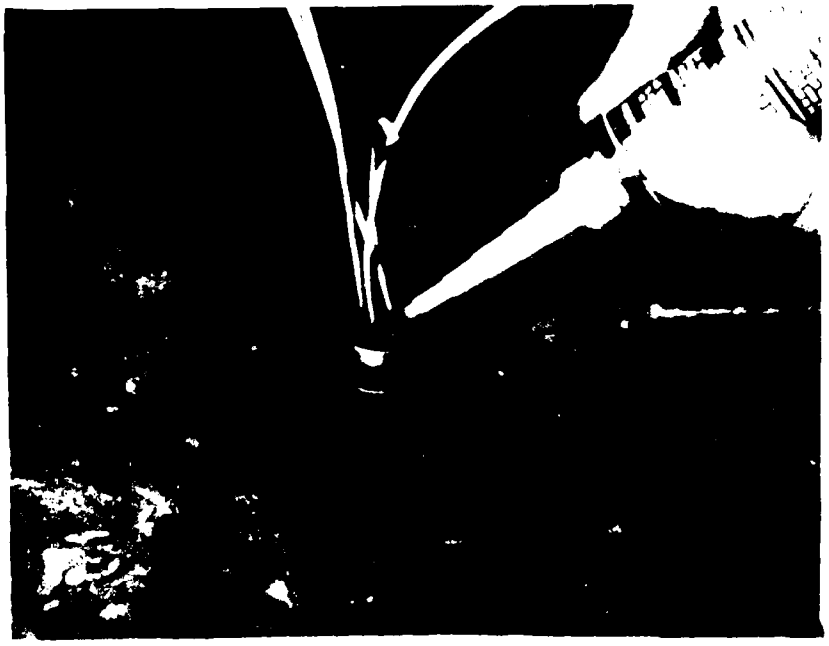

18. RTV 3140 BEING APPLIED TO GROMMET OF ENVIRONMENTAL CONNECTOR

19. WRAPPED NOSE LANDING GEAR WHEEL WELL
EXTREME WET AREA

20. TYPE "W" CONNECTOR SEALED GROMMET TREATED AND WRAPPED. OPENED FOR INSPECTION AFTER TWO DEPLOYMENTS

21. VERTICAL MOUNTED CONNECTOR WITH MINIMUM PROTECTION IN A NAVAL ENVIRONMENT

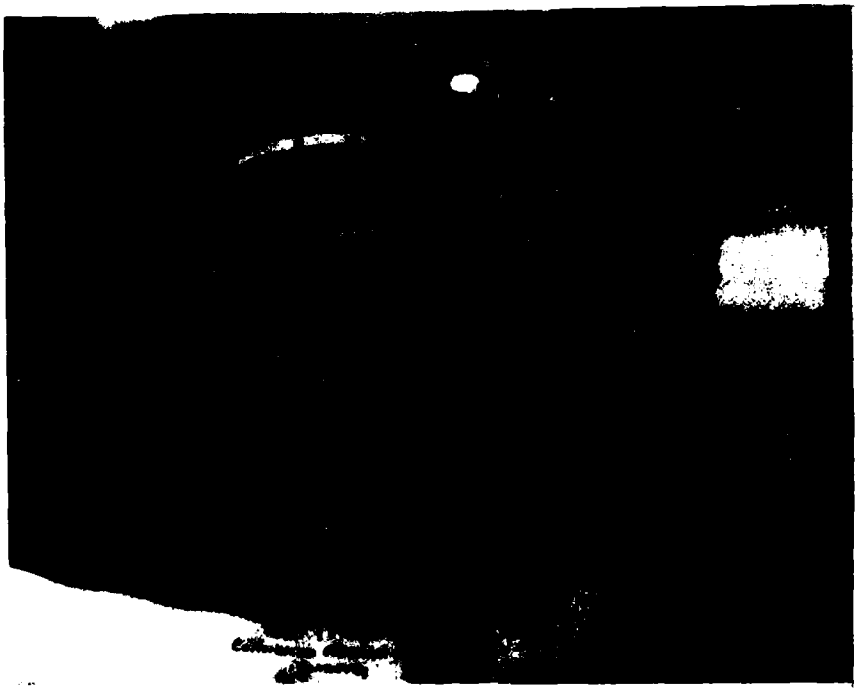

22. ELECTROLESS NICKEL PLATE DAMAGE CORROSION STARTED

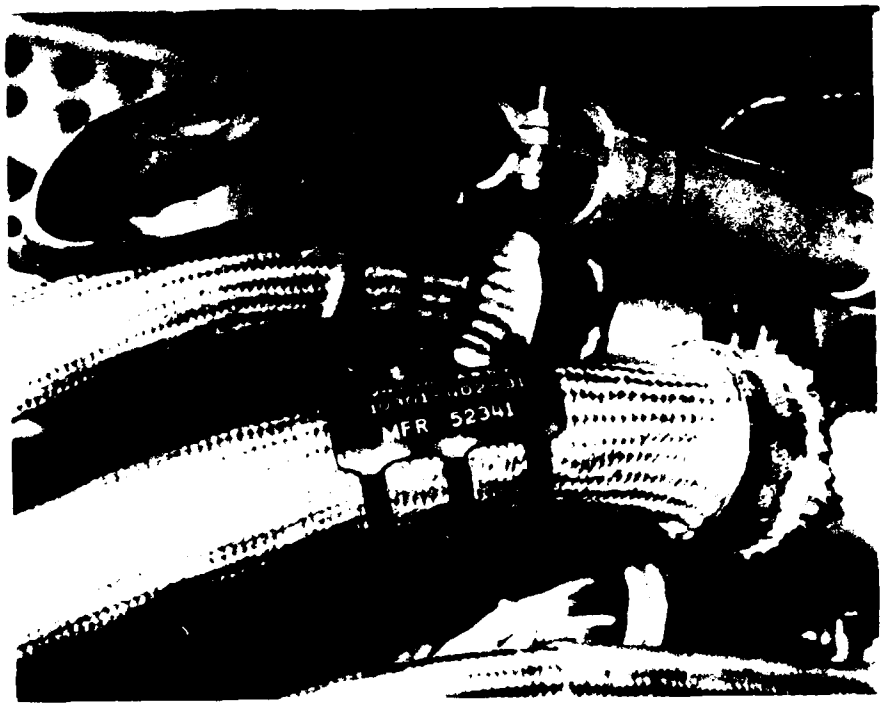

23. COMBINATIONS OF MATERIAL RESULT IN CORROSION IN A NAVAL ENVIRONMENT

24.

25. CORROSION UNDER BERRYLIUM COPPER BONDING STRIP

26. PPS COMPOSITE ENVIRONMENTAL CONNECTOR AFTER FOUR YEAR OPERATION INSTALLED IN MAIN LANDING GEAR WHEEL WELL OF F-14 AIRCRAFT.

SHIELDING EFFECTIVENESS

OF

METALLIC JOINTS

VERSUS

CORROSION PREVENTION

Presented at the

1987 TRI-SERVICE CORROSION CONFERENCE

AIR FORCE ACADEMY

May, 1987

Written by

Jan W. Gooch

Energy and Materials Sciences Laboratory

John K. Daher

Electronics and Computer Systems Laboratory

Georgia Tech Research Institute
Atlanta, Georgia 30332

31 August 1987

1.0 Introduction

1.1 Background

Under present service conditions, Air Force aircraft and weapon systems are experiencing corrosion between metal surfaces such as joints. This problem is two-fold. First, corrosion between metal surfaces in existing aircraft and weapon systems create structural weaknesses which undermine the effectiveness of structure. Secondly, the corrosive process produces non-conductive products which destroy the nuclear-hardening capability of the structure.

At present, the Type 3, MIL-C-5541, chemical conversion coating procedure used on aluminum surfaces is the only protective finish that meets the existing electromagnetic pulse (EMP)/ electromagnetic interference (EMI) requirements. However, this method allows moisture to be trapped between two metal surfaces which causes corrosion of the surfaces. The products of corrosion are non-conductive materials which increase the electrical resistance of the bond or joint between surfaces, resulting in impedance high enough to destroy the nuclear hardness of many aircraft and weapon systems.

From the above description of the problem, it is apparent that corrosion protection materials and/or processes are required which are compatible with the existing and/or modified nuclear-hardened weapon systems.

A primary requirement for effective bonding is that a low resistance path be established between the two joined objects. The resistance of this path must remain low with use and with time. The limiting value of resistance at a particular junction is a function of the current expected to pass through the path. For example, where the bond serves only to prevent static charge buildup, relative high bond resistances, i.e., above a few hundred ohms, may be acceptable. On the other hand, bonds for shock hazard protections are commonly limited to 0.1 ohms resistance. Where RF interference may result from a poor bond between equipment and its mounting surface, the bond resistance is limited by MIL-STD-5087B to 2.5 milliohms.

The imposition of low values of bond resistance helps ensure that impurities are removed from the mating surfaces and that sufficient surface contact area is provided to establish a reliable path for currents to flow while limiting voltage differentials across the bond junction. It is these voltage

differentials that lead to unwanted energy coupling into protected volumes. It is widely recognized that a low dc resistance is not a reliable indicator of the performance of the bond at high frequencies such as those in the upper portions of the EMP spectrum, above the hf communications band, and in the radar bands. Inherent conductor inductance and stray capacitance, along with the associated standing wave effects and path resonances, will determine the total impedance of the bond. An additional factor in bond performance is the bond aperture dimensions relative to the wavelength of incident energy. As an example, a spot welded bond can easily meet the 2.5 milliohm requirement and, yet, if the welds are widely spaced, appreciable electromagnetic energy can reach the interior of the bonded region and produce upset or damage. It is for this reason that most EMP control documents do not specify a resistance performance criterion for bonds -- they, instead, specify the method of construction (typically continuously welded).

1.2 Objectives

What is generally missing in the discussion of bond resistance is a carefully established correlation between measured bond resistance and the shielding effectiveness achieved by the bond. Clearly such a correlation needs to be established.

A straight forward approach to validating joint shielding versus bond resistance would be to measure the shielding effectiveness of several bonds having controlled (and carefully measured) resistance values. To perform such an extensive bond evaluation program with sufficient depth to establish adequate evidence to counter over decades of tradition and experience in the application of MIL-STD-5087B (and the various other standards which have adopted the 2.5 milliohm bond resistance limit either by default or for uniformity of requirements) would indeed require a substantial investigative effort over an extended period of time. In fact, it is not possible to define with precision exactly the magnitude or duration of such an effort because the results cannot be predicted in advance. For example, the investigation could show that the shielding necessary to provide EMP protection can only be realized with bonding resistances LESS THAN 2.5 milliohm, or it may show that adequate protection is produced by bonds of 10 milliohms, 20 milliohms or even higher resistances. (It should be pointed out that there is little prior data on which to base a conclusion in advance of substantive measurements.)

With the evident difficulty of achieving the 2.5 milliohm dc resistance while maintaining a corrosion-free

bond for an extended period, there clearly is a definite need to seriously examine the relative need of such a low resistance in order to produce an EMP-hardened system. An iterative approach was, therefore, taken which was structured toward establishing a carefully planned and documented technology base that demonstrates the relationship between bond dc resistance, corrosion protection and the electromagnetic protection offered by the bond.

The above efforts required identification and, ultimately, optimization of corrosion prevention materials and/or processes. These materials must necessarily be capable of protecting metal surfaces from air/moisture corrosion over a specified period of time. In addition, electrically conductive corrosion prevention materials that are capable of maintaining nuclear-hardening capabilities of weapon systems needed to be identified.

With these capabilities, existing weapon systems can be protected from further corrosion, and existing nuclear-hardened weapon systems can be retrofitted with a corrosion prevention material.

2.0 Assessment of the Validity of the MIL-B-5087B Class R Bonding

The electrical bonding requirements for limiting RF potentials (Class R bonding) as set forth in MIL-B-5087B, "Military Specification -- Bonding, Electrical and Lightning Protection for Aerospace Systems," require that the vehicle skin be designed to produce a uniform low-impedance surface through inherent RF bonding and that the contractor demonstrate by test that the bonding method results in a dc resistance of less than 2.5 milliohms. In addition, current Air Force design practice (per AFSC Design Handbook DH 1-4, Design Note 5D1) requires the contractor to meet the conductivity requirements independent of the use of conductive fasteners, thereby necessitating intimate metal-to-metal contact. Consequently, the finishes which are commonly used to meet existing electromagnetic pulse (EMP)/ electromagnetic interference (EMI) requirements for aluminum surfaces are tin plating or MIL-C-5541, Type 3 chemical conversion coatings. However, these methods allow moisture to be trapped between metal surfaces which can lead to severe corrosion problems in the field. Corrosion between metal surfaces has reportedly been so severe as to create structural weaknesses which undermine the effectiveness of the structure [1]. Further, the products of corrosion are nonconductive materials which increase the electrical resistance/impedance of the bond and, thus, can destroy the nuclear hardness of aircraft and weapon systems.

Consequently, the 2.5 milliohm bonding requirement was questioned. [illegible] higher resistance value could provide the necessary conductivity for nuclear hardening, a variety of conductive sealant materials would be available which could be used to reduce corrosion between faying surfaces. Furthermore, the use of conductive sealants could enable a low resistance and effective bond (both electrically and mechanically) to be maintained over the useful life of the weapon system. Therefore, a study was undertaken to:

1. determine the basis and rationale behind the 2.5 milliohm bonding requirement,
2. determine the relationship (if any) between the dc resistance and EMI/EMP hardness of a bonded joint, and
3. perform measurements to determine the effects of weathering on the dc resistance and EMI/EMP hardness of aluminum joints bonded with and without the use of conductive sealant materials.

2.1 Basis/Rationale Behind the 2.5 Milliohm Bonding Requirement

The basis and rationale behind the 2.5 milliohm requirement given in MIL-B-5087B for Class R bonding was investigated. A thorough review of bonding-related documents was undertaken, and valuable information was also obtained from personal communications with individuals involved with the development of the original MIL-B-5087 bonding specification. The most useful information came from discussions with Mr. C. E. Seth of Wright Patterson Air Force Base, Aeronautical Systems Division (WPAFB/ASD). WPAFB/ASD was the custodian of the original MIL-B-5087 specification, and Mr. Seth was involved in the development of this specification from its inception. Much of the information with regard to the original purpose and intent of the 2.5 milliohm requirement was obtained from Mr. Seth of WPAFB/ASD.

The original purpose of the 2.5 milliohm requirement was to ensure adequate bonding of metal joints to provide lightning protection, RF shielding and system electromagnetic compatibility (EMC). The rationale behind this requirement was that the 2.5 milliohm dc resistance was a value that:

1. could be readily achieved using accepted bonding practices,
2. could be readily verified through measurement, and
3. would force the contractor to properly clean the surfaces before assembly and maintain adequate pressure between the mating surfaces to ensure good metal-to-metal contact.

Higher values of resistance tend to relax the surface preparation and assembly requirements.

One of the oldest cited references to the 2.5 milliohm resistance limit is Volume I of a report prepared in 1964 by the Filtron Company, Inc., for the U. S. Army Electronics Laboratories. This report, which is entitled, "Interference Reduction Guide for Design Engineers," states on pages 2-20 that, "The dc resistance of an adequate bond should be between 0.00025 and 0.0025 ohm." No further rationale is provided for the recommended range of dc resistances. However, the authors do concede that "The effectiveness of a bond at radio frequencies is neither fully dependent upon nor measurable only in terms of its dc electrical resistance; especially at high frequencies..." and that dc measurements are employed since "...it is more convenient to measure the dc resistance rather than the ac impedance of a bond...".

The overall role and function of bonding is discussed in Design Note 5D1 of AFSC DH 1-4:

> "Electrical bonding is the process of mechanically connecting certain metal parts so that they will make a good low-resistance electrical contact. Bonding is required to ensure that a system is electrically stable and relatively free from the hazards of lightning, static discharge, and electrical shock and to assist in the suppression of RF interference. Usually, the resistance of electrical bonds should be in the order of 0.0025 ohm."

The implication that a 2.5 milliohm dc resistance is necessary for adequate bonding is cited over and over again in the literature. However, no technical basis is given for this particular resistance value.

The 2.5 milliohm bonding requirement specified in MIL-B-5087B pertains to Class R bonds whose function is to limit RF potentials. Different dc resistance values are specified for other bond classifications depending on their primary function. These requirements are summarized in MIL-HDBK-253, "Guidance for the Design and Test of Systems Protected Against the Effects of Electromagnetic Energy," on page 15, which states:

> "Measurement of the dc resistance of a bond is often used as a guide to the anticipated performance of the bond. Depending on the purpose of the bond, some military documents specify the maximum dc resistance allowable for a good bond. For example, bonds that are installed to prevent shock hazards are required by both MIL-B-5087 and MIL-STD-1310 to have a resistance of less than 0.1 ohm. Bonds for RF purposes are required by MIL-B-5087 to have a resistance of less than 2.5 milliohm. Additionally, in areas prone to explosion or

fire hazards, maximum values of bond resistances are designated; these values are a function of anticipated maximum fault current in the event a power line to ground short occurs. A guideline as far as a good RF bond is concerned is a dc resistance value of between 0.25 and 2.5 milliohm."

Again, the same range of dc resistance values (0.25 to 2.5 milliohm), as in the Filtron report, are recommended for adequate bonding.

Several other documents, in addition to MIL-HDBK-253, AFSC DH 1-4 and the Filtron report, also specify the 2.5 milliohm bonding resistance or reference MIL-B-5087B. These documents include North Atlantic Treaty Organization (NATO) Standardization Agreement No. 3659, MIL-STD-462, MIL-STD-1310, MIL-STD-1512, MIL-STD-1541, MIL-STD-4544 and MIL-E-6051D.

In summary, a large number of documents have been reviewed which appear to substantiate the information obtained from the personal communications. Based on these sources of information, it is concluded that the 2.5 milliohm bonding requirement arose, not from a theoretically or empirically derived basis, but from a practical standpoint and as a means for ensuring proper bond preparation and assembly.

2.2 Investigation of the Relationship Between DC Resistance and Shielding Effectiveness

An essential ingredient of EMP hardening, particularly for airborne systems, is electromagnetic shielding. In practice, shields are rarely formed of single, continuous sheets of metal. Sheets must be joined together to form the shield, and the joints must be properly bonded to provide desirable shielding performance over a broad frequency range. Electromagnetic shielding effectiveness was, therefore, selected as the measure of bond effectiveness with regard to EMI/EMP hardness. A stainless steel test joint was fabricated, and the electromagnetic shielding effectiveness of the test joint was measured as a function of dc resistance. The stainless steel test joint, dc resistance measurements, shielding effectiveness measurements and the measurement results are described below.

2.2.1 Stainless Steel Test Joint for DC Resistance Measurements

In order to determine the relationship, if any, between dc resistance and shielding effectiveness, a specialized test joint was designed and fabricated. The test joint was constructed out of No. 316 stainless steel rather than aluminum because of the superior ability of stainless steel to withstand atmospheric

corrosion. A sketch of the stainless steel test joint is shown in Figure 1. The back plate of the test joint was designed to conform with the flange area of the shielding effectiveness test box (described in Section 2.2.3). Dielectric washers were used to insulate the screw fasteners from the top metal plate and to allow a fixed separation to be maintained between the plates. The use of dielectric washers allowed the resistance between the plates to be controlled by the bulk conductivity of a conductive sealant material which was applied in the 3/4 inch overlap area between the plates. Cylindrical metal posts were welded onto each plate to facilitate the dc resistance measurements.

A front view of the stainless steel test joint is shown in Figure 2. The two overlapping plates connected with screw fasteners are visible as are the two metal posts used for the resistance measurements. Rear and side views of the stainless steel test joint are shown in Figures 3 and 4, respectively. During resistance and shielding effectiveness tests, the air gap (visible in the side view of Figure 4) was filled with conductive sealant of varying resistivity.

The conductive sealants listed in Table 1 were formulated to yield a wide range of resistance values above and below 2.5 milliohms. These materials consist of silver powder dispersed in urethane resins at different volume loadings to vary the resistivity. Sealant 1 is a two-part urethane, whereas the other four sealant types are moisture-cure urethanes. Each sealant was applied to the stainless steel test joint, cured as required, and subsequently measured for electrical resistance and shielding effectiveness. (These sealant types are not intended for actual use on aircraft as silver will corrode aluminum in the presence of moisture.)

2.2.2 DC Resistance Measurements

The dc resistance of the various conductive sealant test samples were measured with a double Kelvin bridge milliohmmeter. The double Kelvin bridge is a four terminal instrument which is capable of accurately measuring very small resistance values (in this case, as low as 0.1 milliohms). For resistance values greater than 1 ohm, the terminals of the milliohmmeter were clipped or contacted directly to the metal plates of the test joint in order to remove the additional resistance associated with the bonded posts from the measurement. All resistance measurements were made after the sealant material had cured so that the resistance value did not vary appreciably with time. The shielding effectiveness tests were run immediately after the resistance measurements were completed.

Note that in some instances it may be desirable to know the resistance per unit area of the test samples. For the test joints used on this program, the overlap area between the plates in which the sealant materials were loaded was approximately 18.0 square inches. Therefore, the resistance per unit area for any of the test samples measured on this program may be calculated simply by dividing the resistance value in milliohms by 18.0 to get the value in units of milliohms/in^2.

2.2.3 Shielding Effectiveness Measurements

The shielding effectiveness of the test joint samples was evaluated as a measure of the EMI/EMP hardness of the bonded joint. The shielding effectiveness of each test sample was determined as the difference (in dB) between the electromagnetic field coupled through an aperture with and without the sample present over the aperture. (This measurement technique conforms to the basic procedure set forth in MIL-STD-285 [2].) A block diagram of the test setup used to make the shielding effectiveness measurements is illustrated in Figure 5. This test setup enabled accurate and repeatable swept frequency measurements to be made on the test joint samples over the 500-1000 MHz frequency range.

A transmitting antenna (capacitively-loaded dipole) was placed in the center of a shielding effectiveness test enclosure, and a receiving antenna (log conical spiral) was positioned outside of the test enclosure at a distance (5-1/2 feet) which meets the far-field criterion over the entire test frequency range. The log conical spiral receiving antenna was directed towards a 6 inch square aperture located in one wall of the enclosure. The purpose of the test chamber was to isolate the transmitting and receiving antennas so that the only coupling between them was through the aperture. To minimize unwanted coupling, all permanent seams of the test enclosure were welded, and finger stock was installed around the lid of the enclosure and around the periphery of the test panel port (aperture). The inside of the test enclosure was lined with ferrite absorbing tiles which served to dampen enclosure resonances and to simulate free space conditions for the transmitting antenna.

The test joint was fastened to the test enclosure and electromagnetically sealed by three rows of finger stock located on the enclosure flange area. Conductive copper tape was also applied around the periphery of the test sample as an additional precautionary measure to prevent the electromagnetic field from leaking round, rather than through, the test sample. A 6-dB attenuator was used at the transmitting antenna input port to ensure a stable 50-ohm impedance at the power amplifier output. A tracking generator was used in conjunction with a spectrum analyzer to provide the swept frequency output source and

receiver. (The tracking generator derives its output signal from the first and third local oscillator outputs of the spectrum analyzer.) A 10-dB pad was used to attenuate the nominal 0 dBm output signal level of the tracking generator to approximately -10 dBm at the power amplifier input. The power amplifier provides approximately 46 dB of RF gain which corresponds to 4 watts output power with -10 dBm input power. A low noise, high gain amplifier (noise figure = 2 dB; gain = 35 dB) was used to improve the sensitivity of the spectrum analyzer and thereby increase the overall dynamic range.

To isolate the test setup from the external electromagnetic environment and to minimize errors due to ground and/or wall reflections, the test enclosure and receiving antenna were located in a shielded anechoic chamber. The isolation characteristics of this chamber were 100 dB or greater over the frequency range of 10 MHz to 1000 MHz and absorption was effective for RF frequencies greater than 300 MHz. The test enclosure was connected to the outside of the anechoic chamber via a 1/2 inch copper pipe/flange assembly, and a coaxial cable routed through the copper pipe connected the power amplifier outside the enclosure to the attenuator and transmitting antenna located inside the test enclosure. This cable routing configuration was used to prevent RF energy leaking from the coaxial cable from coupling to the receiving antenna and swamping the signal which was coupled through the test sample. In this way, a dynamic range of approximately 100 dB was achieved. (The dynamic range of the test setup was the ratio of the signal level coupled to the receiving antenna with the aperture open to the signal level received with a thick metal plate fastened over the aperture.)

2.2.4 Measurement Results on the Relationship Between DC Resistance and Shielding Effectiveness

A composite plot of the shielding effectiveness versus frequency for a variety of sample resistance values is shown in Figure 6. The shielding effectiveness measurement results for the complete set of sealant samples would be too cluttered to fit on a single composite plot. Note from Figure 6 that, in general, (1) shielding effectiveness increases as dc resistance decreases, and (2) shielding effectiveness is not a strong function of frequency over the 500-1000 MHz test frequency range (except for the very low resistance samples which has high shielding effectiveness values near the dynamic range of the test system). For these very low resistance samples, a stronger frequency dependence was noted due to frequency dependent leakage paths which are significant at the higher shielding effectiveness values but insignificant at the lower shielding values.

In order to summarize the findings on a simple 2-dimensional plot, the shielding effectiveness versus frequency curves were reduced to an average shielding effectiveness value in dB (i.e.,

the frequency average of the logarithmic shielding values) and then all of the average values were plotted on a graph of shielding effectiveness versus dc resistance.

The resulting plot of the (average) shielding effectiveness versus dc resistance is illustrated in Figure 7. First, note that there appears to be a limiting shielding effectiveness value for the high resistance samples which corresponds to a minimum shielding effectiveness of approximately 35 dB. This "minimum" shielding effectiveness value is a function of the test frequency range, the electromagnetic wave impedance and, as will be later demonstrated, the particular test joint geometry used. Second, note that there also appears to be a limiting shielding effectiveness value for the low resistance samples which corresponds to a maximum shielding effectiveness of approximately 105 dB. Closer scrutiny of the data indicates that this "maximum" shielding effectiveness value in some instances occurs due to a limitation in the test sample (i.e., RF leakage) but in other instances results from the limited dynamic range of the test system. And, finally, note the sharp decrease in shielding effectiveness from approximately 105 dB to approximately 55 dB as the dc resistance of the test sample increases from approximately 2.5 milliohms to approximately 100 milliohms. Although the test results presented here represent only one test joint geometry and one electromagnetic test environment, the data of Figure 7 strongly suggest that relaxation of the 2.5 milliohm requirement could result in a significant reduction of the EMI/EMP hardness of aircraft and weapons systems.

It should be emphasized that the data presented here by no means is intended to imply that a low dc resistance is the only requirement for a quality bond from an EMI/EMP hardness perspective. To demonstrate this point, the test joint was modified by removing the insulating washers to allow the screw fasteners to establish dc electrical continuity between the metal plates. The resulting dc resistance of the test sample without a conductive sealant in the flange area was extremely low (<0.1 milliohms) whereas, as can be seen from Figure 8, the shielding effectiveness was generally very poor and frequency sensitive. This example clearly shows that a low dc resistance value is not sufficient for good shielding effectiveness and that electrical continuity must be obtained across the entire joint area (resulting in low RF bonding impedance) for effective shielding over a broad frequency range. This requirement is not necessarily met by a low dc resistance value nor can it be verified solely by a dc resistance measurement.

2.2.5 Effect of Plate Separation on Shielding Effectiveness

A brief experiment was conducted to demonstrate the influence of the test joint geometry on the shielding effectiveness test results. The experiment consisted of measuring the shield-

ing effectiveness of the test joint without conductive sealants while varying the separation distance between the metal plates. Fixed separation distances were obtained by placing one or more mylar sheets (minimum thickness = 0.1 mm) in the flange area between the plates. The tests were run with 0.1, 0.3, 0.95 and 2.5 mm plate separation distances, respectively.

Figure 9 shows a composite plot of the average (over frequency) shielding effectiveness values for the various plate separationdistances. Note that the shielding effectiveness is inversely proportional to the plate separation distance. Approximately 15 dB decrease in shielding effectiveness was measured per decade increase in plate separation distance over the range of plate separation distances evaluated. (Intuitively, a 20 dB per decade roll off could be expected from the capacitance between the plates neglecting fringing terms. Fringing terms could reduce the slope of the roll off somewhat since these terms become more significant at greater separation distances.) Also note that the data from Figure 7 was generated with a dielectric spacer around each screw fastener which maintained a fixed 30 mil spacing between the plates. The limiting value for the high resistance test samples was approximately 35 dB, which falls very near the curve shown in Figure 9 for a 0.76 mm (30 mil) plate separation distance.

2.3 Summary and Conclusions on Validity of 2.5 Milliohm Bonding Requirement

In summary, the basis and rationale behind the 2.5 milliohm bonding requirement in MIL-B-5087 has been determined from an extensive literature review and from information obtained through personal communications with individuals involved with the development of the original MIL-B-5087 specification. The 2.5 milliohm bonding requirement arose not from a theoretically or empirically derived basis but from a practical standpoint and as a means for enforcing proper bond preparation and assembly. The relationship between dc resistance and shielding effectiveness has been investigated with the use of a specialized test joint filled with conductive sealants of varying resistivities to obtain the desired range of dc resistance values. The effect of the test joint geometry, in particular the effect of the plate separation distance, on shielding effectiveness was also evaluated. Although the data collected is by no means all encompassing, it strongly suggests that relaxing the 2.5 milliohm requirement could seriously degrade the EMI/EMP hardness of military aircraft and weapon systems.

3.0 Identification and Evaluation of Optimum Sealant Materials

The objective of this task was to identify and evaluate optimum corrosion prevention materials for use on nuclear hardened aircraft and weapon systems. New test joints were designed and fabricated out of 7075 aluminum and fastened using realistic torque values. The aluminum test joints were loaded with the top candidate sealant materials and weathered in a salt fog environment according to ASTM B117 [3]. The dc resistance and shielding effectiveness of the test joints were measured before weathering tests began and periodically during the weathering tests to monitor the corrosion effects on the electrical and electromagnetic performance of the bonds. In addition, control joints (no sealant) were weathered and tested simultaneously to compare the relative merit of the selected sealant materials.

3.1 Identification of Materials

A variety of conductive sealant materials was considered for use as optimum compromises between EMI/EMP hardness and corrosion prevention. The use of metal coated glass spheres was considered early in the program. However, it was later learned that these materials are not suitable for aircraft structural type sealants for the following reasons:

1. The number of contact points between spheres is small compared to that for irregular shaped particles. The greater the number of contact points, the less damage likely to be experienced from vibration.

2. During normal stresses from aircraft, vibration can cause shearing through the thin metal coating on the spheres which will destroy the current path.

3. Temporary current overload or pulsing, such as could be induced by lightning or nuclear EMP, can damage the coating (as shown in Figure 10).

Pure silver powders and flakes are highly desirable conductive particles from an electrical performance point of view for use in EMI gaskets, compounds, coatings and adhesives. However, the metal's relatively high density, constantly fluctuating cost and potential for galvanic corrosion with many substrate materials often prohibit its use. To overcome these problems, the EMI industry has developed hybrid particles that offer the beneficial conductivity characteristics of silver, yet minimize or negate the drawbacks concerning density, cost and galvanic corrosion. For aluminum substrates, a particularly promising material which was identified was silver coated aluminum. This hybrid material,

produced by coating a thin layer of silver on the surface of aluminum particles, has a galvanic potential very near that of aluminum (see Table 2) and, thus, was expected to have superior corrosion characteristics when used on aluminum substrates.

The final list of conductive sealant materials which appeared to be most promising for meeting the program objectives are shown in Table 3. These five conductive sealant materials were therefore selected for evaluation under accelerated environmental test conditions. A salt fog exposure environment per ASTM B117 was selected to simulate accelerated weathering conditions. The dc resistance and shielding effectiveness of the test joints and the control joints were measured before weathering tests began and periodically during the weathering tests to determine the relative degradation in electrical performance as a function of exposure time in the salt fog environment.

3.2 Evaluation of Conductive Sealants in Salt Spray Chamber, ASTM B117

DC resistance measurements were performed on all five conductive sealant types shown in Table 4 at 24 hour time intervals during the salt fog exposure testing. Shielding effectiveness measurements were made on the stainless steel-filled polysulfide sealant (Products Research Proseal RW2-28-71) and the aluminum-filled polyurethane RTV sealant (Chomerics #43429-252) at approximately one week time intervals during the accelerated environmental exposure testing. A description of the aluminum test joints and the results of the dc resistance and shielding effectiveness measurements are presented below.

3.2.1 Aluminum Test Joints

Five aluminum test joints were fabricated for use in the weathering study. The test joints were designed and constructed to fit on the shielding effectiveness test enclosure while being representative of actual joints located on the skin of military aircraft and missile systems. The material chosen for the test joints was standard aircraft 7075, T6 aluminum certified per Federal Specification QQ-A-250/12. The 7075 aluminum was chosen because it is a common aircraft type of aluminum and is most prone to corrosion compared to other types of aluminum. The design of the aluminum test joints was identical to that of the stainless steel test joint with two exceptions:

1. rather than being threaded, the back plate had countersunk holes to allow screw/nut fasteners (described in MIL-STD-QQS267) to be used, and

2. no dielectric spacers were used between the plates.

The cover and base plates of the joint assembly are shown in Figure 11. The fastener assembly, composed of #316 stainless steel screw, silicone tubing "boot," nylon washer, stainless steel washer and stainless steel nut, is shown in Figure 12.

The screw fasteners are electrically insulated from the test joint to enable the metal-to-metal joint to establish the electrical conductivity and to prevent a galvanic cell from being created between the stainless steel fasteners and the aluminum plates. The conductive sealant was applied to the base plate of the test joint as shown in Figure 13. The cover plate was then fastened to the base plate with the screw fastener assembly and torqued to 13 inch-lbs using a torque wrench, as illustrated in Figure 14. The insulation of the screw fasteners was tested by verifying with an ohmmeter than an "open" connection was measured between the screws and the cover plate and between the nuts and the base plate, as illustrated in Figure 15.

3.2.2 Measurement Results of DC Resistance Versus Exposure in Salt Spray Chamber

The salt spray exposure tests for each conductive sealant material were performed with the set of five aluminum test joints. Four of the five test joints were loaded with conductive sealant, and the other test joint (called the control joint) used no sealant. Curing of the sealant was monitored by measuring the resistance across the test joint with a double Kelvin bridge milliohmmeter, as shown in Figure 16. The resistance would decrease with time -- typically stabilizing after 24 hours, at which time the material was cured. The lack of melting transitions from differential scanning calorimetry was also used to indicate total cross linking or curing.

The five (four sealant and one control) test joints were placed in an Atlas Salt Spray (Fog) Chamber, as shown in Figure 17, and exposed to the environment specified in ASTM B117. The salt spray unit was operated continuously, and the resistance of the joints was measured at 24 intervals. The overall dc resistance versus weathering results are tabulated in Table 4. Shown in this table are the dc resistance values (mean and standard deviation) for the control samples and the sealant sample at t = 0 and t = 1000 hours. In general, it can be seen that:

1. the conductive sealant samples outperformed the control (no sealant) sample;
2. the Ag/Al and stainless steel-filled sealants outperformed the aluminum-filled sealants, and

3. the Ag/Al-filled polysilicone RTV sealant had superior dc resistance versus weathering characteristics to the other materials tested.

For example, the dc resistance versus salt fog exposure time for the Chomerics #1038 polysilicone RTV filled with silver-coated aluminum powder is shown in Figure 18. The resistance of the sealed joints stayed extremely low (on the order of 0.1 milliohms), whereas the resistance of the control joint increased measurably after 96 hours, as shown in Figure 19.

3.2.3 Measurement Results of Shielding Effectiveness Versus Exposure in Salt Spray Chamber

Shielding effectiveness measurements were made at periodic time intervals on two of the five conductive sealant materials shown in Table 4: (1) the Al/Ni-filled polysulfide sealant (Products Research Proseal RW2-28-71) and (2) the aluminum-filled polyurethane sealant (Chomerics #4329-25-2). Shielding effectiveness was measured over the 500-1000 MHz frequency range using the test procedure outlined in Section 2.2.3.

The individual shielding effectiveness results were averaged over frequency and plotted as a function of salt fog chamber exposure time. The overall results for the Al/Ni-filled polysulfide RTV sealant and the aluminum-filled polyurethane RTV sealant are shown in Figures 20 and 21, respectively, which show the mean (denoted with a dot or star) and standard deviation (denoted with a vertical line and horizontal end caps) of the shielding effectiveness data. It can be seen from Figure 20 that the shielding effectiveness of the Al/Ni-filled polysulfide material slowly degraded from approximately 95 dB at t = 0 to approximately 87 dB after nearly 1000 hours' exposure time. The shielding performance of the stainless steel-filled polysulfide RTV test samples were far superior to the control samples, which also began (at t = 0) at approximately 95 dB but degraded more rapidly to approximately 68 dB after 1000 hours of exposure.

It can be seen from Figure 21 that the shielding effectiveness of the aluminum-filled polyurethane RTV sealant degraded from approximately 97 dB at t = 0 to approximately 87 db after only 360 hours of salt fog exposure time. (In this case, the weathering tests were terminated after 360 hours due to the presence of severe corrosion and high dc resistance readings for the test samples.) It is interesting to note that, despite the presence of severe corrosion products and high dc resistance values, the shielding effectiveness of the sealant samples degraded only 10 dB. Also note that the control samples had a mean value of shielding effectiveness equal to approximately 60 dB after 1000 hours, despite the very high resistance values and severe corrosion that took place in these joints. The primary

reason for these surprisingly high shielding effectiveness values is believed to be the small separation distance between the plates. For example, extrapolating the curve in Figure 9 to smaller plate separation distances, the shielding effectiveness of 68 dB, which was obtained for the control samples after 1000 hours, could be obtained with zero dc conductivity (i.e., an open circuit between the plates) provided that the plate separation distance were on the order of 5 microns. It should be noted, however, that poorer shielding performance could be expected at microwave frequencies unless uniform electrical continuity is maintained across the entire joint to achieve a low RF bond impedance.

3.3 Summary of Optimum Conductive Sealant Materials

The objective of this task was to identify and evaluate optimum corrosion prevention materials for use on nuclear hardened aircraft and weapon systems. New test joints were designed and fabricated out of 7075 aluminum and fastened using realistic torque values. The aluminum test joints were loaded with five different sealant materials and weathered in a salt spray environment according to ASTM B117. The dc resistance and shielding effectiveness of selected test joints were measured before weathering tests began and periodically during the weathering tests to monitor the corrosion effects on the electrical and electromagnetic performance of the bonds. In addition, control joints (no sealant) were weathered and tested simultaneously to compare the relative merit of the selected sealant material.

In general, it was found that:

1. the conductive sealant samples outperformed the control (no sealant) samples,
2. The Ag/Al and Al/Ni-filled sealants outperformed the aluminum-filled sealants, and
3. the Ag/Al-filled polysilicone RTV sealant had superior weathering characteristics to the other materials tests.

Based on these data, it is recommended that aluminum fillers be avoided and that either silver-coated aluminum or stainless steel fillers be used with an appropriate matrix (e.g., polysilicone RTV or polysulfide) for applications with aluminum substrates. The use of appropriate conductive sealant materials will improve the long term effectiveness (both structural and electrical) of metal-to-metal bonds typically found on exposed surfaces of military aircraft and weapon systems.

4.0 Proposed Changes to Standards, Specification and Handbooks

A major task on this program was to develop proposed changes to military standards, specifications and handbooks to reflect the findings of the experimental investigations. The implementation of changes to military standards, specifications and handbooks is a lengthy and complex process requiring inputs and approvals from numerous groups and agencies. For this reason, the results of this task are proposed changes to the appropriate documents which can then be used as inputs to any modification proceedings. Each recommended change is in a format suitable for direct inclusion in the applicable document.

A large number of military standards, specifications and handbooks were reviewed to determine appropriate documents for consideration on this task. Table 5 is a list of documents which were considered pertinent for modification on this task. The eight documents identified with asterisks were selected as being most relevant for developing proposed changes. These eight documents were later finalized through mutual agreement with Warner Robins ALC/MMEMC. Once confirmation was received from WR-ALC/MMEMC, proposed changes to the mutually agreed upon documents were formulated. The findings and results of the other program tasks were used in the formulation of proposed modifications.

Based on the results obtained from the experimental investigations, a relaxation of the 2.5 milliohm requirement is neither justifiable nor does it appear necessary. The results of the empirical study of the relationship between dc resistance and shielding effectiveness (see Figure 6) indicate that relaxation of the bonding resistance requirement to 10 milliohms could result in a 20-30 dB reduction in shielding effectiveness (relative to a 2.5 milliohm bond) and that relaxation of the bonding resistance to 100 milliohms could result in a 40-55 dB reduction in shielding effectiveness. Furthermore, based on the empirical study of the effects of weathering on electrical performance of the bond, conductive sealants tested from two different vendors (Chomerics silver-coated aluminum-filled polysilicone RTV and Products Research Corporation Al/Ni-filled polysulfide) maintained a bonding resistance well under the 2.5 milliohm requirement with little or no corrosive performance degradation after 1000 hours in the salt fog environment per ASTM B117. Consequently, relaxation of the 2.5 milliohm requirement was not recommended as part of the proposed modifications.

The reader is referred to the Final Reports of Georgia Tech Research Institute, No. A-4324, and Contract No. F02060-85-66007, WR-ALC, Robins Air Force Base.

REFERENCES

(1) Private communications with WRAFB personnel.

(2) MIL-STD-285, "Attenuation Measurements for Enclosures, Electromagnetic Shielding, for Electronic Test Purposes, Method of," 25 June 1956.

(3) ASTM B117, Salt Spray Cabinet, Method A.

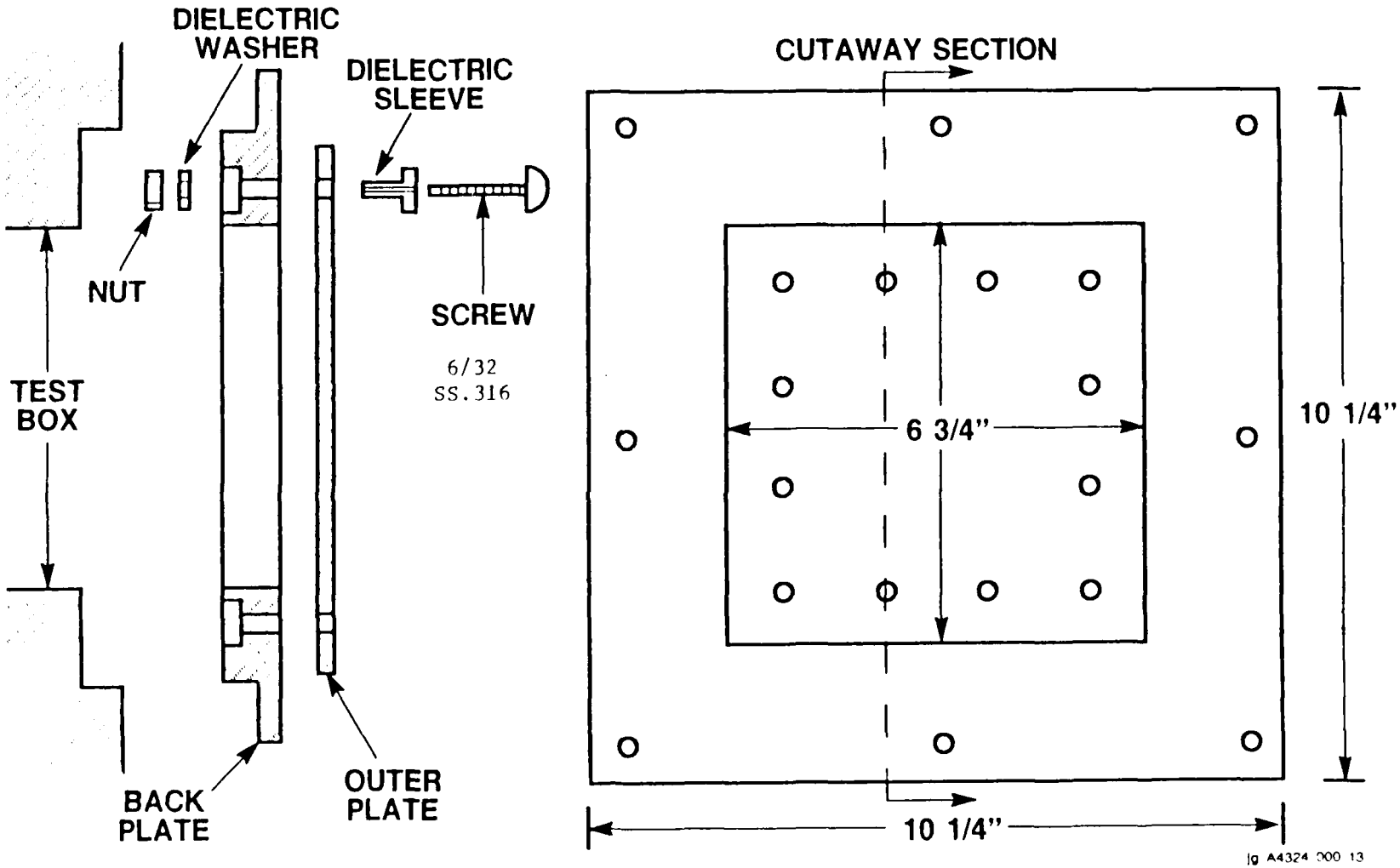

FIGURE 1. SKETCH OF STAINLESS STEEL TEST JOINT

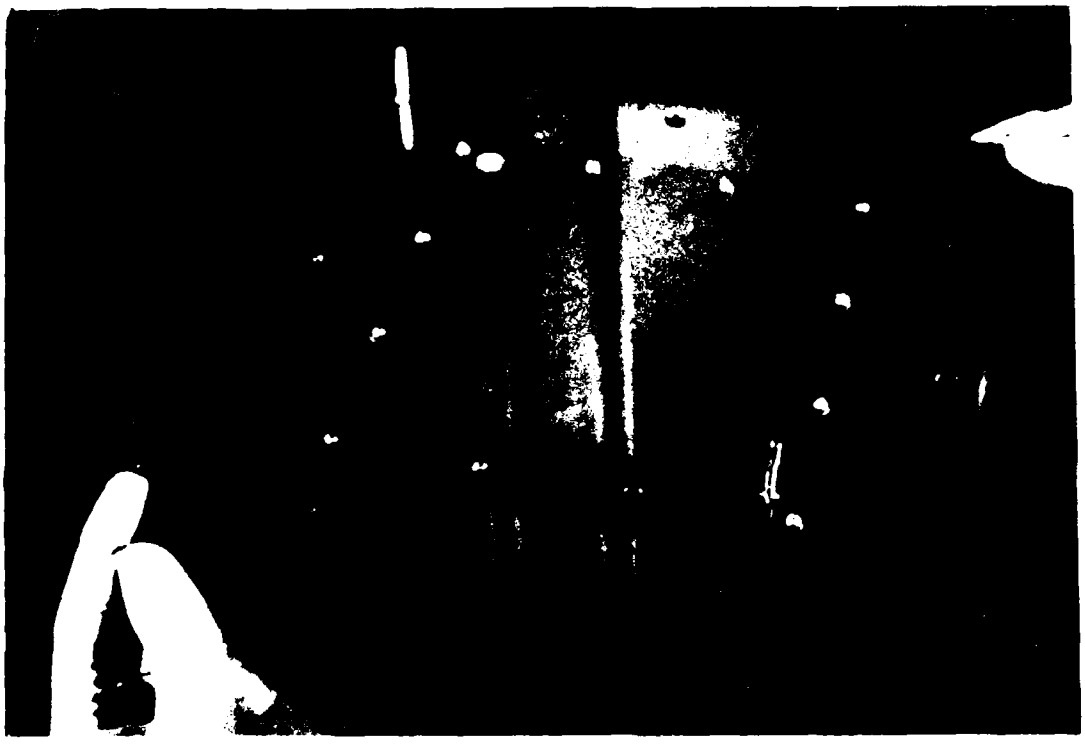

FIGURE 2. FRONT VIEW OF STAINLESS STEEL TEST JOINT

FIGURE 3. REAR VIEW OF STAINLESS STEEL TEST JOINT

FIGURE 4. SIDE VIEW OF STAINLESS STEEL TEST JOINT

TABLE 1. CONDUCTIVE SEALANTS USED TO VARY RESISTANCE OF TEST JOINT

Conductive Sealant Identification	Resistivity, ohm cm	
	10-15 mil	2 mil
1. 2-Part Urethane	--	777
2. Moisture cure Urethane	400	140
3. Moisture cure Urethane	77	76
4. Moisture cure Urethane	23	0.07
5. Moisture cure Urethane	60K	178

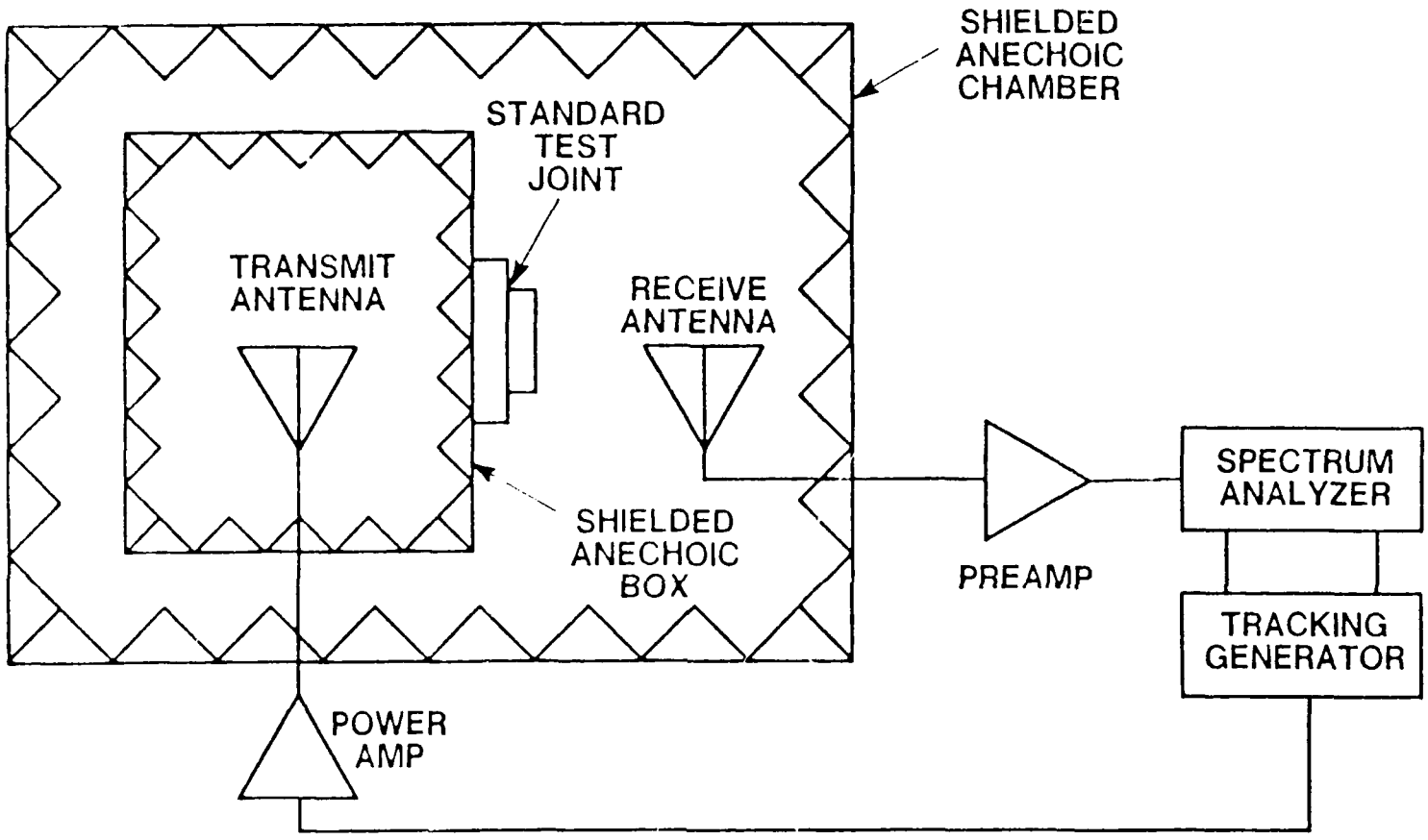

$$S.E.\ (dB) = 10\ LOG\ [P_R(WITHOUT\ SAMPLE) / P_R\ (WITH\ SAMPLE)]$$

FIGURE 5. BLOCK DIAGRAM OF THE SHIELDING EFFECTIVENESS TEST SETUP

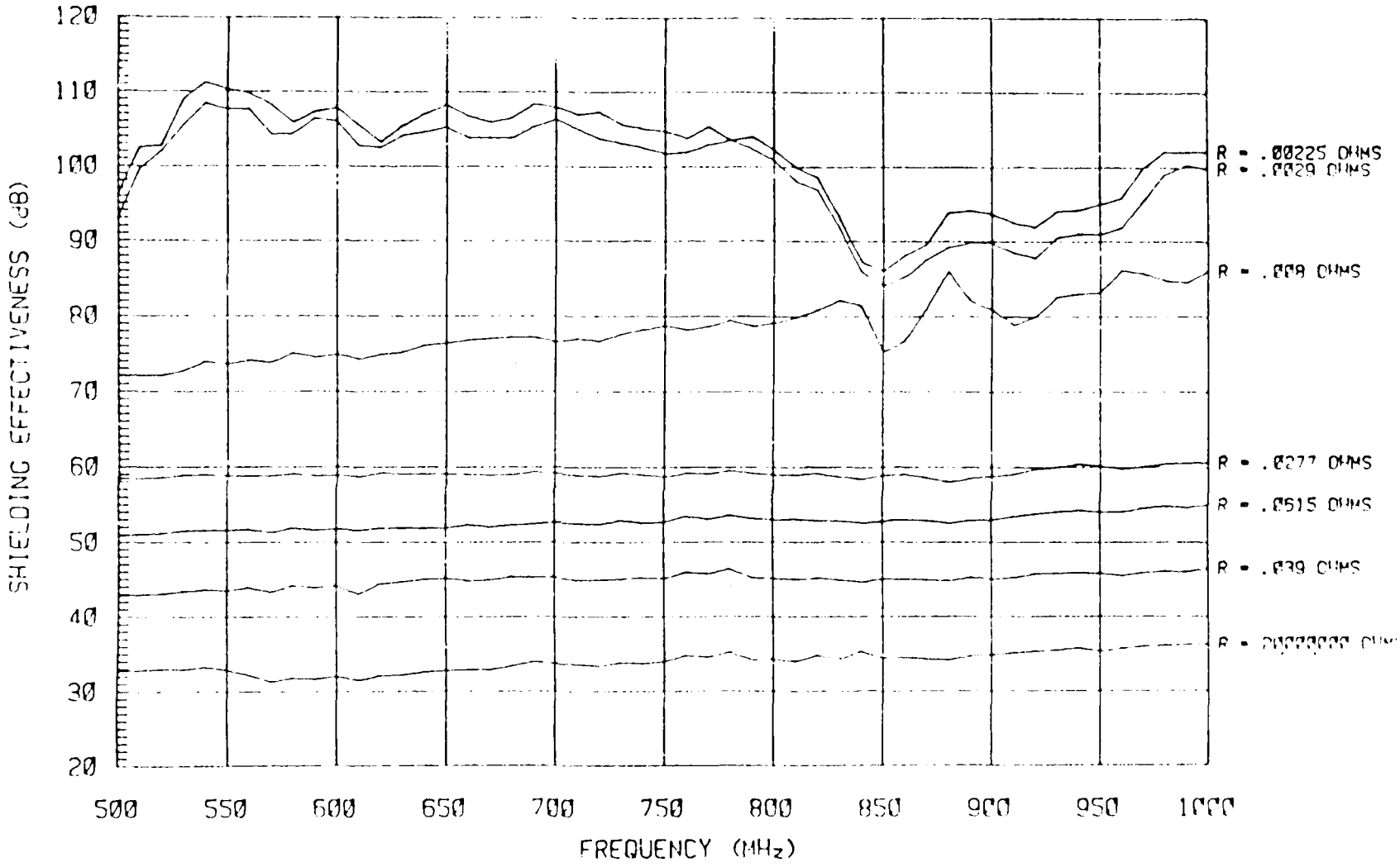

FIGURE 6. SHIELDING EFFECTIVENESS VS. FREQUENCY FOR DIFFERENT BOND RESISTANCES

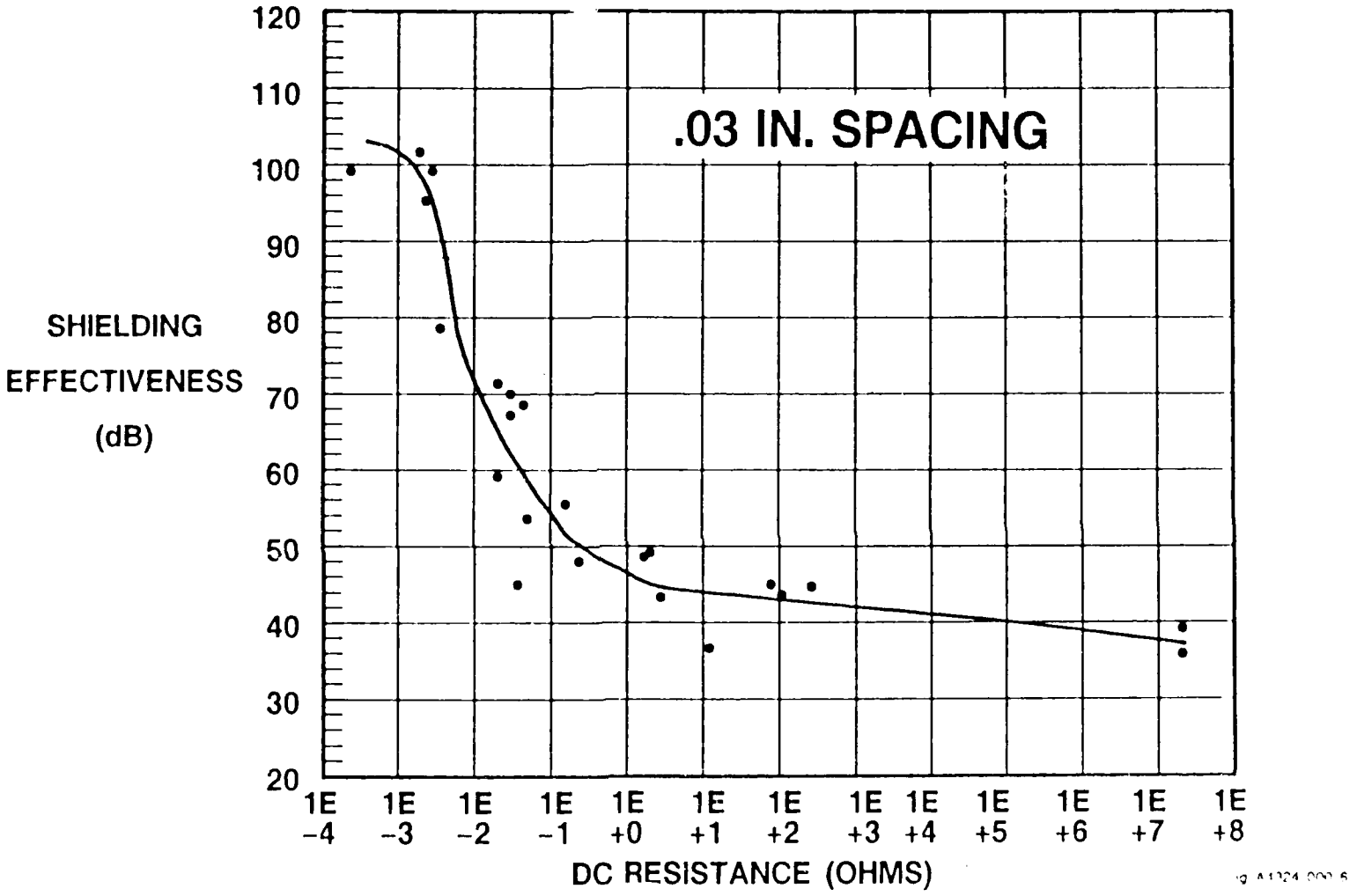

FIGURE 7. SHIELDING EFFECTIVENESS VERSUS DC RESISTANCE

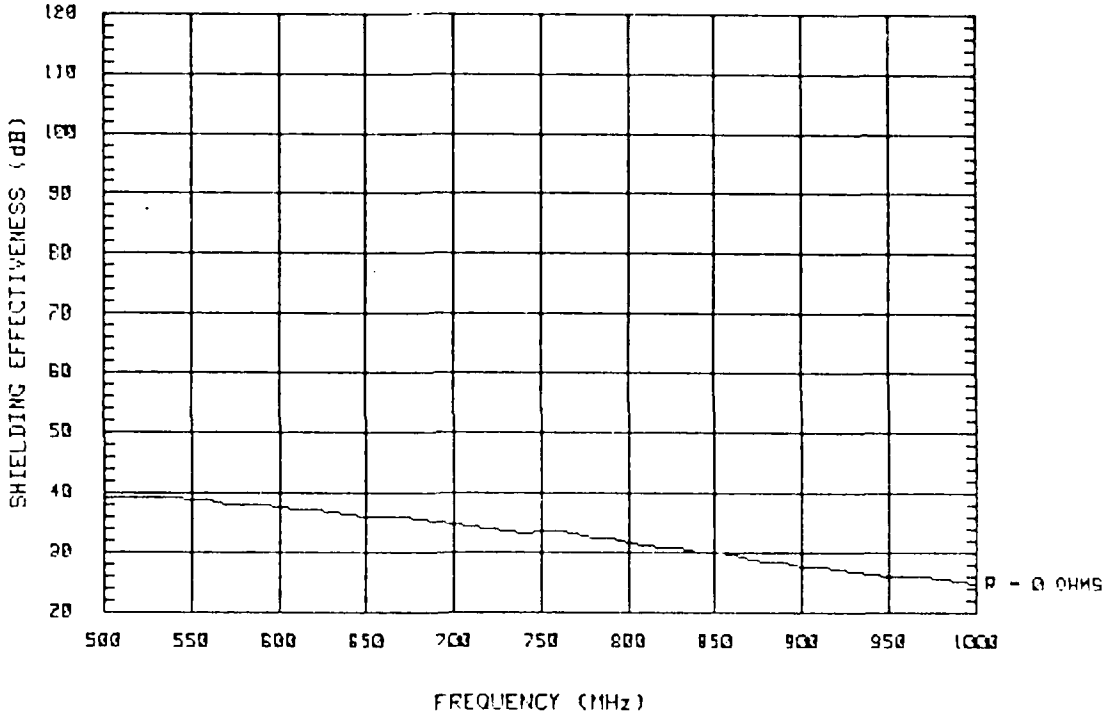

FIGURE 8. SHIELDING EFFECTIVENESS PLOT FOR TEST SAMPLE WITH PLATES SHORT-CIRCUITED TOGETHER THROUGH SCREW FASTENERS BUT HAVING 2.5 MM PLATE SEPARATION

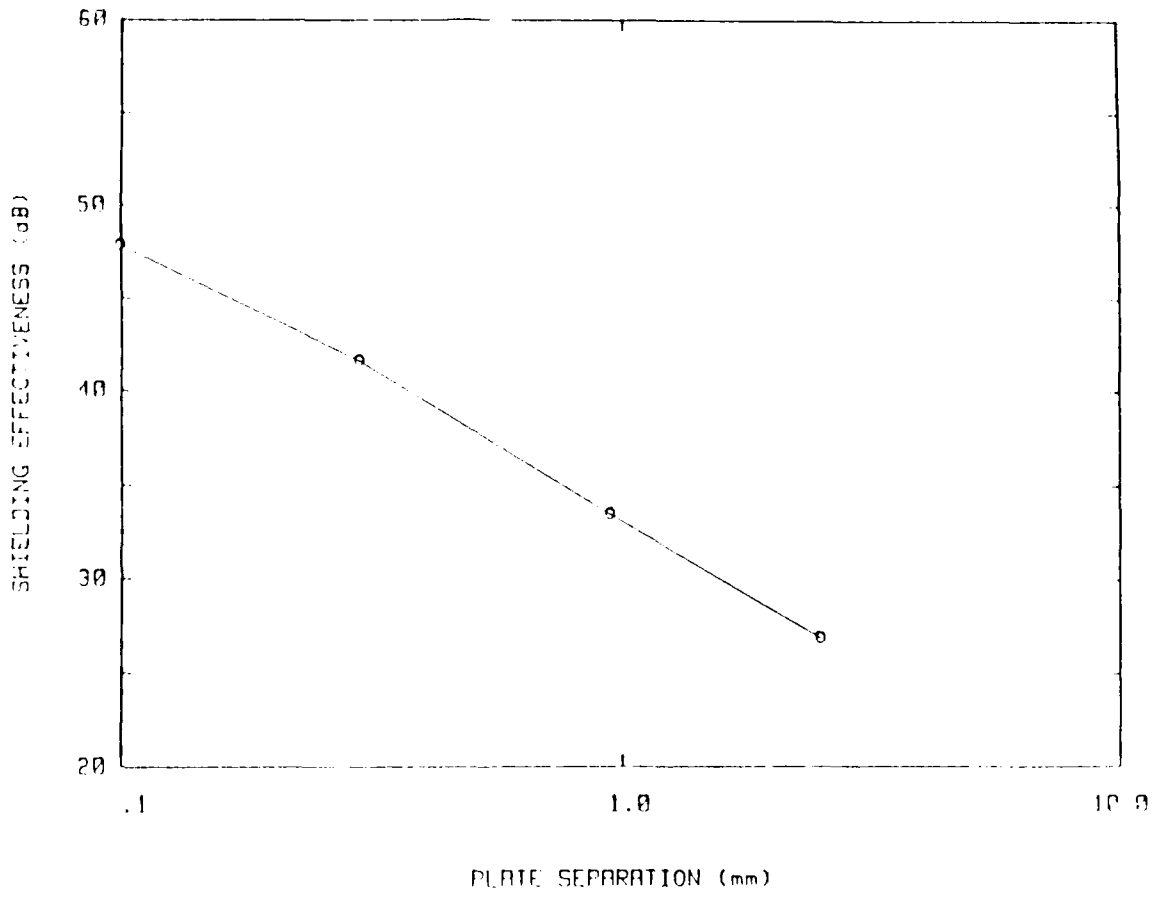

FIGURE 9. SHIELDING EFFECTIVENESS VERSUS PLATE SEPARATION DISTANCE

FIGURE 10. SILVER-COATED GLASS SPHERES AND DAMAGE TO COATING FROM CURRENT OVERLOAD

TABLE 2. CORROSION POTENTIALS OF VARIOUS METALS AND EM GASKET MATERIALS (IN 5% NaCl AT 21°C AFTER 15 MINUTES OF IMMERSION)

MATERIAL	E_{CORR} VS SCE [1] (MILLIVOLTS)
PURE SILVER	-25
SILVER-FILLED ELASTOMER	-50
MONEL MESH	-125
SILVER-PLATED-COPPER FILLED ELASTOMER	-190
COPPER	-244
TIN-PLATED BERYLLIUM-COPPER	-440
TIN-PLATED COPPER-CLAD STEEL MESH	-440
ALUMINUM[2] (1100)	-730
SILVER-PLATE -ALUMINUM FILLED ELASTOMER	-740

[1] GALVANIC POTENTIAL OF TEST CELL MEASURED WITH STANDARD CALOMEL ELECTRODE AS A REFERENCE

[2] ALUMINUM ALLOYS APROXIMATELY -700 TO -840 mV VS SCE IN 3% NaCl. MANSFIELD F. AND KENKEL, J.V., LABORATORY STUDIES OF GALVANIC CORROSION OF ALUMINUM ALLOYS, "GALVANIC AND PITTING CORROSION - FIELD AND LAB STUDIES, ASTM STP 576, 1976, PP. 20-47.

TABLE 3. CONDUCTIVE SEALANT MATERIALS SELECTED FOR TESTING

CONDUCTIVE SEALANT	MANUFACTURER
1. POLYSILICONE RTV #1038, Ag/Al* FILLER	CHOMERICS, INC.
2. POLYSILICONE RTV #1038, Al** FILLER	CHOMERICS, INC.
3 POLYURETHANE RTV #4329-25-1, Ag/Al FILLER	CHOMERICS, INC.
4 POLYURETHANE RTV #4329-25-2 Al FILLER	CHOMERICS, INC.
5. PROSEAL #872 POLYSULFIDE, Al FILLER	PRODUCTS RESEARCH CORP.
6. PROSEAL RW2-28-71 Al / Ni	PRODUCTS RESEARCH CORP.

* SILVER COATED ALMINUM POWDER

** ALUMINUM POWDER

TABLE 4 - MEAN ($\bar{x}$) AND STANDARD DEVIATION (σ) OF DC RESISTANCE VERSUS SALT SPRAY (CHAMBER FOG EXPOSURE TIME

SEALANT MATERIAL	MANUFACTURER	DC RESISTANCE (OHMS) 0 HOURS	1000 HRS
NONE (CONTROL)	--	$\bar{x}$ = 1.0E-4	22-
POLYSILICONE #1038, Ag/Al[1]	CHOMERICS	$\bar{x}$ = 1.0E-4[6] σ = 0	$\bar{x}$ = 1.12E-4[6] σ = 0.22 E-4[7]
POLYURETHANE #4329-25-1, Ag/Al[1]	CHOMERICS	$\bar{x}$ = 1.43E-4 σ = 0.78E-4	$\bar{x}$ = 3.63 E-1 σ = 4.64 E-1
POLYURETHANE #4329-25-2, Al[2,4]	CHOMERICS	$\bar{x}$ = 1.0E-4[6] σ =	$\bar{x}$ = 21[7] σ =
POLYURETHANE #872, Al [2,5]	PRODUCT RESEARCH	$\bar{x}$ = 1.63E-4 σ = 1.63E-4	$\bar{x}$ = [illegible][4] σ = [illegible]
PROSEAL POLYSULFIDE RW-2126-[illegible], STAINLESS STEEL [3]	PRODUCT RESEARCH	$\bar{x}$ = [illegible] σ = [illegible]	$\bar{x}$ = [illegible] σ = [illegible]

(1) SILVER-COATED ALUMINUM [illegible] FILLER

(2) ALUMINUM POWDER FILLER

(3) STAINLESS STEEL [illegible] FILLER

(4) TESTS TERMINATED AFTER [illegible] DUE TO SEVERE CORROSION

(5) TESTS TERMINATED AFTER [illegible] DUE TO SEVERE CORROSION

(6) ACTUAL VALUE LOWER THAN THAT INDICATED DUE TO LIMITED RANGE OF INSTRUMENTATION

(7) ACTUAL VALUE GREATER THAN THAT INDICATED DUE TO LIMITED RANGE OF INSTRUMENTATION

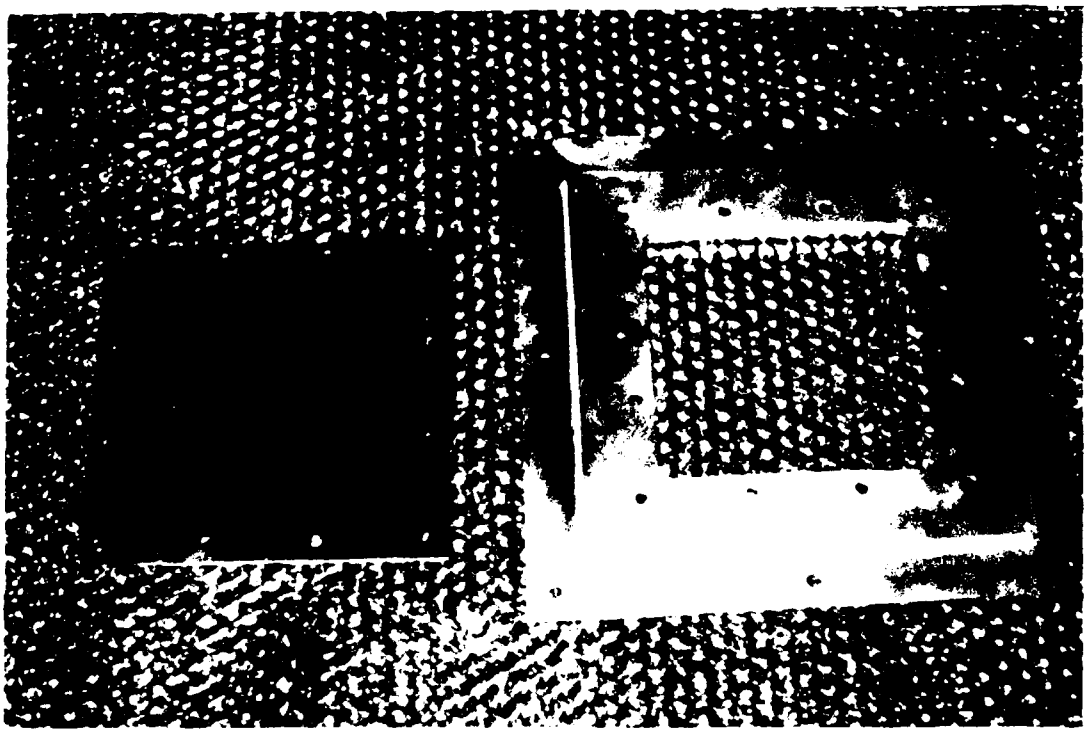

FIGURE 11 TEST JOINT BASE PLATEE (REAR SIDE) AND COVER, POLISHED TO REMOVE OXIDES AND SURFACE DEFECTS, AND CLEANED WITH METHANOL. THE ALUMINUM FLAT SHEET #7065 -76 WAS USED FOR FABRICATIO OF EACH JOINT. THE ALUMINUM FLAT SHEET WAS CERTIFIED PER FEDERAL SPECIFICATION QQ-A-250/12.

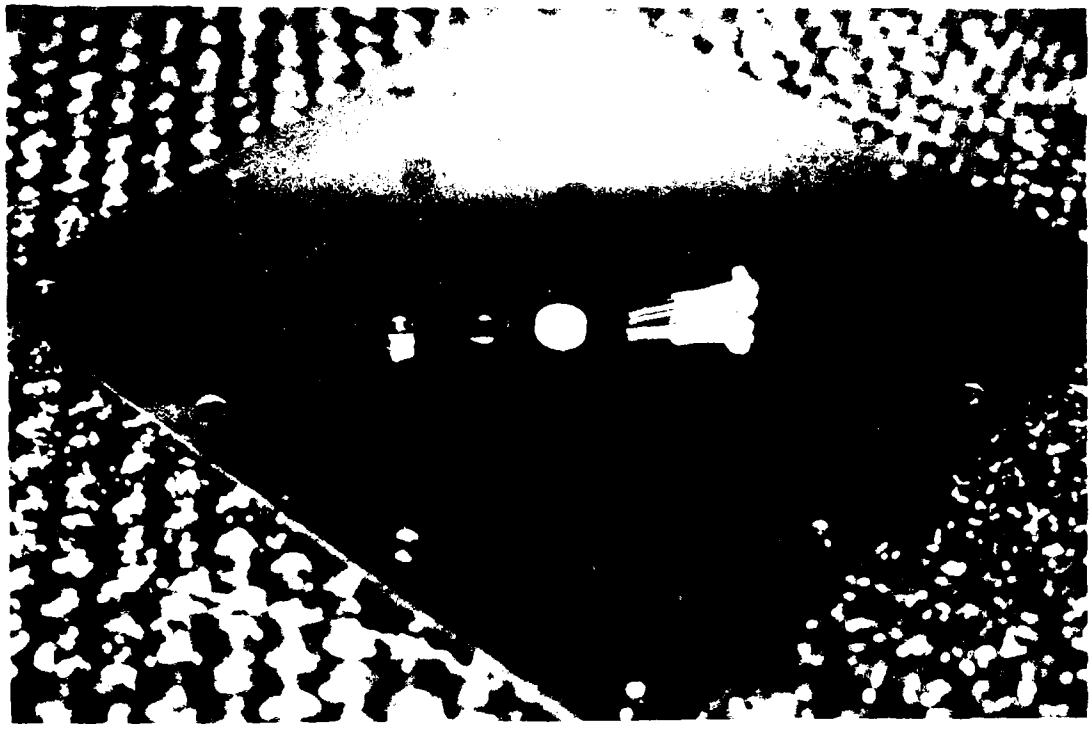

FIGURE 12 FASTENER ASSEMBLY: (1) STAINLESS STEEL #316 6/32 ROUND SLOTTED SCREW INSULATED WITH #6 STAINLESS STEEL WASHER AND; (4) 6/32 HEX-TYPE STAINLESSTEEL NUT. EACH ASSEMBLY WAS TORQUEED TO 13 INCHED-LBS.

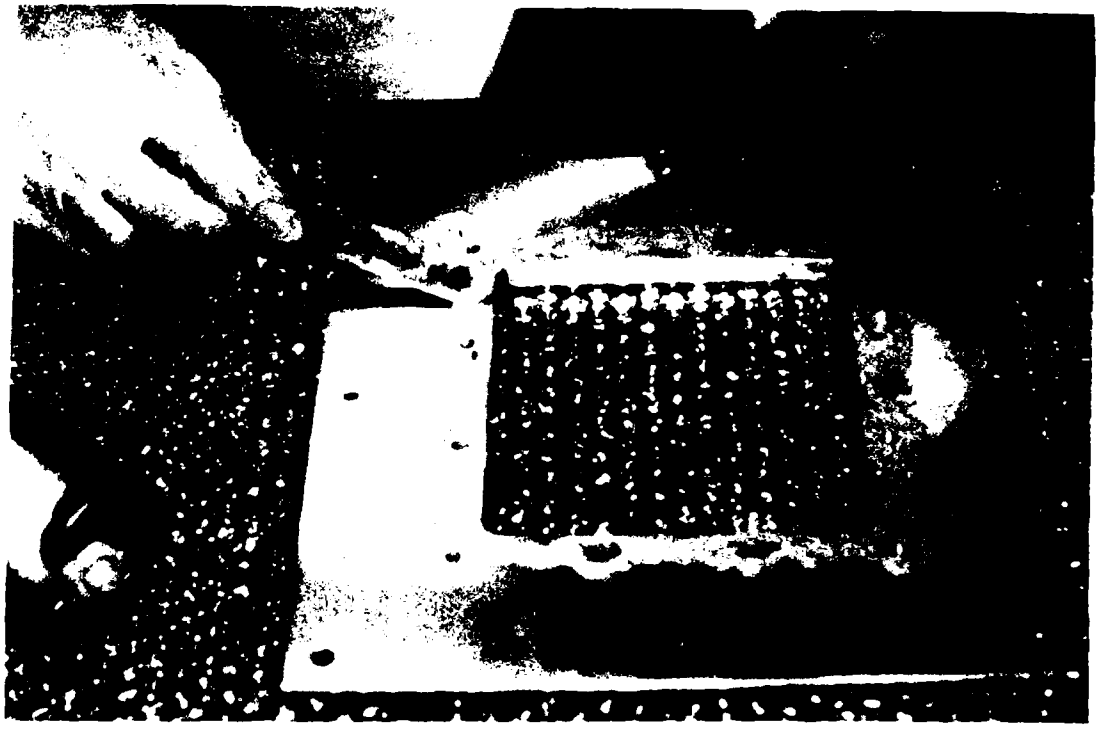

FIGURE 13. APPLICATION OF CONDUCTIVE SEALANT (#1038 Ag/A1 IN RTV POLYSILICONE) APPLIED TO BASE PLATE OF JOINT (FRONT SIDE). THE SEALANTS ARE TYPICALLY VISCOUS AND REQUIRE TROWELING TO COVER THE JOINT AREA.

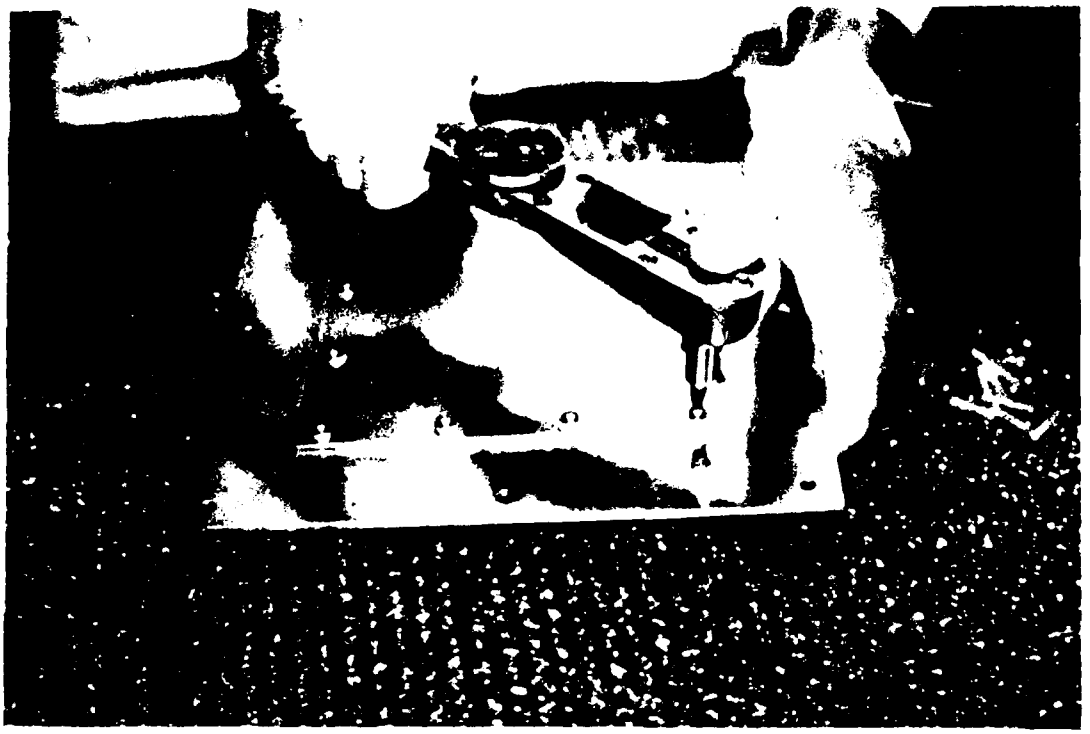

FIGURE 14 FASTENER ASEMBLY TORQUED TO 13 INCH-LBS USING A TORQUE WRENCH

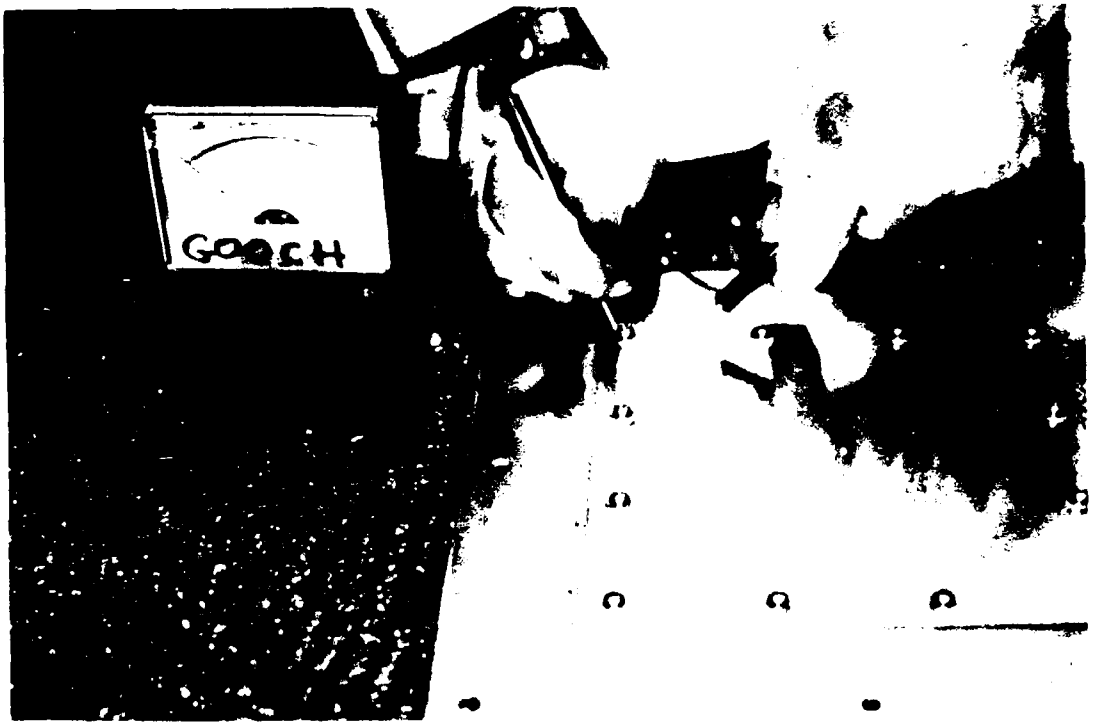

FIGURE 15 TESTING OF INSULATION FASTENER ASSEMBLY WITH OHM-METER

FIGURE 16 RESISTANCE MEASUREMENT OF TEST JOINT USING A GENERAL ELECTRIC DOUBLE KELVIN BRIDGE MILLIOHM-METER

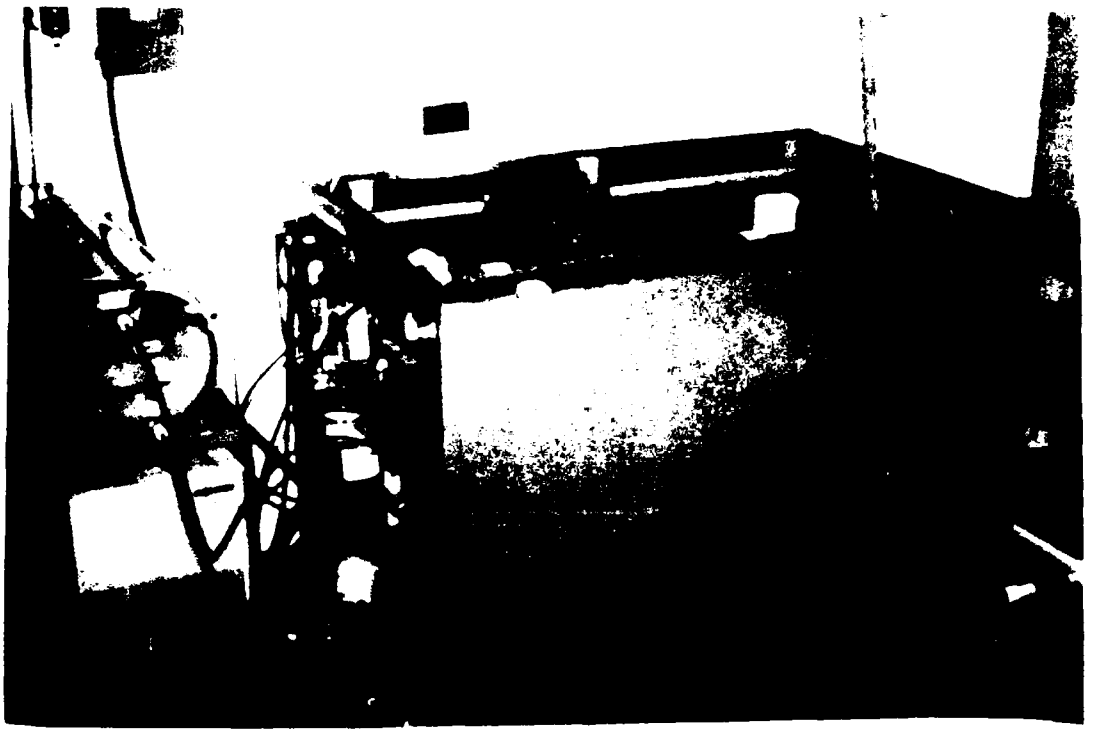

FIGURE 17 ATLAS SALT SPRAY (FOG) CABINET (ASTM B117) FOR CORROSION TESTING OF ALUMINUM JOINTS

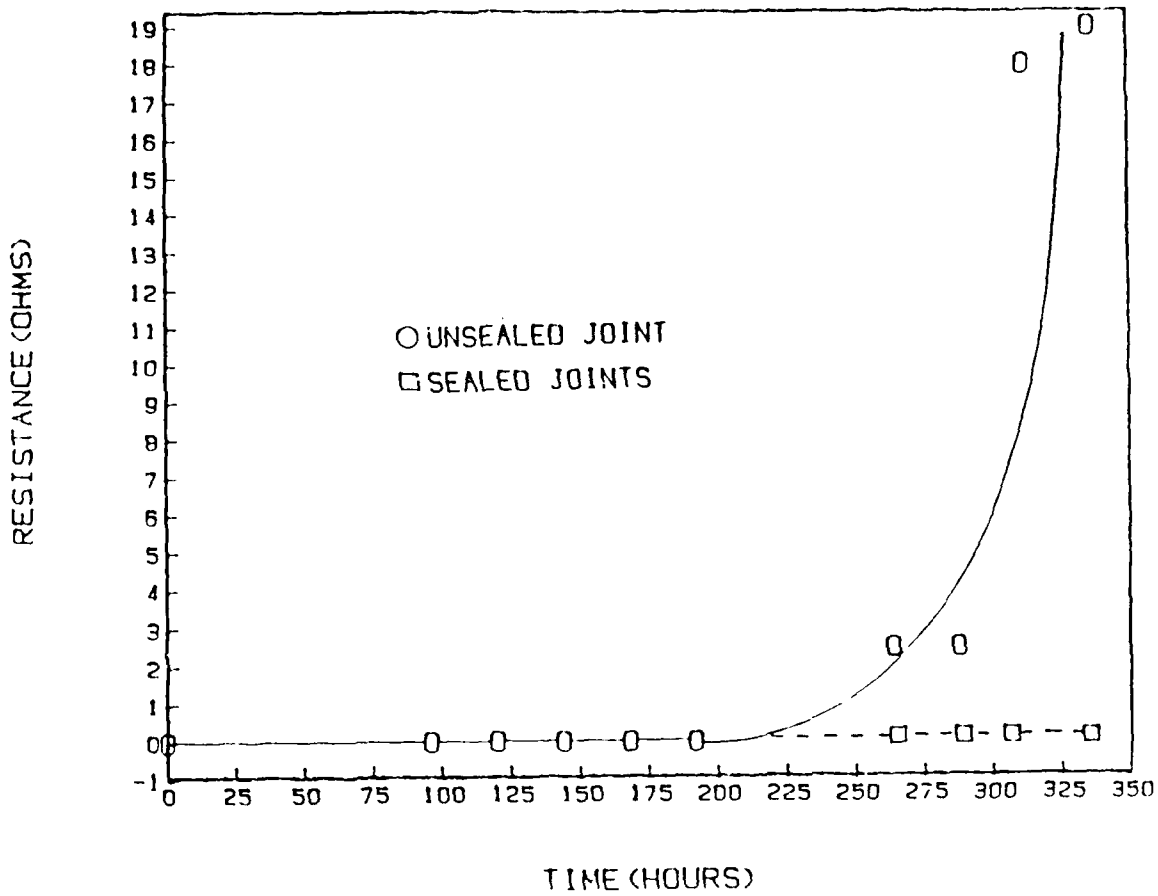

FIGURE 18. DC RESISTANCE VERSUS SALT SPRAY EXPOSURE TIME FOR CONTROL AND CHOMERICS #1038 JOINTS.

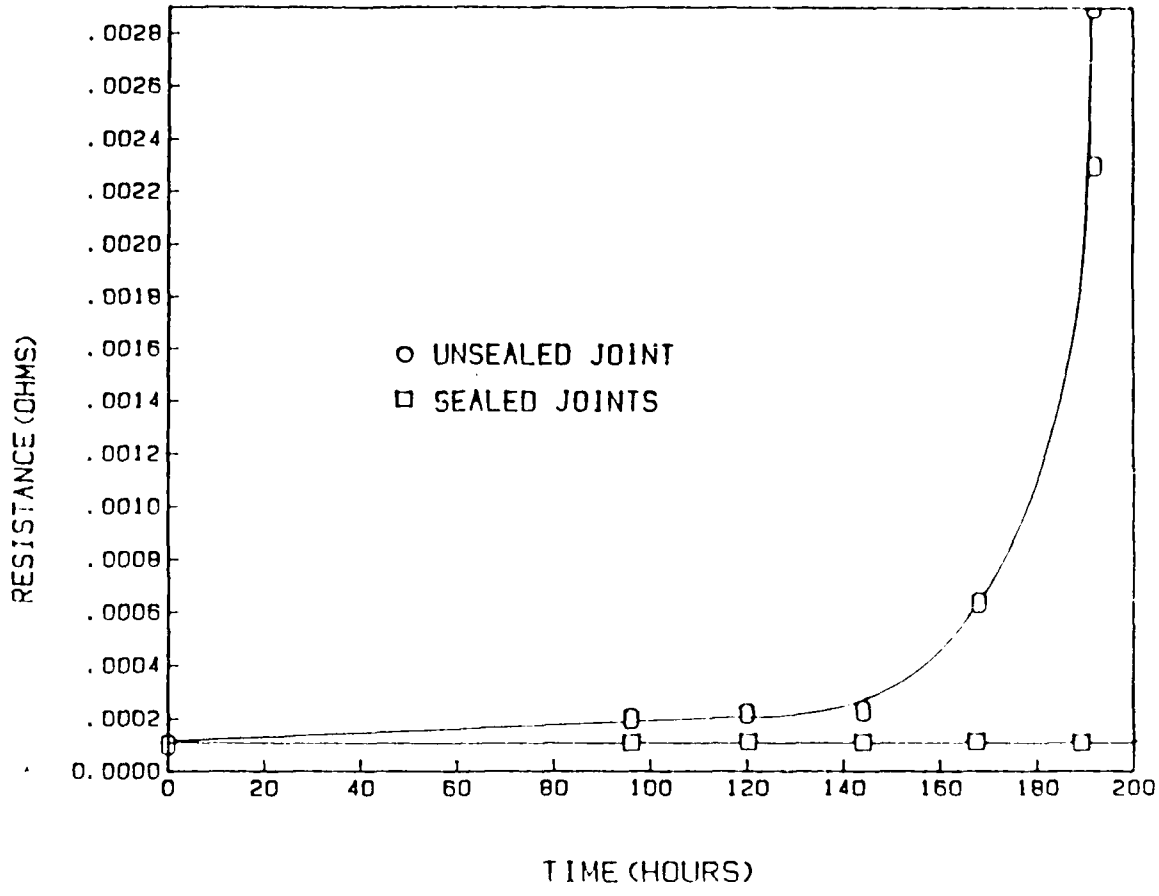

FIGURE 19. DC RESISTANCE VERSUS SALT SPRAY EXPOSURE TIME FOR CONTROL AND CHOMERICS #1038 JOINTS (LOW RESISTANCE REGION).

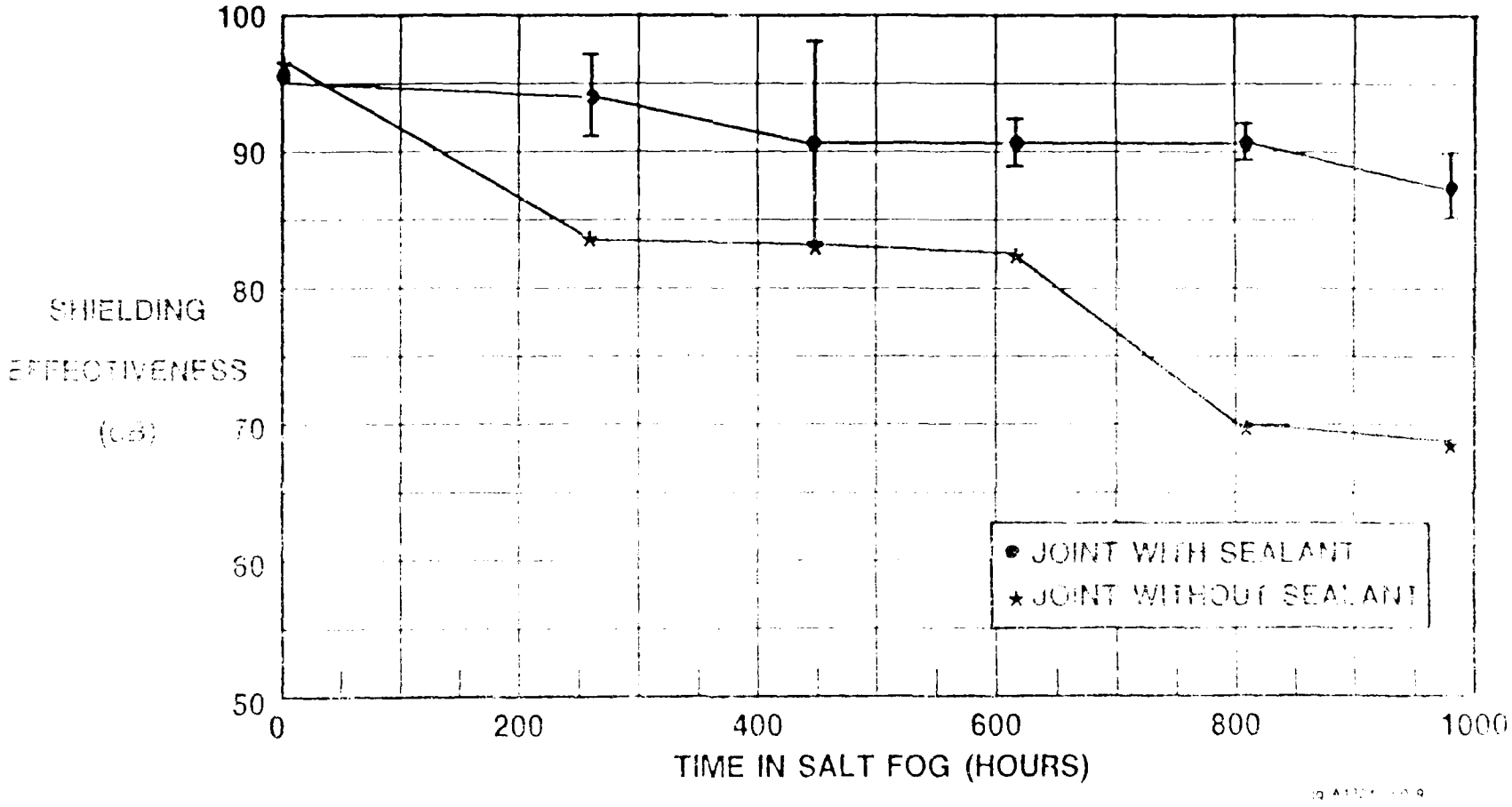

FIGURE 20. SHIELDING EFFECTIVENESS OF CONTROL AND PRODUCTS RESEARCH CORP #RW2-28-71 TEST JOINTS VERSUS SALT SPRAY EXPOSURE TIME

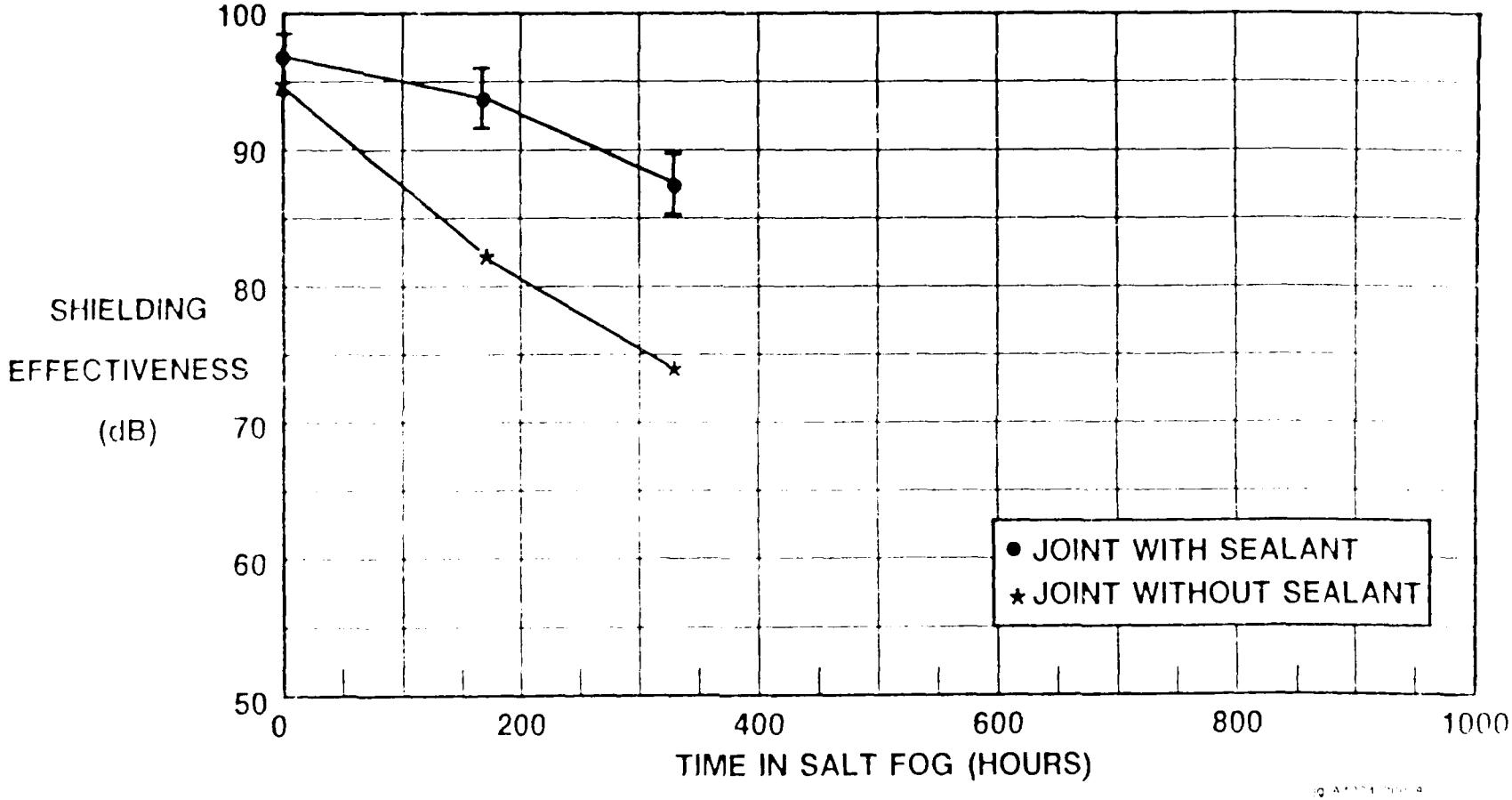

FIGURE 21. SHIELDING EFFECTIVENESS OF CONTROL AND ALUMINUM - FILLED POLYURETHANE TEST JOINTS VERSUS SALT SPRAY EXPOSURE TIME

TABLE 5. DOCUMENTS UNDER CONSIDERATION FOR TASK 3

DOCUMENT IDENTIFIER	DOCUMENT TITLE
MIL-B-5087B*	BONDING, ELECTRICAL, AND LIGHTNING PROTECTION FOR AEROSPACE SYSTEMS
MIL-STD-188-124A*	GROUNDING, BONDING AND SHIELDING
MIL-STD-1310D	SHIPBOARD BONDING, GROUNDING, AND OTHER TECHNIQUES FOR ELECTROMAGNETIC CAPABILITY AND SAFETY SHIELDING
MIL-STD-1542*	ELECTROMAGNETIC COMPATIBILITY (EMC) AND GROUNDING REQUIREMENTS FOR SPACE SYSTEM FACILITIES
MIL-STD-1857	GROUNDING, BONDING, AND SHIELDING DESIGN PRACTICES
MIL-STD-454J*	STANDARD GENERAL REQUIREMENTS FOR ELECTRONIC EQUIPMENT
MIL-STD-462	ELECTROMAGNETIC INTERFERENCE CHARACTERISTICCS, MEASUREMENT OF
MIL-HDBK-253	GUIDANCE FOR THE DESIGN AND TEST OF SYSTEMS PROTECTED AGAINST THE EFFECTS OF ELECTROMAGETIC ENERGY
MIL-E-6051D	ELECTROMAGNETIC COMPATIBILITY REQUIREMENTS, SYSTEMS
NATO STANAG	BONDING AND IN-FLIGHT LIGHTNING PROTECTION FOR AIRCRAFT
MIL-STD-1541*	ELECTROMAGNETIC COMPATIBILITY REQUIREMENTS FOR SPACE SYSTEMS
AFSC DH 1-4*	ELECTROMAGNETIC COMPATIBILITY
MIL-HDBK-335	MANAGEMENT AND DESIGN GUIDANCE, ELECTROMAGNETIC RADIATION HARDNESS FOR AIR LAUNCHED ORDINANCE SYSTEMS
DARCOM-P 706-410	ENGINEERING DESIGN HANDBOOK, ELECTROMAGNETIC COMPATIBILITY
NAVAIR AD 1115	ELECTROMAGNETIC COMPATIBILITY DESIGN GUIDE FOR AVIONICS AND RELATED GROUND SUPPORT EQUIPMENT
DCA NOTICE 310-70-1	DCS INTERIM GUIDANCE ON GROUNDING BONDING, AND SHIELDING
MIL-HDBK-419	GROUNDING, BONDING, AND SHIELDING FOR ELECTRONIC EQUIPMENTS AND FACILITIES

* DOCUMENTS FOR WHICH MODIFICATIONS WERE PROPOSED

Georgia Institute of Technology
Georgia Tech Research Institute

BIOGRAPHICAL SKETCH

GOOCH, JAN W.--Senior Research Scientist
Energy and Materials Sciences Laboratory

Education

Ph.D., Polymer Science, University of Southern Mississippi	1980
B.S., Chemical Engineering, Arkansas Polytechnic College	1971

Employment History

Georgia Institute of Technology Senior Research Scientist	1983-Present
Cook Paint & Varnish Co., Group Leader	1982
Bechtel Group, Inc., Senior Engineer	1979-1982
Wrape Enterprises, Inc., Technical Director	1971-1976

Experience Summary: At Georgia Tech, conducts applied research in coatings and polymer science in the Materials Science Division of the Energy and Materials Sciences Laboratory. With Cook Paint & Varnish, performed and supervised research and development of resins for industrial coatings and fiber-glass composites. At Bechtel, provided technical services in areas of industrial coatings and polymeric materials. Graduate research at the University of Southern Mississippi involved polymer synthesis, characterization, kinetics studies, viscometry and coatings formulation. As Technical Director with Wrape Enterprises, performed research and development in industrial air pollution control systems.

Current Fields of Interest

Polymer-solvent intermolecular reactions; design and testing of composite materials; water-borne and high solids coatings for corrosion protection of metal substrates in chemically aggressive atmospheres; dispersion technology for generating polymer/solid and polymer/polymer systems, filled polymers and interpenetrating polymeric networks materials.

Professional Affiliations

American Chemical Society
National Association of Corrosion Engineers
Society of Plastics Engineers
Sigma Xi Scientific Research Society
Southern Society of Coatings Technology
Who's Who in Frontiers of Science and Technology

Patents:

1. "A Process for Generating Coatings by Autoxidatively Polymerizing Emulsified Oils and Alkyds," U.S. Patent 4,119,130, with C. G. Bufkins and G. C. Wildman

Patents (continued):

2. "A Process of Nucleating and Collecting Dust Particles by Injecting Aerosolized Liquids in an Air Stream, U.S. Patent No. 3,993,460 (1976), with A. J. Wrape, Jr.
3. "A Process for Extracting Organic Waste from Industrial Effluent by Treatment with Dissolved Ammonia," U.S. Patent No. 3,803,290 (1973)
4. "A Process for Agglomerating and Coagulating Waste Material," (1971); initially filed 1968, Under same title: U.S. Patent No. 3,586,627 and 3,733,269; Mexico 109,571; Canada 905,027; Great Britain 1,259,821; Australia 417,206, with P. P. Paladino

Major Reports and Publications

1. "Investigation of Acrylonitrile-Butadiene-Styrene Resins for Manufacture of Plastic Pipe," Final Report prepared for Slocomb Pipe Company of Atlanta, Georgia, 21 October 1985
2. "Thermal Techniques for Service Evaluation of Polymer and Coating Materials," presented at the 14th Annual Conference, North American Thermal Analysis Society, San Francisco, CA, September 1985
3. "Characterization fo Magnetic Dispersions," Journal of Coating Technolgoy (in press), 1985
4. "Dewaxing, Slurry Adhesion and Inclusion Identification in Investment Molding," Final Report, TRW Corporation, Douglas, GA, July 1985
5. "Testing of Polymeric Films and Resins," Final Report, Gateway Plastics Company, Doraville, GA, June 1985
6. "Evaluation of Crumpled Thin Films for TREESS Application, and Thin Films for Reflecting Thermal Infrared for TREESS", with T. B. Wells, J. P. Montgomery, and T. L. Starr, Final Report, U. S. Army Mobility Equipment Research and Development Command Procurement and Production Directorate, Ft. Belvoir, Virginia, April 1984
7. "Autooxidative Crosslinking of Vegetable Oils and Alkyd Emulsions", with G. C. Wildman and B. G. Bufkin, Journal of Coatings Technology, Vol. 56, No. 711, April 1984
8. "Field Microscope and Coatings", J. W. Gooch, Coatings Magazine, March 1984 and Corrosion Control, March 1984
9. "Thermal Analysis of Coatings," Presented at the Practical Thermal Analysis Symposium sponsored by the Society of Plastics Engineers, March 1984, Georgia Institute of Technology
10. "Studies of Magnetic Particle Dispersion Mechanisms", with B. R. Livesay, Final Report prepared for TDK Electronics Co., Ltd. of Tokyo, Japan, December 1983
11. "Field Microscopy for Improved Inspection of Cleaned and Coated Steel," Presented at the 3rd World Contress - Coatings Systems for Bridges and Steel Structures, 2-3 November 1983, St. Louis, Missouri
12. "A Microscopic Examination of Abrasively Cleaned Steel Surfaces," Materials Performance, (in press)
13. "Processing of Emulsified Oils and Alkyds to Generate Polymers," Chapter in USE OF RENEWABLE MATERIALS FOR COATINGS AND PLASTICS, L. Sperling, ed., Plenum Press, New York, New York, 1982, with B. G. Bufkin and G. C. Wildman

Major Reports and Publications

14. "Evaluation of an Acrylate Based Pipe Thread Sealant," Materials Performance 20, (October 1981)
15. "Processing of Emulsified Oils and Alkyds to Generate Polymers," Organic Coatings and Plastics Chemistry Preprints, Volume 45, Part 2, 1981, with B. G. Bufkin and G. C. Wildman
16. "Survey of Water Chemistry at Arkansas Navigational System Lock and Dams," Arksansas Tech University Library, 1971

Georgia Institute of Technology
Georgia Tech Research Institute

BIOGRAPHICAL SKETCH

DAHER, JOHN K.--Research Engineer II
Electronics and Computer Systems Laboratory

Education

M.S.E.E., Georgia Institute of Technology	1982
B.E.E., University of Dayton	1979
B.A., Mathematics, Oberlin College	1977

Employment History

Georgia Institute of Technology	
Research Engineer II	1983-Present
Research Engineer I	1979-1983
Monarch Marking Systems, Lab Technician	1977-1978
Cox Heart Institute, Researcher's Assistant	1977

Experience Summary: At Georgia Tech, was recently involved in the design of a wideband receiver for a millimeter wave near field antenna range. Project director on a program concerned with evaluating the shielding effectiveness of conductive plastics and also on a program to measure the electromagnetic shielding of a computer building in order to make recommendations on improving the shielding effectiveness to within specification. Assistant project director on a program to investigate the EMI/EMC characteristics of electric vehicles and also on a program to develop a generalized model for nonlinear metal-insulator-metal (MIM) junction sources of intermodulation products. Was recently involved with the design, fabrication, and evaluation of two prototype antenna configurations for a VHF communication system. Major contributor to programs involved in conducted emission measurements on the TOMAHAWK Vertical Launch System; the design of digital data communications equipment; definition and analysis of the electromagnetic susceptibility of integrated circuits including VLSIC and VHSIC devices; evaluation of various radiated modeling of intermodulation generation in passive components; development of integrated electromagnetic environmental effects (E^3) specialty tests; evaluation of electromagnetic pulse (EMP) protection measures for defense electronics installations; and measurement and evaluation of various VHF/UHF antennas, preamplifiers, and transmission line components. With Monarch Marking Systems, was active in the testing and evaluation of novel materials (porous rubbers, inks, etc.). With the Cox Heart Institute, conducted a computer-aided statistical analysis of research data.

Current Fields of Interest

Electromagnetic susceptibility and compatibility; antenna design; electroacoustics; and filter design.

Major Reports and Publications

1. "TOMAHAWK VLS CE03 Test Report," Project A-4025, Contract No. SCEEE/NSWC/84-B006, November 1984
2. "Design Guidelines for the Mitigation of EMP Effects in Electronic Circuits," Final Report, Contract No. DNA 001-82-C-0347, October 1984, with others
3. "Field Survey Measurements," Final Letter Report, Federal Express Corporation, Project A-3780, July 1984
4. "Integrated Circuit Technology Assessment (ICTA) Project," Final Technical Report: Definition Phase, Project A-3657, Contract No. F41621-83-C-5015, April 1984, with others
5. "VHSIC/VLSIC Technology Summary, Integrated Circuit Technology Assessment (ICTA) Project," Project A-3657, Contract No. F41621-83-C-5015, December 1983, with others
6. "High Altitude Electromagnetic Pulse (EMP) Protection Criteria for C^3 Power Plants in a Cold War Environment," Final Technical Report, Contract No. DACW88-83-M-0840, Project A-3572, November 1983, with others
7. "Investigation of the EMI Aspects of Electric Vehicles," Proceedings of the IEEE 1983 International Symposium on Electromagnetic Compatibility, Washington, D. C., 22-25 August 1983, coauthor
8. "Antenna Design and Mechanical Feasibility Analyses," Final Technical Report, Contract No. DAAH01-83-D-A013, Project A-3503, April 1983, with others
9. "Investigation of Electric Vehicle EMI/EMC and Its Control," Final Technical Report, Project A-3089, March 1983, coauthor
10. "Evaluation of Radiated Emission and Susceptibility Measurement Techniques," Proceedings of the 1982 IEEE International Symposium on Electromagnetic Compatibility, pp. 244-251, Santa Clara, California, 8-10 September 1982, with others
11. "Evaluation of Shielding Effectiveness Test Methods for Conductive Plastics," Proceedings of the International Conference on Plastics in Telecommunications III, Paper No. 30, London, England, 15-17 September 1982, coauthor
12. "EMC/EMI Investigations on Jet Industries' Electrica," Interim Technical Report, Project A-3089, July 1982, coauthor
13. "Limitation in Swept Receiver Scan Rates for Impulsive Noise Measurements," Technical Report, Project A-3089, February 1982
14. "Evaluation of Radiated Emission and Susceptibility Measurement Techniques," Final Report, Contract No. DAAK80-81-K-0006, January 1982, with others
15. "Shielding Effectiveness Evaluations of Thermoformable Laminates," Final Report, Project A-2897, July 1981
16. "Evaluation of EMP Protection Measures for Defense Electronics Installations," Final Report, Contract No. DNA 001-80-C-0292, 30 May 1981, with others
17. "Identification of Aircraft Passive Nonlinear Interference," Interim Technical Report, IM Measurement Scheme Development, Project A-2845, April 1982, coauthor
18. "Identification of Aircraft Passive Nonlinear Interference," Test Plan I, IM Measurement Procedures, Project A-2845, April 1981, coauthor

Major Reports and Publications (continued)

19. "Integration of Electromagnetic Environmental Effects (E^3) Test and Evaluation," Final Technical Report, Project A-2641, November 1980, with others
20. "EMR Hardness Design Guidance," Final Technical Report, Contract No. F30602-79-C-0132, November 1980, with others
21. MANAGEMENT AND DESIGN GUIDANCE--ELECTROMAGNETIC RADIATED HARDNESS FOR AIR LAUNCHED ORDNANCE SYSTEMS, Military Handbook, 15 November 1980, with others
22. "Program to Improve UHF Television Reception," Final Report, Project A-2475, September 1980, with others

"Corrosion Problems Associated with Computer Disk Packs"

J.F. McIntyre, B.C. Beard, and S.M. Hoover
Naval Surface Weapons Center
Corrosion Technology Group
Codes R32/R33
Silver Spring, MD 20903-5000

ABSTRACT

The nature and source of corrosion observed between recording disks and sector plates in direct contact have been identified in this study. Recordings disks and unanodized sector plates exposed to high relative humidity, chloride ions, and/or a commercial cleaning solution experienced accelerated corrosion; accelerated corrosion was attributed to the tight crevice formed between the recording disk and sector plate. Surface analytical techniques were used to characterize the nature of the corrosion and to identify the source of corrosion. Results confirmed that accelerated corrosion was due to water and cleaning solution entrapped between the recording disk and the sector plate after exposure to a commercial disk pack washer.

INTRODUCTION

The objective of this report is to recognize and outline potential corrosion problem areas which could adversely affect the integrity of computer disk packs (DP). A computer disk pack is composed of ten recording disks where the bottom recording disk (RD) of each DP is located directly on top of the sector plate (SP). This arrangement provides a potential site for crevice corrosion. Crevice corrosion involves attack in an area shielded from a bulk environment usually restricting the flow of oxygen and other reactants and, in most cases, a region of high acidity develops causing rapid attack within the crevice. Crevice corrosion is often the most insidious form of localized attack and alloys which are easily passivated, such as aluminum alloys, are especially susceptible to severe crevice attack.

The SP is an aluminum alloy, AA-5086, which, in some cases, is anodized to provide additional corrosion protection. In general, aluminum alloys exhibit good corrosion resistance and uniformly corrode at a low rate; however, under certain circumstances an environment or structural configuration favors localized attack, i.e., crevice or pitting. The reliability of a DP will be compromised if corrosion between the RD and the SP leads to a breach of the RD surface and/or induced pressures caused by corrosion product build-up leads to a warping or cracking of the RD. The RD is comprised of a polished aluminum disk that is subsequently coated with γ-Fe_2O_3, a magnetic recording material.

The iron oxide, γ-Fe_2O_3, is the most protective iron oxide and least reactive; it is stable in a number of environments, such as water, alkali, and dilute chloride solutions; however, γ-Fe_2O_3 is dissolved by most acids, particularly hydrochloric and nitric acid.

EXPERIMENTAL

Laboratory studies involved exposing computer disks to high and low relative humidity, total immersion in distilled water and exposure to a commercial cleaning solution (Liquinox). Corrosion rates were determined using the polarization resistance (Rp) technique, and potentiodynamic pitting scans were used to determine pitting susceptibility of the SPs. Analysis of the localized corrosion occurring between the SP and the RD was performed by three surface sensitive techniques: Auger electron spectroscopy (AES), scanning electron microscopy (SEM), and X-ray photoelectron spectroscopy (XPS). Test samples studied using surface analytical techniques were taken from a DP which had been exposed to multiple passes through a wash cycle in a commercial DP washer. The DP was carefully opened and disassembled to avoid altering the original surface condition. A corrosion free disk was removed to use as a control, i.e., a RD not adjacent to the SP; in addition, the SP and the bottom RD were removed together then separated. The disk surfaces were not subjected to pre-treatments, but were analyzed in the "as received" condition. The disks were cut into smaller sections for analysis.

Three sets of samples were exposed to 80% R.H. and 24% R.H. A saturated solution of ammonium chloride was used to simulate an 80% R.H. and the 24% R.H. environment was simulated using a saturated solution of $CaCl_2 \cdot 2H_2O$. Test samples were cut from normal size disks in order to conveniently expose them to the two environments. Prior to testing all samples were cleaned with acetone to remove grease and oil and the shear edges were coated with an epoxy to prevent interference from edge corrosion. The three test sample surfaces included: unanodized AA-5086 SPs, anodized AA-5086 SPs, and RDs. For exposure to 80% R.H., samples designated A and B were exposed in the "as-is" condition and left undisturbed for the duration of the test; for samples C and D, water was deliberately introduced between the RD and the SP every 48 hours; and for samples E and F a commercial cleaning solution was introduced between the RD and the SP using the same procedure as used for samples C and D (see Table 1). Samples A-D were exposed to 80% R.H. for three and a half months, while samples E and F were exposed to "Liquinox" cleaning solution for three months. For exposure to 24% R.H., the experimental set-up was identical to that used for samples exposed to 80% R.H. Therefore, six samples were exposed to 80% R.H. and six samples to 24% R.H. for a total of twelve samples. A tabular summary of the results for 24% R.H. exposure is not provided, but the observed corrosion behavior is described later.

For immersion testing, small sections of the RD and SP were mounted in an acrylic polymer and the edges were coated with an epoxy to eliminate edge corrosion. These samples were fully immersed in either distilled water or cleaning solution and visual observations were made. This experiment was designed to test the uniform corrosion behavior of the materials.

A uniform corrosion rate was determined for the unanodized AA-5086 SP in 3.5% NaCl, using the Rp technique. Briefly, the Rp technique involves the application of a controlled-potential scan over a small range, typically $\pm$ 5mV with respect to the corrosion potential. In this potential range, the applied potential and current are linearly related to a close approximation. The resulting current is plotted against the applied potential and the slope of the straight line at the corrosion potential is equal to Rp. The resultant Rp value is inversely proportional to the corrosion current (1). The calculated corrosion current can be expressed as a corrosion rate using the Faraday equation (2). The corrosion rate can be expressed in two familiar forms: "milli-inches per year" (MPY) and "milli-grams per decimeter per day" (MDD).

RESULTS AND DISCUSSION

RELATIVE HUMIDITY EXPOSURE. Test results for 80% R.H. exposures indicated that some corrosion product build-up between the RD and the SP had occurred for each of the samples. The corrosion product build-up was found in highly localized areas, above sites of growing pits, and generally close to the edge. The corrosion products were white in appearance and extremely adherent, probably $Al(OH)_3$. A summary of qualitative results are presented in Table 1. Most of the pits were shallow and small in diameter; however, for samples B and E several deep pits were found on the sector plate and for samples D, E, and F a deep pit was found on the underside of each RD. From Table 1, it can be seen that no pits were found on anodized SPs as compared to the large number of pits observed on the unanodized SPs. Attack on the underside of the RD occurred randomly and did not appear to be influenced by the nature of the SP.

Upon closer inspection of the sample disks using a stereomicroscope it was discovered that a number of pits were actually deep. A photograph of a representative pit for sample F can be seen in Figure 1; this pit was located near the RD edge with a measured depth of, ca. 25 mils. A similar photograph for sample E can be seen in Figure 2; as observed for sample F, this pit was located near the RD edge with a measured depth of, ca. 4 mils. It was observed that the deeper pits were located near the RD edge, i.e., environmental access to this area was greater. In addition, "filiform-like" corrosion was found on several sample surfaces. Typical "filiform-like" corrosion located on the underside of the RD for sample B can be seen in Figure 3. At 25X, the size of these corrosion tracts can be realized by comparison to the milli-meter

scale in the photograph. Filiform corrosion occurs beneath protective coatings in high relative humidity environments, i.e., 60-90%. Filiform corrosion has been observed beneath organic and metallic coatings on steel, aluminum, and magnesium (2). In general, filiform corrosion is not detrimental to a metal's integrity because this corrosion is superficial in nature; however, if the filiform corrosion track breaches the protective coating the exposed metal surface may provide sites for pit initiation. Since γ-Fe_2O_3 is a protective oxide much like other protective coatings and because this environment, i.e., 80% R.H., supports filiform corrosion, the appearance of "filiform-like" corrosion on these disks was not surprising. Observations using the stereo-microscope revealed that a number of "filiform-like" corrosion areas had exposed metal, located adjacent to growing pits.

Identifiable white corrosion spots were observed after one week of exposure on samples exposed to cleaning solution at 24% and 80% R.H.; however, the extent of attack appeared to be worse at 80% R.H. After two weeks, some extremely small white corrosion spots were observed on the "as-is" samples exposed to 80% R.H. During this same period, samples exposed to distilled water revealed some localized attack with areas of dark stains; in addition, the extent of corrosion was more pronounced for samples exposed to 80% R.H.

After one month, no corrosion was detected on the "as-is" samples exposed to 24% R.H. and the "as-is" samples exposed to 80% R.H. showed no acceleration of the initial corrosion. Samples exposed to distilled water in both 24% and 80% R.H. environments exhibited accelerated corrosion with a concurrent build-up of white corrosion product between the disks; in each of these cases, the anodized SP exhibited good corrosion resistance, but localized attack did occur on the underside of the RD. As observed in earlier experiments, the samples exposed to cleaning solution at 24% and 80% R.H. showed signs of extensive localized attack on the underside of the RDs; the unanodized SPs were significantly less resistant to attack as compared to the anodized SPs.

Exposure at 80% R.H. proved to be much more detrimental and the extent of corrosion between the RDs and the SPs was greater than observed at 24% R.H. For samples exposed to 24% R.H., the "as is" samples showed no signs of corrosion between the SPs and RDs. Significant corrosion was detected between the SPs and RDs for samples exposed to distilled water and cleaning solution, although the severity of attack was slightly less pronounced at 24% R.H.

DIRECT IMMERSION TESTING. Representative SPs and RDs were exposed to distilled water and cleaning solution for three months. Visual observations revealed that no corrosive attack occurred on the SPs in both environments. On the other hand, two small diameter pits were observed on the RD exposed to distilled water and no attack was observed on the RD exposed to cleaning solution. These results indicated that uniform corrosion of the SPs and RDs was less severe than observed for crevice samples exposed to R.H. testing.

UNIFORM CORROSION. The corrosion rate for an unanodized SP AA-5086 was determined by the Rp technique. Results from this test are summarized in Table 2. Anodic and cathodic Tafel constants are normally required to calculate a corrosion current (1). Tafel constants can be obtained from laboratory experiments, the literature or a reasonable range of Tafel values can be selected to calculate a range of corrosion rates. Results using the latter method are summarized in Table 3. Only a range of anodic Tafel constants, B_a, was selected for testing because under the experimental conditions the cathodic Tafel constant, B_c, can be assumed to be equal to infinity. The average corrosion rate over this range of anodic Tafel constants for AA-5086 was 0.101 MPY or 0.187 MDD. The corrosion rate for AA-5083 (an aluminum alloy with a composition similar to that of AA-5086) in 3.5% NaCl was determined by Pickens (3) using a weight-loss method. The value given by Pickens was 0.143 MDD for 30 days of exposure, a value close to the corrosion rate determined in our studies. It must be remembered that the corrosion rates determined using Rp or weight-loss techniques are designed to measure the uniform corrosion rate; therefore, the localized corrosion behavior cannot be ascertained using these techniques. For example, Table 4 lists some measured values of pit depth for three samples exposed to 80% R.H. The pits were located on the underside of the RD (the thickness of the RD is approximately 49 mils). For sample E, a pit depth of 25 mils was found after 106 days of exposure to 80% R.H. This was equivalent to a corrosion rate of 86 MPY, thus, it would take only 212 days to penetrate the RD. This corrosion rate was much greater than the uniform corrosion rate determined for AA-5086 using the Rp technique. In addition, the pit depths determined for samples D and F were 4 and 6 mils, respectively. Pit depths of this magnitude corresponded to corrosion rates of 11.1 and 20.7 MPY. Therefore, it would take 2.5 and 4.5 years to failure, respectively. From these experiments, it was obvious that pitting corrosion, although small in area of influence, could occur rapidly and with catastrophic consequences.

PITTING. Electrochemical experiments using DC techniques were not utilized to study the anodized SP because of its high resistant oxide film, ca. 2×10^8 ohms (the use of AC Impedance techniques are better suited for studies of protective coatings). Results obtained for 80% R.H. exposure and total immersion tests revealed that little or no corrosive attack occurred on the anodized SP. A potentiodynamic pitting scan was obtained for a anodized SP sample in de-aerated 0.1M NaCl and a typical curve is shown in Figure 4. The current values were extremely low, in the range of 0.1 μA, and indicated that up to -.200 V (SCE) no pitting had occurred. However, this observed absence of pitting susceptibility was supported by the lack of pitting on the high R.H. and totally immersed samples. On the other hand, a typical potentiodynamic pitting scan obtained for unanodized AA-5086 can be seen in Figure 5. A breakdown of the oxide film, i.e., pitting, occurred at about -700 mV (SCE) as indicated by the rapid increase in current. This observation suggested that the unanodized SP was highly susceptible to

pitting. In fact, visual inspection of 80% R.H. exposed samples showed a propensity for pitting.

SURFACE ANALYSIS. The use of AES was limited due to surface charging. Spectra obtained from an area adjacent to a corrosion pit indicated the presence of a heavy layer of organic material, masking information from depths greater than 50 Å. Individual disks (not in contact with the SP) taken from the same DP did not have this high level of contamination, suggesting that close contact between the bottom RD and the SP entrapped some of the washing solution. AES images of the magnetic disk surface facing the SP (anodized) showed corrosion product build-up that followed regular curved paths duplicating the pattern of the milling marks on the surface of the SP. The ingress of water between the bottom SP and the RD apparently followed the milling marks on the SP. The marks were clearly visible on inspection with the unaided eye. Indeed, on both surfaces the corrosion areas were square or rectangular in shape, bordered by the milling cuts which acted as traps for the wash solution. Point analysis of the corrosion products on the magnetic disk revealed the presence of aluminum; suggesting that transfer of corrosion products from the SP had occurred. Argon ion sputter depth profiling of the RD indicated the presence of a homogeneous surface film composed of carbon, oxygen, and iron (representing the iron oxide magnetic material and an organic binder). High initial concentrations of carbon were observed and were attributed to contamination on the surface of the disk. Red-orange stains on the SP suggested that iron was transferred from the RD to the SP during the corrosion process. The insulating anodized oxide and heavy contamination on the SP made the analysis for iron by Auger electron spectroscopy impossible.

XPS analysis was more successful because charging induced by X-ray excitation was significantly less intense. Analysis of a sample taken from an uncorroded RD found carbon, oxygen, and iron. High resolution spectra of these peaks enabled the identification of the chemical state of the elements; both the carbon and oxygen spectra had multiple components, indicative of different chemical states. The carbon (1s) spectrum had a major peak attributable to carbon singly bonded to two oxygens. These functionalities were attributed to the organic polymer used to bind the magnetic oxide. The O(1s) spectrum had three components: the lowest binding energy component and narrowest peak was due to iron oxide at a characteristic binding energy of 530.0 eV and the two higher binding energy components were assigned to oxygen in the polymeric binder. Angle dependent studies revealed no variation in the relative intensities of these three peaks, thus, eliminating surface adsorbed water or hydroxyls as possible species contributing to the higher binding energy O(1s) components. The angle dependent results were consistent with the Auger sputter-depth profile results indicating that a homogeneous recording film was present. The iron spectrum demonstrated the expected complex spectral pattern for iron oxide, i.e., γ-Fe_2O_3. See Figure 6.

XPS analysis of the corroded magnetic disk indicated a different surface chemistry. The presence of sulfur, chlorine, silicon, magnesium, and aluminum contaminants were observed. See Figure 7. The C(1s) was predominantly one peak appearing at 287.7 eV. The oxygen signal was also predominantly a single peak at 535.0 eV. The spectrum from the iron (2p) region, which was very weak, suggested charging on the order of 3 eV from the anticipated oxide binding energy (Fe_2O_3 $2p_{3/2}$ iron peak is well characterized (4 and 5)). Correcting for this amount of charging, the carbon peak then fell at a binding energy corresponding to hydrocarbons and the oxygen and aluminum peaks corresponding to values characteristic of aluminum oxide. Therefore, the underside of the bottom RD was contaminated by aluminum oxide from SP corrosion and hydrocarbon contamination originating from the wash.

Figure 8 shows a low magnification SEM image of the pitted region of the SP. The deep milling mark in the surface is visible on the left side of the photo corresponding to the border of the corrosion area. The corrosion area clearly followed the milling marks on the surface of the SP as suggested by visual observation. SEM mapping of the SP surface, Figure 9, revealed clear evidence for the transfer of iron into the corrosion pit and along the border of the corrosion region as the red-brown color observed by visual inspection suggested. Close inspection of the border region demonstrated the build-up of corrosion product. See Figure 10.

Several contaminants on the SP not observed by XPS were detected using SEM, including: phosphorous, magnesium, manganese, and chromium. The phosphorous may have originated from the wash solution or as a contaminant due to improper handling. Magnesium, manganese, and chromium, are common alloying elements used in aluminum alloys; therefore, these probably appeared as a result of the corrosion of the aluminum alloy substrate. Alternatively, these elements may have been directly detected from the substrate because SEM X-ray analysis probes several microns into the bulk metal.

SEM imaging of a typical corrosion spot on the underside of the bottom RD is shown in Figure 11. This photograph was representative of a typical corrosion pit. The regularly shaped boundary of the corroded region attributed to the deep milling marks in the surface of the SP and the build-up of corrosion product in this area were easily observed. An aluminum elemental distribution map in this area illustrated the cross-over of aluminum from the SP to the RD was due to the corrosion process. See Figure 12. High magnification of the deposited corrosion products revealed a thick film, ca. 1.5 μm, exhibiting a "mud-crack" pattern caused by the dehydration of water in the film. See Figure 13.

SUMMARY

Laboratory studies indicated that rapid deterioration of RDs occurred in a relatively short period of time, provided the

relative humidity was high and chloride ions were present. Measured pit depths on the underside of several RDs revealed that penetration could occur in as little as 0.58 year. Although the anodized SP had greatly improved corrosion resistance over the unanodized SP, this did not reduce attack on the RD. The appearance of corrosion between the disks was not surprising since this configuration favors crevice and/or pitting corrosion. Exposure to 24% R.H. did not result in attack between the SP and RD for the "as-is" samples. This suggested that storage at low relative humidity will not be detrimental. The R.H. exposure tests also revealed that the cleaning solution was very aggressive and even the anodized SP (which did not exhibit corrosion susceptibility to the cleaning solution in the freely corroding state) was found to corrode when in close contact with the RD.

Surface analytical studies revealed that the surface of the RD and SP, which were in close contact, exhibited pitting corrosion. The white corrosion products found between these disks were identified as aluminum oxide or aluminum hydroxide. RDs that were not in contact with a SP showed no signs of corrosion and an absence of a contaminated layer. However, between the RD and SP, the presence of contamination by hydrocarbons and other impurities demonstrated that the wash solution was deposited onto these surfaces. Transfer of elements from the SP to RD and vice-versa was observed by both AES and SEM. Therefore, the evidence overwhelmingly proved that water retention between these disks and contamination from the wash solution provided a situation where rapid localized attack occurred.

REFERENCES

1. Stern, M. and Geary, A.L., Electrochemical Society Journal 104, 56 (1957).

2. Fontana, M.G. and Greene, N.D., Corrosion Engineering, (New York: McGraw-Hill Co., 1978), p. 45.

3. Pickens, J.R., "Rapidly Solidified Powder Aluminum Alloys", in Proceedings of ASTM B-9 Conference, Philadelphia, PA, April 1984.

4. McIntyre, N.S. and Zetraruk, D.G., Analytical Chemistry 49(11), 1521 (1977).

5. Asami, K. and Hashimoto, K., Corrosion Science 17, 559 (1977).

ACKNOWLEDGMENTS

The authors wish to express their gratitude to Ronnie Hall for his valuable technical support.

TABLE 1. CORROSION RESULTS FOR COMPUTER DISK EXPOSURE TO 80% R.H.

Sample	Type Sector Plate	Conditions	# Pits Between Disks RD	SP
A	Anodized	As Received	4	**
B	Unanodized	As Received	9	15
C	Unanodized	Water	3	10
D	Anodized	Water	15	**
E	Unanodized	Cleaning Soln	10	25
F	Anodized	Cleaning Soln	5	**

TABLE 2. POLARIZATION RESISTANCE VALUES OBTAINED FOR AA-5086 EXPOSED TO 3.5% NaCl FOR 11 DAYS.

Time (hours)	Rp (ohms)
23	91,000
49	65,800
71	94,900
95	17,300
117	13,500
167	35,500
190	27,400
212	35,400
238	45,000
260	48,000

TABLE 3. CORROSION RATE CALCULATIONS FOR A RANGE OF ANODIC TAFEL CONSTANT VALUES FOR A DIFFUSION CONTROLLED REACTIONS.

B_a (mV/decade)	i_{corr} ($\mu A.cm^2$)	MPY	MDD
50	0.155	.067	.125
55	0.171	.074	.137
60	0.186	.081	.150
65	0.202	.087	.162
70	0.217	.094	.175
75	0.232	.101	.187
80	0.248	.108	.200
85	0.263	.115	.212
90	0.279	.121	.225
95	0.295	.128	.235
100	0.310	.135	.250
	Average:	.101	.187

Surface Area = 2.92 cm^2 B_c = oo

TABLE 4. MEASURED PIT DEPTHS ON SEVERAL RECORDING DISK SAMPLES EXPOSED TO 80% R.H.

Sample	Pit Depth (mils)	Mils/Year	Years to Failure
E	25	86.0	0.58
D	6	20.7	2.50
F	4	11.1	4.50

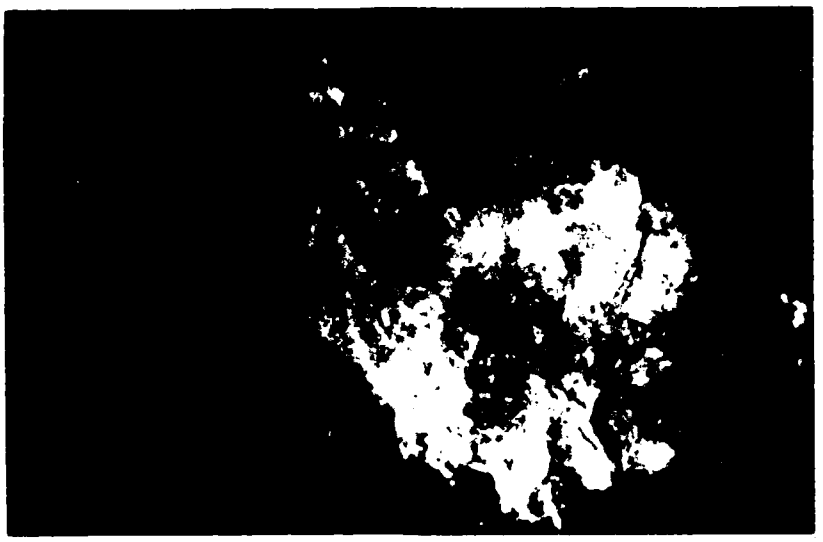

FIGURE 1. CORROSION PIT ON THE UNDERSIDE OF A RECORDING DISK. EXPOSURE OF SAMPLE F TO 80% R.H. FOR 106 DAYS.

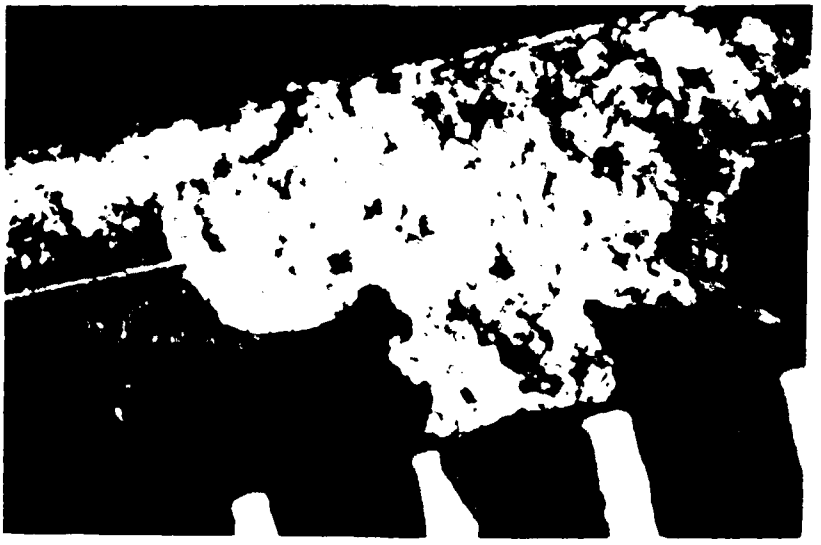

FIGURE 2. CORROSION PIT ON THE UNDERSIDE OF A RECORDING DISK USING A STEREO-MICROSCOPE (25X). EXPOSURE OF SAMPLE E TO 80% R.H. FOR 106 DAYS.

FIGURE 3. "FILIFORM-LIKE" CORROSION ON THE UNDERSIDE OF A RECORDING DISK. EXPOSURE OF SAMPLE B TO 80% R.H. FOR 132 DAYS.

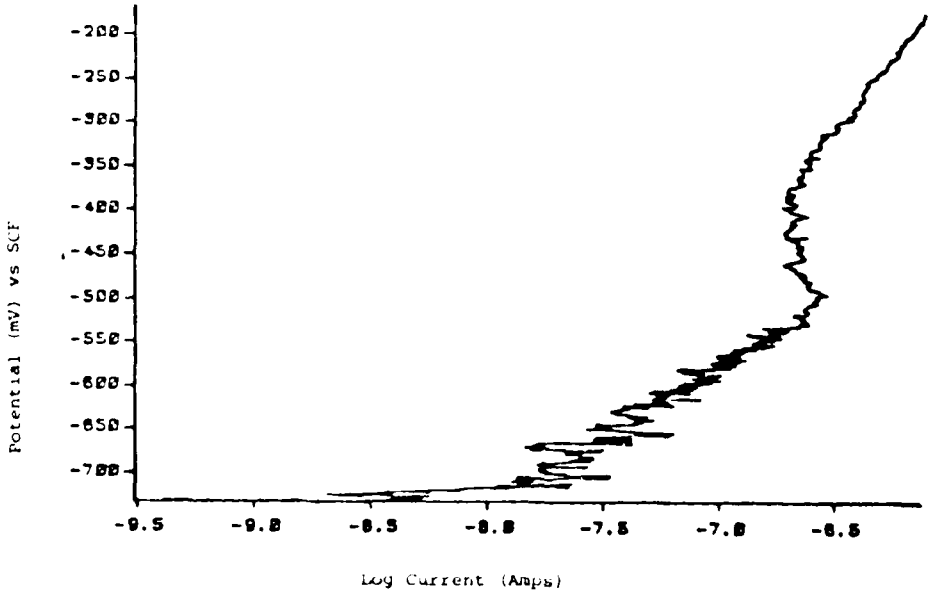

FIGURE 4. POTENTIODYNAMIC PITTING SCAN FOR ANODIZED AA-5086 SECTOR PLATE EXPOSED TO DE-AERATED 0.1M NaCl.

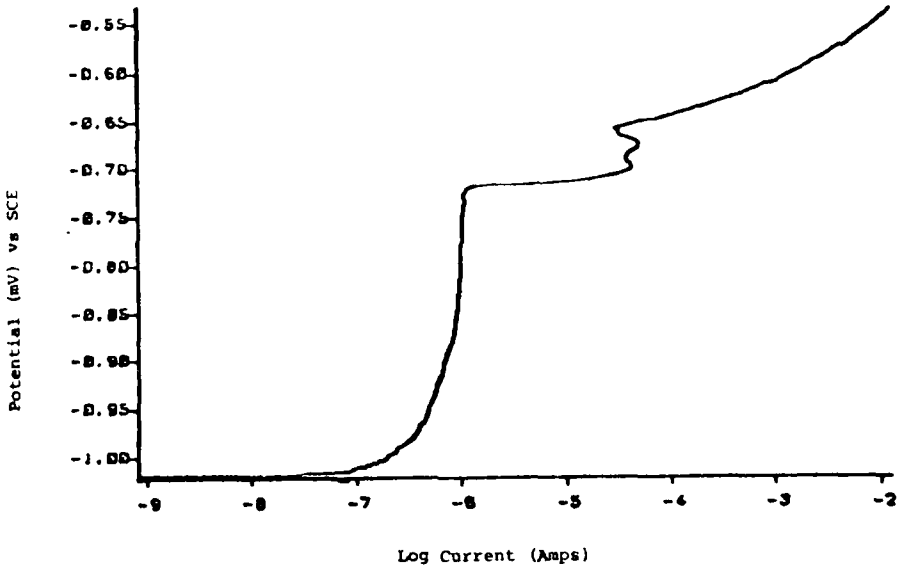

FIGURE 5. POTENTIODYNAMIC PITTING SCAN FOR UNPROTECTED AA-5086 SECTOR PLATE EXPOSED TO DE-AERATED 0.1M NaCl.

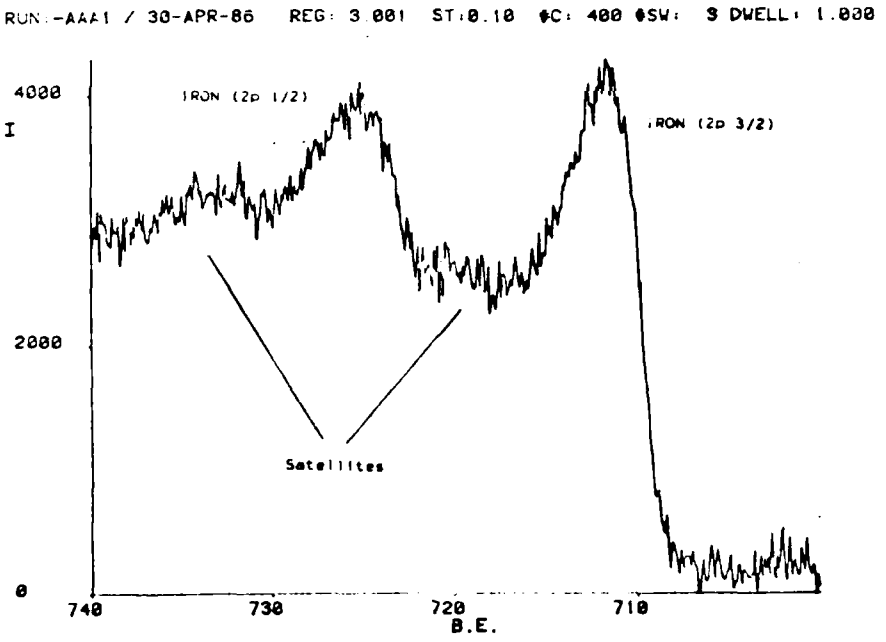

FIGURE 6. XPS SPECTRUM OF A VIRGIN RECORDING DISK.

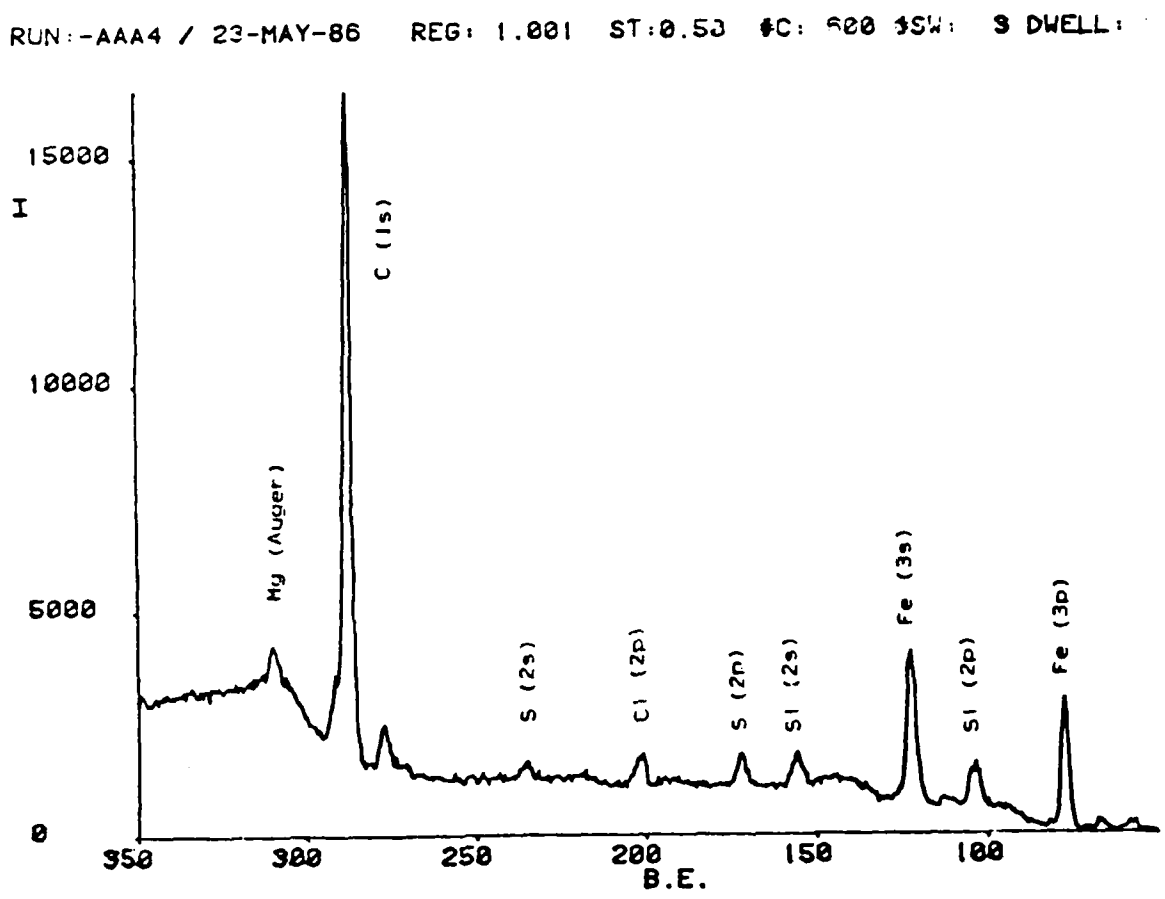

FIGURE 7. XPS SPECTRUM OF A CORROSION SPOT ON THE UNDERSIDE OF A RECORDING DISK.

FIGURE 8. LOW MAGNIFICATION SEM IMAGE OF A PITTED REGION ON AN ANODIZED SECTOR PLATE.

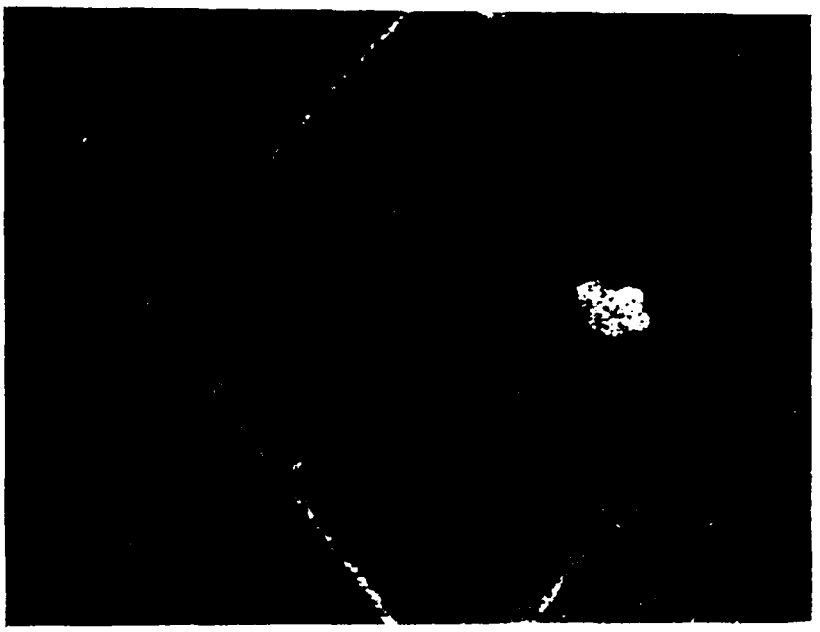

FIGURE 9. SEM IRON MAP ON AN ANODIZED SECTOR PLATE.

FIGURE 10. SEM PHOTOGRAPH OF CORROSION PRODUCTS ON AN ANODIZED SECTOR PLATE.

FIGURE 11. SEM PHOTOGRAPH OF A CORROSION SPOT ON THE UNDERSIDE OF A RECORDING DISK.

FIGURE 12. SEM ALUMINUM MAP ON THE UNDERSIDE OF A RECORDING DISK.

FIGURE 13. SEM PHOTOGRAPH OF CORROSION PRODUCTS ON THE UNDERSIDE OF A RECORDING DISK.

PAPER NUMBER

340

Corrosion 87

March 9-13, 1987
Moscone Center / San Francisco, California

ELECTRONIC FAILURE ANALYSIS-CORROSION OF AVIONICS

Lt M. Marchese, E. White, G. Slenski, B. Dobbs
Air Force Wright Aeronautical Laboratories
Materials Laboratory
Wright-Patterson AFB, OH 45433

ABSTRACT

Six examples of corrosion failure in aircraft electrical and electronic devices are described. Our experience indicates that about 20% of the failed devices submitted for examination are caused by corrosion.

INTRODUCTION

The Electronic Failure Analysis Group at the Air Force Wright Aeronautical Laboratories' Materials Laboratory has investigated a large number of electronic and electrical failures (Reference 1, 2, 3 and 4). It has been established that about 83% of these failures are caused by materials and manufacturing process defects. Also, it has been verified that about 20% of the failures are caused by corrosion.

The examples of corrosion related failures include resistors contaminated with chlorides, circuit boards contaminated with solder flux residues, exposed iron transformer cores, contaminated connector pins, polyvinyl chloride wiring insulation, and heat shrinkable tubing. These items were investigated and analyzed so that appropriate recommendations could be made in terms of material selections and manufacturing improvements.

EXAMPLES OF CORROSION RELATED FAILURES

After environmental testing, it was reported that iron core transformers were exhibiting severe corrosion. It was suspected that the cores were not adequately coated with a protective material (Figure 1). In an effort to determine if the applied coatings were adequate for protection of the transformers, two of the coated transformers were placed in an environmental chamber and subjected to humidity and temperature cycling according to MIL-STD-810C, Method 507, Procedure II. The units were turned on at intervals to verify that they were still working. This 48 hour cycle was between 65°C and 20°C with the relative humidity adjusted to 95%. The transformers were exposed to 5 cycles. Figure 2 shows the transformer core before the test and Figure 3 shows

the same core after the test. The coating was too thin to protect the iron core.

Another test was made to determine the extent that a good coating could protect the cores. Another transformer was selected and thoroughly cleaned with a solvent. Two different coatings were applied to about one third of the core length on the left of opposite sides of the transformer as shown in Figures 4 and 5. This transformer was placed in a 48 hour salt fog test, which is much more severe in terms of corrosion than the five cycles of the humidity and temperature cycling test. The transformer core was photographed after the salt fog test in Figures 6 and 7.

These results indicate that proper cleaning and coating of the iron transformer cores will prevent corrosion.

CHLORIDE CONTAMINATION IN HERMETICALLY SEALED RNR RESISTORS

RNR

Hermetically sealed resistors (Figure 8) were found to be contaminated with chlorides. This is undesirable because a small amount of moisture, perhaps inadvertently sealed inside the resistor, may cause corrosion sufficient to cause an open circuit. The resistors were cross-sectioned (Figure 9). Characteristic X-ray analysis indicated that the chloride contamination was between the brass endcap and the alumina cylinder which had a corkscrew-like nichrome film on it. A very slight amount of corrosion on the resistor could result in failure. The most likely source of chlorine is from a silver plating bath used to plate the brass endcaps. (Figure 10)

CORROSION ON BATTERY CHARGER PRINTED WIRING BOARDS

Several failed battery chargers were examined and corrosion was easily identified on the printed wiring boards (Figures 11, 12 and 13). The green corrosion products shown in Figure 13 were identified as copper abietate which results from the copper conductors and the abietic acid in the rosin solder flux. These type problems usually result from poor cleaning procedures that are used on the boards before conformal coating. Adequate cleaning of the boards before conformal coating will eliminate the problem, while improving the adhesion of the conformal coating.

POLYVINYL CHLORIDE (PVC) WIRING INSULATION

Chlorides from various sources are usually detrimental to electronic systems since small amounts of moisture may combine with the chlorides to cause corrosion. One method used to establish the extent that a material will emit chlorides, or to determine the safe (corrosion free) operating temperatures of the material, is called the copper mirror corrosion test, ASTM Standard D 2671-85, Procedure C. A one inch long specimen of wire with PVC insulation intact was placed in the bottom of a twelve inch test tube. With the tube in a vertical position, a copper mirror was suspended by a copper wire six inches above the bottom of the test tube. The top of the tube was sealed with aluminum foil and the tube was placed in a temperature controlled oil bath. The temperature of the oil bath was selected then maintained for sixteen hours. After the test, the mirrors were examined to determine if there was any corrosion. Figure 14 shows the test result. The bottom mirror was maintained at 175°C for sixteen hours and the top mirror was used as control. The control mirror was placed in a tube that did not have a wire sample in it, but otherwise was treated the same as the wire specimens. It is evident from Figure 14 that the PVC insulation material failed the test.

HEAT SHRINKABLE TUBING

Some heat shrinkable tubing emits gases that create problems, such as corrosion, with electronic equipment. One type of heat shrinkable tubing was analyzed (Figure 15). The tubing was analyzed and found to be a vinyl acetate-ethylene material internally coated with a polyamide. At elevated temperatures it was found to emit forms of sulfur, usually sulfur dioxide. These substances may cause corrosion, also, heat

shrinkable tubing containing sulfur has been shown to prevent the proper cure of silicone potting compounds. Generally, heat shrinkable tubing which emits sulfides should not be used.

PRINTED WIRING BOARD EDGE CONNECTORS

The printed wiring board edge connectors (Figure 16) may exhibit evidence of corrosion (Figure 17) when exposed to certain contaminates. The connector pins are copper base with 1.5 to 2.0 microns plating of nickel and 1.0 to 1.5 microns of gold plating. The wire is usually silver plated copper wire. A cleaning procedure that proved effective in cleaning the residues was determined as follows:

a. a ten second dip in 10-15% HCl
b. agitated tap water rinse at ambient temperatures
c. flowing cold water rinse
d. hot water rinse, 160°F, followed by compressed air dry
e. oven dry at 160°F for one hour

This type of cleaning procedure eliminates many contaminates that when present in sufficient amounts with humidity, may cause an electrical failure of the edge connector.

CONCLUSIONS

Most electronic systems are susceptible to corrosion. The corrosion can result in leakage currents and opens which can eventually lead to electrical failures. The use of dissimilar metals, small dimensions and voltage gradients greatly accelerate the corrosion process in electronic hardware. In some cases, the corrosion of one picogram of metal may result in the circuit failing. This extreme sensitivity of electronics to corrosion requires special consideration for cleanliness and moisture content.

REFERENCES

1. B. Dobbs, AFWAL/ML Electronic/Electrical Failure Analysis Systems Support, Technical Report AFWAL-TR-80-4119, November 1980, DTIC No. B053846L

2. J. A. Snide and B. Dobbs, Proceedings of 13th Congress of the International Council of the Aeronautical Sciences with AIAA Aircraft Systems and Technology Conference, Seattle, Washington, August 22-27, 1982, ICAS-82-3.8.4, p. 1406-1414

3. Bill Dobbs and George Slenski, Materials Performance, 23, No. 3, p. 35-38 (1984)

4. Ken McClure, Phil Holbrook, Chuck Mrizek, Jr., George Slenski and Bill Dobbs, Corrosion 185, Preprint No. 329, National Association of Corrosion Engineers, Houston, TX (1985)

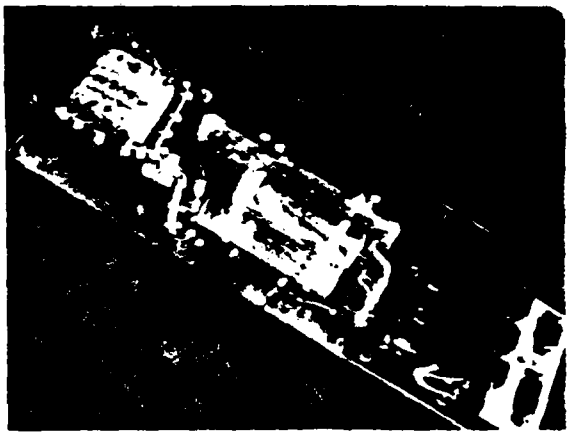

Figure 1 - Overall view of the transformer on the circuit board

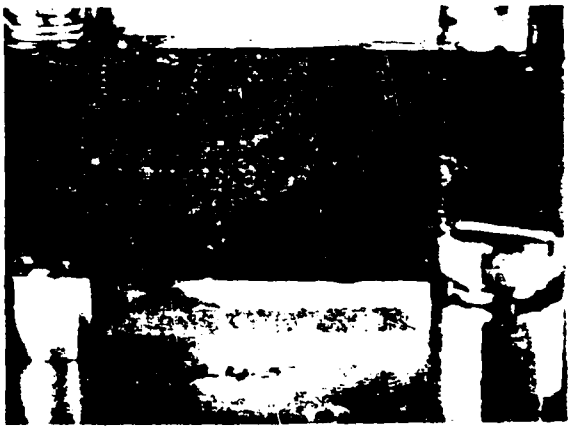

Figure 2 - Coated transformer core before humidity and temperature cycling

Figure 3 - Same core shown in Figure 2 after testing

Figure 6 - Transformer shown in Figure 4 after 48 hour salt fog test. Note lack of corrosion in the coated section

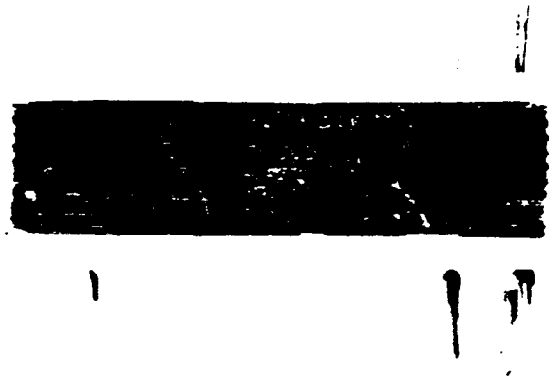

Figure 4 - Transformer core with special coating on left 1/3 of length before testing

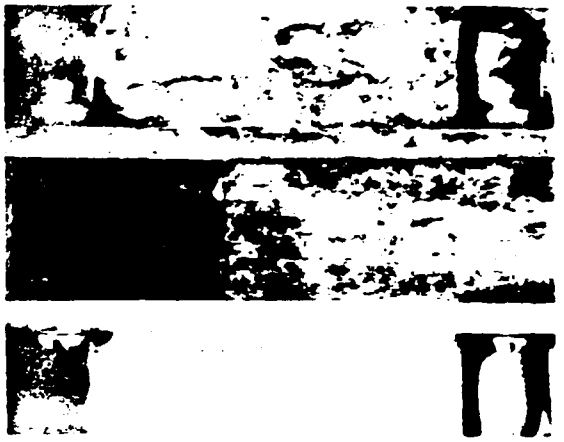

Figure 7 - Transformer shown in Figure 5 after 48 hour salt fog test. Note lack of corrosion in the coated section

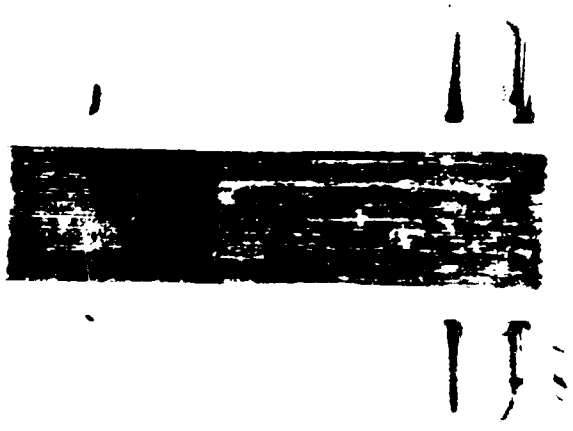

Figure 5 - Opposite side of transformer core show in in Figure 4 with a different type coating on left 1/3 of core length

Figure 8 - Hermetically sealed RNR resistor

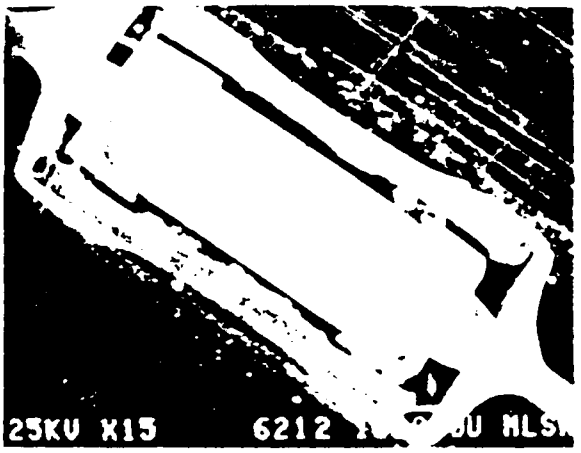

Figure 9 - Micrograph of resistor cross-section

Figure 12 - Corrosion around glass diodes causes exposed copper on the conductor traces

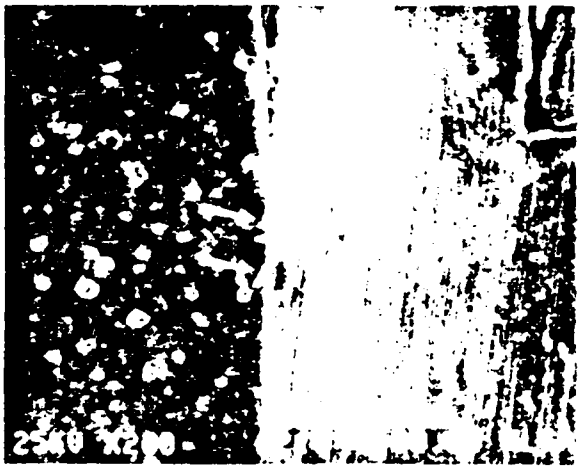

Figure 10 - Arrow marks chloride contamination between brass endcap and alumina insulator with corkscrew-like nichrome resistor element on it

Figure 13 - Green corrosion residue causes short betwen DIP leads

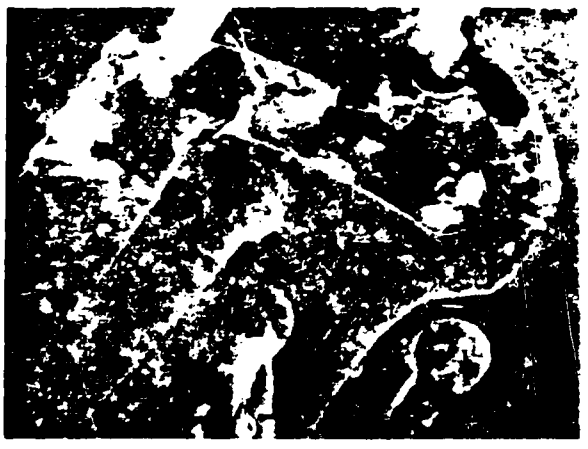

Figure 11 - Corrosion residues on and between conductor traces of battery charger printed wiring board

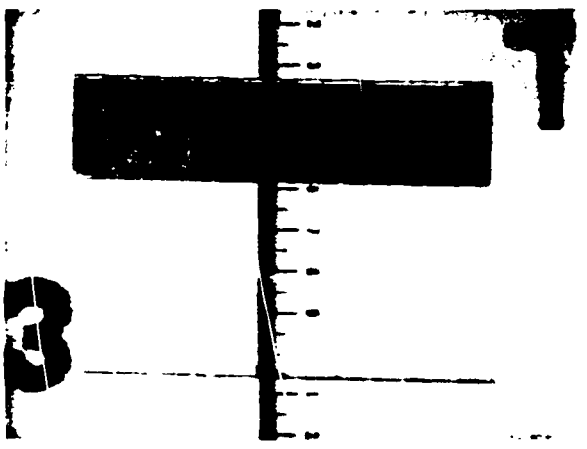

Figure 14 - Results of copper mirror corrosion test at 175 C. Top mirror is the control mirror and the bottom mirror is the actual mirror which was placed over the PVC wire sample. Note that the PVC wire sample failed the test

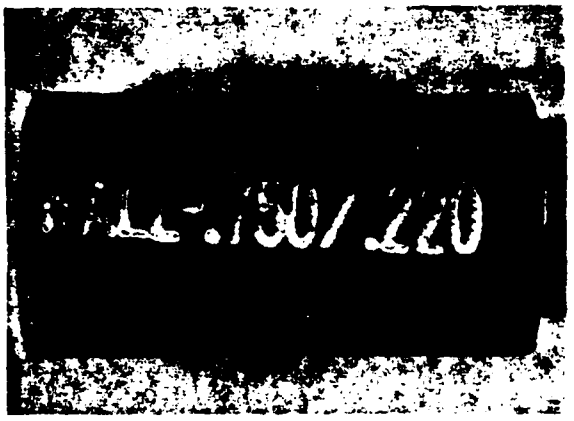

Figure 15 - Heat shrinkable tubing

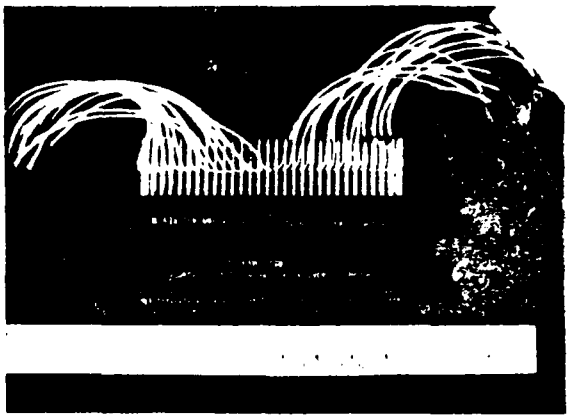

Figure 16 - Printed wiring board edge connector

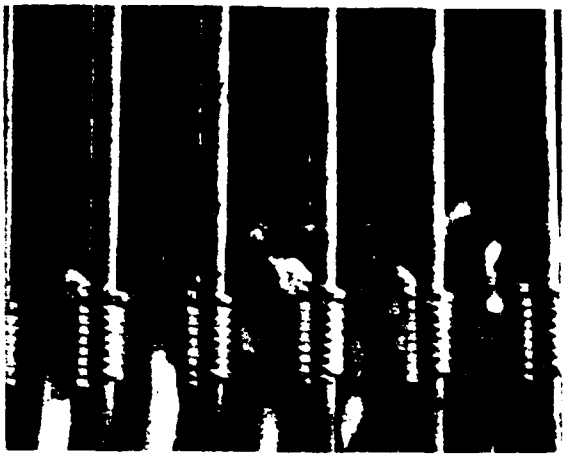

Figure 17 - Corrosion residue on edge connector pins

Low Cost Corrosion Sensors

Frank Ansuini
Dynaco Corporation
P. O. Box 3209
Derry, NH 03038

ABSTRACT

In response to an increased interest in corrosion monitoring, Dynaco has started a program to develop a series of low-cost corrosion sensing systems. These systems are designed for specific applications and use well established corrosion measurement techniques. Their intended use is those applications not presently being served by commercially available corrosion monitoring systems. This paper describes work in progress to develop a high sensitivity system for benign environments such as electronic and ordinance enclosures.

* * * * *

INTRODUCTION

Interest in corrosion monitoring has grown in recent years as the real costs of corrosion become apparent. These costs include direct costs, such as replacement of equipment which has failed due to corrosion, and indirect costs, such as maintenance and inspection for the purpose of minimizing the effects of corrosion. The science of corrosion prevention is now quite sophisticated. If the operating environment is known, systems can be designed so that the effects of corrosion can be minimized. Yet, failures still occur and these failures are often the result of an unexpected change in the operating environment. Thus, the purpose of a corrosion monitoring system is to provide an early warning of a change in the expected behavior so that timely corrective action can be taken.

There are several excellent corrosion monitoring systems on the market today. These systems are designed to operate in a wide range of environments and report corrosion rates and losses to a high degree of accuracy. Chemical processing plants represent the primary application for such systems where the very high cost of the equipment being protected can justify the expense of a sophisticated monitoring system.

Many additional applications exists where corrosion monitoring would be valuable, but use of presently available systems cannot be economically justified. It was with this need in mind that we started a project to develop a series of low cost, state-of-the-art monitoring systems. Certain of the concepts embodied in these novel systems are proprietary. The course of our development project has been guided by the following principles:

1. Design for specific applications. The output of the sensor in a given application can be predicted to within one or two orders of magnitude. This greatly simplifies the design of the electronic control circuits and allows the elimination of range switches.

2. Use established corrosion monitoring techniques. This is primarily to aid user acceptance.

3. Re-design sensor heads to allow their manufacture by photofabrication. This permits low cost, high precision replication of the sensors. Precision photofabrication is also what we do best.

4. Design dedicated electronics matched to the sensor output. This results in simple functional circuits which are inherently lower in cost than those designed to accommodate a wide range of sensor designs.

5. Provide innovative read-outs to reduce technical knowledge required by the user. In many potential corrosion monitoring applications, the user will not be a trained corrosion engineer. It is important, nevertheless, to clearly alert him to the existence of an abnormal situation in which the advice of a knowledgeable person is required.

MEASURING PRINCIPLES

Many different techniques have been developed over the years to measure corrosion. Sensors described in this paper concurrently use two different techniques: electrical resistance and linear polarization resistance.

Electrical Resistance - The electrical resistance (ER) method of monitoring corrosion has been around for several decades. A metal shape of uniform cross section is exposed to the operating environment. As corrosion proceeds, the cross section is reduced which causes an increase in the electrical resistance of the shape. As shown in Table 1, the law of parallel resistors can be applied to this situation and solved for the thickness loss. The corrosion data output from this type of measurement is cumulative metal loss which can be converted into a corrosion rate, if desired, by accounting for the time interval between readings.

Electronically, the primary signal output from this type of sensor is an electrical resistance value which can be measured by any of the commonly used techniques. This measurement can be processed by the circuit to yield a voltage which is proportional to cumulative metal loss.

Linear Polarization Resistance - Linear polarization resistance (LPR) is also a well established method for monitoring corrosion. A small bias voltage, Ea, applied between two electrodes causes a current, Im, to flow between them (see Table 2, Eqn. [1]). The ratio between them is called the polarization resistance, Rp, and is inversely proportional to the corrosion current, Ic. The corrosion current can be equated to a mass loss rate, Eqn. [3], or a corrosion rate, Eqn. [4]. The expression can be greatly simplified, without an unacceptable loss of accuracy, so that the corrosion rate can be equated to the measured current through a proportionality constant, K, Eqn. [6, 7]. Thus, the LPR technique yields an instantaneous corrosion rate; this is in contrast to the ER technique which yields cumulative metal loss. Each quantity, however, can be approximately converted to the other by accounting for the time interval.

The electronic control circuit for LPR measurements must be capable of applying a steady bias voltage to the sensor and measuring the current necessary to maintain that voltage. This current level can then be processed by the circuit to a voltage directly proportional to the instantaneous corrosion rate. Further processing can be done to yield the current-time integral (coulombs) which is directly proportional to cumulative metal loss.

SENSOR DESIGN

Figure 1 shows one of the early sensors designed in this project. It consists of two distinct adjacent traces, or electrodes. Each trace starts out in a broad area, reduces to a narrow serpentine section, and then opens up to a broad area once again. The broad areas are for the LPR measurements; the sensor output in this mode is directly proportional to exposed area. The serpentine parts are for the ER measurements. One trace is

exposed to the environment, the other shielded to provide temperature compensation. Since the purpose of this design was proof of concept, it was deliberately made oversized so as to supply strong signals to the electronics which were being concurrently developed.

The output of dual mode sensors of this type can be quantified using the relationships in Tables 1 and 2. A standard computer spreadsheet program can therefore be used as a design aid for both sizing the sensor and predicting the interactions between the ER and LPR areas. Table 3 shows a sample of this spreadsheet for the sensor shown in Figure 1. Rows 1 - 8 contain the constants for the particular sensor/application combination. Rows 10 - 13 allow prediction of the LPR output current as a function of sensor geometry and bias level. Rows 15 - 20 are for design of the ER part of the sensor. Finally, cells F20, B24 and B25 show the geometric interference each part of the pattern (ER and LPR) has on measurements produced by the other.

SENSOR FABRICATION

Sensors are fabricated using standard photofabrication techniques similar to those used in circuit board manufacture. The first step is artwork preparation in which an oversized rendition of the sensor pattern is prepared by any of several suitable methods. The artwork is photo-reduced to final size and replicated to yield a working negative. Concurrently, the metal foil is prepared by laminating it to a carrier, usually Kapton, and coated with a photo-resist, a light sensitive chemical. The negative and foil are brought into intimate contact and given a controlled exposure to ultra-violet light which alters the chemical structure of the resist. A chemical dip is used to remove the resist from the exposed areas after which the laminate is sprayed with ferric chloride or other etchant which dissolves all the metal except that which is still covered by the resist. A second chemical dip removes the remaining resist. The sensor is now ready for quality inspection, terminations and testing.

ELECTRONICS

The electronic control circuit consists of three major components: The LPR circuit, the ER circuit and the display. These can be designed around the predicted sensor output range calculated in the spreadsheet.

LPR Circuit - A very simple op-amp based potentiostat circuit, as first published by Baboian in Materials Performance, is shown in Figure 2. It is intended for three electrode work, with the bias voltage being set at P1 and the output current monitored at A. An enhanced version of this circuit, created for the electronic development part of the project, is shown in Figure 3. It can be configured by dip switch settings to function as a two or three electrode potentiostat or as a zero resistance ammeter, according to the needs of the particular experiment. It also has a signal capture range of about seven orders of magnitude and can either measure the current directly or supply a voltage proportional to the measured current. The final circuit for the LPR sensors will be mid-way in complexity between these two circuits.

ER Circuit - A simple bridge circuit suitable for measuring the response of the ER portion of the sensor is shown in Figure 4. This circuit produces an output voltage proportional to differential input resistance. Circuits of this type are commonly used in strain gage work. Since a goal of this project is to miniaturize the sensors to the greatest degree practical, it is possible that the ER trace resistance could be of the same order of magnitude as the lead wire resistance. This could necessitate the use of the so-called four-wire technique to measure resistance in order to back out the lead wire resistance. This technique involves putting a constant current through the resistor trace with one pair of lead wires and measuring the resultant voltage drop across the resistor through a very high input impedance meter with the other pair of lead wires.

Display - A stated goal of this project is to reduce the technical knowledge required by users of these sensors. The display, therefore, must provide an indication of when things are "normal" as well as a stronger indication of when things become "abnormal". A useful analogy can be found in the engine idiot lights on an automobile which provide an alarm when a condition exists requiring the services of someone knowledgeable in automotive mechanics.

At the present stage of development, the ER and LPR circuits are being designed to supply a voltage signal proportional to the cumulative metal loss (ER) and the instantaneous corrosion rate (LPR). These voltages will then be displayed on a twin LCD bar graph. If the reading exceeds a preset alarm level, the display will latch into a blinking mode. This display technique will provide one significant digit of corrosion data. While this level of resolution is clearly not sufficient for laboratory or development work, it is considered adequate for the intended purpose of these sensors: to inexpensively provide a warning of abnormal or unexpected corrosion activity.

Additional signal processing circuits can be added to convert the ER measured cumulative loss to interval or cumulative corrosion rates. Similarly, the LPR measured instantaneous corrosion rate can be converted to interval or cumulative metal loss. An advantage to the conversion step is that it will allow the direct comparison of the same quantity measured by two independent methods. A disadvantage is that it adds to the cost and complexity of the electronics. Also, it is well known in the corrosion field that such simple numerical conversions of one type measurement to another can be fraught with danger if they are performed without a sound understanding of what is actually happening on the sensor surface.

WORK TO DATE

Proof of Concept Experiments - The sensor pattern shown in Figure 1 and described in Table 3 was fabricated in 90/10 copper nickel and tested for sixty days in aerated ASTM synthetic seawater. The enhanced potentiostat previously described was used for LPR measurements while the four wire method was used for ER measurements. A set of weight loss panels was concurrently exposed for verification. ER and WL data was converted to interval corrosion rates so as to allow direct comparison with the LPR measured rates. Good agreement was noted among in the results obtained by the various methods, as shown in Figure 5.

The upturn in corrosion rates noted toward the end of the experiment was a fortuitous artifact of the test setup. The copper concentration in the tank continued to increase during the test and, since the tank was well aerated, cupric ions were the most likely species. The cupric ion itself can attack copper metal surfaces, a reaction which is put to good use in the photofabrication business. The most probable explanation for the increased corrosion rates toward the end of the test is the secondary attack by cupric ions.

Current Work - At present we are working [illegible] contract to develop a qualified corrosion [illegible] earlier work. The intended [illegible] such as ordinance and electronics [illegible] intended to measure cumulative [illegible] high humidity or condensing conditions, [illegible] failed hermetic seal, using the [illegible] be battery powered so as to [illegible] remote areas.

The development [illegible] into separate [illegible] would then be [illegible] the end of the [illegible]

Procedure: [illegible]

AD-A191 295 PROCEEDINGS OF THE TRI-SERVICE CONFERENCE ON CORROSION (1987) HELD AT THE.. (U) AIR FORCE WRIGHT AERONAUTICAL LABS WRIGHT-PATTERSON AFB OH.. F H MEYER MAY 87 6/6

UNCLASSIFIED AFWAL-TR-87-4139-VOL-1 F/G 11/6.1 NL

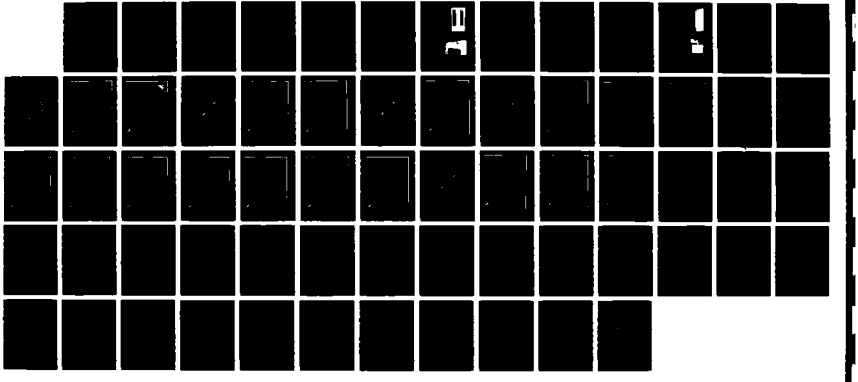

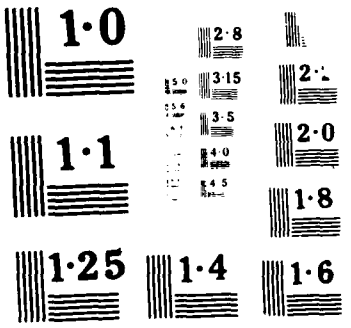
1·0
1·1
1·25
1·4
1·6
1·8
2·0
2·8
3·15
3·5
4·0
4·5

the not unexpected result that large aspect (width:thickness) ratios gave more accurate results since it minimized the effect of attack on the trace side wall. The limit to miniaturizing this part of the sensor will depend primarily on the detection limits of the ER circuit.

A prime requirement for the LPR part of the sensor was that it be able to detect corrosion activity in high humidity environments. Translated to corrosion terms, this means that the corrodent would have a very high resistivity so solution IR drop could interfere with the readings. This effect can be minimized by minimizing the distance over which the ionic current must travel when the sensor is energized. In geometric terms, the gap between the electrodes should be as small as possible. Similarly, the electrode width should also be small to ensure that the entire surface of the electrode participates in the reaction, not just the edges near the gap.

These considerations were experimentally verified by preparing three patterns, all with the same exposed area. Sensors were fabricated from 2 mil steel foil. Pattern C, shown in Figure 6, had a 60 mil trace with a 15 mil gap. The active area is the two parallel bars in the center; the rest of the pattern are termination leads or gage marks which were masked before testing. Pattern B was identical to pattern C except that the gap was reduced to 3 mils. Pattern D, shown in Figure 7, kept the 3 mil gap but reduced the trace width from 60 mils to 6 mils. It was necessary to use an interdigitated shape for the electrodes in pattern D so that metallic IR drop would not interfere with the operation.

The sensors were tested for 30 days in aerated distilled water which would be similar in corrosivity to atmospheric condensation. The results, shown in Figure 8, verified that small is better as the fine geometry sensors gave a stronger signal than those with coarser features. The heightened sensitivity of pattern B vs. C is believed to be strictly due to the reduced gap width of the former. The results from pattern D reflect both the reduced trace width and a side wall effect.

The plan view area of the three sensors (length times width) was identical: 0.774 sq. cm. The area of the side walls is also available for reaction and hence will contribute to the current output. Since the patterns were etched from 2 mil foil, the B and C electrodes had an effective width of 64 mils (60 + 2 + 2) which gives an actual reaction area of about 0.83 sq. cm. Pattern D has an effective trace width of 10 mils (6 + 2 + 2) which gives an actual area of 1.29 sq. cm. Thus, if all other conditions were equal, the side wall effect alone would cause pattern D to put out about 50% more current than patterns B or C. The rest of the increased current output of pattern D can be attributed to the effect of the narrower trace.

FUTURE WORK

The next step in this project is to recombine the ER and LPR patterns into a single composite pattern. Unlike the composite pattern shown in Figure 1 which has the ER trace in the middle of the LPR trace, the new pattern will have the ER and LPR portions located in separate areas of the sensor surface. One reason for the change is to eliminate the geometric interference shown in Table 3. The other reason is to eliminate electronic interference between the two modes during reading events. The new pattern will have four or seven lead wires, depending on the ER measurement technique selected. It appears very likely that the new sensor pattern will occupy an area about the size of a commemorative postage stamp. Other remaining tasks include investigation of various surface treatments to enhance sensor sensitivity, qualification tests in which the sensor's response is measured as a function of relative humidity, and correlation tests to relate the sensor's response to weight loss corrosion rates of many common metals.

Table 1 - *Calculation of Thichness Loss from Electrical Resistivity Measurements.*

Appreach: *Treat as parallel resistors where R_i = initial resistance, R_c = resistance of the corroded portion, R_b = resistance of the remaining portion.*

$$\frac{1}{R_i} = \frac{1}{R_c} + \frac{1}{R_b} \quad == \quad \frac{1}{R_c} = \frac{1}{R_i} - \frac{1}{R_b} \qquad [1]$$

For d much less than t, the cross section of the corroded area can be approximated by a slab d thick by $(w_i + 2t)$ wide. Therefore

$$R_c = \frac{\rho * l}{d * (w_i + 2t)} \qquad \text{where } \rho = \text{resistivity} \qquad [2]$$

$$\frac{1}{R_c} = \frac{d * (w_i + 2t)}{\rho * l} = \left(\frac{1}{R_i} - \frac{1}{R_b}\right) \qquad [3]$$

$$d = \frac{\rho * l}{(w_i + 2t)} * \left(\frac{1}{R_i} - \frac{1}{R_b}\right) \qquad [4]$$

For w_i much greater than t, $w_i \cong (w_i + 2t)$
Eqn. [4] can be simplified to:

$$d = \frac{\rho * l}{w_i} * \left(\frac{1}{R_i} - \frac{1}{R_b}\right) \qquad [5]$$

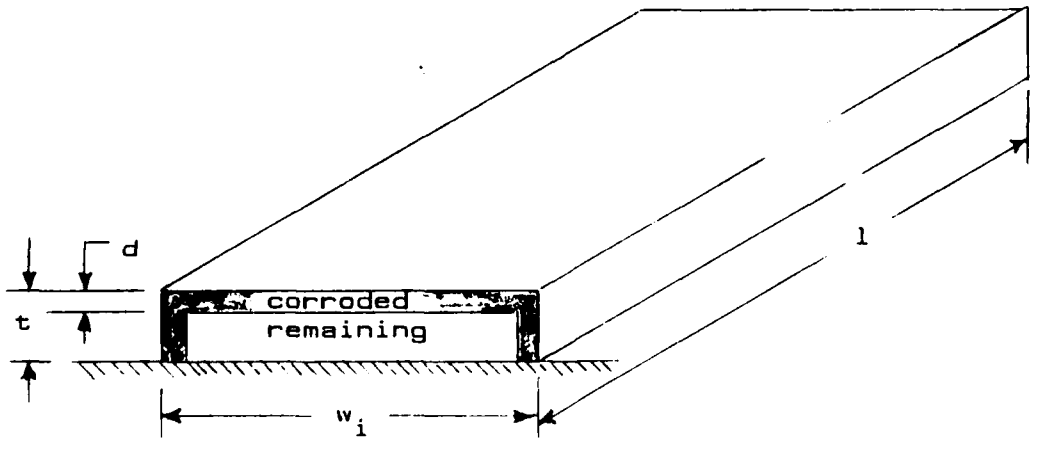

Table 2 Calculation of Corrosion Rate from Linear Polarization Resistance Measurements

When a small bias voltage, Ea, is applied between two electrodes, a measureable current, Im, will flow. For bias voltages less than about 20 mV, the current will be directly proportional to the voltage. This proportionality is termed the polarization resistance, Rp, and is inversely proportional to the corrosion current, Ic. The proportionality constant is known as the polarization constant, B:

$$dEa/dIm = Rp = B/Ic \qquad [1]$$

For the case when Im = 0 when Ea = 0, equation [1] reduces to:

$$Ea/Im = Rp = B/Ic \qquad [2]$$

The corrosion current can be directly converted to a mass loss rate, MLR, by means of a proportionality constant known as the Electrochemical Equivilant, EE:

$$MLR = (EE)*(Ic) \qquad [3]$$

Mass loss rate is converted to corrosion rate by accounting for the area, A, and density, D, of the metal:

$$CR = MLR/(A*D) \qquad [4]$$

Substituting equations [2] and [3] into equation [4], the corrosion rate can be expressed in terms of constants or dirctly measurable quantities:

$$CR = [(EE)*B*(Im)]/[A*D*(Ea)] \qquad [5]$$

In a given experimental setup, EE, B, A, and D would be constants. Therefore:

$$CR = K*(Im)/(Ea) \qquad [6]$$

If Im = 0 when Ea = 0, then Ea can also be set as a constant:

$$CR = K'*(Im) \qquad [7]$$

Table 3 *Sample output from computer spreadsheet used to design the prototype corrosion sensors.*

Rows 5 - 8: Input material constants.
Rows 11 - 12: Input LPR design variables.
Row 13: Output sensor's LPR response.
Row 16: Input ER design variables.
Row 17: Output choke point resistance.
Row 19: Output resistance of LPR portion and area of choke point.
Row 20: Output total trace resistance and percent contribution of LPR portion.
Row 24: Output LPR constant, LPR trace only.
Row 25: Output LPR constant, total trace.

:	A ::	B ::	C ::	D ::	E ::F:
1:	Sensor Sizing SS, Variable Input - CuNi				
2:	Final Design: 2/18/85				
3:	L,W&A=LPR dim'n; l,w&a=ER dim'n				
4:	----------				
5:	Alloy: CuNi706	Density: 8.94	gm/cc		
6:	Media: Seawater	ElRes: 19.10	uOcm		
7:	B,mV: 26	ElChmEqv: .000327	gms/coul		
8:	Thk,mils: 10.00				
9:					
10:	LinPolRes Outputs - Variable Inputs				
11:	CR,mpy: 1.00	#W,in: .490			
12:	#Bias,mV: 10	#L,in: 10.000			
13:	Imeas,uA: 26.82	#A,sqin: 4.900			
14:					
15:	ElRes Outputs - Variable Inputs				
16:	w,mils: 30.00	l,in: 22.963			
17:	R,ohms: .576				
18:	R,ohms, for LPR trace using dimensions				
19:	at # above: .015	a,sq.in: .689			
20:	Tot R/trace,ohms: .591	%Rlpr: 2.60			
21:					
22:	K' Calculation				
23:	For inputs at # above				
24:	mpy/uA: .037	LPR only			
25:	mpy/uA: .033	LPR and ER			

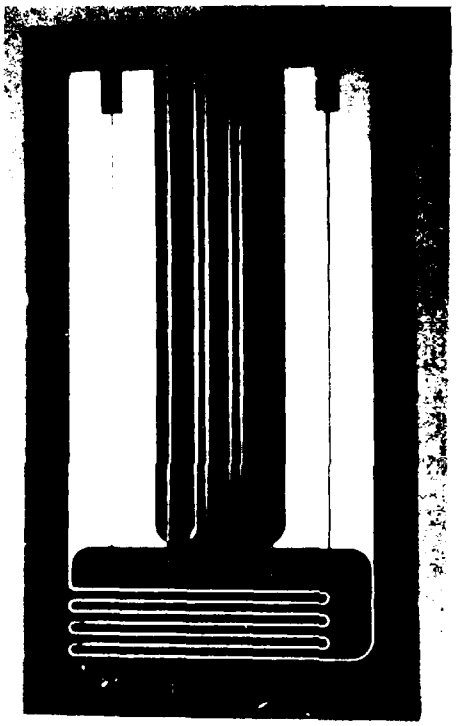

Figure 1 *Early proof-of-concept sensor. The broad bands are the LPR reaction areas; the serpentine traces are the ER reaction areas. The center serpentine is masked from the environment; its function is to provide temperature compensation to the exposed trace.*

Both photos approximately 1/2 x.

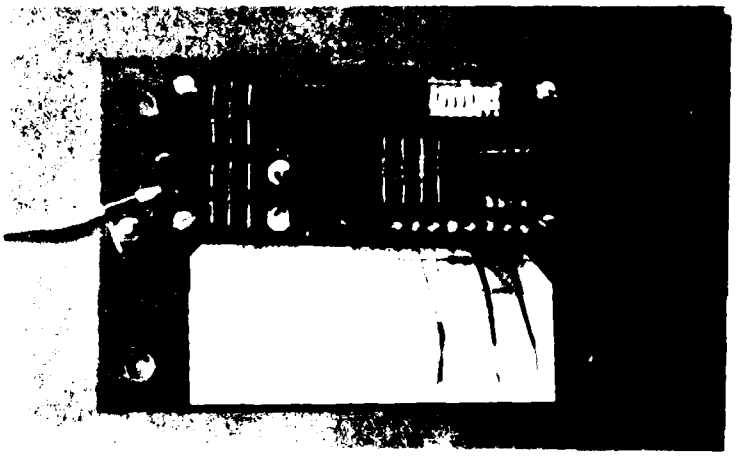

Figure 3 *Enhanced version of potentiostat shown in Figure 2. Changes included: addition of resistors to convert response current to voltage; input offset bias adjustment for the op-amp; a more sensitive bias voltage setting; additional switches to configure the circuit for use as a two or three electrode potentiostat or as a zero resistance ammeter.*

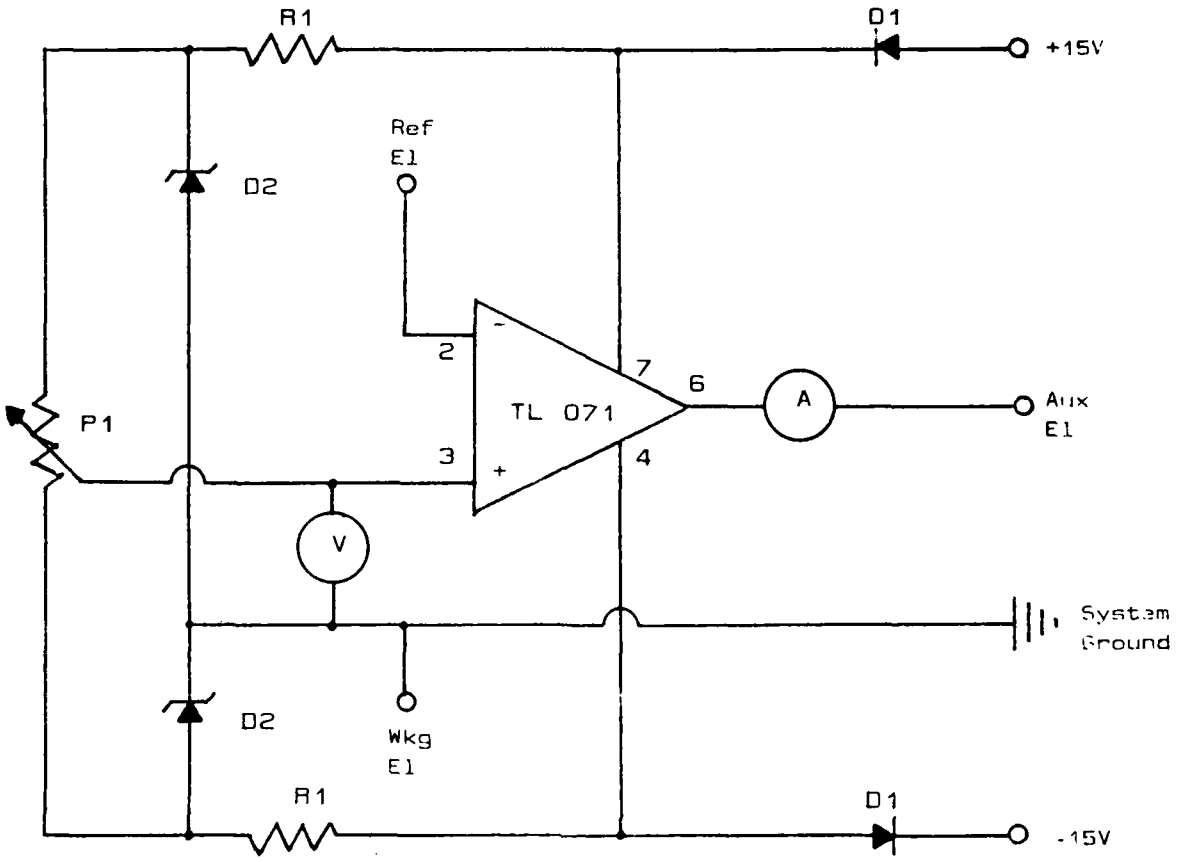

Parts List		No. Required
D1	1N4006 Si Rectifier, 1A 800 PIV	2
D2	1N4742 Zener diode, 12V 5% 1W	2
R1	2.2 kilo ohm resistor	2
P1	100 kilo ohm 15 turn potentiometer	1
TL 071	Low noise JFET input op amp	1

Figure 2 *Op-amp based potentiostat. The desired bias potential is set by adjusting P1. The circuit will supply current through the auxiliary electrode to the working electrode to keep the working electrode at the desired bias potential. [Ref.: Babaian et. al.; "Effect of Modern Electronics on Corrosion Technology"; Materials Performance; December, 1979.]*

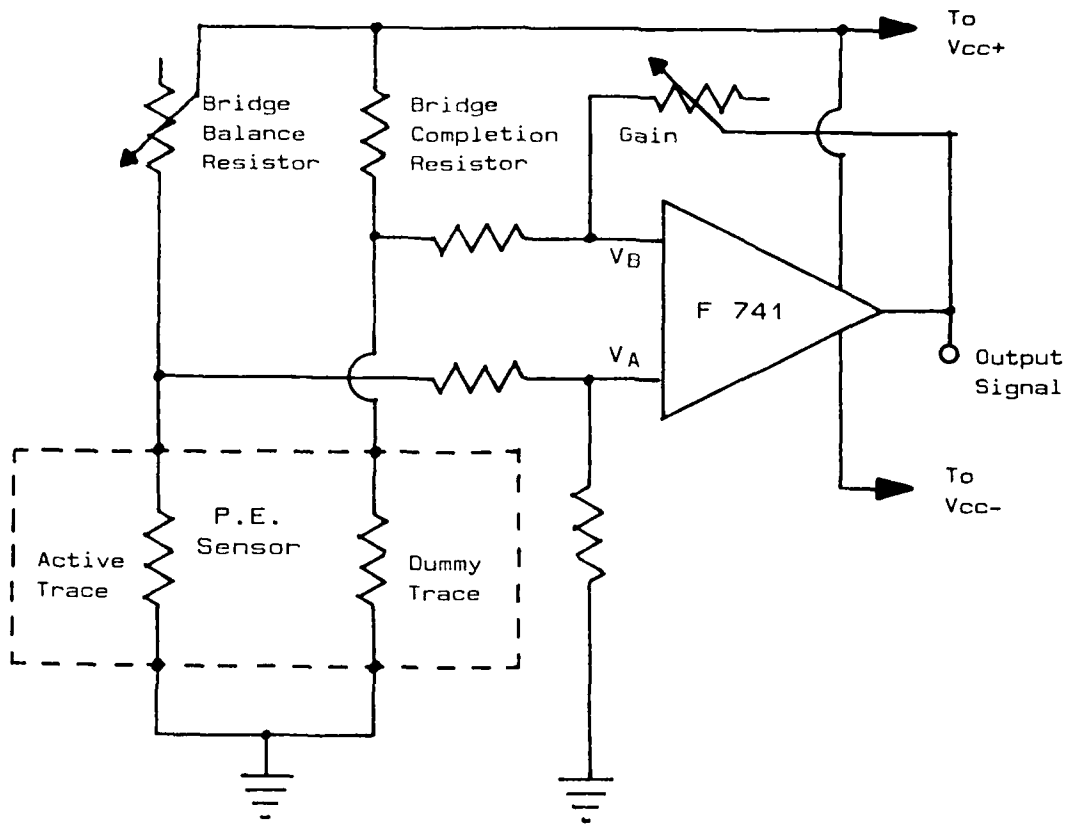

Figure 4 *Typical Bridge Circuit. The output signal from this circuit is proportional to the differential resistance between the active and the dummy trace. The resistance of the active trace increases as metal is lost to corrosion. The dummy trace is shielded from the environment and serves to compensate for changes in resistance due to temperature fluctuations.*

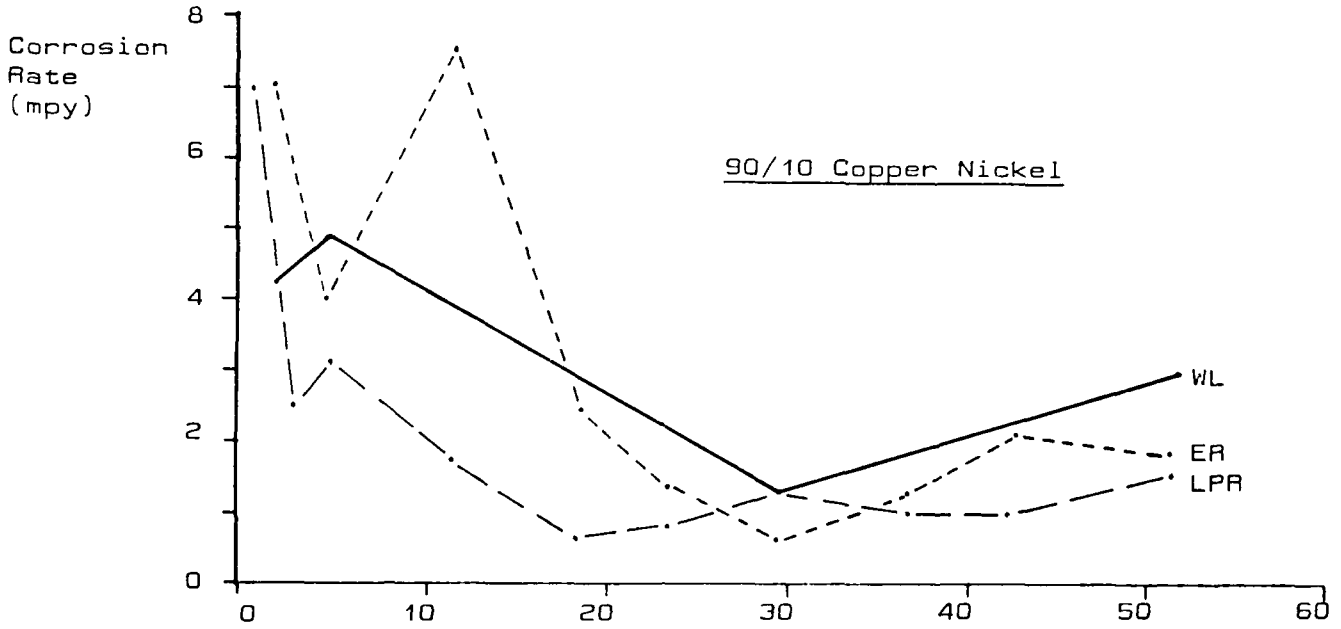

Figure 5 *Comparison of interval corrosion rates in synthetic seawater as determined by weight loss measurements and the prototype sensors operating in the Electrical Resistance and Linear Polarization Resistance modes.*

Patterns Used For LPR Trace Development.

Figure 6 *The active area of Pattern C is the two parallel bars in the center. Each bar is 60 mils wide by 2 inches long. The gap between them is 15 mils. Pattern B (not shown) is identical to C except that the gap has been reduced to 3 mils.*

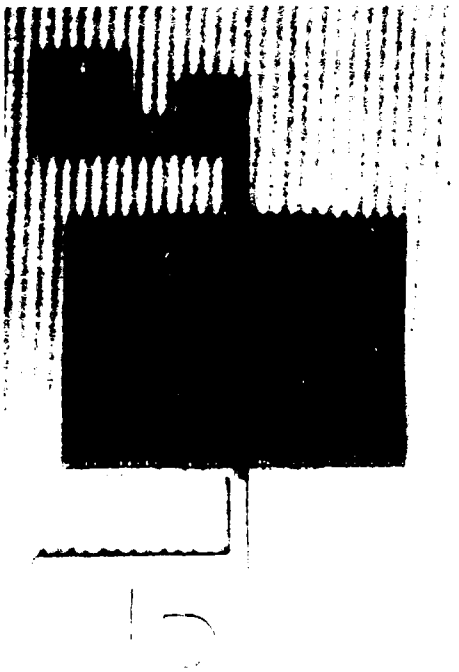

Figure 7 *Pattern D has the same area and gap width as Pattern B. The trace width, however, has been reduced to 6 mils. The interdigitated arrangement of the electrodes shown was necessary to reduce metallic IR drop in the narrow traces. This was the most sensitive of the patterns tested (see Figure 8).*

Approx. 2X

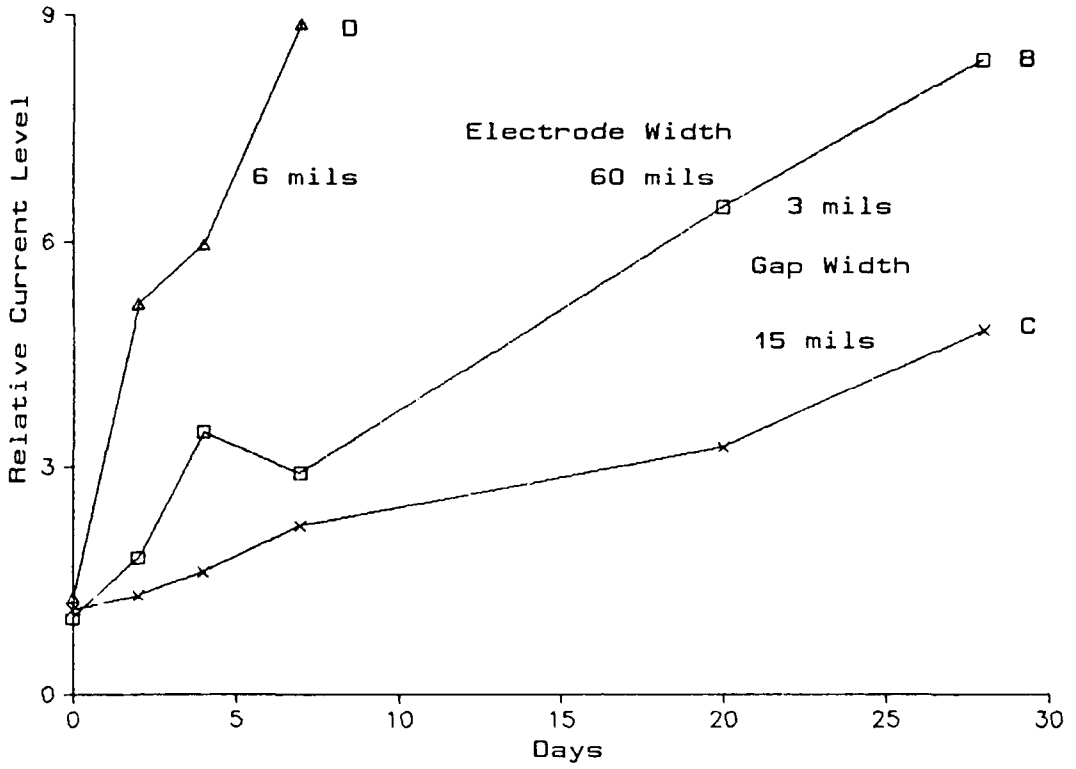

Figure 8 *Relative response currents of three sensor designs showing the effects of electrode width and gap width. The reduced response of C vs. B is believed to be primarily due to the effect of IR drop across the gap. The heightened response of D vs. B is primarily due to the side wall effect (see text) and, to a lesser extent, the reduced IR drop across the electrode width.*

BIOGRAPHY

NAME: Frank Ansuini

PRESENT AFFILIATION: Has been an Independent Consultant in Corrosion and Metallurgy since 1980

TITLE: Registered Professional Corrosion Engineer

FIELD OF INTEREST/RESPONSIBILITIES: Assists companies with developing products for the corrosion market and holds several alloy, process and and device patents. Has been involved in both research and marketing of corrosion resistant alloys

PREVIOUS AFFILIATIONS/TITLES: Has been associated with the International Nickel Co. and Kennecott Copper Co.

ACADEMIC BACKGROUND: BSc degree from the Massachusetts Institute of Technology and an MSc degree from New York University where he also took post graduate courses in Ocean Engineering

SOCIETY ACTIVITIES/OFFICES/AWARDS: Past chairman of the Boston Section of the National Association of Corrosion Engineers and is also active in the Marine Technology Society, American Society for Metals, Society for Naval Architects and Marine Engineers, and the Boston Computer Society.

PUBLICATIONS/PAPERS: Publications on the subjects of alloy and product development and materials selection.

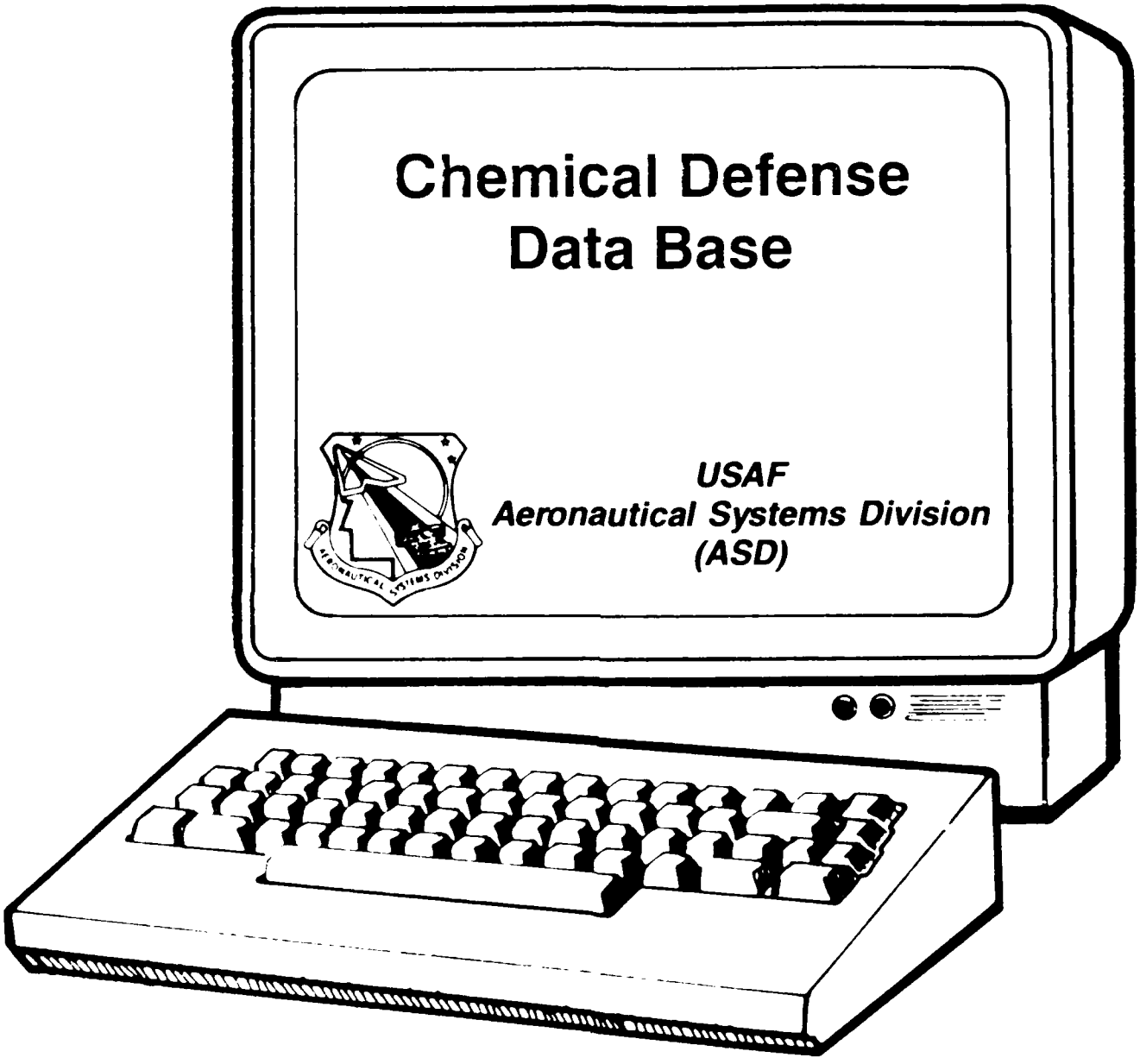
Chemical Defense
Data Base
USAF
Aeronautical Systems Division
(ASD)

Introduction

The Battelle Memorial Institute
Columbus Division

Battelle

Under Contract With the

USAF
Aeronautical Systems Division
(ASD)

to

Develop a Chemical Defense Data Base

Program Sponsor

USAF
Aeronautical Systems Division
(ASD)

* * * * * *

Fred Meyer
AFWAL Materials Laboratory

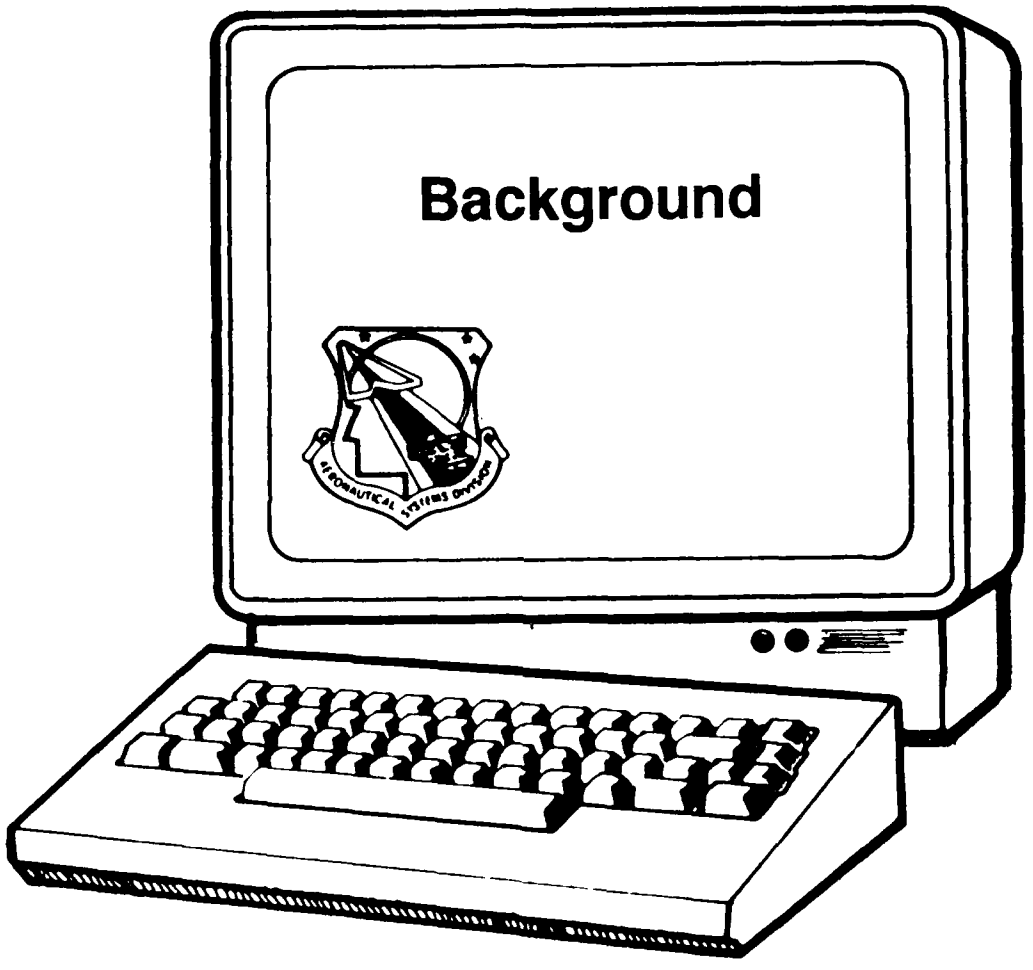
Background

NBC Contamination Vulnerability of Materiel

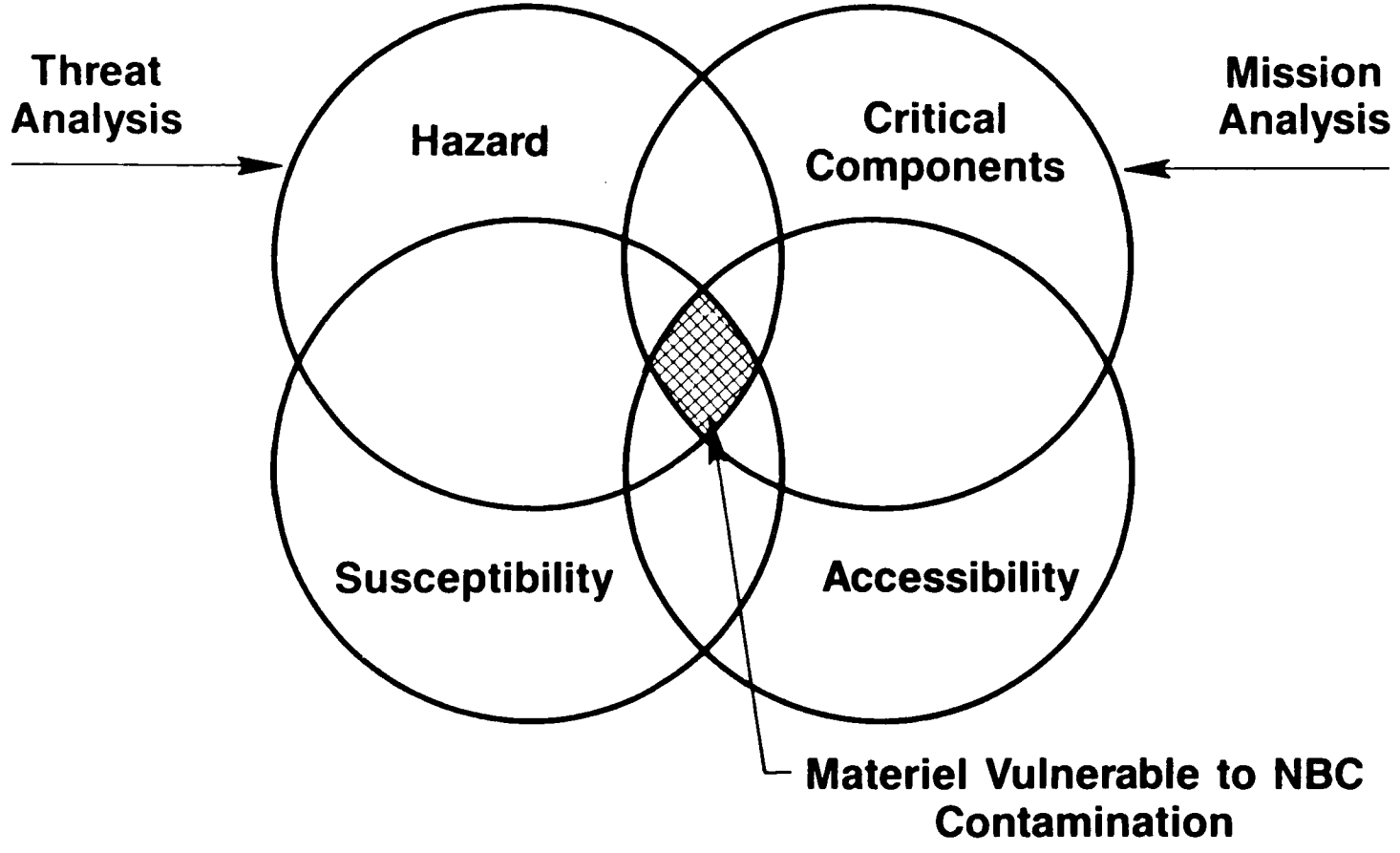

The Materiel Problem

- Chemical Warfare Agents and Decontaminants Alter Material Properties
- Alteration May Lead to System Malfunction
- Malfunction May Lead to Mission Failure
- Design Engineering Solutions Are Limited by Data Which Are Incomplete, Inconsistent, and Not Readily Available

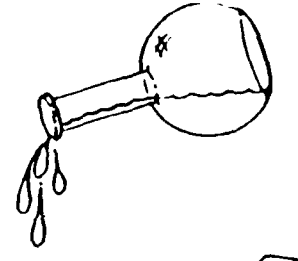

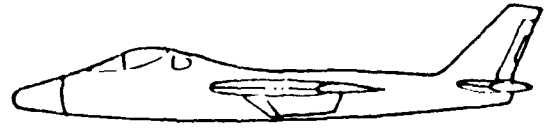

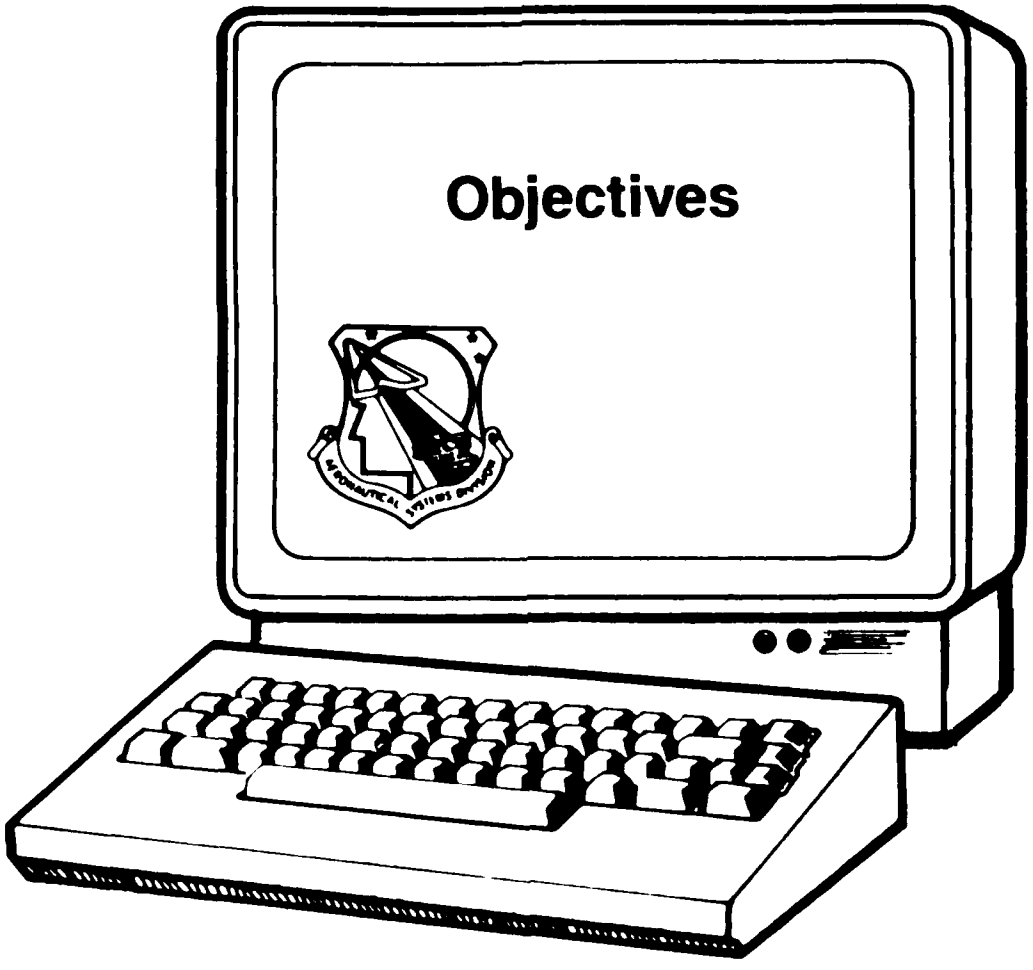
Objectives

Program Objectives

- Develop Mechanism for Information
  - Storage
  - Retrieval and Dissemination
  - Expansion
- Collect, Organize and Incorporate Relevant Data
- Develop Comprehensive Test Approach
  - Structure
  - Coordination

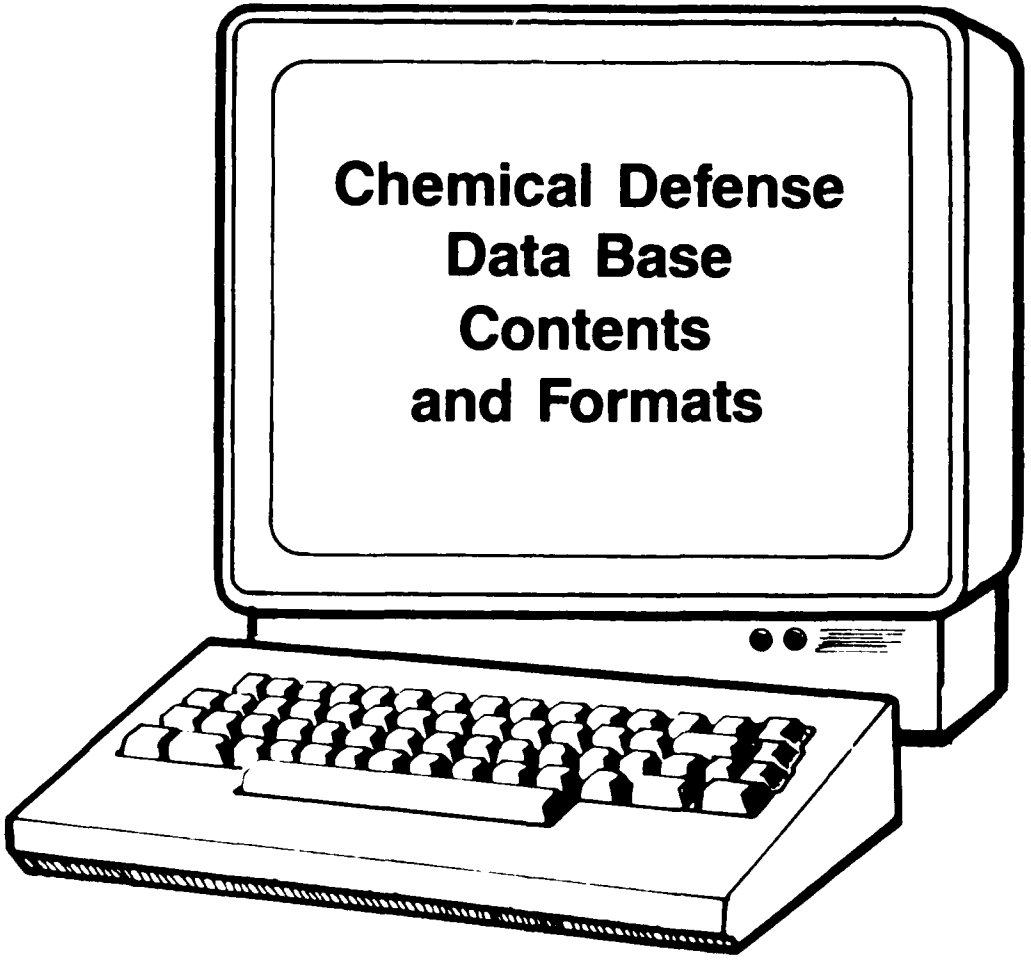
Chemical Defense
Data Base
Contents
and Formats

Data Base Contents

- Effects of CW Agents, Decontaminants, and Simulants On:
  - — Materials
  - — Subsystems/Systems
- Abstracts of Source Documents
- Properties of CW Agents, Decontaminants and Simulants
- Listing of CSM Test Facilities
- Planned Test Schedule
- Listing of CW Survivability Community Members

Chemical Defense Data Base Records

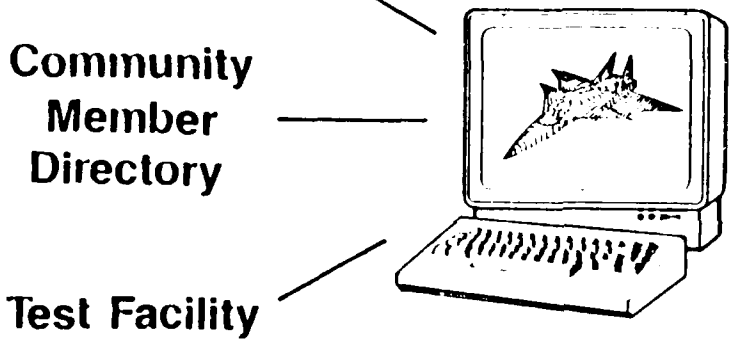

Document

Community Member Directory

Test Facility Directory

Test Schedule

Material Degradation

Component Degradation

Chemical Properties

Bibliographic Main Table

UNCLASSIFIED
MAIN TABLE

Reference Number	:	1
Record Classification	:	UNCLASSIFIED
Title	:	(U): Interaction of Chemical Warfare Agent with Polymers of Military Interest
Personal Authors	:	Pfau, J. P.; Sharpe, R. E.; Jewett, S. K.; Huggins, R. L.; Dick, R. J.
Performing Organization	:	Battelle Columbus Division, Tactical Technology Center, Columbus, Ohio 43220
PO Report Number	:	BATT-CSL-48-1
Sponsoring Organization	:	Chemical Systems Laboratory, Aberdeen Proving Ground, MD 21010
SO Report Number	:	ARCSL-CR-82039
Contract Number	:	DAAH01-81-C-A2777, MIPR No. 1.38199
Publication Date	:	82/03/00
Classification	:	UNCLASSIFIED
Availability	:	LIMITED-C
Government Accession Number	:	ADB068512

**********PLEASE ENTER CHOICE**********
* NEXT ABSTR SUBJECT MATERIEL EXIT *
****

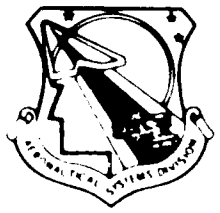

Descriptive Summary Table

UNCLASSIFIED
Degradation Descriptive Summary Table
LEVEL 1

Reference Number	:	242
Component Name	:	-0-
Material Code	:	A92024
Chemical Code	:	STB
Test Type Number	:	4
Interaction Rating	:	MAJOR
Rating Confidence	:	HIGH

General Remarks
(U): MAJOR RATING RESULTS FROM ROOM TEMP (23 DEGREES C). AT 23 DEGREES C, SEVERE EFFECTS ON MAX.ELO & RED.AREA, MAJOR EFFECTS ON YLD.STR & TN.STR.BRK & MD.ELA.T, NEGLIGIBLE EFFECT ON WEIGHT. AT 71 DEGREES C, MAJOR EFFECTS ON MAX.ELO & RED.AREA & MD.ELA.T WHILE REMAINING PROPERTIES HAVE NEGLIGIBLE EFFECTS. HIGH CONFIDENCE RATING DUE TO USE OF ASTM METHOD & CONTROL SAMPLES. AT BOTH TEMPS (23 & 71 DEGREES C), SAMPLES WERE GRAY WITH SLIGHT PITTING BY BASELINE EXPOSURE TIME.

PLEASE ENTER CHOICE

NEXT TESTSPEC MATSPEC CHEMSPEC COMPSPEC CHEMSYN MATLSYN
RATCRIT REMARKS LISTING CONDSUM EXIT

Conditional Summary Table

UNCLASSIFIED
Conditional Summary Table
LEVEL 2

REFERENCE NUMBER	: 242		
COMPONENT NAME	: -0-		
MATERIAL CODE	: A92024	CHEMICAL CODE	: STB
TEST TYPE NUMBER	: 4	TEST RUN NUMBER	: 1
NUMBER OF SAMPLES	: 5	EXPOSURE STATE	: LIQUID
EXPOSURE CONCENTRATION	: IMMERSED	EXPOSURE UNITS	: NA
EXPOSURE TEMPERTURE	: 23. C	EXPOSURE TIME	: 24. (HRS)
CONDITIONAL RATING	: MAJOR		

DATA REMARKS:
(U): MAJOR RATING DUE TO: SEVERE EFFECTS ON MAX.ELO AND RED.AREA; MAJOR EFFECTS ON YLD.STR AND TN.STR.BRK AND MD.ELA.T; NEGLIGIBLE EFFECT ON WEIGHT.

IMMMMMMMMMMMMMMMMMMMMMMMMPLEASE ENTER CHOICEMMMMMMMMMMMMMMMMMMMMMMMM;
: NEXT CHEMSYN MATLSYN LISTING PROPSUM DEGSUM EXIT :
HMMMMMMMMMMMMMMMMMMMMMMMMMMMMMMMMMMMMMMMMMMMMMMMMMMMMMMMMMMMMMMMMMMMM<

Property Summary Table

UNCLASSIFIED
PROPERTY SUMMARY TABLE
LEVEL 3

REFERENCE NUMBER	: 242		
COMPONENT NAME	: -0-		
MATERIAL CODE	: A92024	CHEMICAL CODE	: STB
TEST TYPE NUMBER	: 4	TEST RUN NUMBER	: 1
PROPERTY CODE	: MAX.ELO		

PROPERTY UNIT	: %
TEST SPECIFICATION	: ASTM E-8
TOTAL PROPERTY CHANGE	: -29.9
PROPERTY RATING	: SEVERE

PLEASE ENTER CHOICE

NEXT CHEMSYN MATLSYN PROPERTY PROPDATA CONDSUM DEGSUM
EXIT

Property Data Table

UNCLASSIFIED
PROPERTY DATA TABLE
LEVEL 4

REFERENCE NUMBER : 242
COMPONENT NAME : -0-
MATERIAL CODE : A92024 CHEMICAL CODE : STB
TEST TYPE NUMBER : 4
TEST RUN NUMBER : 1
PROPERTY CODE : MAX.ELO

TIME VALUE	PROPERTY VALUE	STANDARD DEVIATION	PCT. CHANGE
0.5 (hrs)	15.6	0.	-4.9
1. (hrs)	14.1	0.	-14.
6. (hrs)	14.	0.	-14.6
24. (hrs)	11.5	0.	-29.9

PRESS ANY KEY TO CONTINUE

Chemical Synonym Table

CHEMICAL SYNONYM TABLE

CHEMICAL CODE	:STB
COMMON NAME	:SUPER TROPICAL BLEACH
CHEMICAL CLASSIFICATION	:DECONTAMINANTS
CHEMICAL FAMILY	:N/A
CHEMICAL NAME	:-0-
CHEMICAL FORMULA	:-0-
CHEMICAL COMPOSITION	:BLEACHING POWDER CONSISTING PRIMARILY OF DOUBLE SALTS Ca(OCL)2-2Ca(OH)2 AND CaCl2-Ca(OH)2-H2O WITH CaO ADDED AS A DESICCANT. NORMALLY DISSOLVED IN WATER: 566 GRAMS STB IN 1 LITER OF WATER.
OTHER CHEMICAL NAMES	:CHLORINATED LIME, BLEACHING POWDER

PRESS ANY KEY TO CONTINUE

Material Synonym Table

MATERIAL SYNONYM TABLE

MATERIAL NAME :WROUGHT ALUMINUM ALLOY 2024

MATERIAL CODE :A92024

MATERIAL CATEGORY :METALS

MATERIAL FAMILY :ALUMINUM

TRADE NAME :-0-

PRESS ANY KEY TO CONTINUE

Chemical Property Table

SUBRECORD CLASSIFICATION : UNCLASSIFIED
CHEMICAL CODE : HD

CHEMICAL PROPERTY	PROPERTY VALUE		REFERENCE NUMBER
APPEARANCE	NA	PALE YELLOW LIQUID	125
BOILING POINT	217 EST	DEG C(DECOMPOSES AT 149-177 C)	125
DENSITY (LIQUID)	1.27	G/ML	125
DENSITY (SOLID CRYSTAL)	1.37	G/ML @ 0 DEG C	125
DENSITY (VAPOR)	5.5	AIR-1 (RELATIVE TO AIR)	125
DIFFUSION COEFFICIENT OF VAPOR IN AIR	.060 EST	CM^2/SEC	479
FLASH POINT	105	DEG C	125
FREEZING POINT	14.45	DEG C	125
HEAT OF COMBUSTION	-4752.5	CAL/G	125
HEAT OF VAPORIZATION	94	CAL/G	125
LATENT HEAT OF FUSION	26.5	CAL/G	125
LATENT HEAT OF SUBLIMATION	116.92	CAL/G @ 14.5 DEG C	479
MOLECULAR WEIGHT	159.08	G/MOLE	125
ODOR	NA	GARLIC-LIKE	125
OXYGEN INDEX	17.18	ND	125
REFRACTIVE INDEX	1.5252 EST	ND	479
SOLUBILITY IN WATER	.920	G/100 G WATER @ 22 DEG C	478
SOLUBILITY PARAMETER	10.6	HILDEBRANDS	479
SPECIFIC HEAT	.317 (SOL)	CAL/G/DEG C @ 0 DEG C	479
SPECIFIC HEAT	.358 (LIQ)	CAL/G/DEG C @ 19 DEG C	479
SURFACE TENSION	42.520	DYNES/CM	479
THERMAL CONDUCTIVITY	.316E-3	CAL/CM^2/CM/DEG C/SEC @20DEG C	479
VAPOR PRESSURE	.11	MMHG	125
VISCOSITY	3.95	CENTISTOKES	125
VOLATILITY	920	MG/M^3	125

Note : Property values are at 25 degrees C except where noted.

Material Property Synonym Table

MATERIAL PROPERTY SYNONYM TABLE

MATERIAL CATEGORY:METALS

MATERIAL PROPERTY	CODE	TEST SPECIFIC.	PROPERTY UNITS	RATING METHOD
APPEARANCE	APPEAR	NS	ALPHANUMERIC	VISUAL
BARCOL HARDNESS	BARCOL.HRD	ASTM D3648	NA	STANDARD
BEARING STRENGTH	BR.STR	ASTM E238	PSI	STANDARD
BEARING YIELD STRENGTH	BR.YLD.STR	ASTM E238	PSI	STANDARD
BREAKING LOAD	BRK.LOAD	NS	PSI	STANDARD
BRINELL HARDNESS	BRIN.HRD	ASTM E10	NA	STANDARD
BULK MODULUS OF ELASTICITY	BLK.MD.ELA	NS	PSI	STANDARD
CHEMICAL PURITY DEGRADATION	CHM.PUR.DG	NS	%	STANDARD
COLOR	COLOR	NS	ALPHANUMERIC	VISUAL
COMPRESSIVE STRENGTH	CMPRSV.STR	ASTM E9	PSI	STANDARD
CORROSION RATE	CORR.RATE	NS	MIL/YR	CORROSION
CREEP RUPTURE STRENGTH	CRP.RP.STR	ASTM E139	PSI	STANDARD
CREEP STRENGTH	CRP.STR	ASTM E139	PSI	STANDARD
DIAMETER	DIAM	NS	%	STANDARD
ELONGATION (YIELD)	ELO.YLD	NS	%	STANDARD
FATIGUE STRENGTH	FAT.STR	NS	PSI (n CYCLES)	STANDARD
IMPACT STRENGTH (CHARPY)	IM.STR.CHY	ASTM E23	FT LB	STANDARD
IMPACT STRENGTH (IZOD-NOTCHED)	IM.STR.IZN	ASTM E23	FT LB	STANDARD
IMPACT STRENGTH (IZOD-UNNOTCH)	IM.STR.IZU	NS	FT LB	STANDARD
KNOOP HARDNESS	KNOOP.HRD	ASTM E384	PSI	STANDARD
LENGTH	LENGTH	NS	%	STANDARD

Community Member Record

COMMUNITY MEMBER RECORD

FIRST NAME	FRED
LAST NAME	MEYER
TITLE	MATERIALS ENGINEER, CDDB PROJECT MANAGER
ORGANIZATION	U.S. AIR FORCE - AFWAL/MLSA
MAILING ADDRESS	AFWAL/MLSA
	-0-
	-0-
CITY	WRIGHT-PATTERSON AFB
STATE	OH
COUNTRY	USA
ZIP CODE	45433-6533
PHONE	(513)255-5108

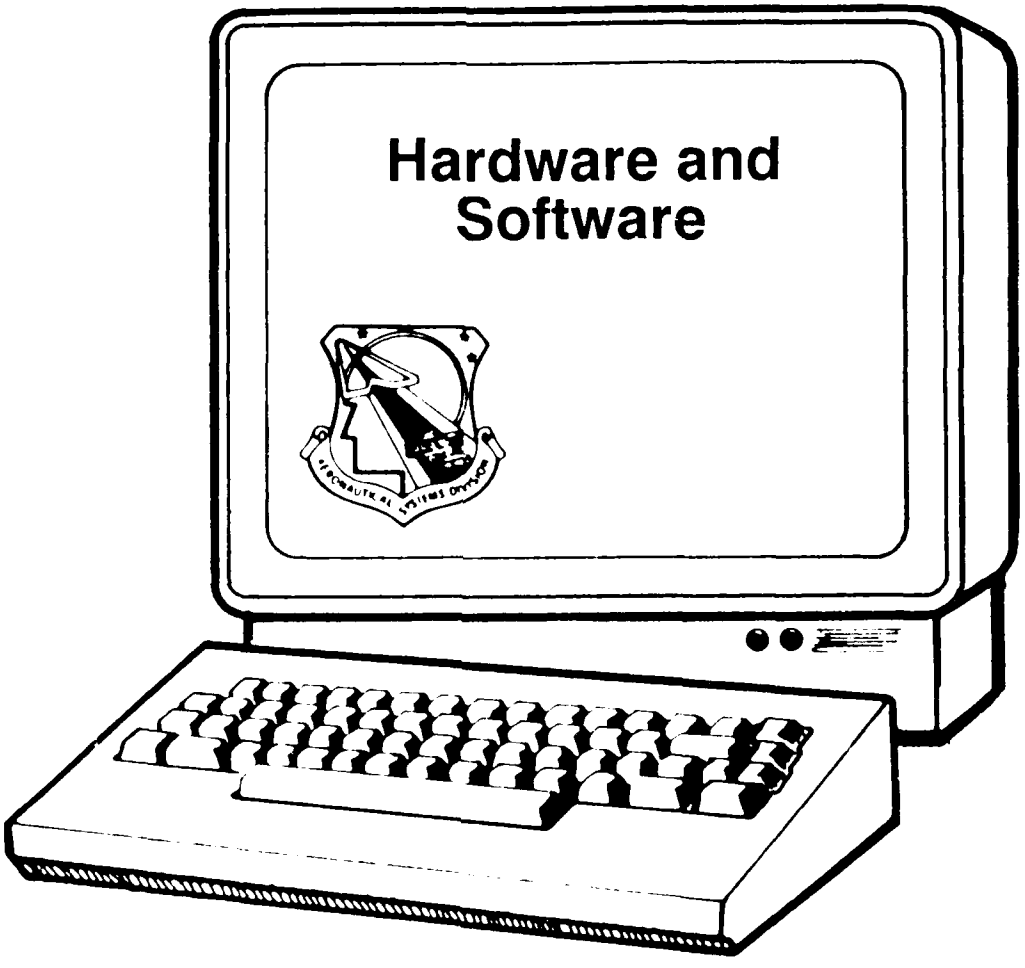
Hardware and
Software

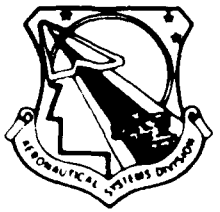

Data Base System Desirables

- Personal Computer Based System
- Large Data Storage Capabilities
- Input Proprietary Data
- Access Wide Variety of Information
- Accommodate Periodic Data Base Updates
- Meet Security Requirements
- Multi-Level Data Access
- Flexible for Future Hardware/Software Upgrading

CDDB Hardware/ Software Requirements

- IBM PC, XT, AT or 100% compatible
- Bernoulli Box (20 megabyte cartridge)
- RBASE System V Relational Database

Chemical Defense Data Base (CDDB) Security Requirements

- CDDB - SECRET NOFORN
- Industrial Contractors Must Get Following Approvals
  - Defense Investigative Service (DIS) - Standard Practice Procedure, (SPP) - DoD 5220.22-M
  - TEMPEST Certification if required - Approval of Designated Approving Authorities (DAA)

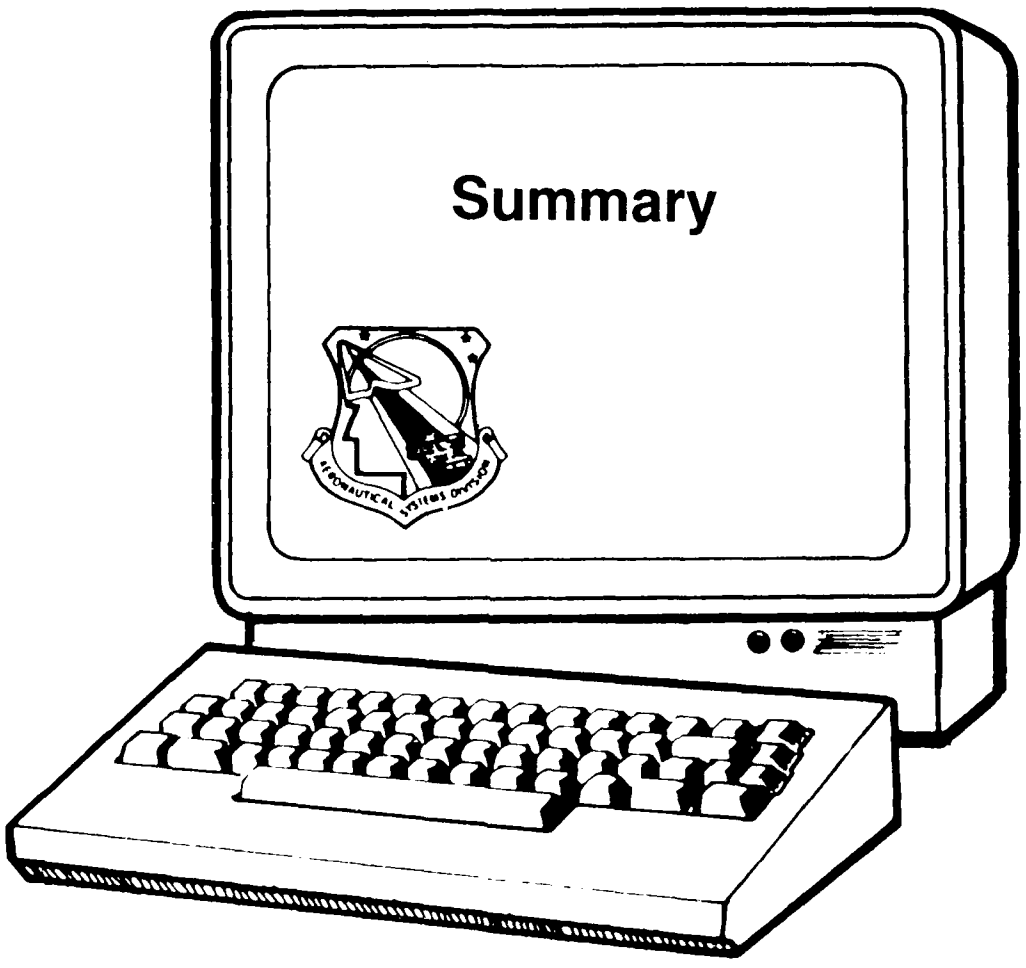
Summary

Degradation Data Entered

- 1450 Descriptive Summaries
  - 252 Materials
  - 79 Chemicals
- 1608 Conditional Summaries
- 6907 Property Data Tables

Current Effort

- Incorporate CLOUT
- Add Data
- Add Menus
- Investigate CD ROM
- Add Graphics Capability

Corrosion Information and Analysis

A Special Task Under Contract No. DLA900-83-C-1744
For The Operation of The
Metals and Ceramics Information Center (MCIC)
(MCIC Is a DoD Information Analysis Center)

Harold Mindlin
Dr. Gerhardus Koch

Battelle

Scope

- Metal Alloys
- Finishes
  - Paints
  - Organic/Metallic/Ceramic Coatings
- Sealants
- Chemical Treatments
- Design Action
- Environmental/Stress Effects
- Direct Chemical Attack

- U.S. Aircraft
- Foreign Aircraft
- Missiles
- Surface Vehicles
- Ships
- Subsystems
- Support Equipment

Functions

Collection
Storage
Review
Analysis
Appraisal
Summarization
Dissemination

Corrosion Information and Data

Scientific
Technical
Commercial

Promotion Efforts

- Actions
  - Visits – Key panel members and major DoD facilities
  - Announcements and interest survey

- Results
  - 17 visits to DoD facilities
  - 2 conferences (Triservice and ADPA CPC)
  - Interest profile – field needs
  - Topics for SOARs and handbooks
  - Separate corrosion mailing list

Acquisition and Input of Source Information

- Collection (Started With 7403 MCIC Records)
  - U.S. and foreign literature
  - Information from services and contractors
  - DROLS (through MCIC)
  - Commercial databases

- Review and analysis of 750 corrosion documents
  - 492 journal articles
  - 177 government technical reports
  - 81 technical papers

- Estimated 900-1000 documents per year

Products and Services

Handbooks and databooks

State-of-the-art reports

Critical reviews and technology assessments

Technical and bibliographic inquiries

Current awareness

Failure analysis database

Handbooks and Databooks

- Collected and reviewed over 80 percent of identified DoD publications (incl. limited distribution)
- Recommended two topics
  - Design procedures for corrosion prevention in aircraft
  - Recognition of forms of corrosion: a manual for technicians and engineers
- Prepared detailed outlines, estimated costs, and schedules
- Prepared list of other possible topics

State-Of-The-Art Reports (SOAR)

- Coverage
  - Current technology and information
  - Limited scope
- Data sources
  - Technical expert(s)
  - Pertinent literature review
- Two completed and distributed
  - "Corrosion of Electrical Connectors"
  - "Environmental Performance of Ceramic Coatings"
- Prepared list of other possible SOARs

Critical Reviews and Technologies

Respond to individual requests

Can be similar to SOAR

Usually funded separately

Technical and Bibliographic Inquiries

Technical	Bibliographic
Battelle technical staff	Utilitize DTIC/MCIC/Corrosion database Direct access by DoD or contractors to MCIC database Through MCIC (Commercial DBs through MCIC)

Technical and Bibliographic Inquiries

Responses	Costs
Oral	Free
↓	↓
Written Reports	Costs Incurred

43 inquiries from government and industry

Current Awareness Program

- Rapid dissemination of current information
- Topics within scope of task
  - Extended reviews of specific topics, significant publications, or major research programs
  - Summaries of significant meetings
  - Brief reviews of current literature
  - State-of-the-art summaries
- 14 inserts to MCIC "Current Awareness Bulletin"

Failure Analysis Database

- Objectives
  - Corrosion-related failure information
  - Computerization
  - Analysis

Failure Analysis Database

- Reviewed 556 failure reports
  - 431 laboratory failure analysis reports (WR-ALC)
  - 125 Corrosion reports (AFWAL)

- Standard input format (16 items)
  - Source-data
  - Cause, mode
  - System, subsystem, component
  - Material, related specifications
  - Part no. and manufacturer

Failure Analysis Database

Computerization

- Data review
  - Transformations
- Examples
  - C-141A, C-141B→C-141
  - C-123J, C-123K→C-123
  - Subsystems
  - Mode of failure

Failure Analysis Database

- Statistical analysis (SAS)
  - Frequency counts
  - Cross correlations

- Examples
  - Generation of frequency bar charts
  - Subsystem, component, mode
  - System, mode, subsystem, part no., material

SYS=AIRCRAFT/C-141

TABLE OF MATRL BY MODE

MODE

MATERIAL

FREQUENCY PERCENT ROW PCT COL PCT	GENERAL CORROSIO	HIGH TEN PERATURE	HYDROGEN EMBRITT	INTERGRA NULAR ST	INTERGRA NULAR TY	N/A	OVERLOAD	PITTING CORROSIO	STRESS C ORROSION	WEAR	TOTAL
6061 AL ALLOY	0 0.00 0.00 0.00	0 0.00 0.00 0.00	0 0.00 0.00 0.00	0 0.00 0.00 0.00	0 0.00 0.00 0.00	0 0.00 0.00 0.00	0 0.00 0.00 0.00	1 0.59 100.00 4.55	0 0.00 0.00 0.00	0 0.00 0.00 0.00	1 0.59
6R7 STEEL ALLOY	0 0.00 0.00 0.00	0 0.00 0.00 0.00	0 0.00 0.00 0.00	0 0.00 0.00 0.00	0 0.00 0.00 0.00	0 0.00 0.00 0.00	0 0.00 0.00 0.00	1 0.59 100.00 4.55	0 0.00 0.00 0.00	0 0.00 0.00 0.00	1 0.59
6AL-4V TI ALLOY	0 0.00 0.00 0.00	0 0.00 0.00 0.00	0 0.00 0.00 0.00	0 0.00 0.00 0.00	0 0.00 0.00 0.00	0 0.00 0.00 0.00	0 0.00 0.00 0.00	0 0.00 0.00 0.00	0 0.00 0.00 0.00	0 0.00 0.00 0.00	1 0.59
7075 AL ALLOY	0 0.00 0.00 0.00	0 0.00 0.00 0.00	0 0.00 0.00 0.00	0 0.00 0.00 0.00	0 0.00 0.00 0.00	0 0.00 0.00 0.00	0 0.00 0.00 0.00	0 0.00 0.00 0.00	2 1.18 66.67 2.63	0 0.00 0.00 0.00	3 1.78
7075 AL ALLOY	0 0.00 0.00 0.00	0 0.00 0.00 0.00	0 0.00 0.00 0.00	0 0.00 0.00 0.00	0 0.00 0.00 0.00	0 0.00 0.00 0.00	0 0.00 0.00 0.00	0 0.00 0.00 0.00	1 0.59 50.00 1.32	0 0.00 0.00 0.00	2 1.18
7075 AL ALLOY	0 0.00 0.00 0.00	0 0.00 0.00 0.00	0 0.00 0.00 0.00	8 5.33 12.50 84.28	1 0.59 1.39 100.00	0 0.00 0.00 0.00	1 0.59 1.39 100.00	0 0.00 0.00 0.00	48 28.40 66.67 63.16	0 0.00 0.00 0.00	72 42.60
7079 AL ALLOY	0 0.00 0.00 0.00	0 0.00 0.00 0.00	0 0.00 0.00 0.00	0 0.00 0.00 0.00	0 0.00 0.00 0.00	0 0.00 0.00 0.00	0 0.00 0.00 0.00	0 0.00 0.00 0.00	1 0.59 100.00 1.32	0 0.00 0.00 0.00	1 0.59
TOTAL	2 1.18	2 1.18	8 4.73	14 8.28	1 0.59	4 2.37	1 0.59	22 13.02	76 44.97	4 2.37	169 100.00

(CONTINUED)

SYS=AIRCRAFT/C-141

TABLE OF SUBSYS BY MODE

MODE

SUBSYSTEM

FREQUENCY PERCENT ROW PCT COL PCT	GENERAL CORROSIO	HIGH TEM PERATURE	HYDROGEN EMBRITT	INTERGRA NULAR ST	INTERGRA NULAR TY	N/A	OVERLOAD	PITTING CORROSIO	STRESS C ORROSION	WEAR	TOTAL
FUSELAGE	0 0.00 0.00 0.00	0 0.00 0.00 0.00	0 0.00 0.00 0.00	2 1.18 28.57 14.29	0 0.00 0.00 0.00	0 0.00 0.00 0.00	0 0.00 0.00 0.00	0 0.00 0.00 0.00	4 2.37 57.14 5.26	0 0.00 0.00 0.00	7 4.14
GUNNER WING (MON	0 0.00 0.00 0.00	0 0.00 0.00 0.00	1 0.59 100.00 12.50	0 0.00 0.00 0.00	0 0.00 0.00 0.00	0 0.00 0.00 0.00	0 0.00 0.00 0.00	0 0.00 0.00 0.00	0 0.00 0.00 0.00	0 0.00 0.00 0.00	1 0.59
HORIZONTAL STABI	0 0.00 0.00 0.00	0 0.00 0.00 0.00	0 0.00 0.00 0.00	0 0.00 0.00 0.00	0 0.00 0.00 0.00	0 0.00 0.00 0.00	0 0.00 0.00 0.00	0 0.00 0.00 0.00	1 0.59 100.00 1.32	0 0.00 0.00 0.00	1 0.59
LANDING GEAR	0 0.00 0.00 0.00	0 0.00 0.00 0.00	0 0.00 0.00 0.00	0 0.00 0.00 0.00	0 0.00 0.00 0.00	0 0.00 0.00 0.00	0 0.00 0.00 0.00	0 0.00 0.00 0.00	2 1.18 100.00 2.63	0 0.00 0.00 0.00	2 1.18
LOWER SPOILER AS	0 0.00 0.00 0.00	0 0.00 0.00 0.00	0 0.00 0.00 0.00	0 0.00 0.00 0.00	0 0.00 0.00 0.00	0 0.00 0.00 0.00	0 0.00 0.00 0.00	0 0.00 0.00 0.00	0 0.00 0.00 0.00	0 0.00 0.00 0.00	1 0.59
MAIN FRAME (FS 8	0 0.00 0.00 0.00	0 0.00 0.00 0.00	0 0.00 0.00 0.00	0 0.00 0.00 0.00	0 0.00 0.00 0.00	1 0.59 100.00 25.00	0 0.00 0.00 0.00	0 0.00 0.00 0.00	0 0.00 0.00 0.00	0 0.00 0.00 0.00	1 0.59
MAIN FRAME 1058	0 0.00 0.00 0.00	0 0.00 0.00 0.00	0 0.00 0.00 0.00	0 0.00 0.00 0.00	0 0.00 0.00 0.00	0 0.00 0.00 0.00	0 0.00 0.00 0.00	0 0.00 0.00 0.00	1 0.59 100.00 1.32	0 0.00 0.00 0.00	1 0.59
MAIN LANDING GEA	0 0.00 0.00 0.00	0 0.00 0.00 0.00	0 0.00 0.00 0.00	1 0.59 6.67 7.14	0 0.00 0.00 0.00	1 0.59 6.67 25.00	1 0.59 6.67 100.00	0 0.00 0.00 0.00	4 2.37 26.67 5.26	0 0.00 0.00 0.00	15 8.88
TOTAL	2 1.18	2 1.18	8 4.73	14 8.28	1 0.59	4 2.37	1 0.59	22 13.02	76 44.97	4 2.37	169 100.00

(CONTINUED)

SAS

SYS=AIRCRAFT/C-130

FREQUENCY BLOCK CHART

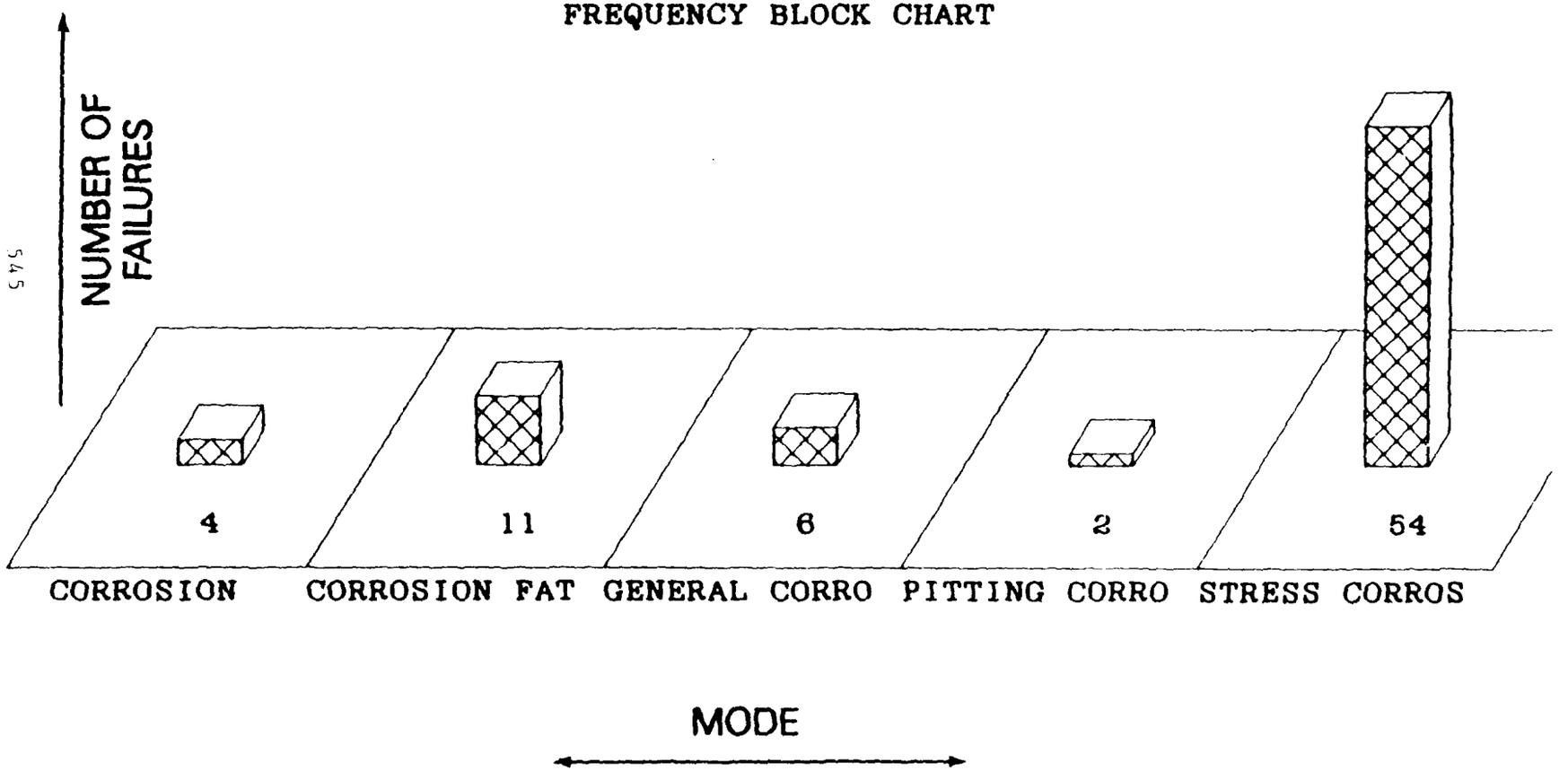

Corrosion Information and Analysis Status

- Task completed (April 85- December 86)
- Corrosion Information Analysis Center
  - Procurement cancelled
- Corrosion coverage by MCIC
  - Literature
  - CAB
  - Inquiries
  - Latest SOAR "Corrosion of Metals in Marine Environments"

References

AFWAL-TR-87-4062 (July 1987) Corrosion Information and Analysis Special Task

AFWAL-TR-87-4054 (July 1987) Development of a Corrosion-Related Failure Analysis Database

THE NACE-NBS CORROSION DATA PROGRAM

David B. Anderson
National Bureau of Standards
Gaithersburg, MD 20899

ABSTRACT

The National Association of Corrosion Engineers (NACE) and the National Bureau of Standards (NBS) have established a collaborative program to collect, analyze, evaluate and disseminate corrosion data. The multi-faceted effort centers on compilation of computerized materials performance information and corrosion database development. A user friendly computer database combining both rate (kinetic) and stability (thermodynamic) data will be a key component with emphasis on numeric corrosion data for metals and nonmetals exposed to a wide range of industrial and laboratory environments using formats and descriptors compatible with other material property/performance databases. Output programs include search parameters designed to give the user easy access to the required information in a number of graphical and tabular formats. Expert systems are also being developed to provide interpretive analysis to guide users in critical areas.

Program Justification

Corrosion has been estimated to cost developed countries 3-5% of their annual gross national product and 15% of that is considered avoidable using present technology ([1]). In the USA, it is estimated that at least $25 billion a year could be saved if existing information was effectively applied. The NACE-NBS corrosion data program was established to collect, evaluate and disseminate the comprehensive materials performance information base needed to address this need. The technical credibility of the corrosion data disseminated will be maximized by the broad-based, multi-disciplinary support provided by the expertise and resources of the NACE membership and the NBS staff.

Program Activities

Initial activities have included demonstration projects aimed at the complexities of compilation, evaluation and presentation of various types of corrosion data. The NACE Corrosion Data Survey publications on metals and nonmetals have been translated into electronic format as Cor-Sur software for PC use. The programs provide tabular and graphical outputs with unique search capabilities to characterize material compatibilities with a wide variety of environments as a guide to identification of candidate materials to meet specific corrosion requirements.

A Corrosion Data Workshop attracted sixty experts from a variety of disciplines ([2]). Discussions centered on (a) how corrosion data are used , (b) who uses corrosion data, (c) sources of corrosion data, (d) how can existing data be made more useful, (e) how to evaluate corrosion data, (f) what types of corrosion data are most useful, (g) requirements for establishment of a standard format for reporting corrosion data to facilitate database development and (h) database user benefits. These discussions have provided direction to the corrosion data program in its efforts to address the needs of industry and the corrosion community in general.

Current activities center on the following:

1. Establishment of consensus guidelines for compilation of corrosion data from multiple sources to assure meaningful database output. This includes adequate material, environment and corrosion data descriptors with assurance of compatibility with other material/performance databases. Broad-based guidance is gained through Task Groups within both NACE and ASTM.

2. Development of corrosion data evaluation techniques and procedures to insure accuracy and consistency in compiled data outputs.

3. Development of database output formats, both tabular and graphic, to aid user in understanding and interpretation of complex corrosion data.

4. Software development to utilize thermodynamic stability concepts for data interpolations.

5. Software addressing complex calculation of economics considerations in materials selection for corrosion control.

6. Computerized indexing of corrosion literature

7. Development of expert systems to guide problem solving in materials selection for critical applications where corrosion is a key factor.

References

1. J. H. Payer et al, "Economic Effects of Metallic Corrosion in the United States", NBS Special Publications 511-1 and 511-2, May 1978

2. E. D. Verink, J. Kolts, J. Rumble and G. M. Ugiansky, "Corrosion Data Program Workshop Summary", Materials Performance, April 1987, pp 55-60

BIOGRAPHY

NAME:

David B. Anderson

PRESENT AFFILIATION:

Corrosion Group
National Bureau of Standards
Gaithersburg, MD 20899

TITLE:

Physical Scientist

FIELD OF INTEREST/RESPONSIBILITIES:

Corrosion , database development

PREVIOUS AFFILIATIONS/TITLES:

International Nickel Co. various positions in corrosion research and marketing

ACADEMIC BACKGROUND:

B. S. Yale University
Graduate Studies - North Carolina State Univ.

SOCIETY ACTIVITIES/OFFICES/AWARDS:

Active in NACE and ASTM

PUBLICATIONS/PAPERS:

24 papers

☆ U.S. GOVERNMENT PRINTING OFFICE 1987 548-054 80612

1 Atch

END

DATE

FILMED

5-88

DTIC